

2012

Total synthesis of a virotoxin and analogs for conformational studies

Benson Jumba Edagwa

Louisiana State University and Agricultural and Mechanical College, bedagw1@tigers.lsu.edu

Follow this and additional works at: https://digitalcommons.lsu.edu/gradschool_dissertations



Part of the [Chemistry Commons](#)

Recommended Citation

Edagwa, Benson Jumba, "Total synthesis of a virotoxin and analogs for conformational studies" (2012). *LSU Doctoral Dissertations*. 804.

https://digitalcommons.lsu.edu/gradschool_dissertations/804

This Dissertation is brought to you for free and open access by the Graduate School at LSU Digital Commons. It has been accepted for inclusion in LSU Doctoral Dissertations by an authorized graduate school editor of LSU Digital Commons. For more information, please contact gradetd@lsu.edu.

TOTAL SYNTHESIS OF A VIROTOXIN AND ANALOGS FOR CONFORMATIONAL STUDIES

A Dissertation

Submitted to the Graduate Faculty of the
Louisiana State University and
Agricultural and Mechanical College
in partial fulfillment of the
requirements for the degree of
Doctor of Philosophy

in

The Department of Chemistry

By
Benson Jumba Edagwa
BSc, Moi University, Kenya, 2005

May 2012

ACKNOWLEDGEMENTS

I would like to express my gratitude to my advisor, Dr. Carol Taylor, for her invaluable guidance and support during my research studies. I would also like to thank my committee members Dr. William Crowe, Dr. Graca Vicente, Dr. Evgueni Nesterov and Dr. Frederick Enright for their advice and meaningful suggestions. Sincere thanks to Dr. Dale Treleaven and Dr. Thomas Weldeghiorghis for their help with NMR studies.

My appreciation goes to my wife Teresa Mutahi for her moral support. It is because of her understanding that I am able to complete my degree. My gratitude goes to my parents, brothers, sisters and the Kamau family. Without their encouragement and faith in me, I would not have made it this far.

I thank members of the Taylor research group, Doug, Ning, Chamini, Saroj, Chyree, Molly and Jarret for the discussions, friendship and encouragement. I also thank Stefan of Dr. Crowe group and Kevin of Dr. Macnaughtan group for their good friendship. My gratitude goes to the department of Chemistry, Louisiana State University for their financial support.

TABLE OF CONTENTS

ACKNOWLEDGEMENTS	ii
LIST OF TABLES	v
LIST OF FIGURES	vi
LIST OF SCHEMES	viii
LIST OF ABBREVIATIONS AND SYMBOLS	xi
ABSTRACT	xv
 CHAPTER 1. BACKGROUND AND SIGNIFICANCE.....	 1
1.1 STRUCTURE AND OCCURRENCE OF AMANITA TOXINS	1
1.2 BIOLOGICAL ACTIVITY AND POTENTIAL APPLICATIONS	3
1.3 BIOSYNTHESIS	6
1.4 PREVIOUS SYNTHETIC STUDIES AND ANALOGS.....	8
1.4.1 Kahl and Coworkers	9
1.4.2 Zanotti and Coworkers.....	11
1.4.3 Ongoing Synthetic Studies.....	13
1.4.3.1 Guy and Coworkers	13
1.4.3.2 Schuresko and Lokey	15
1.5 GOALS OF THE CURRENT WORK	15
 CHAPTER 2. SYNTHESIS OF A DIHYDROXYLEUCINE-VALINE DIPEPTIDE	 19
2.1 PREVIOUS SYNTHESIS OF THE 4,5-DIHYDROXYLEUCINE RESIDUE	20
2.2 THE SHARPLESS ASYMMETRIC DIHYDROXYLATION.....	20
2.3 PREPARATION OF (2 <i>S</i>)-4,5-DIHYDROXYLEUCINE RESIDUE	27
2.4 THE DIHYDROXYLATION REACTION	30
2.4.1 Stereochemical Analysis of the Dihydroxylation Reaction	38
2.4.2 Summary	40
2.5 EXPERIMENTAL SECTION	41
2.5.1 General Methods	41
2.5.2 Spectra.....	51
 CHAPTER 3. THE PEPTIDE FRAGMENTS	 76
3.1 Overview	76
3.2 2-METHYLSULFONYL-TRYPTOPHAN AND THE TETRAPEPTIDE FRAGMENT.....	77
3.3 THE PROLINE BUILDING BLOCKS AND THE TRIPEPTIDE FRAGMENTS.....	82
3.3.1 <i>L</i> -Proline Benzyl Ester Hydrochloride.....	83
3.3.2 <i>L</i> -4- <i>cis</i> -Hydroxyproline Building Block.....	83
3.3.3 <i>L</i> -3- <i>trans</i> -Hydroxyproline Building Block.....	85
3.3.4 <i>L</i> -2,3- <i>trans</i> -3,4- <i>trans</i> -3,4-Dihydroxyproline	86

3.3.5 Completion of the Tripeptide Fragments	89
3.3.6 Summary	92
3.4 EXPERIMENTAL SECTION	93
3.4.1 General Methods	93
3.4.2 Spectra and HPLC Chromatograms	120
CHAPTER 4. FRAGMENT CONDENSATION AND CYCLIZATIONS	173
4.1 THE LINEAR HEPTAPEPTIDES	173
4.1.1 Overview	173
4.1.2 The Risk of Epimerization in Fragment Condensation	174
4.1.3 Execution of the Condensations	177
4.2 THE CYCLIZATIONS	178
4.2.1 The Importance of Cyclic Peptides	178
4.2.2 Types of Peptide Cyclization	179
4.2.3 Suppressing Epimerization of the C-Terminal Residue	181
4.2.4 Conformational Control to Facilitate Cyclization	184
4.2.5 Cyclizations and Deprotections	188
4.2.6 Summary/Conclusions	193
4.3 EXPERIMENTAL SECTION	194
4.3.1 General Methods	194
4.3.2 Spectra and HPLC Chromatograms	202
CHAPTER 5. CONFORMATION	219
5.1 NMR, CD AND X-RAY STUDIES	219
5.1.2 Bhaskaran and Yu	221
5.1.3 Kobayashi and coworkers	222
5.1.4 Zanotti and coworkers	226
5.1.5 Zanotti and coworkers	228
5.1.6 Falcigno and coworkers	230
5.2 CONFORMATION OF THE PROLINE CONTAINING TRIPEPTIDES	233
5.2.1 Overview	233
5.2.2 Computational Studies	238
5.2.3 NMR Assignments and CD of Alloviroidin Analogs	244
5.2.4 Summary	248
5.2.5 Future Work	250
5.3 EXPERIMENTAL SECTION	251
5.3.1 General Methods	251
REFERENCES	253
APPENDIX: LETTERS OF PERMISSION	269
VITA	274

LIST OF TABLES

Table 1.1	Natural virotoxins isolated from <i>Amanita</i> species	2
Table 1.2	Natural virotoxins isolated from <i>Amanita suballiacea</i>	2
Table 1.3	The virotoxin analogs and their constituent amino acid residues.	9
Table 1.4	Cyclization yields and actin affinities of viroisin analogs relative to viroisin.....	12
Table 2.1	Turning the mismatched into the matched case via protecting group tuning	24
Table 2.2	Asymmetric dihydroxylation of 1,1-disubstituted allyl alcohol derivatives.....	25
Table 2.3	Examples reagent-controlled dihydroxylations	26
Table 2.4	Conditions for the aminolysis of lactone 103 with <i>L</i> -valine ethyl ester (104)	33
Table 4.1	Effect of coupling reagent and base during peptide bond formation.....	176
Table 4.2	Ehrlich and co-workers' cyclization of all <i>L</i> -pentapeptide.....	182
Table 5.1	The <i>cis</i> -to- <i>trans</i> isomerization across the prolyl-serine peptide bond.....	235
Table 5.2	The <i>cis</i> -to- <i>trans</i> isomerization across the prolyl-serine peptide bond in CDCl ₃	237
Table 5.3	The energies and equilibrium constants of the optimized dipeptide geometries	239
Table 5.4	The energies and equilibrium constants of the optimized geometries.....	242
Table 5.5	¹ H NMR chemical shifts of alloviroidin analogs.....	246

LIST OF FIGURES

Figure 1.1	<i>Amanita</i> mushrooms and prototypical members of the phallotoxins and virotoxins	1
Figure 1.2	Fluorescent dyes that have been conjugated to phalloidin	5
Figure 1.3	Conceptual representation of actin polymerization	5
Figure 1.4	Ribosomal cyclic peptide synthesis in a fungus.	7
Figure 1.5	Glu ⁷ phalloidin and a fluorescent conjugate.....	15
Figure 2.1	The Sharpless dihydroxylation mnemonic	21
Figure 2.2	Phthalazine and pyrimidine ligands	22
Figure 2.3	¹⁹ F NMR spectra (CDCl ₃ , 236 MHz) for Mosher amide 88 derived from enzymatically resolved dehydroleucine and racemic dehydroleucine	29
Figure 2.4	Matched and mismatched double diastereoselectivity	31
Figure 2.5	Interconversion of conformations of the γ -lactone 92	31
Figure 2.7	ORTEP diagram of compound 54a (2 <i>S</i> ,4 <i>S</i>).	37
Figure 2.8	Selected region of the ¹ H NMR spectrum of the γ -lactones obtained via different routes.....	37
Figure 3.1	Byproducts arising from Fmoc cleavage.....	81
Figure 3.2	The series of four tripeptide fragments	82
Figure 3.3	Naturally occurring virotoxins	86
Figure 3.4	Generation of molecular hydrogen from triethylsilane/Pd-C and methanol mixture.....	92
Figure 4.1	Selected phosphorous and uronium based coupling reagent.....	175
Figure 4.2	Examples of cyclic peptide drugs. Somatostatin (186) along with hexapeptide analogs (187-194), synthesized by Hirschmann and co-workers.....	178
Figure 4.3	Examples of peptide cyclization approaches.....	179
Figure 4.4	Schmidt and Langner sequence dependence cyclization.....	185
Figure 4.5	TBS deprotection and purification protocol	192
Figure 5.1	The CD spectra of viroidin (A), viroisin (B), and phalloidin (C) sulfone.....	219
Figure 5.2	Viroisin (7) and dethiophalloidin (221)	220
Figure 5.3	Stereo views of viroisin solution conformations showing side chain orientations	222
Figure 5.4	ROE correlations determined from 2D ROESY spectra	223
Figure 5.5	The <i>trans</i> and <i>cis</i> conformations of a <i>D</i> -serine-prolyl amide bond.....	225
Figure 5.6	β -turn regions in viroisin and phalloidin	226
Figure 5.7	Viroisin analogs.....	227

Figure 5.8 Stereodrawing of the molecular model of (Ala ⁷)-phalloidin	228
Figure 5.9 Conformations of hyp ⁴ residue	229
Figure 5.10 Intramolecular hydrogen bonds (dotted lines) observed by X-ray analysis	230
Figure 5.11 Phalloidin analogs analyzed by Falcigno and co-workers	230
Figure 5.12 <i>P</i> - and <i>M</i> - helical configurations of a 2-indolylthioether	231
Figure 5.13 A stereodrawing of analog 226 illustrating a U-type structure	232
Figure 5.14 The <i>cis</i> and <i>trans</i> conformations of a <i>D</i> -serine-prolyl amide bond.....	233
Figure 5.15 Conformations of hyp ⁴ residue	234
Figure 5.16 Pyrrolidine conformation in compound 171	236
Figure 5.17 Pyrrolidine conformation in compounds 173 and 174	236
Figure 5.18 Pyrrolidine conformation in compounds 47 , 49 and 50	237
Figure 5.19 Optimized geometries of dipeptides 231 and 232	239
Figure 5.20 Optimized geometries of dipeptides 235 and 236	242
Figure 5.21 The NH-H α cross peaks in the TOCSY spectrum of compound 43 in 90 % H ₂ O/10 % D ₂ O (pH 3.0) at 25 °C and 700 MHz.....	245
Figure 5.22 The NH-H α cross peaks in the TOCSY spectrum of compound 44 in 90 % H ₂ O/10 % D ₂ O (pH 3.0) at 25 °C and 700 MHz.....	246
Figure 5.23 Circular dichroism spectra of hyp (45) and Pro (43) analogs in water (1.4 x 10 ⁻⁴ M)	248

LIST OF SCHEMES

Scheme 1.1	Simplified rendition of key degradation reactions	4
Scheme 1.2	Derivatization of phalloidin and attachment to a fluorophore	4
Scheme 1.3	Sequence of reactions that would convert a phalloxin-type precursor into a virotoxin.....	6
Scheme 1.4	Partial synthesis of phalloidin from the natural product	8
Scheme 1.5	Formation of peptide bonds via a mixed anhydride method.....	8
Scheme 1.6	Synthesis of virotoxin analogs 20 and 21	10
Scheme 1.7	Synthesis of virotoxin analogs 22 and 23	11
Scheme 1.8	Synthesis of viroisin analog 21	13
Scheme 1.9	Guy and co-workers' retrosynthetic analysis of Ala ⁷ phalloidin	14
Scheme 1.10	Retrosynthetic analysis of alloviroidin and analogs.....	17
Scheme 1.11	The conformation of the prolyl peptide bond and cyclization	18
Scheme 2.1	Retrosynthetic analysis of alloviroidin and analogs.....	19
Scheme 2.2	Wieland and Weiberg dihydroxyleucine synthesis	20
Scheme 2.3	Retrosynthetic analysis of dihydroxylation of an (<i>S</i>)-dehydroleucine derivative	21
Scheme 2.4	Matched and mismatched double diastereoselectivity	23
Scheme 2.5	Wade and co-workers' dihydroxylation of 4,5-dehydroisoxazoles	25
Scheme 2.6	Morikawa and Sharpless dihydroxylation of a carbohydrate-derived olefin ester.....	26
Scheme 2.7	Diastereoselectivity in the asymmetric dihydroxylation of an <i>L</i> -proline derived 1,1-disubstituted alkene.....	27
Scheme 2.8	Preparation of the dehydroleucine residue	28
Scheme 2.9	Undesired lactone formation	28
Scheme 2.10	Mosher amide formation	29
Scheme 2.11	Dihydroxylation of the dehydroleucine residue	30
Scheme 2.12	Diketopiperazine formation	32
Scheme 2.13	Examples of γ -lactone opening by <i>N</i> -nucleophiles	32
Scheme 2.14	Formation of the γ,γ -dimethyl- γ -valerolactone and reaction with the valine ethyl ester	34
Scheme 2.15	Lactone ring opening by hydrolysis	34
Scheme 2.16	Proposed rcemization mechanism	35
Scheme 2.17	Dihydroxylation of hindered esters	35

Scheme 2.18	Dihydroxylation of the dehyLeu-Val dipeptide	36
Scheme 2.19	Cleavage of peptides containing γ -hydroxyamino acids under mild acid conditions	38
Scheme 2.20	Protection of the dipeptide diol	38
Scheme 2.21	Dihydroxylation of the dehydroamino ester.....	39
Scheme 2.22	Dihydroxylation of the dehyLeu-Val dipeptide	39
Scheme 3.1	Retrosynthetic analysis of alloviroidin and analogs.....	76
Scheme 3.2	Retrosynthetic analysis of the tetrapeptide.....	77
Scheme 3.3	Takase and co-workers synthesis of the 2-thiomethyl derivative of Cbz- <i>L</i> -Trp-OMe	77
Scheme 3.4	Dillard and co-workers' synthesis of indole-3-acetamides	78
Scheme 3.5	Preparation of the 2-methylsulfonyl-tryptophan	79
Scheme 3.6	Preparation of the tetrapeptide fragment.....	79
Scheme 3.7	Acid activation by HATU	80
Scheme 3.8	Cleavage of the Fmoc group via β -elimination.....	81
Scheme 3.9	Preparation of the proline building block.....	83
Scheme 3.10	Preparation of the hydrochloride salt of 4-hyp building block	84
Scheme 3.11	Preparation of the trifluoroacetate salt of 4-hyp building block	85
Scheme 3.12	Preparation of the trifluoroacetate salt of 3-Hyp building block	85
Scheme 3.13	Kahl and Wieland synthesis of two naturally occurring dihydroxyproline diastereomers	87
Scheme 3.14	Synthesis of 2,3- <i>trans</i> -3,4- <i>trans</i> -3,4-dihydroxyproline residue.....	87
Scheme 3.15	Silyl ether migration upon reductive opening of the lactone ring.....	88
Scheme 3.16	Pyrrolidine ring formation.....	88
Scheme 3.17	The synthesis of the Fmoc- <i>D</i> -Thr- <i>D</i> -Ser dipeptide.....	89
Scheme 3.18	Preparation of the tripeptides	90
Scheme 3.19	Hydrogenolysis of the benzyl ester	91
Scheme 4.1	Retrosynthetic analysis of allovroidin and analogs.....	173
Scheme 4.2	Racemization through oxazolone	174
Scheme 4.3	The [3 + 4] fragment condensations.....	177
Scheme 4.4	Crich and Sasaki's head to tail cyclization of a pentapeptide	180
Scheme 4.5	Anseth and co-workers' side chain to tail cyclization on a solid phase.....	180
Scheme 4.6	Smith and co-workers' side chain to side chain cyclization on a solid phase.....	180

Scheme 4.7	Zhang and Tam's head to side chain cyclization	181
Scheme 4.8	EDC activation	183
Scheme 4.9	Schmidt and Langner's C-terminal epimerization of all <i>L</i> residues.....	184
Scheme 4.10	Extended and circular conformations of the peptide	185
Scheme 4.11	Jolliffe and co-workers' synthesis utilizing pseudoproline as turn inducers	186
Scheme 4.12	van Maarseveen and co-workers' site isolation mechanism using carbosilane dendrimeric carbodiimide	187
Scheme 4.13	Abdel-Magid and co-workers hydrolysis of polypeptide esters.....	188
Scheme 4.14	Wipf and Uto's synthesis of trunkamide A	189
Scheme 4.15	Cyclizations and global desilylation	190
Scheme 4.16	Kaburagi and Kishi's synthesis of halichondrin	191
Scheme 5.1	Derivatization of alloviroidin with a fluorophore	251

LIST OF ABBREVIATIONS AND SYMBOLS

Å	Angstrom
Ac	Acetyl
AD-mix- α	1 kg contains: K ₃ Fe(CN) ₆ , 699.6 g; K ₂ CO ₃ , 293.9 g; and [(DHQ) ₂ -PHAL], 5.52g; and K ₂ O ₅ O ₂ (OH) ₄ , 1.04 g
AD-mix- β	Contents are as for AD-mix- α except the ligand: [(DHQD) ₂ -PHAL]
AOP	(7-azabenzotriazol-1-yl)oxytris-(dimethyl amino)phosphonium hexafluorophosphate
Bg	<i>N</i> -benzhydrylglycolamide
Bn	benzyl
Boc	<i>tert</i> -butyloxycarbonyl
BOP	benzotriazol-1-yloxytris(dimethylamino)-phosphonium hexafluorophosphate
^t Bu	<i>tert</i> -butyl
° C	degrees Celsius
Cbz	carbobenzyloxy
COSY	correlation spectroscopy
mCPBA	<i>meta</i> -chloroperoxybenzoic acid
DCC	dicyclohexylcarbodiimide
<i>de</i>	diastereomeric excess
Ddz	α,α -dimethyl-3,5-dimethoxybenzyloxycarbonyl
(DHQ) ₂ -PHAL	dihydroquinine-phthalazine
(DHQD) ₂ -PHAL	dihydroquinidine-phthalazine
DIEA	<i>N,N</i> -diisopropylethylamine

DMAP	4-dimethylaminopyridine
DMF	dimethylformamide
DMSO	dimethylsulfoxide
DPPA	diphenylphosphoryl azide
EDC	1-(3-dimethylaminopropyl)-3-ethylcarbodiimide hydrochloride
<i>ee</i>	enantiomeric excess
ESI	electrospray ionization
Fmoc	9-fluorenylmethoxycarbonyl
HAPyU	<i>O</i> -(7-azabenzotriazol-1-yl)-1,1,3,3-tetramethylenuronium hexafluorophosphate
HATU	<i>O</i> -(7-azabenzotriazol-1-yl)-1,1,3,3-tetramethyluronium hexafluorophosphate
HBPyU	<i>O</i> -(benzotriazol-1-yl)oxybis-(pyrrolidino)uronium hexafluorophosphate
HBTU	<i>O</i> -(benzotriazol-1-yl)-1,1,3,3-tetramethyluronium hexafluorophosphate
HMBC	heteronuclear multiple bond coherence
HOAt	1-hydroxy-7-azabenzotriazole
HOBt	1-hydroxybenzotriazole
HPLC	high performance liquid chromatography
HRMS	high resolution mass spectrometry
HSQC	heteronuclear single quantum correlation
hyLeu	γ -hydroxy- <i>L</i> -leucine
dihyLeu	4,5-dihydroxyleucine
aHyp	<i>allo</i> -hydroxyproline (<i>cis</i> -4-hydroxy- <i>L</i> -proline)
Lac	internal γ -lactone

MA	mixed anhydride
MEM	β -methoxyethoxymethyl
Ms	methanesulfonyl
MS	mass spectrometry
MTPA	α -methoxy- α -trifluoromethylphenylacetic acid
NHS	<i>N</i> -hydroxysuccinimide
NMM	<i>N</i> -methylmorpholine
NMR	nuclear magnetic resonance
nOe	nuclear Overhauser effect
PMA	phosphomolybdic acid
ppm	parts per million
PyAOP	[(7-azabenzotriazol-1-yl)oxy]tri-(pyrrolidino)phosphonium hexafluorophosphate
PyBOP	benzotriazol-1-yloxytri(pyrrolidino)phosphonium hexafluorophosphate
PyBroP	bromotri(pyrrolidino)phosphonium hexafluorophosphate
PyCloP	chlorotri(pyrrolidino)phosphonium hexafluorophosphate
R_f	retention factor
rt	room temperature
s	singlet
q	quartet
TAEA	<i>tris</i> (2-aminoethyl)amine
TATU	<i>O</i> -(7-azabenzotriazol-1-yl)-1,1,3,3-tetramethyluronium tetrafluoroborate
TBAF	tetra- <i>n</i> -butylammonium fluoride

TBAH	tetra- <i>n</i> -butylammonium hydroxide
TBDMS/TBS	<i>t</i> -butyldimethylsilyl
TBTU	<i>O</i> -benzotriazol-1-yl-1,1,3,3-tetramethyluronium tetrafluoroborate
TFA	trifluoroacetic acid
TFFH	tetramethylfluoroformamidinium hexafluorophosphate
THF	tetrahydrofuran
TLC	thin layer chromatography
TOF	time of flight
UV	ultraviolet

Standard 3 letter codes are utilized throughout the document for amino acids

ABSTRACT

This dissertation describes the first total synthesis of alloviroidin in trace amounts, along with that of three analogs containing *L*-proline (Pro), *trans*-3-hydroxyproline (3-Hyp) or *cis*-4-hydroxyproline (4-hyp) residue substituting for 2,3-*trans*-3,4-*trans*-dihydroxyproline in the natural product.

We report herein an efficient strategy that provides a dipeptide containing a (2*S*,4*S*)-4,5-dihydroxy-leucine (diHyLeu) residue, including a diastereoselective dihydroxylation. *N*-α-Carbobenzyloxy-(2*S*)-4,5-dehydroleucine was coupled with valine ethyl ester to give a dipeptide that was subjected to a Sharpless asymmetric dihydroxylation to introduce the diol. The relative configuration at C4 was assigned as *S* by X-ray crystallography after derivatization as an α-amino-γ-lactone hydrochloride salt.

The preparation of the 2-(methylsulfonyl)tryptophan residue is described followed by incorporation into a tetrapeptide, Fmoc-Ala-[2-MeSO₂]-Trp-diHyLeu(OTBS)-Val-OEt. An efficient synthesis of four tripeptide fragments is also described: Fmoc-*D*-Thr(OTBS)-*D*-Ser(OTBS)-Pro*-OBn, where Pro* represents Pro, 3-Hyp, 4-hyp and DHP. These tripeptides were assembled via a [2+1] coupling between Fmoc-*D*-Thr(O^tBu)-*D*-Ser(O^tBu)-OH and the appropriate proline benzyl ester. The acid labile side-chain protecting groups were swapped out for fluoride-labile silyl ethers.

Linear heptapeptides were prepared via [3+4] fragment condensations between the series of four tripeptide acids Fmoc-*D*-Thr(OTBS)-*D*-Ser(OTBS)-Pro*-OH and the tetrapeptide amine H-Ala-[2-MeSO₂-Trp]-diHyLeu(OTBS)-Val-OEt. Deprotection of the *N*- and *C*-termini, followed by cyclization and global side chain deprotection generated our target cyclopeptides. Removal of excess TBAF reagent and salts formed as byproducts during ethyl ester and silyl ether deprotections was achieved by treatment with DOWEX 50WX8-400 H⁺ resin and calcium carbonate. This procedure led to reasonable

yields of the three analogs but afforded only trace amounts of the natural product after HPLC purification.

We examined the conformational preferences of dipeptide fragments Ac-*D*-Ser-Pro*-NHMe (in both free and TBS protected side chains of *D*-Ser and Pro* residues) using computational studies. The computational analyses confirm that the ratio of *trans:cis* conformers varies with the degree, regio- and stereochemistry of proline hydroxylation. These equilibrium constant about the prolyl amide bond calculated for these dipeptides are in qualitative agreement with those determined by NMR for tripeptides Fmoc-*D*-Thr-*D*-Ser-Pro*-OBn (in both free and TBS protected side chains).

CHAPTER 1: BACKGROUND AND SIGNIFICANCE

1.1 STRUCTURE AND OCCURRENCE OF AMANITA TOXINS

The virotoxins are cyclic heptapeptides derived from species of mushrooms known as *Amanita virosa*¹ and *Amanita suballiacea*,² also commonly referred to as the “destroying angels.” The name “destroying angel” refers to the fact that even though *Amanita* is pure, like an angel’s veil, and strikingly beautiful, it turns out to be deadly.³ These species share several toxic peptides with those isolated from *Amanita phalloides*, the “death cap.”

Virotoxins closely resemble phallotoxins morphologically and pathogenetically.^{4, 5} The major structural difference is that the virotoxins are monocyclic in nature, while the phallotoxins are bicyclic. Furthermore, three of the seven amino acids of the virotoxins differ from the corresponding residues in phallotoxins (Fig. 1.1). These are the 2,3-*trans*-3,4-*cis*-3,4-dihydroxyproline vs. *cis*-4-*(allo)*hydroxyproline in position 4 (hyp), *D*-serine vs. *L*-cysteine in position 3, and finally, the thioether bridge between tryptophan and cysteine in the phallotoxins is replaced by a non-bridging 2'-(methylsulfonyl)tryptophan in the virotoxins. The variation in side chains, leading to the six different virotoxins, and their proportions, as isolated from *Amanita virosa*, are given in Table 1.1.¹

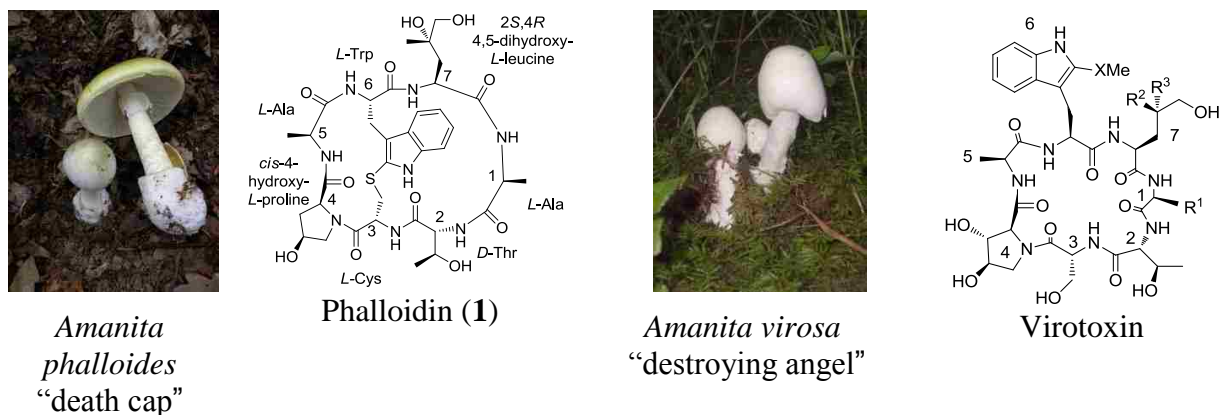


Figure 1.1. *Amanita* mushrooms and prototypical members of the phallotoxins and virotoxins.

Table 1.1: Natural virotoxins isolated from *Amanita* sp. R¹-R³ and X are as defined in Figure 1.1.

Compound Number	Name	X	R ¹	R ²	R ³	Percent of total*
2	Viroidin	SO ₂	CH(CH ₃) ₂	OH	CH ₃	18
3	Alloviroidin	SO ₂	CH(CH ₃) ₂	CH ₃	OH	**
4	Desoxoviroidin	SO	CH(CH ₃) ₂	CH ₃	OH	4
5	Ala ¹ -viroidin	SO ₂	CH ₃	CH ₃	OH	} 10
6	Ala ¹ -desoxoviroidin	SO	CH ₃	CH ₃	OH	
7	Viroisin	SO ₂	CH(CH ₃) ₂	CH ₂ OH	OH	49
8	Desoxoviroisin	SO	CH(CH ₃) ₂	CH ₂ OH	OH	19

* Of extract from *Amanita virosa*.¹

** Isolated from *Amanita suballiacea*.²

In the nomenclature of the virotoxins and phallotoxins, the suffix “-din” denotes a two-fold hydroxylated side chain of residue seven and “-sin”, a three-fold hydroxylated one.⁶ From Figure 1.1 and Table 1.1, it can be seen that the features common to both phallotoxins and virotoxins are the *D*-threonine in position two, *L*-alanine in position five, and *L*-leucine, with a varying degree of hydroxylation in position seven.

Although virotoxins were initially isolated from, and presumed unique to, *Amanita virosa*,¹ Little *et al.* demonstrated that these compounds exist in *Amanita suballiacea* too.² They found that, of the virotoxins (1.3 mg/g of dry weight tissue) in *Amanita suballiacea*, viroisin represented 75% of the total; alloviroidin and viroidin represented 15 and 9-10% respectively, while Ala¹-viroidin was detected in levels of less than 1% (Table 1.2).²

Table 1.2: Natural virotoxins isolated from *Amanita suballiacea*.² R¹-R³ and X are as defined in Fig. 1.1.

Compound Number	Name	X	R ¹	R ²	R ³	Percent of total
2	Viroidin	SO ₂	CH(CH ₃) ₂	CH ₃	OH	9-10
3	Alloviroidin	SO ₂	CH(CH ₃) ₂	OH	CH ₃	15
5	Ala ¹ -viroidin	SO ₂	CH ₃	CH ₃	OH	<1
7	Viroisin	SO ₂	CH(CH ₃) ₂	CH ₂ OH	OH	75

It was established that alloviroidin and viroidin have identical molecular weights and affinity for actin. The only difference between alloviroidin and viroidin lies in the configuration at C4 in the 4,5-dihydroxyleucine residue. This was found to be 2*S*,4*S* in alloviroidin, in contrast to 2*S*,4*R* in viroidin and phalloidin.²

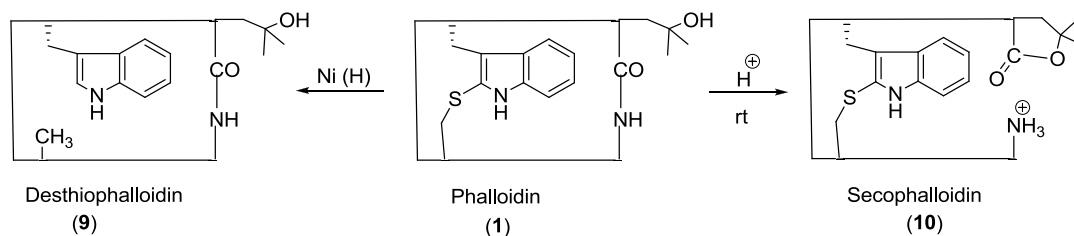
1.2 BIOLOGICAL ACTIVITY AND POTENTIAL APPLICATIONS

Mushrooms of the genus *Amanita* account for most of the fatal intoxications by mushrooms following ingestion. In his book on peptides of poisonous *Amanita* mushrooms, Theodor Wieland states that, “the actual number of victims due to poisonous *Amanita* mushrooms throughout history is unknown.”⁶ The term *fungus* is derived from the Latin word *funus* (= funeral). High concentrations of toxins are found in the carpophores (fruiting body). Biological studies have shown that one mature destroying angel or death cap can contain a fatal dose of 10-12 mg of toxin.^{1, 7, 8} According to Wieland,¹ both phallotoxins and virotoxins cause the death of experimental white mice within two to five hours of administration. The toxins target the liver, causing it to swell due to hemorrhage.⁹ It is speculated that the mechanism of intoxication of these peptides involves binding to the liver cell actin.¹ The physiological role of these peptides in mushrooms is not well understood, however, it is presumed that phallotoxins and virotoxins could be playing a role in cellular functions involving contractile apparatus.¹

The phallotoxins bind and stabilize filamentous F-actin, lowering the critical concentration of actin monomers in solution. This is fascinating, since derived monocyclic compounds, such as desthiophalloidin do not show affinity for actin. Monocyclic derivatives of phallotoxins can be generated by either cleavage of a peptide bond or removal of the sulfur atom forming the thioether bridge (Scheme 1.1). According to Wieland,¹⁰ the peptide bond between γ -hydroxylated side chain 7 and the amino acid in position 1 was readily cleaved upon treatment with mild acid to generate

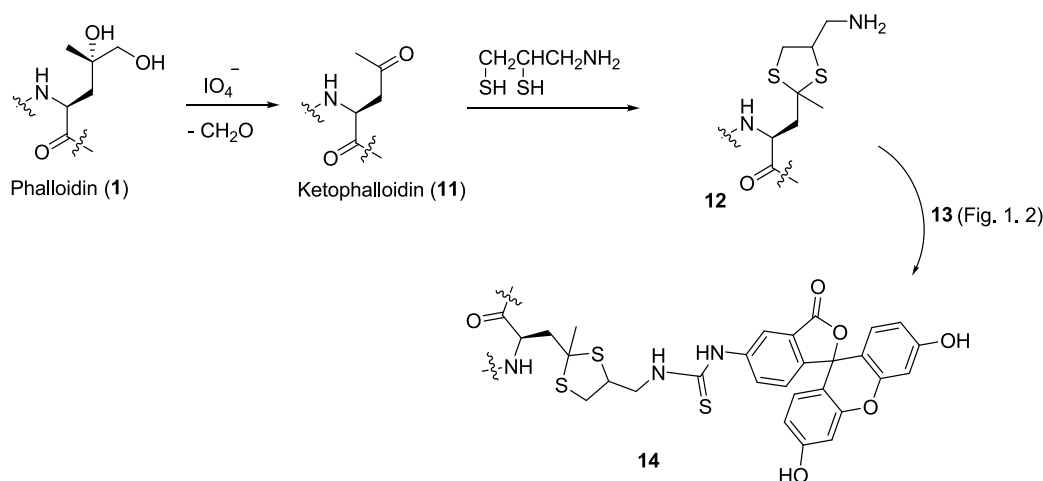
secophalloidin (**10**) that was found to be non-toxic. Also, hydrogenolysis with Raney nickel assisted in removal of the sulfur atom forming part of the thioether bridge and delivered monocyclic desthiophalloidin (**9**) that was also biologically inactive (Scheme 1.1).

Scheme 1.1. Simplified rendition of key degradation reactions.



Phalloidin is widely used to study actin dynamics *in vitro* and its fluorescent analogs¹¹⁻¹⁴ have been used for microscopic visualization of the actin cytoskeleton. Structure-activity studies have shown that the γ,δ -dihydroxyleucine residue is not essential for actin binding^{15, 16} and therefore the hydroxyl side chain of this amino acid has been derivatized to generate fluorescent analogs of phalloidin.^{11, 13, 17, 18} Wieland and co-workers oxidized phalloidin to ketophalloidin (**11**), and subsequently derivatized with 2,3-dimercaptopropylamine introducing an amino nucleophile that served as a link to a fluorescein (Scheme 1.2).¹⁹

Scheme 1.2 Derivatization of phalloidin and attachment to a fluorophore.



Some of the examples of commercial dyes that have been used to synthesize fluorescent phallotoxin derivatives are shown below (Fig. 1.2).

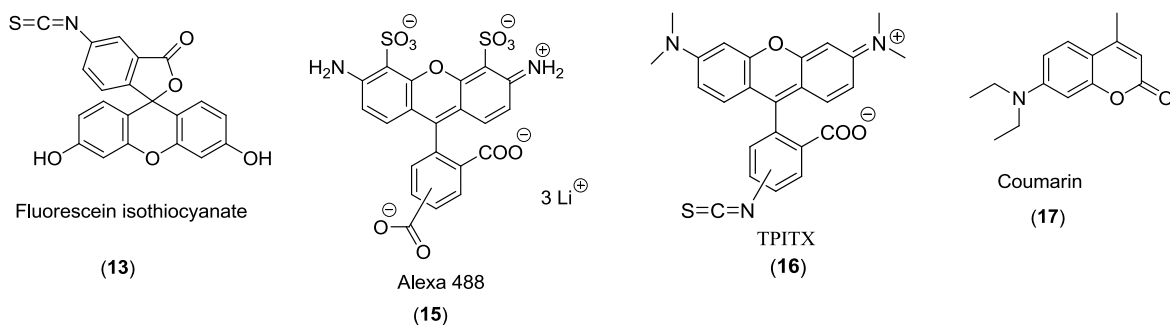


Figure 1.2. Fluorescent dyes that have been conjugated to phalloidin.

Visualization of actin fibers in mammalian cells revealed that phallotoxins bind to filamentous actin forming a 1:1 complex with each protomer in the filament.¹ However, the molecular mechanism of virotoxin interaction with actin was presumed to be different given the monocyclic nature of these natural products.

Actin is a dynamic network of filaments made up of a monomeric 43 kDa protein, known as G-actin that self assembles into polymeric F-actin (Fig. 1.3).²⁰ Actin plays a major role in the process of cell division, migration and transmission of signals by tethering protein complexes to specific domains of the plasma membrane.²¹

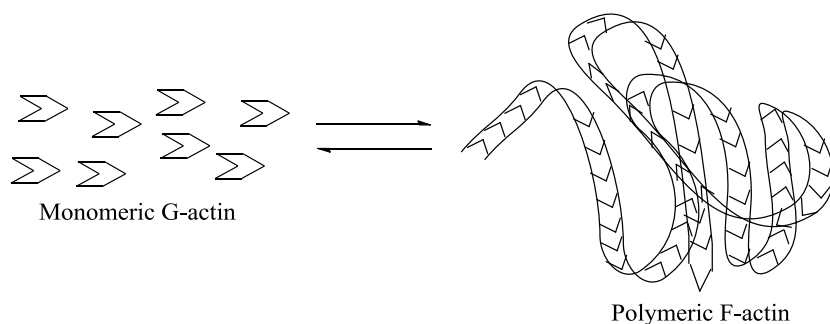


Figure 1.3. Conceptual representation of actin polymerization.

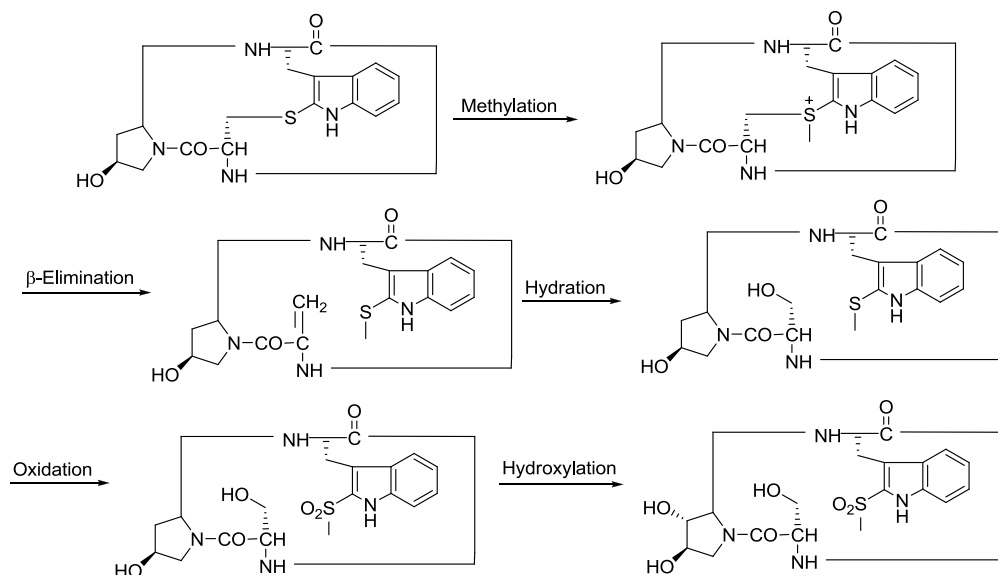
In 2003, Giganti and Friederich noted that structural and functional perturbations of the actin cytoskeleton in cancer cells correlate with higher proliferation rates and uncontrolled movement.²¹

These authors pointed out that small molecules targeting the actin cytoskeleton are possible candidates for cancer chemotherapy. Also, compounds that act on actin may be used in designing anti-parasitic drugs since unicellular and multicellular parasites rely on the actin cytoskeleton for invasion and reproduction in the host.²¹ In addition to their potential as therapeutic compounds, inhibitors of cell motility are invaluable research probes for understanding the process of cell movement and its roles in the biology of the organism.²²

1.3 BIOSYNTHESIS

A biosynthetic route to virotoxin from phallotoxin was proposed by Faulstich *et al.* (Scheme 1.3).¹ Methylation of the thioether bridge, followed by a β -elimination, hydration of the dehydroalanine, oxidation of the sulfur atom and hydroxylation of the hyp residue would generate viroidin.¹ It is worth mentioning that the order of events toward the end of the pathway could vary.

Scheme 1.3. Sequence of reactions that would convert a phallotoxin-type precursor into a virotoxin.¹



A recent genomic study by Hallen *et al.* to identify genes involved in the biosynthesis of the amatoxins and phallotoxins demonstrated that these compounds, produced by *Amanita bisporigera* –

another destroying angel – are the first known example of cyclic peptides to be produced by ribosomal peptide synthesis in a fungus.²³ The genome of *Amanita bisporigera* was shotgun-sequenced to approximately two times the coverage of the genome by a combination of automated Sanger sequencing and pyrosequencing. The sequences were then compared to known bacterial and fungal nonribosomal peptide synthetases, in addition to searching the genome for DNA encoding amanitins' amino acid sequence. It was established that the genome of *Amanita bisporigera* contains related sequences that are characterized by a conserved “toxin” region of seven to ten amino acids (Fig. 1.4). The presence of proline residues immediately upstream of the toxin region and as the last amino acid in the toxin region suggested the involvement of a proline peptidase in the initial post-translational processing of these proproteins.²⁴ The toxins are therefore conceived to be synthesized as proproteins from which they are predicted to be cleaved by a prolyl oligopeptidase (Fig. 1.4). The report concludes that the fungi have evolved a unique mechanism of combinatorial biosynthesis that gives them the ability to biosynthesize cyclic peptides.

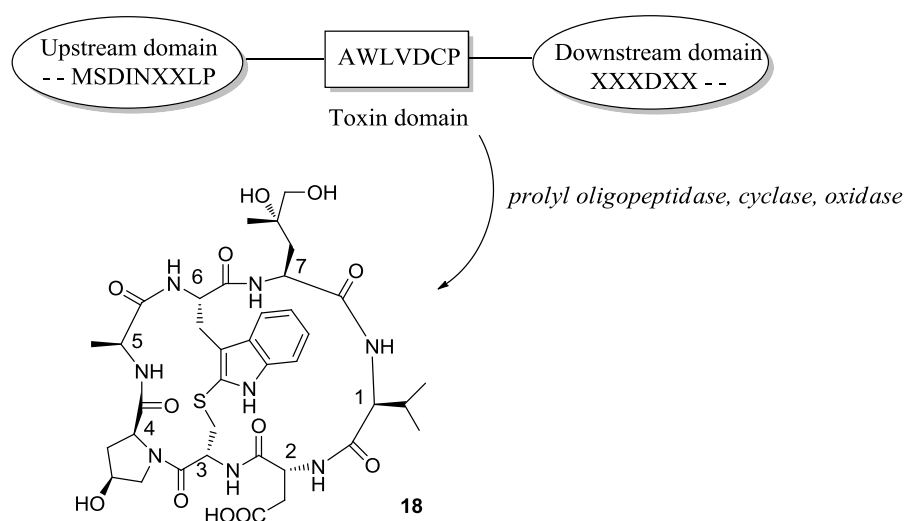
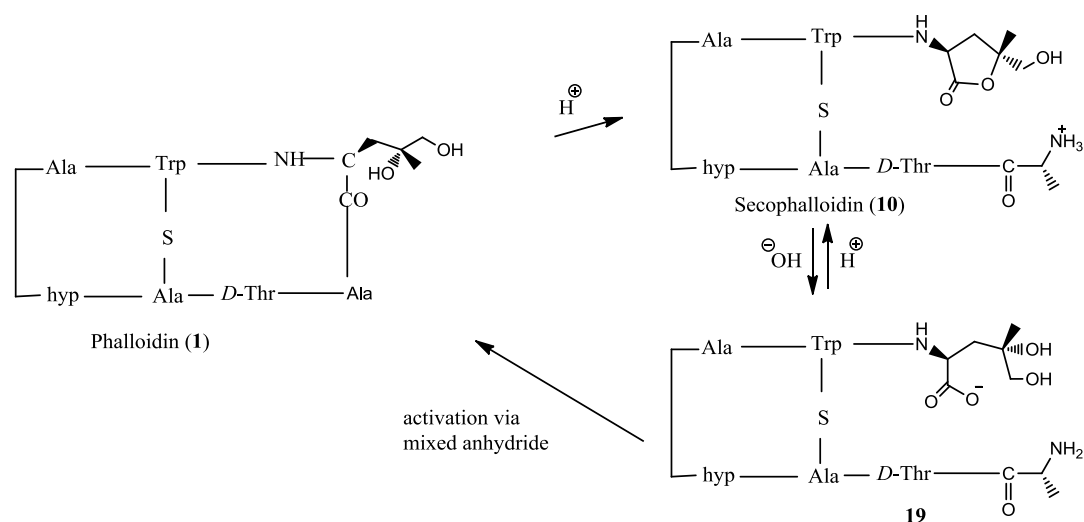


Figure 1.4. Ribosomal cyclic peptide synthesis in a fungus.

1.4 PREVIOUS SYNTHETIC STUDIES AND ANALOGS

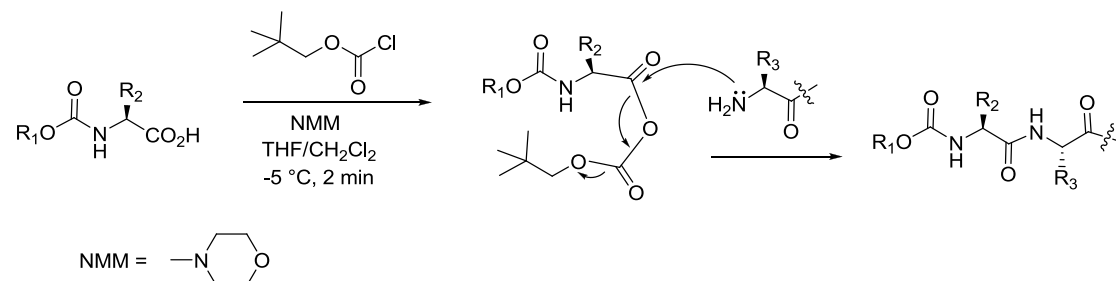
Earlier attempts at the generation of *Amanita* toxins involved partial synthesis from the natural product. The peptide bond between residues 1 and 7 was readily cleaved upon treatment with acids, accompanied by lactonization of the dihydroxyleucine residue (*vide supra*, Scheme 1.1). Hydrolysis of the lactone, followed by recyclization using the mixed anhydride method regenerated the natural product (Scheme 1.4).²⁵

Scheme 1.4. Partial synthesis of phalloidin from the natural product.



Typically, formation of peptide bonds via a mixed anhydride involves separate activation of the acid by adding isobutyl chloroformate to a solution of the peptide acid and *N*-methylmorpholine (Scheme 1.5).²⁶⁻²⁸ The amine nucleophile is then added in the second step to form the peptide bond.

Scheme 1.5. Formation of peptide bonds via a mixed anhydride method.



1.4.1 Kahl and Coworkers²⁹

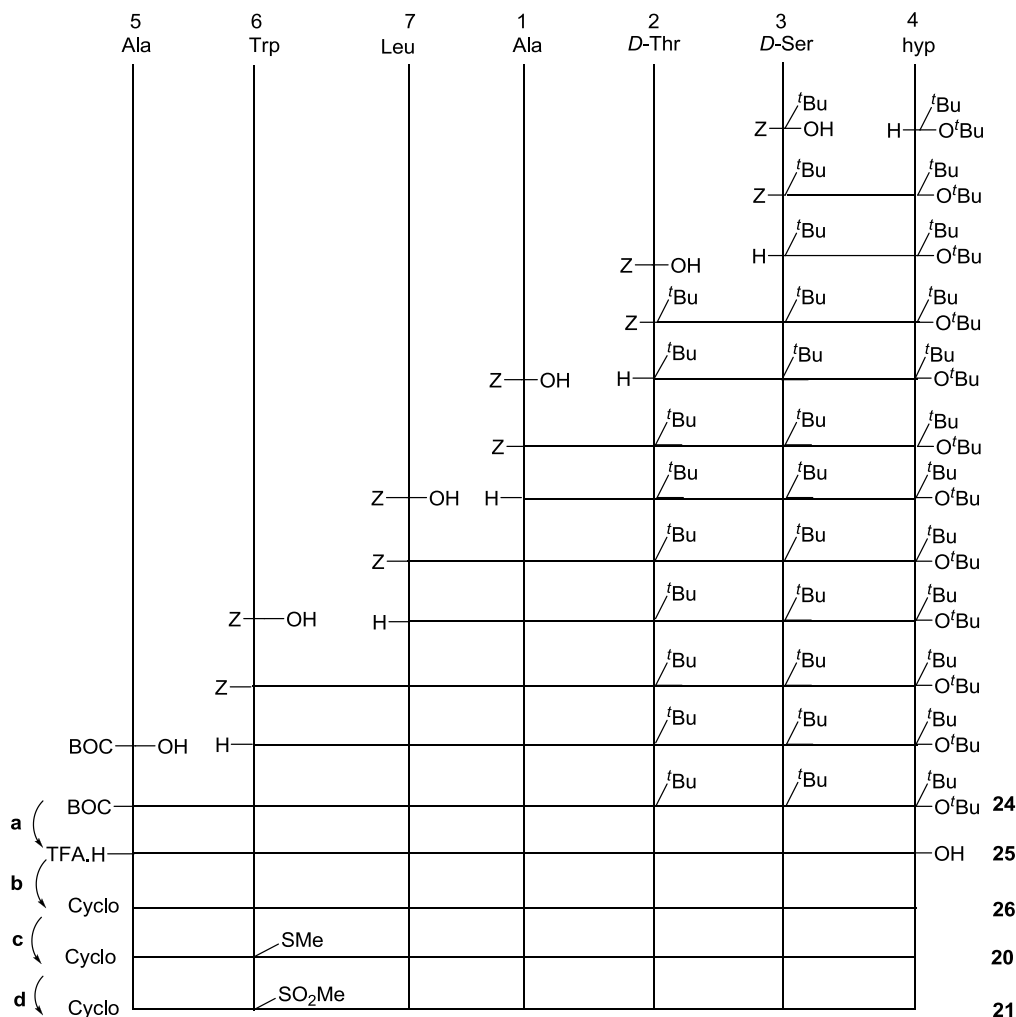
In 1983, Kahl and co-workers reported the synthesis of four virotoxin-like, F-actin-binding heptapeptides with *cis*-4-hydroxy-*L*-proline substituting for dihydroxyproline. The dihydroxyleucine residue of the natural toxins was replaced with either *L*-leucine or hydroxyleucine, after being found not to be vital for biological activity.¹ Two of these analogs, **22** and **23**, were found to have an affinity for F-actin ca. five times lower than that of viroisin. None of the analogs was toxic up to 10 mg/kg body weight of the white mouse.

Table 1.3: The virotoxin analogs and their constituent amino acid residues.

Residue Analog	1	2	3	4	5	6	7
20	Ala	<i>D</i> -Thr	<i>D</i> -Ser	hyp	Ala	2-MeS-Trp	Leu
21	Ala	<i>D</i> -Thr	<i>D</i> -Ser	hyp	Ala	2-MeSO ₂ -Trp	Leu
22	Val	<i>D</i> -Thr	<i>D</i> -Ser	hyp	Ala	2-MeS-Trp	hyLeu
23	Val	<i>D</i> -Thr	<i>D</i> -Ser	hyp	Ala	2-MeSO ₂ -Trp	hyLeu

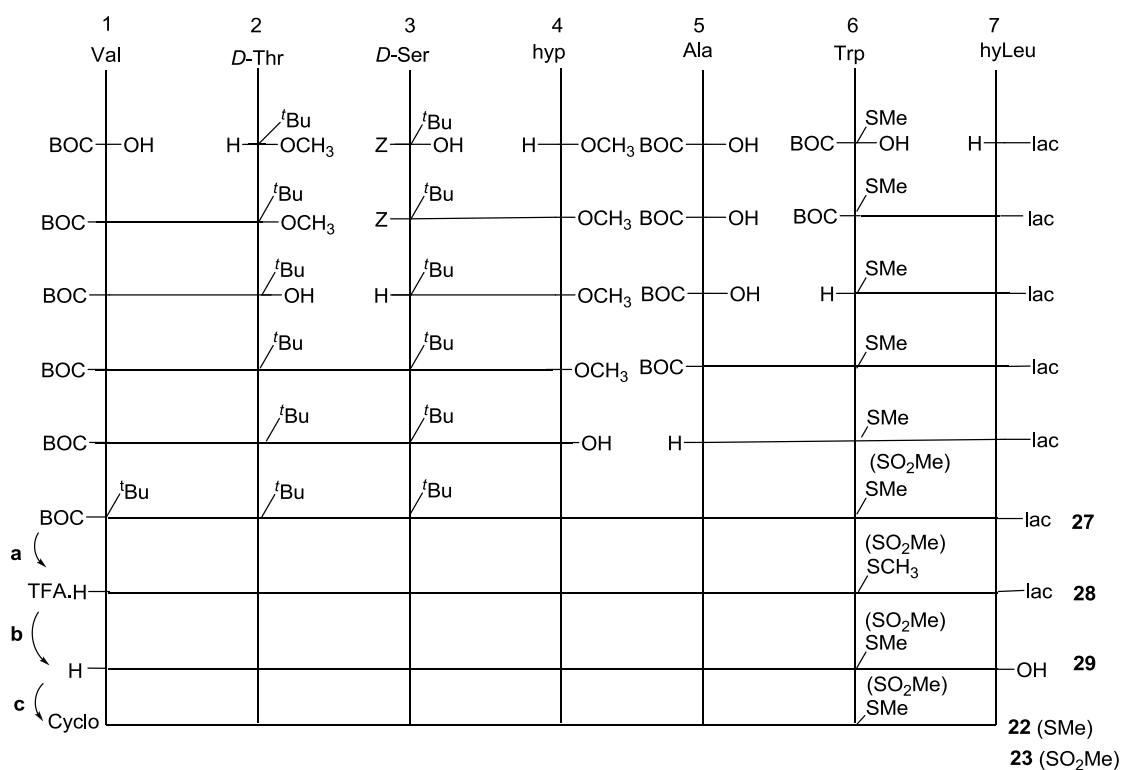
Synthesis of analogs **20** and **21** was conducted according to Scheme 1.6. The linear precursor, with *allo*-hydroxyproline at the C-terminus, was chosen, since this residue would not racemize during peptide bond formation. Generation of the required linear heptapeptide **24** was achieved through stepwise C→N elongation using DCC/HOBt as coupling reagents. The linear heptapeptides were then cyclized using the mixed anhydride method (*i.e.*, **25**→**26**, Scheme 1.6). Cyclization was followed by modification of the Trp residue to give analogs **20** and **21** that differ in the oxidation state of sulfur.

Scheme 1.6. Synthesis of virotoxin analogs **20** and **21**. Reagents for advanced steps: **a.** TFA; **b.** 1. t BuOCOC_l, DMF, THF, 2. NMM; **c.** MeSC_l, HOAc; **d.** 30 % H₂O₂, HOAc.



Analogs **22** and **23** were prepared via fragment condensation, substituting Val for Ala at position 1 (Table 1.3). Their fragment condensation synthesis is summarized in Scheme 1.7. For the synthesis of these γ -hydroxyleucine containing analogs, ring closure between the hydroxyleucine as the C-terminal site and valine was said to be “inevitable to avoid cleavage of peptide bonds via lactonization under acidic conditions (*vide supra*).”²⁹ Lower yields were obtained for the cyclization step, than in Scheme 1.6, since both valine and the hydroxyleucine residues are sterically demanding.

Scheme 1.7. Synthesis of virotoxin analogs **22** (9 % cyclization yield) and **23** (2.6 % cyclization yield). Reagents: **a.** TFA/CH₂Cl₂; **b.** Sephadex LH-20, 0.004M NH₃; **c.** 1. ^tBuOCOC₂H₅, DMF, THF, 2. NMM. Compound **23** was prepared in analogous fashion.

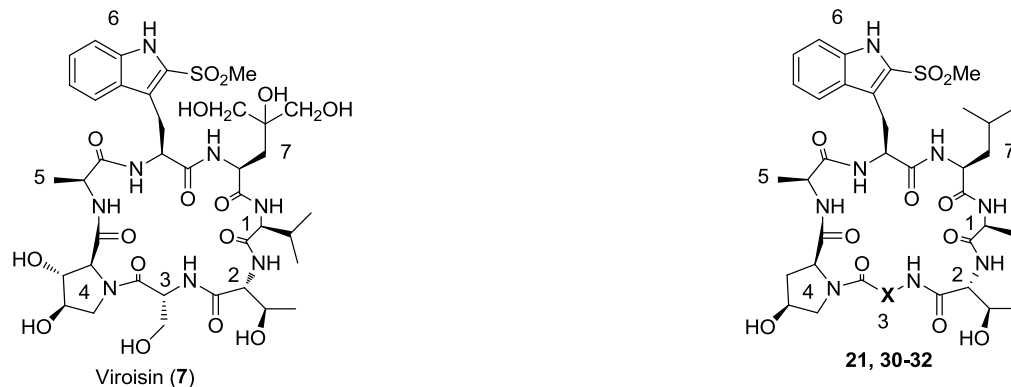


During the synthesis of analogs **20** and **21**, the methylsulfonyl group was introduced onto the indole ring after cyclization of the tryptophan-containing heptapeptide, while for analogs **22** and **23**, the 2-methyl-thio-L-Trp was incorporated at the level of the building block.

1.4.2 Zanolotti and Coworkers³⁰

In 1999, Zanolotti and coworkers concluded that the configuration of the amino acid preceding the prolyl residue is vital for the biological activity of virotoxins (*vide supra*). Four viroisin analogs (**21**, and **30-32**), were synthesized by cyclizing the linear heptapeptides H-Ala-D-Thr-**X**-hyp-Ala-2-MeSO₂Trp-Leu-OH and these cyclic heptapeptides were subjected to conformational analysis by NMR as well as to an actin binding assay (Table 1.4).

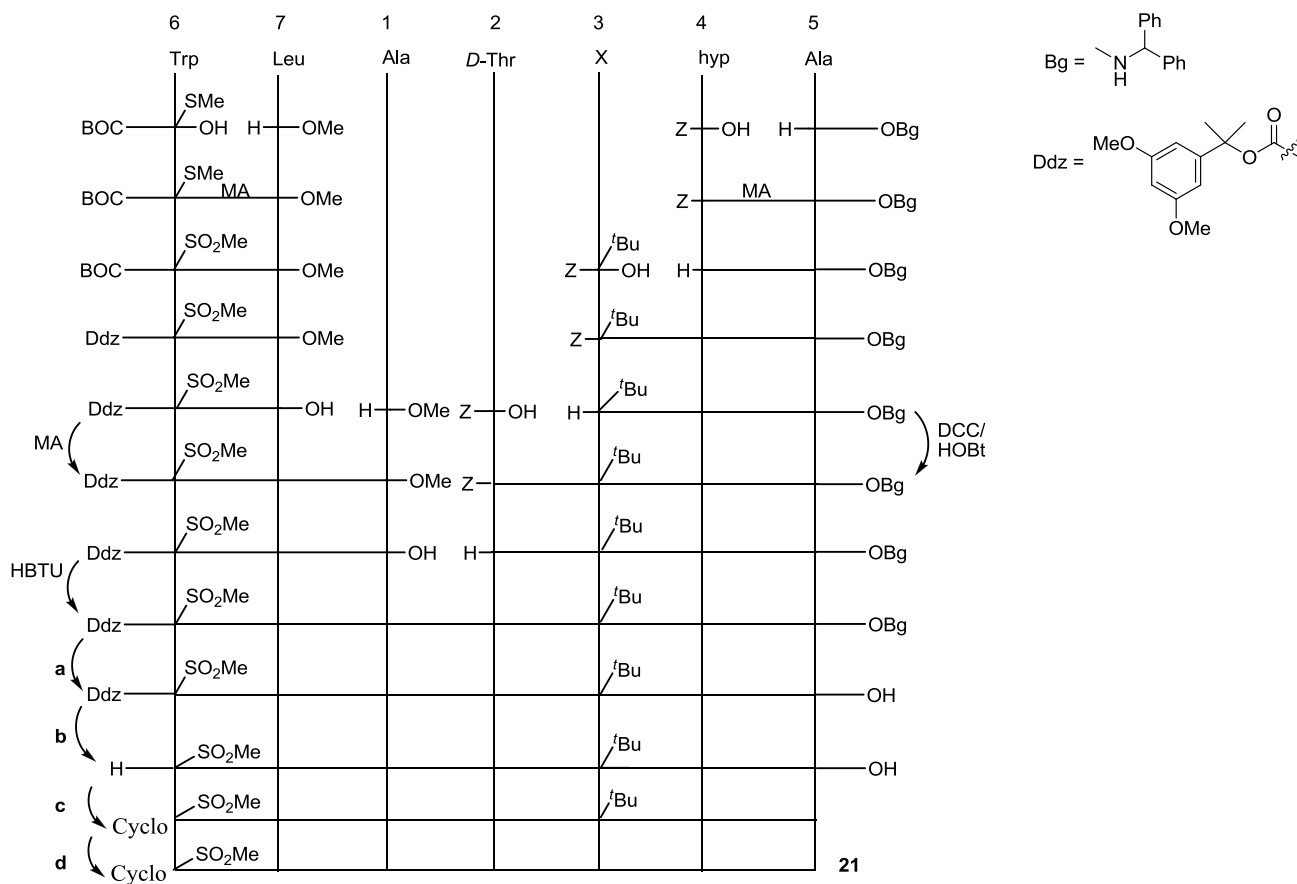
Table 1.4: Cyclization yields and actin affinities of viroisin analogs relative to viroisin.



Entry	Compound	X	Cyclization Yield (%)	Relative affinity for actin analog Viroisin=1.0
1	7 (viroisin)	-	-	1.0
2	21	<i>D</i> -Ser	19	0.2
3	30	<i>D</i> -Ala	32	0.076
4	31	<i>L</i> -Ser	13	0.005
5	32	<i>L</i> -Ala	16	<0.001

In their study, *L*-valine was replaced by *L*-alanine for ease of coupling, while commercially available *L*-allo-hydroxyproline and leucine served as surrogates for dihydroxyproline and dihydroxyisovaline respectively. Their best analog **21** loses half an order of magnitude binding affinity for actin relative to viroisin (Table 1.4, entry 2). Synthesis of **21**, and **30-32** was performed in the solution phase, although with a different strategy to that of Kahl and coworkers.²⁹ Of particular note, was that the 2-methylthio-substituent was introduced into the Trp building block prior to incorporation into the peptide. In addition, the heptapeptide was generated through condensation of tripeptide and tetrapeptide fragments. The tri- and tetrapeptide fragments were assembled using the mixed anhydride method with typical coupling yields of 46-100 %. A [3+4] fragment condensation between Ala/*D*-Thr residues was carried out using HBTU to generate linear heptapeptides with yields of 60-75 %. The cyclization was conducted using HBTU and the yields for compounds **21**, and **30-32** are shown in Table 1.4. Details of the synthetic work are shown in Scheme 1.8.

Scheme 1.8. Synthesis of viroisin analog **21**. Reagents: **a.** 0.4 mmol K₂CO₃, DMF; **b.** 10 eq. TFA, CH₂Cl₂; **c.** HBTU, DMF, DIEA; **d.** = neat TFA. Compounds **30-32** were prepared in analogous fashion.



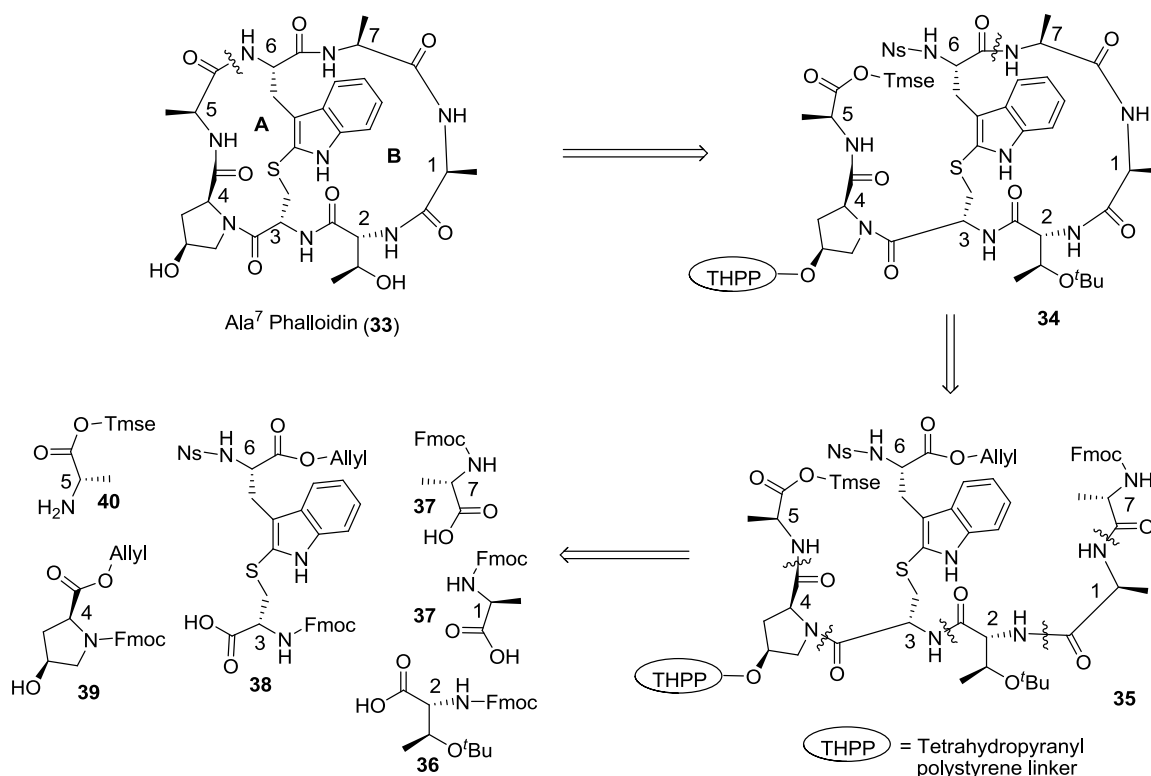
1.4.3 Ongoing Synthetic Studies

1.4.3.1 Guy and Coworkers³¹

In 2005, Guy and co-workers used a solid-phase synthesis approach to prepare Ala⁷ phalloidin (Scheme 1.9).³¹ These authors were interested in developing a rapid and efficient approach to phallotoxins that would allow the synthesis of a diverse library of compounds. According to their retrosynthetic analysis (Scheme 1.9), the initial plan involved disconnecting ring **A** between the Trp⁶ amino group and Ala⁵ carboxyl group to reveal orthogonally protected intermediate **34**. The second

disconnection between the Trp⁶ and Ala⁷ residues led to intermediate **35**, which was disconnected further according to Scheme 1.9.

Scheme 1.9. Guy and co-workers' retrosynthetic analysis of Ala⁷ phalloidin³¹



In their synthesis, the hydroxyl side chain of hyp⁴ was utilized as the point of attachment to the resin via the acid labile tetrahydropyranyl polystyrene linker (THPP). The amino acid building blocks with orthogonal protecting groups were prepared in solution, followed by a sequence of solid-phase peptide couplings involving two key macrocyclization reactions. The order of cyclizing the two rings was based on literature work on the solution-phase synthesis of phallotoxin.^{12, 15, 32} The final cyclization step generated two compounds that were conceived to be atropisomers based on spectroscopic data, computational studies and circular dichroism analysis. One of the atropisomers, designated as “natural,” had positive Cotton effects similar to phalloidin, while the “non-natural” bicyclopeptide had negative Cotton effects. The yields for the “natural” and “non-natural” atropisomers were quantified as 1.3% and

3.2 % respectively. These low yields were accounted for by the two challenging cyclization reactions, specifically the second cyclization step (ring **A**, Scheme 1.9) and losses during separation of the two atropisomers.

1.4.3.2 Schuresko and Lokey³³

A recent report by Schuresko and Lokey described an efficient solid-phase synthesis of Glu⁷-phalloidin (Fig. 1.5) with an overall yield of 50 %.³³ This report provides the highest yield reported to-date for the syntheses of phalloidin/viroidin analogs either in solution or the solid phase. The side chain of the glutamic acid in position 7 was used as a handle for linkage to the solid phase, and then later derivatized to generate a fluorescent, bioactive analog that stained F-actin in fixed cells at a concentration comparable to that of commercial phalloidin based probes.

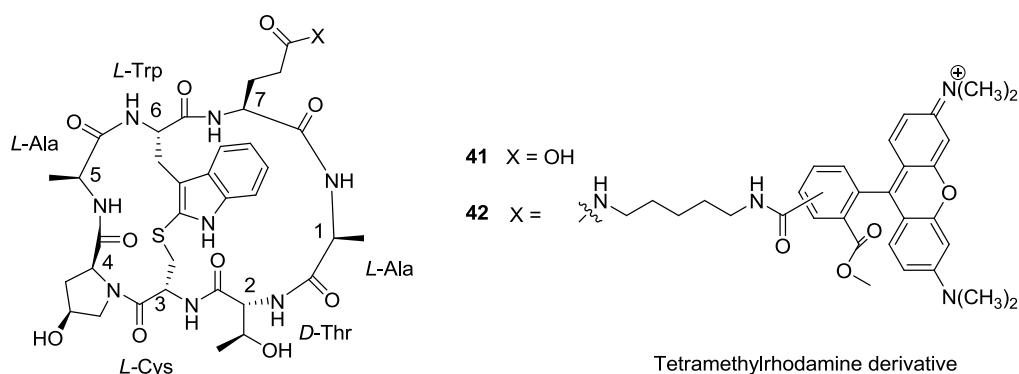


Figure 1.5. Glu⁷ phalloidin and a fluorescent conjugate.

1.5 GOALS OF THE CURRENT WORK

The natural source of virotoxins is selected species of mushrooms that are considered uncultivable due to slow growth and failure to produce carpophores in culture,⁶ and therefore, an efficient chemical synthesis of these compounds offers an alternative. Despite the production of many

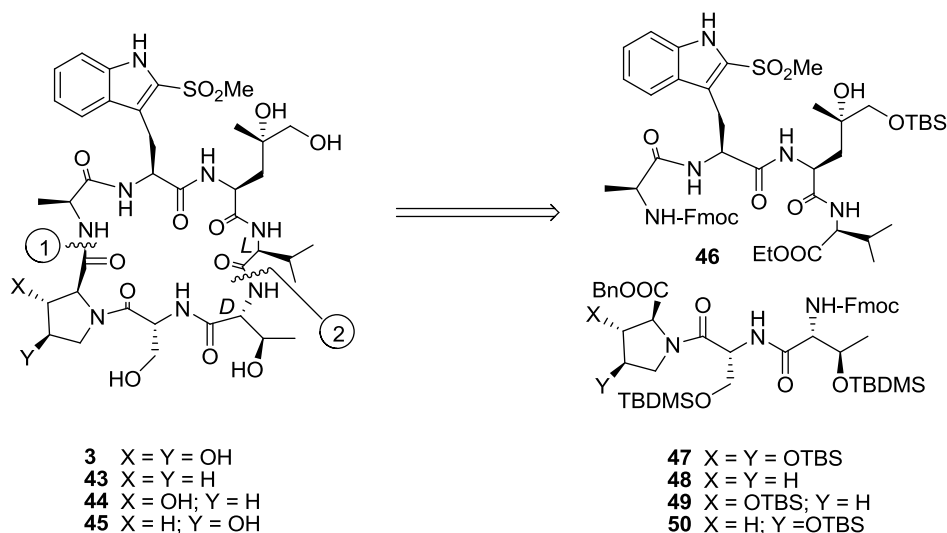
phalloidin and viroidin analogs, and biological and structural studies, a total synthesis of a naturally occurring virotoxin has yet to be reported, due to inaccessibility of the 3,4-dihydroxyproline and 4,5-dihydroxy-*L*-leucine residues. Moreover, there are issues and uncertainties in handling these highly functionalized residues in peptide synthesis without protecting the hydroxyl groups.

Conjugated to fluorophores,¹⁹ phalloidin is widely used to study the dynamics of actin filaments. As seen in section **1.4.3**, in the twenty-first century, efforts are ongoing to produce synthetic phallotoxins, in useful amounts, to make these experiments more affordable and accessible. A synthetic, fluorescent virotoxin would serve as a new probe for the visualization of actin. A solution phase synthesis would have the additional potential to provide analogs and other conjugates with desirable biological properties. Solution phase peptide synthesis permits the incorporation of the uncoded amino acids in a controlled manner.

In addition to the synthesis of a natural product, we sought to prepare three analogs, to specifically investigate the role of proline hydroxylation in the conformation and related biological activity of these compounds. At the outset, we selected viroidin (**2**) as our target but our stereoselective synthesis of the 4,5-dihydroxyleucine residue dictated that we synthesize the equally potent alloviroidin (see Chapter 2). To facilitate these studies, we prepared three tripeptide fragments with either a proline (Pro), *trans*-3-hydroxyproline (3-Hyp), *cis*-4-hydroxyproline (hyp) or 2,3-*trans*-3,4-*trans*-dihydroxyproline (DHP) residue (*vide infra*). All building blocks were commercially available, with the exception of the 2-methylsulfonyl-tryptophan, 2,3-*trans*-3,4-*trans*-dihydroxy-proline³⁴ and dihydroxyleucine residues.³⁵ The previous virotoxin analog syntheses did not incorporate the 2,3-*trans*-3,4-*trans*-dihydroxy-proline,³⁴ valine and dihydroxyleucine residues.^{29, 30} These analogs that were more easily synthesized demonstrated that a replacement of the DHP residue for hyp, dihydroxyleucine for leucine and alanine for valine led to compounds that were five times less active (*vide supra*).²⁹ We are therefore

in a unique position to produce the natural product and analogs via synthesis as presented in Scheme 1.10.

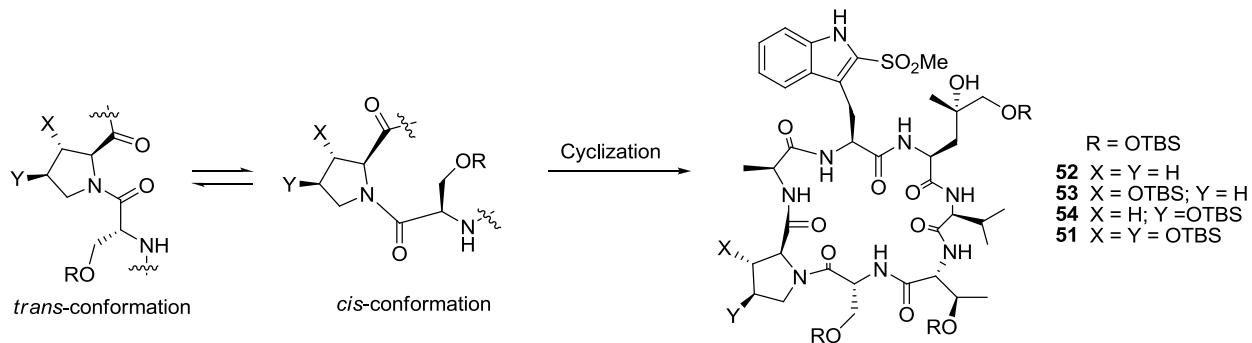
Scheme 1.10. Retrosynthetic analysis of alloviroidin and analogs.



Nuclear magnetic resonance studies will enable us to investigate the conformational preference of the prolyl peptide bond in linear peptides and how this influences the structure and ease of cyclization of the heptapeptides. X-ray studies by Zanotti³² and coworkers (*vide supra*) revealed that the *cis*-4-hydroxyproline adopts a C^{γ} -*endo* type conformation. Our work will predict conformations adopted by pyrrolidine rings of proline, 2,3-*trans*-3,4-*trans*-dihydroxy-proline, *cis*-4-hydroxyproline and *trans*-3-hydroxyproline residues when incorporated into linear and cyclic peptides, and the impact this would have on the conformation of the Ser³-Pro^{*}-Ala⁵-Trp⁶ peptide region and its propensity to facilitate cyclization. Similar work on factors influencing conformation in proline-containing peptides was conducted by Taylor *et al.*³⁶

Computational studies together with the experimental data will allow us to predict the low energy conformations of the cyclic peptides and thereby relate the contribution of each hydroxyl group to the bioactive conformation of the cyclic heptapeptide.

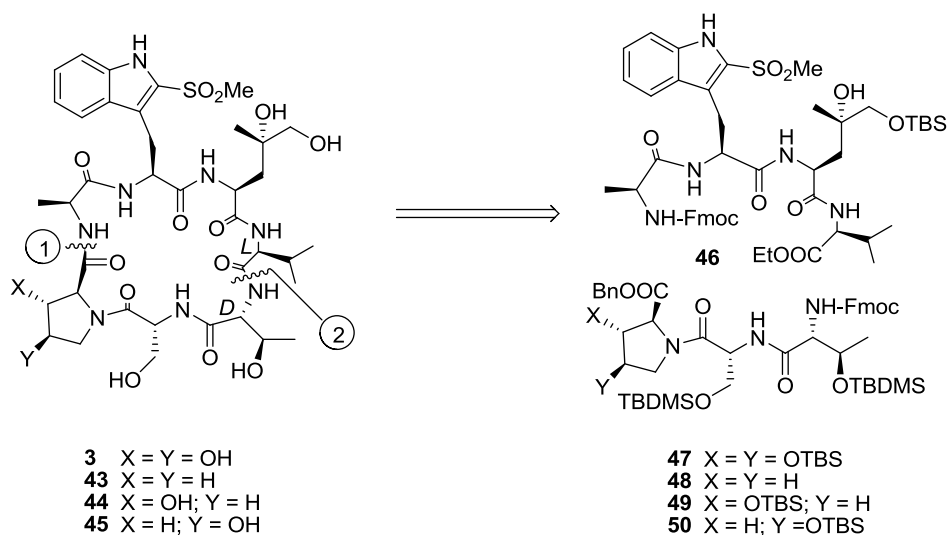
Scheme 1.11. The conformation of the prolyl peptide bond and cyclization.



CHAPTER 2: SYNTHESIS OF A DIHYDROXYLEUCINE-VALINE DIPEPTIDEⁱ

Our retrosynthetic analysis of alloviroidin is presented in Scheme 2.1. Disconnections between the proline/alanine and valine/*D*-threonine residues leads to the tetrapeptide **46** and tripeptide fragments **47-50**. In a forward direction, the first peptide bond to be formed will constitute a [3+4] fragment condensation at the position labeled '1,' between carboxyl component derived from **47-50** and the amino component derived from **46**, followed by a cyclization of the linear heptapeptide at the disconnection labeled '2' (Scheme 2.1). Formation of linkage 1 is appealing, since the *C*-terminal proline is not susceptible to racemization during peptide bond formation. Furthermore, ease of cyclization (formation of linkage 2) is expected to be enhanced by the presence of a turn inducing³⁷ proline residue, and the opposite configuration of the *D*-Thr/*L*-Val residues.

Scheme 2.1. Retrosynthetic analysis of alloviroidin and analogs.



Fragments **46** and **47** are of approximately equal complexity, each containing one synthetically valuable amino acid. We employed an orthogonal protecting group strategy, utilizing

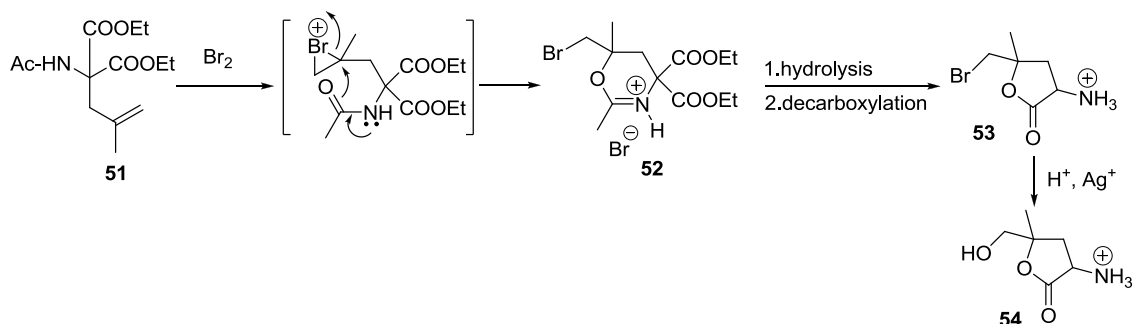
ⁱ Parts of this Chapter are reprinted with permission from the American Chemical Society.

fluoride-labile side chain protection (*viz.*, *tert*-butyl-dimethylsilyl ethers), the base labile Fmoc group, and benzyl or ethyl esters for the protection of the amino and carboxy termini respectively.

2.1 PREVIOUS SYNTHESIS OF THE 4,5-DIHYDROXYLEUCINE RESIDUE

A single synthesis of the 4,5-dihydroxyleucine residue appeared in the literature in 1957.³⁸ Wieland and Weiberg reported the preparation of a mixture of all four stereoisomers of this amino acid via bromination of compound **51** to give **52** (Scheme 2.2). Subsequent hydrolysis and decarboxylation delivered **53** that was reacted with acid in the presence of silver ions to give **54** as a mixture of stereoisomers. The two racemates (*2S,4S*; *2R,4R*) and (*2S,4R*; *2R,4S*) were separated by crystallization and then resolved into enantiomers, through crystallization of salts formed with ditoluoyl tartaric acid.³⁹

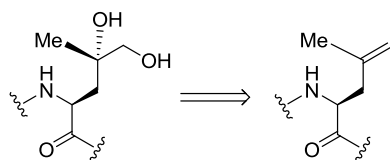
Scheme 2.2. Wieland and Weiberg dihydroxyleucine synthesis.³⁸



2.2 THE SHARPLESS ASYMMETRIC DIHYDROXYLATION

We hoped to prepare a single stereoisomer of this key amino acid via a diastereoselective dihydroxylation of an (*S*)-dehydroleucine derivative (Scheme 2.3).

Scheme 2.3. Retrosynthetic analysis of dihydroxylation of an (*S*)-dehydroleucine derivative.



The Sharpless asymmetric dihydroxylation reaction has emerged as one of the most efficient methods for forming optically active 1,2-diols from olefins in a predictable and controlled manner.⁴⁰⁻⁴⁷ The reaction proceeds via a *syn* addition, whereby the hydroxyl groups are delivered to the same face of the double bond (Fig. 2.1). This dihydroxylation reaction is easy to perform since a premix of all reactants is commercially available in two antipodal forms: AD-mix- α and AD-mix- β .

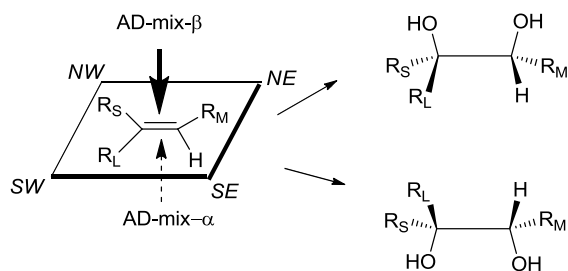


Figure 2.1. The Sharpless dihydroxylation mnemonic.

The mnemonic proposed by Sharpless and co-workers to explain the outcome of the dihydroxylation (Fig. 2.1) has proven to be reliable at predicting the enantiofacial selectivity for a wide range of olefinic substrates.⁴⁸ The olefin substrate is positioned to allow for an aromatic or sterically demanding aliphatic substituent (R_L) to occupy the southwest quadrant of the empirical mnemonic, whereas the northeast quadrant is occupied by aliphatic substituents of moderate size (R_M). The diastereofacial selectivity can be rationalized on the basis of the type of ligand used (Fig. 2.2), *e.g.*, AD-mix- β , with the chiral dihydroquinidine (DHQD) ligand, brings about dihydroxylation from the top face.

AD-mix- α , on the other hand contains the pseudoenantiomeric dihydroquinine (DHQ) derived ligand and dihydroxylates the olefin from the bottom face. Sharpless and co-workers⁴⁹ have shown that the dihydroxylation of prochiral olefins proceeds with high levels of enantioselectivity. When chiral olefins are dihydroxylated, the situation is more complicated.

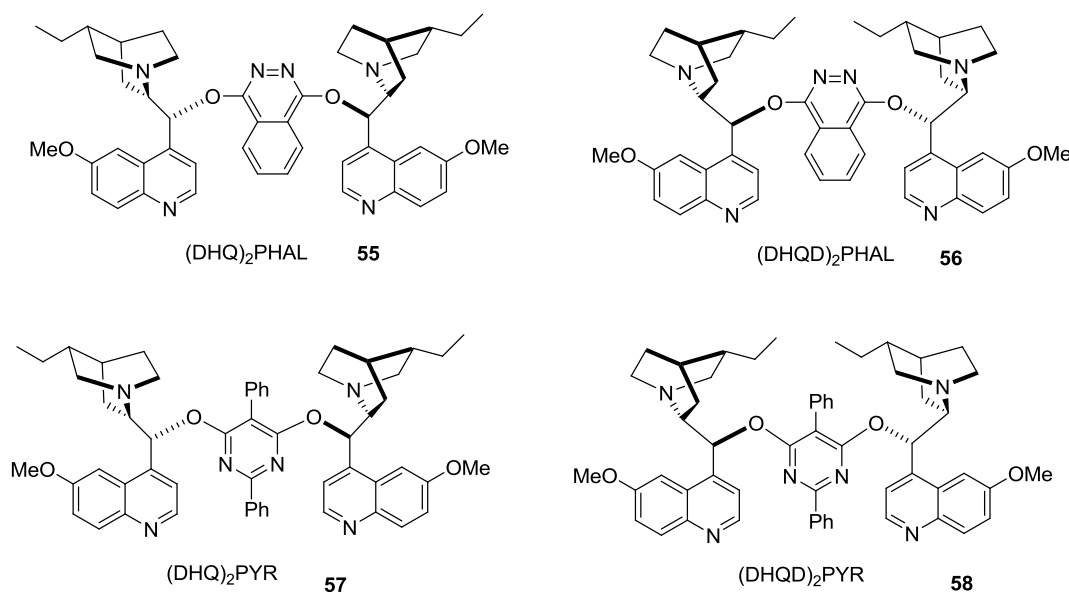
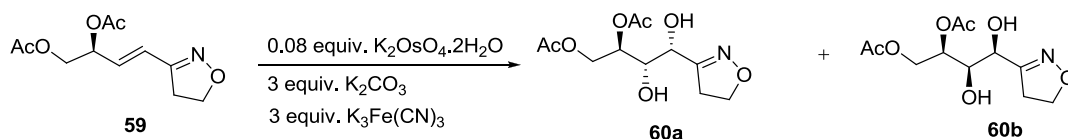


Figure 2.2. Phthalazine and pyrimidine ligands.

There have been cases reported of matched and mismatched double diastereoselectivity during the asymmetric dihydroxylation of chiral olefins.⁵⁰⁻⁵² The concept of matched and mismatched pairs can be explained by first comparing the reaction in the absence of any chiral ligand. As illustrated in Scheme 2.4 (Entry 1), dihydroxylation of **59** under ligand free conditions generated 76% of **60a** and 24% of **60b**. This selectivity arises from the intrinsic bias of **59** *i.e.* K_2OsO_4 approaches the double bond of the substrate from the less hindered face furnishing **60a** as the major product.

Scheme 2.4. Matched and mismatched double diastereoselectivity.

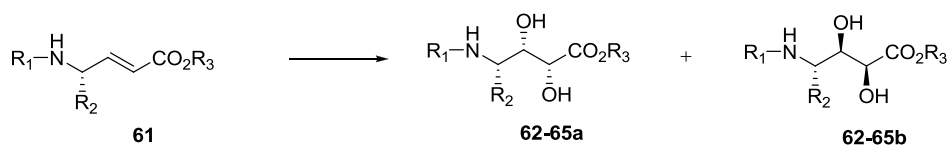


Entry	Reaction conditions	Ligand	Product ratio of 60a:60b	
1	<i>t</i> BuOH/H ₂ O (1:1),	No ligand	76	24
2		0.4 equiv. (DHQD) ₂ PHAL	98	2
3	MeSO ₂ NH ₂ , 20 °C	0.4 equiv. (DHQ) ₂ PHAL	5	95

A matched pair is a reaction using a chiral ligand that leads to the same facial selectivity as the substrate's intrinsic bias. For example, dihydroxylation of **59** in the presence of (DHQD)₂PHAL (Scheme 2.4, Entry 2) enhances selectivity of **60a/60b** from 76/24 to 98/2 (Entries 1 and 2 respectively). Therefore, the diastereofacial selectivity of **59** and (DHQD)₂PHAL represents a matched pair. However, facial selectivity of the chiral ligand in a mismatched case is opposite to that of intrinsic bias of the substrate (Scheme 2.4, Entry 3). In this case, the diastereofacial selectivities of substrate **59** and the chiral ligand (DHQ)₂PHAL are counteracting each other. Weak substrate intrinsic bias, as in Scheme 2.4, can be overridden by a chiral ligand, while moderate to strong substrate bias could result in poor selectivity. The outcome of the reaction is thereby influenced by the chirality of both the reagents and the substrates.

Reetz and co-workers have examined the dihydroxylation of chiral γ -amino α,β -unsaturated esters and shown that tuning of the amine protecting group can be used to transform the mismatched into a matched case (Table 2.1). A comparison between the *N*-Boc- and *N,N*-dibenzyl-protected substrates revealed different levels of stereoselectivity of the products formed.⁵³

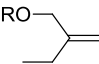
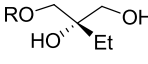
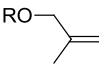
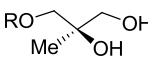
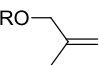
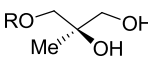
Table 2.1: Turning the mismatched into the matched case via protecting group tuning.⁵³ AD-mix- α always favors **62-65a**; AD-mix- β always favors **62-65b**.



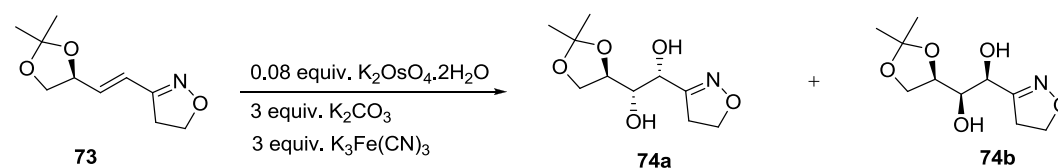
	R₁	R₂	R₃	AD-mix	62-65a: b
62	Boc	CH ₃	CH ₃ CH ₂	α β	97:3 9:91
63	Boc	PhCH ₂	CH ₃	α β	94:6 11:89
64	Bn ₂	CH ₃	CH ₃ CH ₂	α β	92:8 6:94
65	Bn ₂	PhCH ₂	CH ₃	α β	88:12 14:86

Facial selectivity of the dihydroxylation is affected by the substitution of the double bond. Unexpected results have been observed during the dihydroxylation of 1,1-disubstituted allylic alcohol derivatives⁵⁴ and chiral 1,1-disubstituted olefins.⁵⁵ Karl Hale and co-workers conducted studies on 1,1-disubstituted allylic alcohols and recorded the unexpected trend summarized in Table 2.2.⁵⁴ From these results, it can be concluded that the Sharpless facial selectivity rule is unpredictable for allylic ethers and strongly affected by the protecting group.

Table 2.2: Asymmetric dihydroxylation of 1,1-disubstituted allyl alcohol derivatives.⁵⁴

Substrate		R	AD-mix	% ee	Product
	66	<i>t</i> BuPh ₂ Si	β	91	
	67	Bn	β	31	
	68	Pv	β	11	
	69	<i>t</i> BuPh ₂ Si	α	47	
	70	<i>t</i> BuMe ₂ Si	α	43	
	71	Pv	α	15	
	72	Bn	α	45	

During their investigation of 4,5-dehydroisoxazoles as intermediates for amino sugar synthesis, Wade and co-workers noted that optically active alkene substrates constitute a double asymmetric synthesis during dihydroxylation using chiral ligands.⁵⁶ The authors were able to overcome the intrinsic bias of the substrate in their reactions by employing the standard phthalazine class of ligands (Scheme 2.5).

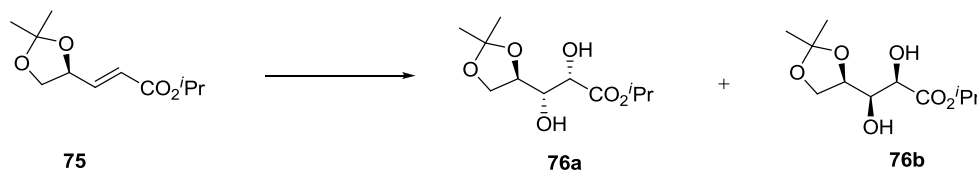
Scheme 2.5. Wade and co-workers' dihydroxylation of 4,5-dehydroisoxazoles.⁵⁶

Reaction conditions	Ligand	Product ratio of 74a : 74b	
<i>t</i> BuOH/H ₂ O (1:1), MeSO ₂ NH ₂ , 20 °C	No ligand	77	23
	0.4 equiv. (DHQD) ₂ PHAL	96	4
	0.4 equiv. (DHQ) ₂ PHAL	11	89

Similarly, Morikawa and Sharpless assessed the extent of matching and mismatching in the asymmetric dihydroxylation of a carbohydrate-derived olefin ester using phthalazine and pyrimidine

ligands.⁵⁷ According to the findings recorded in Scheme 2.6, phthalazine ligands performed better for the matched reaction (Entry 1), while pyrimidine derivatives gave improved results in the mismatched case (Entry 4).

Scheme 2.6. Morikawa and Sharpless dihydroxylation of a carbohydrate-derived olefin ester.⁵⁷



Entry	Ligand (mol %)	Product ratio of 76a:76b	
1	(DHQD) ₂ PHAL (1)	39	1
2	(DHQ) ₂ PHAL (1)	1	1.3
3	(DHQD) ₂ PYR (5)	6.9	1
4	(DHQ) ₂ PYR (5)	1	4.1

Enantioselectivity studies by Sharpless and co-workers recommended phthalazine based ligands for the dihydroxylation of 1,1-disubstituted, 1,2-*trans*-disubstituted and trisubstituted classes of olefins.⁴⁰ The examples represent reagent-controlled dihydroxylations (Table 2.3).

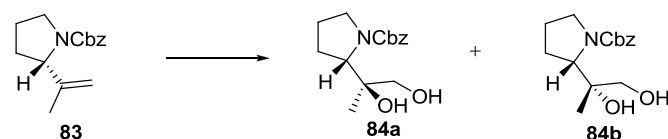
Table 2.3. Examples reagent-controlled dihydroxylations⁴⁰

	Olefin		Product	(DHQD) ₂ -PHAL % <i>ee</i>	(DHQ) ₂ -PHAL % <i>ee</i>
77		78		94 (<i>R</i>)	93 (<i>S</i>)
79		80		99 (2 <i>S</i> ,3 <i>R</i>)	96 (2 <i>R</i> ,3 <i>S</i>)
81		82		98 (<i>R</i>)	95 (<i>S</i>)

Gardiner and co-workers demonstrated that the asymmetric dihydroxylation of an *L*-proline-derived 1,1-disubstituted alkene proceeds with the same sense of diastereoselectivity using both phthalazine based ligands (Scheme 2.7).⁵⁵ It was hypothesized that the orientation of the substrate in the

mnemonic device was altered by the sterically hindered pyrrolidine group and that a ligand switch in this case does not influence the facial selectivity but instead leads to a matching enhancement.

Scheme 2.7: Diastereoselectivity in the asymmetric dihydroxylation of an *L*-proline derived 1,1-disubstituted alkene.⁵⁵



Chiral ligand	84a:84b*
None	1.1:1
(DHQ) ₂ PHAL	1.9:1
(DHQD) ₂ PHAL	3.5:1
(DHQ) ₂ PYR	1.8:1
(DHQD) ₂ PYR	1:2.5

* Ratios determined by gas chromatography after diol derivatization.

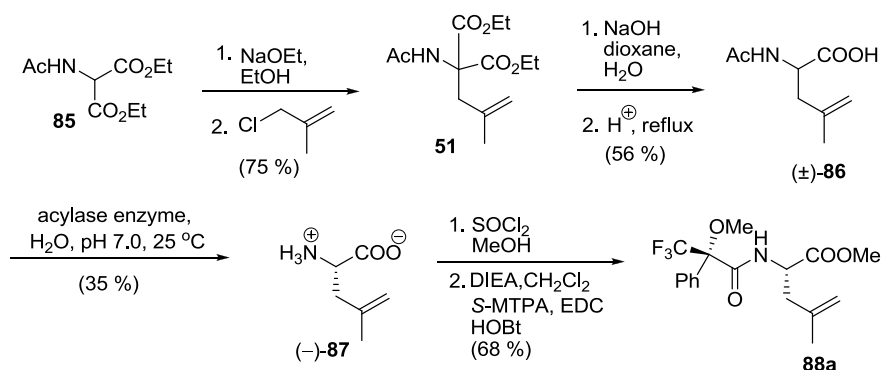
With this background, we set about our synthesis of 4,5-dihydroxyleucine employing a Sharpless asymmetric dihydroxylation.

2.3 PREPARATION OF (2*S*)-4,5-DIHYDROLEUCINE RESIDUE

The preparation of our dehydroleucine began with condensation of the anion of ethyl acetamidomalonate (**85**) with methylal chloride to give **51** (Scheme 2.8).⁵⁸

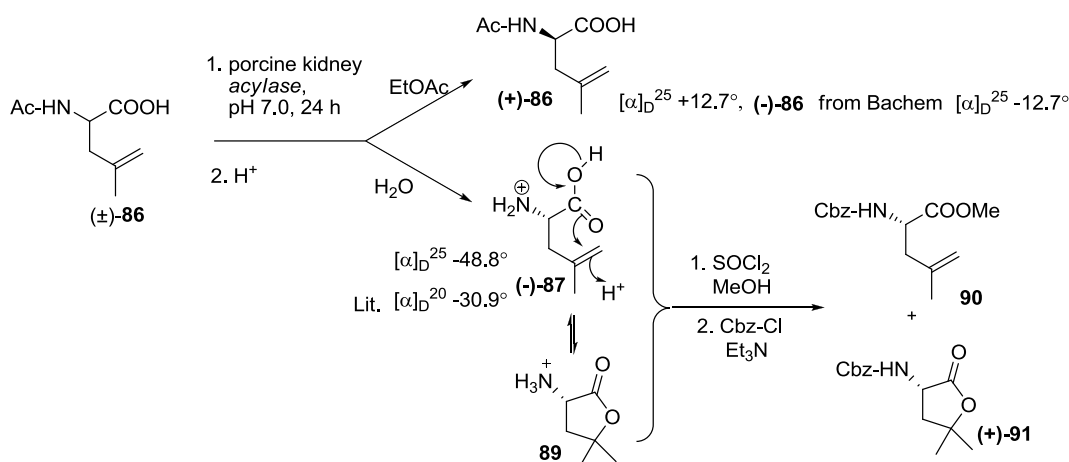
Hydrolysis of the esters, acidification and decarboxylation resulted in racemic *N*-acetyldehydroleucine (**86**). According to the work of Schmidt and Schmidt, who utilized (*S*)-dehydroleucine in their synthesis of eponemycin,⁵⁹ we conducted an enzymatic resolution of this amino acid at room temperature, with strict control of pH between 7 and 8 for no more than 24 hours. We then acidified the reaction mixture and extracted the unreacted (*R*)-*N*-acetyl-dehydroleucine with ethyl acetate and an optical rotation measurement demonstrated this compound to be enantiopure (Scheme 2.9).

Scheme 2.8. Preparation of the dehydroleucine residue.



Schmidt and Schmidt made note that “the temperature should not exceed 40 °C” during concentration of the acidic, aqueous layer.⁵⁹ We noticed that (*S*)-dehydroleucine was invariably contaminated with another, less polar compound that stained with ninhydrin. The amount of this byproduct was reduced, but not completely eliminated, by freeze-drying instead of evaporation at < 40 °C on a rotary evaporator. We reacted the product mixture with thionyl chloride in methanol, followed by carbobenzyloxychloride, according to Scheme 2.9. Following this derivatization, we were able to separate two compounds and identify the undesired compound as a γ -lactone that was later used in model studies (*vide infra*). The lactone presumably arises via protonation of the double bond to form the tertiary carbocation and intramolecular attack by the carboxylate to form the lactone **89**.

Scheme 2.9. Undesired lactone formation.



Neutralization of the reaction mixture, with Amberlite IRA-67 (HO^-) ion exchange resin, before freeze-drying prevented this side reaction but was still not optimal. We were subsequently able to isolate (*S*)-dehydroleucine (**87**) in high optical purity according to the recommended protocol of Chenault *et al.*⁶⁰ Specifically, the acidic layer, without neutralization, was applied directly to a column of Dowex-50 (H^+), the column was washed with water, followed by elution of the amino acid with aqueous ammonium hydroxide solution.

The free amino acid (-)-**87** was converted to its methyl ester, followed by Mosher amide formation (Scheme 2.8).⁶¹ The stereochemical make-up of **88** was determined by ^{19}F NMR analysis to be 98 % *de* in favor of the *S*-configuration at C_α (Fig. 2.3). We also prepared and analyzed the Mosher amide of the racemic material (\pm)-**88** in an analogous manner after deacetylation of (\pm)-**86** with aqueous 2.5N NaOH solution (Scheme 2.10).

Scheme 2.10. Mosher amide formation.

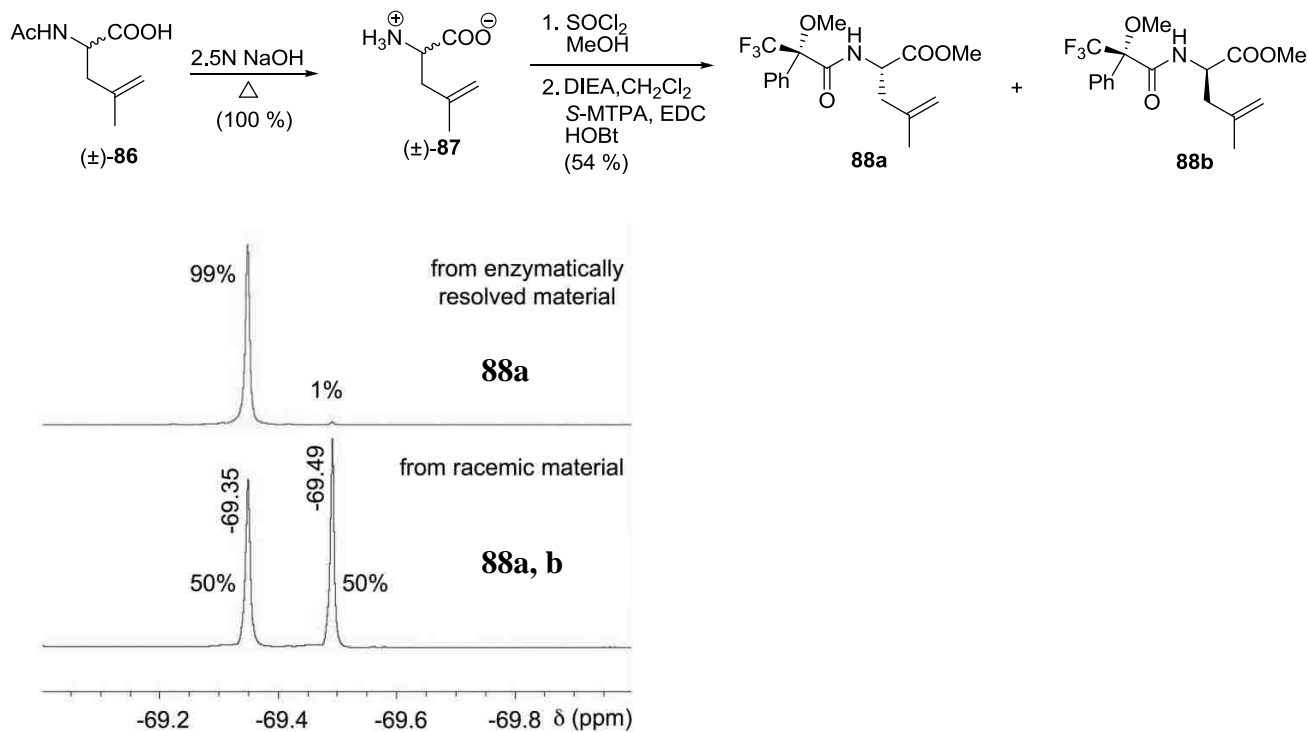


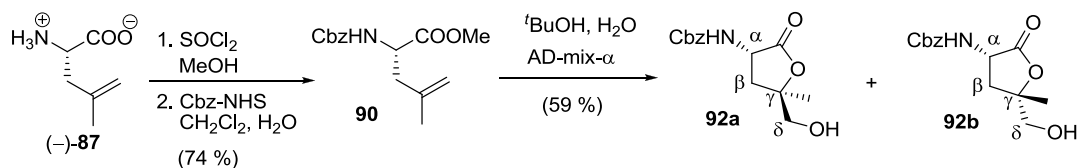
Figure 2.3. ^{19}F NMR spectra (CDCl₃, 236 MHz) for Mosher amide **88** derived from enzymatically resolved dehydroleucine and racemic dehydroleucine.

2.4 THE DIHYDROXYLATION REACTION

The methyl ester of **87** was protected as its Cbz derivative **90** (Scheme 2.11). With useful quantities of enantiopure dehydroamino ester **90** in hand, we were in a position to investigate the dihydroxylation reaction. We hoped that the aromatic ring would be attracted to bind in the hydrophobic southwest binding pocket of the ligand during the asymmetric dihydroxylation (see Fig. 2.1). Given the examples presented in section 2.2,^{54, 55} we were reluctant to predict which of the AD-mixes would give the desired diastereomer. We were uncertain what impact the existing C α stereocenter would have on the stereochemical course of the reaction. In general, dihydroxylation of γ,δ -unsaturated esters results in the isolation of γ -lactones^{62, 63} and we hoped that lactone **92a** would be a useful building block for peptide synthesis.

Dihydroxylation of **90** with AD-mix- β , under the standard conditions of the Sharpless asymmetric dihydroxylation,⁴⁹ gave **92** in a 1:1 diastereomeric ratio. However, treatment of alkene **90** with AD-mix- α yielded an inseparable mixture of diastereomers of **92** in a ratio of 6.5:1.0 (Scheme 2.11). Considerable effort was directed toward determining the configuration of C γ in the major diastereomer. Also, attempts to separate and characterize the diastereomers were unsuccessful, although the configuration at C γ was later determined to be 4*R* (*vide infra*).

Scheme 2.11. Dihydroxylation of the dehydroleucine residue.



Analysis of the proton NMR of the product mixture derived from the AD-mix- α reaction revealed a single signal for the two H δ protons of the major diastereomer. Two distinct doublets were observed for the minor diastereomer. The single signal of the major diastereomer indicated that the two H δ protons were equivalent and implied that the CbzNH and CH₂OH were on opposite faces of the

lactone ring, *i.e.* diastereomer **92a** (*2S*, *4R*) as occurs in viroidin. If the NHCbz and CH₂OH substituents were on the same face of the lactone ring, hydrogen bonding between them could lead to restricted rotation about C γ -C δ bond giving rise to two distinct H δ signals, as observed for the minor diastereomer. Wieland⁶⁴ used the same reasoning to distinguish between diastereomers of the free aminolactone (Fig. 2.4).



Figure 2.4. Hydrogen bonding in the lactone ring.

To prove this hypothesis, standard NMR experiments (NOESY and ROESY) were recorded at a variety of mixing times and temperatures to establish the relative stereochemistry of the substituents on the five-membered ring. Unfortunately, only weak signals were observed, implying that the interconversion of conformations of the γ -lactone occurs at rates faster than mixing times.

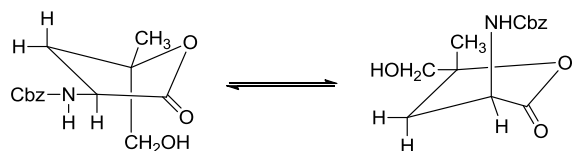
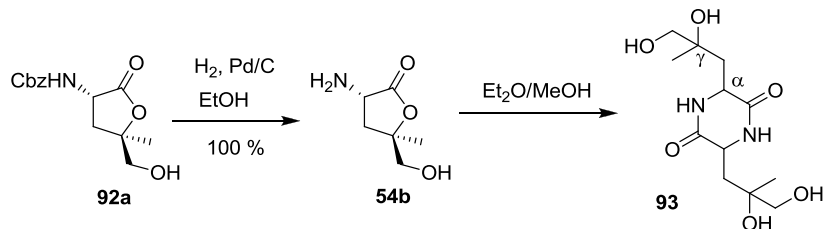


Figure 2.5. Interconversion of conformations of the γ -lactone **92a**.

Attempts to prepare crystalline derivatives from **92a**, **b** by derivatizing the primary alcohol with 4-bromobenzoic acid or hydrogenolysis of the Cbz group in the presence of ditoluoyl tartaric acid were both unsuccessful. Deprotection of the Cbz group under standard hydrogenolysis conditions resulted in the isolation of crystalline diketopiperazine **93** (Scheme 2.12).⁶⁵ Unfortunately, the structure of **93** could not be properly refined due to the poor quality of the crystals. However, the data hinted that C α was of the *S*-configuration and C γ of the *R*-configuration.

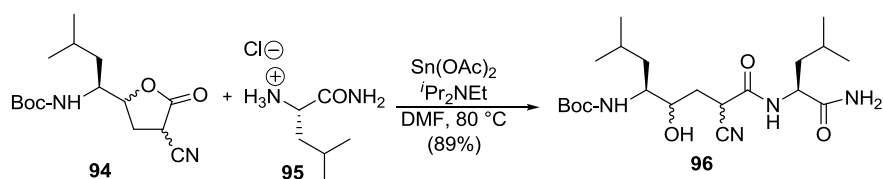
Scheme 2.12. Diketopiperazine formation.



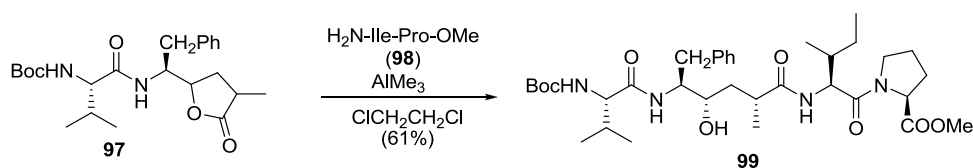
While trying to clarify this issue of stereochemistry, we simultaneously sought to investigate methods for formation of the dihyLeu-Val peptide bond, as occurs in the toxin, without prior opening of the lactone ring. There are scattered reports of the reaction of γ -lactones being opened by *N*-nucleophiles (examples are illustrated in Scheme 2.13): under neutral conditions,^{66, 67} in the presence of bases,^{68, 69} Lewis acid catalysis,^{70, 71} catalysis by 2-hydroxypyridine,^{72, 73} a modification of the Weinreb method,^{74, 75} and catalysis by *p*-toluenesulfonic acid.⁷⁶

Scheme 2.13. Examples of γ -lactone opening by *N*-nucleophiles.

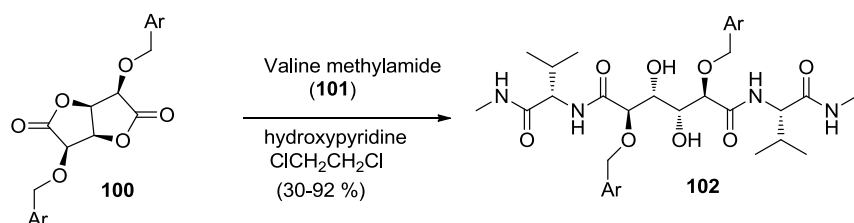
(a)⁷⁰



(b)⁷⁴



(c)⁷²



We decided to explore this strategy, to minimize the number of steps and protecting group manipulations associated with the dihydroxyleucine residue. Prior to investing our synthetically valuable lactone **92a**, we screened a number of methods using (±)-valerolactone (**103**) and valine ethyl ester (**104**) and found that the conditions of Hansen *et. al.* (Scheme 2.13, **a**)⁷⁰ gave the best results for our substrates (Table 2.4, entry 2).

Table 2.4. Conditions for the aminolysis of lactone **103** with *L*-valine ethyl ester (**104**). All reactions were conducted at 80 °C.

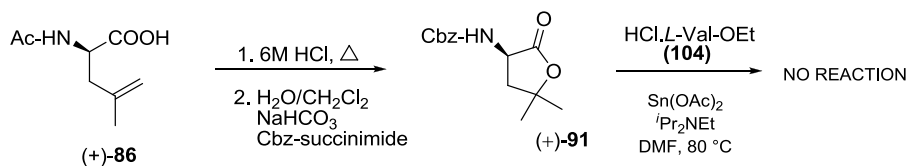


Entry	Reaction Conditions	Solvent	Yield (%)
1	2-hydroxypyridine, <i>i</i> Pr ₂ NEt	DMF	10
2	Sn(OAc) ₂ , <i>i</i> Pr ₂ NEt	DMF	65
3	Sn(OAc) ₂ , <i>i</i> Pr ₂ NEt	ClCH ₂ CH ₂ Cl	53
4	Cs ₂ CO ₃ , Et ₃ N	Toluene	4
5	Cs ₂ CO ₃	DMF	-
6	MeAlCl ₂ , <i>i</i> Pr ₂ NEt	ClCH ₂ CH ₂ Cl	24

We also explored compound (-)-**91** as a model system. Acid hydrolysis of the acetamide in compound (+)-**86** (stockpiled from the enzymatic resolution, Schemes 2.8 and 2.9) resulted in lactonization yielding α-amino-γ,γ-dimethyl-γ-valerolactone that was protected as its Cbz derivative (-)-**91** (Scheme 2.14). Attempts to open (+)-**91** using the optimized conditions from Table 3 were unsuccessful. Indeed, none of the examples cited in Scheme 2.13 involve a γ-lactone bearing a carbamate protected amine at Cα; substituents at Cα were invariably small (*e.g.*, H, Me, OMe, CN) and

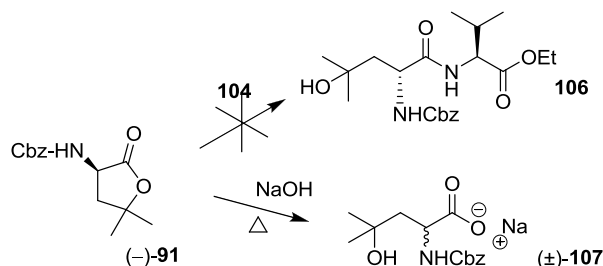
there were no examples with γ -disubstitution. This suggested to us that lactone (+)-**91** was stable⁷⁷ to ring opening reactions due to steric hindrance at the C α and C γ positions.

Scheme 2.14. Formation of the γ,γ -dimethyl- γ -valerolactone and reaction with the valine ethyl ester.⁷⁰



We decided to open the lactone ring in compound (+)-**91** by hydrolysis to give **107**⁷⁸ (Scheme 2.15) and then couple to valine ethyl ester via a conventional peptide bond formation. Unfortunately, ring opening was likely to be accompanied by racemization.

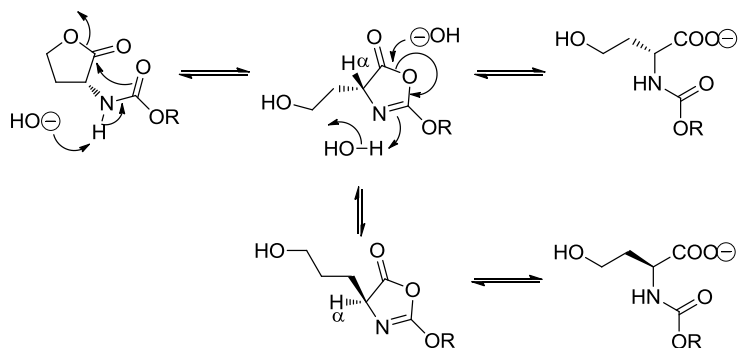
Scheme 2.15. Lactone ring opening by hydrolysis.



Michl demonstrated that *N*-acyl α -amino- γ -lactones epimerize at C α , even under weakly basic conditions.⁷⁹ Further studies by Michl revealed a similar trend with *N*-alkoxycarbonyl derivatives of the lactones under basic conditions; however, γ -lactones with an unprotected amine at C α resisted racemization. The mechanism proposed by Michl involves the formation of an oxazolone intermediate,

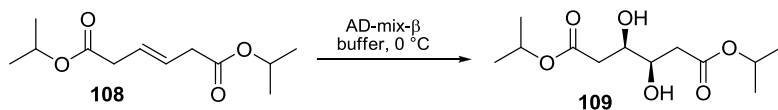
with a readily exchangeable H_α (Scheme 2.16). In light of these unfortunate results, we concluded that the γ -lactone generated via the dihydroxylation of β,γ -unsaturated ester **90** was unlikely to be a useful synthetic intermediate for peptide synthesis.

Scheme 2.16. Proposed rcemization mechanism.⁷⁹



During dihydroxylation of β,γ -unsaturated esters, concomitant lactonization is prevented by sterically hindered esters (Scheme 2.17).⁸⁰

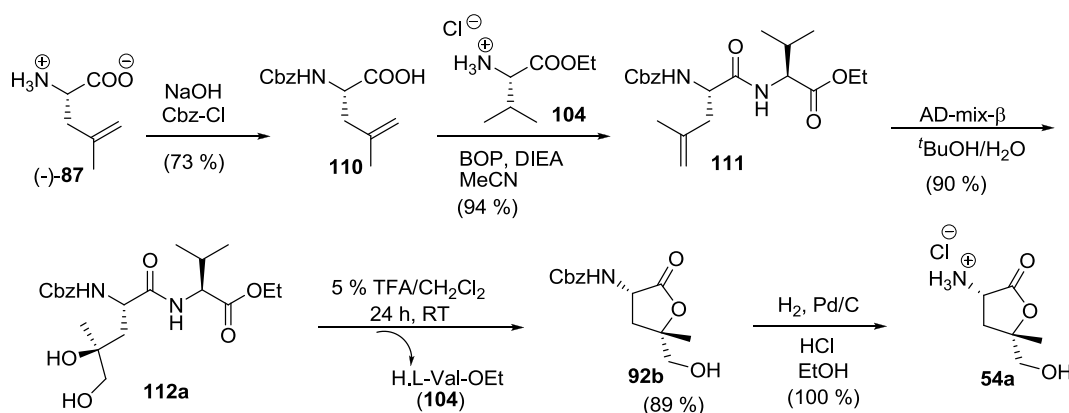
Scheme 2.17. Dihydroxylation of hindered esters.



We reasoned that an amide bond would also be resistant to spontaneous lactonization. We decided to change our approach by forming the dehyLeu-Val peptide bond prior to dihydroxylation (Scheme 2.18). The dipeptide olefin **111** was prepared and subjected to dihydroxylation reactions using both AD-mixes and OsO_4 to probe the extent of substrate control. Dihydroxylation with AD-mix- β gave us a single

peptide **112a** while AD-mix- α and OsO₄ formed mixtures of diastereomers that were not synthetically useful. While phthalazine ligands perform better for 1,1- and 1,2-*trans*-disubstituted class of olefins, it might have been worthwhile to investigate diastereoselectivities of PYR ligands.

Scheme 2.18. Dihydroxylation of the dehyLeu-Val dipeptide.



We were again unsuccessful at establishing the configuration of the dipeptide diol **112a** by crystallization of derivatives (4-bromobenzoate) of the primary alcohol or following hydrogenolysis of the Cbz group in the presence of ditoluoyl tartaric acid. Treatment of **112a** with TFA promoted lactonization and concomitant cleavage of the peptide bond forming valine ethyl ester **104** and lactone **92b** as a single diastereomer (Scheme 2.18). Gratifyingly, hydrogenolysis of **92b** in the presence of hydrochloric acid gave the hydrochloride salt of **54a**, a compound that Wieland had previously described as crystalline.³⁹ The crystal structure of **54a** revealed that the α -NH₃⁺ and γ -CH₂OH substituents were on the same face of the ring (Fig. 2.7). Thus the configuration of **54a** is (2*S*,4*S*) as

occurs in alloviroidin (**3**). The proton NMR spectrum (Figure 2.8) indicated that **92b** is the minor diastereomer obtained from the dihydroxylation of the dehydroleucine residue **90** (Scheme 2.11).

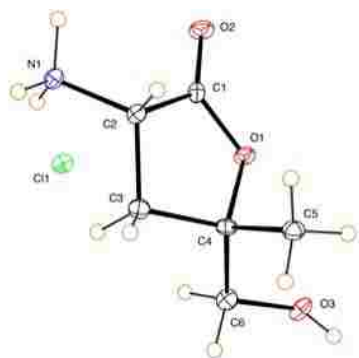


Figure 2.7. ORTEP diagram of compound **54a** (2*S*,4*S*).

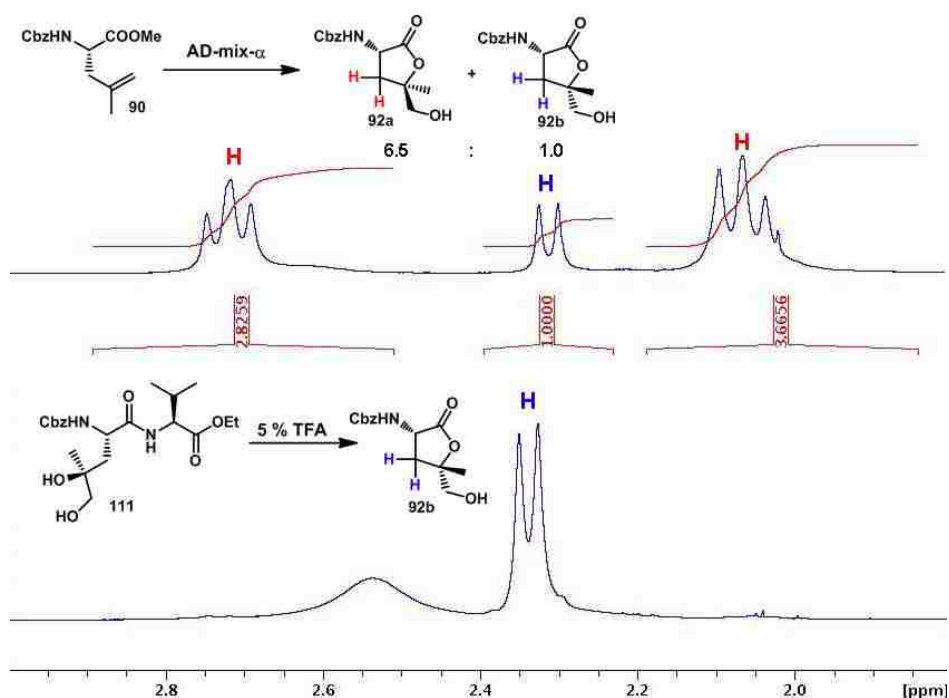
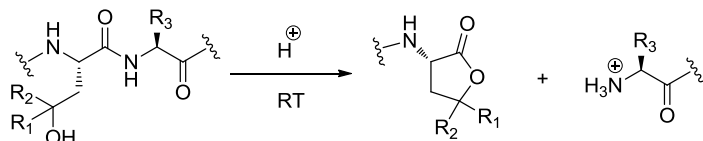


Figure 2.8. Selected region of the ^1H NMR spectrum of the γ -lactones obtained via different routes.

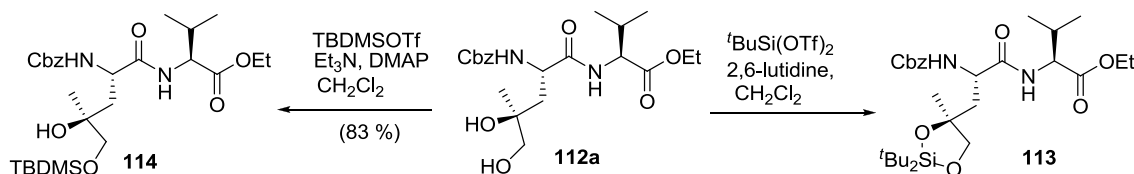
A careful choice of the side chain diol protecting group was necessary since peptides containing γ -hydroxyamino acids are prone to cleavage under mild acid conditions to give the γ -lactone and amine (Scheme 2.19).⁸¹ Thus, *tert*-butyl ethers, typically used in combination with Fmoc peptide synthesis are inappropriate.

Scheme 2.19. Cleavage of peptides containing γ -hydroxyamino acids under mild acid conditions.



Protection of the diol as a silyl acetal delivered **113** (Scheme 2.20). Unfortunately, the di-*tert*-butylsilyl acetal protecting group was partially cleaved during purification by silica gel chromatography, regenerating the starting material, **112a**. Corey and Hopkins had observed that the di-*tert*-butylsilylene derivatives of 1,3- and 1,4-diols are more stable than those of 1,2-diols.⁸² Given the problem associated with protecting both primary and tertiary alcohols as a silyl acetal, we decided to selectively protect the primary alcohol of **112a** as the fluoride-labile TBS ether derivative **114** (Scheme 2.20) to improve solubility. Protecting the primary alcohol was possible since it is less hindered and therefore easily transformed into the corresponding TBS ether in high yields as compared to the tertiary alcohol. It should also be noted that primary TBS ethers are readily cleaved under mild conditions as opposed to hindered tertiary TBS ethers. We hoped that the hindered nature of the remaining free alcohol would make it unlikely to participate as a nucleophile in side reactions associated with the larger peptide synthesis.

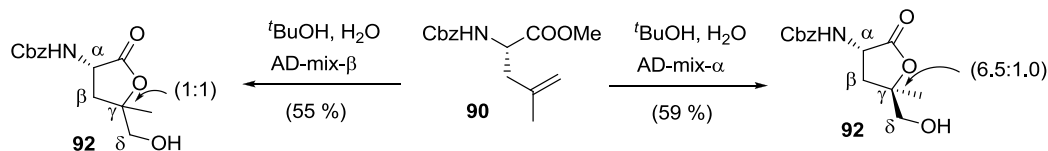
Scheme 2.20. Protection of the dipeptide diol.



2.4.1 Stereochemical Analysis of the Dihydroxylation Reaction

In our synthesis of the dihydroxy-leucine residue (*vide supra*), the dihydroxylation of the dehydroamino ester **90** using AD-mix- β gave a diastereomeric ratio of 1:1, whereas the AD-mix- α reagent resulted into an enhanced diastereomeric ratio of 6.5:1 (Scheme 2.21).

Scheme 2.21. Dihydroxylation of the dehydroamino ester.

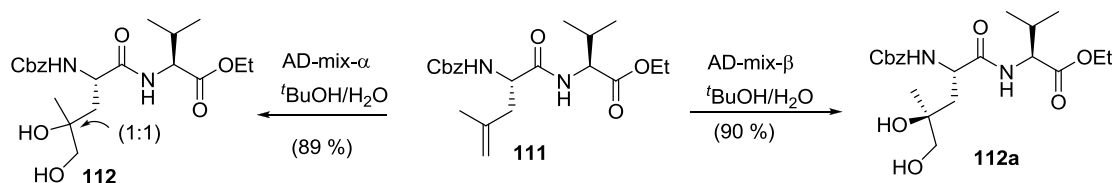


The poor diastereoselectivity observed using the AD-mix-β reagent represents a mismatched pair, *i.e.*, the chiral reagent (DHQD) was unable to overcome the intrinsic diastereofacial bias of the substrate. AD-mix-α-mediated dihydroxylation of **90** comprised a matched pair with the chiral reagent (DHQ), surmounting the intrinsic preference of the substrate, leading to the formation of the diol with fairly good diastereoselectivity.

Sharpless and co-workers have recommended the use of the aforementioned AD-mixes containing phthalazine based ligands for the dihydroxylation of 1,1-disubstituted olefins,⁴⁹ however, it was noted that predicting the stereochemical outcome for these class of olefins using the empirical mnemonic was less reliable since the two substituents compete for the ligand's hydrophobic, southwest quadrant, resulting in low enantioselectivities. The observed stereochemical outcome led us to speculate that the stereocenter in our dehydroleucine substrate has a significant influence on the ligand-substrate interaction and thus the stereochemical course of the reaction.

Upon changing our dihydroxylation substrate from dehydroleucine to the dehyLeu-Val dipeptide, the mismatched case turned into a matched pair (Scheme 2.22).

Scheme 2.22. Dihydroxylation of the dehyLeu-Val dipeptide.



It was astonishing to note that the dihydroxylation of the dehyLeu-Val dipeptide **111** using AD-mix-β afforded a single diastereomer, while the reaction of the same substrate **111** with AD-mix-α led to a 1:1

diastereomeric ratio, in contrast to the observation made for the dehydroleucine residue. These outcomes demonstrated that the nature of the substituents on our 1,1-disubstituted olefin substrates had a great impact on the stereochemical course of the reaction. We also investigated the dihydroxylation of **111** using OsO₄ in the absence of the chiral ligands, and again observed an almost equal mixture of diastereomers slightly favoring the diastereomer obtained using the AD-mix- β reagent. This is in agreement with the observed diastereomeric ratios using the chiral reagents, with AD-mix- β giving enhanced diastereofacial selectivity, suggesting that both steric effects and the two chiral centers present in our dipeptide substrate have a significant role in governing the facial selectivity of the reaction. It should be noted that the dihydroxylation of the dehyLeu-Val dipeptide substrate under all the investigated conditions produced high chemical yields in comparison to the single residue, dehydroleucine substrate **90**. A possible explanation for the low yield recorded during the dihydroxylation of the dehydroleucine **90** could be as a result of partial decomposition of the olefin substrate and losses during the aqueous work-up since the starting material was never recovered.

2.4.2 Summary

In summary, an efficient strategy that provides a dipeptide containing (2*S*,4*S*)-4,5-dihydroxyleucine residue via a diastereoselective dihydroxylation has been described. The dihydroxyleucine residue in its γ -lactone form was found not to be a useful building block for peptide synthesis, since it was unreactive toward amines. Also, hydrolytic opening of the γ -lactone posed the risk of epimerization at the C α position. We incorporated dehydroleucine into a dipeptide and performed a Sharpless asymmetric dihydroxylation to introduce the diol. The (2*S*,4*R*) diastereomer could not be generated through the same protocol.

2.5 EXPERIMENTAL SECTION

2.5.1 General Methods: All reactions were performed under a dry nitrogen atmosphere unless otherwise noted. Reagents were obtained from commercial sources and used directly; exceptions are noted. Diisopropylethylamine and triethylamine were dried and distilled from CaH_2 and stored over KOH pellets. Ethanol and Methanol were distilled from Mg turnings and stored over 4 Å molecular sieves. Flash chromatography was performed using flash silica gel (32-63 μ) from Dynamic Adsorbents Inc. Reactions were followed by TLC on precoated silica plates (200 μm , F-254 from Dynamic Adsorbents Inc.). The compounds were visualized by UV fluorescence or by staining with phosphomolybic acid, ninhydrin or KMnO_4 stains. NMR spectra were recorded on Bruker DPX-250 or AV-400-liquid spectrometers. Proton NMR data is reported in ppm downfield from TMS as an internal standard. Disodium 3-trimethylsilyl-1-propane-sulfonate (DSS) was used to reference ^1H NMR spectra run in D_2O . High resolution mass spectra were recorded using either time-of-flight or electrospray ionization.

L-Dehydroleucine, (-)-**87**, was prepared according to previously published procedures.^{58, 59, 83}

• **Ethyl 2-Acetamido-2-ethoxycarbonyl-4-methyl-4-pentenoic acid (51).** To a solution of diethylacetamido malonate (**85**) (10.00 g, 46.0 mmol, 1 equiv.) in EtOH (60 mL) at rt under N_2 was cautiously added Na (1.165 g, 50.64 mmol, 1.1 equiv.). The mixture was heated at reflux at which point followed the addition of 2-methyl-2-propenyl chloride (6 mL, 60 mmol, 1.3 equiv.) over 30 min. Heating at reflux was continued further for 2 h, concentrated, partitioned between EtOAc (60 mL) and H_2O (20 mL). The aqueous layer was extracted further with ethyl acetate (2×25 mL). The organic layers were combined, filtered through MgSO_4 and concentrated to a volume of 10 mL. Hexane (60 mL) was then added, with vigorous stirring, to give **51** as colorless crystals (9.384 g, 75 %); mp 88-88.5 °C,

Lit.⁵⁸ 92-93°, Lit.⁵⁹ 90-91 °C. ¹H NMR (250 MHz, CDCl₃) δ 1.27 (t, *J* = 7.1 Hz, 6H), 1.66 (s, 3H), 2.03 (s, 3H), 3.10 (s, 2H), 4.25 (qd, *J* = 7.1, 1.1 Hz, 4H), 4.69 (d, *J* = 0.9 Hz, 1H), 4.86 (t, *J* = 1.78 Hz, 1H), 6.81 (br. s, 1H); ¹³C NMR (62.5 MHz, CDCl₃) δ 13.9, 22.9, 23.2, 39.6, 62.4, 66.1, 115.9, 139.9, 167.9, 168.8.

• **(±)-2-Acetamido-4-methyl-4-pentenoic acid (±)-(86).** Aqueous NaOH (2M, 20 mL) was added to a solution of **51** (4.00 g, 15 mmol) in dioxane (20 mL) and the mixture heated at 50 °C for 3 d. The solution was concentrated, acidified to pH 1 with 6M HCl and partitioned between EtOAc (40 mL) and H₂O (30 mL). The aqueous layer was extracted further with EtOAc (3 × 30 mL). The organic layers were combined, dried over MgSO₄ and concentrated. The colorless residue was decarboxylated by heating at reflux in H₂O (15 mL) at 100 °C for 4 h. The solution was cooled and extracted with EtOAc (40 mL). The aqueous layer was extracted further with EtOAc (3 x 20 mL). The organic layers were combined, dried over MgSO₄ and concentrated to a volume of 10 mL. Hexane (~30 mL) was then added with vigorous stirring to give **(±)-86** (1.409 g, 56 %) as colorless shiny crystals upon standing at rt.; mp 154-154.8 °C, Lit.⁵⁹ 155-156 °C. ¹H NMR (250 MHz, CD₃OD): δ 1.75 (s, 3H), 1.96 (s, 3H), 2.37 (dd, *J* = 14.2, 9.9 Hz, 1H), 2.57 (dd, *J* = 14.2, 4.9 Hz, 1H), 4.57 (dd, *J* = 9.9, 4.9 Hz, 1H), 4.77 (d, *J* = 0.62 Hz, 1H), 4.82 (br, 1H); ¹³C NMR (62.5 MHz, CD₃OD) δ 20.9, 21.2, 39.8, 51.0, 113.1, 141.3, 172.2, 174.2.

• **(S)-γ,δ-Dehydroleucine (-)-87** and **(R)-2-Acetamido-4-methyl-4-pentenoic acid (+)-(86).** Compound **(±)-86** (400 mg, 2.34 mmol) and phenol red (1 drop from a Pasteur pipette) were suspended in H₂O (13 mL) at rt. Aqueous NH₄OH solution (~ 2 mL) was added dropwise to attain a pH of 7 (monitored by UIP) at which point the compound went into solution. Acylase enzyme (6.9 mg, activity

720 $\mu\text{mol}/\text{mg}$ protein from pork kidney' Sigma A8376) was added and the mixture stirred at rt for 24 h. The solution was acidified to pH 1 (monitored by UIP) with 6M HCl, concentrated to ~ 40 mL and extracted with EtOAc (3×15 mL). The organic layers were combined, filtered through MgSO_4 and concentrated to give (*R*)-2-acetamido-4-methyl-4-pentenoic acid (+)-**86** as a colorless amorphous solid (184 mg, 46 %). $[\alpha]_{\text{D}}^{25} +12.7^\circ$ (*c* 1.0, CH_3OH) [*S*-2-acetamido-4-methyl-4-pentenoic acid (-)-**86**, purchased from Bachem gave $[\alpha]_{\text{D}}^{25} -12.7^\circ$ (*c* 1.0, CH_3OH)]. ^1H and ^{13}C NMR spectra were as described above for the racemic material.

The aqueous layer was applied to a column (25 mm diameter, 30 mm high) of Dowex-50 (H^+), rinsed with water (~ 250 mL), eluted with 1N aqueous NH_4OH solution and fractions monitored by TLC, staining with ninhydrin. Relevant fractions were concentrated on a freeze-drier to deliver (-)-**87** as a colorless amorphous powder (104 mg, 35 %). R_f 0.53 (3:3:3:1 $^n\text{BuOH}/\text{EtOH}/\text{NH}_3/\text{H}_2\text{O}$); $[\alpha]_{\text{D}}^{25} -48.3^\circ$ (*c* 1.0, H_2O), Lit.⁵⁹ $[\alpha]_{\text{D}}^{20} -30.9^\circ$ (*c* 1.04, H_2O). ^1H NMR (400 MHz, D_2O): δ 1.77 (s, 3H), 2.50 (dd, $J = 14.5, 9.5$ Hz, 1H), 2.68 (dd, $J = 14.5, 9.5$ Hz, 1H), 3.85 (dd, $J = 9.5, 4.5$ Hz, 1H), 4.90 (s, 1H), 5.00 (t, $J = 1.4$ Hz, 1H); ^{13}C NMR (100 MHz, D_2O) δ 20.8, 39.1, 52.7, 115.5, 140.1, 174.6.

- (\pm)- γ,δ -Dehydroleucine (**87**): Compound (\pm)-**86** (100 mg, 0.58 mmol) was suspended in aqueous NaOH (2.5 N) and refluxed for 4 h. The solution was neutralized to pH 7 (monitored by UIP) with 6 M HCl, applied to a column (25 mm diameter, 30 mm high) of Dowex-50 (H^+), rinsed with water (~ 150 mL), eluted with 1N aqueous NH_4OH solution and fractions monitored by TLC, staining with ninhydrin. Relevant fractions were concentrated on a freeze-drier to deliver (\pm)-**87** as a colorless amorphous powder in quantitative yield. R_f 0.53 (3:3:3:1 $^n\text{BuOH}/\text{EtOH}/\text{NH}_3/\text{H}_2\text{O}$). ^1H and ^{13}C NMR spectra were as described above for compound (-)-**87**.

- **Lactone (+)-91:** (+)-**86** (500 mg, 2.9 mmol) was suspended in 2 M HCl (7.5 mL). The mixture was refluxed for 2 h and concentrated to dryness. The residue was dissolved in a mixture of CH₂Cl₂ (7 mL) and H₂O (3.5 mL) and cooled at 0 °C at which point NaHCO₃ (1.6 g, 19.3 mmol, 6.6 equiv.) and *N*-(benzyloxycarbonyloxy)succinimide (874 mg, 3.5 mmol, 1.2 equiv.) were added in that order. The reaction mixture was gradually warmed to rt overnight and partitioned between CH₂Cl₂/H₂O (30 mL each). The aqueous layer was back extracted with CH₂Cl₂ (2 × 30 mL). The organic extracts were combined, filtered through MgSO₄ and concentrated. The residue was purified by flash chromatography eluting with 1:1 Hex/EtOAc to give (+)-**91** as a colorless solid (641 mg, 83 %). *R*_f 0.47 (1:1 Hexanes/EtOAc); [α]_D²⁴ +26.6° (*c* 1.0, CH₃OH), Lit.⁵⁸ [α]_D²⁰ -33.1° (*c* 1.0, CH₃OH). ¹H NMR (400 MHz, CDCl₃): δ 1.45 (d, *J* = 28.7 Hz, 6H), 1.99 (t, *J* = 12.1 Hz, 1H), 2.65 (t, *J* = 10.5 Hz, 1H), 4.60 (dd, *J* = 16.2, 9.6 Hz, 1H), 5.12 (s, 2H), 5.36 (s, 1H), 7.31-7.36 (m, 5 H); ¹³C NMR (100 MHz, CDCl₃) δ 26.9, 28.9, 42.3, 51.6, 67.3, 82.4, 128.1, 128.3, 128.5, 135.9, 156.0, 174.0

- **Mosher amide (-)-88a.** Thionyl chloride (112 μL, 184 mg, 1.5 mmol, 2.0 equiv.) was added dropwise to a solution of dehydroleucine (-)-**87** (100 mg, 0.77 mmol, 1.0 equiv.) in anhydrous methanol (3 mL) at -10 °C under N₂. The solution was warmed to rt and left to stir overnight. The mixture was concentrated to give dehydroleucine methyl ester hydrochloride as a colorless oil (136 mg, 98 %).

N-Methyl morpholine (67 μL, 62 mg, 0.61 mmol, 1.1 equiv.) was added to a solution of dehydroleucine methyl ester hydrochloride (100 mg, 0.56 mmol, 1 equiv.) in THF (2 mL) at 0 °C under N₂. (*S*)-(-)-Methoxy(trifluoromethyl)phenyl acetic acid (MTPA) (143 mg, 0.61 mmol, 1.1 equiv.) and *N,N'*-dicyclohexyl carbodiimide (DCC) (138 mg, 0.67 mmol, 1.2 equiv.) were added. The mixture was stirred at 0 °C for 3 h and then at rt overnight. The resulting *N,N'*-dicyclohexyl urea was removed by filtration and the filtrate concentrated. The residue was dissolved in ethyl acetate (15 mL) and washed

successively with 10 % citric acid (10 mL), 5% NaHCO₃ (10 mL) and brine (10 mL). The organic layer was filtered through MgSO₄ and concentrated. The residue was purified by flash chromatography, eluting with 5:1 Hex/EtOAc to give **88a** as an oil (123 mg, 62%). *R_f* 0.53 (2:1 Hexanes/EtOAc); [α]_D²⁸ +16.5° (*c* 0.85, CHCl₃). ¹H NMR (400 MHz, CDCl₃): δ 1.67 (s, 3H), 2.39 (dq, *J* = 8.8, 5.2 Hz, 1H), 2.56 (dd, *J* = 14.0, 5.1 Hz, 1H), 3.51 (dd, *J* = 3.3, 1.6 Hz, 3H), 3.80 (s, 3H), 4.60 (d, *J* = 0.8 Hz, 1H), 4.70 (app. t, *J* = 1.5 Hz, 1H), 4.80 (dt, *J* = 8.6, 4.4 Hz, 1H), 7.35-7.58 (m, 5H); ¹⁹F NMR (236 MHz, CDCl₃) δ -69.34 (br, 3F), -69.49 (br, 3F); ¹³C NMR (100 MHz, CDCl₃) δ 21.6, 40.4, 50.1, 55.2, 83.7, 84.0, 114.8, 122.1, 125.0, 127.5, 128.4, 129.4, 132.7, 140.0, 166.2, 172.0. HRMS (+TOF) calcd for C₁₇H₂₁NO₄F₃ (M + H)⁺: 391.2227; obsd: 391.2240.

- **Mosher amides 88a,b.** Compound (±)-**86** (100 mg, 0.58 mmol) was suspended in aqueous NaOH (2.5 N, 3 mL) and heated at reflux for 4h. The solution was neutralized to pH 7 (monitored with UIP) by the addition of 6M HCl. The solution was then loaded onto a column (25 mm diameter, 30 mm high) of Dowex-50 (H⁺), rinsed with water (150 mL), eluted with 1N aqueous NH₄OH. Fractions were monitored by TLC, staining with ninhydrin. Relevant fractions were freeze-dried to give (±)-**87** as a colorless, amorphous powder in quantitative yield. A portion of this material (50 mg) was derivatized with MTPA, as described above, to give a 1:1 mixture of diastereomers (75 mg, 54 %). ¹⁹F NMR (236 MHz, CDCl₃) δ -69.35, -69.49.

- **Cbz-dehydroleucine-OMe (90).** Thionyl chloride (229 μ L, 376 mg, 3.2 mmol, 2 equiv.) was gradually added to a suspension of the amino acid (-)-**87** (204 mg, 1.6 mmol, 1 equiv.) in MeOH (4 mL) at -10 °C under N₂. The solution was gradually warmed to rt, stirred for 2 d, and concentrated. The residue was dissolved in a mixture of CH₂Cl₂ (3 mL) and H₂O (1.5 mL) and cooled to 0 °C at which

point NaHCO₃ (728 mg, 8.7 mmol, 6.6 equiv.) and *N*-(benzyloxycarbonyloxy)succinimide (393 mg, 1.6 mmol, 1.2 equiv.) were added sequentially. The reaction mixture was gradually warmed to rt overnight and diluted with CH₂Cl₂/H₂O (20 mL each). The aqueous layer was back extracted with EtOAc (2 × 15 mL). The organic extracts were combined, filtered through MgSO₄ and concentrated. The residue was purified by flash chromatography eluting with 2:1 Hex/EtOAc to give **90** as a colorless oil (266 mg, 73 %). *R_f* 0.50 (3:1 Hexanes/EtOAc); [α]_D²⁷ +7.3° (*c* 1.2, CHCl₃). ¹H NMR (400 MHz, CDCl₃): δ 1.73 (s, 3H), 2.38 (dd, *J* = 14.0, 8.4 Hz, 1H), 2.54 (dd, *J* = 14.0, 5.4 Hz, 1H), 3.73 (s, 3H), 4.49 (td, *J* = 8.1, 5.6 Hz, 1H), 4.75 (br, 1H), 4.84 (app. t, *J* = 1.5 Hz, 1H), 5.10 (s, 2H), 5.27 (d, *J* = 7.8 Hz, 1H), 7.27-7.38 (m, 5 H); ¹³C NMR (100 MHz, CDCl₃) δ 21.7, 40.6, 52.1, 52.2, 66.9, 114.6, 127.9, 128.0, 128.4, 136.2, 140.2, 155.7, 172.6. HRMS (+TOF) calcd for C₁₅H₂₀NO₄ (*M* + H)⁺: 278.1386; obsd: 278.1387.

- **Lactones 92a,b.** AD-mix-α (1.833 g) was added to a mixture of ^tBuOH (6.5 mL) and H₂O (6.5 mL) at rt. The clear orange solution was cooled to 0 °C and Cbz-dehydroleucine-OMe (**90**) (363 mg, 1.31 mmol) was added. The reaction mixture was stirred at 0 °C for 24 h, quenched with Na₂SO₃ (1.964 g), stirred for an additional 1 h at rt, and extracted with CH₂Cl₂ (6 × 30 mL). The organic layers were combined, filtered through MgSO₄ and concentrated. The residue was purified by flash chromatography, eluting with 95:5 CH₂Cl₂/MeOH, to give **92a,b** (215 mg, 59 %) as a mixture of diastereomers. *R_f* 0.55 (9:1 CH₂Cl₂/CH₃OH); ¹H NMR (400 MHz, CDCl₃): δ 1.41 (s, 3H), 2.08 (t, *J* = 11.7 Hz, 1H), 2.35 (br, 1H), 2.77 (t, *J* = 11.2 Hz, 1H), 3.54 (d, *J* = 12.0 Hz, 1H), 3.70 (d, *J* = 12.0 Hz, 1H), 4.69 (dd, *J* = 17.1, 9.6 Hz, 1H), 5.10 (s, 2H), 5.49 (d, *J* = 6.3 Hz, 1H), 7.29-7.38 (m, 5H); ¹³C NMR (100 MHz, CDCl₃) δ 23.4, 35.8, 38.0, 52.3, 67.2, 68.6, 84.9, 128.1, 128.2, 128.5, 136.0, 156.1, 174.9. HRMS (+TOF) calcd for C₁₅H₁₄N₅O (*M* + H)⁺: 280.1179; obsd: 280.1183.

• **Amide 105.** Diisopropylethylamine (182 μ L, 142 mg, 1.10 mmol, 1.1 equiv.), γ -valerolactone (**103**) (95 μ L, 100 mg, 1.00 mmol, 1 equiv.) and Sn(OAc)₂ (47 mg, 0.20 mmol, 0.2 equiv.) were added sequentially to a solution of *L*-valine ethyl ester hydrochloride (**104**) (272 mg, 1.50 mmol, 1.5 equiv.) in DMF (3 mL) at 0 °C under N₂. The mixture was warmed to 80 °C and stirred for 44 h, concentrated, and the product isolated by flash chromatography eluting with 95:5 CH₂Cl₂/MeOH to give **105** as a 1:1 mixture of diastereomers (159 mg, 65%). *R_f* 0.37 (95:5 CH₂Cl₂/MeOH); ¹H NMR (400 MHz, CDCl₃): δ 0.91 (dd, *J* = 6.9, 0.6 Hz, 3H), 0.94 (d, *J* = 6.9 Hz, 3H), 1.98 (d, *J* = 1.2 Hz, 1.5H), 1.21 (d, *J* = 1.2, Hz, 1.5H), 1.29 (t, *J* = 7.1 Hz, 3H), 1.66-1.75 (m, 1H), 1.80-1.89 (m, 1H), 2.12-2.20 (m, 1H), 2.37-2.48 (m, 1H), 2.42 (t, *J* = 6.8 Hz, 1H), 2.43 (t, *J* = 7.3 Hz, 1H), 3.27 (br, 1H), 3.81-3.87 (m, 1H), 4.14-4.26 (m, 2H), 4.53 (dd, *J* = 8.7, 5.0 Hz, 1H), 6.48 (br, 1H); ¹³C NMR (100 MHz, CDCl₃) δ 14.1, 17.7, 18.8, 23.5, 31.1, 33.0, 34.2, 57.0, 61.2, 67.1 & 67.2, 172.1 & 172.2, 173.6. HRMS (+TOF) calcd for C₁₂H₂₄NO₄ (M + H)⁺: 244.1554; obsd: 244.1549.

• **Cbz-dehydroleucine-OH (110).** Aqueous NaOH (2M, 10 mL) was added dropwise to a suspension of dehydroleucine (-)-**87** (380 mg, 2.94 mmol, 1 equiv.) in THF (5 mL) at 0 °C. Benzyl chloroformate (497 μ L, 602 mg, 3.53 mmol, 1.2 equiv.) was added dropwise over 30 min, with vigorous stirring. The cloudy reaction mixture was left to stir overnight at rt and concentrated to remove THF. The residue was diluted with H₂O (20 mL), extracted with ether (2 \times 10 mL), acidified with 6M HCl to pH 1 and extracted with EtOAc (3 \times 25 mL). The organic layers were combined, washed with brine (25 mL) and concentrated to give **110** as a colorless oil (630 mg, 81%). *R_f* 0.35 (9:1 CH₂Cl₂/MeOH); [α]_D²⁷ +4.4° (*c* 1.2, CH₃OH). ¹H NMR (400 MHz, CD₃OD): δ 1.75 (s, 3H), 2.38 (dd, *J* = 14.1, 10.0 Hz, 1H), 2.56 (dd, *J* = 14.1, 4.7 Hz, 1H), 4.36 (dd, *J* = 10.0, 4.8 Hz, 1H), 4.78 (br, 1H), 4.81 (br, 1H), 4.95 (br, 1H), 5.07 (s, 2H), 7.26-7.35 (m, 5 H); ¹³C NMR (100 MHz, CD₃OD) δ 20.0, 38.9, 51.7, 65.5, 112.3, 126.7, 126.9,

127.4, 136.2, 140.3, 156.5, 173.7. HRMS (+TOF) calcd for $C_{14}H_{18}NO_4$ ($M + H$)⁺: 264.1230; obsd: 264.1224.

• **Cbz-dehydroleucine-Val-OEt (111).** Diisopropylethylamine (1.2 mL, 910 mg, 7.04 mmol, 2.0 equiv.) was added to a solution of Cbz-protected dehydroleucine (**110**) (618 mg, 2.3 mmol, 3.0 equiv.), valine ethyl ester hydrochloride (426 mg, 2.3 mmol, 1.0 equiv.) and BOP reagent (1.1 g, 2.6 mmol, 1.1 equiv.) in acetonitrile (15 mL). The mixture was stirred at 0 °C for 1 h and then at rt overnight. The mixture was concentrated and the product isolated by flash chromatography eluting with 2:1 Hex/EtOAc, to give **111** as a colorless solid (851 mg, 93 %). R_f 0.53 (2:1 Hexanes/EtOAc); $[\alpha]_D^{30}$ -2.4° (c 1.05, $CHCl_3$). 1H NMR (400 MHz, $CDCl_3$): δ 0.88 (d, J = 6.9 Hz, 3H), 0.91 (d, J = 6.9 Hz, 3H), 1.27 (t, J = 7.1 Hz, 3H), 1.75 (s, 3H), 2.16 (app. pd, J = 6.9, 4.8 Hz, 1H), 2.39 (dd, J = 14.2, 8.8 Hz, 1H), 2.56 (dd, J = 14.2, 5.8 Hz, 1H), 4.14-4.24 (m, 2H), 4.31 (br, 1H), 4.50 (dd, J = 8.7, 4.8 Hz, 1H), 4.80 (br, 1H), 4.87 (t, J = 1.4 Hz, 1H), 5.11 (s, 2H), 5.26 (br, 1H), 6.63 (d, J = 7.8 Hz, 1H), 7.29-7.37 (m, 5 H); ^{13}C NMR (100 MHz, $CDCl_3$) δ 14.1, 17.7, 18.8, 21.9, 31.3, 40.4, 53.2, 57.2, 61.2, 67.1, 114.5, 127.9, 128.1, 128.5, 136.2, 140.8, 156.1, 171.3, 171.5. HRMS (+TOF) calcd for $C_{21}H_{31}N_2O_5$ ($M + H$)⁺: 391.2227; obsd: 391.2240.

• **Compound 112a.** AD-mix- β (563 mg) was dissolved in t BuOH (2 mL) and H_2O (2 mL) at rt. The clear orange solution was cooled to 0 °C and dipeptide olefin **111** (157 mg, 0.4 mmol) was added. The mixture was stirred for 48 h at 0 °C, quenched with Na_2SO_3 (604 mg), stirred for 1 h at rt, diluted with H_2O (10 mL) and extracted with EtOAc (6 \times 15 mL). The organic layers were combined, dried over $MgSO_4$ and concentrated. The crude product was purified by flash chromatography eluting with 20:1 EtOAc/MeOH, to give **112a** as a colorless solid (154 mg, 90 %). R_f 0.32 (9:1 CH_2Cl_2 /MeOH); $[\alpha]_D^{29}$ -

25.8° (*c* 0.95, CH₃OH). ¹H NMR (400 MHz, CD₃OD): δ 0.93 (d, *J* = 2.3 Hz, 3H), 0.95 (d, *J* = 2.3 Hz, 3H), 1.19 (s, 3H), 1.26 (t, *J* = 7.1 Hz, 3H), 1.77 (dd, *J* = 14.8, 8.7 Hz, 1H), 2.03 (dd, *J* = 14.6, 3.3 Hz, 1H), 2.15 (app. qd, *J* = 13.1, 6.5 Hz, 1H), 3.38 (dd, *J* = 15.9, 11.1 Hz, 2H), 4.10-4.21 (m, 2H), 4.30 (d, *J* = 5.5 Hz, 1H), 4.39 (dd, *J* = 8.4, 3.8 Hz, 1H), 5.09 (s, 2H), 7.25-7.36 (m, 5 H); ¹³C NMR (100 MHz, CD₃OD) δ 12.5, 16.3, 17.4, 22.3, 29.8, 39.0, 50.8, 57.2, 60.2, 65.7, 68.6, 71.1, 126.8, 127.0, 127.5, 136.2, 156.2, 170.9, 173.5. HRMS (+TOF) calcd for C₂₁H₃₃N₂O₇ (M + H)⁺: 425.2282; obsd: 425.2280.

- **Lactone **92b**.** A mixture of trifluoroacetic acid (100 μL) and CH₂Cl₂ (2 mL) was added to compound **112a** (43 mg, 0.10 mmol) at 0 °C under N₂. The mixture was gradually warmed to rt overnight, concentrated, and the product isolated by flash chromatography eluting with 95:5 CH₂Cl₂/MeOH to give **92b** (23 mg, 82 %). *R_f* 0.53 (9:1 CH₂Cl₂/CH₃OH); [α]_D²⁵ -5.7° (*c* 1.0, CHCl₃). ¹H NMR (400 MHz, CDCl₃): δ 1.35 (s, 3H), 2.34 (d, *J* = 9.5 Hz, 1H), 2.54 (br, 1H), 3.44 (d, *J* = 8.0 Hz, 1H), 3.73 (d, *J* = 12.2 Hz, 1H), 4.70 (dd, *J* = 17.1, 8.8 Hz, 1H), 5.11 (dd, *J* = 18.5, 12.2 Hz, 2H), 5.79 (d, *J* = 7.3 Hz, 1H), 7.30-7.36 (m, 5H); ¹³C NMR (100 MHz, CDCl₃) δ 22.5, 29.7, 35.8, 51.1, 67.3, 67.4, 84.6, 128.1, 128.2, 128.5, 136.0, 156.1, 174.9. HRMS (+TOF) calcd for C₁₅H₁₄N₅O (M + H)⁺: 280.1179; obsd: 280.1183.

- **Hydrochloride salt of Lactone (2*S*,4*S*)-**54a**.** Concentrated HCl (48 μL) and 10 % Pd/C (22 mg, 0.206 mmol) were added to a solution of **92b** (70 mg, 0.25 mmol) in EtOH (2.4 mL) at rt under N₂. The mixture was hydrogenated for 4h, then filtered through Celite, and concentrated to give the hydrochloride salt as a colorless solid. Recrystallization from ethanol/ether yielded colorless crystals (46 mg, 100 %); *R_f* 0.46 (3:3:3:1 ⁿBuOH/EtOH/NH₃/H₂O); mp 210-213 °C, Lit.³⁹ 205-207 °C. [α]_D²³ -7.4° (*c* 0.75, 6N HCl), Lit.³⁹ [α]_D²⁰ -12° (*c* 2, 6N HCl). ¹H NMR (400 MHz, D₂O): δ 1.45 (s, 3H), 2.43

(dd, $J = 13.0, 10.4$ Hz, 1H), 2.60 (dd, $J = 13.2, 9.6$ Hz, 1H), 3.61 (d, $J = 12.7$ Hz, 1H), 3.77 (d, $J = 12.7$ Hz, 1H), 4.64 (t, $J = 9.9$ Hz, 1H); ^{13}C NMR (100 MHz, D_2O) δ 20.9, 32.8, 49.4, 65.9, 87.5, 173.2. HRMS (+TOF) calcd for $\text{C}_6\text{H}_{12}\text{NO}_3(\text{M} - \text{HCl})^+$: 146.0811; obsd: 146.0813.

- **Hydrochloride salt of Lactone 54a,b.** Lactone **92a,b** (32 mg) was treated, as for the diastereomer, to cleave the Cbz group to give the hydrochloride salt of aminolactone **54a,b** (18 mg, 86 %) as a 6.5:1.0 mixture of diastereomers. mp 197-200 °C, Lit.³⁹ 199-200 °C. $[\alpha]_{\text{D}}^{23} -22^\circ$ (c 0.45, 6N HCl), Lit.³⁹ $[\alpha]_{\text{D}}^{20} -35.5^\circ$ (c 2, 6N HCl). NMR spectra are reported for the major (2*S*,4*R*) diastereomer. ^1H NMR (400 MHz, D_2O): δ 1.46 (s, 3H), 2.24 (dd, $J = 13.4, 11.0$ Hz, 1H), 2.88 (dd, $J = 13.4, 9.8$ Hz, 1H), 3.65 (d, $J = 12.6$ Hz, 1H), 3.71 (d, $J = 12.7$ Hz, 1H), 4.64 (t, $J = 10.3$ Hz, 1H); ^{13}C NMR (100 MHz, D_2O) δ 22.1, 35.3, 50.0, 66.9, 87.9, 173.7.

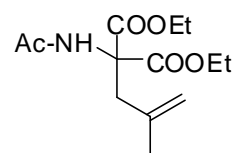
- **Silyl ether protection 114.** Triethylamine (273 μL , 199 mg, 1.96 mmol, 2.4 equiv.), DMAP (20 mg, 0.16 mmol, 0.2 equiv.) and TBDMSOTf (206 μL , 238 mg, 0.90 mmol, 1.1 equiv.) were added to a solution of **112a** (347 mg, 0.82 mmol, 1 equiv.) in CH_2Cl_2 (4 mL) at 0 °C under N_2 . The mixture was warmed to rt overnight, concentrated, and the product isolated by flash chromatography eluting with 2:1 Hex/EtOAc to give **114** (368 mg, 84 %). R_f 0.42 (2:1 Hex/EtOAc); ^1H NMR (400 MHz, CDCl_3): δ 0.07 (d, $J = 4.4$ Hz, 6H), 0.88 (d, $J = 6.8$ Hz, 3H), 0.89 (s, 9H), 0.93 (d, $J = 6.8$ Hz, 3H), 1.26 (t, $J = 8.8$ Hz, 3H), 1.29 (s, 3H), 1.76 (dd, $J = 14.8, 4.2$ Hz, 1H), 1.84 (br, 1H), 2.13 (d, $J = 6.6$ Hz, 1H), 2.14-2.23 (m, 1H), 3.29 (br, 1H), 3.43 (app.t, $J = 10.6$ Hz, 2H), 4.08-4.24 (m, 3H), 4.42 (br, 1H), 4.48 (q, $J = 8.8$ Hz, 1H), 5.12 (dd, $J = 10.9, 6.1$ Hz, 2H), 6.12 (d, $J = 10.9, 5.4$ Hz, 1H), 7.28-7.36 (m, 5 H); ^{13}C NMR (100 MHz, CDCl_3) δ -5.5, 14.2, 17.5, 18.3, 19.0, 23.6, 25.8, 30.9, 41.1, 51.1, 57.3, 61.1, 66.8, 70.6, 72.2,

128.0, 128.1, 128.4, 136.3, 156.0, 171.8, 172.4. HRMS (+TOF) calcd for $C_{27}H_{46}N_2O_7Si$ ($M + H$)⁺: 538.3074; obsd: 538.3065.

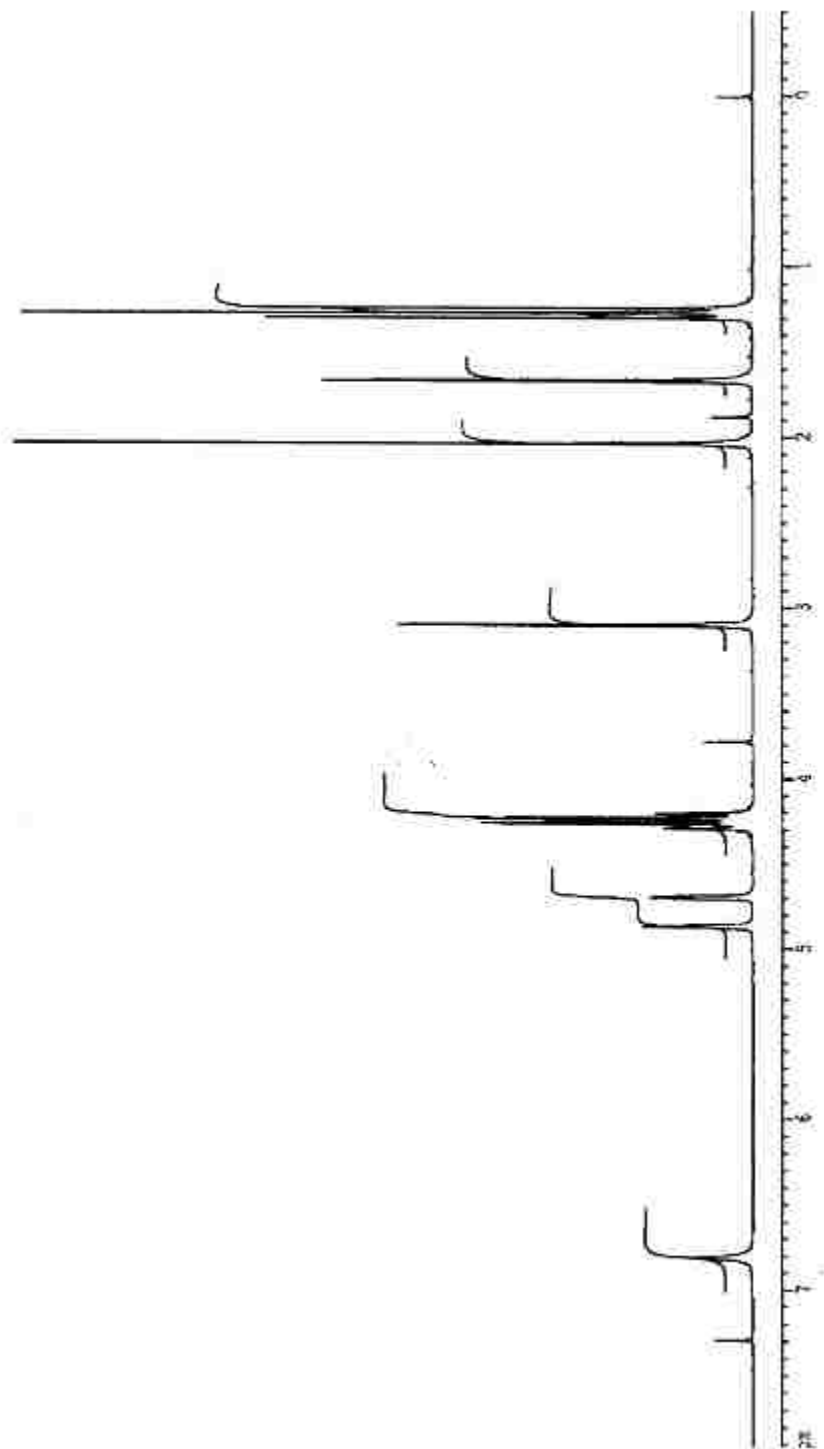
2.5.2 Spectra

¹ H NMR spectrum of compound 51	52
¹³ C NMR spectrum of compound 51	53
¹ H NMR spectrum of compound (±)- 86	54
¹³ C NMR spectrum of compound (±)- 86	55
¹ H NMR spectrum of compound (-)- 87	56
¹³ C NMR spectrum of compound (-)- 87	57
¹ H NMR spectrum of compound 88a	58
¹³ C NMR spectrum of compound 88a	59
¹ H NMR spectrum of compound 110	60
¹³ C NMR spectrum of compound 110	61
¹ H NMR spectrum of compound 90	62
¹³ C NMR spectrum of compound 90	63
¹ H NMR spectrum of compound 105	64
¹³ C NMR spectrum of compound 105	65
¹ H NMR spectrum of compound (+)- 91	66
¹³ C NMR spectrum of compound (+)- 91	67
¹ H NMR spectrum of compound 111	68
¹³ C NMR spectrum of compound 111	69
¹ H NMR spectrum of compound 112a	70
¹³ C NMR spectrum of compound 112a	71
¹ H NMR spectrum of compound 92b	72
¹³ C NMR spectrum of compound 92b	73
¹ H NMR spectrum of compound 114	74
¹³ C NMR spectrum of compound 114	75

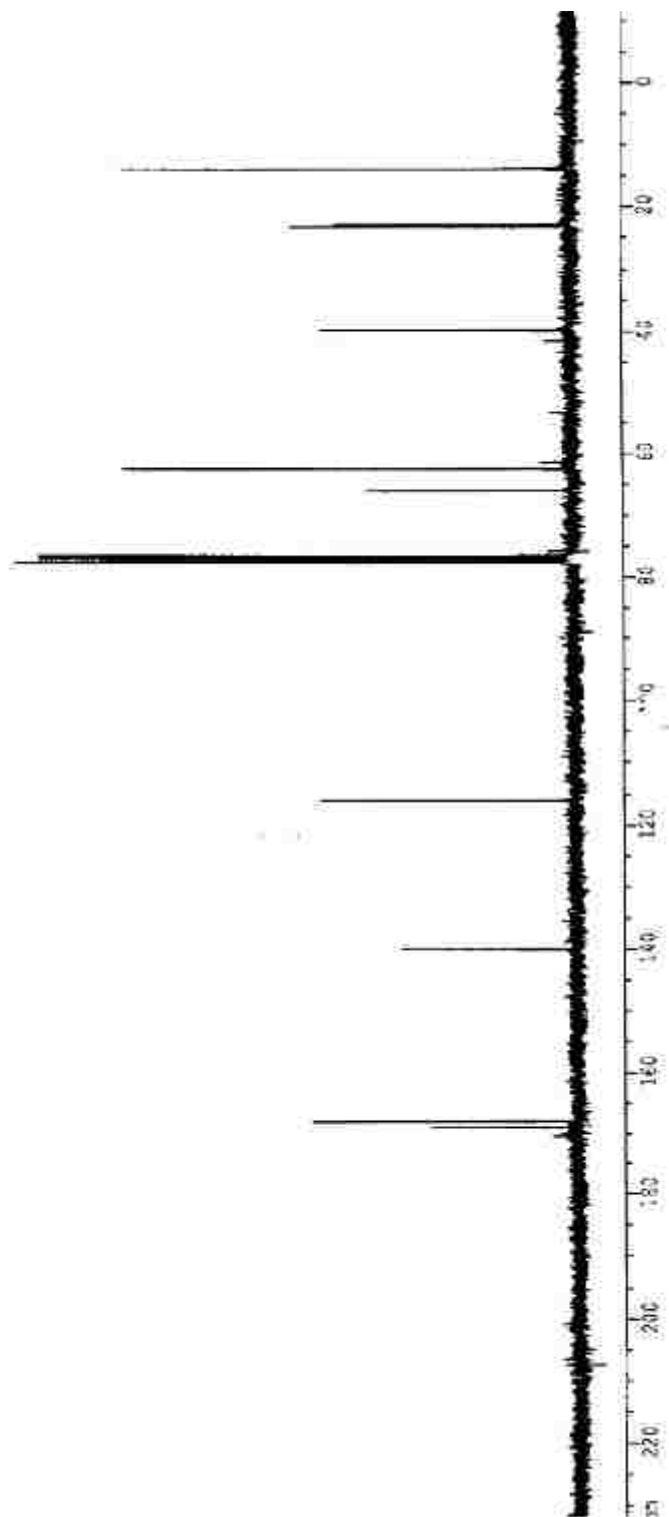
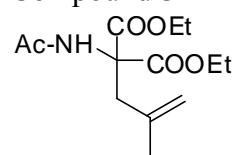
Compound **51** – ^1H NMR in CDCl_3 at 250 MHz



bej-1/142a

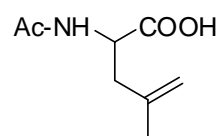


Compound **51** – ^{13}C NMR in CDCl_3 at 62.5 MHz

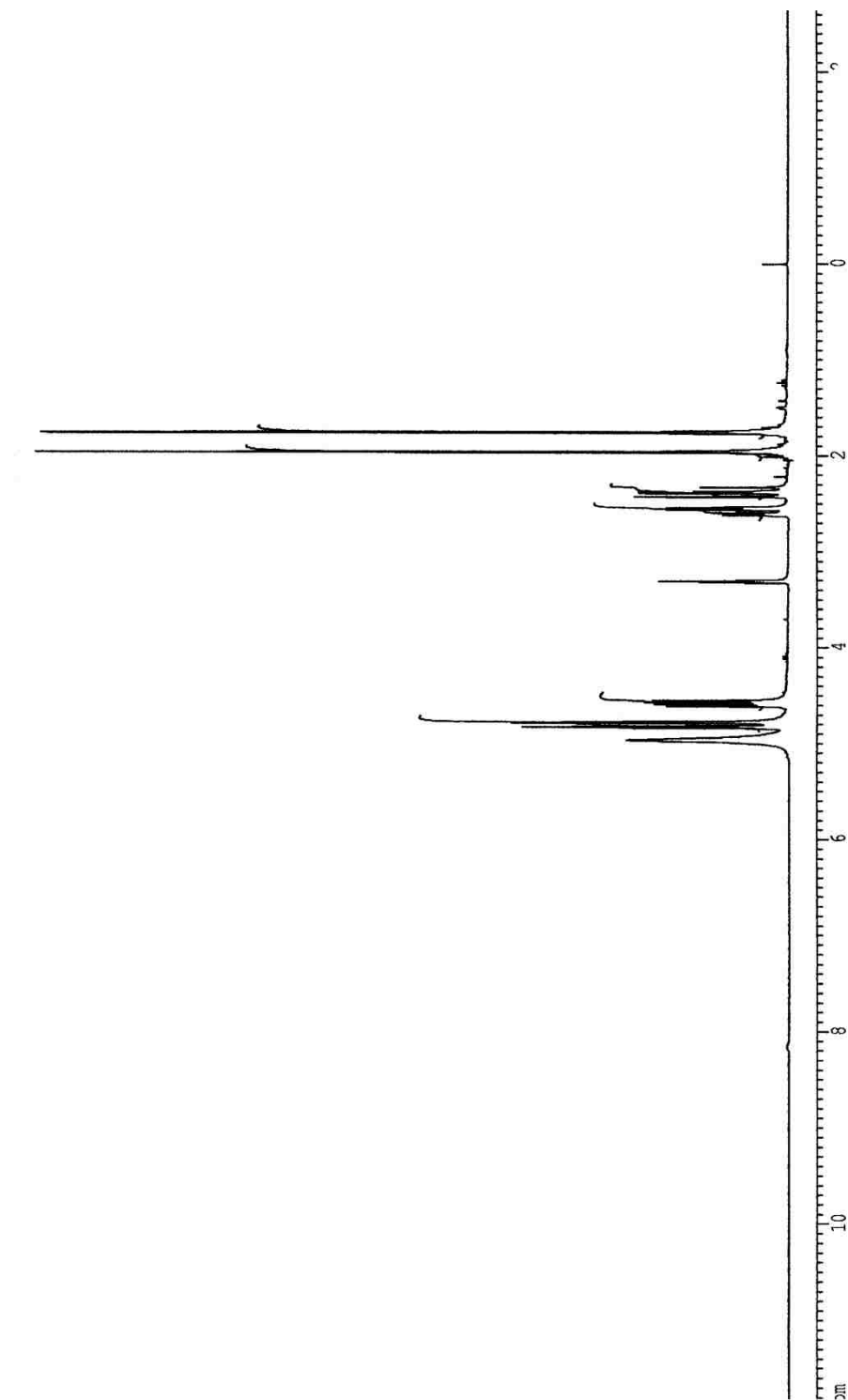


067-1/95A

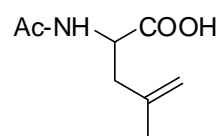
Compound (±)-**86** – ^1H NMR in CD_3OD at 250 MHz



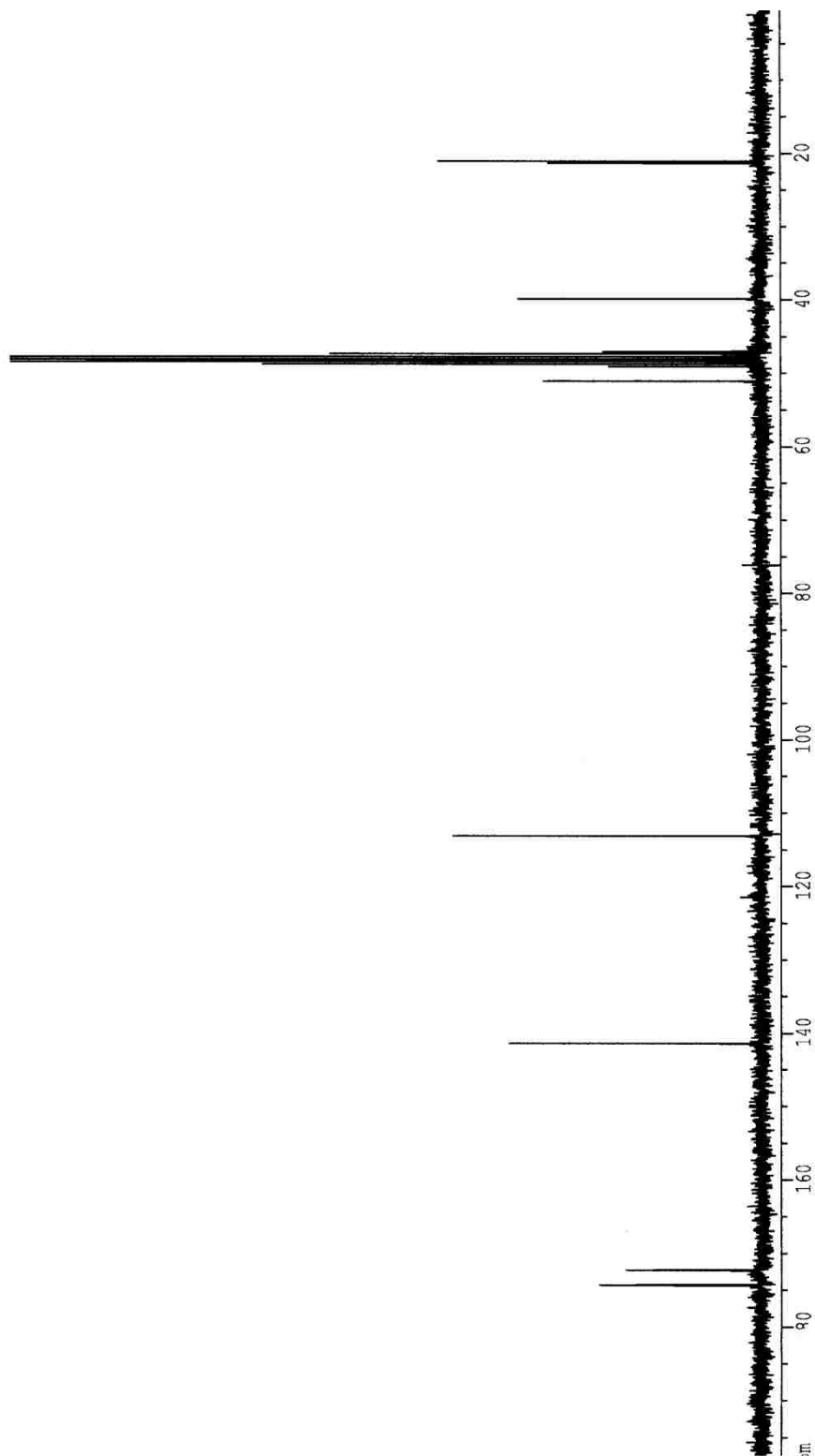
bej-1/100b



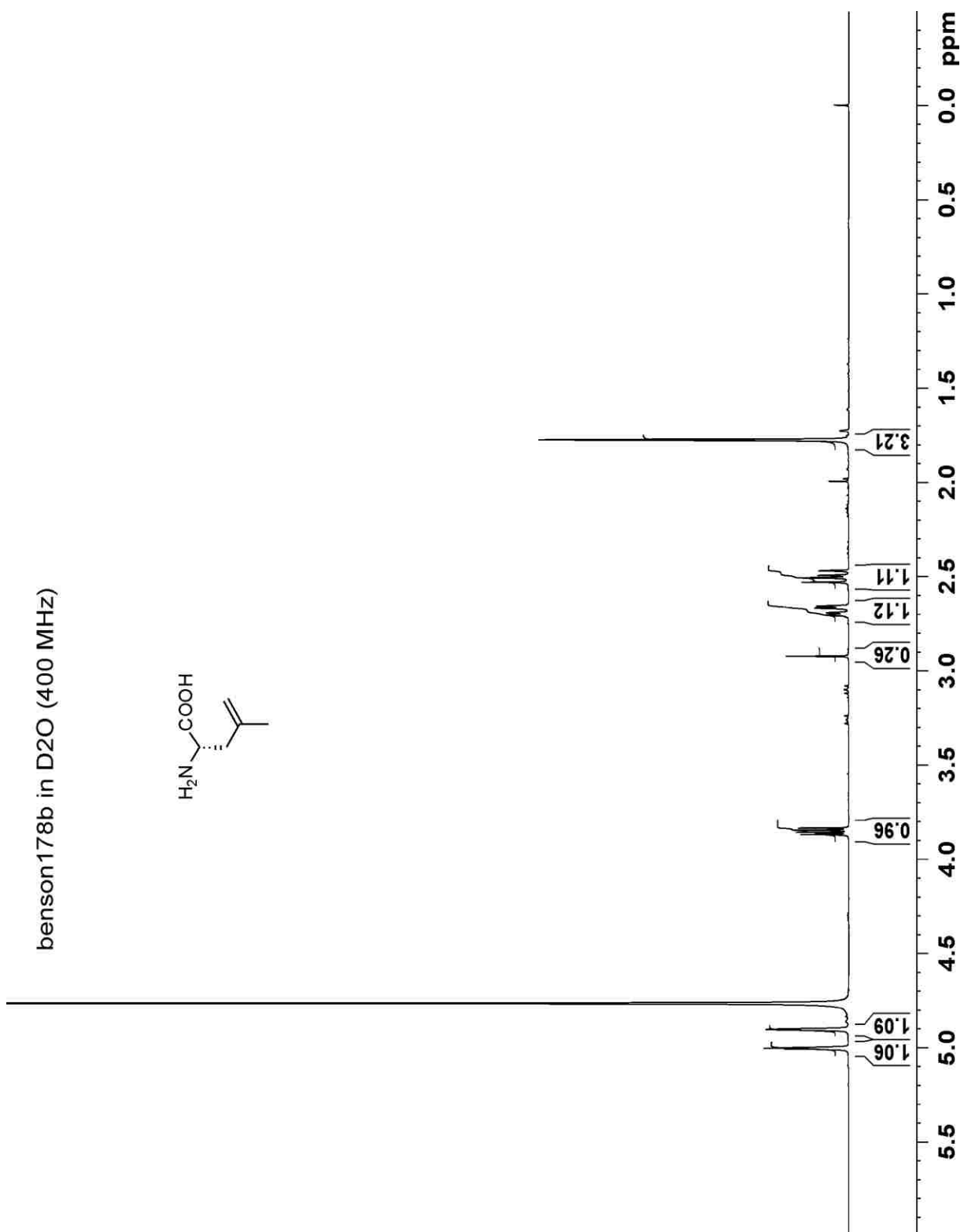
Compound (±)-**86** – ^{13}C NMR in CD_3OD at 62.5 MHz



bej-1/101b

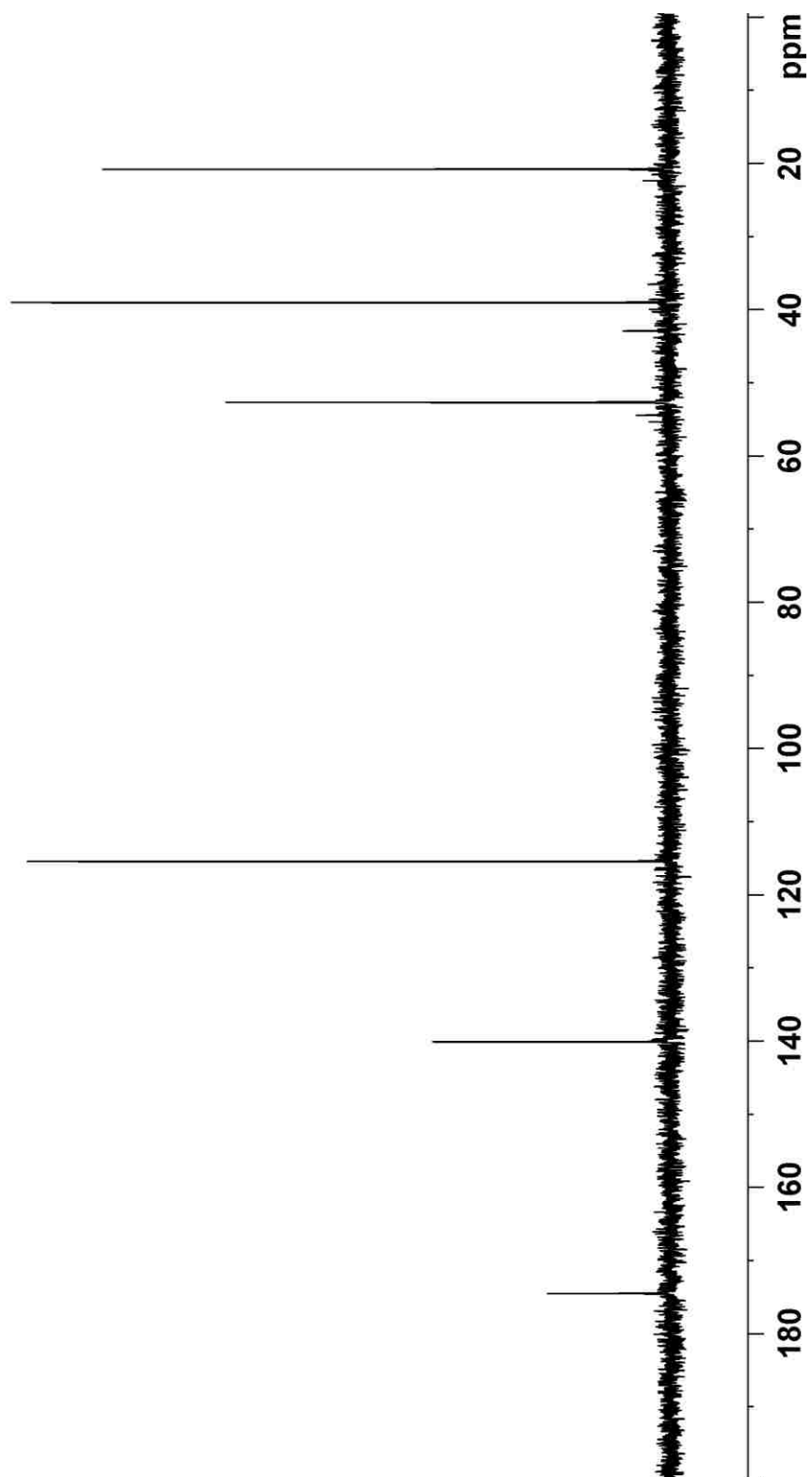
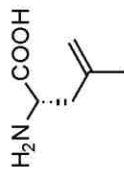


Compound (-)-**87** – ^1H NMR in D_2O at 400 MHz

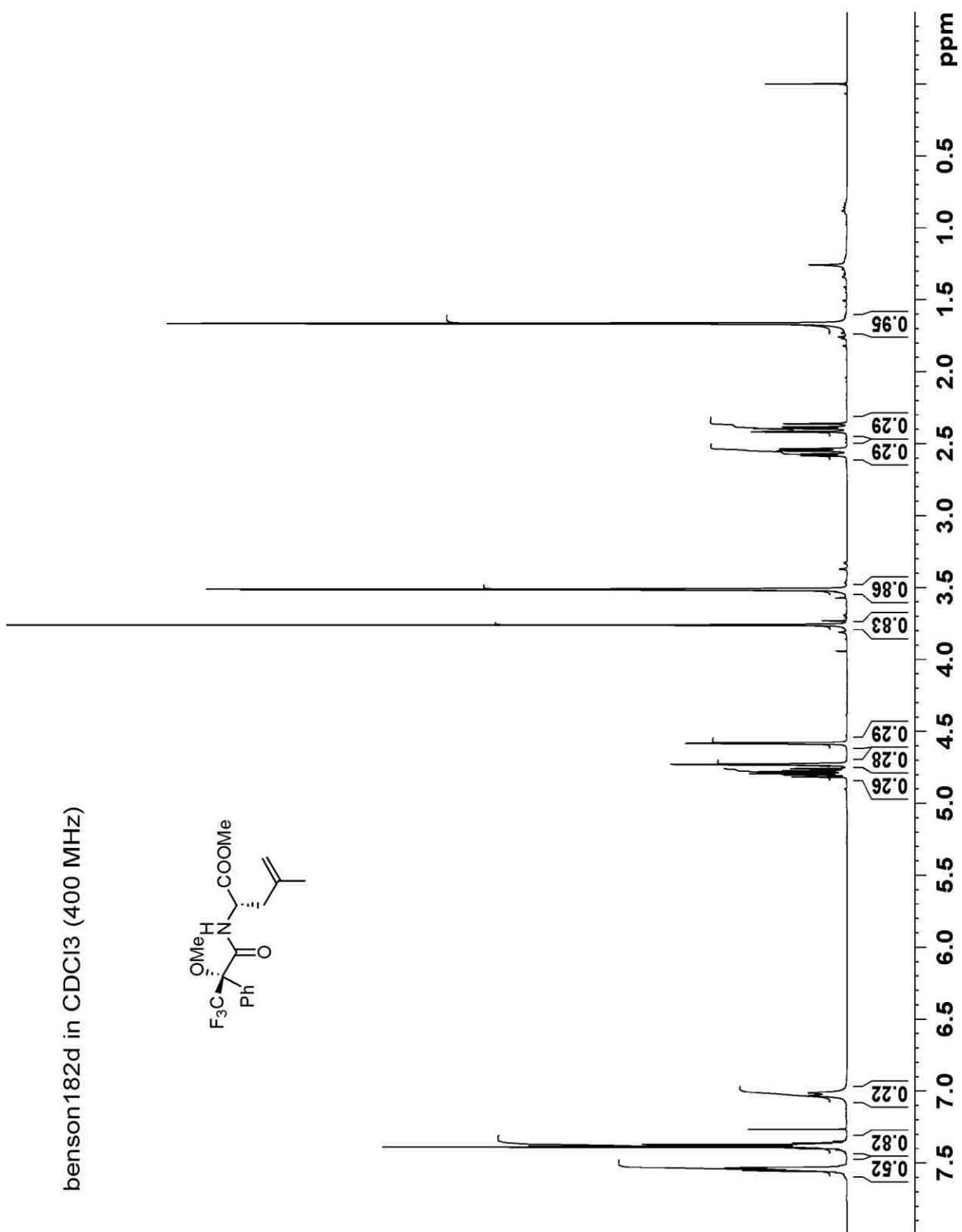


Compound (-)-**87** – ^{13}C NMR in D_2O at 100 MHz

benson178b in D2O (100 MHz)

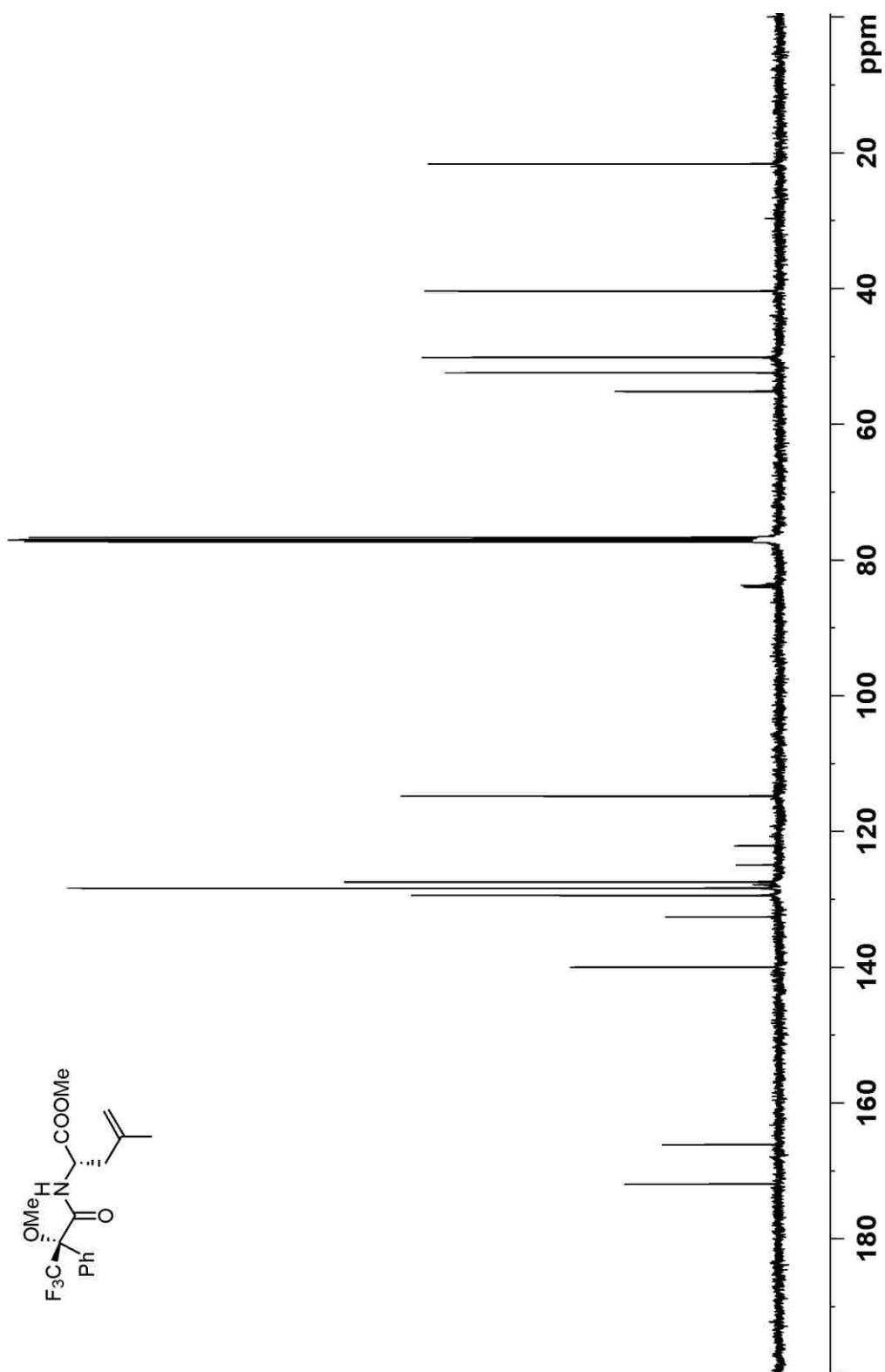


Mosher amide **88a** – ^1H NMR in CDCl_3 at 400 MHz



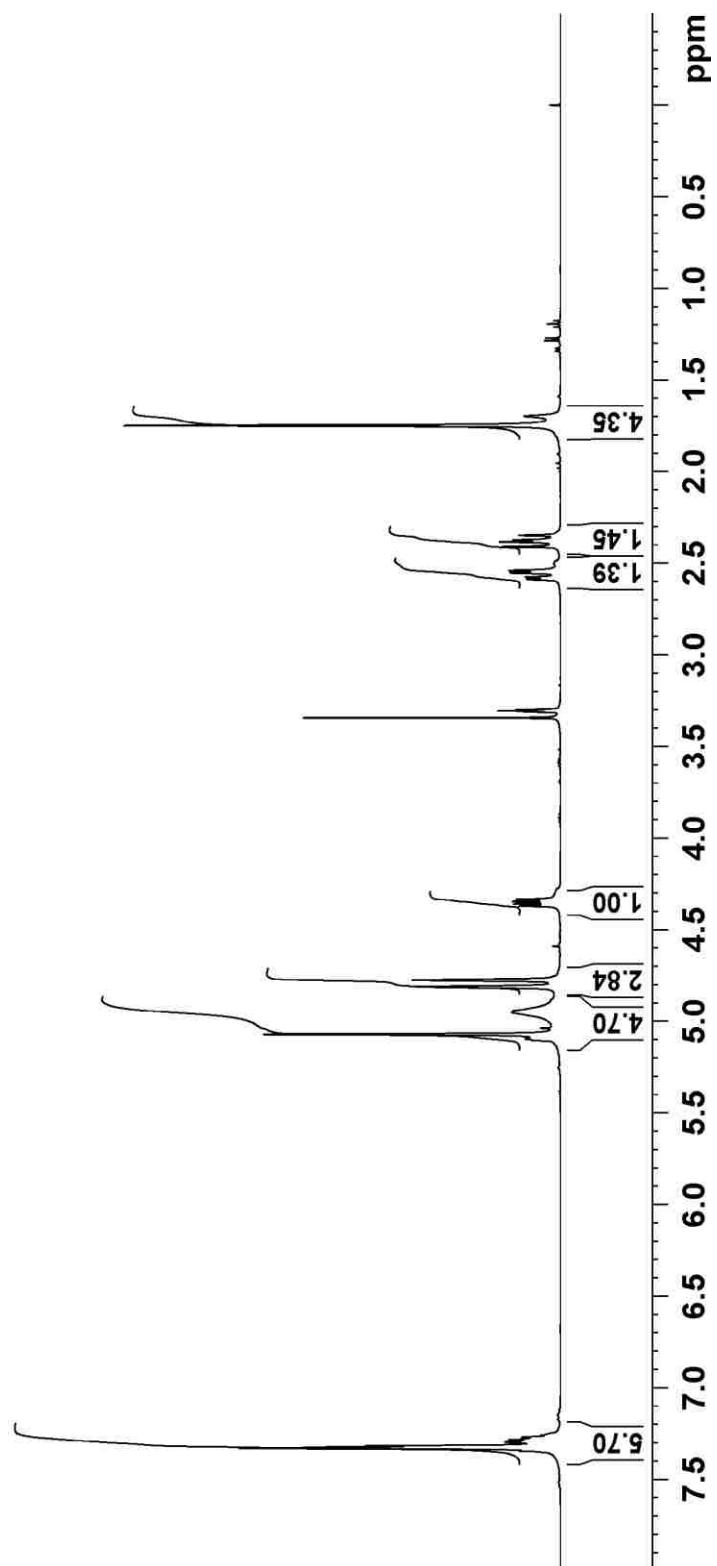
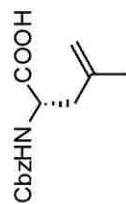
Mosher Amide **88a** – ^{13}C NMR in CDCl_3 at 100 MHz

benson182d in CDCl_3 (100 MHz)



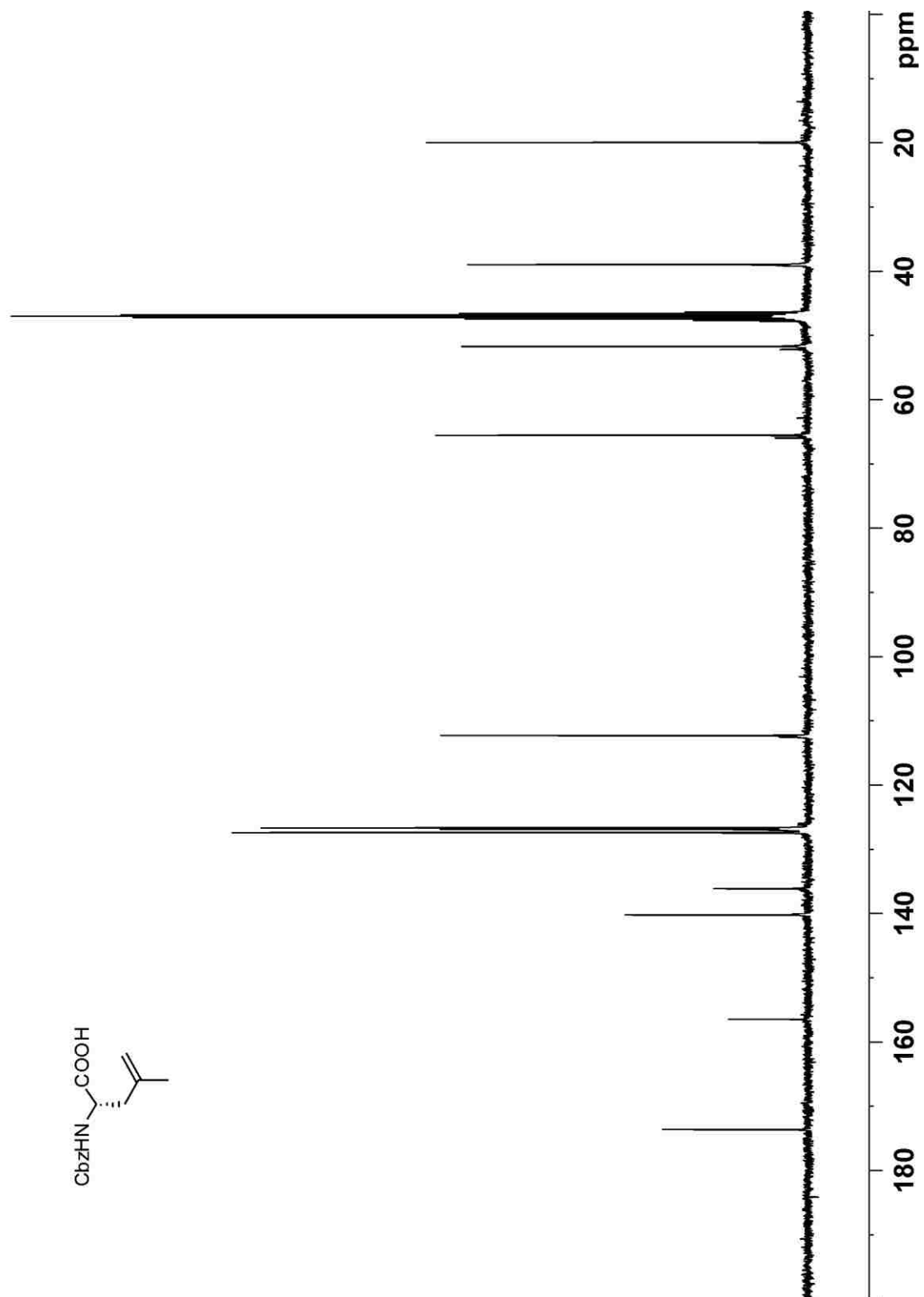
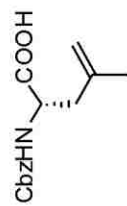
Compound **110** – ^1H NMR in CD_3OD at 400 MHz

benzon179d in CD_3OD (400 MHz)

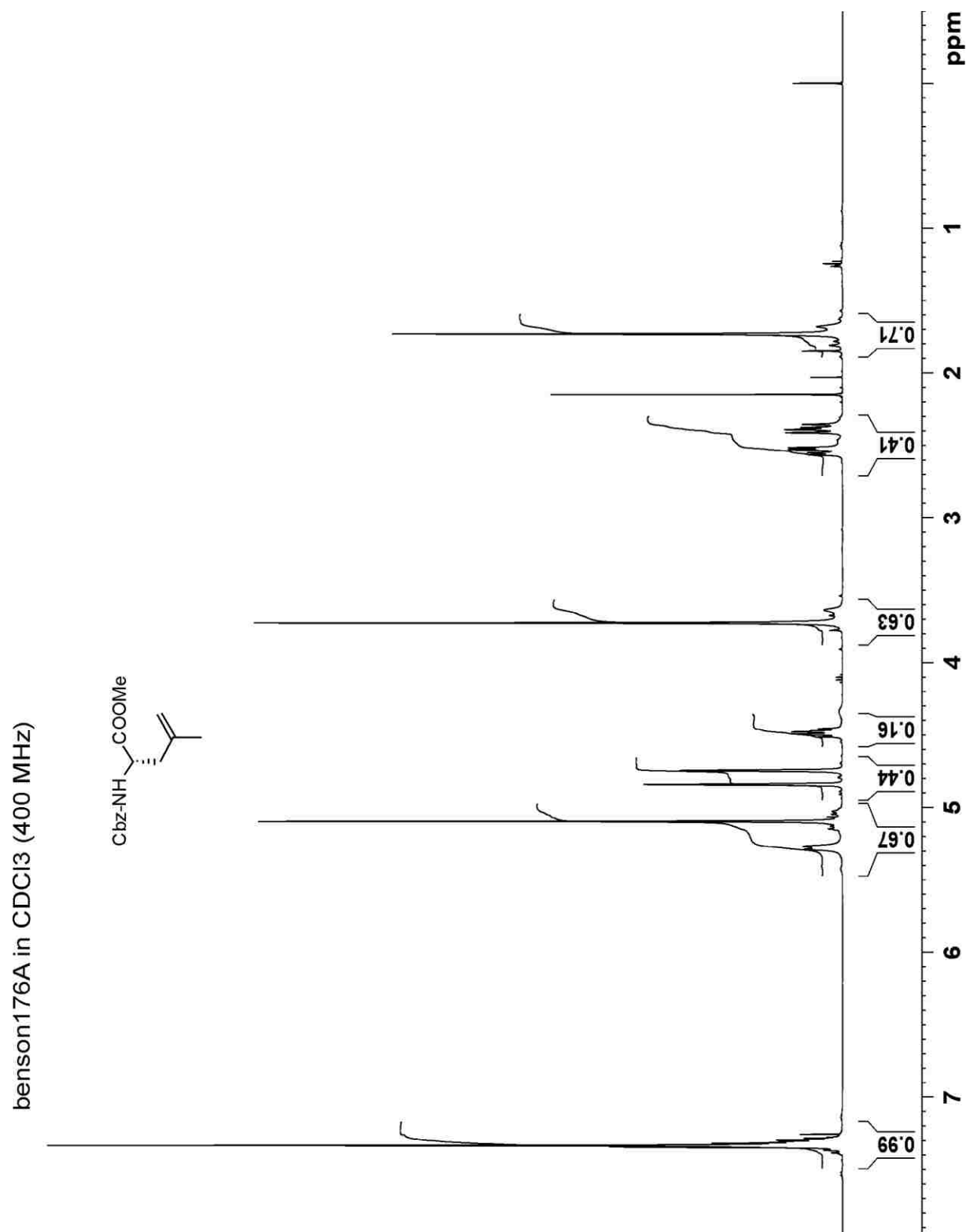


Compound **110** – ^{13}C NMR in CD_3OD at 100 MHz

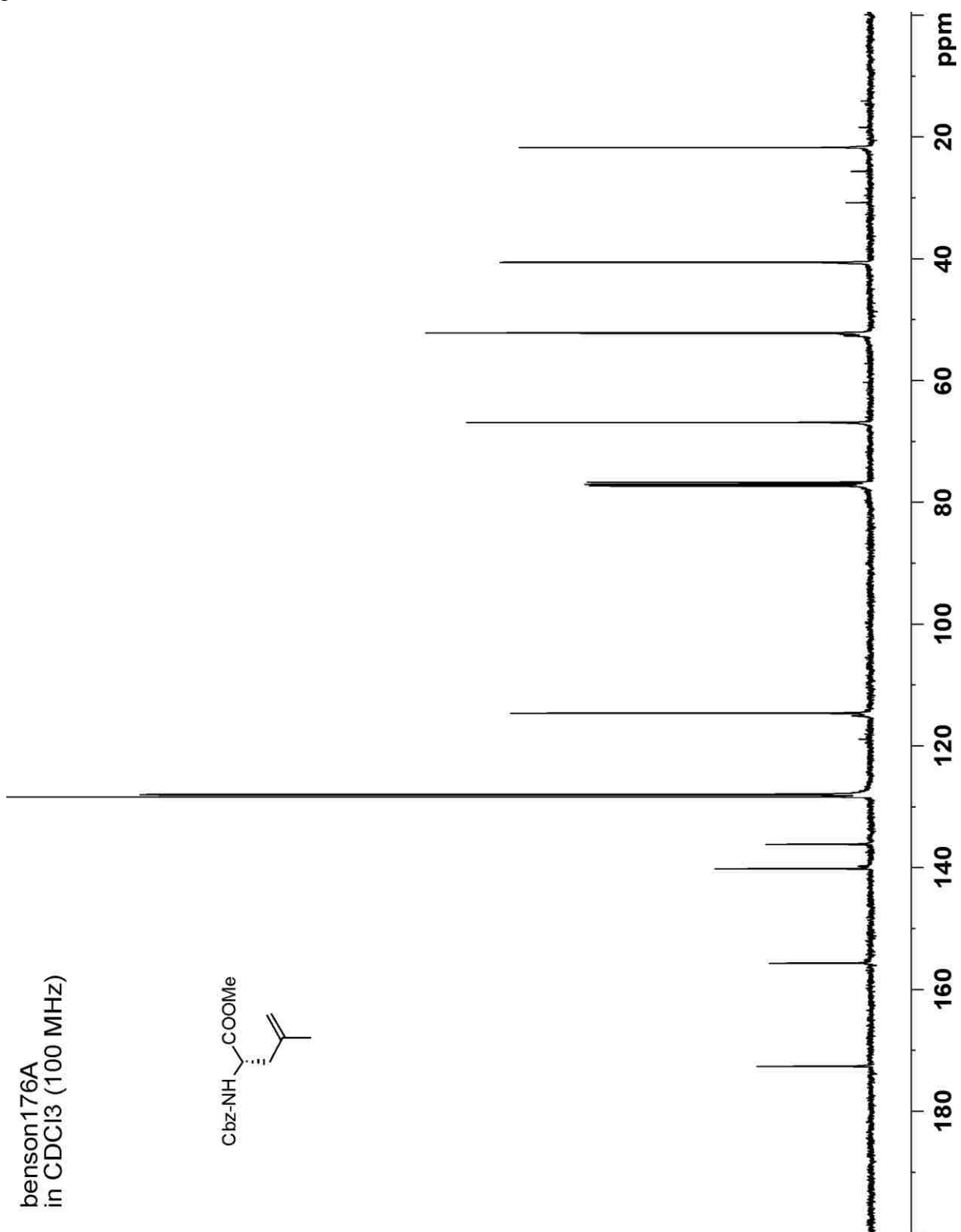
benson179d in CD_3OD (100 MHz)



Compound **90** – ^1H NMR in CDCl_3 at 400 MHz

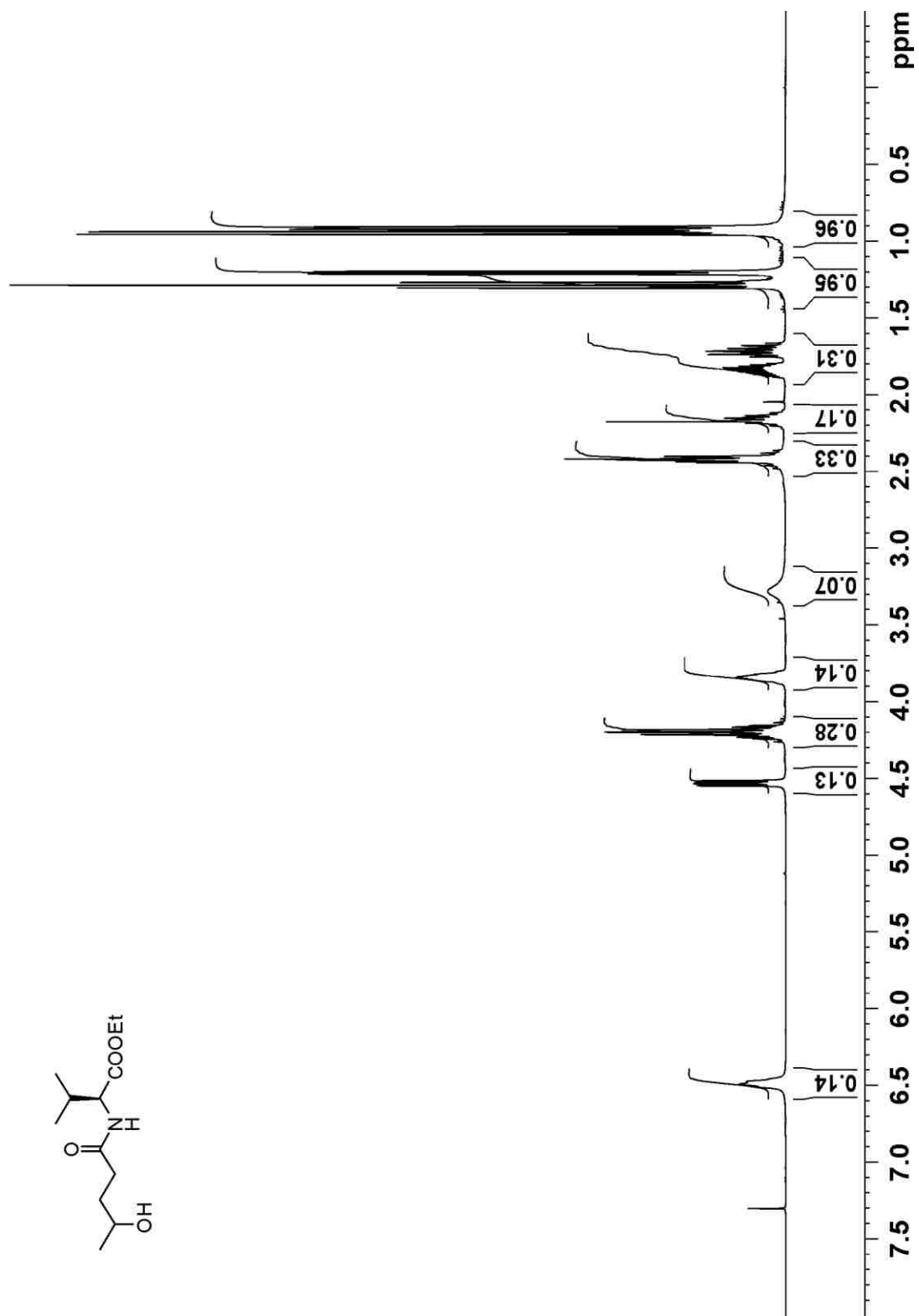


Compound **90** – ^{13}C NMR in CDCl_3 at 100 MHz



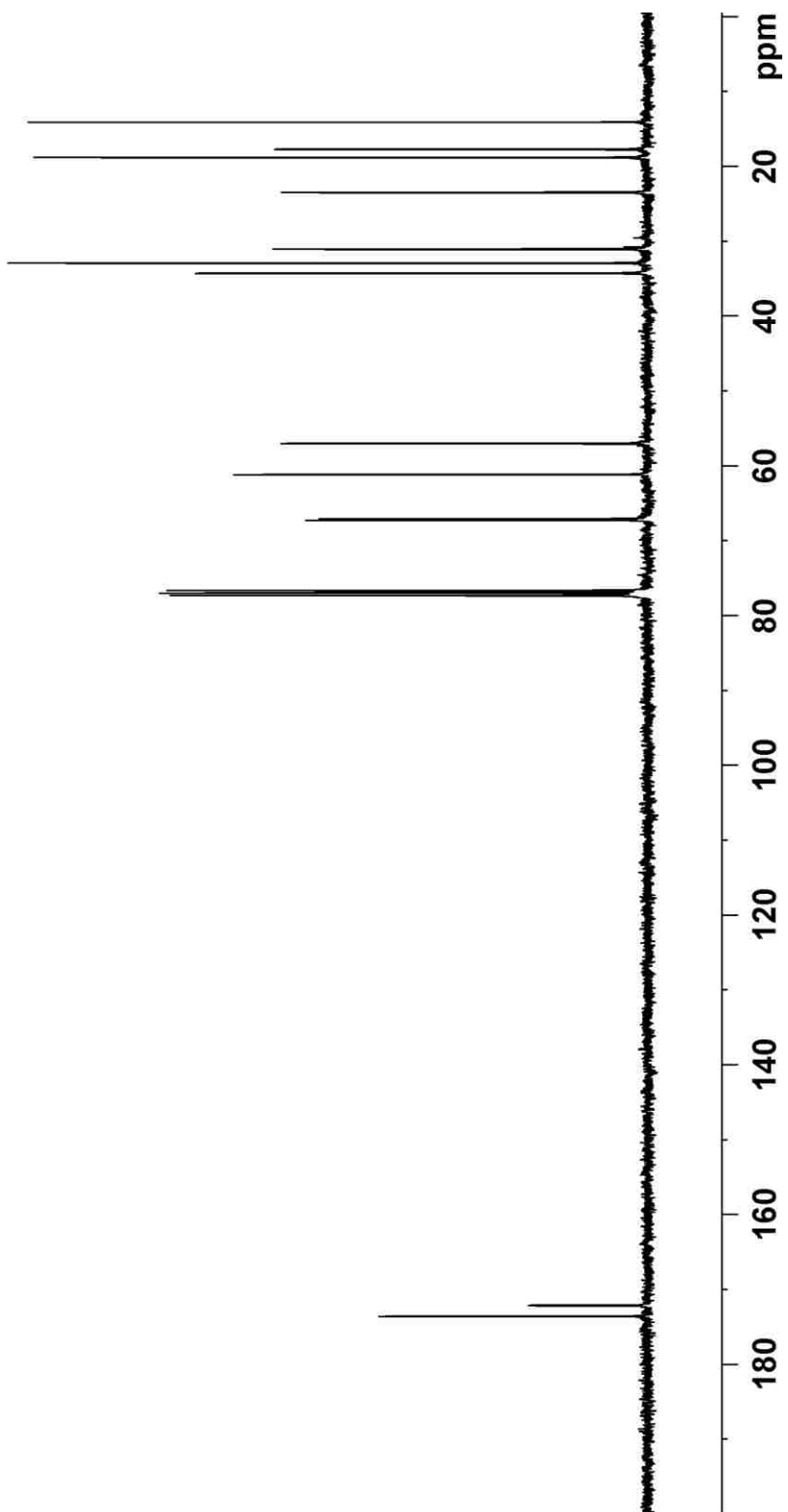
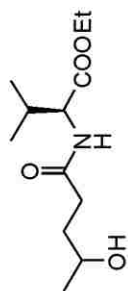
Compound **105** – ^1H NMR in CDCl_3 at 400 MHz

benson107a2 in CDCl_3 (400 MHz)



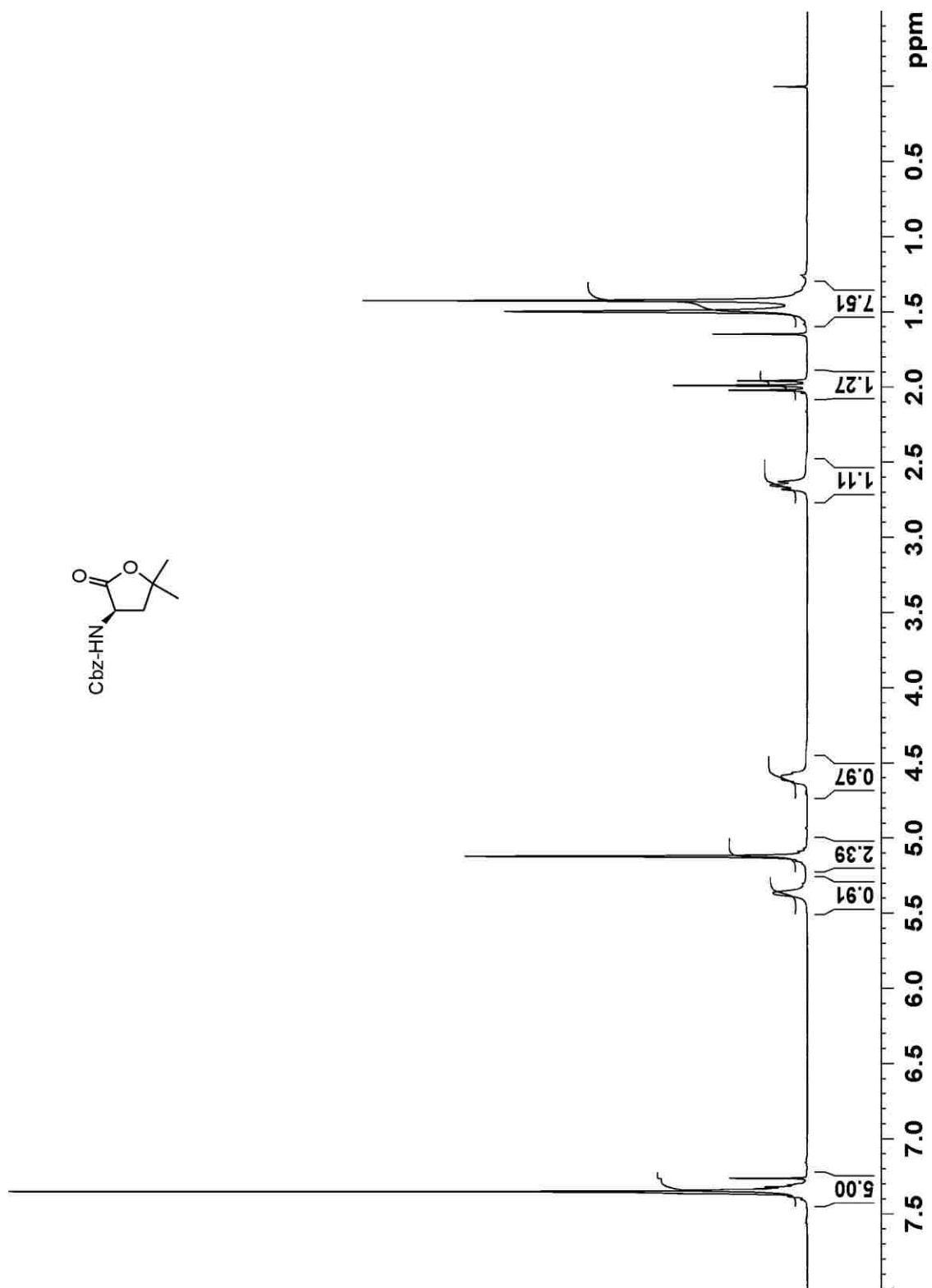
Compound **105** – ^{13}C NMR in CDCl_3 at 100 MHz

benson1072 in CDCl_3 (100 MHz)

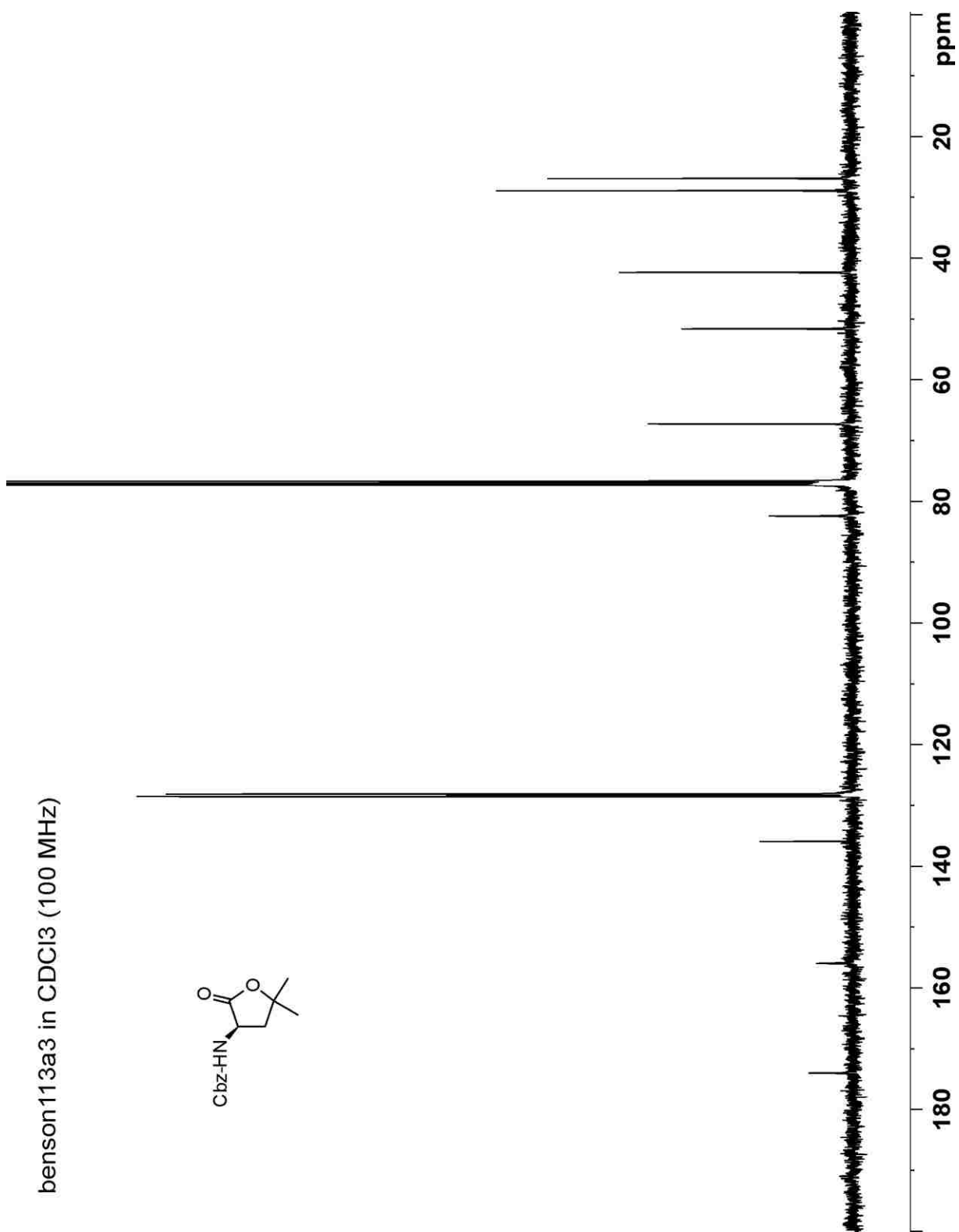


Compound (+)-**91** – ^1H NMR in CDCl_3 at 400 MHz

benson113a3 in CDCl_3 (400 MHz)

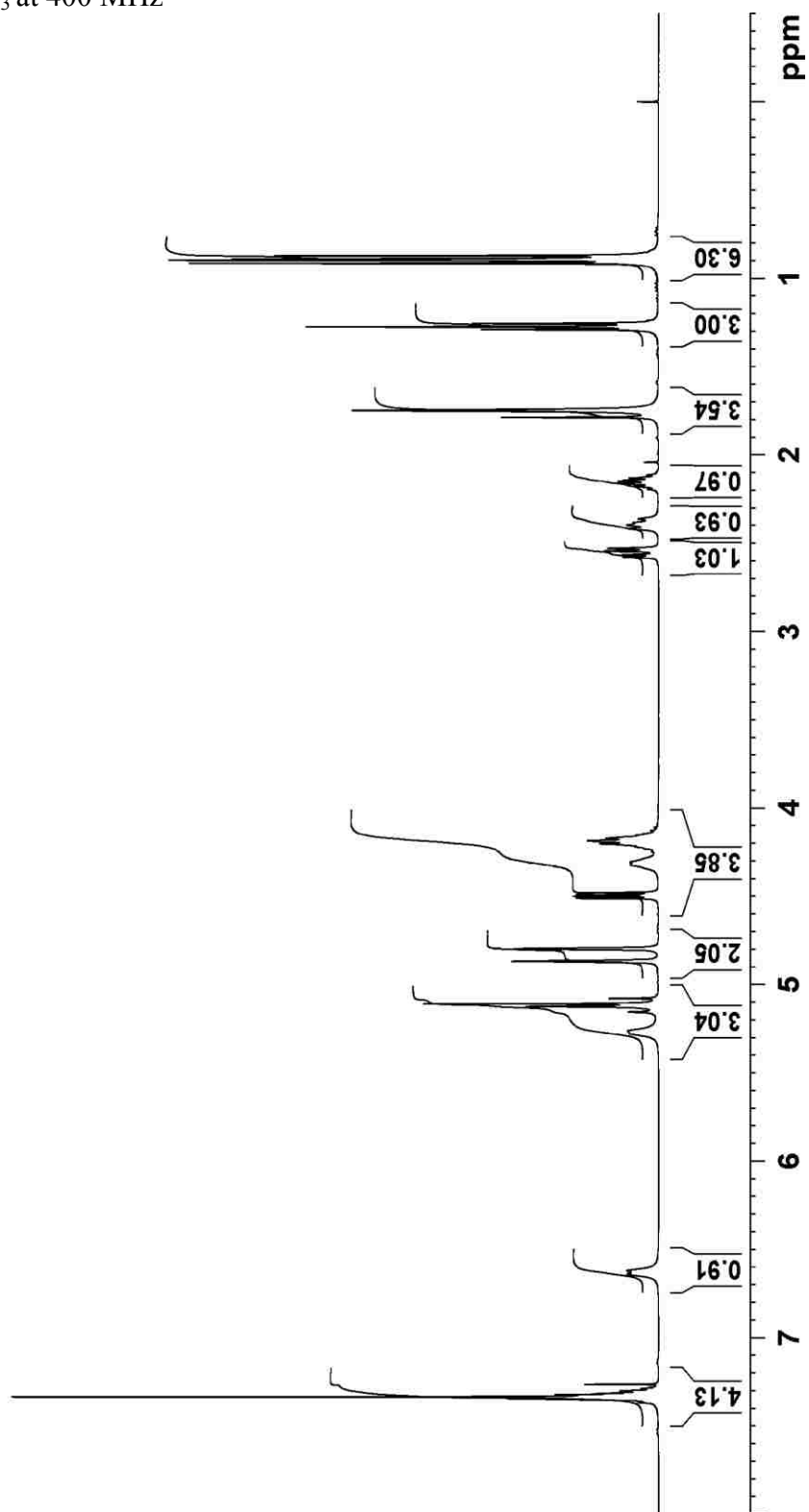
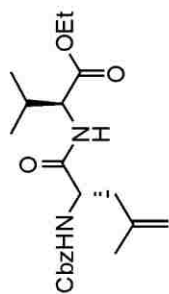


Compound (+)-**91** – ^{13}C NMR in CDCl_3 at 100 MHz



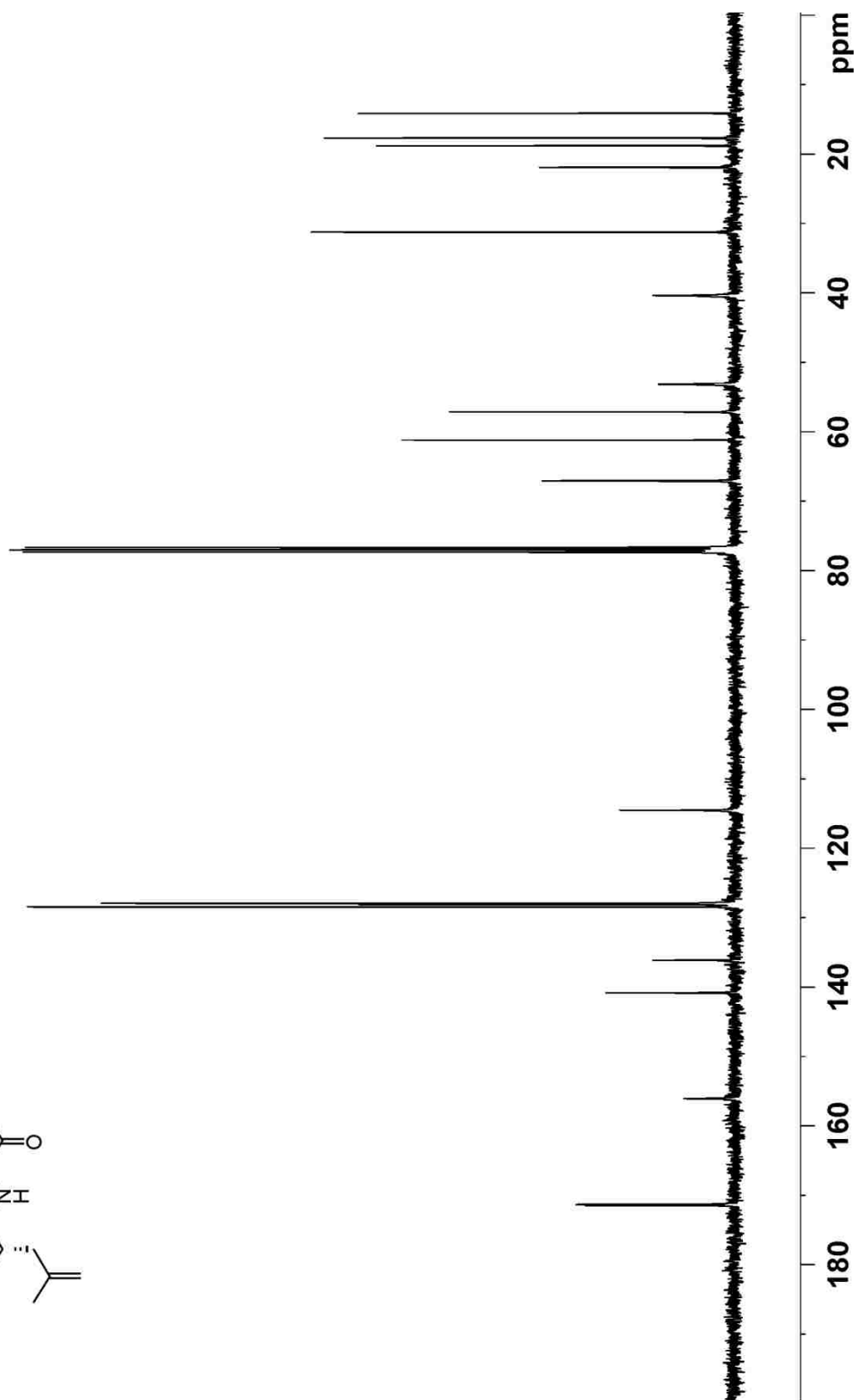
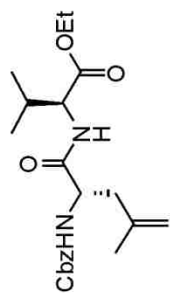
Dipeptide **111** – ^1H NMR in CDCl_3 at 400 MHz

benson171e in CDCl_3 (400MHz)



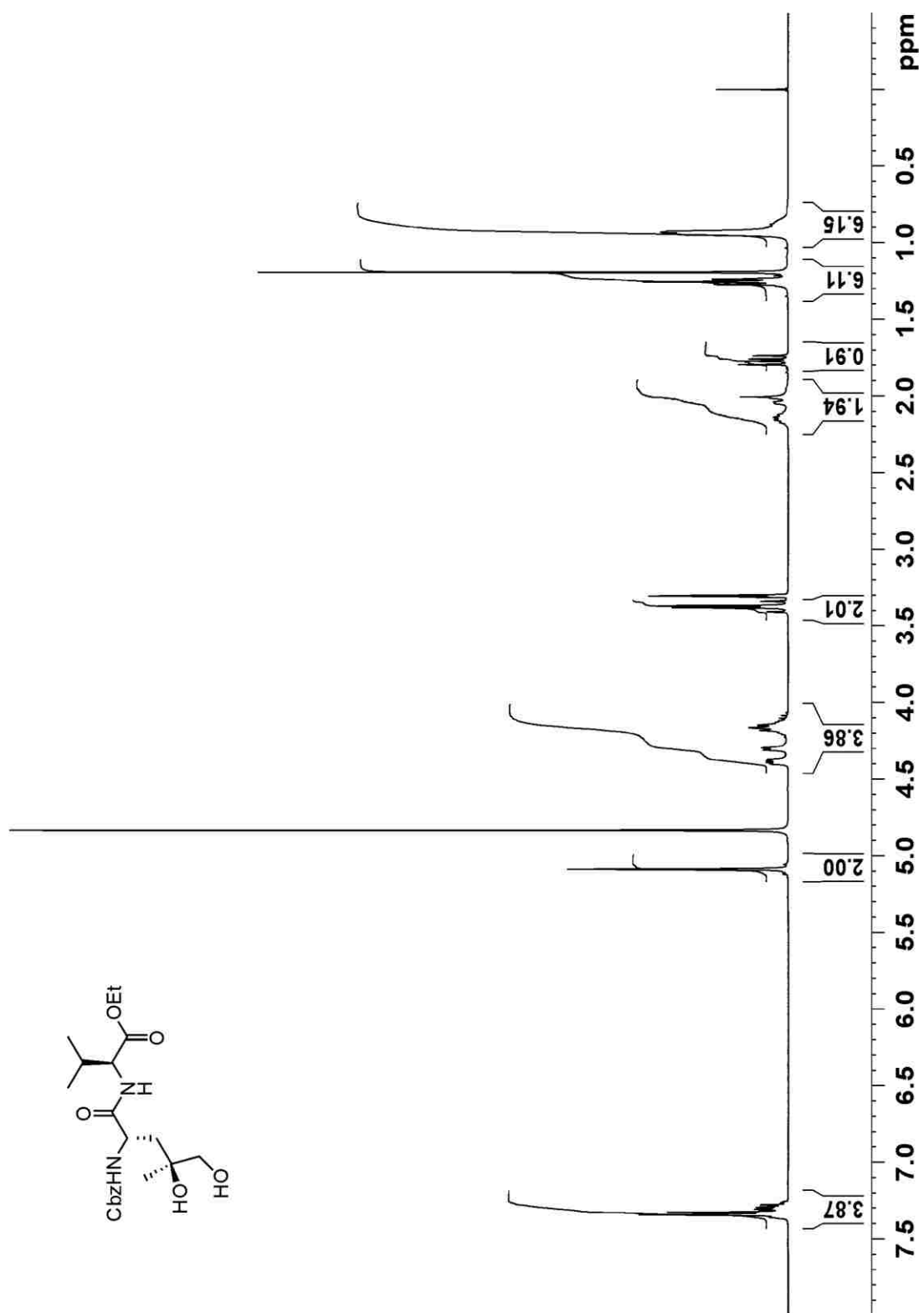
Dipeptide **111** – ^{13}C NMR in CDCl_3 at 100 MHz

benson168e in CDCl_3 (400 MHz)

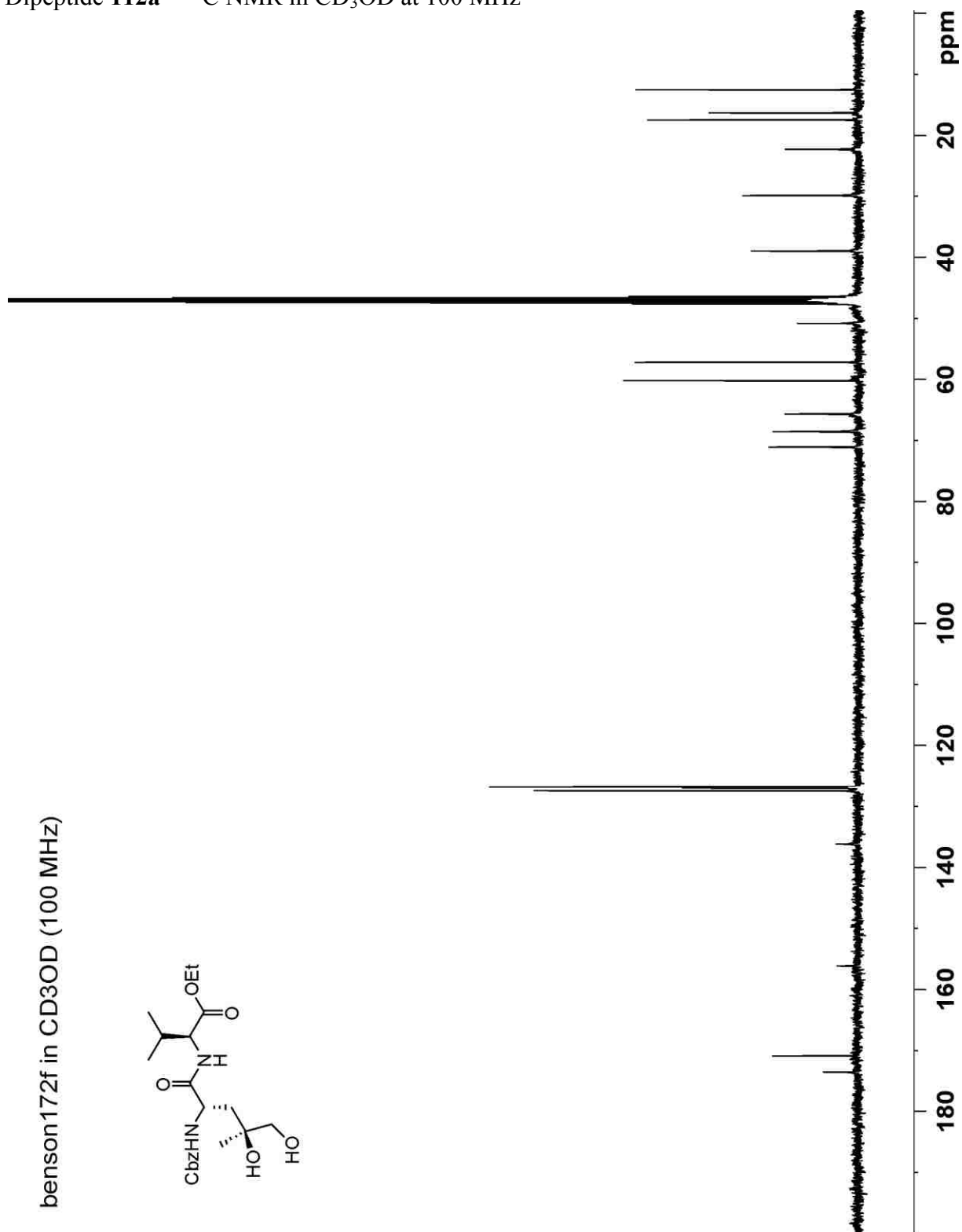


Compound **112a** – ^1H NMR in CD_3OD at 400 MHz

benson172f in CD_3OD (400 MHz)

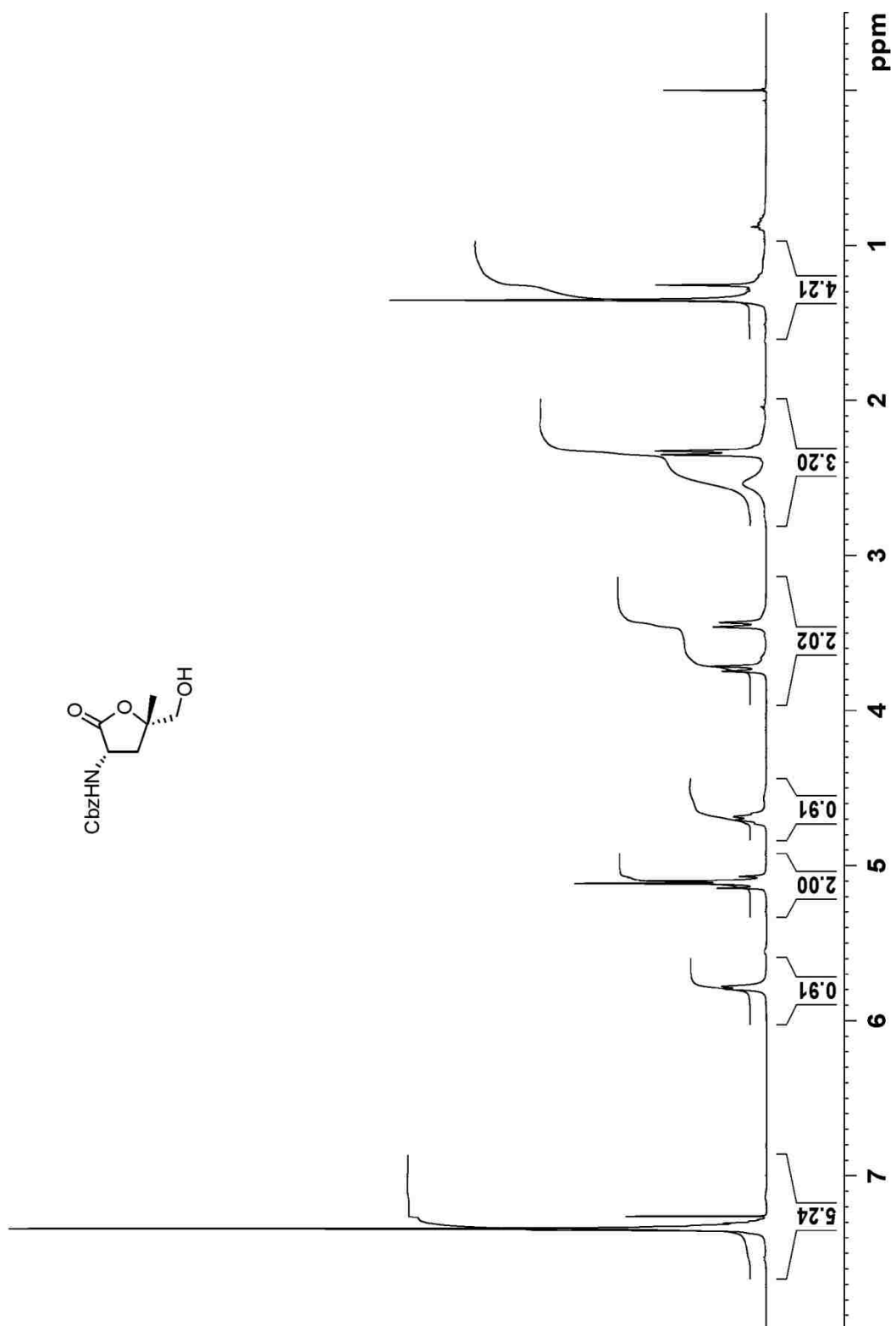


Dipeptide **112a** – ^{13}C NMR in CD_3OD at 100 MHz



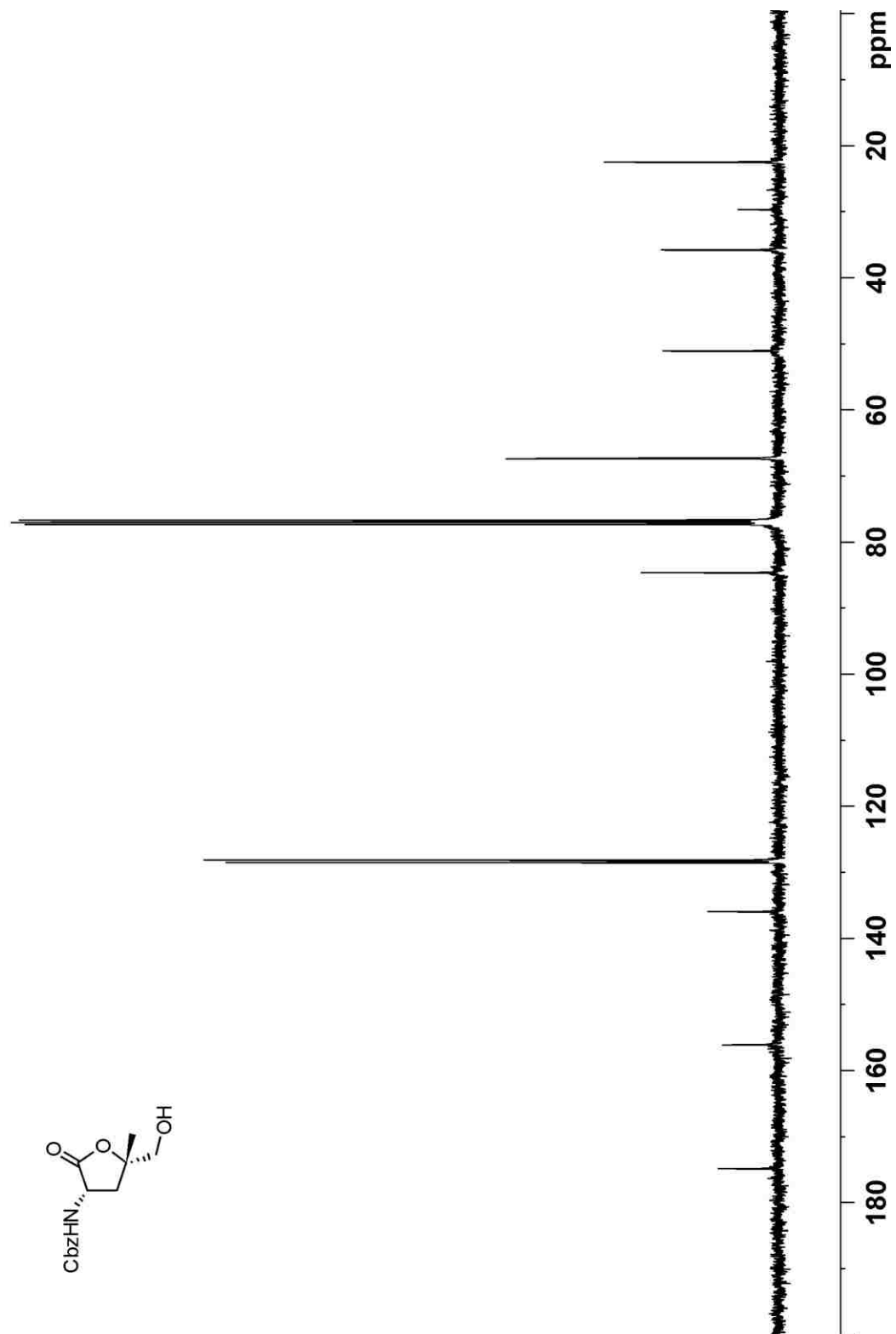
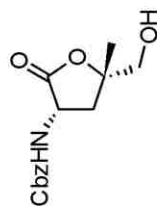
Compound **92b** – ^1H NMR in CDCl_3 at 400 MHz

benson187g1 in CDCl_3 (400 MHz)

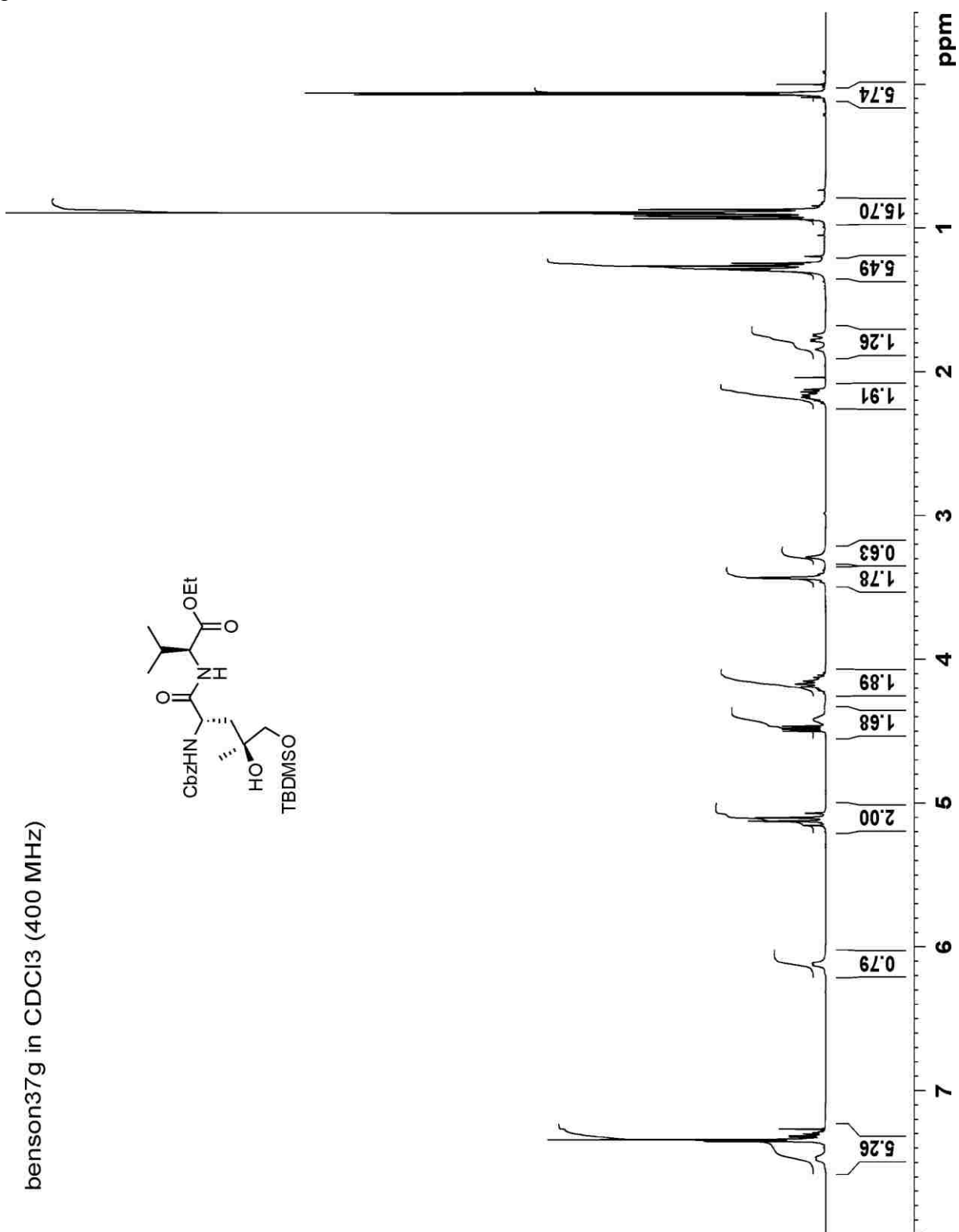


Compound **92b** – ^{13}C NMR in CDCl_3 at 100 MHz

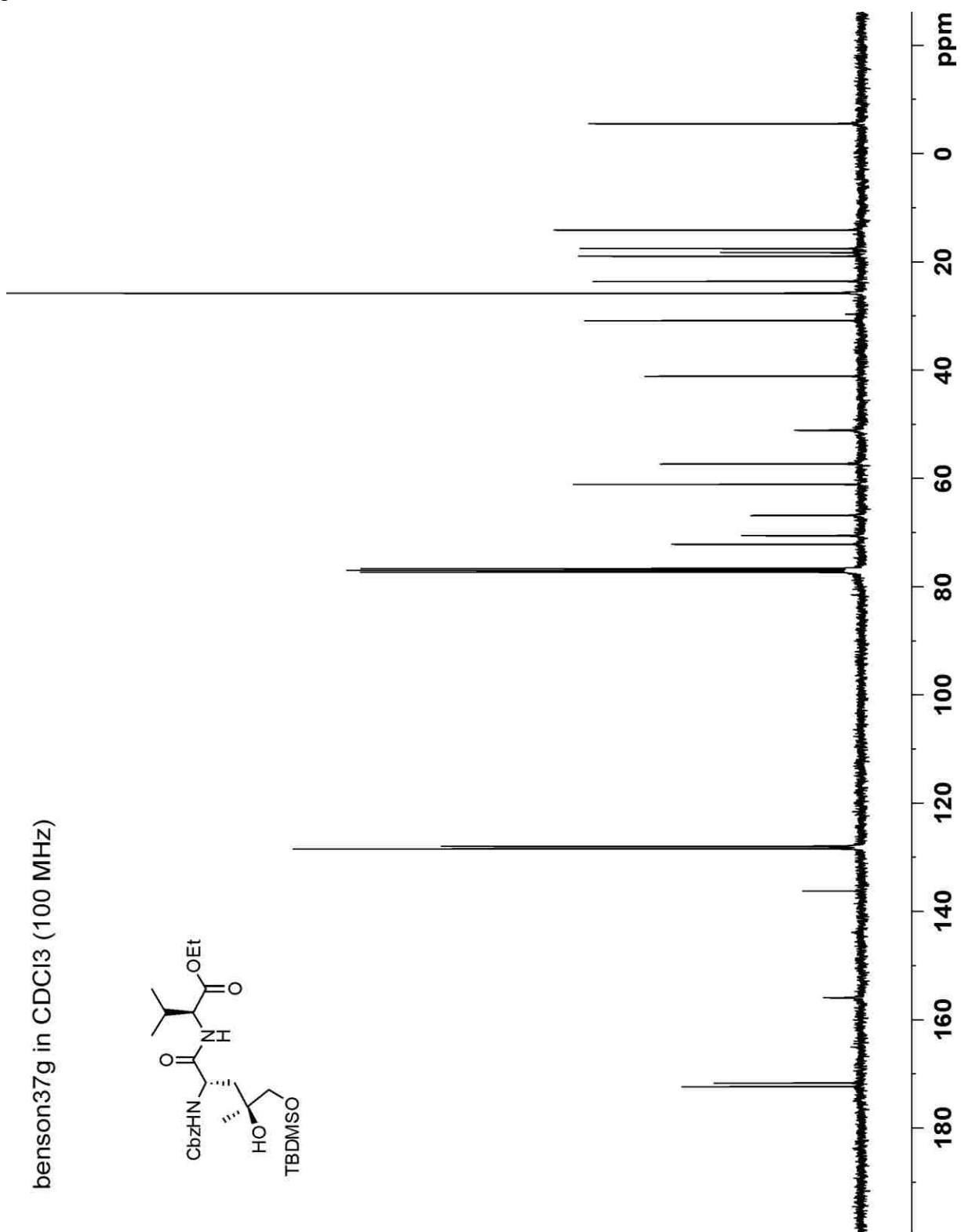
benson187g1 in CDCl_3 (100 MHz)



Compound **114** – ^1H NMR in CDCl_3 at 400 MHz



Compound **114** – ^{13}C NMR in CDCl_3 at 100 MHz

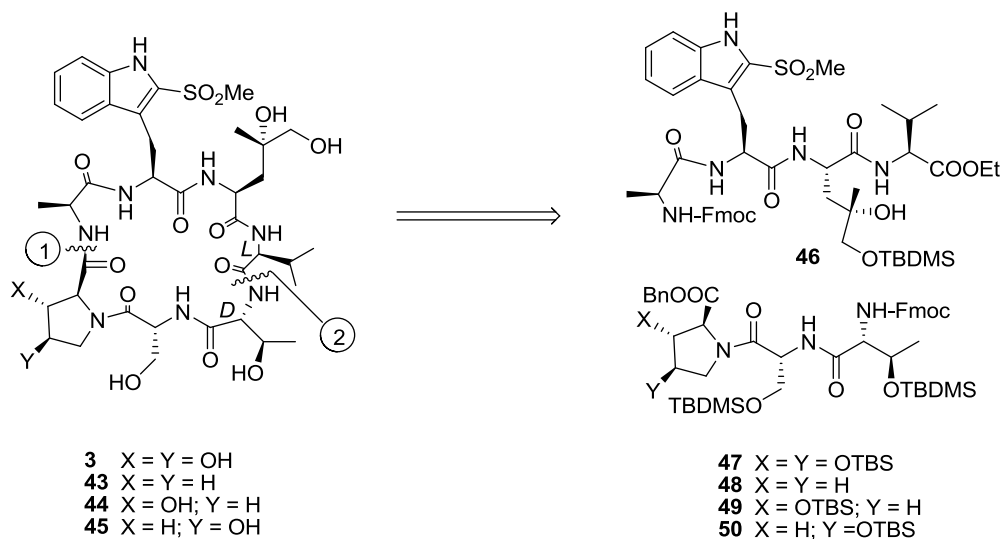


CHAPTER 3: THE PEPTIDE FRAGMENTS

3.1 OVERVIEW

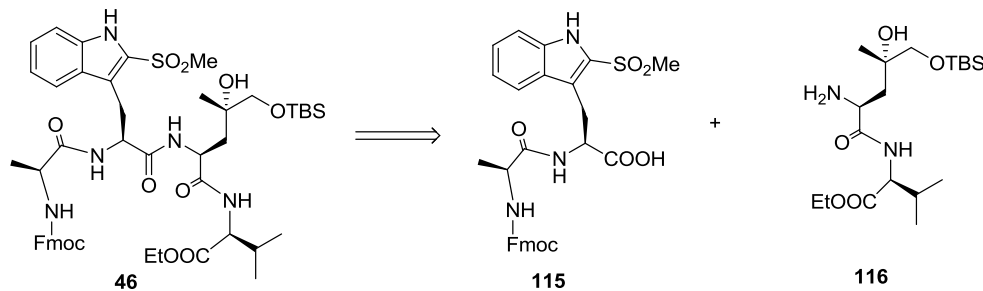
Revisiting our retrosynthetic analysis from (Scheme 3.1) Chapter 2, we recall that our approach to alloviroidin and the three analogs involves coupling of the tripeptide acids derived from **47-50** and the amino component derived from tetrapeptide **46**. According to this strategy, the tetrapeptide fragment **46** is common to the natural product and the analogs. However, examination of the tripeptide fragments **47-50** reveals that the natural product and the three analogs are distinguished by the degree and regiochemistry of proline hydroxylation.

Scheme 3.1. Retrosynthetic analysis of alloviroidin and analogs.



Prerequisites to the synthesis of the tetrapeptide fragment **46** were the efficient preparation of the (2*S*,4*R*)-4,5-dihydroxyleucine³⁵ (Chapter 2) and 2-methylsulfonyl-tryptophan (*vide infra*) residues. We designed a strategy that incorporated each of these residues into a dipeptide, followed by a [2 + 2] fragment condensation to deliver the tetrapeptide (Scheme 3.2).

Scheme 3.2. Retrosynthetic analysis of the tetrapeptide.

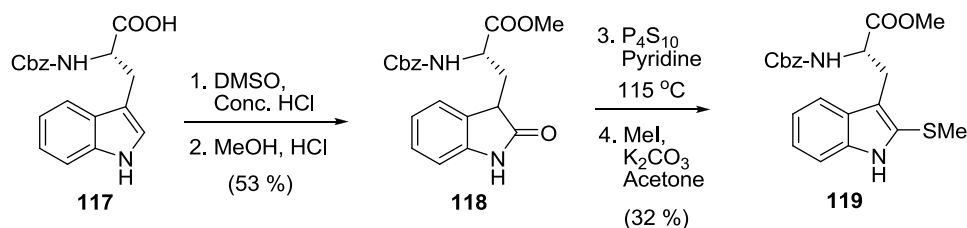


The next section describes the preparation of the 2-methylsulfonyl-tryptophan residue and formation of the Fmoc-Ala-[2-MeSO₂-Trp]-OH dipeptide fragment. We shall also describe the assembly of the tetrapeptide fragment.

3.2 2-METHYLSULFONYL-TRYPTOPHAN AND THE TETRAPEPTIDE FRAGMENT

During their total synthesis of amauromine, Takase *et al.* described the synthesis of the 2-thiomethyl derivative of Cbz-*L*-Trp-OMe in four steps with an overall yield of 17 % (Scheme 3.3).^{84, 85} The 2-thiomethyl functional group was introduced by heating compound **118** with phosphorus pentasulfide in pyridine at reflux to generate the corresponding 2-thione, which was then treated with methyl iodide to give the desired building block (Scheme 3.3).

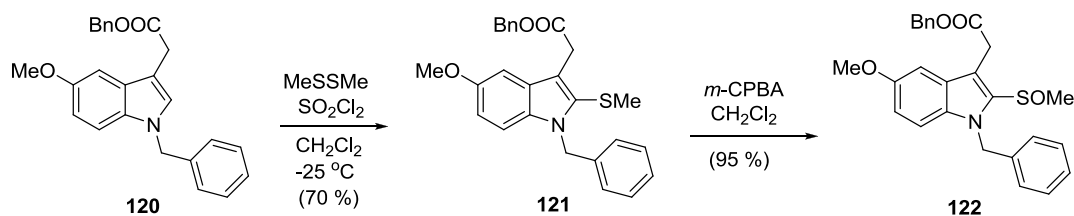
Scheme 3.3. Takase and co-workers synthesis of the 2-thiomethyl derivative of Cbz-*L*-Trp-OMe.⁸⁵



In 1996, Dillard and coworkers described the synthesis and structure-activity relationships of indole-3-acetamides and derivatives as potential therapeutic inhibitors of human nonpancreatic secretory phospholipase A₂, an enzyme that is involved in the biosynthesis of eicosanoid products. In one of the

lead compounds, the methylsulfenyl group was introduced onto the indole ring according to Scheme 3.4.⁸⁶

Scheme 3.4. Dillard and co-workers' synthesis of indole-3-acetamides.

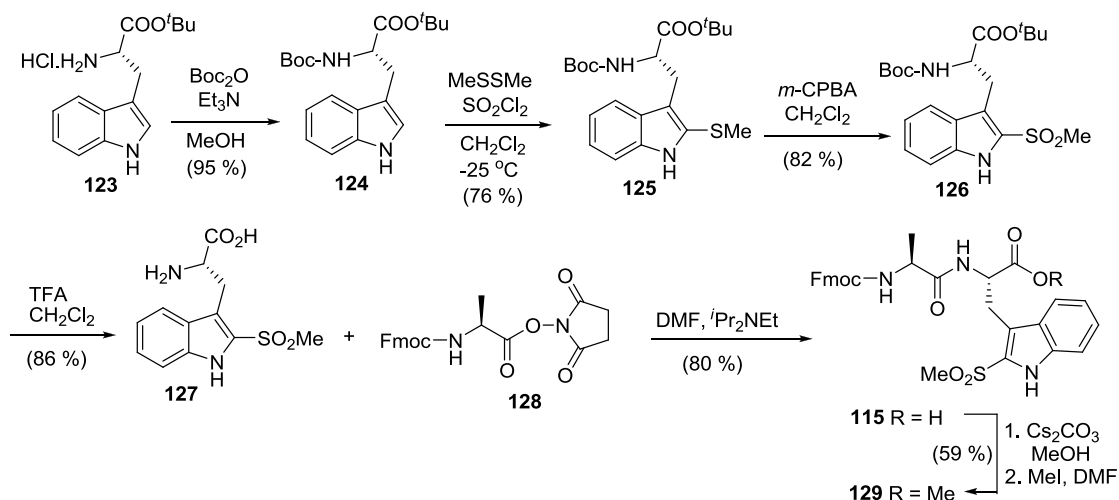


Our approach to 2-methylsulfonyl-tryptophan involved four steps from commercially available *L*-tryptophan *tert*-butyl ester **123** (Scheme 3.5) utilizing the same approach as Dillard. The amino group was protected as its Boc (*tert*-butoxycarbonyl) derivative to give compound **124**,⁸⁷ anticipating simultaneous acid cleavage of the two protecting groups at a later stage. We followed the above protocol of Dillard *et al.* to introduce the thiomethyl group; this involved *in situ* generation of methylsulfenyl chloride from sulfonyl chloride and dimethyl disulfide. Compound **125** was found to be unstable, hence all the data reported was collected on the same day it was prepared. The methylthioether group of **125** was oxidized to afford the corresponding sulfone **126** with two equivalents of *m*-chloroperbenzoic acid in dichloromethane.⁸⁶ Analysis of the oxidation reaction by thin layer chromatography indicated the conversion of the starting material into a sulfoxide intermediate prior to sulfone formation. Mass spectrometry and NMR analysis provided evidence that the desired product had been formed. Specifically, an examination of the ¹H NMR spectra of compounds **125** and **126** revealed a singlet at δ 2.34 (for **125**) and 3.24 (for **126**), integrating for three protons, of the thiomethyl and methanesulfonyl groups respectively. The observed shift, downfield, for the methanesulfonate derivative is influenced by the two electron withdrawing oxygen atoms introduced on sulfur.

Removal of the protecting groups was accomplished in good yield by treatment with TFA/CH₂Cl₂, in the presence of thioanisole as a carbocation scavenger, to give **127**. This free Trp

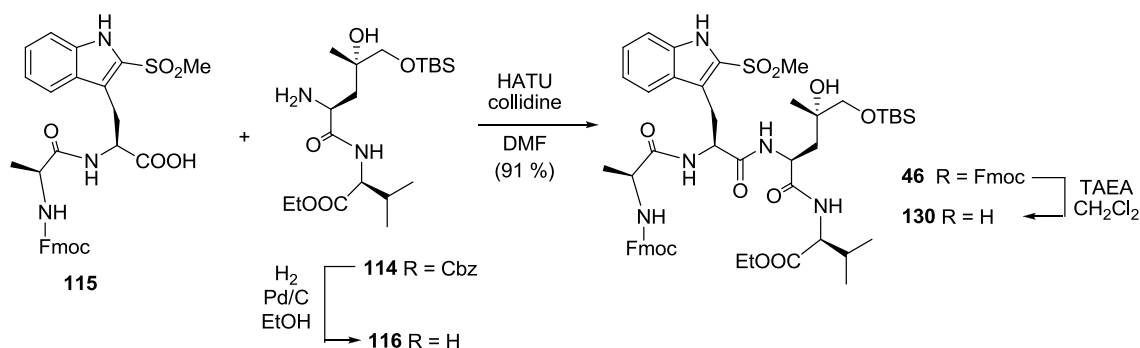
derivative was then coupled with the preformed *N*-hydroxysuccinimide ester **128** (from commercially available Fmoc-Ala-OH via the traditional NHS/DCC protocol) to give dipeptide acid **115**, which was routinely used in the next step without further purification. A portion of **115** was converted into the corresponding methyl ester **129** to allow for purification by column chromatography and characterization.

Scheme 3.5. Preparation of the 2-methylsulfonyl-tryptophan.



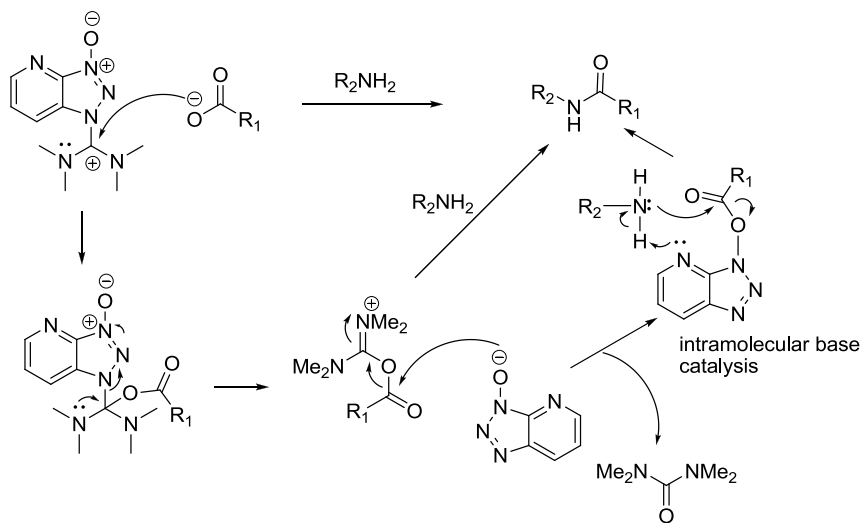
Having secured the two dipeptide fragments **115** (Scheme 3.5) and **116** (Chapter 2), we next turned to the preparation of the tetrapeptide fragment **46** according to Scheme 3.6.

Scheme 3.6. Preparation of the tetrapeptide fragment.



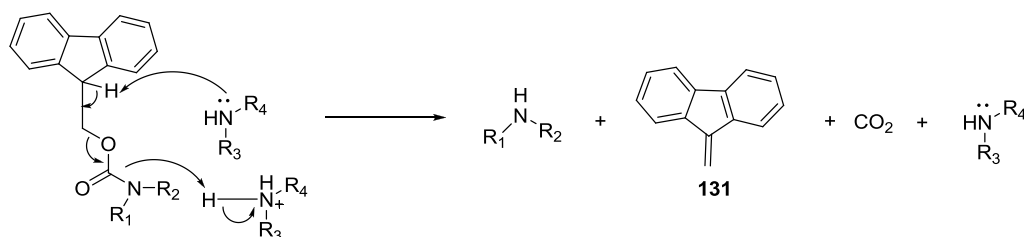
This effort began with the hydrogenolysis of the Cbz group from compound **114** to furnish the free dipeptide amine **116** that was coupled to dipeptide acid **115** (from Scheme 3.5) to generate tetrapeptide **46**. This [2 + 2] coupling was effected by HATU⁸⁸ in the presence of the weak base 2,4,6-collidine, chosen to limit the potential problem of racemization⁸⁹ of the Trp residue. The HATU reagent is the most reactive guanidium peptide coupling reagent and has proven effective for difficult reactions. With this reagent, acid activation proceeds according to Scheme 3.7. The azabenzotriazole ester intermediate can facilitate coupling via intramolecular base catalysis, and is considered responsible for the high reactivity and chemical yields associated with HATU couplings.⁸⁸

Scheme 3.7. Acid activation by HATU.⁸⁸



The fluorenylmethoxycarbonyl (Fmoc) group is widely used for temporary amino protection in peptide synthesis.⁹⁰ This protecting group is stable to acids but readily cleaved with mild bases via β -elimination of dibenzofulvene (Scheme 3.8).⁹¹⁻⁹⁵ For the removal of the Fmoc group from the *N*-terminus of **46** (Scheme 3.6), we explored the use of diethylamine (DEA), piperidine and *tris*(2-aminoethyl)amine (TAEA).

Scheme 3.8. Cleavage of the Fmoc group via β -elimination.



The major drawback associated with the Fmoc protecting group during solution phase synthesis is the removal of the byproduct arising from addition of the secondary amine to dibenzofulvene (Fig. 3.1). Removal of this byproduct requires either purification of the free amino peptide by column chromatography or aqueous workup, sometimes characterized by emulsions or large volumes of solvents during extraction. In the case of TAEA, the excess reagent and dibenzofulvene adduct are removed by extraction into a phosphate buffer solution of pH 5.5.⁹⁶ The low boiling point of diethylamine makes it a reagent of choice since it can be used in excess and removed by evaporation upon completion of the deprotection. Although this does not remove the adduct, this is often found not to adversely affect the subsequent coupling reaction. Piperidine is also an effective base for Fmoc cleavage, however, this reagent cannot be completely eliminated on a rotavap and therefore the excess amine and the dibenzofulvene adduct (**133**) can be removed by column chromatography. Failure to remove excess reagents used for Fmoc cleavage could lead to side reactions during coupling since they could serve as competing nucleophiles. In some cases, effective peptide couplings could be conducted in the presence of the dibenzofulvene adduct. In our studies, TAEA generated the free amine **130**, in excellent yields setting the stage for fragment condensation.

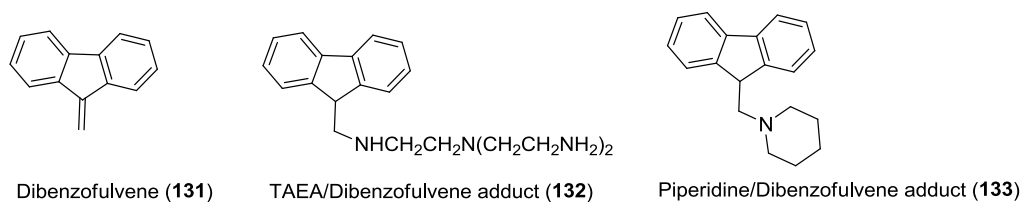


Figure 3.1. Byproducts arising from Fmoc cleavage.

3.3 THE PROLINE BUILDING BLOCKS AND THE TRIPEPTIDE FRAGMENTS

Proline plays an important role in protein folding by inducing a reversal in backbone conformation.⁹⁷ Our initial goal, when we started this work, was to synthesize a virotoxin. But in the course of these studies, the concept of accessing three analogs containing proline, *cis*-4-hydroxyproline and *trans*-3-hydroxyproline evolved (*vide infra*). Prior to investing our synthetically valuable 2,3-*trans*-3,4-*trans*-3,4-dihydroxyproline residue, we sought to investigate an efficient way of incorporating this building block into peptides. We decided to utilize *L*-proline and *cis*-4-hydroxyproline residues as model systems but later realized that these compounds could also serve as the basis for understanding the effect of proline hydroxylation on the conformation of the cyclic peptides. For complete comparison, we decided to incorporate a *trans*-3-hydroxyproline residue in our peptides, as this would explain the influence of the *trans* hydroxyl group at C β of the dihydroxyproline residue. A noteworthy feature of the syntheses is the use of the same protecting group strategy utilized during the preparation of 2,3-*trans*-3,4-*trans*-3,4-dihydroxyproline residue to the proline building blocks incorporated into the virotoxin analogs.

According to our retrosynthetic analysis given in Scheme 3.1, a series of four tripeptide fragments (Fig. 3.2), incorporating different proline residues was synthesized prior to heptapeptide formation (*vide infra*).

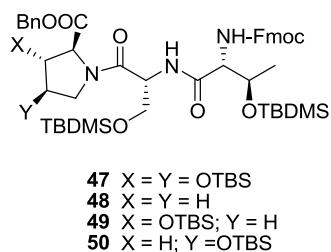
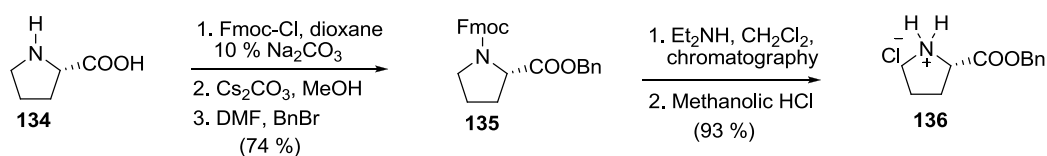


Figure 3.2. The series of four tripeptide fragments.

3.3.1 L-Proline Benzyl Ester Hydrochloride

Although the hydrochloride salt of *L*-proline benzyl ester residue is inexpensive and commercially available, we sought to prepare proline residues that mimicked the protecting group strategy of 2,3-*trans*-3,4-*trans*-3,4-dihydroxyproline in order to provide experience of peptide couplings and associated manipulations involving this building block (*vide supra*). The preparation of *L*-proline benzyl ester hydrochloride residue is presented in Scheme 3.9. The nitrogen of commercially available proline (**134**) was protected with the 9-fluorenylmethyloxycarbonyl group (Fmoc) under standard conditions,⁹⁰ followed by benzylation of the crude carboxylic acid to deliver **135** in good yield. We encountered challenges handling the prolyl amine after Fmoc cleavage using standard conditions. Deprotection of the Fmoc group was best achieved using diethylamine, followed by chromatography and formation of the hydrochloride salt **136**. The salt formation eliminated a side reaction experienced in our initial attempts to utilize the free amine directly to form tripeptides. The side reaction involved dimerization of the proline benzyl ester, leading to poor yields of the desired tripeptide. Handling the proline residue as the hydrochloride salt greatly improved our overall coupling yield (*vide infra*).

Scheme 3.9. Preparation of the proline building block.

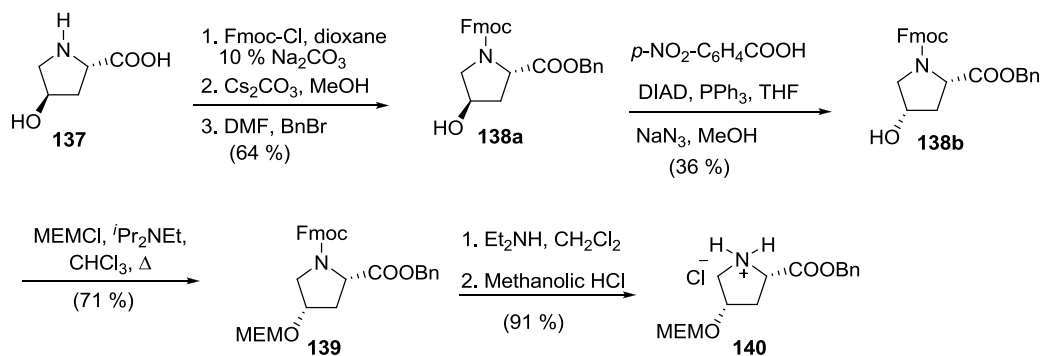


3.3.2 L-4-cis-Hydroxyproline Building Block

While *L*-*cis*-4-hydroxyproline is commercially available, this building block is expensive (\$561.00/g, from Sigma). We therefore followed previously developed procedures for the generation of *cis*-4-hydroxyproline derivatives.⁹⁸ After introducing the 9-fluorenylmethyloxycarbonyl and the benzyl ester protecting groups (Scheme 3.10) to the *trans*-4-hydroxyproline residue (**138a**), we conducted the

Mitsunobu reaction with *p*-nitrobenzoic acid to invert the stereochemistry at the hydroxyl-bearing center. The use of *p*-nitrobenzoic acid is well known to increase the efficiency of inversion in sterically hindered secondary alcohols,^{99, 100} and the development of a mild and selective method of cleaving the *p*-nitrobenzoate ester intermediates using sodium azide in methanol¹⁰¹ has increased the utility of *p*-nitrobenzoates in Mitsunobu reactions. However, in our hands, we recorded poor yields for this reaction under the same conditions as Gomez-Vidal and co-workers.¹⁰¹ The low yield of product from the Mitsunobu reaction of Fmoc protected substrate **138b** (Scheme 3.10) was used in the subsequent steps as an alternative source of the 4-*cis*-hydroxyproline building block. The hydroxyl group was protected as its MEM ether derivative, followed by Fmoc cleavage and hydrochloride salt formation as described above.

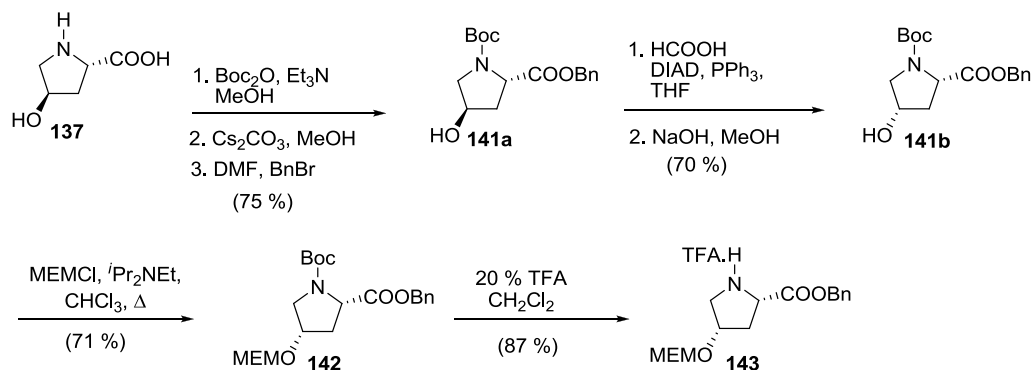
Scheme 3.10. Preparation of the hydrochloride salt of 4-hyp building block.



Switching from the Fmoc to the Boc protecting group and formation of the formate ester instead of the previously used *p*-nitrobenzoate ester, tremendously improved our yield for the Mitsunobu reaction as indicated in Scheme 3.11. A possible explanation for the poor yield with the Fmoc protected derivative could be due to instability of the protecting group under these conditions. This change in strategy was further justified by the ease of hydrolysis of the less hindered formate ester of the *N*-Boc derivative to give the inverted alcohol in high yields. Protection of the hydroxyl group as its MEM ether

derivative, followed by removal of the Boc protecting group under mild acidic conditions set the stage for tripeptide formation.

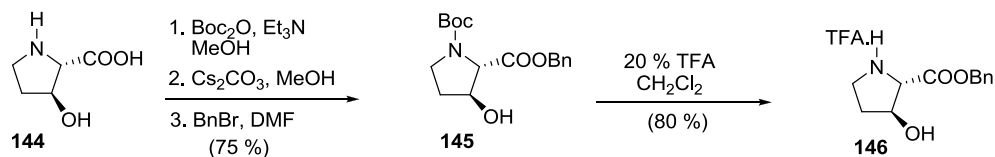
Scheme 3.11. Preparation of the trifluoroacetate salt of 4-hyp building block.



3.3.3 *L*-3-*trans*-Hydroxyproline Building Block

The preparation of this residue from commercially available **144** proceeded as outlined in Scheme 3.12. Protection of the two functionalities, as previously described for the *cis*-4-hydroxyproline building block (Scheme 3.11), generated **145**. Having demonstrated that the MEM ether could be cleaved under the same conditions as the side chain protected *tert*-butyl ethers using the 4-*cis*-hydroxyproline residue (*vide supra*), we decided to handle the β -hydroxyl group of 3-*trans*-hydroxyproline in its unprotected form at the initial tripeptide coupling level. Trifluoroacetic acid mediated Boc-deprotection of **145** gave the corresponding trifluoroacetate salt **146** that was routinely used in the next step without further purification.

Scheme 3.12. Preparation of the trifluoroacetate salt of 3-Hyp building block.



3.3.4 *L*-2,3-*trans*-3,4-*trans*-3,4-Dihydroxyproline³⁴

All naturally occurring virotoxins contain this amino acid (Fig. 3.3). One of the major obstacles to the synthesis of these natural products has been the availability of the 2,3-*trans*-3,4-*trans*-3,4-dihydroxyproline residue, which was not commercially available and considered inaccessible via synthesis. A report by Kahl and coworkers demonstrated that substituting *cis*-4-hydroxyproline for the dihydroxyproline residue generates a synthetic analog that is five times less active (*vide supra*).²⁹

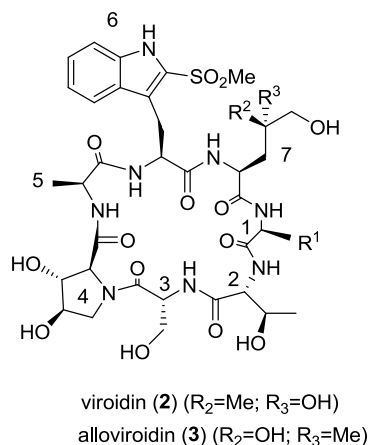
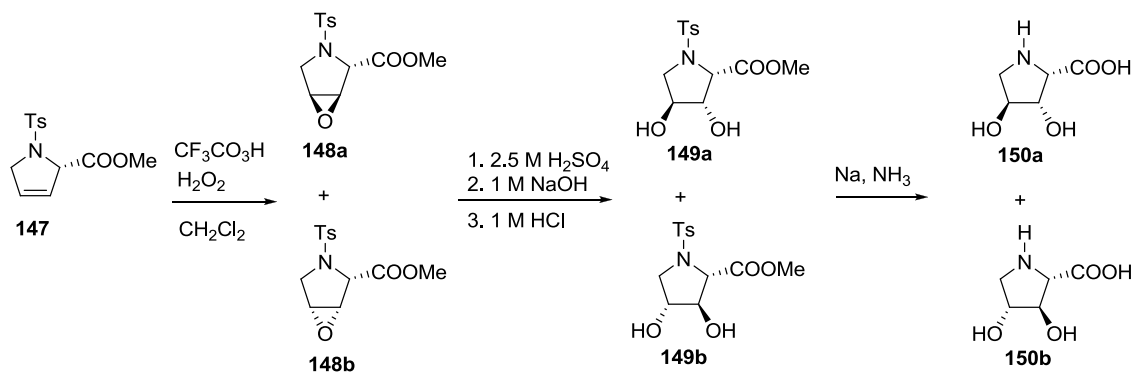


Figure 3.3. Naturally occurring virotoxins.

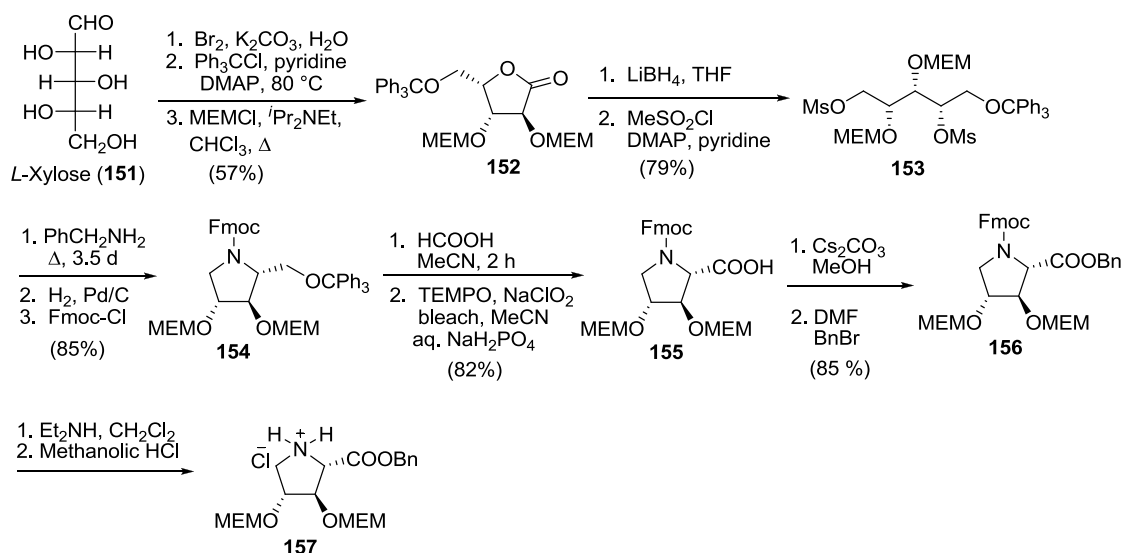
A notable amount of synthetic work on dihydroxyprolines can be found in literature.¹⁰²⁻¹⁰⁴ Most of these approaches are not capable of delivering the eight stereoisomers of 3,4-dihydroxyproline. In 1981, Kahl and Wieland synthesized two naturally occurring dihydroxyproline diastereomers **150a** and **150b**. Their aim was to correlate structural data of the synthetic and natural compounds. Epoxidation of *N*-tosyl-3,4-dehydro-*L*-proline methyl ester (**147**) with trifluoroperacetic acid generated the 3,4-epoxy esters **148a** and **148b**, which were ring-opened and hydrolyzed without separation to give **149a** and **149b**. Removal of the tosyl protecting group with sodium in liquid ammonia afforded the free dihydroxyprolines **150a** and **150b** (Scheme 3.13).¹⁰⁵ This strategy was laborious and not efficient at generating sufficient quantities of the dihydroxyproline building block required for a virotoxin synthesis.

Scheme 3.13. Kahl and Wieland synthesis of two naturally occurring dihydroxyproline diastereomers.¹⁰⁵



Significant efforts in the Taylor laboratory developed an efficient way to produce orthogonally protected dihydroxyproline building blocks in gram quantities.^{34, 106, 107} We utilized this approach to produce more of the 2,3-*trans*-3,4-*trans*-3,4-dihydroxyproline residue as described below (Scheme 3.14).³⁴

Scheme 3.14. Synthesis of 2,3-*trans*-3,4-*trans*-3,4-dihydroxyproline residue.ⁱⁱ

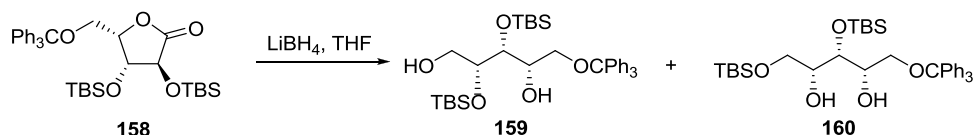


Commercially available *L*-xylose (**151**) was oxidized to give a γ -lactone. Selective protection of the primary alcohol as its triphenylmethyl ether, followed by protection of the secondary alcohols as MEM¹⁰⁸ ethers, using conditions optimized by Chantelle Jones, involved heating at reflux in chloroform

ⁱⁱ Procedures for the preparation of compound **155** followed the literature and are not reiterated in this dissertation.

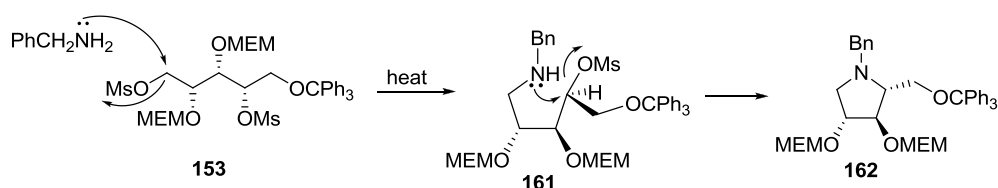
with 5 equivalents of the alkylating reagent³⁴ to give compound **152**. Initial studies in our group utilized *tert*-butyldimethylsilyl (TBS) ethers for protection of the secondary alcohols, however, silyl ether migration upon reductive opening of the lactone ring in **158** (Scheme 3.15) and partial cleavage of this protecting group under the acidic conditions used for triphenylmethyl ether cleavage adversely affected the chemical yield of the desired product.¹⁰⁷

Scheme 3.15. Silyl ether migration upon reductive opening of the lactone ring.



Reductive opening of lactone **152** with lithium borohydride gave the open chain diol that was converted to *bis*-mesylate **153** by adding a solution of the diol in pyridine to a precooled mixture of methanesulfonyl chloride and DMAP. Treatment with benzylamine displaced the primary mesylate, followed by an $\text{S}_{\text{N}}2$ attack at the secondary mesylate to produce the pyrrolidine (Scheme 3.16).

Scheme 3.16. Pyrrolidine ring formation.



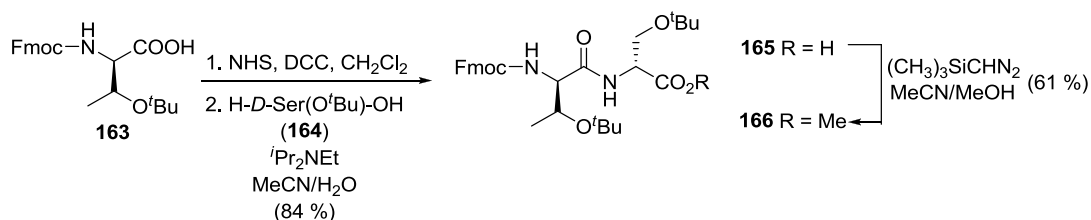
At this point, the replacement of the *N*-benzyl group for Fmoc was necessary for stability and compatibility in the subsequent oxidation and peptide synthesis steps.¹⁰⁶ Hydrogenolysis of the benzyl group from **162**, followed by treatment of the crude secondary amine with fluorenylmethyl chloroformate in toluene using triethylamine as a base, gave **154** in good yields (Scheme 3.14). The trityl ether was then cleaved with formic acid followed by oxidation of the resulting alcohol to give the

corresponding carboxylic acid **155** that was protected as its benzyl ester derivative **156**, the building block required for virotoxin synthesis.

3.3.5 Completion of the Tripeptide Fragments

With the four proline building blocks in-hand, our next goal was the synthesis of the Fmoc-*D*-Thr-*D*-Ser-OH dipeptide. The preparation of the dipeptide acid **165** proceeded from the *tert*-butyl ether derivatives of the two *D*-amino acids (Scheme 3.17) that were obtained from commercial sources. Formation of the activated *N*-hydroxysuccinimide ester of the threonine residue was accomplished using NHS and DCC.¹⁰⁹ This intermediate was subsequently coupled with the amino acid **164** to provide the corresponding dipeptide acid **165** that was routinely used in the next step without further purification. For the purposes of characterization, we again converted a portion of the acid to the corresponding methyl ester using trimethylsilyldiazomethane.

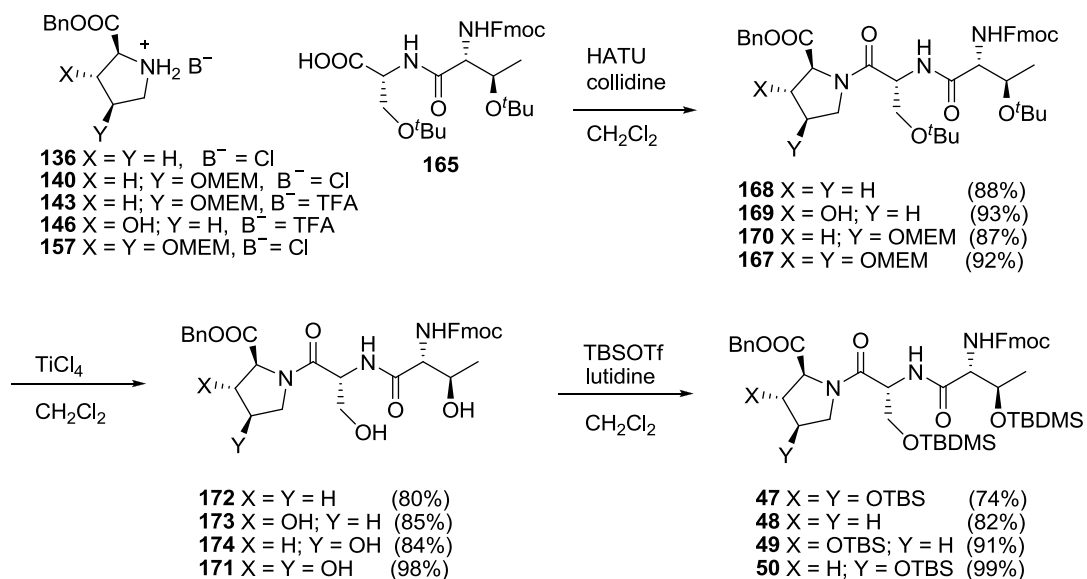
Scheme 3.17. The synthesis of the Fmoc-*D*-Thr-*D*-Ser dipeptide.



Having generated the Fmoc-*D*-Thr-*D*-Ser-OH dipeptide (**165**), the stage was now set for the amalgamation with each of the four proline building blocks and a final elaboration to deliver the series of four tripeptides. The assembly of the tripeptides began with coupling the dipeptide acid **165** with the salts of proline (**136**), 3-*trans*-hydroxyproline (**146**), 4-*cis*-hydroxyproline (**140/143**), and 2,3-*trans*-3,4-*trans*-3,4-dihydroxyproline (**157**) building blocks using HATU/collidine to furnish the corresponding tripeptide fragments **167-170** (Scheme 3.18) in high yields. We relied on this remarkable coupling

reagent since earlier studies by Carpino and co-workers had demonstrated that acid activation by HATU in the presence of collidine as a base gave little or no epimerization even in difficult cases.⁸⁹

Scheme 3.18. Preparation of the tripeptides.

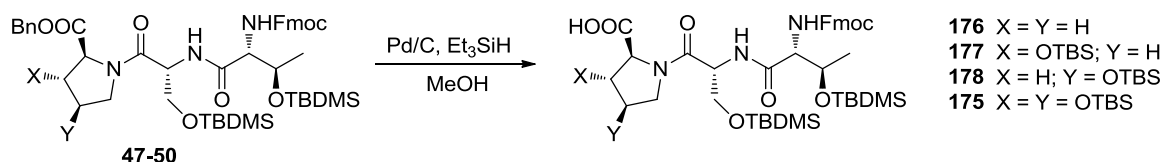


At this point, an exchange of the acid labile *tert*-butyl and MEM ether protecting groups for silyl ethers was considered vital. Acid labile protecting groups are not compatible with the tendency of the γ -hydroxylated dihyLeu to lactonize under acidic conditions causing cleavage of the peptide bond (*vide supra*, Scheme 2.18).⁸¹ Attempts to employ either neat trifluoroacetic acid, or this reagent in combination with CH₂Cl₂ or 2M HCl, to cleave both MEM and *tert*-butyl ethers in a one-pot process were plagued by incomplete deprotection of the MEM group, even after prolonged reaction times that resulted in partial cleavage of the benzyl ester. Gratifyingly, the use of titanium tetrachloride¹¹⁰ afforded a smooth deprotection of both protecting groups, within a short time, in high yields. We then protected the alcohols as the fluoride-labile silyl ethers using the highly reactive silylating reagent; *t*-butyldimethylsilyl trifluoromethanesulfonate and 2,6-lutidine in dichloromethane (Scheme 3.18). Analysis of the proline, 3-*trans*-hydroxyproline, 4-*cis*-hydroxyproline and 2,3-*trans*-3,4-*trans*-3,4-dihydroxyproline containing tripeptides by ¹H and ¹³C NMR spectra revealed the existence of two

conformers. This could be explained in terms of the *cis*→*trans* isomerization about the serine-prolyl peptide bond. The position of this equilibrium depends on the degree and stereochemistry of proline hydroxylation.³⁶ This phenomenon is also associated with carbamate protecting groups that gives rise to the *cis* and *trans* rotamers in solution. The purity of the four tripeptides was found to be greater than 96% by HPLC analysis (see experimental section for the HPLC traces), an indication that our couplings and deprotections proceeded smoothly.

Having synthesized the tripeptide fragments, we next set about cleaving the benzyl ester in preparation for the [3+4] fragment condensation to give heptapeptides. Attempts to employ standard catalytic hydrogenolysis conditions led to considerable cleavage of the Fmoc group and incomplete debenzylation of the 2,3-*trans*-3,4-*trans*-3,4-dihydroxyproline containing tripeptide, presumably due to steric effects introduced by the additional *O*-TBS group at the C β -position of the pyrrolidine ring. A similar Fmoc cleavage in peptide synthesis had been reported earlier by Bodanszky and co-workers during hydrogenolysis of Fmoc protected amino acids.¹¹¹ Bodanszky *et al.* identified the side product as 9-methyl-fluorene and hypothesized that the quality of the palladium catalyst dictated the stability of the Fmoc group to hydrogenolysis, *i.e.*, a partially poisoned catalyst could be active enough to reduce a benzyl group leaving the Fmoc group intact.¹¹¹ Gratifyingly, cleavage of the benzyl esters by transfer hydrogenolysis with triethylsilane¹¹² liberated the tripeptide acids in high yields without affecting the *N*-terminal Fmoc (Scheme 3.19).

Scheme 3.19. Hydrogenolysis of the benzyl ester.



Addition of triethylsilane to the palladium/carbon catalyst generates molecular hydrogen *in situ*, avoiding the use of an external source of hydrogen gas (Fig. 3.4) during the reduction process.¹¹³

An extensive study by McMurray and Mandal has revealed that a wide range of substrates, including both acid- and base-sensitive substrates tolerated these conditions.¹¹²

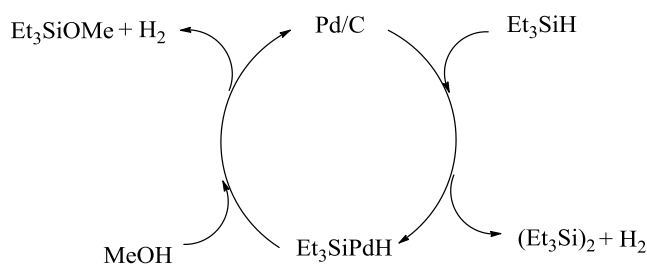


Figure 3.4.¹¹³ Generation of molecular hydrogen from triethylsilane/Pd-C and methanol mixture.

3.3.6 Summary

In this Chapter, we have described the preparation of the 2-methylsulfonyl-tryptophan residue **127** in four steps with an overall yield of 51% starting from commercially available *L*-tryptophan *tert*-butyl ester. We then performed coupling to generate Fmoc-Ala-[2-SO₂Me-Trp]-OH dipeptide **115**, that was condensed with (2*S*,4*S*)-4,5-dihyLeu-Val-OEt from Chapter 2 to give the tetrapeptide fragment.

We have also described an efficient synthesis of the four tripeptide fragments required for the assembly of alloviroidin and analogs utilizing the same strategy by substituting the appropriate proline residue into each fragment. The coupling conditions permitted the synthesis of the tripeptides in acceptable yields. Also, the overall yield per tripeptide fragment compares favorably with couplings involving regular amino acids. Orthogonal protection of the final tripeptide fragments was accomplished with the base labile Fmoc group for temporary amino protection, the fluoride-labile silyl ether for permanent side chain protection, and the benzyl ester for temporary protection of the C-terminus.

3.4 EXPERIMENTAL SECTION

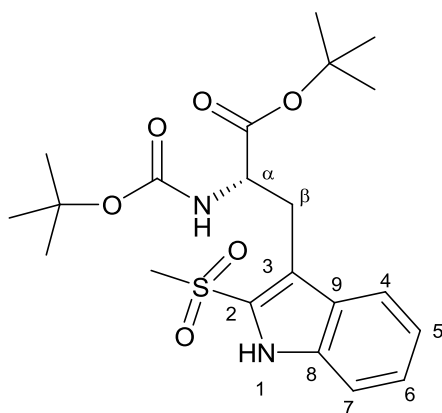
3.4.1 General Methods: As for Chapter 2 with the following additions and modifications: 2,4,6-collidine and 2,6-lutidine were dried and distilled from CaH₂ and stored over KOH pellets. The compounds were visualized by UV fluorescence or by staining with Ehrlich reagent, phosphomolybdic acid, ninhydrin or KMnO₄ stains.

- **Boc-*L*-Trp-O^tBu (124).** *L*-tryptophan *tert*-butyl ester hydrochloride (3.00 g, 10.1 mmol, 1.0 equiv.) was added gradually to a solution of triethylamine (15 mL, 10.92 g, 107.92 mmol, 10.7 equiv.) in methanol (120 mL) at rt under N₂. The mixture was stirred for a further 30 min after the addition was complete. Di-*tert*-butyl-dicarbonate (2.646 g, 12.1 mmol, 1.2 equiv.) was then added in a single portion, with vigorous stirring. The temperature was raised to 40 °C for 1 h, and then cooled to rt for another 1 h. The reaction mixture was concentrated and partitioned between ethyl acetate (150 mL) and 2M HCl (75 mL, diluted to 190 mL with ice cold water). The aqueous layer was extracted further with ethyl acetate (4 × 50 mL). The organic extracts were combined, filtered through MgSO₄ and concentrated. The residue was purified by flash chromatography, eluting with 2:1 Hexanes/EtOAc to give **124** as a colorless solid (3.476 g, 95 %). *R_f* 0.45 (2:1 Hexanes/EtOAc). [α]_D²⁵ +16.5° (*c* 1.0, CHCl₃). ¹H NMR (250 MHz, CDCl₃) δ 1.37 (s, 9H), 1.41 (s, 9H), 3.24 (br, 2H), 4.54 (q, *J* = 13.2 Hz, 1H), 5.08 (d, *J* = 7.5 Hz, 1H), 6.99 (s, 1H), 7.10 (t, *J* = 7.5 Hz, 1H), 7.18 (t, *J* = 7.5 Hz, 1H), 7.33 (d, *J* = 7.5 Hz, 1H), 7.61 (d, *J* = 7.5 Hz, 1H), 8.26 (br, 1H); ¹³C NMR (62.5 MHz, CDCl₃) δ 27.9, 28.3, 54.7, 79.5, 81.7, 110.4, 111.0, 119.0, 119.3, 122.0, 122.7, 127.9, 136.0, 155.3, 171.4. HRMS (+TOF) calcd for C₂₀H₂₉N₂O₄ (M + H)⁺: 361.2121; obsd: 361.2116.

- **Boc-*L*-Trp(SMe)-O^tBu (125).** Sulfuryl chloride (368 μ L, 612 mg, 4.5 mmol, 1 equiv.) was added dropwise to a solution of Me₂S₂ (443 μ L, 470 mg, 5.0 mmol, 1.1 equiv.) in CH₂Cl₂ (10 mL) at -25 °C (ethylene glycol-dry ice) under N₂. The mixture was stirred for 30 min, then warmed to rt. This solution of methylsulphenyl chloride was then added gradually to a solution of **124** (3.27 g, 9.1 mmol, 2 equiv.) in CH₂Cl₂ (150 mL) under N₂ at rt. After stirring for 2.5 h, the solution was washed with 10% aq. Na₂CO₃ (150 mL), and brine (150 mL). The organic layer was filtered through MgSO₄ and concentrated. The residue was purified by flash chromatography eluting with 3:1 Hex/EtOAc to give **125** as light green foam (2.50 g, 68%). *R_f* 0.48 (3:1 Hexanes/EtOAc). [α]_D²⁵ +3.6° (*c* 1.0, CHCl₃). ¹H NMR (400 MHz, CDCl₃) δ 1.32 (s, 9H), 1.38 (s, 9H), 2.34 (s, 3H), 3.26 (dq, *J* = 6.2, 7.8 Hz, 1H), 4.53 (q, *J* = 15.5 Hz, 1H), 5.19 (d, *J* = 8.2 Hz, 1H), 7.08 (t, *J* = 7.5 Hz, 1H), 7.16 (t, *J* = 7.2 Hz, 1H), 7.26 (d, *J* = 7.9 Hz, 1H), 8.38 (br, 1H); ¹³C NMR (100 MHz, CDCl₃) δ 19.8, 27.8, 28.1, 28.2, 54.8, 79.4, 81.6, 110.5, 119.2, 119.7, 122.8, 127.9, 128.0, 136.5, 155.1, 171.6. HRMS (+TOF) calcd for C₂₁H₃₁N₂O₄S (M + H)⁺: 407.1999; obsd: 407.2009.

- **Boc-*L*-Trp(SO₂Me)-O^tBu (126).** *meta*-Chloroperbenzoic acid (405 mg, 1.8 mmol, 2 equiv., 77 %) was added in one portion to a solution of the thioether **125** (367 mg, 0.9 mmol, 1 equiv.) in CH₂Cl₂ (100 mL) at 0 °C under N₂. The mixture was stirred further at this temperature for 1.5 h, and then washed with 10% aq. Na₂CO₃ (100 mL). The aqueous layer was extracted further with CH₂Cl₂ (3 \times 50 mL). The organic extracts were combined, filtered through MgSO₄ and concentrated. The residue was purified by flash chromatography eluting with 1:1 Hex/EtOAc to give **126** (302 mg, 76%). *R_f* 0.59 (1:1 Hexanes/EtOAc). [α]_D²⁵ -10.6° (*c* 1.0, CHCl₃). ¹H NMR (400 MHz, CDCl₃) δ 1.29 (s, 9H), 1.39 (s, 9H), 3.24 (s, 3H), 3.39 (t, *J* = 10.2 Hz, 1H), 3.54 (dd, *J* = 4.5, 4.6 Hz, 1H), 4.50 (t, *J* = 4.0 Hz, 1H), 5.44 (d, *J*

= 8.1 Hz, 1H), 7.19 (d, $J = 1.04$ Hz, 1H), 7.21 (t, $J = 1.1$ Hz, 1H), 7.23 (d, $J = 1.0$ Hz, 1H), 7.35 (d, $J = 1.0$ Hz, 1H), 7.37 (t, $J = 1.1$ Hz, 1H), 7.39 (d, $J = 1.0$ Hz, 1H), 7.43 (d, $J = 8.3$ Hz, 1H), 7.77 (d, $J = 8.0$ Hz, 1H), 9.25 (br, 1H); ^{13}C NMR (100 MHz, CDCl_3) δ 25.5, 26.6, 44.6, 55.2, 112.8, 115.3, 120.6, 121.3, 126.4, 126.5, 129.4, 136.3, 173.7. HRMS (+TOF) calcd for $\text{C}_{21}\text{H}_{31}\text{N}_2\text{O}_6\text{S}$ ($\text{M} + \text{H}$) $^+$: 439.1902; obsd: 439.1902.



NMR Assignments

Position	^1H (ppm)	J (Hz)	^{13}C (ppm)
C=O COO t Bu			171.2
C=O Boc			155.3
H α	4.50	q (8.6, 4.6)	54.9
H β	3.39	dd (10.6, 2.8)	27.2
	3.54	dd (13.2, 3.8)	
C2			118.1
C3			129.4
C4	7.41	d (8.3)	112.3
C5	7.37	ddd (8.2, 7.0, 1.1)	121.4
C6	7.21	ddd (8.1, 7.0, 1.1)	126.5
C7	7.77	d (8.0)	121.2
C9			127.5
C8			135.9
SOOCH $_3$	3.24	s	45.7
C(CH $_3$) $_3$ x 2			79.5, 82.0
C(CH $_3$) $_3$ x 2			27.9, 28.1

- **H-L-Trp(SO₂Me)-OH (127).** Trifluoroacetic acid (3 mL) was added gradually to a stirred solution of **126** (400 mg, 0.91 mmol, 1 equiv.) in CH₂Cl₂ (3 mL) at 0 °C under N₂. Thioanisole (107 µL, 113 mg, 0.91 mmol, 1 equiv.) was then added and the resultant solution stirred and gradually warmed to rt overnight. The mixture was concentrated and the residue dissolved in a minimum volume of H₂O (~ 3 mL), loaded onto a Dowex-50 (H⁺) column, rinsed with water (~ 250 mL), and the product eluted with 1N aqueous NH₄OH solution. The relevant fractions were combined and concentrated on a freeze-drier to deliver **127** (249 mg, 76 %). *R_f* 0.31 (6:4:1 CHCl₃/CH₃OH/H₂O). [α]_D³¹ +12.3° (*c* 1.0, H₂O). ¹H NMR (400 MHz, D₂O) δ 3.36 (s, 3H), 3.53 (dd, *J* = 14.8, 8.2 Hz, 1H), 3.72 (dd, *J* = 14.9, 5.9 Hz, 1H), 4.08 (dd, *J* = 7.8, 6.2 Hz, 1H), 7.29 (t, *J* = 7.6 Hz, 1H), 7.47 (t, *J* = 7.7 Hz, 1H), 7.57 (app. d, *J* = 8.4 Hz, 1H), 7.71 (d, *J* = 7.8 Hz, 1H), 7.83 (d, *J* = 8.2 Hz, 1H); ¹³C NMR (100 MHz, D₂O) δ 27.1, 27.9, 28.1, 45.7, 54.9, 79.5, 81.9, 112.3, 118.1, 121.2, 121.4, 126.4, 127.4, 129.4, 135.9, 155.3, 171.2; HRMS (+TOF) calcd for C₁₂H₁₅N₂O₄S (M + H)⁺: 283.07470; obsd: 283.07495.

- **Fmoc-Ala-Trp(SO₂Me)-OH (115).** *N,N'*-Dicyclohexyl carbodiimide (DCC) (235 mg, 1.14 mmol, 1.0 equiv.) and NHS (132 mg, 1.14 mmol, 1.0 equiv.) were added to a solution of Fmoc-*L*-Ala-OH (355 mg, 1.14 mmol, 1.0 equiv.) in CH₂Cl₂ (15 mL) at 0 °C under N₂. The reaction mixture was stirred and gradually warmed to rt for 4 h. The resulting *N,N'*-dicyclohexyl urea was removed by filtration and the filtrate concentrated, dissolved in a mixture of MeCN (4 mL) and H₂O (2 mL) and cooled to 0 °C. To this solution was added H-*L*-Trp-(SO₂Me)-OH (323 mg, 1.14 mmol, 1.0 equiv.), then diisopropylethylamine (377 µL, 295 mg, 2.28 mmol, 2.0 equiv.). The mixture was stirred and gradually warmed to rt overnight, and then partitioned between EtOAc (40 mL) and 2M HCl (40 mL). The aqueous layer was extracted further with ethyl acetate (3 × 30 mL). The organic extracts were combined,

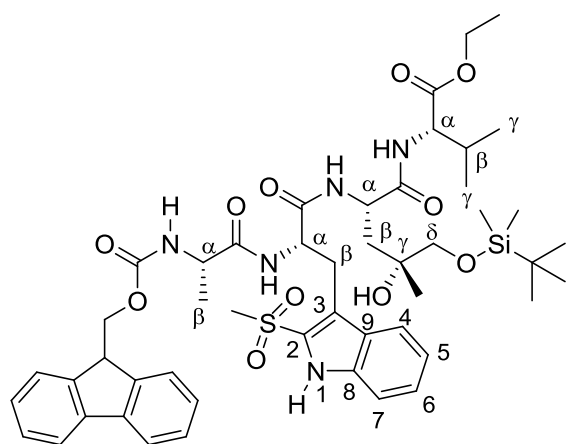
washed with H₂O (40 mL), filtered through MgSO₄ and concentrated to give compound **115** (642 mg, 98 %), which was used directly in the next reaction. For the purposes of characterization, a sample was converted to corresponding methyl ester.

• **Fmoc-Ala-Trp(SO₂Me)-OMe (129).** Cesium carbonate (17 mg, 0.05 mmol, 0.5 equiv.) was added to a solution of Fmoc-Ala-Trp(SO₂Me)-OH (**115**) (60 mg, 0.10 mmol, 1.0 equiv.) in MeOH (2 mL). The mixture was stirred for 2 h and concentrated. The residue was suspended in DMF (2 mL) and cooled to 0 °C. Methyl iodide (8 µL, 18 mg, 0.13 mmol, 1.2 equiv.) was added and the reaction mixture was stirred and gradually warmed to rt overnight, diluted with EtOAc (15 mL) and washed successively with H₂O and brine (15 mL each). The organic layer was dried over MgSO₄, filtered and concentrated. The product was isolated by flash chromatography eluting with 1:1 Hex/EtOAc to give **129** (36 mg, 59 %). *R_f* 0.47 (4:1 EtOAc/Hex). [α]_D²⁷ -15.6° (*c* 1.0, CHCl₃). ¹H NMR (400 MHz, CDCl₃) δ 1.32 (d, *J* = 6.7 Hz, 3H), 3.17 (s, 3H), 3.41 (dd, *J* = 10.0, 4.2 Hz, 1H), 3.58 (dd, *J* = 14.2, 4.3 Hz, 1H), 3.72 (s, 3H), 4.12-4.40 (m, 4H), 4.77-4.84 (m, *J* = 10.2 Hz, 1H), 5.44 (d, *J* = 7.5 Hz, 2H), 7.16-7.33 (m, 7H), 7.38 (t, *J* = 7.5 Hz, 2H), 7.58 (t, *J* = 7.1 Hz, 1H), 7.74 (d, *J* = 7.5 Hz, 2H), 9.27 (s, 1H); ¹³C NMR (100 MHz, CDCl₃) δ 18.9, 26.3, 45.6, 47.1, 50.3, 52.6, 53.0, 67.0, 112.6, 116.7, 119.9, 120.6, 121.7, 125.2, 126.8, 127.0, 127.6, 129.9, 136.0, 141.2, 143.8, 144.0, 155.7, 171.6, 172.5. HRMS (+TOF) calcd for C₃₁H₃₂N₃O₇ (M + H)⁺: 590.1955; obsd: 590.1943.

• **Dipeptide amine 116.** To a solution of Cbz-deHyleu (δ-OTBS)-Val-OEt (**114**) (180 mg, 0.33 mmol) in EtOH (3 mL) was added 10 % Pd/C (29 mg). The reaction vessel was evacuated and then opened to

an atmosphere of hydrogen gas. The suspension was stirred at rt overnight, filtered through Celite™, washed with methanol and then concentrated to give **116** (134 mg, 99 %), that was used in the next step without further purification.

• **Tetrapeptide 46.** Collidine (52 μ L, 48 mg, 0.40 mmol, 1.2 equiv.), and HATU (151 mg, 0.40 mmol, 1.2 equiv.) were added to a solution of the dipeptide amine **116** (134 mg, 0.33 mmol, 1.0 equiv.) and acid **115** (229 mg, 0.40 mmol, 1.2 equiv.) in DMF (3 mL) at 0 °C under N₂. The mixture was stirred and warmed to rt overnight, concentrated, and the product isolated by flash chromatography eluting with 4:1 EtOAc/Hex to give **46** (291 mg, 91 %). *R_f* 0.40 (4:1 EtOAc/Hex). $[\alpha]_D^{25}$ -17.0° (*c* 1.0, CHCl₃). ¹H NMR (400 MHz, CDCl₃) δ 0.00 (s, 3H), 0.01 (s, 3H), 0.85 (s, 9H), 0.93 (d, *J* = 6.5 Hz, 3H), 0.94 (d, *J* = 6.5 Hz, 3H), 1.15 (s, 3H), 1.23 (d, *J* = 7.1 Hz, 3H), 1.25 (t, *J* = 7.1 Hz, 3H), 1.70 (dd, *J* = 14.7, 4.7 Hz, 1H), 1.76 (s, 3H), 1.90 (dd, *J* = 14.7, 6.2 Hz, 1H), 2.19 (app. sept. *J* = 6.5 Hz, 1H), 3.16 (s, 3H), 3.26 (d, *J* = 9.7 Hz, 1H), 3.30 (d, *J* = 9.7 Hz, 1H), 3.39 (dd, *J* = 14.4, 10.4 Hz, 1H), 3.65 (dd, *J* = 14.4, 2.8 Hz, 1H), 4.10-4.19 (m, 1H), 4.12 (q, *J* = 7.1 Hz, 2H), 4.21 (t, *J* = 6.8 Hz, 1H), 4.32-4.36 (m, 2H), 4.42 (dd, *J* = 8.6, 5.4 Hz, 1H), 4.56-4.62 (m, 2H), 5.42 (d, *J* = 6.1 Hz, 1H), 7.20 (t, *J* = 6.5 Hz, 2H), 7.31 (t, *J* = 7.4 Hz, 2H), 7.39 (dd, *J* = 15.1, 7.2 Hz, 3H), 7.63 (d, *J* = 7.3 Hz, 2H), 7.70-7.86 (m, 3H), 9.16 (s, 1H); ¹³C NMR (100 MHz, CDCl₃) δ -6.5, 13.2, 17.0, 17.2, 17.4, 18.0, 22.6, 24.7, 24.9, 29.7, 38.0, 44.6, 46.0, 49.2, 50.2, 53.6, 56.8, 60.0, 66.3, 69.6, 71.3, 111.4, 119.0, 120.2, 120.8, 124.2, 126.0, 126.7, 128.7, 135.0, 140.2, 142.9, 155.2, 169.2, 170.5, 171.2, 172.4. HRMS (+TOF) calcd for C₄₉H₆₇N₅O₁₁SSi (M + H)⁺: 962.4399; obsd: 962.4396.



NMR Assignments

Position	^1H (ppm)	Multiplicity (J , Hz)	^{13}C (ppm)
Residue 1 –Fmoc-Ala-			
Ala C=O			173.4
Ala α	4.10-4.19		51.2
Ala β	1.23	d (7.1)	18.2
Ala NH	5.42	d (6.1)	
Fmoc C=O			156.2
Fmoc CH ₂	4.32-4.36		67.3
Fmoc CH	4.21	t (6.8)	47.0
Fmoc CH	7.63	d (7.3)	
Fmoc CH	7.76	d (7.5)	
Fmoc CH	7.31	t (7.4)	
Fmoc CH	7.36-7.44		
Fmoc C 4°			141.2
Fmoc C 4°			141.3
Fmoc C 4°			143.8
Fmoc C 4°			143.9
Residue 2 –(2 MeSO ₂ -Trp)-			
Trp C=O			172.2
Trp α	4.56-4.62		54.6
Trp β	3.39 3.65	dd (14.4, 10.4) dd (14.4, 2.8)	25.7
Trp NH	7.72-7.86		
NH1	9.16	s	
C2			121.2
C3			129.7
C4	7.36-7.44		112.4
C5	7.36-7.44		121.8
C6	7.21	t (6.7)	
C7	7.81	d (8.2)	120.0

C9			
C8			136.0
TrpSO ₂ CH ₃	3.16	s	45.6
Residue 3 –HyLeu-			
HyLeu C=O			171.5
HyLeu α	4.56-4.62		50.2
HyLeu β	1.70 1.90	dd (14.7, 4.7) dd (14.7, 6.2)	39.1
HyLeu γ			72.3
HyLeu γ- CH ₃	1.15		23.6
HyLeu δ	3.26 3.30	d (9.7) d (9.7)	70.6
HyLeu NH	7.72-7.86		
Si(CH ₃) ₂	0.00 0.01	s s	-5.5
SiCCH ₃			18.4
SiC(CH ₃) ₃	0.85	s	25.8
Residue 4 –Val-OEt			
OCH ₂ CH ₃	1.25	t (7.1)	14.2
OCH ₂ CH ₃	4.12	q (7.1)	61.0
Val C=O			171.2
Val α	4.42	dd (8.6, 5.4)	57.8
Val β	2.19	app sept. (6.5)	30.7
Val γ	0.93, 0.94	d (6.5) d (6.5)	18.0
Val NH	7.36-7.44		

• **Boc-4-Hyp-OBn (141a).** Di-*tert*-butyl dicarbonate (3.329 g, 15.252 mmol, 2 equiv.) was added to a solution of *trans*-4-hydroxyproline (1 g, 7.626 mmol, 1 equiv.) and triethylamine (1.648, 1.2 mL, 16.286 mmol, 2.1 equiv.) in methanol (12 mL) at room temperature under N₂. The reaction mixture was stirred and heated at reflux for 1 h, cooled and concentrated. The residue was cooled to 0 °C at which point NaH₂PO₄ (100 mg) and 1 M HCl were added to adjust the pH to 2. The mixture was extracted with EtOAc (4 x 35 mL). The organic extracts were combined, filtered through MgSO₄ and concentrated. Cesium carbonate (1.243 g, 3.810 mmol, 0.5 equiv.) was added to the residue in dry methanol (15 mL). The solution was stirred at rt under N₂ for 2 h and concentrated. The residue was

dissolved in DMF (10 mL), treated with benzyl bromide (1.1 mL, 1.566 g, 9.150 mmol, 1.2 equiv.) and stirred at rt under N₂ for 16 h. The suspension was diluted with EtOAc (35 mL) and washed successively with H₂O and brine (35 mL each). The organic layer was dried over MgSO₄, filtered and concentrated. The product was isolated by flash chromatography, eluting with 1:1 Hex/EtOAc, then 2:1 EtOAc/Hex to give Boc-4-Hyp-OBn (**141a**) as a colorless foam (1.833 g, 75 % over two steps). *R_f* 0.42 (1:1 Hex/EtOAc). $[\alpha]_D^{25}$ -48.2° (*c* 1.0, CHCl₃). NMR spectra are recorded for the major conformer. ¹H NMR (400 MHz, CDCl₃) δ 1.34 (s, 9H), 2.02-2.12 (m, 1H), 2.20-2.34 (m, 1H), 3.45 (d, *J* = 11.6 Hz, 1H), 4.40-4.54 (m, 2H), 5.14 (d, *J* = 12.2 Hz, 1H), 5.18 (d, *J* = 12.2 Hz, 1H), 7.30-7.40 (m, 5H); ¹³C NMR (100 MHz, CDCl₃) δ 28.1, 38.2, 53.3, 57.6, 66.6, 69.0, 80.1, 127.9, 128.1, 128.4, 135.3, 154.0, 172.6. HRMS (+TOF) calcd for C₁₇H₂₄NO₅ (*M* + *H*)⁺: 322.1642; obsd: 322.1649.

- **Boc-4-hyp-OBn (141b).** A solution of Boc-4-Hyp-OBn (**141a**) (1.220 g, 3.796 mmol, 1 equiv.) and formic acid (293 μL, 351 mg, 2.01 equiv.) in dry THF (5 mL) was added dropwise to a mixture of diisopropyl azodicarboxylate (1.5 mL, 1.543 g, 7.630 mmol, 2.01 equiv.) and triphenylphosphine (2.000 g, 7.630 mmol, 2.01 equiv.) in dry THF (15 mL) under N₂ at 0 °C. The reaction mixture was warmed to rt for 2 h, concentrated and the residue was partially purified by flash chromatography eluting with 2:1 Hex/EtOAc to generate the corresponding formate ester that was directly hydrolyzed.

Aqueous NaOH (1 N, 3.4 mL) was added dropwise to a solution of the formate ester in MeOH (15 mL) at 0 °C. The reaction mixture was stirred for 30 min, acidified with 10 % aqueous KHSO₄ (30 mL), concentrated to remove methanol and extracted with EtOAc (3 × 40 mL). The organic extracts were combined, washed successively with H₂O (2 × 30 mL) and brine (30 mL), dried over MgSO₄, concentrated and purified by flash chromatography, eluting with 1:1 Hex/EtOAc to give Boc-4-hyp-OBn (**141b**) as a colorless solid (860 mg, 70 % over two steps). *R_f* 0.42 (1:1 Hex/ EtOAc). $[\alpha]_D^{25}$ -10.3°

(*c* 1.0, CHCl₃). NMR spectra are recorded for the major conformer. ¹H NMR (400 MHz, CDCl₃) δ 1.33 (s, 9H), 2.02-2.13 (m, 1H), 2.23-2.37 (m, 1H), 3.26 (d, *J* = 9.4 Hz, 1H), 3.49-3.68 (m, 1H), 4.29-4.44 (m, 2H), 5.12 (d, *J* = 12.3 Hz, 1H), 5.29 (d, *J* = 12.3 Hz, 1H), 7.31-7.39 (m, 5H); ¹³C NMR (100 MHz, CDCl₃) δ 28.3, 38.0, 55.6, 58.0, 67.6, 70.4, 80.5, 128.3, 128.4, 128.8, 135.3, 153.9, 174.8. HRMS (+TOF) calcd for C₁₇H₂₄NO₅ (M + H)⁺: 322.1643; obsd: 322.1649.

• **Boc-4-hyp-(OMEM)-OBn (142).** MEMCl (719 μL, 785 mg, 6.30 mmol, 2.5 equiv.) was added dropwise to a solution of Boc-4-hyp-OBn (**141b**) (810 mg, 2.52 mmol, 1.0 equiv.) and diisopropylethylamine (1.1 mL, 814 mg, 6.30 mmol, 2.5 equiv.) in chloroform (10 mL) at rt under N₂. The mixture was then heated at reflux for 16 h, cooled, diluted with chloroform (50 mL), washed successively with 10 % aqueous citric acid, saturated aqueous NaHCO₃ and brine (50 mL each).³⁴ The organic layer was dried over MgSO₄, concentrated and purified by flash chromatography, eluting with 2:1 EtOAc/Hex to give **142** as a colorless oil (862 mg, 84 %). *R_f* 0.35 (2:1 EtOAc/Hex). [α]_D²⁵ -38.3° (*c* 1.0, CHCl₃). NMR spectra are recorded for the major conformer. ¹H NMR (400 MHz, CDCl₃) δ 1.36 (s, 9H), 2.18-2.43 (m, 2H), 3.37 (s, 3H), 3.46-3.74 (m, 6H), 4.25-4.31 (m, 1H), 4.35 (dd, *J* = 3.7, 9.0 Hz, 1H), 4.57-4.62 (m, 1H), 5.05 (d, *J* = 12.4 Hz, 1H), 5.27 (d, *J* = 12.4 Hz, 1H), 7.29-7.39 (m, 5H); ¹³C NMR (100 MHz, CDCl₃) δ 28.3, 35.8, 51.9, 57.6, 66.8, 71.8, 73.9, 80.2, 94.1, 128.2, 128.3, 128.5, 135.9, 153.9, 171.9. HRMS (+TOF) calcd for C₂₁H₃₁NNaO₇ (M + Na)⁺: 432.1993; obsd: 432.1996.

• **CF₃COOH.4-hyp-(OMEM)-OBn (143).** Trifluoroacetic acid (2 mL) was added dropwise to a stirred solution of Boc-4-hyp-(OMEM)-OBn (**142**) (300 mg, 0.73 mmol) in CH₂Cl₂ (10 mL) at -25 °C

(ethylene glycol-dry ice) under N₂ for 2 h. The reaction was quenched with aqueous saturated NaHCO₃ (~ 3 mL), diluted with H₂O (20 mL) and extracted with CH₂Cl₂ (4 × 25 mL). The organic extracts were combined, dried over MgSO₄ and concentrated to give the trifluoroacetate salt of 4-hyp-(OMEM)-OBn (**143**) that was used in the next step without further purification.

- **Boc-3-Hyp-OBn (145).** Di-*tert*-butyl dicarbonate (666 mg, 3.05 mmol, 2 equiv.) was added to a solution of *trans*-3-hydroxyproline (200 mg, 1.53 mmol, 1 equiv.) and triethylamine (300 µL, 218 mg, 2.15 mmol, 1.4 equiv.) in methanol (3 mL) at room temperature under N₂. The reaction mixture was stirred and heated at reflux for 1 h, cooled and concentrated. The residue was cooled to 0 °C at which point NaH₂PO₄ (20 mg) and 1 M HCl (-1 mL) were added to adjust the pH to 2. The mixture was extracted with EtOAc (4 x 20 mL). The organic extracts were combined, filtered through MgSO₄ and concentrated to give Boc-3-Hyp-OH that was used in the next step without further purification.

Cesium carbonate (248 mg, 0.76 mmol, 0.5 equiv.) was added to a suspension of Boc-3-Hyp-OH (352 mg, 1.52 mmol, 1.0 equiv.) in dry methanol (4 mL). The solution was stirred at rt under N₂ for 2 h and concentrated. The residue was dissolved in DMF (3 mL), treated with benzyl bromide (312 mg, 219 µL, 1.83 mmol, 1.2 equiv.) and stirred at rt under N₂ for 16 h. The suspension was diluted with EtOAc (30 mL) and washed successively with H₂O and brine (30 mL each). The organic layer was dried over MgSO₄, filtered and concentrated. The product was isolated by flash chromatography eluting with 1:1 Hex/EtOAc to give Boc-3-Hyp-OBn (**145**) as a mixture of two conformers (366 mg, 75 %). *R*_f 0.38 (1:1 Hex/ EtOAc). [α]_D²⁵ -23.6° (*c* 1.0, CHCl₃). NMR spectra are reported for the major conformer. ¹H NMR (400 MHz, CDCl₃) δ 1.32 (s, 9H), 1.86-1.94 (m, 1H), 2.20-2.12 (m, 1H), 2.73 (d, *J* = 4.4 Hz, 1H), 3.58-

3.68 (m, 2H), 4.22 (app. b, 1H), 4.38-4.46 (m, 1H), 5.13 (d, $J = 12.2$ Hz, 1H), 5.19 (d, $J = 12.2$ Hz, 1H), 7.30-7.38 (m, 5H); ^{13}C NMR (100 MHz, CDCl_3) δ 28.2, 32.2, 44.4, 67.0, 68.0, 74.0, 80.3, 128.1, 128.5, 128.7, 135.5, 154.2, 170.9. HRMS (+TOF) calcd for $\text{C}_{17}\text{H}_{24}\text{NO}_5$ ($\text{M} + \text{H}$) $^+$: 322.1640; obsd: 322.1649.

• **Fmoc-DHP-(OMEM) $_2$ -OBn (156).** Cesium carbonate (97 mg, 0.30 mmol, 0.50 equiv.) was added to a suspension of Fmoc-DHP(OMEM) $_2$ -OH (**155**) (326 mg, 0.598 mmol, 1 equiv.) residue in dry methanol (4 mL). The solution was stirred at rt under N_2 for 2 h and concentrated. The residue was dissolved in DMF (3 mL), treated with benzyl bromide (86 μL , 123 mg, 0.718 mmol, 1.2 equiv.) and stirred at rt under N_2 for 17 h. The suspension was diluted with EtOAc (50 mL) and washed successively with H_2O and brine (50 mL each). The organic layer was dried over MgSO_4 , filtered and concentrated. The product was isolated by flash chromatography, eluting with 2:1 Hex/EtOAc, then 2:1 EtOAc/Hex to give Fmoc-DHP(OMEM) $_2$ -OBn (**156**) as a colorless foam (305 mg, 80 %). R_f 0.50 (2:1 EtOAc/Hex). $[\alpha]_{\text{D}}^{25}$ -19.2° (c 0.9, CHCl_3). ^1H NMR (400 MHz, CDCl_3) δ 3.37 (s, 6H), 3.47-3.86 (m, 10H), 4.13-4.62 (m, 10H), 5.16 (d, $J = 12.3$ Hz, 1H), 5.25 (d, $J = 12.3$ Hz, 1H), 7.26-7.44 (m, 2H), 7.54 (d, $J = 7.4$ Hz, 2H), 7.61 (t, $J = 7.4$ Hz, 2H), 7.77 (t, $J = 8.6$ Hz, 2H); ^{13}C NMR (100 MHz, CDCl_3) δ 47.3, 51.0, 59.2, 64.5, 67.2, 67.4, 67.7, 71.8, 78.6, 81.5, 83.0, 94.5, 94.8, 120.1, 125.3, 127.2, 127.9, 128.4, 128.5, 128.6, 135.9, 141.5, 144.0, 144.3, 155.3, 169.0. HRMS (+TOF) calcd for $\text{C}_{35}\text{H}_{41}\text{NNaO}_{10}$ ($\text{M} + \text{Na}$) $^+$: 658.2623; obsd: 658.2614.

• **HCl.DHP-(OMEM) $_2$ -OBn (157).** Diethylamine (1.6 mL) was added to a solution of Fmoc-DHP-(OMEM) $_2$ -OBn (**156**) (135 mg, 0.21 mmol) in CH_2Cl_2 (8 mL) and the mixture stirred at rt under N_2 for 30 min. The mixture was concentrated, and the product isolated by flash chromatography eluting with

2:1 EtOAc/Hex, then 9:1 CH₂Cl₂/MeOH. The relevant fractions were combined, treated with methanolic HCl (0.21 mmol) solution (prepared by dropwise addition of acetyl chloride (15 μ L, 17 mg, 0.21 mmol) to MeOH (1 mL) at 0 °C under N₂) and concentrated to give HCl.DHP-(OMEM)₂-OBn (**157**) that was used in the next step without further purification.

- **Fmoc-*D*-Thr-(O'ⁱBu)-*D*-Ser(O'ⁱBu)-OH (165).** *N,N'*-Dicyclohexyl carbodiimide (DCC) (311 mg, 1.51 mmol, 1.0 equiv.) and NHS (174 mg, 1.51 mmol, 1.0 equiv.) were added to a solution of Fmoc-*D*-Thr-(O'ⁱBu)-OH (600 mg, 1.51 mmol, 1.0 equiv.) in CH₂Cl₂ (15 mL) at 0 °C under N₂. The reaction mixture was stirred and gradually warmed to rt for 4 h. The resulting *N,N'*-dicyclohexyl urea was removed by filtration and the filtrate concentrated, dissolved in a mixture of MeCN (4 mL) and H₂O (2 mL) and cooled to 0 °C. To this solution was added H-*D*-Ser(O'ⁱBu)-OH (243 mg, 1.51 mmol, 1.0 equiv.), then diisopropylethylamine (249 μ L, 195 mg, 1.51 mmol, 1.0 equiv.). The mixture was stirred and gradually warmed to rt overnight, then partitioned between EtOAc (40 mL) and 2M HCl (40 mL). The aqueous layer was extracted further with ethyl acetate (3 \times 35 mL). The organic extracts were combined, washed with H₂O (40 mL), filtered through MgSO₄ and concentrated to give compound **165** (684 mg, 84 %), which was used directly in the next reaction. For the purposes of characterization, a sample was converted to corresponding methyl ester.

- **Fmoc-*D*-Thr-(O'ⁱBu)-*D*-Ser(O'ⁱBu)-OMe (166).** Trimethylsilyldiazomethane (359 mg, 0.5 mL, 1.04 mmol, 4.8 equiv., 2.0 M solution in hexanes) was added gradually to a solution of Fmoc-*D*-Thr-(O'ⁱBu)-*D*-Ser(O'ⁱBu)-OH (**165**) (136 mg, 0.22 mmol, 1.0 equiv.) in a mixture of MeCN (2.7 mL) and MeOH (0.3 mL) at 0 °C under N₂. The reaction mixture was stirred and gradually warmed to rt over 1 h, and then concentrated. The product was isolated by flash chromatography eluting with 3:1 Hex/EtOAc to

afford **166** (85 mg, 61 %). R_f 0.26 (3:1 Hex/EtOAc). $[\alpha]_D^{25}$ -23.3° (c 0.75, CHCl₃). ¹H NMR (400 MHz, CDCl₃) δ 1.14 (s, 9H), 1.17 (d, J = 6.4 Hz, 3H), 1.32 (s, 9H), 3.56 (dd, J = 9.1, 3.1 Hz, 1H), 3.75 (s, 3H), 3.86 (dd, J = 9.1, 3.1 Hz, 1H), 4.12-4.28 (m, 3H), 4.38 (d, J = 7.3 Hz, 2H), 4.67-4.74 (dt, J = 8.4, 3.1 Hz, 1H), 6.04 (d, J = 5.2 Hz, 1H), 7.31 (t, J = 7.4 Hz, 2H), 7.39 (t, J = 7.5 Hz, 2H), 7.61 (d, J = 7.4 Hz, 2H), 7.76 (d, J = 7.6 Hz, 2H), 7.96 (d, J = 8.4 Hz, 1H); ¹³C NMR (100 MHz, CDCl₃) 16.3, 27.3, 28.2, 47.2, 52.1, 53.2, 58.5, 61.9, 66.8, 66.9, 73.4, 75.3, 119.9, 125.1, 127.0, 127.6, 141.3, 143.8, 143.9, 156.0, 169.5, 170.5. HRMS (+TOF) calcd for C₃₁H₄₃N₂O₇ (M + H)⁺: 555.3065; obsd: 555.3074.

- **Fmoc-D-Thr-(O^tBu)-D-Ser(O^tBu)-Pro-OBn (168).** The dipeptide acid **165** (680 mg, 1.26 mmol, 1.2 equiv.) and HCl.Pro-OBn (**136**) (253 mg, 1.05 mmol, 1.0 equiv.) were dissolved in CH₂Cl₂ (3 mL), and the solution cooled to 0 °C. Collidine (332 μ L, 305 mg, 2.52 mmol, 2.4 equiv.) and HATU (478 mg, 1.26 mmol, 1.2 equiv.) were added sequentially to the reaction mixture. The resultant solution was stirred at 0 °C for 1 h and then at rt overnight. The mixture was concentrated and the product isolated by flash chromatography eluting with 1:1 Hex/EtOAc, to give **168** (671 mg, 88 %). R_f 0.37 (1:1 Hex/EtOAc). $[\alpha]_D^{25}$ -36.6° (c 1.0, CHCl₃). ¹H NMR (400 MHz, CDCl₃, signals are reported for the major rotamer only) δ 1.03 (d, J = 6.3 Hz, 3H), 1.14 (s, 9H), 1.27 (s, 9H), 1.80-2.10 (m, 3H), 2.12-2.25 (m, 1H), 3.45 (t, J = 8.6 Hz, 1H), 3.62 (dd, J = 8.4, 5.3 Hz, 2H), 3.71-3.79 (m, 1H), 3.88-3.98 (m, 1H), 4.06-4.26 (m, 3H), 4.38 (dd, J = 7.2, 2.2 Hz, 1H), 4.52 (dd, J = 8.3, 4.3 Hz, 1H), 4.91 (dq, J = 7.6, 5.3 Hz, 1H), 5.05 (d, J = 12.4 Hz, 1H), 5.16 (d, J = 12.4 Hz, 1H), 5.95 (d, J = 5.8 Hz, 2H), 7.26-7.43 (m, 9H), 7.61 (d, J = 7.1 Hz, 2H), 7.76 (d, J = 7.6 Hz, 2H); ¹³C NMR (100 MHz, CDCl₃) δ 17.1, 24.7, 27.3, 28.2, 29.3, 47.2, 51.4, 58.8, 59.1, 63.0, 66.5, 66.6, 67.0, 73.5, 75.1, 119.9, 125.2, 127.0, 127.7, 127.9, 128.1, 128.5, 128.7, 135.8, 141.3, 141.4, 143.7, 144.0, 156.0, 169.1, 169.3, 171.6. HRMS (+TOF) calcd for C₄₂H₅₄N₃O₈ (M + H)⁺: 728.3905; obsd: 728.3909.

- **Fmoc-*D*-Thr-(*O*^tBu)-*D*-Ser(*O*^tBu)-*trans*-3-Hyp-OBn (169).** The dipeptide acid **165** (504 mg, 0.93 mmol, 1.2 equiv.) and CF₃COOH.3Hyp-OBn (**146**) (172 mg, 0.78 mmol, 1.0 equiv.) were dissolved in CH₂Cl₂ (3 mL), and the solution cooled to 0 °C. Collidine (247 µL, 226 mg, 1.87 mmol, 2.4 equiv.) and HATU (354 mg, 0.93 mmol, 1.2 equiv.) were added sequentially to the reaction mixture. The resultant solution was stirred at 0 °C for 1 h and then at rt overnight. The mixture was concentrated and the product isolated by flash chromatography eluting with 2:1 EtOAc/Hex, to give **169** (538 mg, 93 %). *R*_f 0.51 (2:1 EtOAc/Hex). [α]_D²⁵ -23.8° (*c* 1.0, CHCl₃). ¹H NMR (400 MHz, CDCl₃): δ 1.03 (d, *J* = 6.3 Hz, 3H), 1.15 (s, 9H), 1.27 (s, 9H), 1.91-2.03 (m, 1H), 2.10-2.20 (m, 1H), 3.48 (t, *J* = 8.5 Hz, 1H), 3.53-3.67 (m, 4H), 3.87 (app. t, *J* = 9.2 Hz, 1H), 4.02-4.62 (m, 6H), 4.94 (app. dd, *J* = 8.0, 13.3 Hz, 1H), 5.07 (d, *J* = 12.4 Hz, 1H), 5.17-5.20 (m, 1H), 5.96 (d, *J* = 5.8 Hz, 1H), 7.25-7.43 (m, 9H), 7.61 (app. d, *J* = 7.2 Hz, 2H), 7.76 (app. d, *J* = 7.2 Hz, 2H); ¹³C NMR (100 MHz, CDCl₃) δ 17.3, 27.5, 28.4, 33.0, 45.3, 47.4, 51.6, 59.0, 60.6, 63.0, 66.9, 67.1, 68.2, 73.5, 75.3, 120.2, 125.4, 127.3, 127.9, 128.2, 128.5, 128.8, 141.4, 143.9, 156.3, 169.4, 169.7, 170.1. HRMS (+TOF) calcd for C₄₂H₅₃N₃NaO₉(M + Na)⁺: 766.3680; obsd: 766.3688.

- **Fmoc-*D*-Thr-(*O*^tBu)-*D*-Ser(*O*^tBu)-*cis*-4-hyp(OMEM)-OBn (170).** The dipeptide acid **165** (375 mg, 0.69 mmol, 1.2 equiv.) and HCl.hyp(OMEM)-OBn (**140**) (200 mg, 0.58 mmol, 1.0 equiv.) were dissolved in CH₂Cl₂ (4 mL), and the solution cooled to 0 °C. Collidine (183 µL, 168 mg, 1.39 mmol, 2.4 equiv.) and HATU (264 mg, 0.69 mmol, 1.2 equiv.) were added sequentially to the reaction mixture. The resultant solution was stirred at 0 °C for 1 h and then at rt overnight. The mixture was concentrated and the product isolated by flash chromatography eluting with 2:1 EtOAc/Hex, to give **170** (163 mg, 87 %). *R*_f 0.40 (2:1 EtOAc/Hex). [α]_D²⁵ -33.9° (*c* 1.0, CHCl₃). ¹H NMR (400 MHz, CDCl₃) δ 1.00 (d, *J* = 6.3 Hz, 3H), 1.13 (s, 9H), 1.27 (s, 9H), 2.10-2.45 (m, 2H), 3.30-3.66 (m, 11H), 3.71 (dd, *J* = 11.0, 3.2

Hz, 1H), 4.05-4.45 (m, 5H), 4.54 (d, $J = 7.2$ Hz, 1H), 4.60 (d, $J = 7.0$ Hz, 1H), 4.67 (dd, $J = 8.6, 4.5$ Hz, 1H), 4.90 (dt, $J = 8.4, 4.2$ Hz, 1H), 5.06 (d, $J = 12.4$ Hz, 1H), 5.16 (d, $J = 12.4$ Hz, 1H), 5.93 (d, $J = 5.8$ Hz, 1H), 7.24-7.44 (m, 9H), 7.61 (app.t, $J = 7.4$ Hz, 2H), 7.76 (d, $J = 7.4$ Hz, 2H); ^{13}C NMR (100 MHz, CDCl_3) δ 17.0, 27.3, 28.2, 35.2, 47.2, 52.6, 57.2, 58.5, 59.0, 63.2, 66.6, 67.0, 67.1, 71.6, 72.4, 73.5, 74.6, 75.1, 94.2, 119.9, 125.2, 127.0, 127.7, 128.0, 128.4, 128.6, 135.9, 141.3, 156.0, 169.0, 169.6, 170.7. HRMS (+TOF) calcd for $\text{C}_{46}\text{H}_{62}\text{N}_3\text{O}_{11}(\text{M} + \text{H})^+$: 832.4378; obsd: 832.4378.

- **Fmoc-*D*-Thr-(*O*'Bu)-*D*-Ser(*O*'Bu)-DHP(OMEM)₂-OBn (**167**)**. The dipeptide acid **165** (138 mg, 0.26 mmol, 1.2 equiv.) and HCl.DHP(OMEM)₂-OBn (**157**) (96 mg, 0.21 mmol, 1.0 equiv.) were dissolved in CH_2Cl_2 (3 mL), and the solution cooled to 0 °C. Collidine (68 μL , 62 mg, 0.51 mmol, 2.4 equiv.) and HATU (97 mg, 0.26 mmol, 1.2 equiv.) were added sequentially to the reaction mixture. The resultant solution was stirred at 0 °C for 1 h and then at rt overnight. The mixture was concentrated and the product isolated by flash chromatography eluting with 2:1 EtOAc/Hex, to give **167** (183 mg, 92 %). R_f 0.44 (2:1 EtOAc/Hex). $[\alpha]_D^{25} -22.7^\circ$ (c 1.0, CHCl_3). ^1H NMR (400 MHz, CDCl_3) δ 0.98 (d, $J = 7.3$ Hz, 3H), 1.13 (s, 9H), 1.27 (s, 9H), 3.37 (s, 6H), 3.42-3.83 (m, 11H), 4.03-4.22 (m, 2H), 4.24 (t, $J = 7.0$ Hz, 1H), 4.31 (dd, $J = 11.0, 5.4$ Hz, 1H), 4.34-4.43 (m, 4H), 4.50 (d, $J = 7.2$ Hz, 1H), 4.73-4.84 (m, 4H), 4.92 (ddd, $J = 8.1, 7.6, 4.7$ Hz, 1H), 5.05 (d, $J = 12.4$ Hz, 1H), 5.17 (d, $J = 12.4$ Hz, 1H), 5.92 (d, $J = 5.8$ Hz, 1H), 7.26-7.44 (m, 9H), 7.61 (app.t, $J = 7.2$ Hz, 2H), 7.76 (d, $J = 7.6$ Hz, 2H); ^{13}C NMR (100 MHz, CDCl_3) δ ^{13}C NMR (100 MHz, CDCl_3) δ 17.2, 27.4, 28.4, 47.4, 51.3, 59.2, 63.9, 67.0, 67.2, 67.6, 71.8, 73.8, 75.4, 78.7, 80.9, 94.7, 120.2, 125.4, 127.3, 127.9, 128.3, 128.6, 128.7, 136.0, 141.5, 143.9, 156.2, 168.5, 169.3, 170.3. MALDI-TOF (+TOF) calcd for $\text{C}_{46}\text{H}_{62}\text{N}_3\text{O}_{11}(\text{M} + \text{Na})^+$: 958.467; obsd: 958.526.

- Fmoc-D-Thr-D-Ser-Pro-OBn (172).** Titanium tetrachloride (1.0 M solution in CH₂Cl₂, 1.8 mL, 1.8 mmol, 6.0 equiv.) and thioanisole (35 μ L, 37 mg, 0.30 mmol, 1.0 equiv.) were added sequentially to a solution of **168** (217 mg, 0.30 mmol, 1.0 equiv.) in CH₂Cl₂ (5 mL) at 0 °C under N₂. The reaction mixture was stirred and gradually warmed to rt over 30 min, then quenched with saturated NH₄Cl solution (~ 4 mL) and extracted with EtOAc (3 \times 20 mL). The organic extracts were combined, filtered through MgSO₄ and concentrated. The residue was purified by flash chromatography eluting with 2:1 EtOAc/Hex, then 9:1 CH₂Cl₂/MeOH to give the product as a colorless foam (143 mg, 80 %). *R*_f 0.39 (9:1 CH₂Cl₂/CH₃OH). [α]_D²⁵ -20.0° (*c* 1.0, CH₃OH). ¹H NMR (400 MHz, CD₃OD) δ 1.16 (d, *J* = 6.2 Hz, 3H, Thr CH₃), 1.82-2.08 (m, 3H, Pro 2H β , H γ), 2.14-2.32 (m, 1H, Pro H γ), 3.63-3.87 (m, 4H, Ser 2H β , Pro 2H δ), 4.09-4.17 (m, 1H, Thr H α), 4.23 (t, *J* = 6.8 Hz, 1H, Fmoc CH), 4.38 (d, *J* = 6.8 Hz, 2H, Fmoc CH₂), 4.47 (dd, *J* = 8.7, 3.8 Hz, 1H, Thr H β), 4.82-4.92 (m, 2H, Pro H α , Ser H α), 5.02 (d, *J* = 12.4 Hz, 1H, COOCH₂Ph), 5.06 (d, *J* = 12.4 Hz, 1H, COOCH₂Ph), 7.25-7.34 (m, 7H), 7.38 (t, *J* = 7.5 Hz, 2H), 7.67 (dd, *J* = 12.8, 7.4 Hz, 2H), 7.78 (d, *J* = 7.6 Hz, 2H); ¹³C NMR (100 MHz, CD₃OD) δ 18.1, 23.6, 28.1, 46.4, 52.2, 58.7, 60.0, 60.5, 60.8, 65.8, 66.2, 66.5, 118.9, 124.2, 126.2, 126.8, 127.0, 127.4, 127.7, 135.3, 140.6, 143.1, 156.7, 168.8, 170.8, 171.3. HRMS (+TOF) calcd for C₃₄H₃₈N₃O₈ (M + H)⁺: 616.2653; obsd: 616.2664.

- Fmoc-D-Thr-D-Ser-trans-3-Hyp-OBn (173).** Titanium tetrachloride (1.0 M solution in CH₂Cl₂, 3.8 mL, 3.87 mmol, 6.0 equiv.) was added gradually to a solution of **169** (480 mg, 0.65 mmol, 1.0 equiv.) in CH₂Cl₂ (10 mL) at 0 °C under N₂. The reaction mixture was stirred and gradually warmed to rt over 1 h, quenched with saturated NH₄Cl solution (~ 6 mL), diluted with H₂O (20 mL) and extracted with EtOAc (3 \times 50 mL). The organic extracts were combined, filtered through MgSO₄ and concentrated. The residue was purified by flash chromatography eluting with 9:1 CH₂Cl₂/MeOH to give the product as a

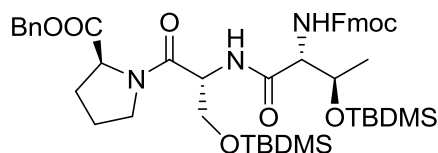
colorless foam (344 mg, 85 %). R_f 0.37 (9:1 CH₂Cl₂/CH₃OH). $[\alpha]_D^{25} +11.2^\circ$ (c 1.0, CH₃OH). ¹H NMR (400 MHz, CD₃OD) δ 1.17 (d, J = 6.1 Hz, 3H, Thr CH₃), 1.90-2.04 (m, 1H, 3-Hyp H γ), 2.08-2.18 (m, 1H, 3-Hyp H γ), 3.75 (dd, J = 11.3, 5.3 Hz, 1H, Ser H β), 3.82 (dd, J = 11.3, 5.0 Hz, 1H, Ser H β), 3.82-3.92 (m, 1H, 3-Hyp H δ), 3.92-4.10 (m, 1H, 3-Hyp H δ), 4.11-4.20 (m, 1H, Thr H α), 4.26 (t, J = 6.8 Hz, 1H, Fmoc CH), 4.34-4.46 (m, 3H, 3-Hyp H β , 3-Hyp H α , Thr H β), 4.41 (d, J = 6.8 Hz, 2H, Fmoc CH₂), 4.94 (app. pentet, J = 11.7, 5.6, Hz, 1H, Ser H α), 5.06 (d, J = 12.5 Hz, 1H, COOCH₂Ph), 5.10 (d, J = 12.5 Hz, 1H, COOCH₂Ph), 5.24 (d, J = 3.2 Hz, 1H, NH Thr), 7.28-7.43 (m, 10H, NH Ser, 4 \times Fmoc CH, 5 \times COOCH₂Ph), 7.70 (dd, J = 11.5, 7.4 Hz, 2H, Fmoc CH), 7.81 (d, J = 7.4 Hz, 2H, Fmoc CH); ¹³C NMR (100 MHz, CDCl₃) δ 18.0, 31.8, 44.4, 52.2, 59.9, 66.0, 66.5, 67.4, 72.0, 118.9, 124.2, 126.2, 127.1, 127.5, 135.1, 140.6, 143.1, 156.6, 169.1, 169.2, 170.9. HRMS (+TOF) calcd for C₃₄H₃₈N₃O₉ (M)⁺: 632.2603; obsd: 632.2594.

- **Fmoc-*D*-Thr-*D*-Ser-*cis*-4-hyp-OBn (174).** Titanium tetrachloride (1.0 M solution in CH₂Cl₂, 3.6 mL, 3.76 mmol, 9.0 equiv.) was added gradually to a solution of **170** (348 mg, 0.42 mmol, 1.0 equiv.) in CH₂Cl₂ (18 mL) at 0 °C under N₂. The reaction mixture was stirred and gradually warmed to rt over 1 h, quenched with saturated NH₄Cl solution (~ 5 mL), diluted with H₂O (15 mL) and extracted with EtOAc (3 \times 30 mL). The organic extracts were combined, filtered through MgSO₄ and concentrated. The residue was purified by flash chromatography eluting with 9:1 CH₂Cl₂/MeOH to give the product as a colorless foam (223 mg, 84 %). R_f 0.29 (9:1 CH₂Cl₂/CH₃OH). $[\alpha]_D^{25} +20.6^\circ$ (c 1.0, CH₃OH). ¹H NMR (400 MHz, CD₃OD) δ 1.16 (d, J = 6.3 Hz, 3H, Thr CH₃), 2.06 (dt, J = 13.3, 3.5 Hz, 1H, hyp H β), 2.38 (ddd, J = 13.5, 9.0, 4.7 Hz, 1H, hyp H β), 3.66-3.81 (m, 3H, Ser 2 H β , hyp H δ), 3.93 (dd, J = 10.9, 5.1 Hz, 1H, hyp H δ), 4.07-4.17 (m, 1H, Thr H α), 4.23 (t, J = 6.8 Hz, 1H, Fmoc CH), 4.33-4.45 (m, 4H, Fmoc CH₂, Thr H β , hyp H γ), 4.54 (dt, J = 7.6, 3.9 Hz, 1H, Ser H α), 4.59 (dd, J = 9.2, 3.8 Hz, 1H, hyp

H α), 5.05 (d, J = 8.5 Hz, 1H, COOCH₂Ph) , 5.20 (d, J = 8.5 Hz, 1H, COOCH₂Ph), 7.20-7.45 (m, 7H), 7.60-7.73 (m, 2H), 7.78 (d, J = 7.4 Hz, 2H), 8.15 (d, J = 8.4 Hz, 2H); ¹³C NMR (100 MHz, CD₃OD) δ 18.1, 36.1, 51.9, 53.9, 57.3, 59.9, 60.8, 65.9, 66.2, 66.5, 67.2, 68.8, 118.9, 124.2, 126.2, 126.7, 127.1, 127.3, 127.5, 135.2, 140.6, 143.1, 156.7, 169.1, 170.9, 171.5. HRMS (+TOF) calcd for C₃₄H₃₈N₃O₉(M + H)⁺: 632.2603; obsd: 632.2614.

• **Fmoc-*D*-Thr-*D*-Ser-DHP-OBn (171).** Titanium tetrachloride (1.0 M solution in CH₂Cl₂, 1.3 mL, 1.28 mmol, 9.0 equiv.) was added gradually to a solution of **167** (133 mg, 0.14 mmol, 1.0 equiv.) in CH₂Cl₂ (6 mL) at 0 °C under N₂. The reaction mixture was stirred and gradually warmed to rt over 1 h, quenched with saturated NH₄Cl solution (~ 3 mL), diluted with H₂O (15 mL) and extracted with EtOAc (3 \times 30 mL). The organic extracts were combined, filtered through MgSO₄ and concentrated. The residue was purified by flash chromatography eluting with 9:1 CH₂Cl₂/MeOH to give the product as a colorless foam (93 mg, 98 %). R_f 0.24 (9:1 CH₂Cl₂/CH₃OH). [α]_D²⁵ +0.8° (c 1.0, CH₃OH). ¹H NMR (400 MHz, CD₃OD, signals are reported for the major conformer only) 1.15 (d, J = 6.2 Hz, 3H, Thr CH₃), 3.62 (dd, J = 7.2, 3.0 Hz, 1H, DHP H δ), 3.71 (d, J = 5.8 Hz, Ser H β), 3.76 (d, J = 5.9 Hz, Ser H β), 4.02 (dd, J = 10.9, 5.0 Hz, 1H, DHP H γ), 4.04-4.26 (m, 4H, Thr H α , Thr H β , Fmoc CH), 4.06 (ap. d J = 4.4 Hz, 1H, DHP H α), 4.31-4.49 (m, DHP H δ , Fmoc CH₂), 4.58 (dd, J = 7.8, 4.4 Hz, 1H, DHP H β), 4.90 (app. t, J = 6.3 Hz, 1H, Ser H α), 5.04 (s, 2H, COOCH₂Ph), 7.22-7.42 (m, 7H), 7.64 (d, J = 7.4 Hz, 2H), 7.77 (d, J = 7.4 Hz, 2H); δ ¹³C NMR (100 MHz, CD₃OD) δ 18.1, 51.9, 60.0, 65.2, 66.0, 66.2, 66.6, 71.9, 74.0, 77.3, 78.8, 118.9, 124.2, 126.2, 126.8, 127.1, 127.3, 127.5, 135.2, 140.6, 143.1, 156.7, 168.4, 169.5, 170.2, 171.0. HRMS (+TOF) calcd for C₄₆H₆₂N₃O₁₁(M + H)⁺: 832.4378; obsd: 832.4378.

• **Fmoc-*D*-Thr-(OTBS)-*D*-Ser(OTBS)-Pro-OBn (48).** 2,6-Lutidine (104 μ L, 96 mg, 0.89 mmol, 9.2 equiv.), followed by TBDMSOTf (102 μ L, 118 mg, 0.45 mmol, 4.6 equiv.) were added to a solution of the tripeptide (60 mg, 0.10 mmol, 1 equiv.) in CH_2Cl_2 (2 mL) at 0 $^\circ\text{C}$ under N_2 . The mixture was stirred and warmed to rt overnight, diluted with CH_2Cl_2 (15 mL), washed with brine (15 mL). The brine layer was extracted further with CH_2Cl_2 (3×10 mL). The organic extracts were combined, filtered through MgSO_4 and concentrated. The residue was purified by flash chromatography eluting with 2:1 Hex/EtOAc to give **48** (67 mg, 82 %). R_f 0.38 (2:1 Hex/EtOAc). $[\alpha]_D^{25}$ -32.5 $^\circ$ (c 1.0, CHCl_3). ^1H NMR (400 MHz, CDCl_3) δ 0.01 (s, 6H, Si- $\text{CH}_3 \times 2$), 0.03 (s, 6H, Si- $\text{CH}_3 \times 2$), 0.85 (s, 9H, SiC(CH_3) $_3$), 0.94 (s, 9H, SiC(CH_3) $_3$), 1.05 (d, J = 6.2 Hz, 3H, Thr CH_3), 1.85-2.25 (m, 4H, Pro 2H β , 2H γ), 3.67 (t, J = 9.1 Hz, 1H, Ser H β), 3.76-3.88 (m, 3H, Ser H β , Pro 2H δ), 4.17 (dd, J = 6.7, 2.8 Hz, 1H, Thr H α), 4.24 (t, J = 7.1 Hz, 1H, Fmoc CH), 4.34 (dd, J = 6.4, 3.1 Hz, 1H, Thr H β), 4.35-4.44 (m, 2H, Fmoc CH_2), 4.52 (dd, J = 8.3, 3.6 Hz, 1H, Pro H α), 4.97 (qd, 9.1, 6.8 Hz, 1H, Ser H α), 5.09 (s, 2H, COOCH_2Ph), 5.76 (d, J = 6.8 Hz, 1H, Thr NH), 7.27-7.43 (m, 9H), 7.61 (t, J = 6.7 Hz, 2H), 7.76 (d, J = 7.5 Hz, 2H); ^{13}C NMR (100 MHz, CDCl_3) δ -5.6, -5.1, -4.7, 17.9, 18.1, 18.2, 24.5, 25.7, 25.8, 29.3, 47.1, 47.2, 52.1, 59.0, 59.4, 64.2, 66.6, 67.0, 68.2, 119.9, 125.2, 127.1, 127.7, 128.0, 128.1, 128.5, 135.8, 141.3, 143.7, 144.0, 156.2, 169.2, 171.4. HRMS (+TOF) calcd for $\text{C}_{46}\text{H}_{66}\text{N}_3\text{O}_8\text{Si}_2$ ($\text{M} + \text{H}$) $^+$: 844.4383; obsd: 844.4385.



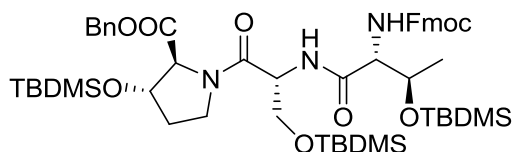
NMR Assignment

Position	^1H (ppm)	Multiplicity (J , Hz)	^{13}C (ppm)
Si(CH_3) $_2 \times 2$	0.01, 0.03	s	-5.6, -5.1, -4.7
SiC(CH_3) $_3 \times 2$	0.85, 0.94	s	17.9, 18.2, 25.7, 25.8
Residue 1 –Fmoc-Thr-			
Thr C=O	-	-	169.2
Thr α (1H)	4.17	dd (6.7, 2.8)	59.4
Thr β (1H)	4.34	dd (6.4, 3.1)	68.2

Thr γ (3H)	1.05	d (6.2)	18.1
Thr NH	5.76	d (6.8)	-
Fmoc C=O	-	-	156.2
Fmoc CH ₂	4.35-4.44	m	67.0
Fmoc CH	4.24	t (7.1)	47.1
Fmoc CH (4H)	7.27-7.43	m	119.9, 125.1, 125.2,
Fmoc CH (2H)	7.61	t (6.7)	127.1
Fmoc CH (2H)	7.76	d (7.5)	
Fmoc C 4°	-	-	141.2, 141.3, 143.7, 144.0
Residue 2 –Ser-			
Ser C=O	-	-	169.2
Ser α (1H)	4.97	qd (9.1, 6.8)	52.1
Ser β (2H)	3.67 3.76-3.88	t (9.1) m	64.2
Ser NH (1H)			-
Residue 3 –Pro-OBn			
Pro C=O	-	-	171.4
Pro α (1H)	4.52	dd (8.3, 3.6)	59.0
Pro β (2H)	1.85-2.25	m	24.5
Pro γ (2H)	1.85-2.25	m	29.3
Pro δ (2H)	3.76-3.88	m	47.2
Bn CH ₂	5.09	s	66.6
Bn C 4°	-	-	135.8
Bn CH (5)	7.27-7.43	m	127.7, 128.0, 128.1, 128.5

• **Fmoc-*D*-Thr-(OTBS)-*D*-Ser(OTBS)-*trans*-3-Hyp(OTBS)-OBn (49).** To a solution of the tripeptide (173 mg, 0.27 mmol, 1 equiv.) in CH₂Cl₂ (3 mL) at 0 °C under N₂, were added 2,6-lutidine (439 μ L, 405 mg, 3.78 mmol, 13.8 equiv.), then TBDMSOTf (434 μ L, 500 mg, 1.89 mmol, 6.9 equiv.). The mixture was stirred and warmed to rt overnight, diluted with CH₂Cl₂ (20 mL), washed with brine (20 mL), and then extracted with CH₂Cl₂ (3 \times 15 mL). The organic extracts were combined, filtered through MgSO₄ and concentrated. The residue was purified by flash chromatography eluting with 2:1 Hex/EtOAc to give **49** (242 mg, 91 %). *R*_f 0.42 (2:1 Hex/EtOAc). [α]_D²⁵ -17.4° (*c* 1.0, CHCl₃). ¹H NMR (400 MHz, CDCl₃) δ 0.02 (s, 6H), 0.03 (s, 6H), 0.12 (s, 3H), 0.14 (s, 3H), 0.84 (s, 9H), 0.86 (s, 9H),

0.93 (s, 9H), 1.05 (d, $J = 6.3$ Hz, 3H, Thr CH₃), 1.82-1.92 (m, 1H, 3-Hyp H γ), 2.06-2.18 (m, 1H, 3-Hyp H γ), 3.74 (app. t, $J = 8.8$ Hz, 1H, Ser H β), 3.81 (dd, $J = 9.4, 5.2$ Hz, 1H, Ser H β), 3.84-3.98 (m, 2H, 3-Hyp H δ), 4.18 (dd, $J = 6.4, 2.9$ Hz, 1H, Thr H α), 4.24 (t, $J = 7.2$ Hz, 1H, Fmoc CH), 4.26-4.39 (m, 2H, Thr H β , 3-Hyp H α), 4.28-4.36 (m, 2H, 3-Hyp H β and Thr H β), 4.39 (d, $J = 7.0$ Hz, 2H, Fmoc CH₂), 4.97 (td, $J = 8.0, 5.3$ Hz, 1H, Ser H α), 5.06 (d, $J = 12.3$ Hz, 1H, COOCH₂Ph), 5.13 (d, $J = 12.3$ Hz, 1H, COOCH₂Ph), 5.80 (d, $J = 6.6$ Hz, 1H, NH Thr), 7.27-7.46 (m, 10H, NH Ser, 4 \times Fmoc CH, 5 \times COOCH₂Ph), 7.61 (t, $J = 6.1$ Hz, 2H, Fmoc CH), 7.75 (d, $J = 7.5$ Hz, 2H, Fmoc CH); ¹³C NMR (100 MHz, CDCl₃) δ -5.6, -5.4, -5.1, -5.0, -4.9, -4.7, 17.9, 18.2, 25.7, 25.8, 25.9, 34.0, 45.6, 52.2, 59.3, 64.4, 66.6, 67.0, 68.2, 70.4, 119.9, 125.1, 127.1, 127.7, 127.8, 128.0, 128.3, 128.4, 128.6, 135.8, 141.3, 143.7, 144.0, 169.1, 169.3, 170.4. HRMS (+TOF) calcd for C₅₂H₇₉N₃O₉Si₃ (M)⁺: 974.5196; obsd: 974.5187.



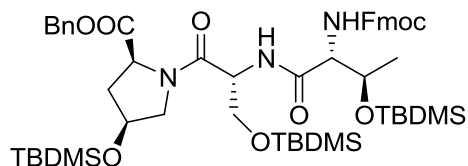
NMR Assignment

Position	¹ H (ppm)	Multiplicity (J , Hz)	¹³ C (ppm)
Si(CH ₃) ₂ x 3	0.02, 0.03, 0.12, 0.14	s	-5.6, -5.4, -5.1, -5.0, -4.9, -4.7
SiC(CH ₃) ₃ x 3	0.84, 0.86, 0.93	s	17.9, 18.1, 25.7, 25.8, 25.9
Residue 1 –Fmoc-Thr-			
Thr C=O			170.4
Thr α (1H)	4.18	dd (6.4, 2.9)	59.3
Thr β (1H)	4.28-4.36	m	68.2
Thr γ (3H)	1.05	d (6.3)	18.3
Thr NH	5.80	d (6.6)	
Fmoc C=O	-	-	156.2
Fmoc CH ₂	4.39	d (7.0)	67.0
Fmoc CH	4.24	t (7.2)	47.1
Fmoc CH (x 4)	7.28-7.47	m	119.9, 125.2, 127.1
Fmoc CH (x 2)	7.61	t (6.2)	127.7, 128.0, 128.2
Fmoc CH (x 2)	7.75	d (7.6)	

Fmoc C 4°(x 4)	-	-	141.3, 143.7, 144.0
Residue 2 –Ser-			
Ser C=O	-	-	169.1
Ser α (1H)	4.97	td (8.0, 5.3)	52.3
Ser β (2H)	3.74 3.81	app. t (8.8) dd (9.4, 5.2)	64.0
Ser NH (1H)	7.27-7.46	m	-
Residue 3 –Pro-OBn			
Pro C=O	-	-	169.3
Pro α (1H)	4.26-4.39	m	45.6
Pro β (1H)	4.28-4.36	m	74.2
Pro γ (2H)	1.82-1.92 2.06-2.18	m m	34.0
Pro δ (2H)	3.84-3.98 4.30-4.34	m m	68.4
Bn CH ₂	5.06 5.13	d (12.3) d (12.3)	66.7
Bn C 4°	-	-	135.6
Bn CH (5)	7.27-7.46	m	127.7, 128.0, 128.2 128.5

• **Fmoc-*D*-Thr-(OTBS)-*D*-Ser(OTBS)-*cis*-4-hyp(OTBS)-OBn (50).** To a solution of the tripeptide (300 mg, 0.48 mmol, 1 equiv.) in CH₂Cl₂ (5 mL) at 0 °C under N₂, were added 2,6-lutidine (761 μL, 702 mg, 6.56 mmol, 13.8 equiv.), then TBDMSOTf (753 μL, 867 mg, 3.28 mmol, 6.9 equiv.). The mixture was stirred and warmed to rt overnight, diluted with CH₂Cl₂ (30 mL), washed with brine (30 mL), and then extracted with CH₂Cl₂ (3 × 25 mL). The organic extracts were combined, filtered through MgSO₄ and concentrated. The residue was purified by flash chromatography eluting with 2:1 Hex/EtOAc to give **50** (460 mg, 99 %). *R_f* 0.40 (3:1 Hex/EtOAc). [α]_D²⁵ -17.4° (*c* 1.0, CHCl₃). ¹H NMR (400 MHz, CDCl₃) δ 0.01-0.14 (Singlets, Si-CH₃ × 6, 18H), 0.84-0.94 (Singlets, SiC(CH₃)₃ × 3, 27H), 1.01 (d, *J* = 6.2 Hz, 3H, Thr CH₃), 2.11 (dt, *J* = 12.9, 4.8 Hz, 1H, hyp Hβ), 2.28 (ddd, *J* = 12.9, 8.3, 5.0 Hz, 1H, hyp Hβ), 3.60 (dd, *J* = 7.2, 4.1 Hz, 1H, hyp Hδ), 3.63 (app.t, *J* = 9.2 Hz, 1H, Ser Hβ), 3.82 (dd, *J* = 9.2, 5.3 Hz, 1H, Ser Hβ), 4.11 (dd, *J* = 10.2, 5.7 Hz, 1H, hyp Hδ), 4.16 (dd, *J* = 7.0, 2.9 Hz, 1H, Thr

H α), 4.24 (t, J = 7.0 Hz, 1H, Fmoc CH), 4.33 (dd, J = 6.4, 2.9 Hz, 1H, Thr H β), 4.34-4.43 (m, 3H, Fmoc CH₂, hyp H γ), 4.62 (dd, J = 8.6, 5.0 Hz, 1H, hyp H α), 4.96 (ddd, J = 9.4, 8.0, 5.3 Hz, 1H, Ser H α), 5.05 (d, J = 12.2 Hz, 1H, COOCH₂Ph), 5.10 (d, J = 12.2 Hz, 1H, COOCH₂Ph), 5.70 (d, J = 7.0 Hz, 1H, NH Thr), 7.27-7.43 (m, 10H, NH Ser, 4 \times Fmoc CH, 5 \times COOCH₂Ph), 7.61 (t, J = 7.0 Hz, 2H, Fmoc CH), 7.75 (d, J = 7.4 Hz, 2H, Fmoc CH); ¹³C NMR (100 MHz, CDCl₃) δ -5.6, -5.4, -5.1, -5.0, -4.9, -4.7, 17.9, 18.2, 25.6, 25.7, 25.8, 38.2, 47.1, 51.8, 55.0, 57.5, 59.4, 64.4, 66.6, 67.0, 68.2, 70.4, 119.9, 125.1, 127.0, 127.7, 127.8, 128.0, 128.3, 128.4, 128.6, 135.8, 141.3, 143.7, 144.0, 156.2, 169.1, 169.3, 170.4. HRMS (+TOF) calcd for C₅₂H₇₉N₃O₉Si₃ (M + H)⁺: 974.5196; obsd: 974.5191.



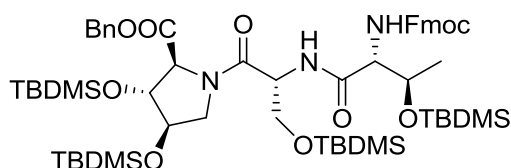
NMR Assignment

Position	¹ H (ppm)	Multiplicity (J , Hz)	¹³ C (ppm)
Si(CH ₃) ₂ x 3	0.00, 0.02, 0.03, 0.05 0.11, 0.13	s	-5.6, -5.4, -5.1, -5.0, -4.9, -4.7
Si(CH ₃) ₃ x 3	0.85, 0.93	s	17.9, 25.6, 25.7, 25.8
Residue 1 –Fmoc-Thr-			
Thr C=O			169.1
Thr α (1H)	4.16	dd (7.0, 2.9)	59.4
Thr β (1H)	4.33	dd (6.4, 2.9)	68.2
Thr γ (3H)	1.01	d (6.2)	18.2
Thr NH	5.70	d (7.0)	
Fmoc C=O	-	-	156.2
Fmoc CH ₂	4.34-4.43	m	67.0
Fmoc CH	4.24	t (7.0)	47.1
Fmoc CH (x 4)	7.27-7.43	m	119.9, 125.1, 127.0
Fmoc CH (x 2)	7.61	t (7.0)	127.7, 127.8
Fmoc CH (x 2)	7.75	d (7.4)	
Fmoc C 4°(x 4)	-	-	141.3, 143.7, 144.0
Residue 2 –Ser-			
Ser C=O	-	-	169.3
Ser α (1H)	4.96	ddd (9.4, 8.0, 5.3)	51.8

Ser β (2H)	3.54-3.68 3.82	m dd (9.0, 5.3)	64.4
Ser NH (1H)	7.27-7.43	m	-
Residue 3 –Pro-OBn			
Pro C=O	-	-	170.4
Pro α (1H)	4.62	dd (8.6, 5.0)	57.5
Pro β (2H)	2.11 2.29	dt (12.9, 4.8) ddd (12.9, 8.3, 5.0)	38.2
Pro γ (1H)	4.34-4.43	m	55.0
Pro δ (2H)	3.82 4.11	dd (9.0, 5.3) dd (10.2, 5.7)	70.4
Bn CH ₂	5.05 5.10	d (12.2) d (12.2)	66.6
Bn C 4°	-	-	135.8
Bn CH (5)	7.27-7.43	m	127.7, 127.8, 128.0, 128.3, 128.4, 128.6

• **Fmoc-*D*-Thr-(OTBS)-*D*-Ser(OTBS)-DHP(OTBS)₂-OBn (47)**. To a solution of the tripeptide (76 mg, 0.12 mmol, 1 equiv.) in CH₂Cl₂ (3 mL) at 0 °C under N₂, was added 2,6-lutidine (251 μ L, 231 mg, 2.16 mmol, 18.4 equiv.), followed by TBDMSOTf (248 μ L, 285 mg, 1.08 mmol, 9.2 equiv.). The mixture was stirred and warmed to rt overnight, diluted with CH₂Cl₂ (25 mL), washed with brine (25 mL). The brine was further extracted with CH₂Cl₂ (3 \times 20 mL). The organic extracts were combined, filtered through MgSO₄ and concentrated. The residue was purified by flash chromatography eluting with 3:1 Hex/EtOAc to give **47** (95 mg, 74 %). *R_f* 0.50 (3:1 Hex/EtOAc). [α]_D²⁵ +6.1° (*c* 0.90, CHCl₃). ¹H NMR (400 MHz, CDCl₃) (M = major rotamer, m = minor rotamer) δ -0.01, 0.02, 0.03, 0.04, 0.05, 0.07, 0.09, 0.13, 0.16, 0.19, 0.20 (singlets, 24H, Si(CH₃)₂ \times 4, M, m), 0.83, 0.84, 0.85, 0.87, 0.88, 0.93, 0.95, 0.98 (singlets, 36H, SiC(CH₃)₃ \times 4, M, m), 1.05 (d, *J* = 6.3 Hz, 3H, Thr CH₃ γ), 3.51 & 3.74 (d, *J* = 12.6 Hz, 1H, DHP H δ , m), 3.72 & 3.84 (d, *J* = 10.6 Hz, 1H, DHP H δ , M), 3.79 (d, 6.7 Hz, 1H, Ser H β , M), 4.00 (dd, *J* = 7.7, 3.8 Hz, 1H, DHP H γ , m), 4.04 (d, *J* = 4.3 Hz, 1H, Ser H β , m), 4.10-4.18 (m, 1H, DHP H α , M), 4.17-4.22 (m, 1H, Thr H α , M, m), 4.25 (t, *J* = 7.5 Hz, 1H, Fmoc CH), 4.31 (s, 1H, DHP

H β , M), 4.33 (app. dd, $J = 7.3, 4.1$ Hz, 1H, Thr H β , M), 4.36-4.50 (m, 1H, Ser H α , m), 4.38 (d, $J = 6.8$ Hz, 2H, Fmoc CH₂), 4.49 (app. s, 1H, DHP H γ , M), 4.58 (app. s, DHP H β , m), 4.97 (app. q, $J = 7.4$ Hz, 1H, Ser H α , M), 5.09 (s, 1H, COOCH₂Ph, M), 5.10 (d, $J = 12.7$ Hz, 1H, COOCH₂Ph, M), 5.17 (s, 1H, COOCH₂Ph, m), 5.24 (d, $J = 12.7$ Hz, 1H, COOCH₂Ph, m), 5.78 (d, $J = 6.6$ Hz, 1H, NH Thr, M), 5.88 (d, $J = 5.3$ Hz, 1H, NH Thr, m), 7.26-7.40 (m, 7H, 2 \times Fmoc CH, 5 \times COOCH₂Ph), 7.40 (t, $J = 7.5$ Hz, 2H, Fmoc CH), 7.49 (d, $J = 8.1$ Hz, 1H, NH Ser, M), 7.52 (d, $J = 8.5$ Hz, 1H, NH Ser, m), 7.60 (d, $J = 6.5$ Hz, 1H, Fmoc CH), 7.63 (d, $J = 6.5$ Hz, 1H, Fmoc CH), 7.77 (d, $J = 7.5$ Hz, 2H, Fmoc CH); ¹³C NMR (100 MHz, CDCl₃) (major/minor rotamer) δ -5.3, -5.2, -5.1, -4.8, -4.7, -4.6, -4.5, 17.1, 18.0, 18.1, 18.2, 18.3, 18.5, 25.7, 25.8, 25.9, 26.0, 26.1, 47.4, 52.4, 53.8, 54.0, 54.1, 58.5, 59.5, 63.0, 64.2, 66.5, 66.8, 67.2, 68.2, 68.5, 74.9, 76.8, 80.3, 81.2, 120.1, 125.4, 127.2, 127.3, 127.9, 128.0, 128.1, 128.5, 128.6, 128.8, 135.5, 136.0, 141.5, 143.9, 144.3, 156.4, 169.2, 169.6, 170.2. HRMS (+TOF) calcd for C₅₈H₉₄N₃O₁₀Si₄ (M + H)⁺: 1104.6011; obsd: 1104.6010.



NMR Assignment

Position	¹ H (ppm) M = major m = minor	Multiplicity (J , Hz)	¹³ C (ppm)
Silyl Ether Protecting Groups			
Si(CH ₃) ₂ x 4	-0.01, 0.03, 0.04, 0.05, 0.07, 0.09, 0.13, 0.20, 0.02, 0.07, 0.16, 0.19	s	-5.3, -5.2, -5.1, -4.8, -4.7, -4.6, -4.5
SiC(CH ₃) ₃ x 4	0.83, 0.84, 0.85, 0.87, 0.88, 0.93, 0.95, 0.98	s	18.0, 18.1, 18.2, 18.3, 18.5, 25.7, 25.8, 25.9, 26.0, 26.1
Residue 1 –Fmoc-Thr-			

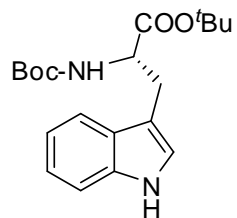
Thr C=O	-	-	169.2
Thr α	4.17-4.22 (M, m)	m	59.5 M, 58.5 m
Thr β	4.33	app. dd (7.3, 4.1)	68.5 M, 68.2 m
Thr γ	1.05	d (6.3)	17.1
Thr NH	5.78 M 5.88 m	d (6.6) d (5.3)	- -
Fmoc C=O	-	-	156.4
Fmoc CH ₂	4.38	d (6.8)	67.2
Fmoc CH	4.25	t (7.5)	47.4
Fmoc CH 2H	7.26-7.40	m	120.1, 125.4, 127.2, 127.3, 127.9, 128.0, 128.1
Fmoc CH 2H	7.40	t (7.5)	
Fmoc CH 1H	7.60	d (6.5)	
Fmoc CH 1H	7.63	d (6.5)	
Fmoc CH 2H	7.77	d (7.5)	
Fmoc C 4°(x 4)	-	-	141.5, 143.9, 144.3
Residue 2 –Ser-			
Ser C=O	-	-	169.6
Ser α	4.97 M 4.36-4.50 m	app. q (7.4) m	52.4 M
Ser β	3.79 M 4.04 m	d (6.7) d (4.3)	64.2 M 63.0 m
Ser NH	7.49 M 7.52 m	d (8.1) d (8.5)	- -
Residue 3 -DHP-OBn			
DHP C=O	-	-	170.2
DHP α	4.10-4.18 M	m	54.0
DHP β	4.31 M 4.58 m	s s	80.3 81.2
DHP γ	4.49 M 4.00 m	app. s dd (7.7, 3.8)	76.8 74.9
DHP δ	3.72 M, 3.84 M 3.51 m, 3.74 m	d (10.6) d (12.6)	54.1 M 53.8 m
Bn CH ₂	5.09 M 5.10 M 5.17 m 5.24 m	s d (12.7) s d (12.7)	66.8 66.5
Bn C 4°	-	-	135.5, 136.0
Bn CH (5)	7.26-7.37	m	128.1, 128.5, 128.6, 128.8

3.4.2 Spectra and HPLC Chromatograms

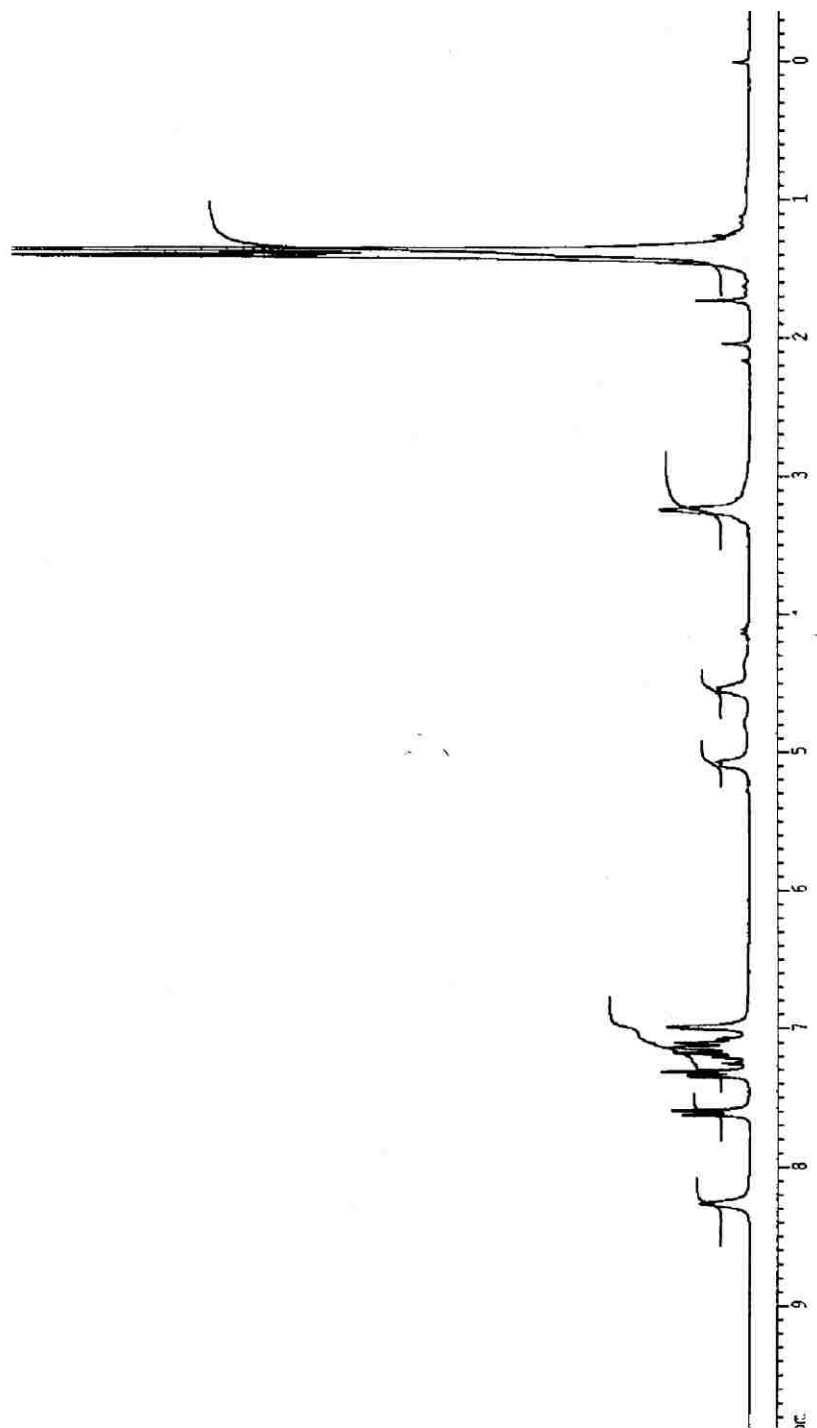
¹ H NMR spectrum of compound 124	122
¹³ C NMR spectrum of compound 124	123
¹ H NMR spectrum of compound 125	124
¹³ C NMR spectrum of compound 125	125
¹ H NMR spectrum of compound 126	126
¹³ C NMR spectrum of compound 126	127
¹ H NMR spectrum of compound 127	128
¹³ C NMR spectrum of compound 127	129
¹ H NMR spectrum of compound 129	130
¹³ C NMR spectrum of compound 129	131
¹ H NMR spectrum of compound 46	132
¹³ C NMR spectrum of compound 46	133
HPLC chromatogram of compound 46	134
¹ H NMR spectrum of compound 141a	135
¹³ C NMR spectrum of compound 141a	136
¹ H NMR spectrum of compound 142	137
¹³ C NMR spectrum of compound 142	138
¹ H NMR spectrum of compound 145	139
¹³ C NMR spectrum of compound 145	140
¹ H NMR spectrum of compound 156	141
¹³ C NMR spectrum of compound 156	142
¹ H NMR spectrum of compound 166	143
¹³ C NMR spectrum of compound 166	144
¹ H NMR spectrum of compound 168	145
¹³ C NMR spectrum of compound 168	146
¹ H NMR spectrum of compound 169	147
¹³ C NMR spectrum of compound 169	148
¹ H NMR spectrum of compound 170	149

¹³ C NMR spectrum of compound 170	150
¹ H NMR spectrum of compound 167	151
¹³ C NMR spectrum of compound 167	152
¹ H NMR spectrum of compound 172	153
¹³ C NMR spectrum of compound 172	154
¹ H NMR spectrum of compound 173	155
¹³ C NMR spectrum of compound 173	156
¹ H NMR spectrum of compound 174	157
¹³ C NMR spectrum of compound 174	158
¹ H NMR spectrum of compound 171	159
¹³ C NMR spectrum of compound 171	160
¹ H NMR spectrum of compound 48	161
¹³ C NMR spectrum of compound 48	162
HPLC chromatogram of compound 48	163
¹ H NMR spectrum of compound 49	164
¹³ C NMR spectrum of compound 49	165
HPLC chromatogram of compound 49	166
¹ H NMR spectrum of compound 50	167
¹³ C NMR spectrum of compound 50	168
HPLC chromatogram of compound 50	169
¹ H NMR spectrum of compound 47	170
¹³ C NMR spectrum of compound 47	171
HPLC chromatogram of compound 47	172

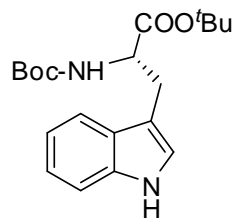
Boc-*L*-Trp-O'Bu (124) – ^1H NMR in CDCl_3 at 250 MHz



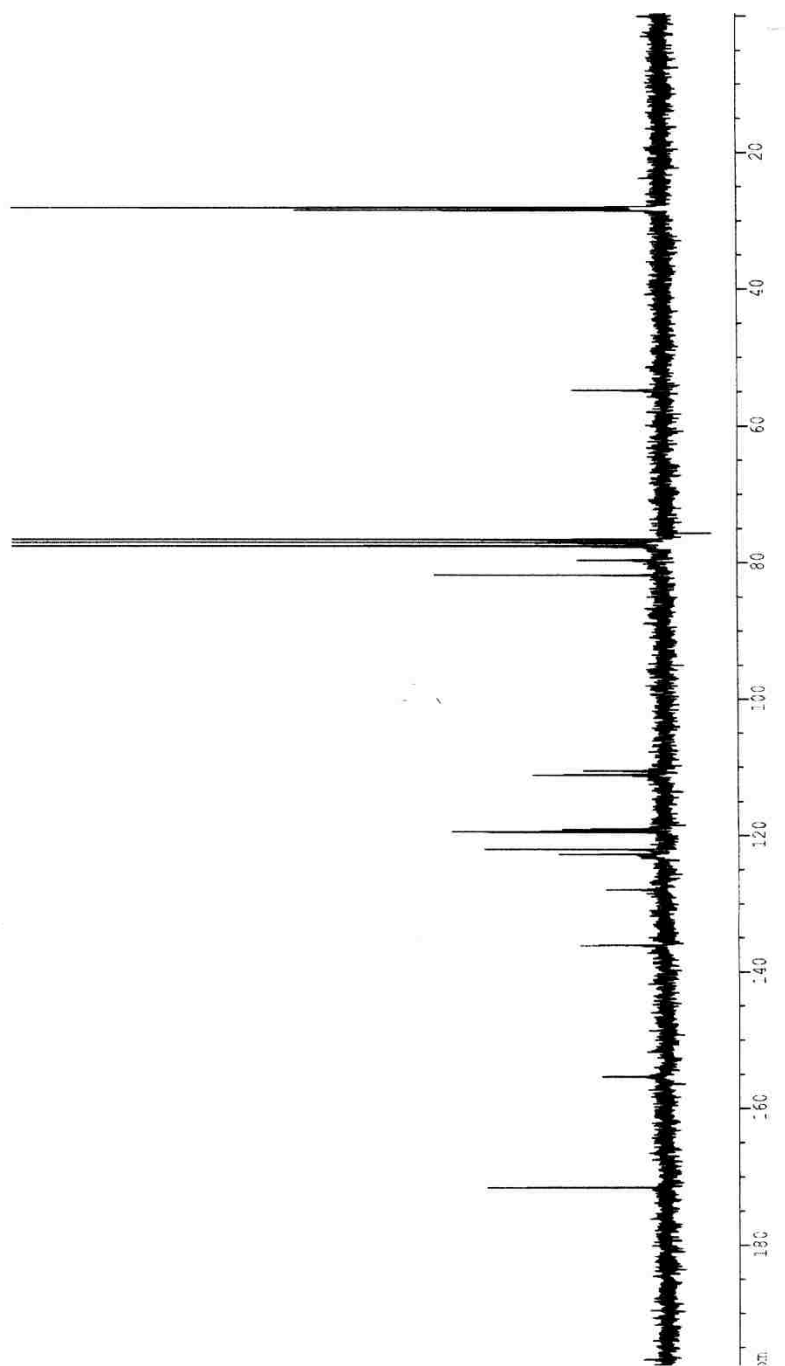
bej-1/77a



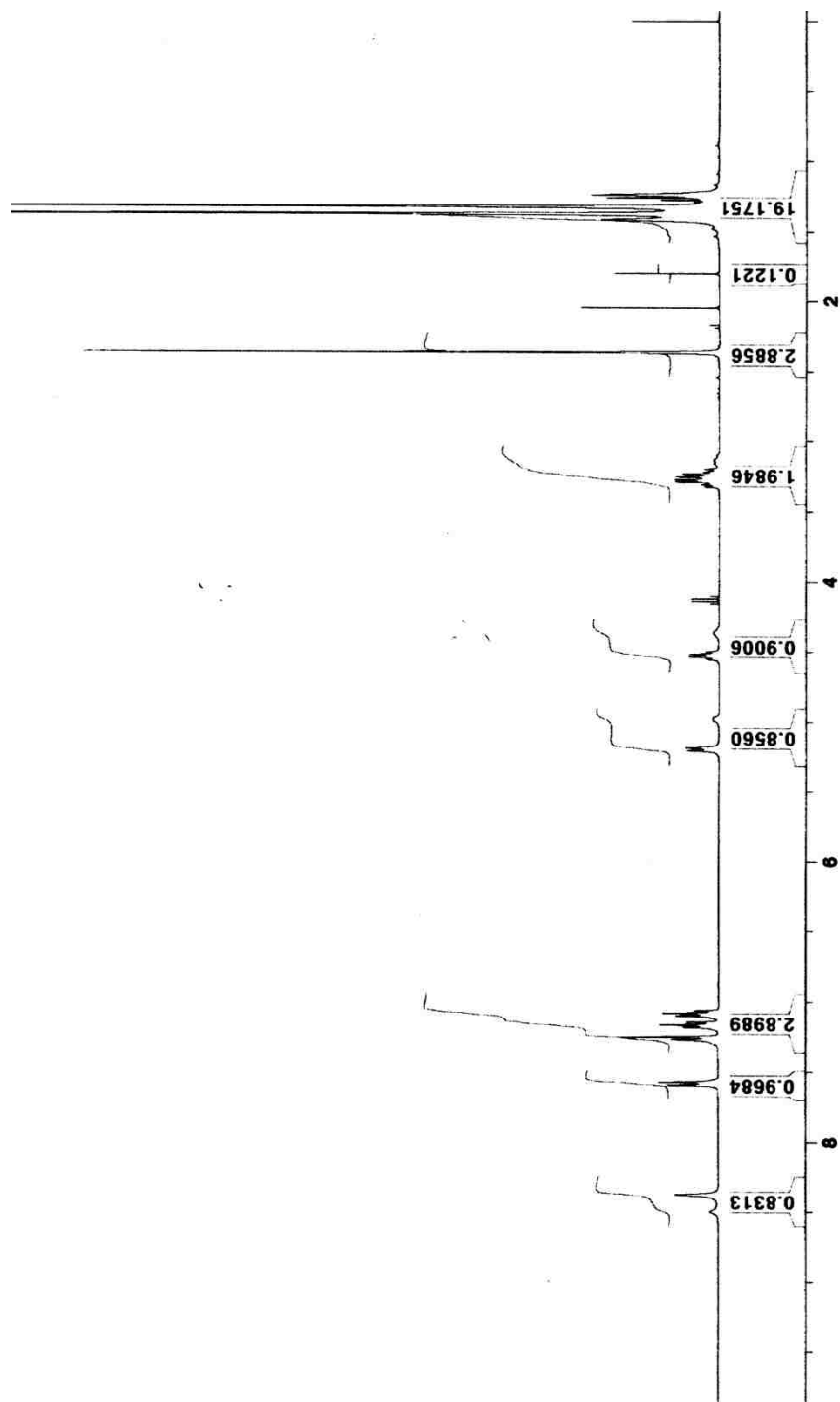
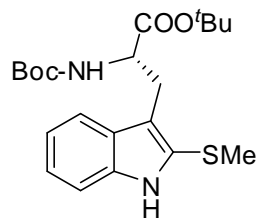
Boc-*L*-Trp-O^tBu (124) – ¹³C NMR in CDCl₃ at 62.5 MHz



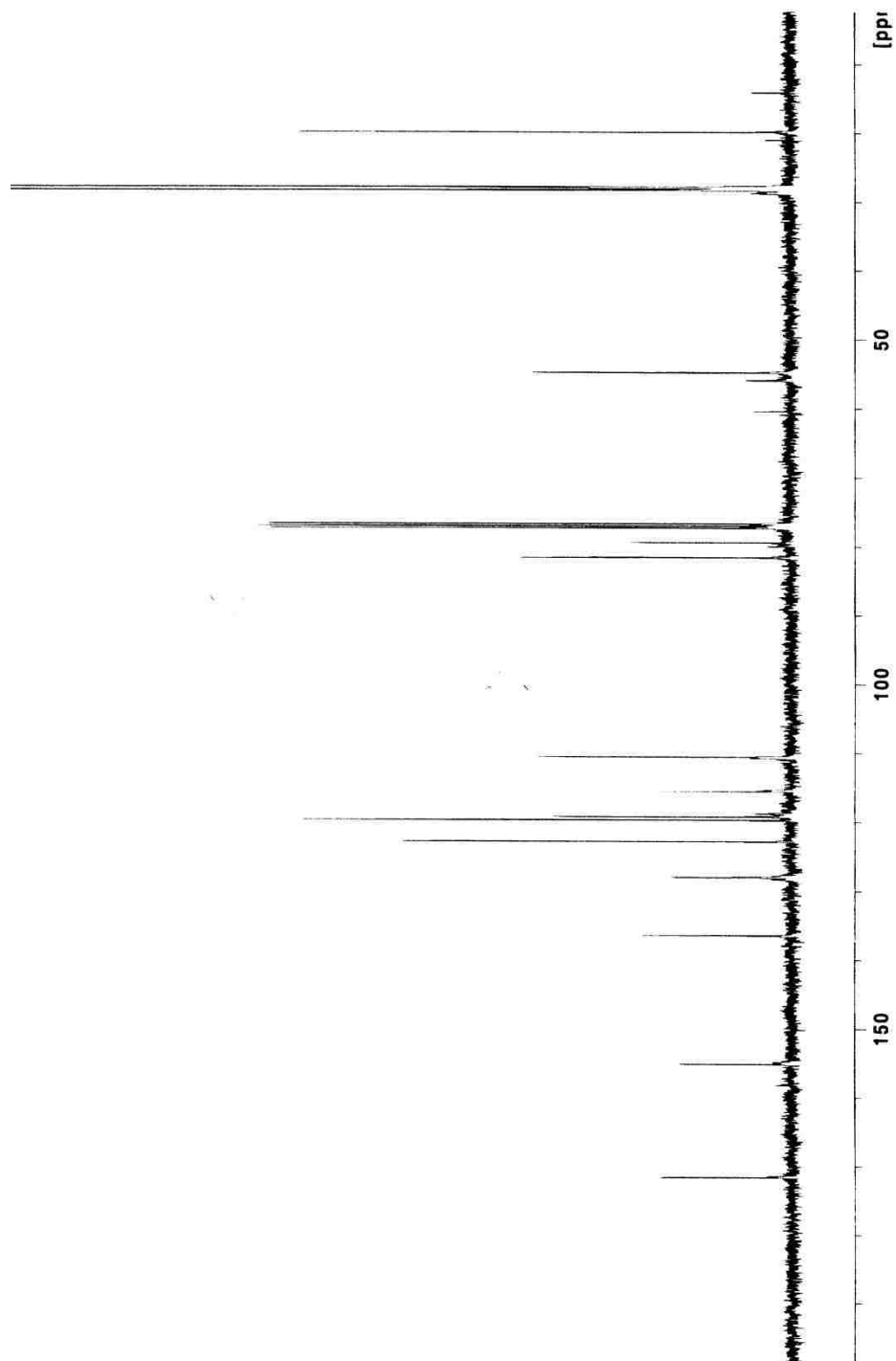
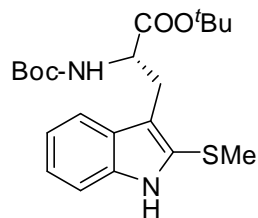
bej-177a



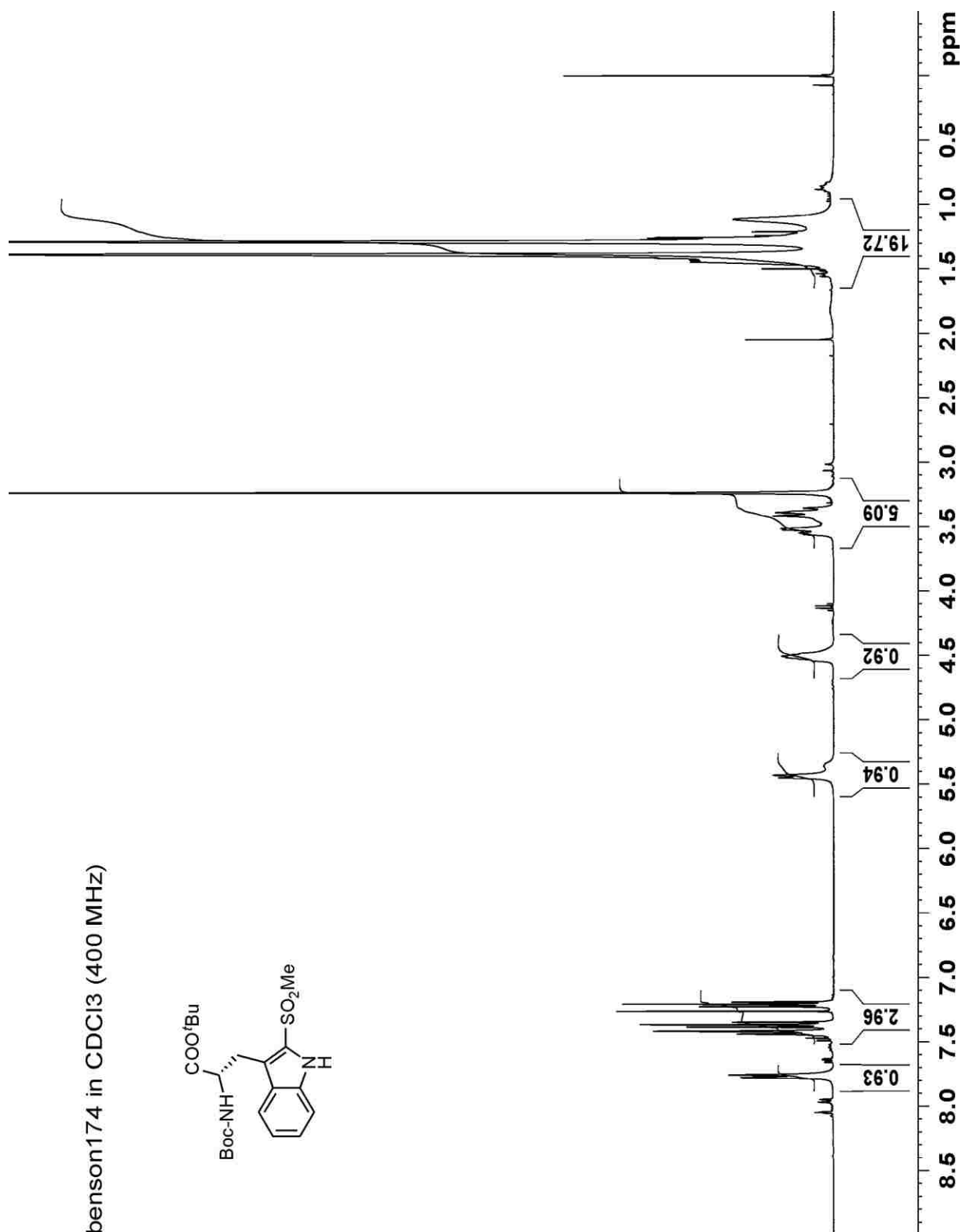
Boc-*L*-Trp(SMe)-O^tBu (125) – ¹H NMR in CDCl₃ at 400 MHz



Boc-*L*-Trp(SMe)-O^tBu (125)–¹³C NMR in CDCl₃ at 100 MHz

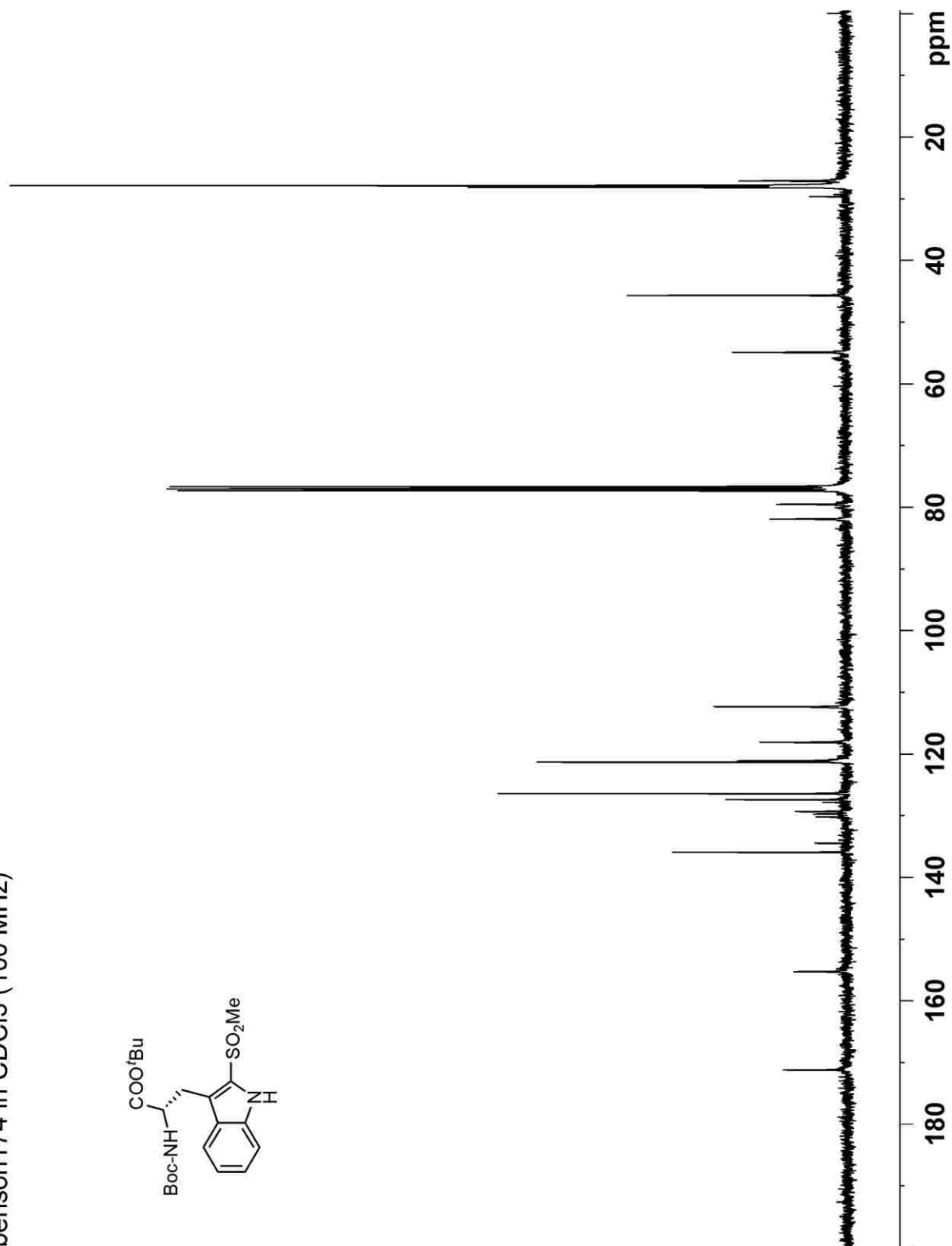
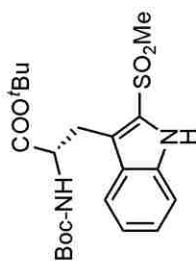


Boc-*L*-Trp(SO₂Me)-O^tBu (126) – ¹H NMR in CDCl₃ at 400 MHz



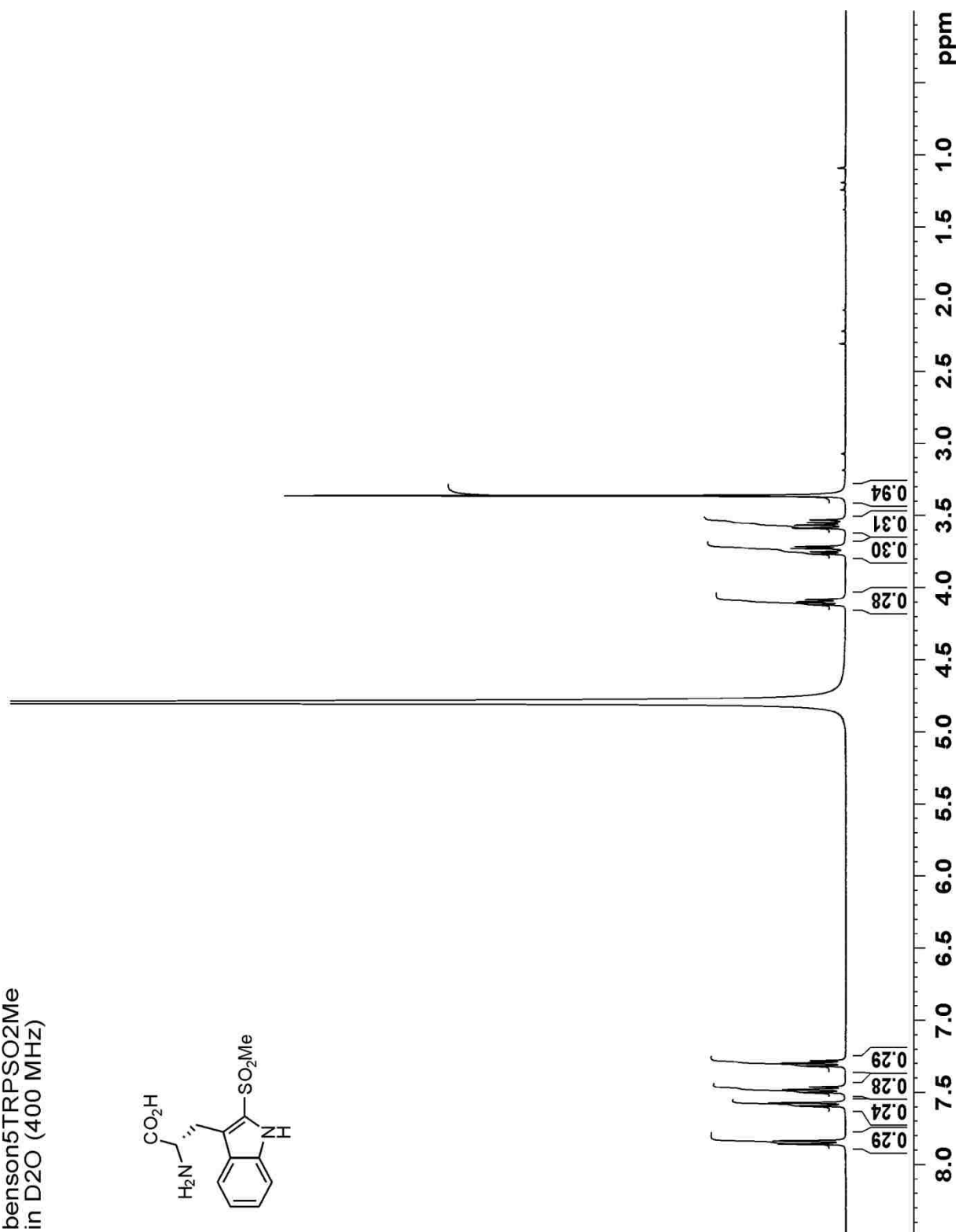
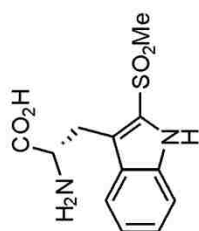
Boc-*L*-Trp(SO₂Me)-O^tBu (126) – ¹³C NMR in CDCl₃ at 100 MHz

beneson174 in CDCl3 (100 MHz)

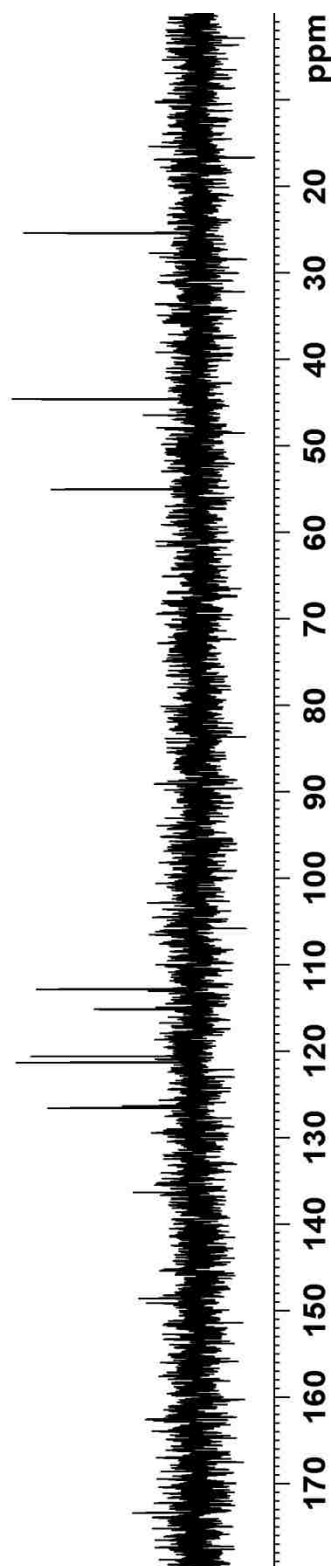
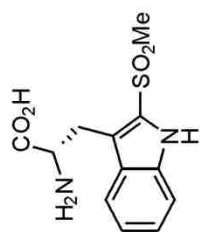


H-L-Trp(SO₂Me)-OH (127) - ¹H NMR in D₂O at 400 MHz

benzon5TRPSO2Me
in D2O (400 MHz)



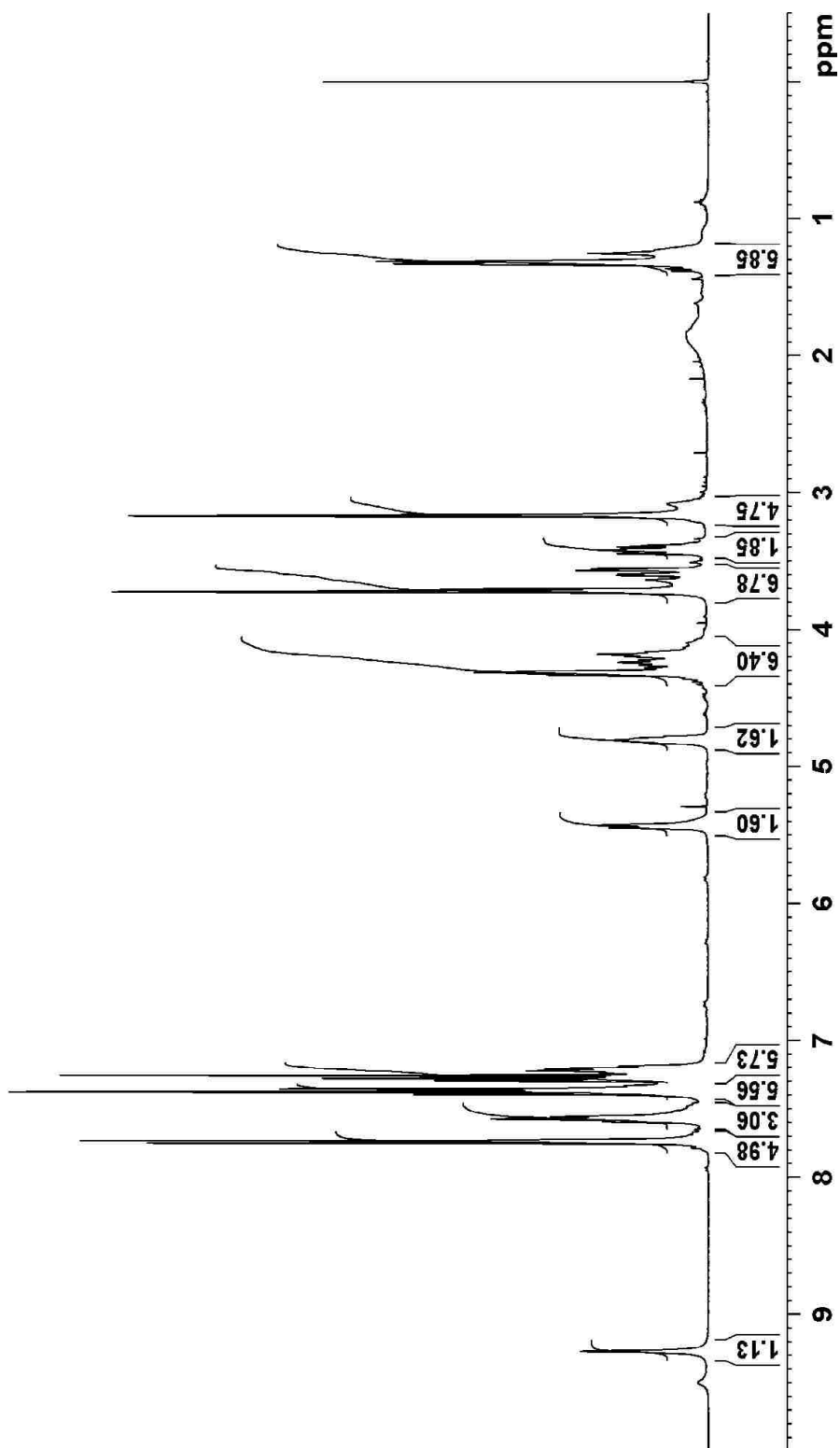
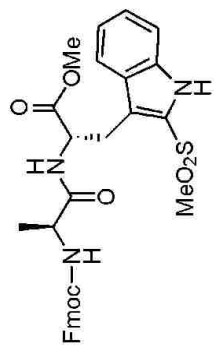
H-L-Trp(SO₂Me)-OH (127) -¹³C NMR in D₂O at 100 MHz



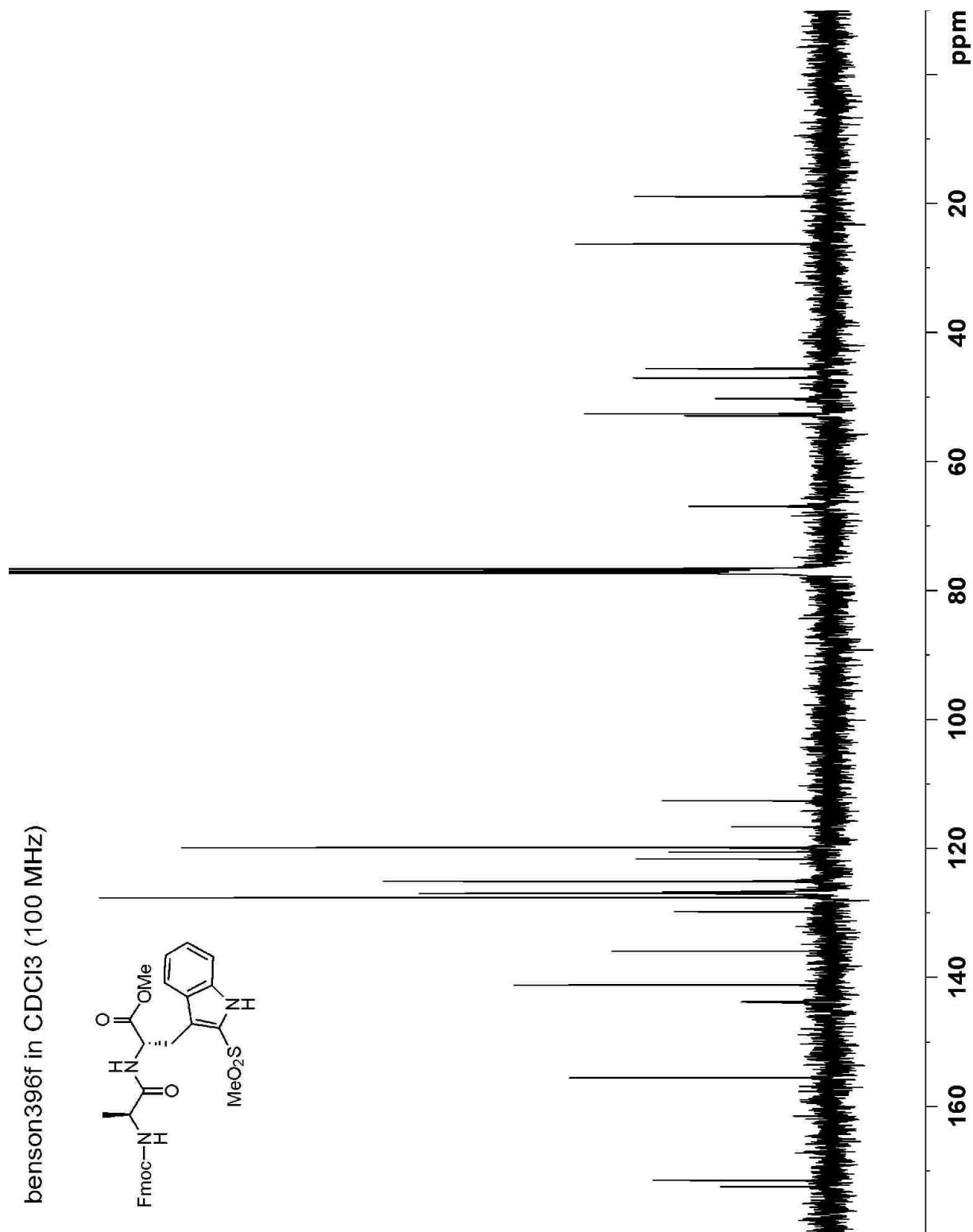
benso5TRPSO2Me
in D2O (100 MHz)

Fmoc-Ala-Trp(SO₂Me)-OMe (129)- ¹H NMR in CDCl₃ at 400 MHz

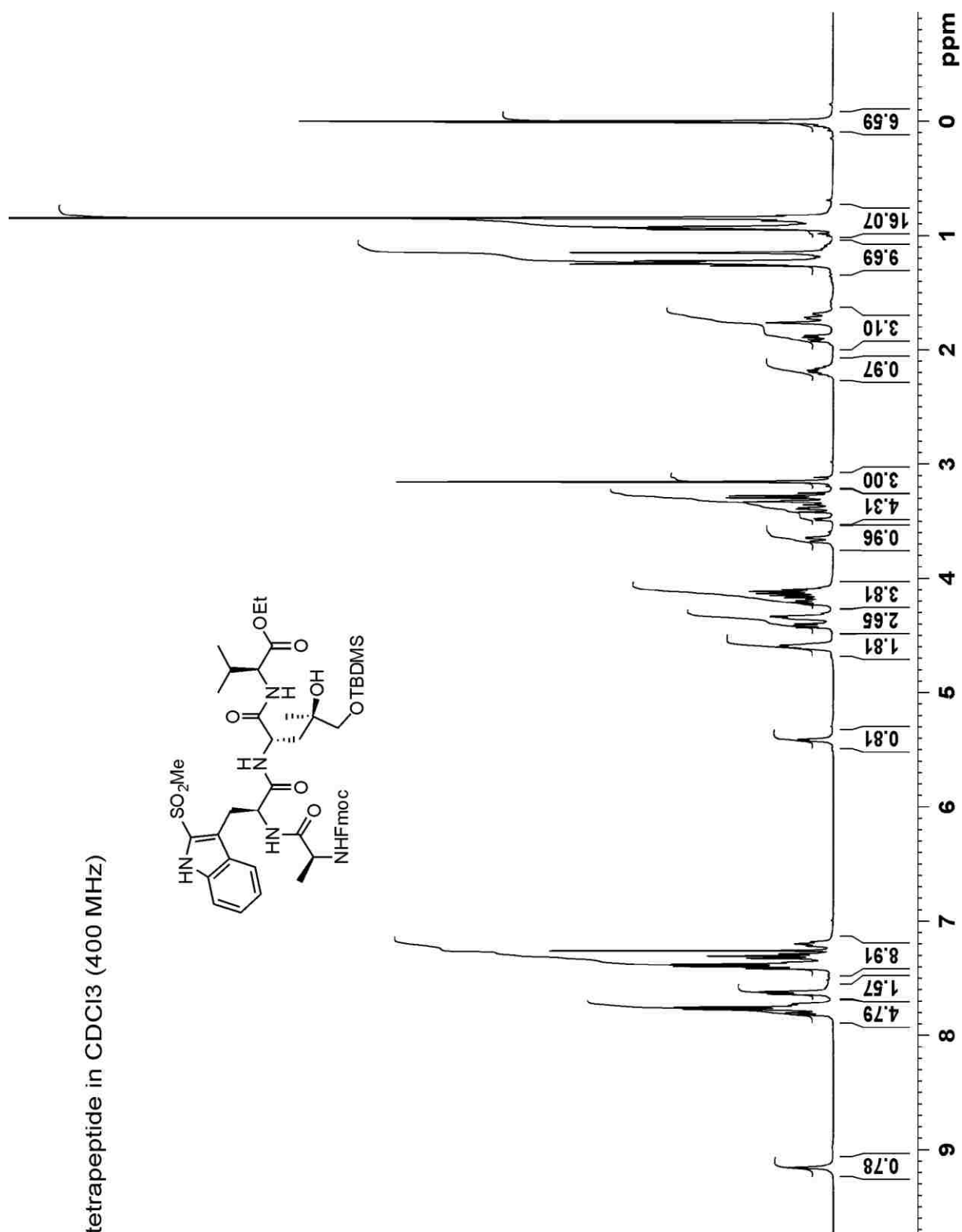
benson396f in CDCl₃ (400 MHz)



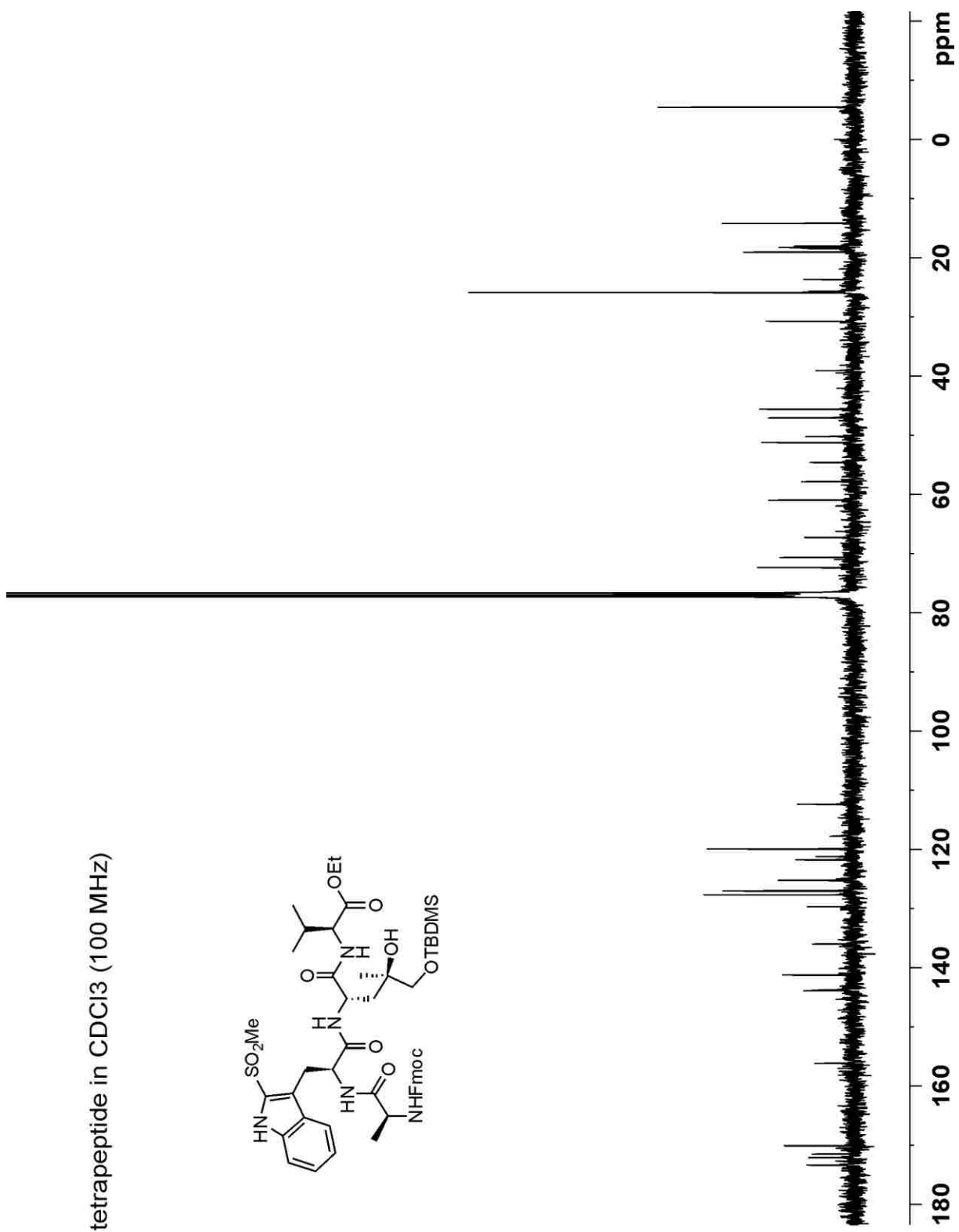
Fmoc-Ala-Trp(SO₂Me)-OMe (129)- ¹³C NMR in CDCl₃ at 100 MHz



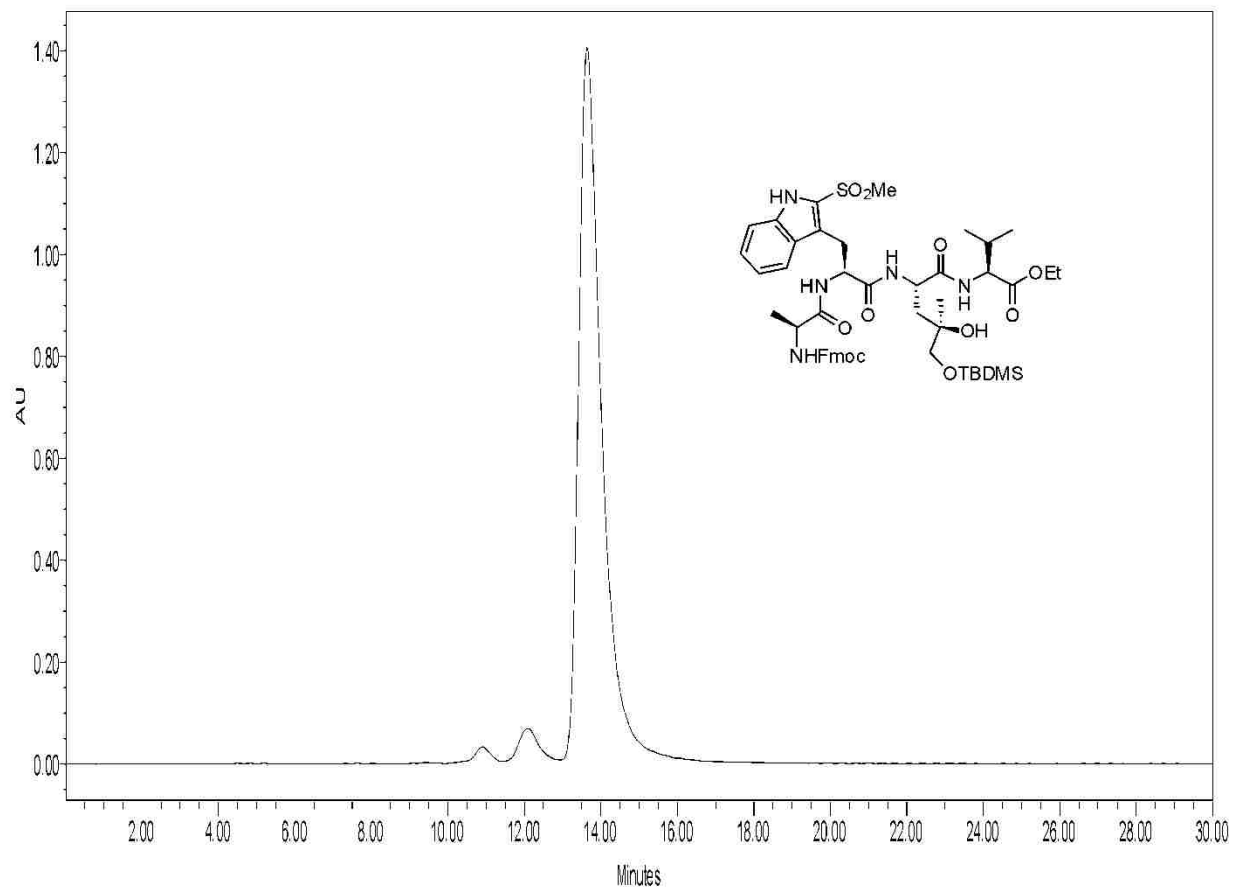
Tetrapeptide 46– ^1H NMR in CDCl_3 at 400 MHz



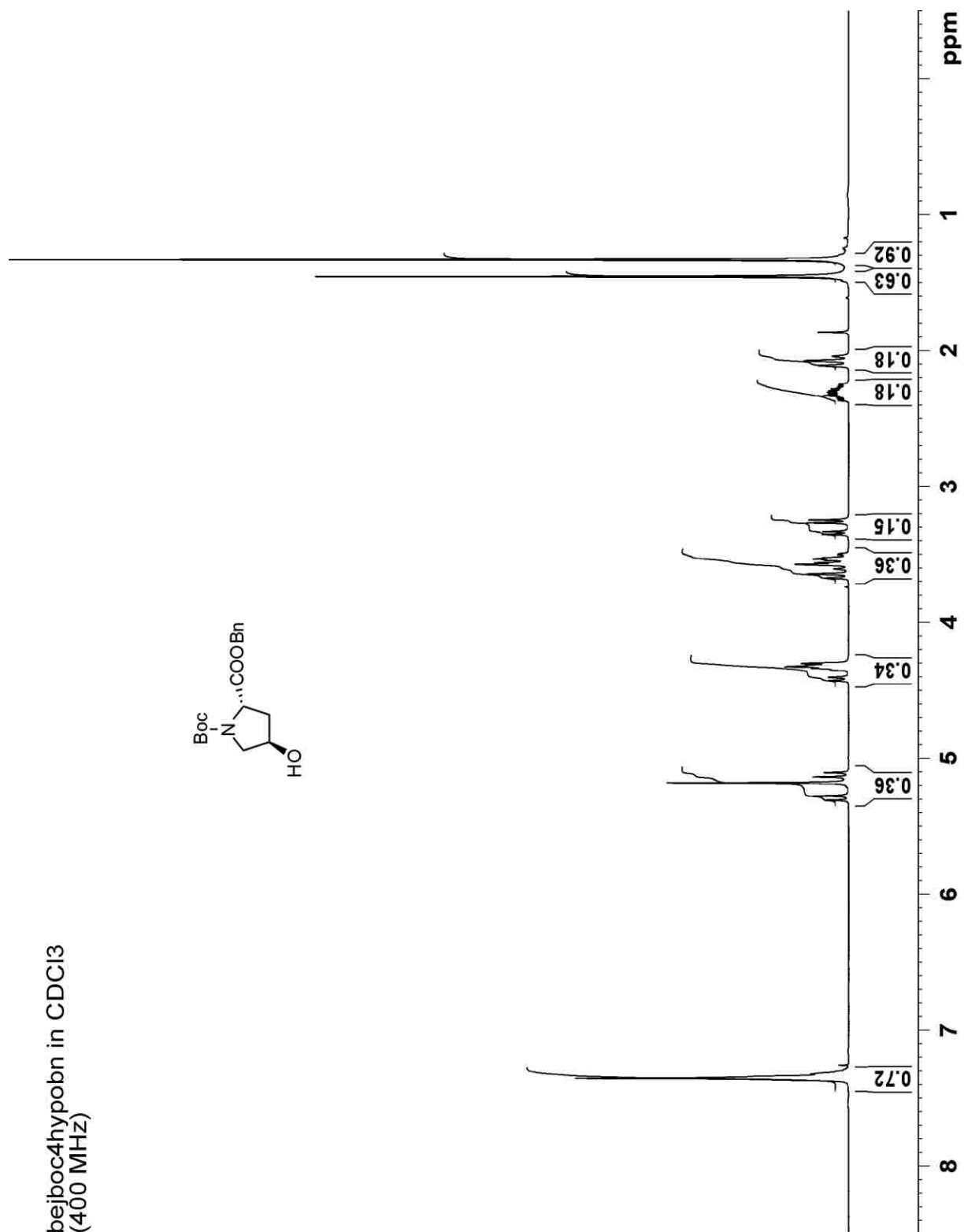
Tetrapeptide 46— ^{13}C NMR in CDCl_3 at 100 MHz



Tetrapeptide (46)– HPLC chromatogram at 254 nm, 75% EtOAc in Hexanes, 10 mm Econosil, 3 mL min⁻¹ (96% pure)

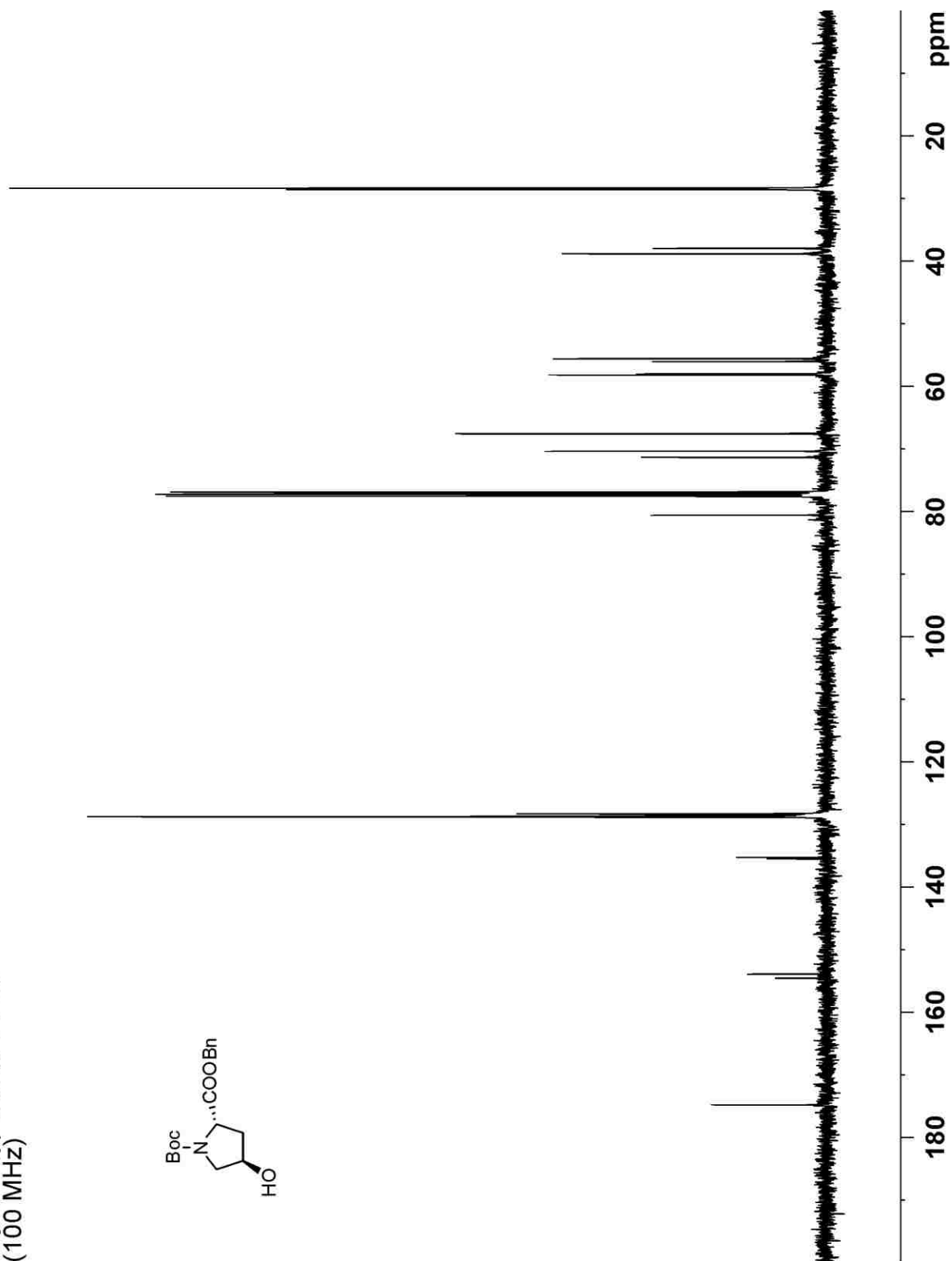
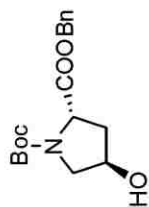


Boc-4-Hyp-OBn (141a) – ^1H NMR in CDCl_3 at 400 MHz



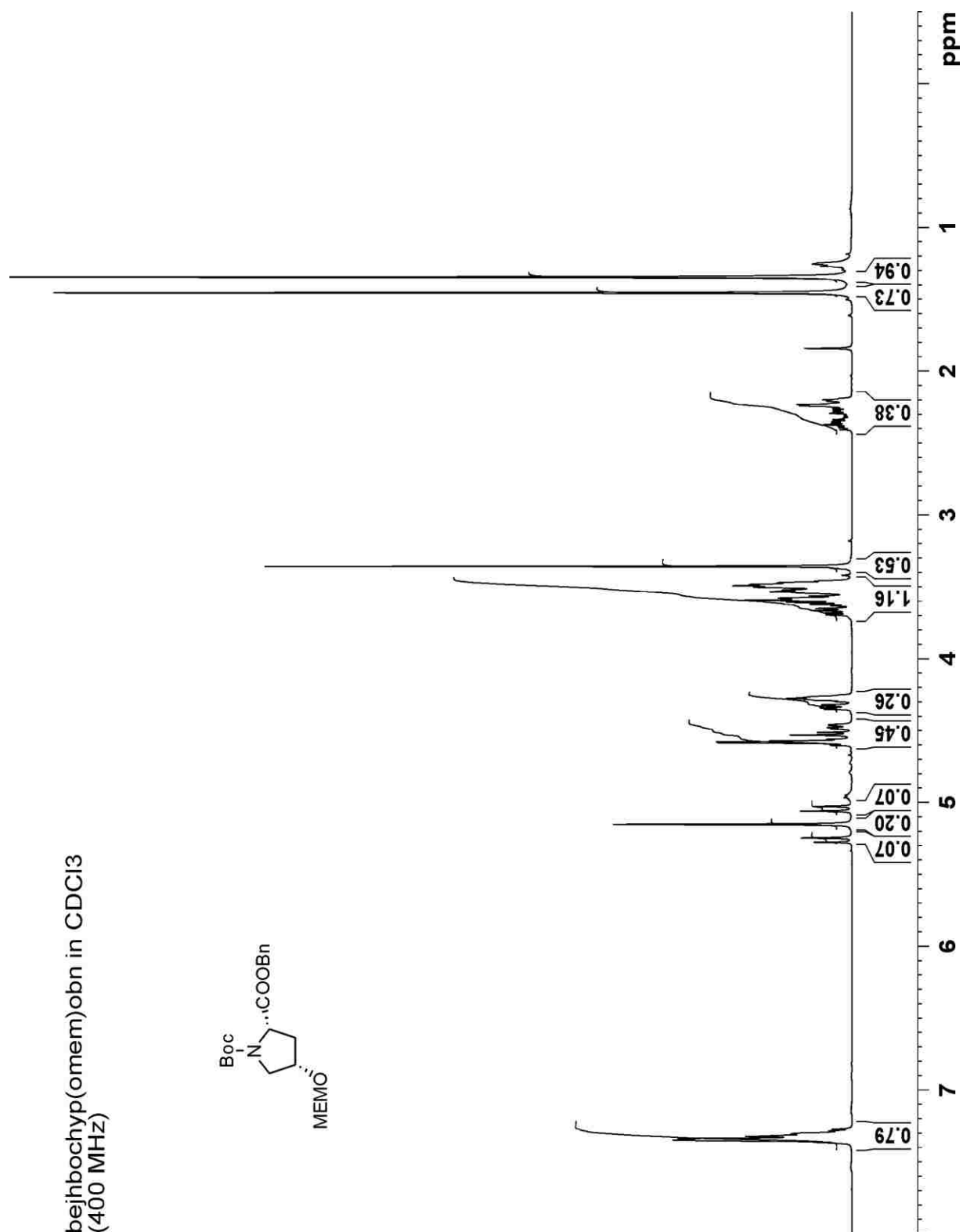
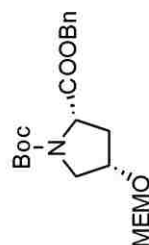
Boc-4-Hyp-OBn (141a) – ^{13}C NMR in CDCl_3 at 100 MHz

bejboc4hypobn in CDCl_3
(100 MHz)



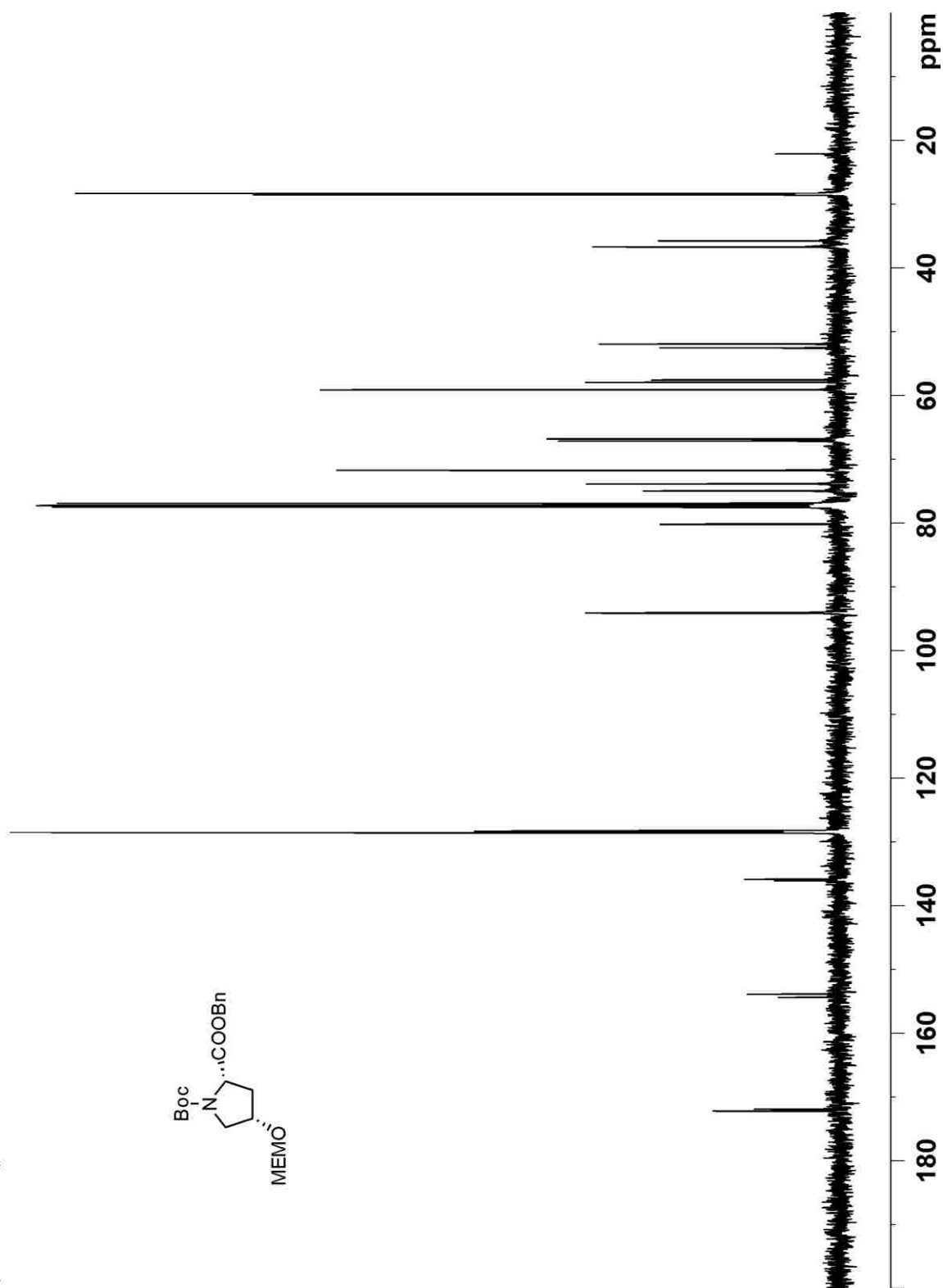
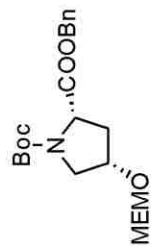
Boc-4-hyp-(OMEM)-OBn (142) – ^1H NMR in CDCl_3 at 400 MHz

bejhbochyp(omem)obn in CDCl_3
(400 MHz)

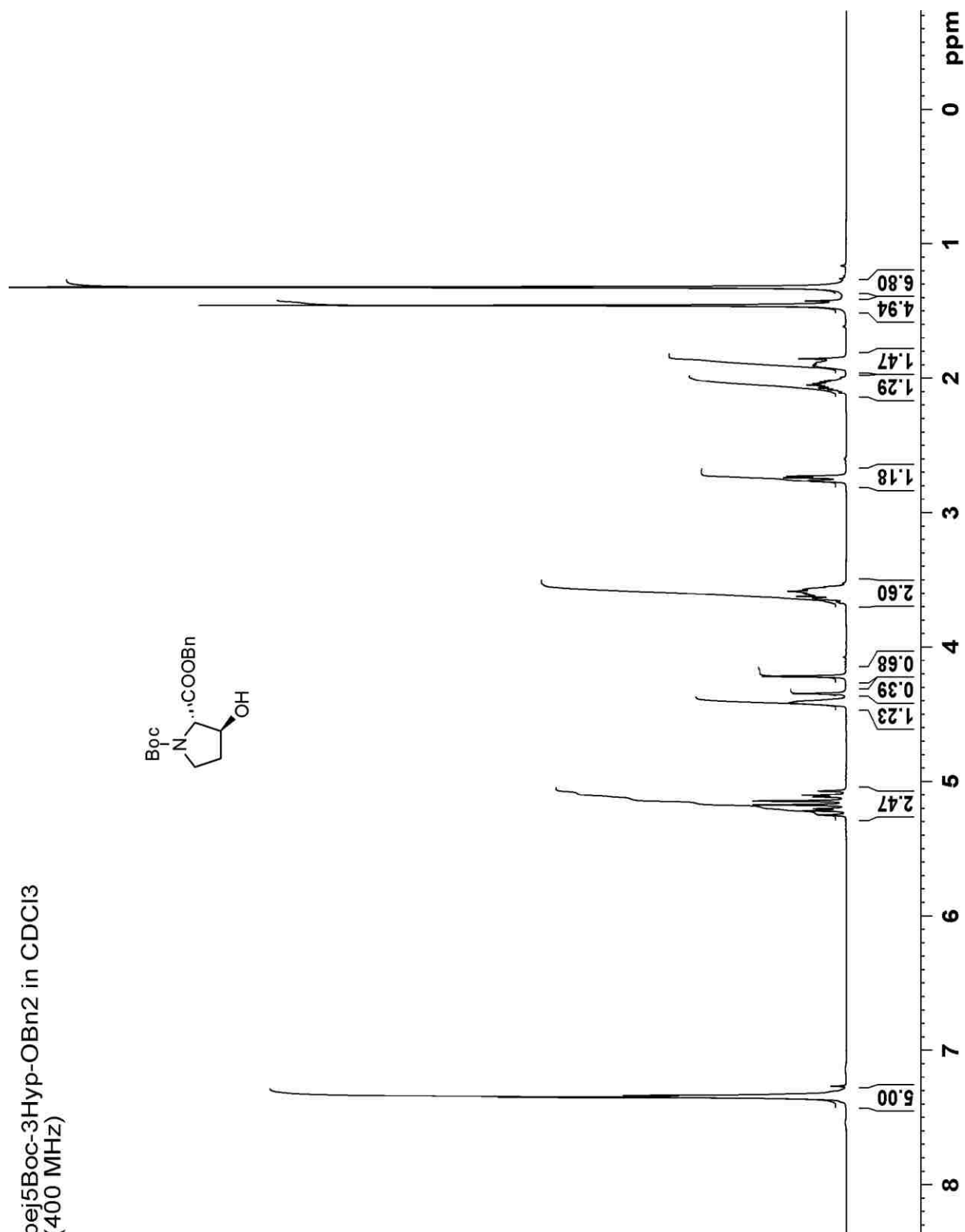


Boc-4-hyp-(OMEM)-OBn (142) – ^{13}C NMR in CDCl_3 at 100 MHz

bejhbochyp(omem)obn in CDCl_3
(100 MHz)

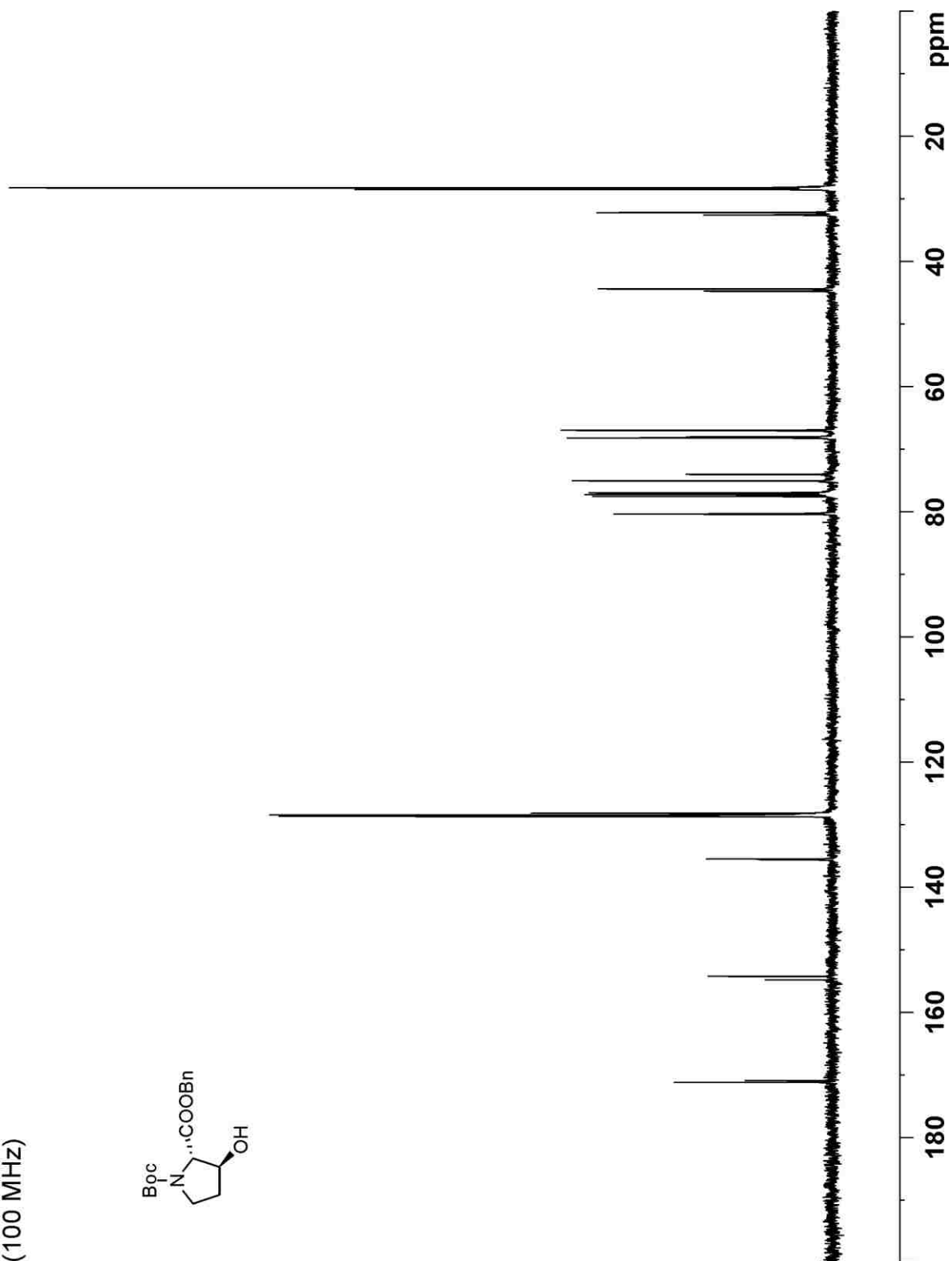
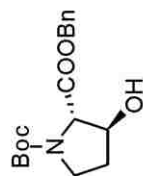


Boc-3-Hyp-OBn (145) – ^1H NMR in CDCl_3 at 400 MHz

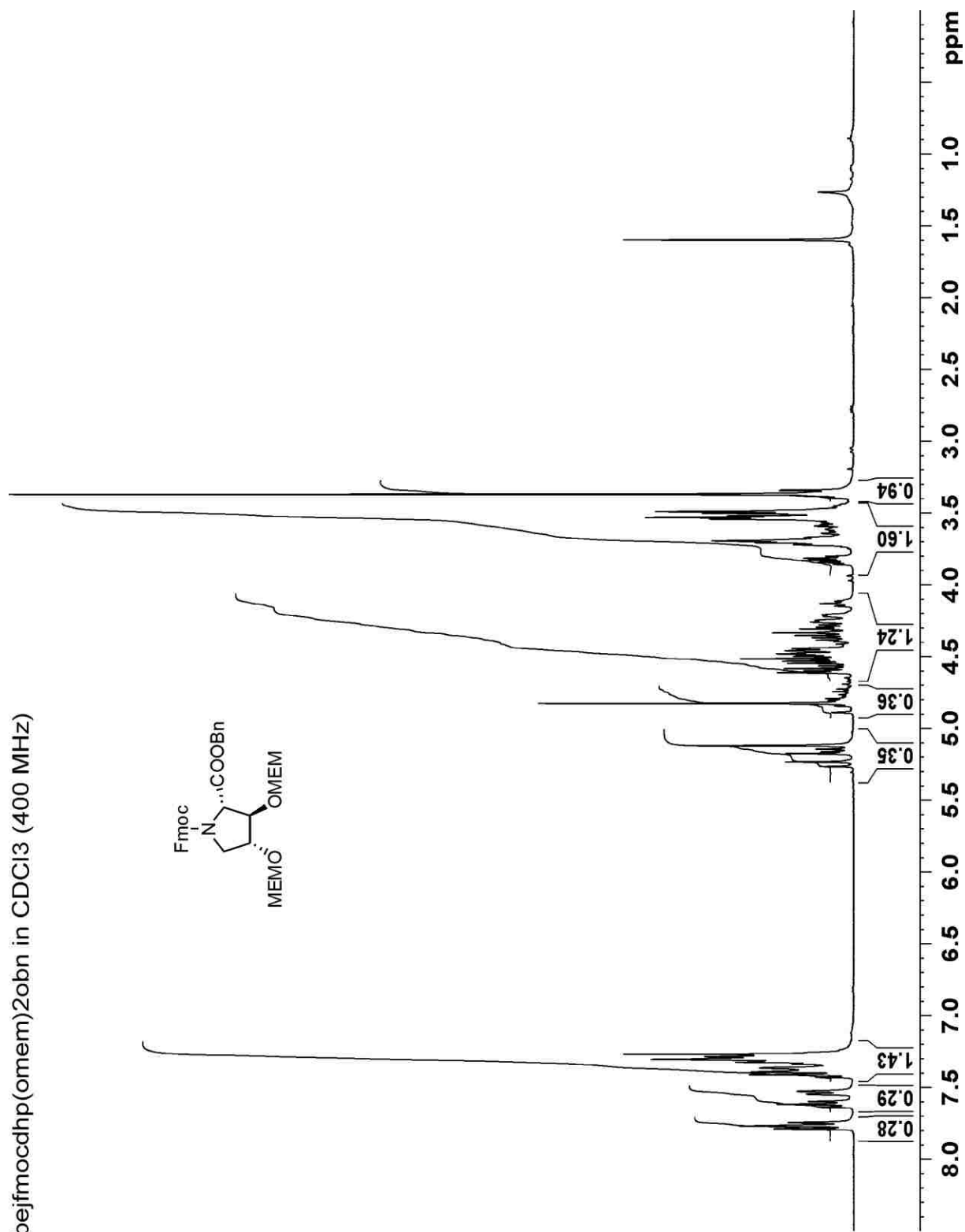


Boc-3-Hyp-OBn (145) – ^{13}C NMR in CDCl_3 at 100 MHz

bej5Boc-3Hyp-OBn in CDCl_3
(100 MHz)

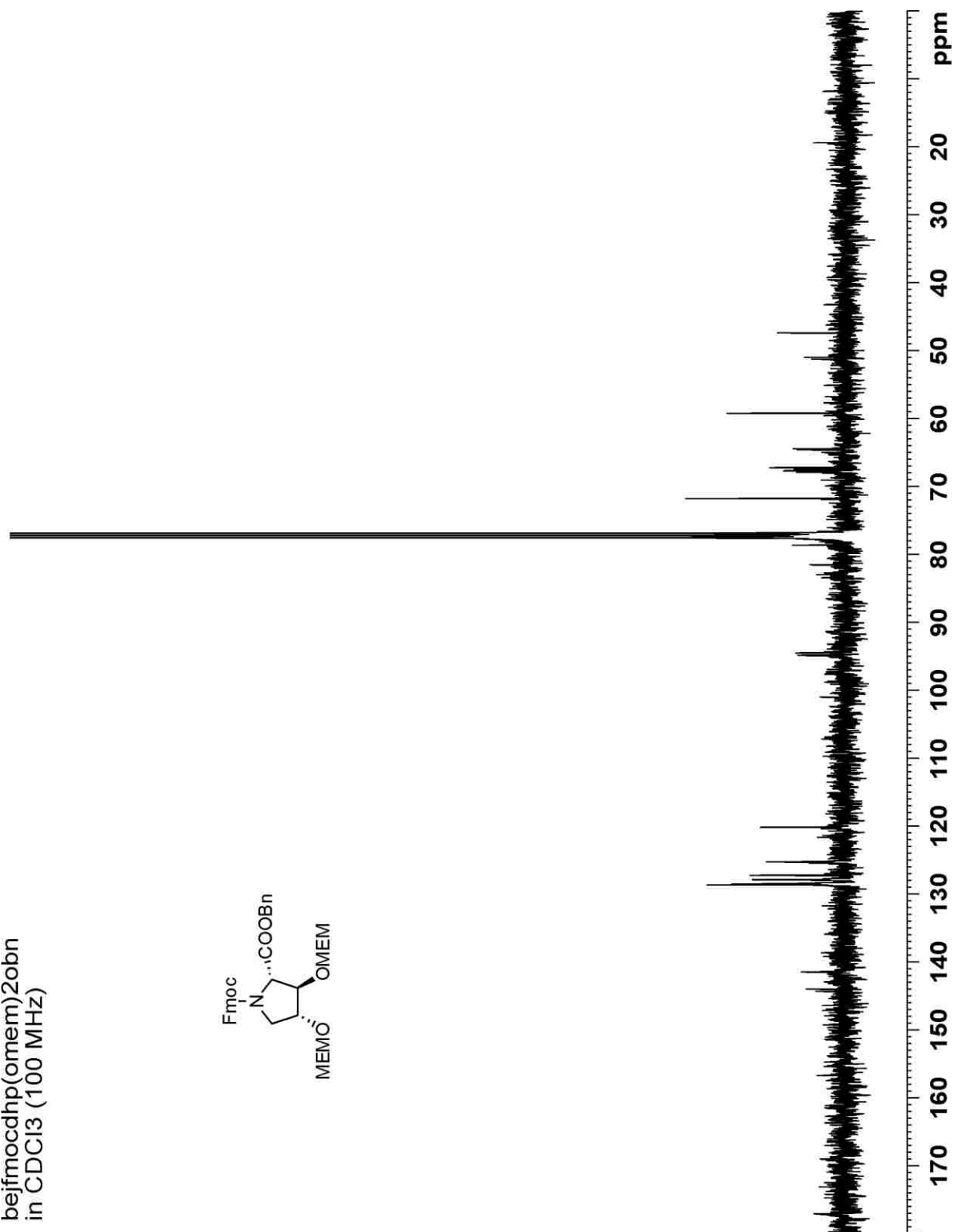
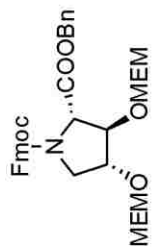


Fmoc-DHP-(OMEM)₂-OBn (156) – ¹H NMR in CDCl₃ at 400 MHz



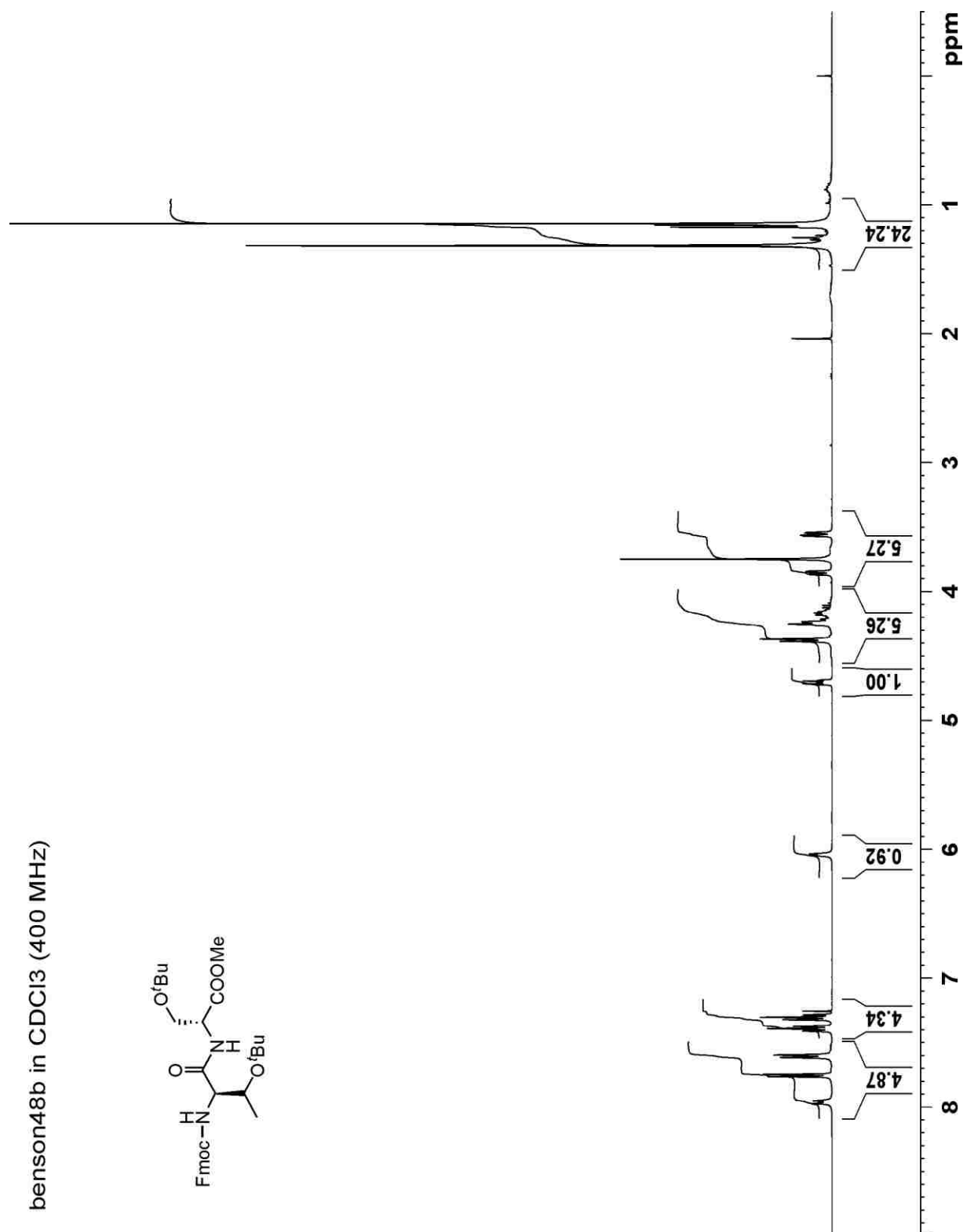
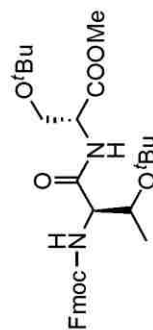
Fmoc-DHP-(OMEM)₂-OBn (156) – ¹³C NMR in CDCl₃ at 100 MHz

bejfmocdhp(omem)2obn
in CDCl₃ (100 MHz)



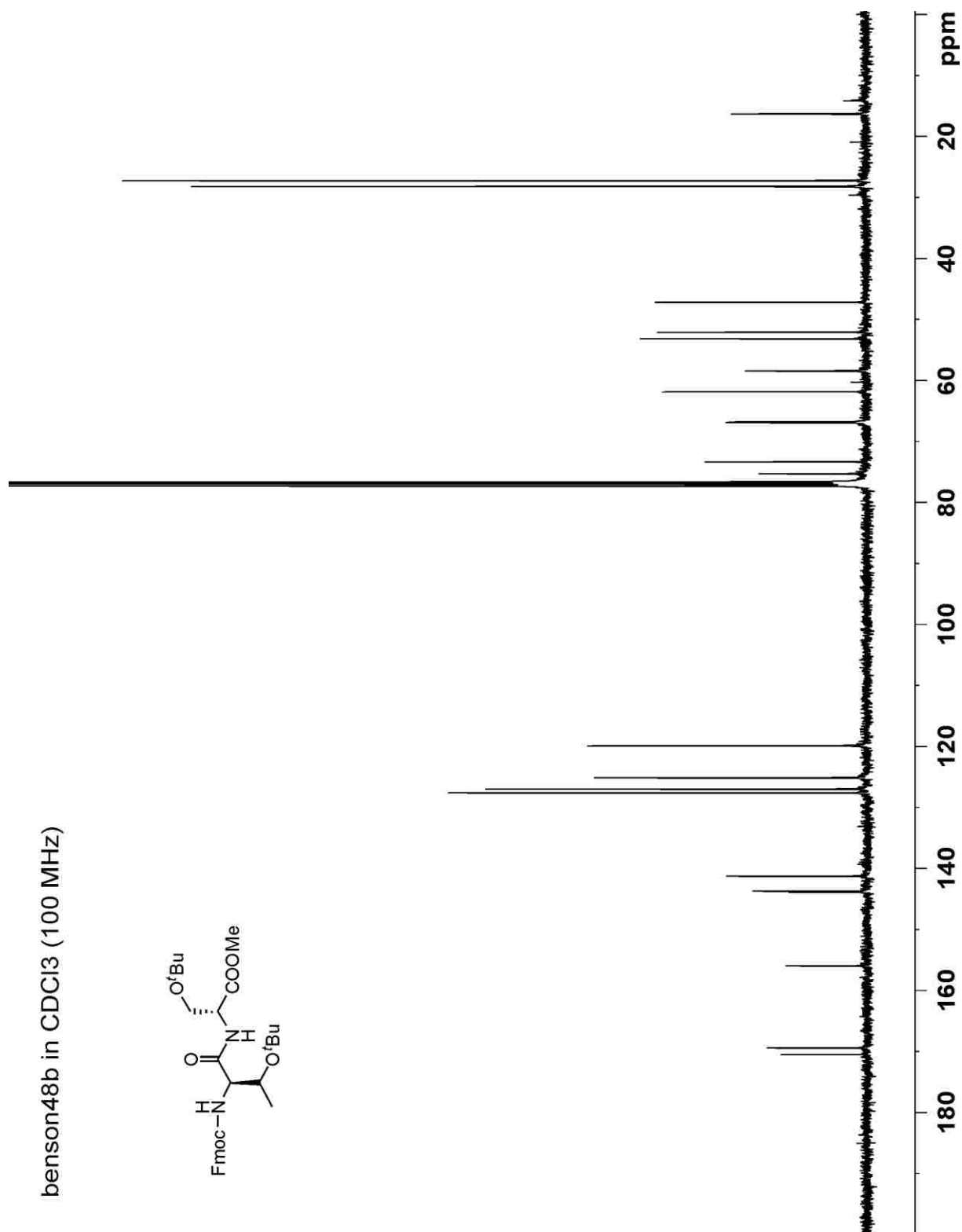
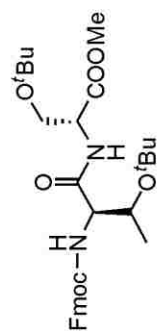
Fmoc-*D*-Thr-(*O*^tBu)-*D*-Ser(*O*^tBu)-OMe (166) – ¹H NMR in CDCl₃ at 400 MHz

benson48b in CDCl₃ (400 MHz)

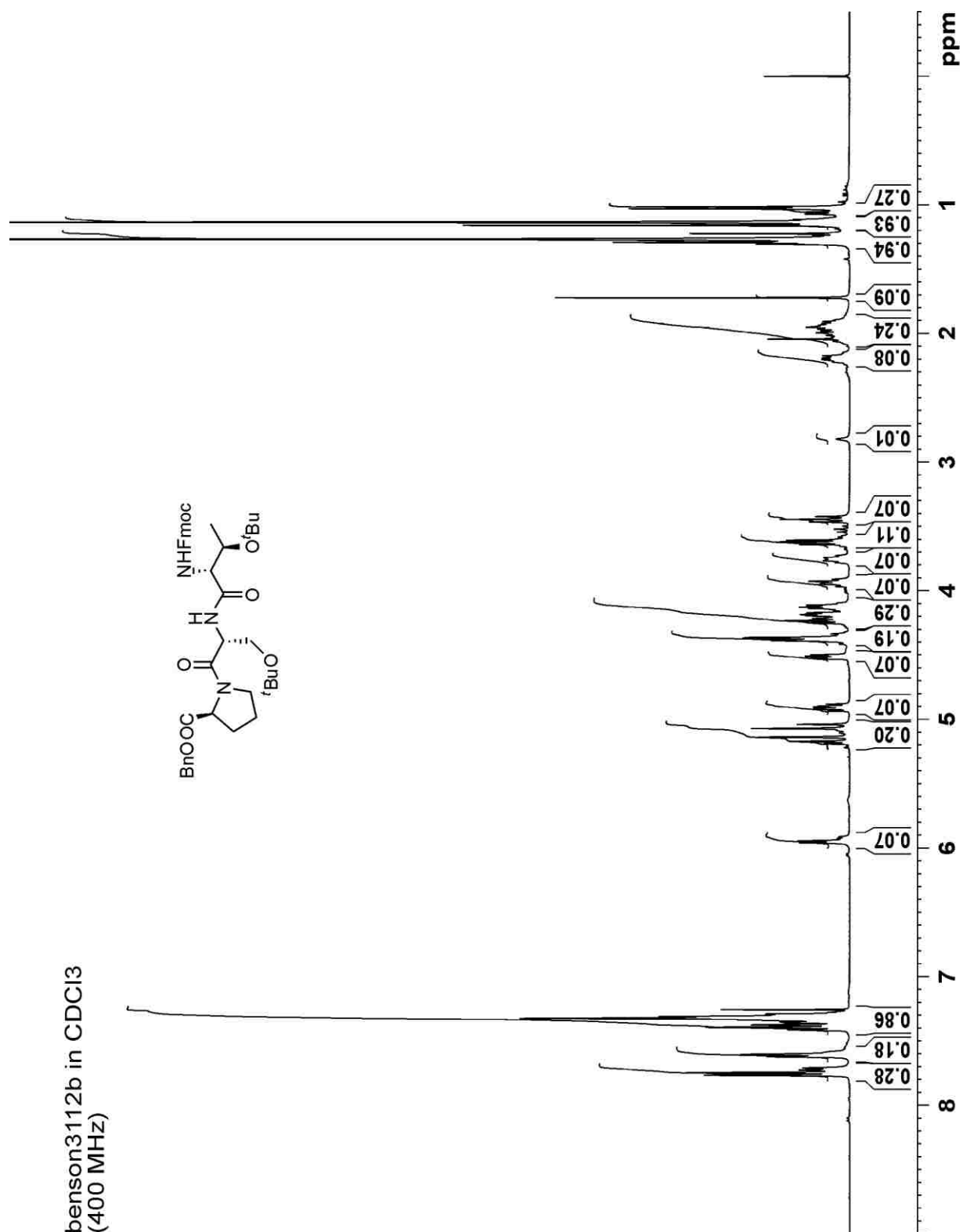


Fmoc-*D*-Thr-(*O*^tBu)-*D*-Ser(*O*^tBu)-OMe (166) – ¹³C NMR in CDCl₃ at 100 MHz

benson48b in CDCl₃ (100 MHz)

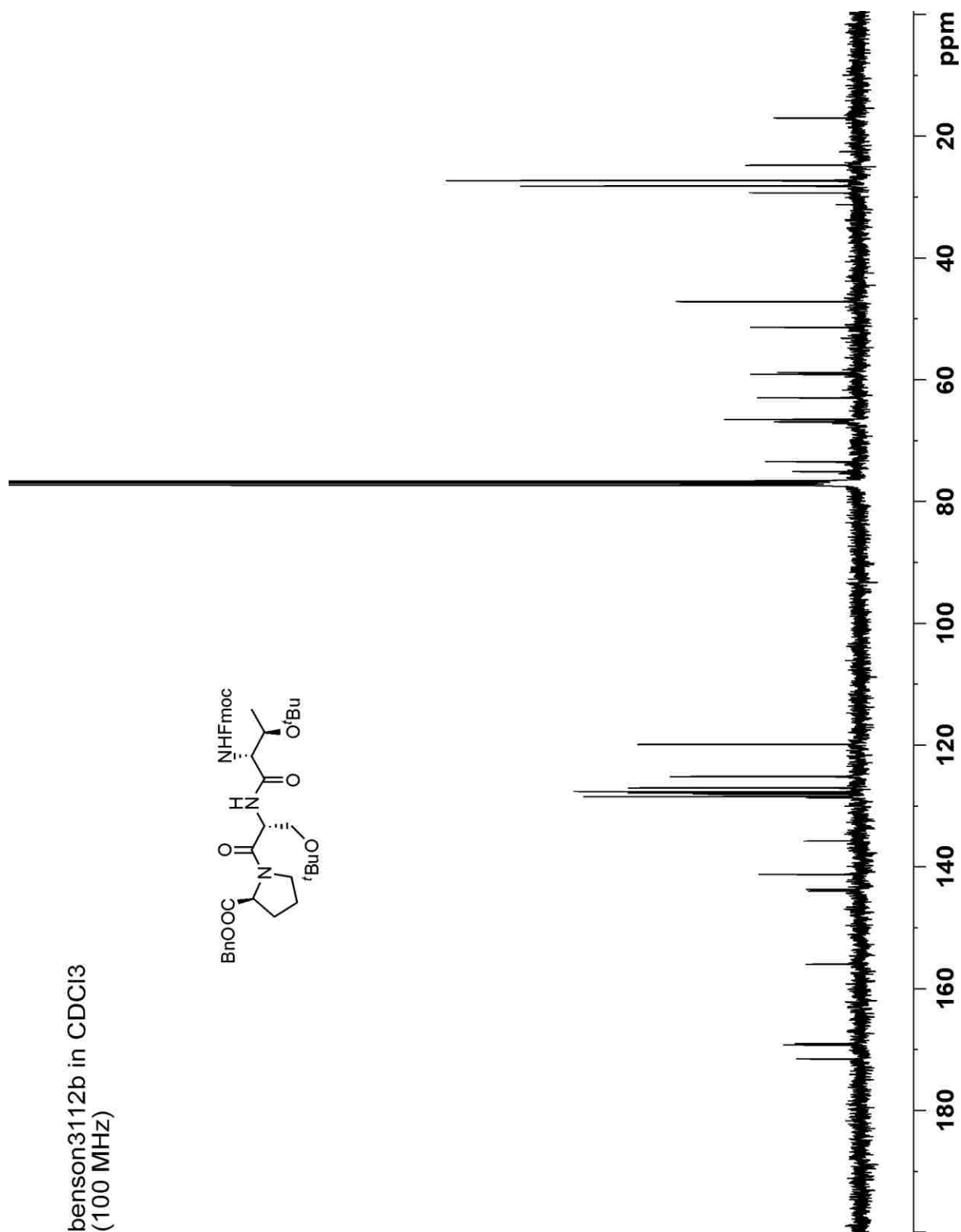
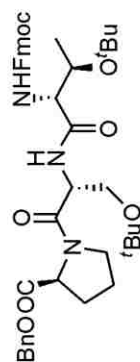


Fmoc-*D*-Thr-(*O*^tBu)-*D*-Ser(*O*^tBu)-Pro-OBn (168) – ¹H NMR in CDCl₃ at 400 MHz

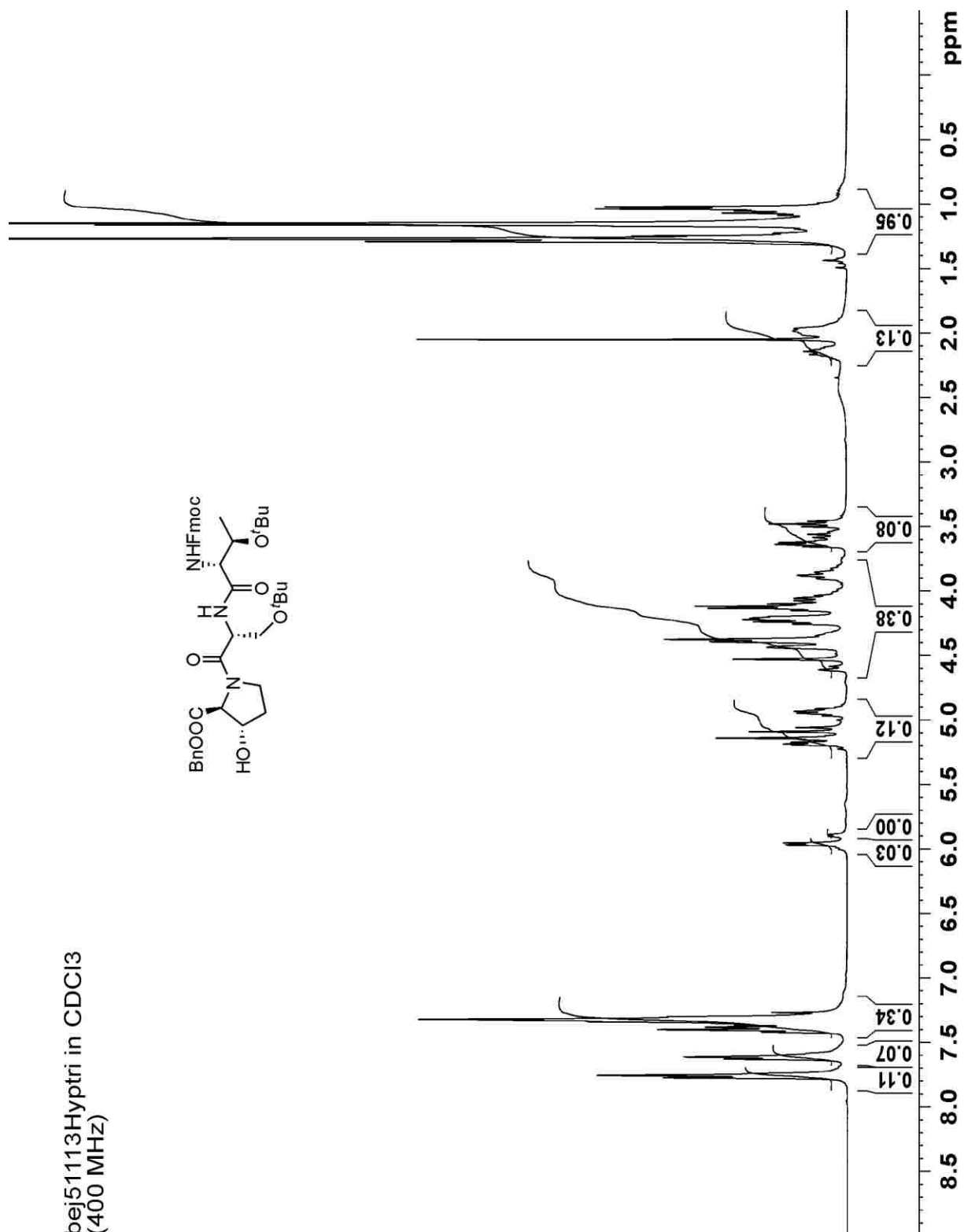


Fmoc-*D*-Thr-(*O*^tBu)-*D*-Ser(*O*^tBu)-Pro-OBn (168) – ¹³C NMR in CDCl₃ at 100 MHz

benso3112b in CDCl₃
(100 MHz)

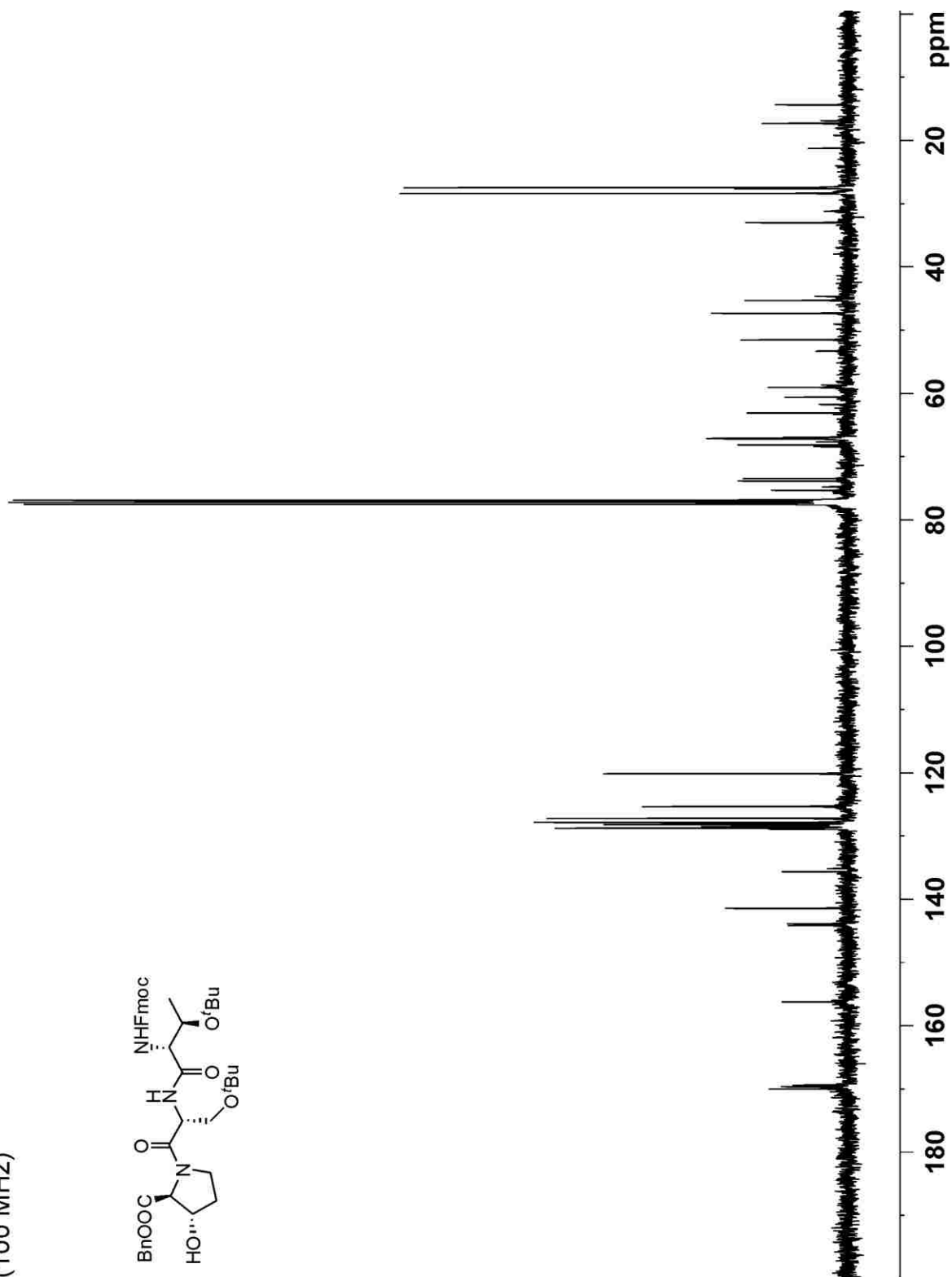
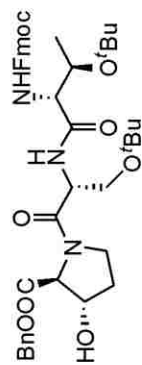


Fmoc-*D*-Thr-(*O*^tBu)-*D*-Ser(*O*^tBu)-*trans*-3-Hyp-OBn (169) – ¹H NMR in CDCl₃ at 400 MHz

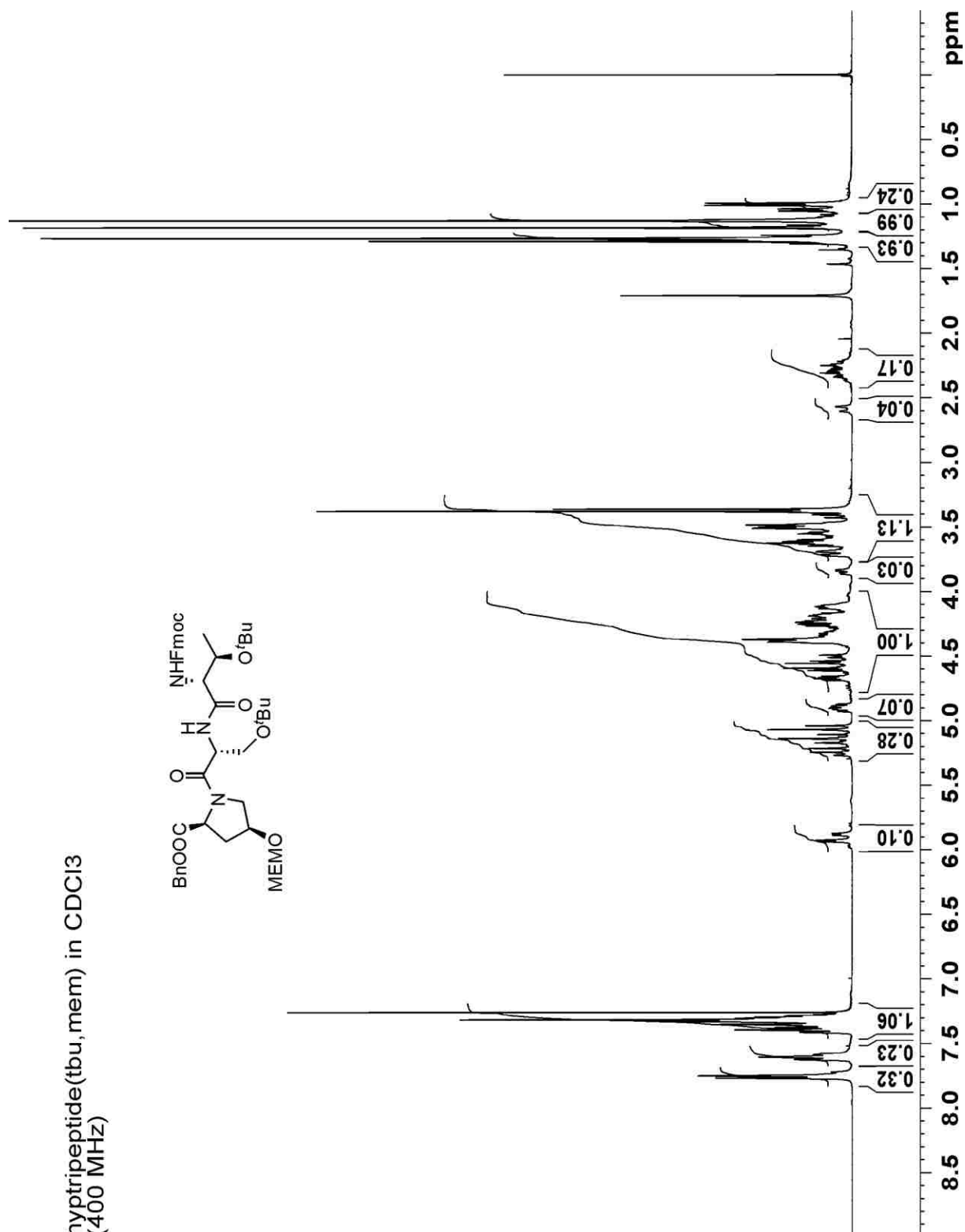


Fmoc-*D*-Thr-(*O*^tBu)-*D*-Ser(*O*^tBu)-*trans*-3-Hyp-OBn (169) – ¹³C NMR in CDCl₃ at 100 MHz

bej51113Hyptri in CDCl₃
(100 MHz)

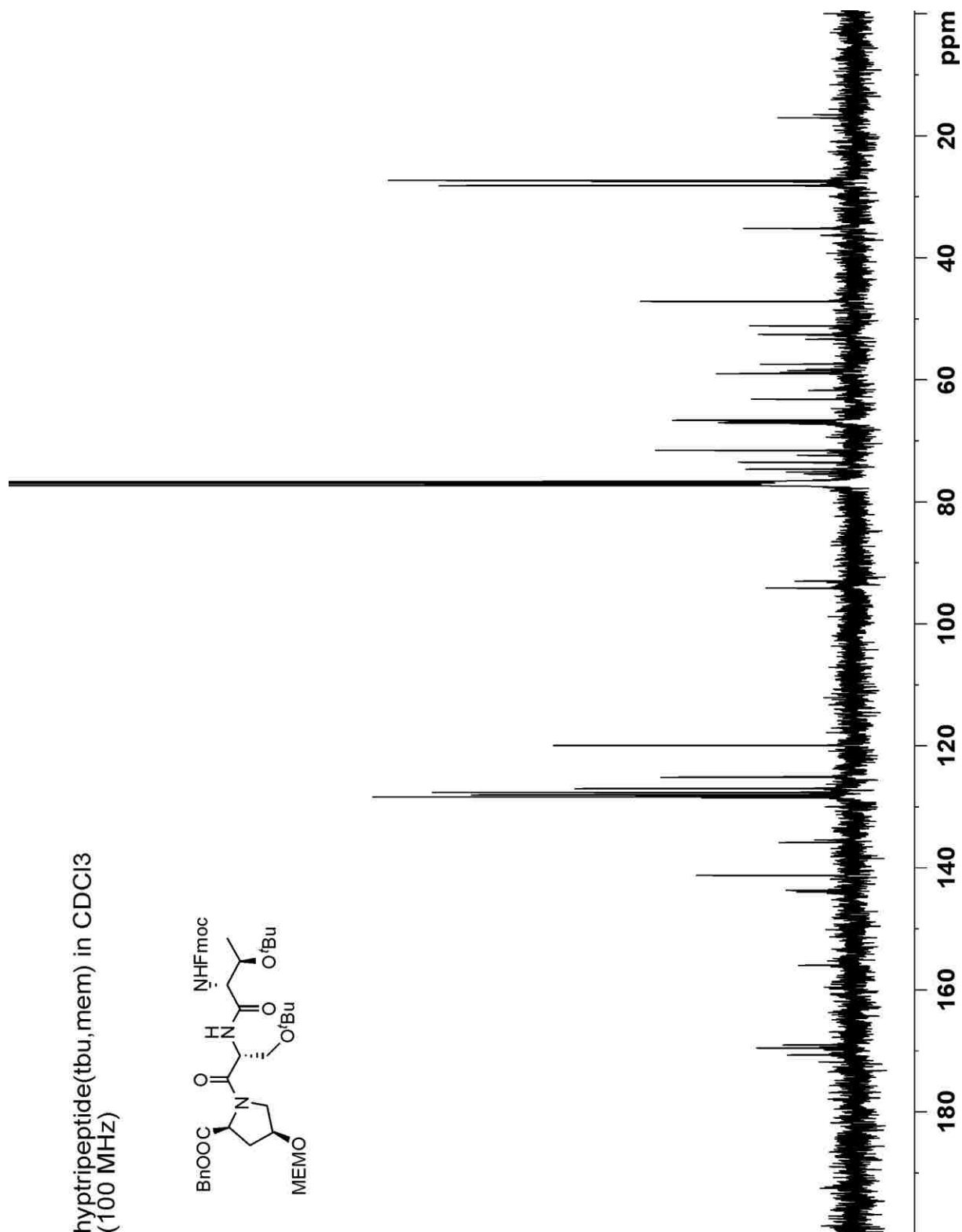
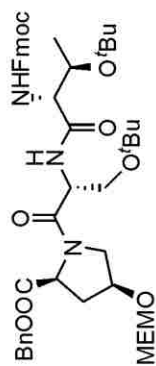


Fmoc-*D*-Thr-(*O*^tBu)-*D*-Ser(*O*^tBu)-*cis*-4-hyp(OMEM)-OBn (170)- ¹H NMR in CDCl₃ at 400 MHz



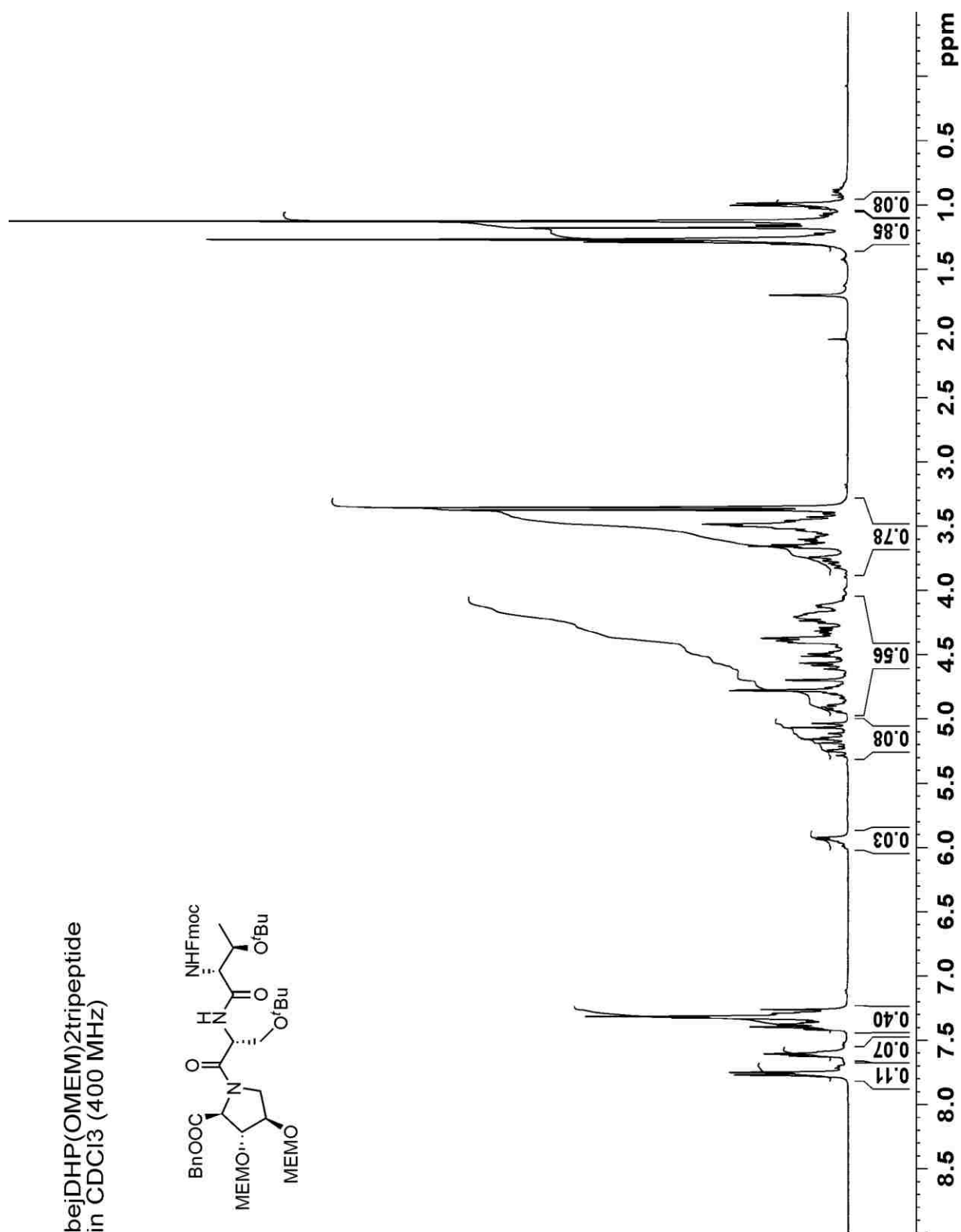
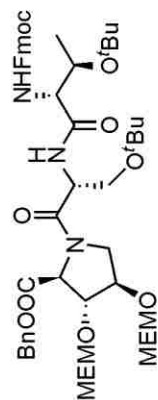
Fmoc-*D*-Thr-(*O*^tBu)-*D*-Ser(*O*^tBu)-*cis*-4-hyp(OMEM)-OBn (170)- ¹³C NMR in CDCl₃ at 100 MHz

hyptripeptide(tbu,mem) in CDCl₃
(100 MHz)



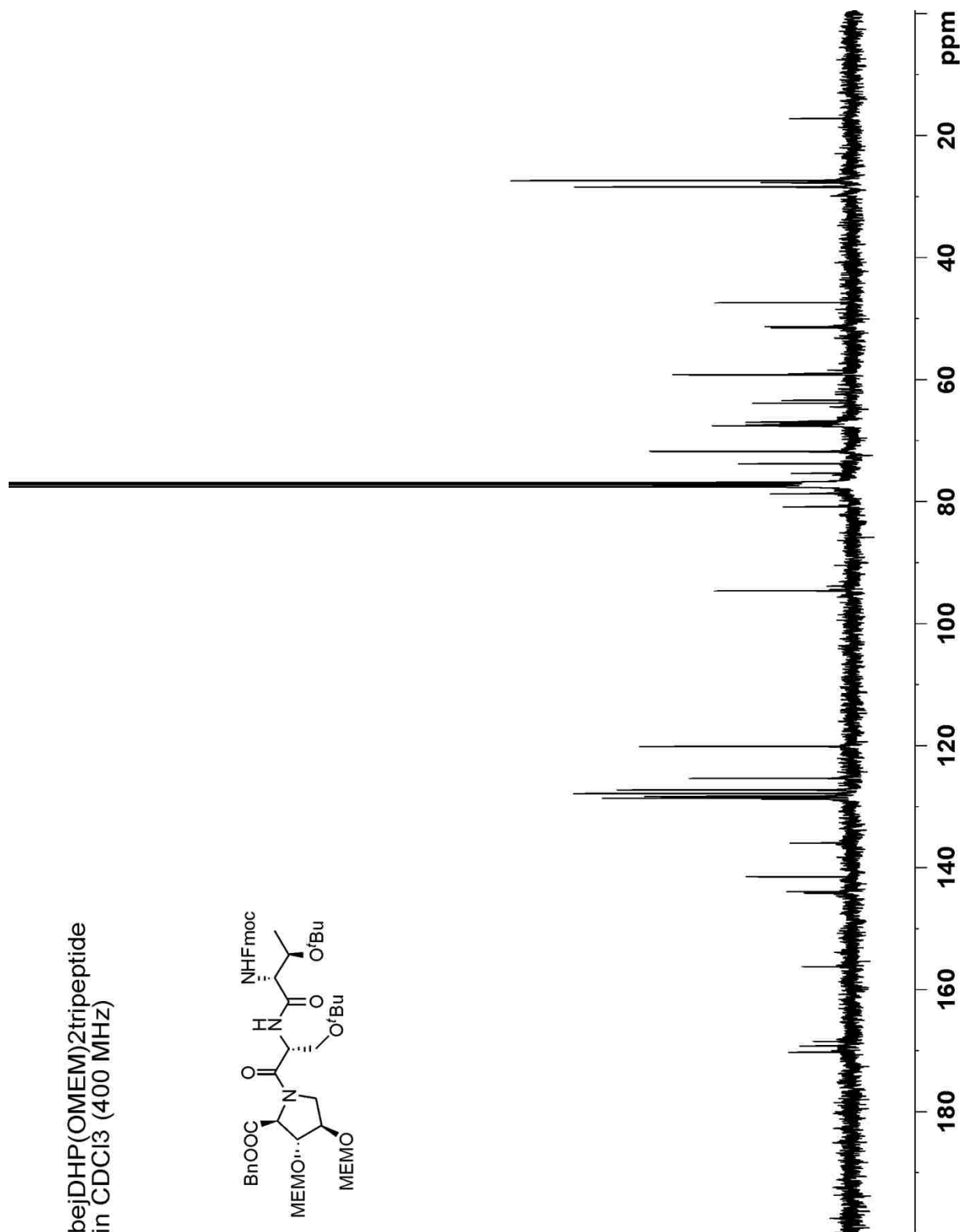
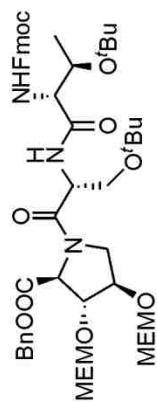
Fmoc-*D*-Thr-(*O*^tBu)-*D*-Ser(*O*^tBu)-DHP(OMEM)₂-OBn (167))- ¹H NMR in CDCl₃ at 400 MHz

bejDHP(OMEM)2tripeptide
in CDCl₃ (400 MHz)

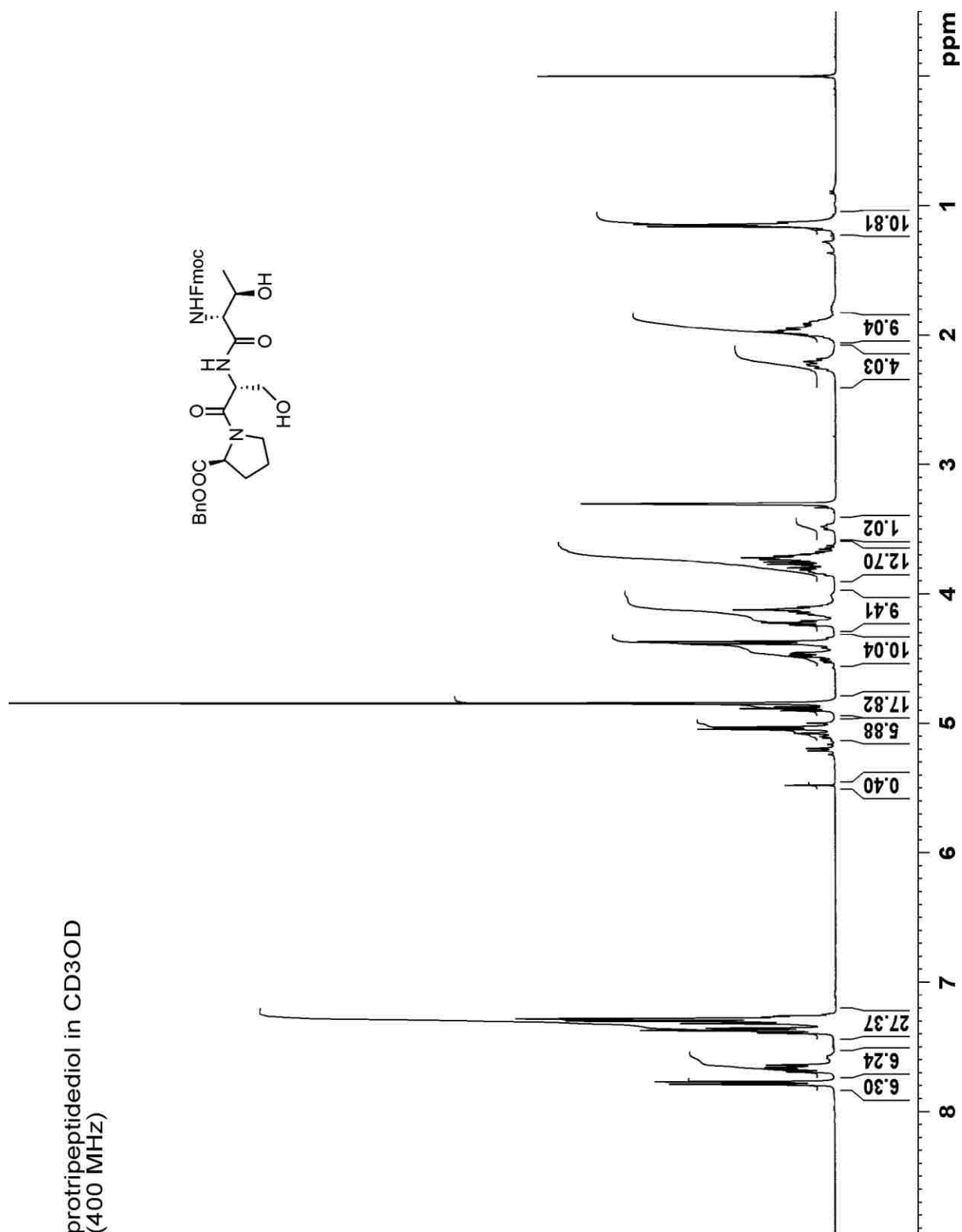


Fmoc-*D*-Thr-(*O*^tBu)-*D*-Ser(*O*^tBu)-DHP(OMEM)₂-OBn (167) - ¹³C NMR in CDCl₃ at 100 MHz

bejDHP(OMEM)₂tripeptide
in CDCl₃ (400 MHz)

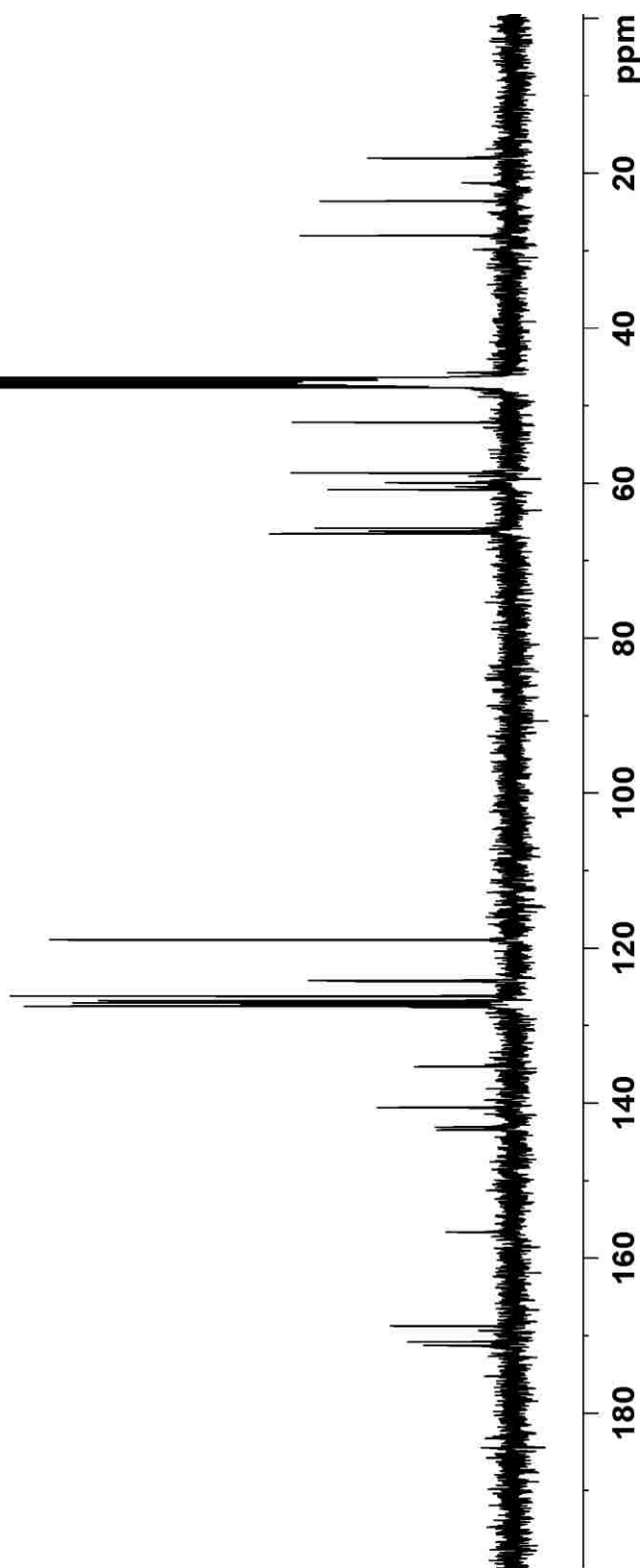
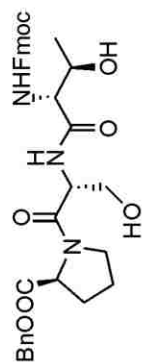


Fmoc-*D*-Thr-*D*-Ser-Pro-OBn (172) – ^1H NMR in CD_3OD at 400 MHz

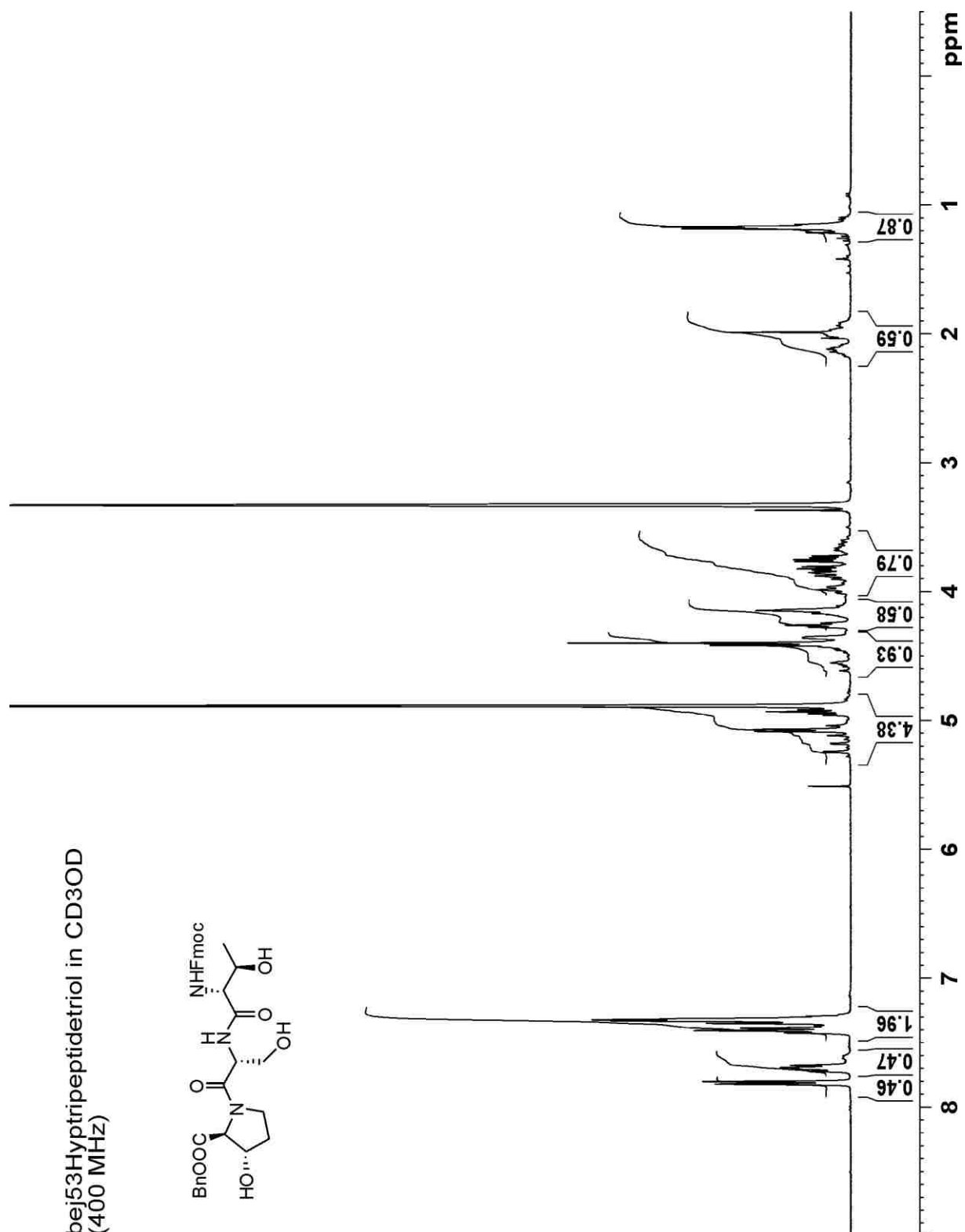


Fmoc-*D*-Thr-*D*-Ser-Pro-OBn (172) – ^{13}C NMR in CD_3OD at 100 MHz

protripeptidediol in CD_3OD
(100 MHz)

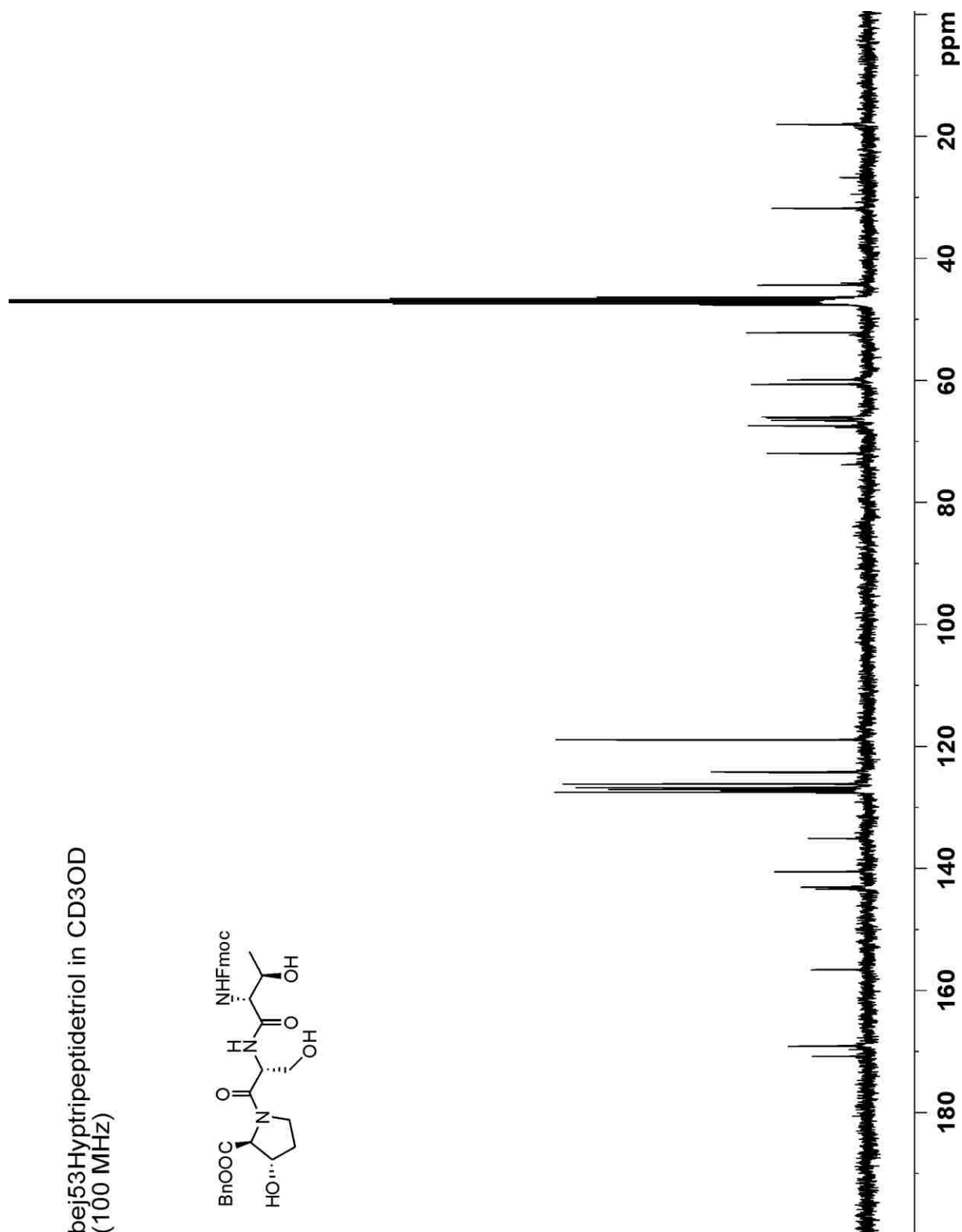
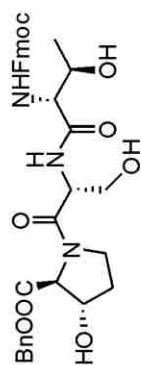


Fmoc-*D*-Thr-*D*-Ser-*trans*-3-Hyp-OBn (173) – ^{13}C NMR in CD_3OD at 400 MHz

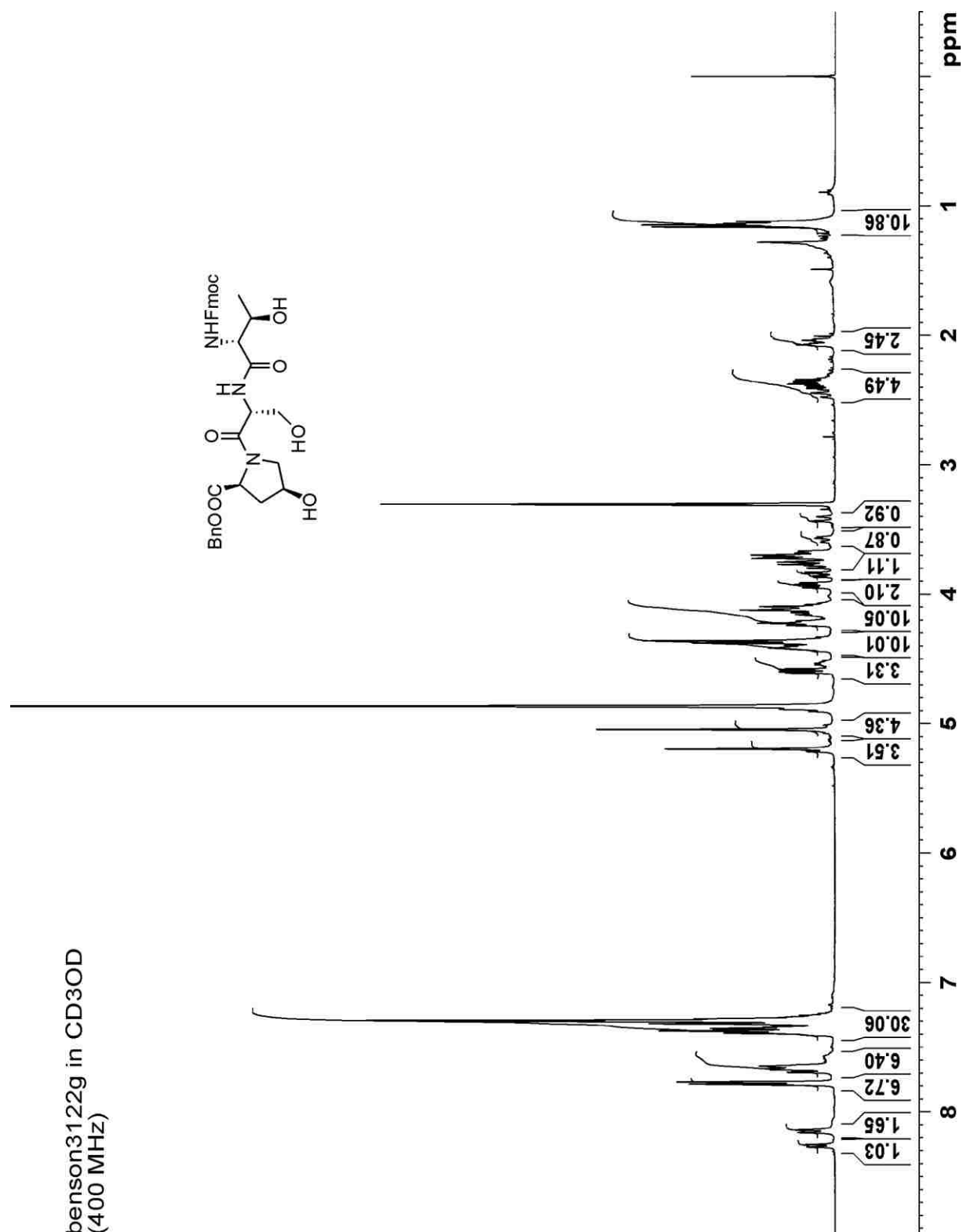


Fmoc-*D*-Thr-*D*-Ser-*trans*-3-Hyp-OBn (173) – ^{13}C NMR in CD_3OD at 100 MHz

bei53Hyptripectidetriol in CD3OD
(100 MHz)

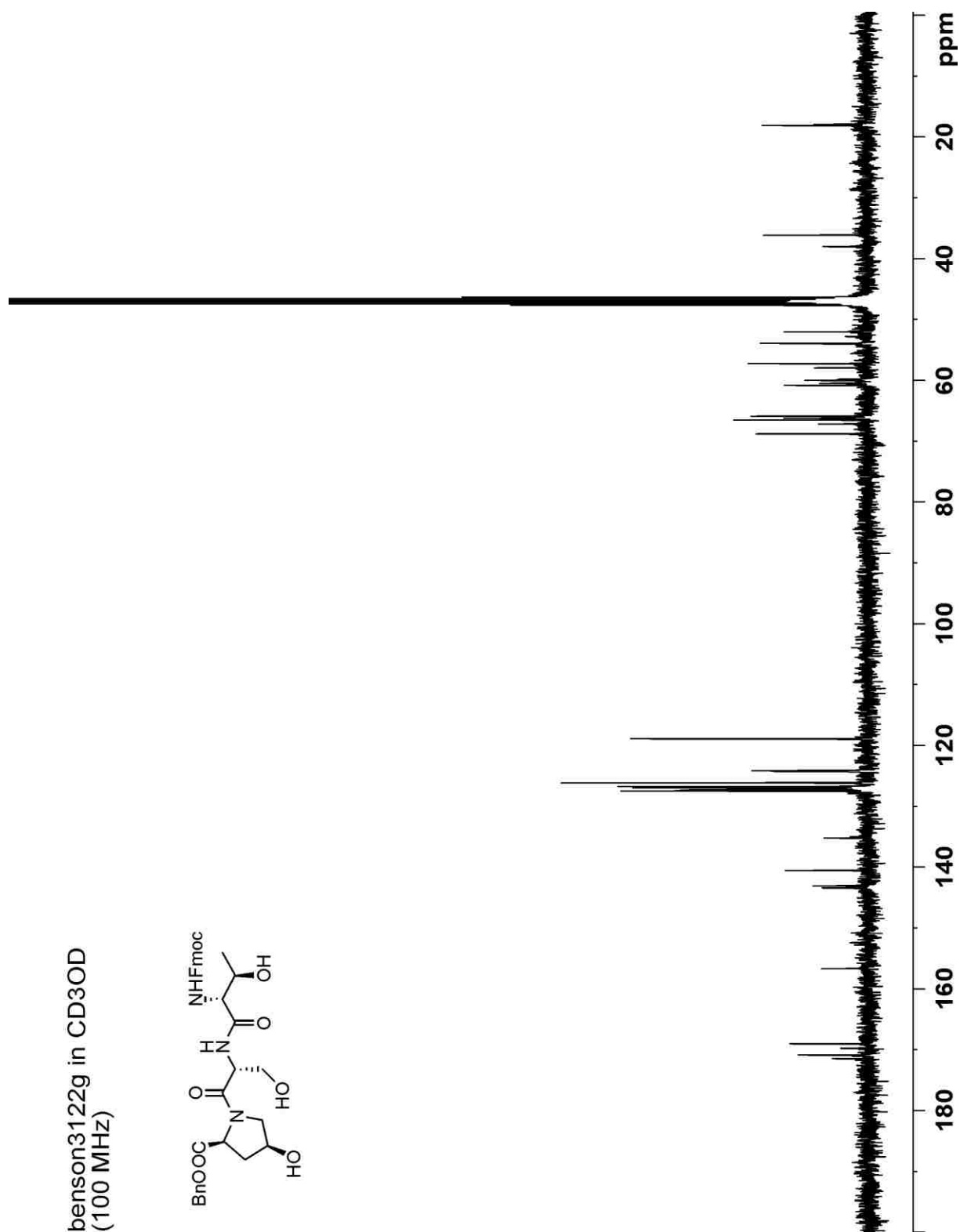
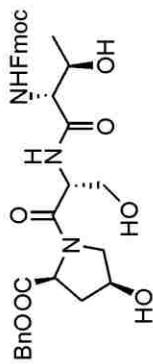


Fmoc-*D*-Thr-*D*-Ser-*cis*-4-hyp-OBn (174) – ^1H NMR in CD_3OD at 400 MHz

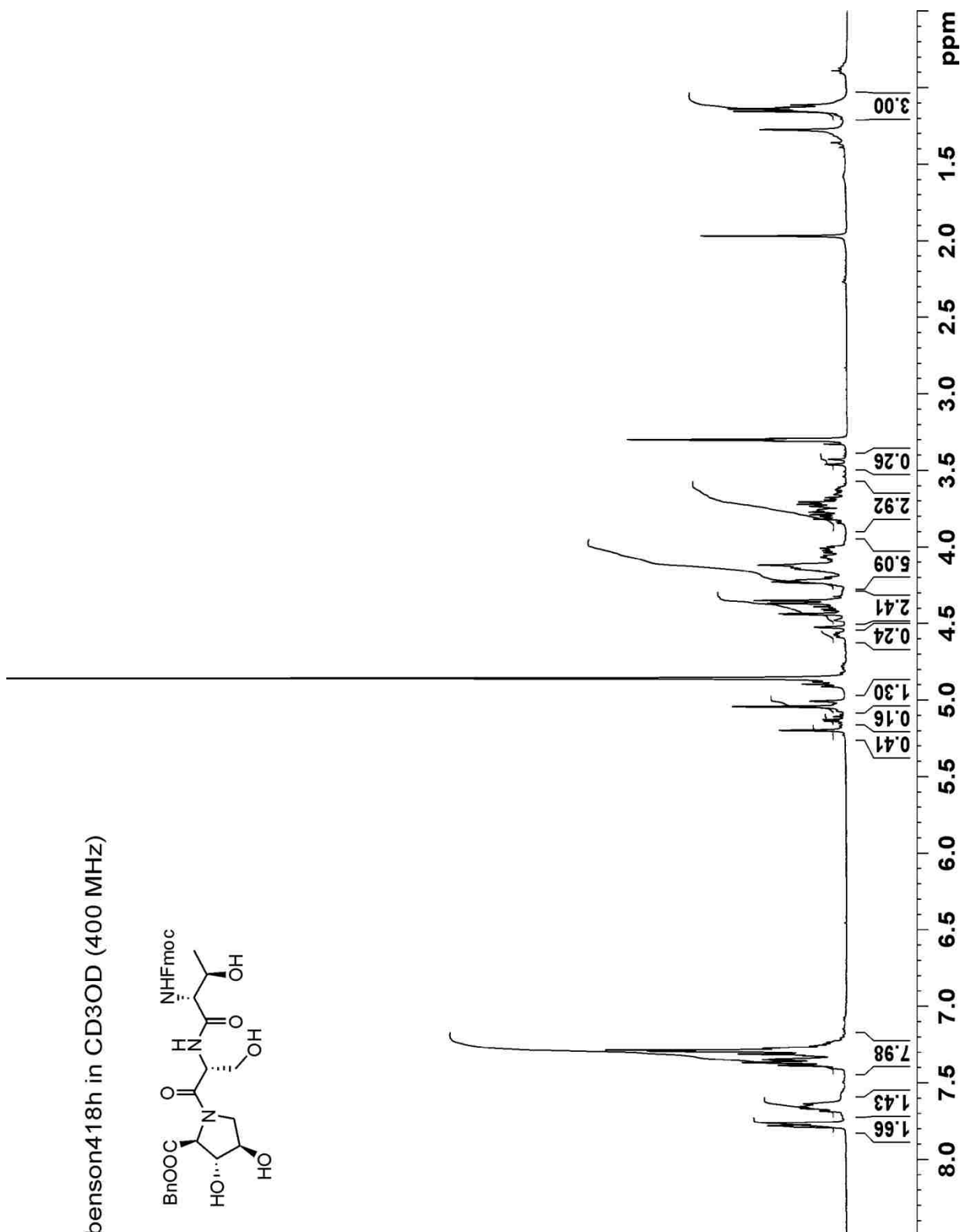


Fmoc-*D*-Thr-*D*-Ser-*cis*-4-hyp-OBn (174) – ^{13}C NMR in CD_3OD at 100 MHz

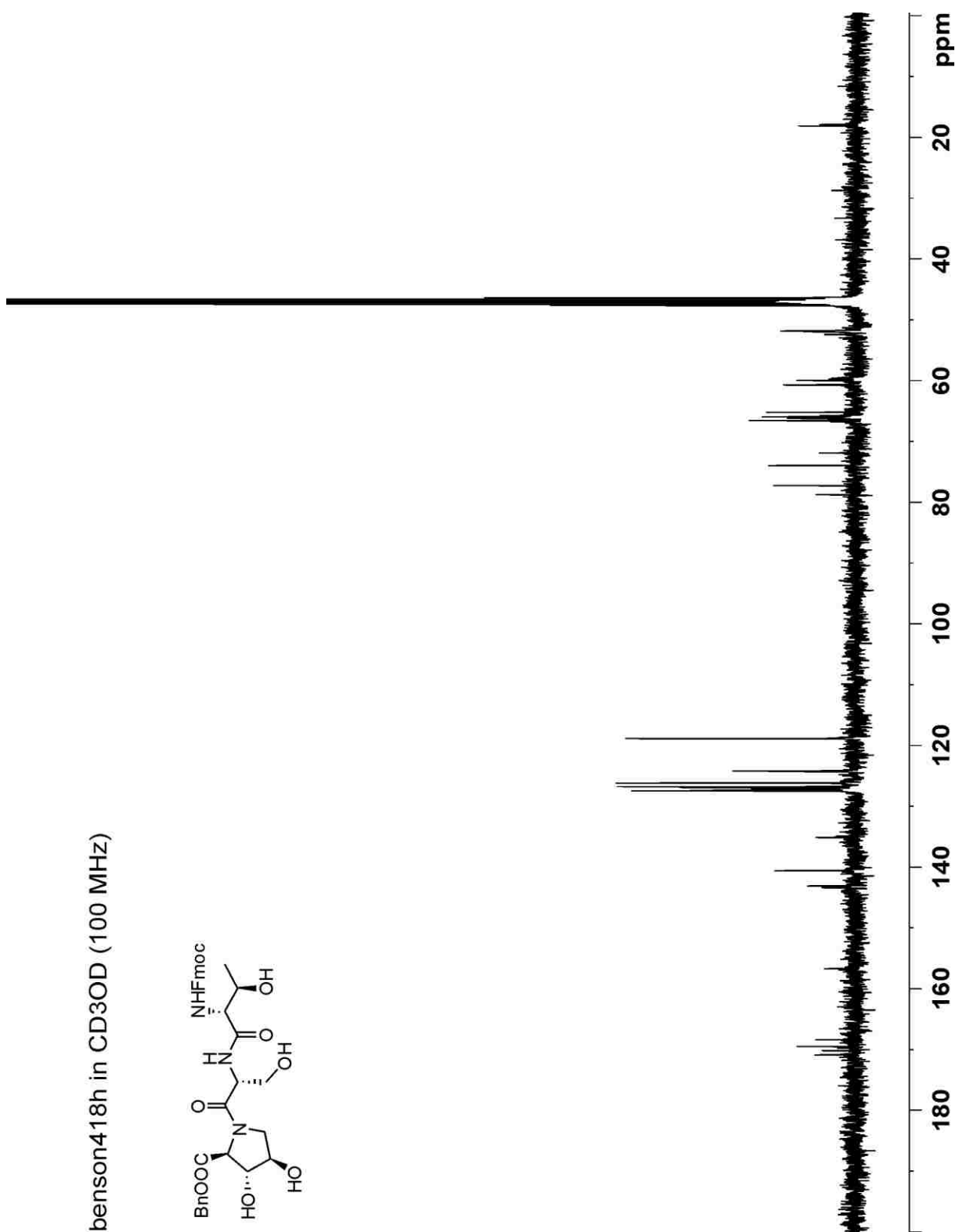
benzon3122g in CD3OD
(100 MHz)



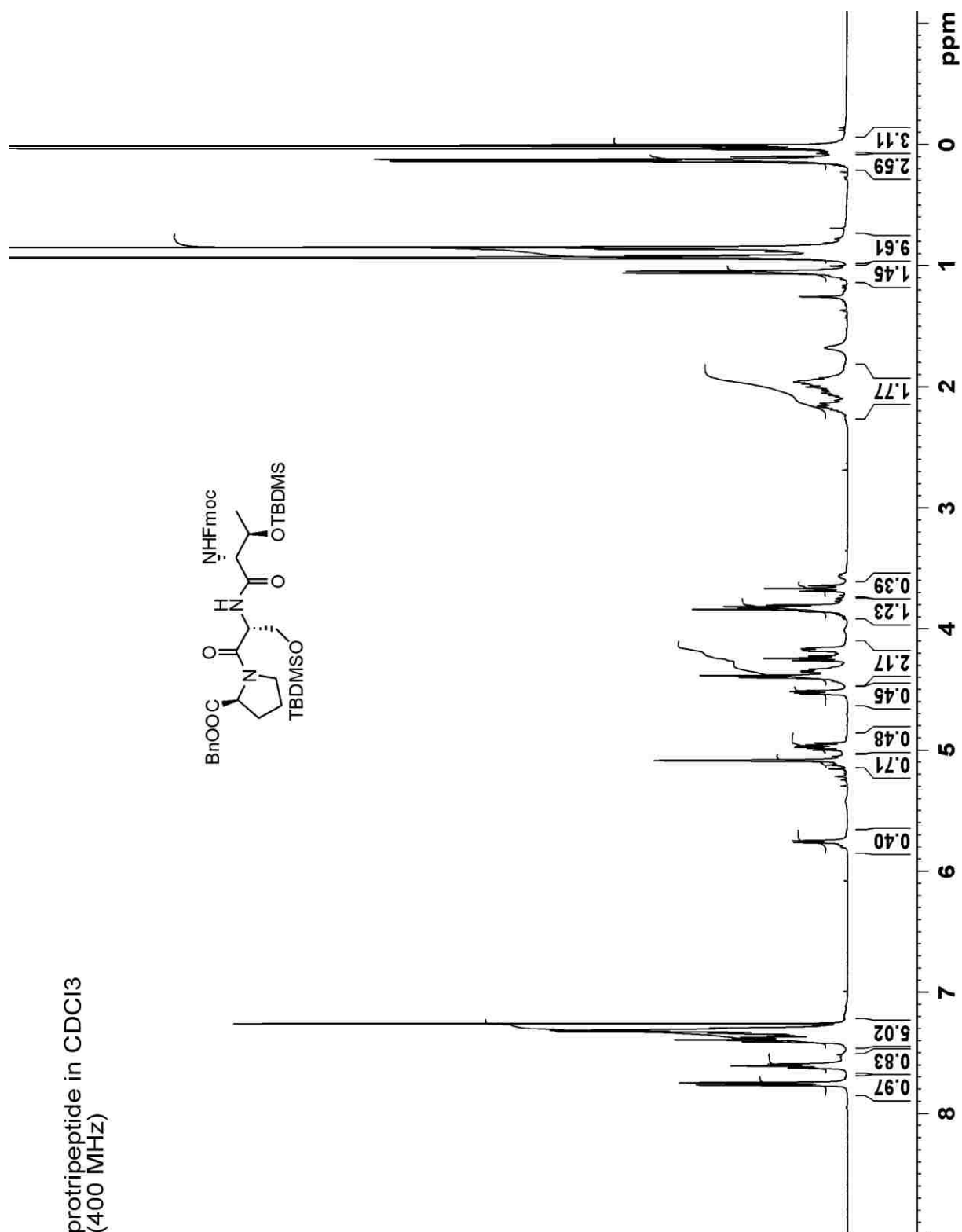
Fmoc-D-Thr-D-Ser-DHP-OBn (171)- ^1H NMR in CD_3OD at 400 MHz



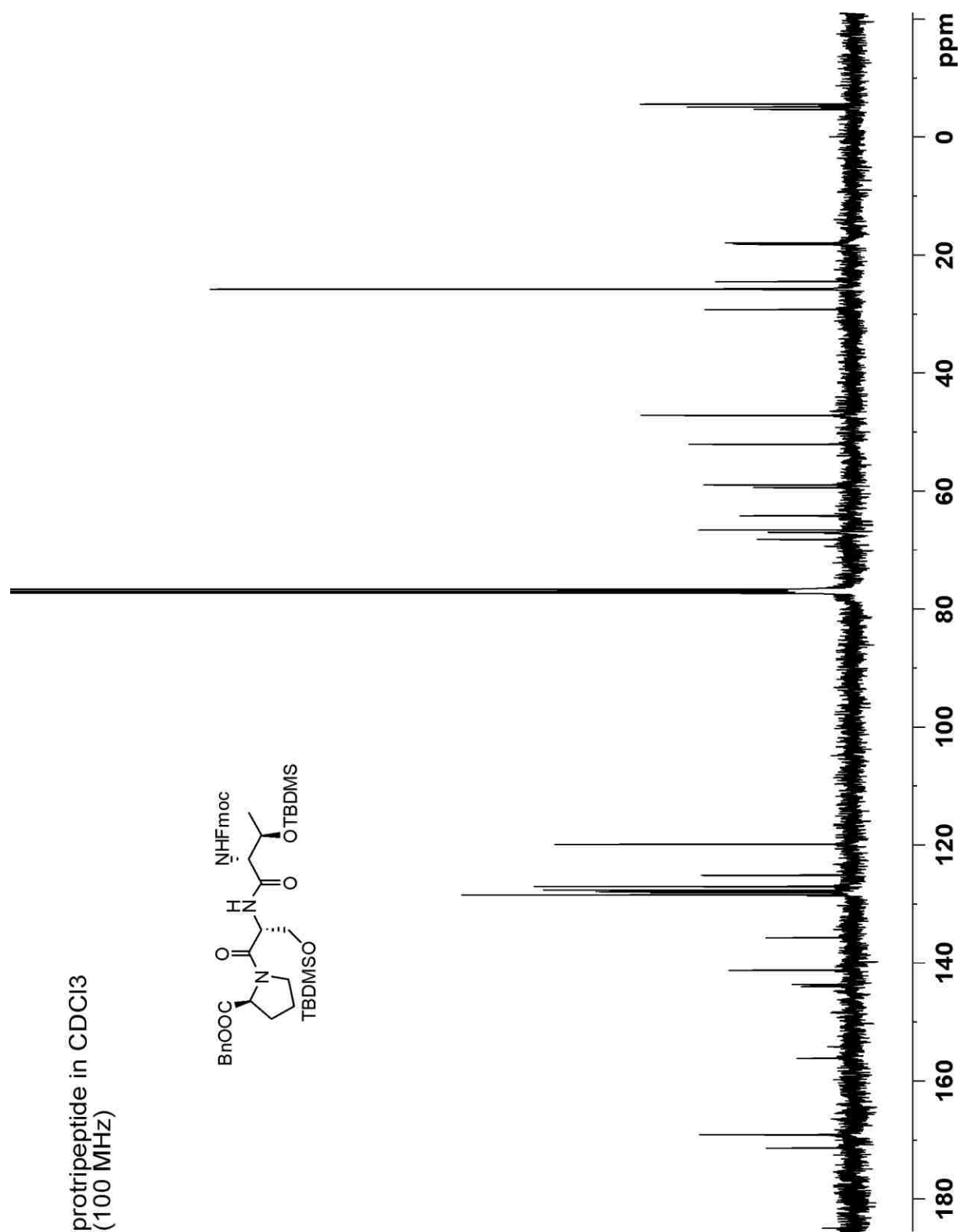
Fmoc-*D*-Thr-*D*-Ser-DHP-OBn (171)- ^{13}C NMR in CD_3OD at 100 MHz



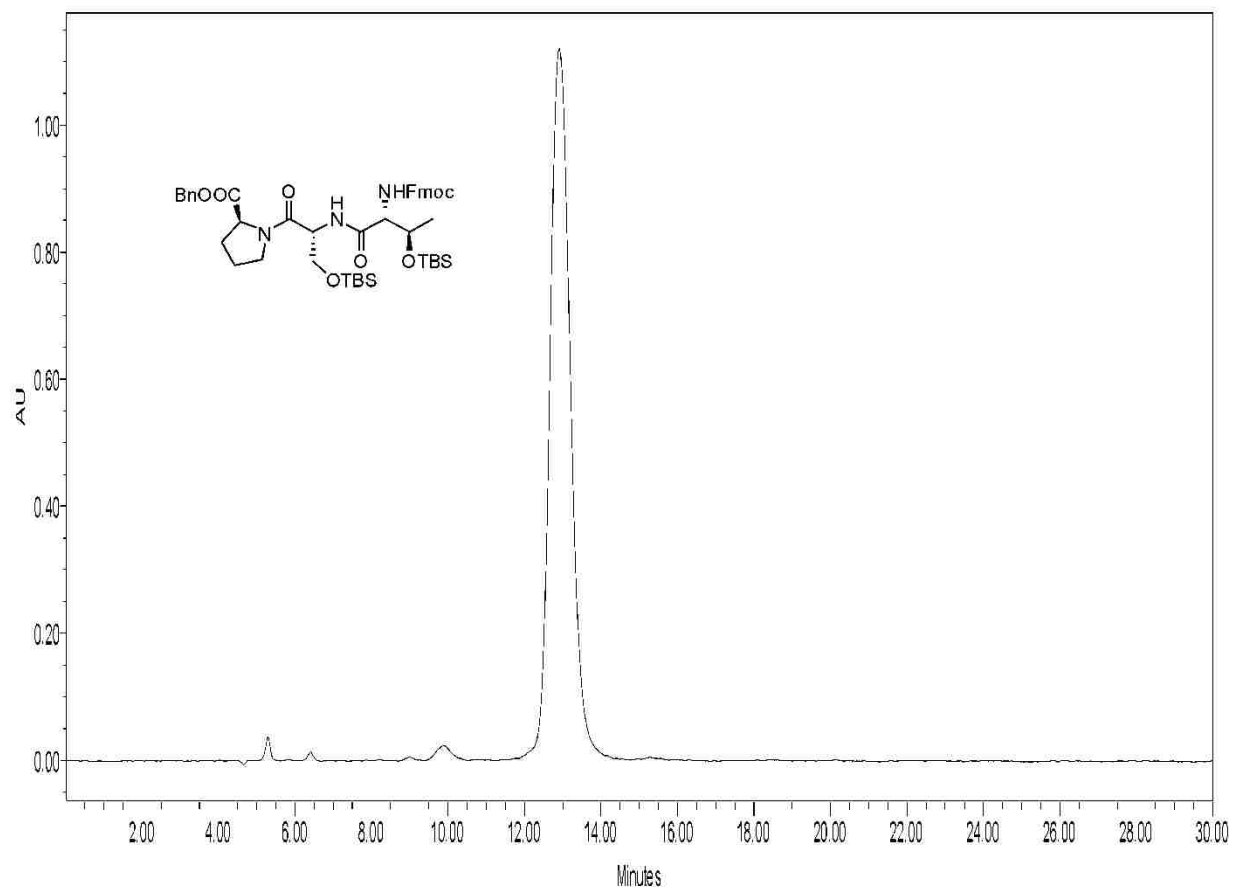
Fmoc-*D*-Thr-(OTBS)-*D*-Ser(OTBS)-Pro-OBn (48) – ^1H NMR in CDCl_3 at 400 MHz



Fmoc-*D*-Thr-(OTBS)-*D*-Ser(OTBS)-Pro-OBn (48) – ^{13}C NMR in CDCl_3 at 100 MHz

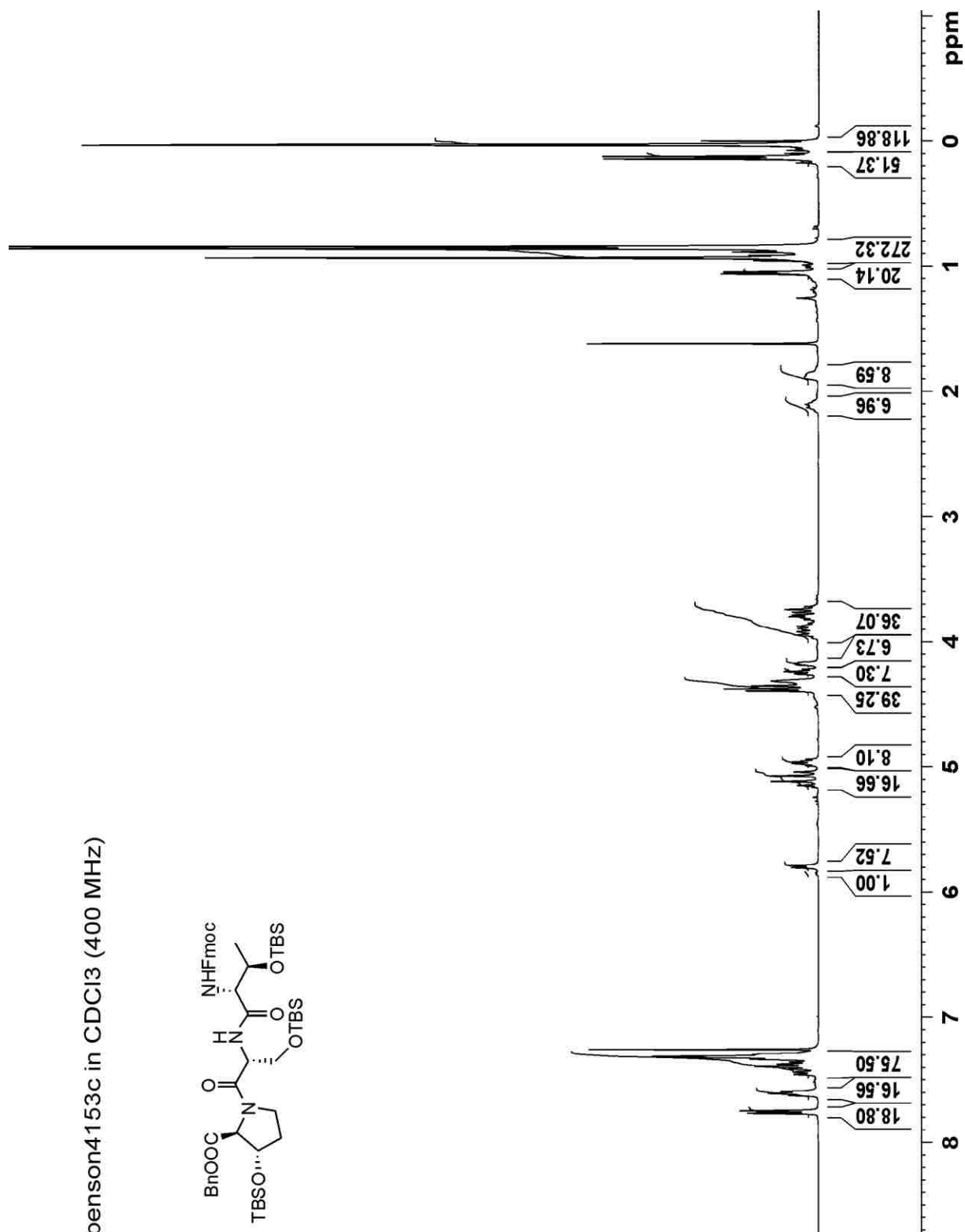
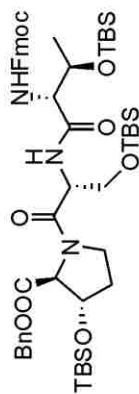


Fmoc-D-Thr-(OTBS)-D-Ser(OTBS)-Pro-OBn (48) – HPLC chromatogram at 254 nm, 30% EtOAc in Hexanes, 10 mm Econosil, 3 mL min⁻¹ (98% pure)

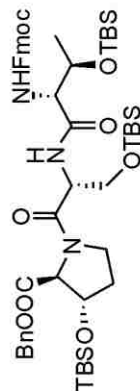


Fmoc-*D*-Thr-(OTBS)-*D*-Ser(OTBS)-*trans*-3-Hyp(OTBS)-OBn (49) – ^1H NMR in CDCl_3 at 400 MHz

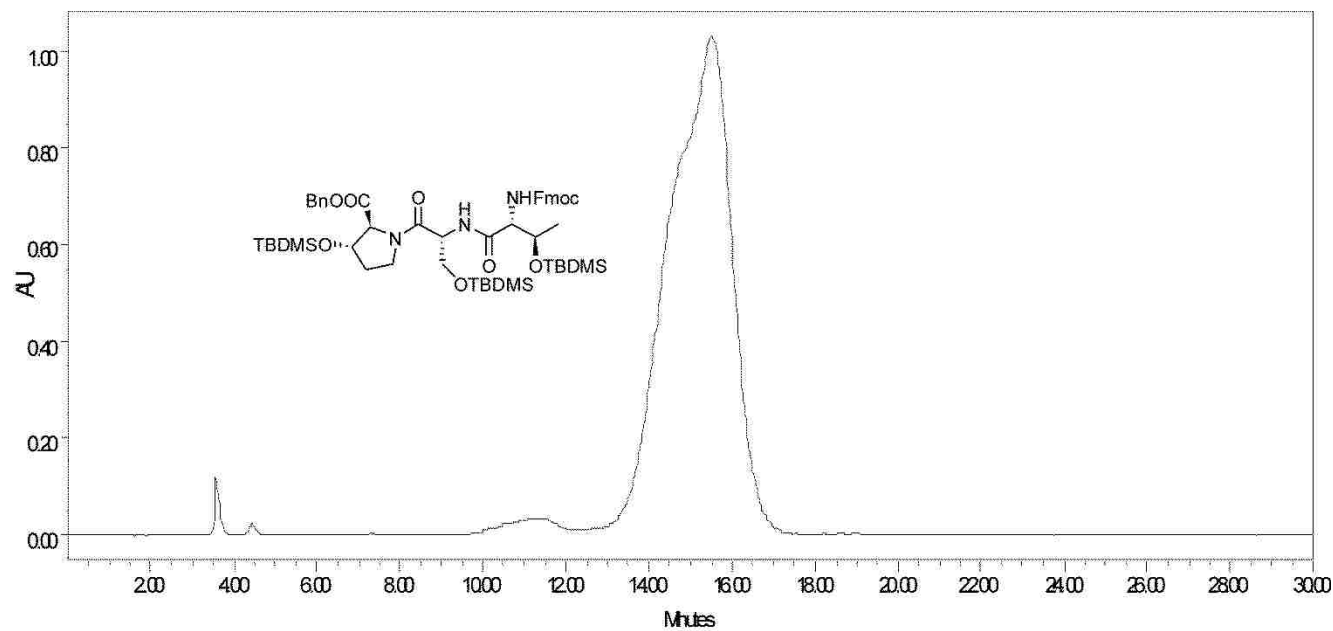
benson4153c in CDCl_3 (400 MHz)



benson4153c in CDCI3 (100 MHz)



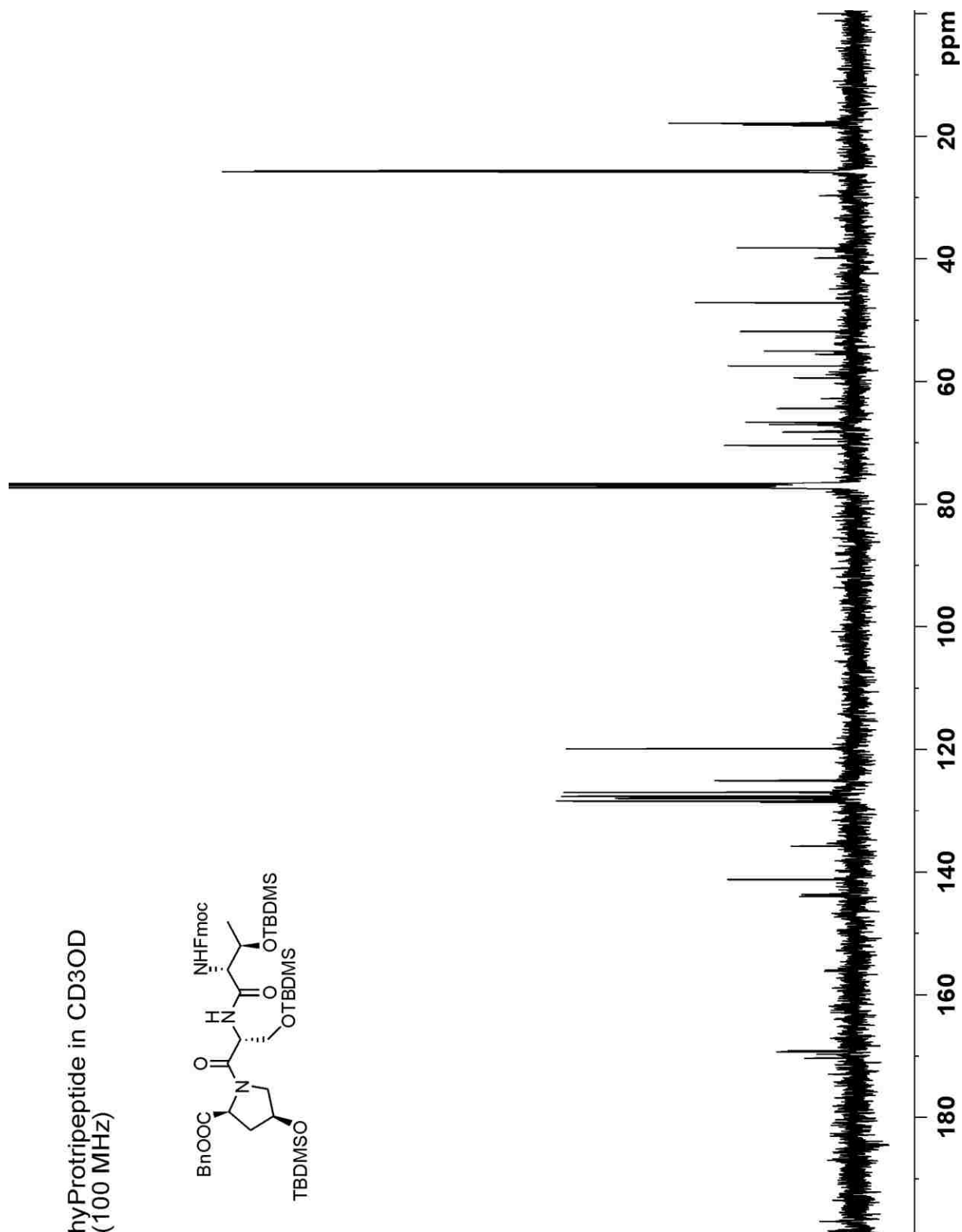
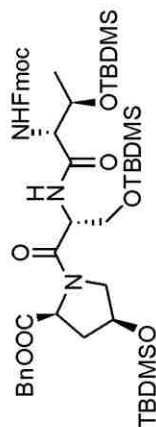
Fmoc-*D*-Thr-(OTBS)-*D*-Ser(OTBS)-3-hyp(OTBS)-OBn (49) – HPLC chromatogram at 254 nm, 20% EtOAc in Hexanes, 10 mm Econosil, 3 mL min⁻¹ (97% pure).



hyProTripeptide in CDCl₃
(400 MHz)

Fmoc-*D*-Thr-(OTBS)-*D*-Ser(OTBS)-*cis*-4-hyp(OTBS)-OBn (50) - ^{13}C NMR in CDCl_3 at 100 MHz

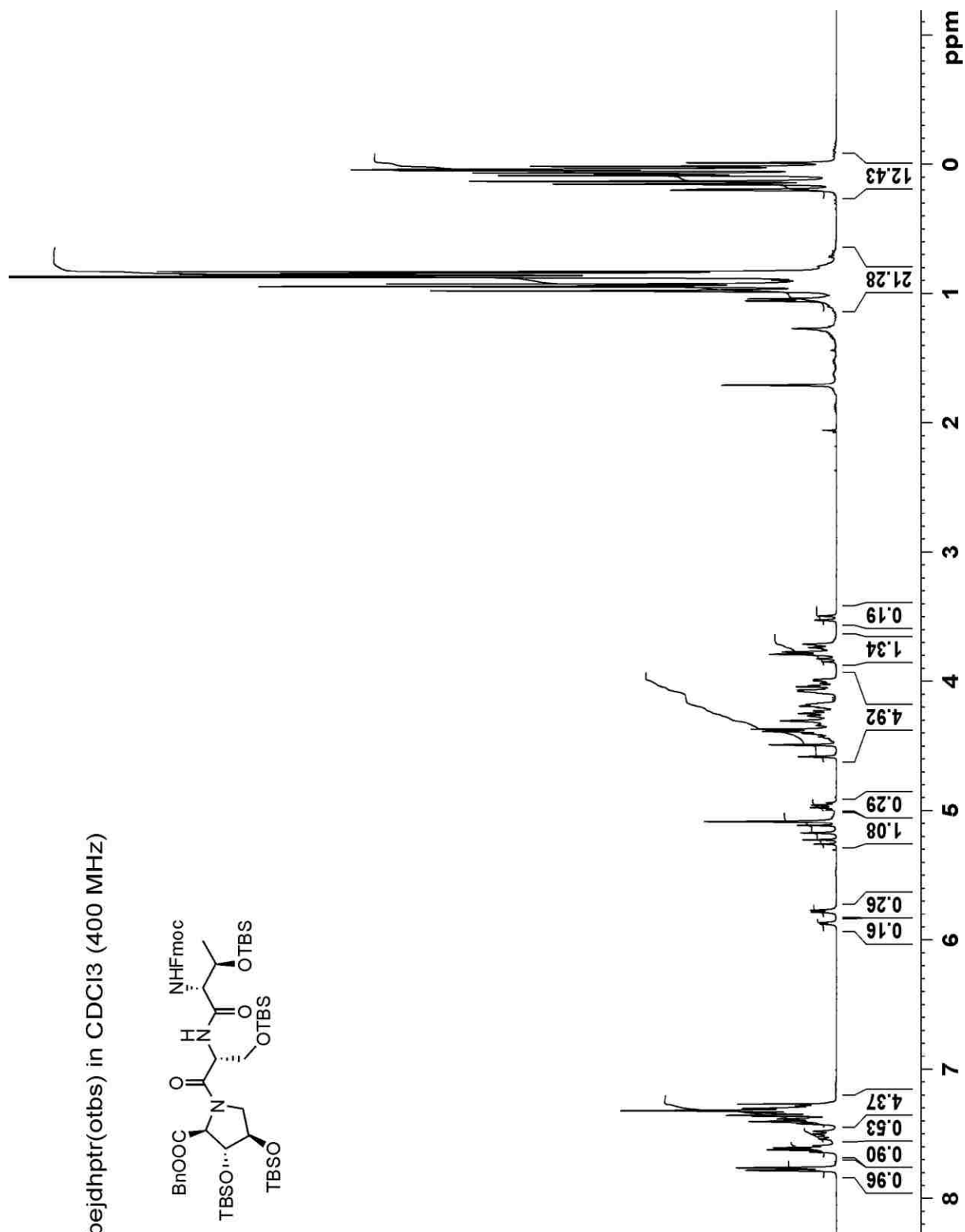
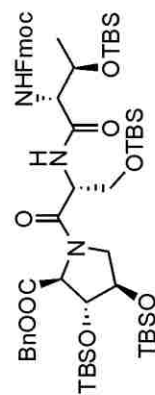
hyProtripeptide in CD_3OD
(100 MHz)



The HPLC chromatogram displays the separation of compound 10. The x-axis represents time in minutes, ranging from 2.00 to 30.00. The y-axis represents absorbance units (AU), ranging from 0.00 to 0.60. A single, sharp, prominent peak is observed at a retention time of 17.1 minutes, reaching an AU of approximately 0.59. Several minor baseline fluctuations are visible between 4 and 16 minutes. The chemical structure of compound 10 is provided as an inset, showing a complex molecule with a benzyl ester, a TBSO group, a Boc-protected amine, and a TBSO-protected alcohol.

Fmoc-*D*-Thr-(OTBS)-*D*-Ser(OTBS)-DHP(OTBS)₂-OBn (47) – ¹H NMR in CDCl₃ at 400 MHz

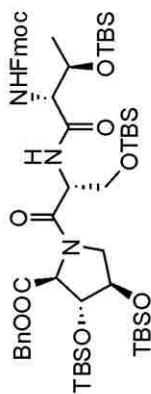
bejdhp(otbs) in CDCl₃ (400 MHz)



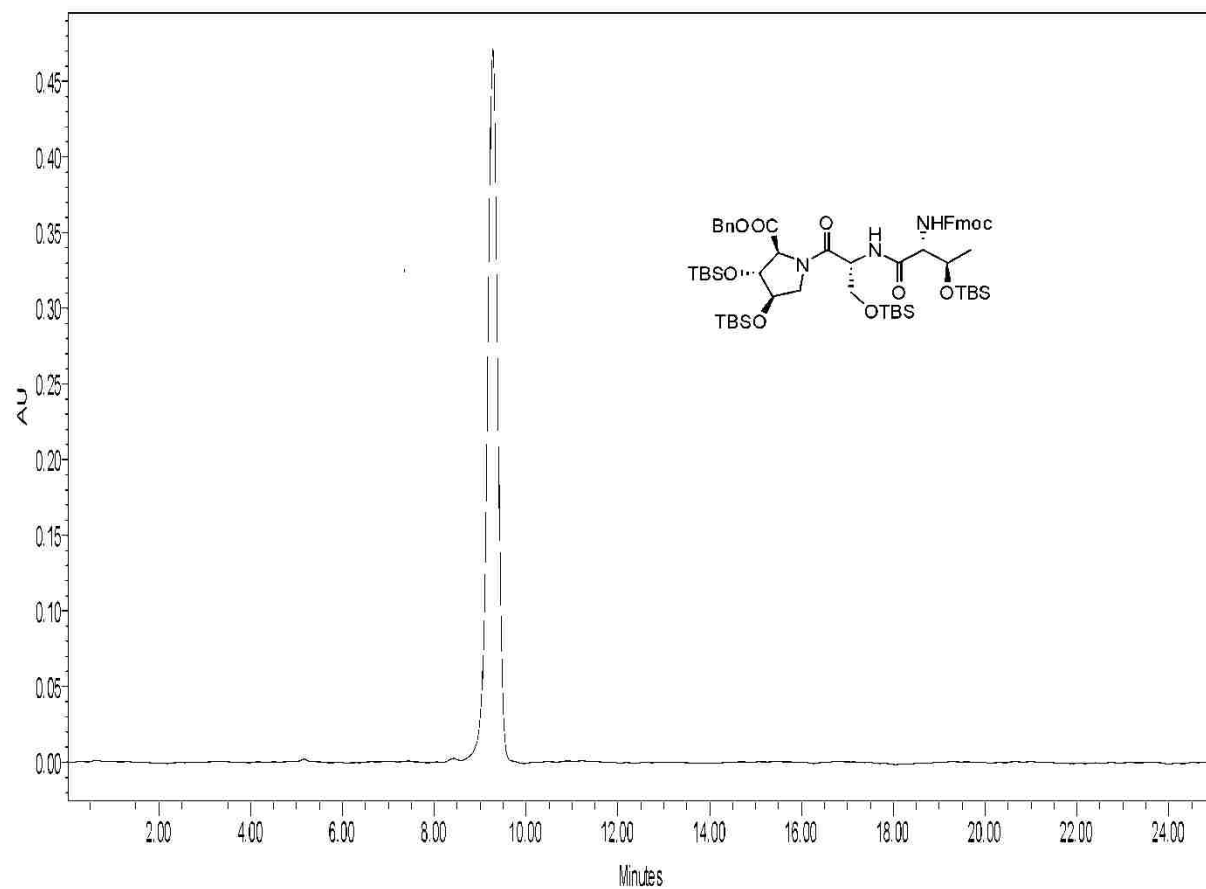
bejdhptr(otbs) in CDCl₃ (100 MHz)

Chemical structure of compound 10j is shown above the spectrum. The structure is a complex molecule with a central carbon atom bonded to a benzyl group (Bn), a tert-butyldimethylsilyl group (TBS), and a dimethylsilyl group (TMS). The central carbon is also bonded to a nitrogen atom, which is part of a five-membered ring containing a carbonyl group (C=O) and a dimethylsilyl group (TMS). The nitrogen atom is also bonded to a dimethylsilyl group (TMS). The structure is labeled with stereochemistry: (R) for the central carbon and (S) for the nitrogen atom.

¹³C NMR spectrum (100 MHz, CDCl₃) of compound 10j. The spectrum shows peaks from 0 to 160 ppm. Key peaks include a large solvent triplet at 77.0 ppm, a carbonyl peak at 165.0 ppm, and various aliphatic and silyl peaks between 10 and 60 ppm.



Fmoc-D-Thr-(OTBS)-D-Ser(OTBS)-DHP(OTBS)₂-OBn (47) – HPLC chromatogram at 254 nm, 14% EtOAc in Hexanes, 10 mm Econosil, 3 mL min⁻¹ (100 % pure).



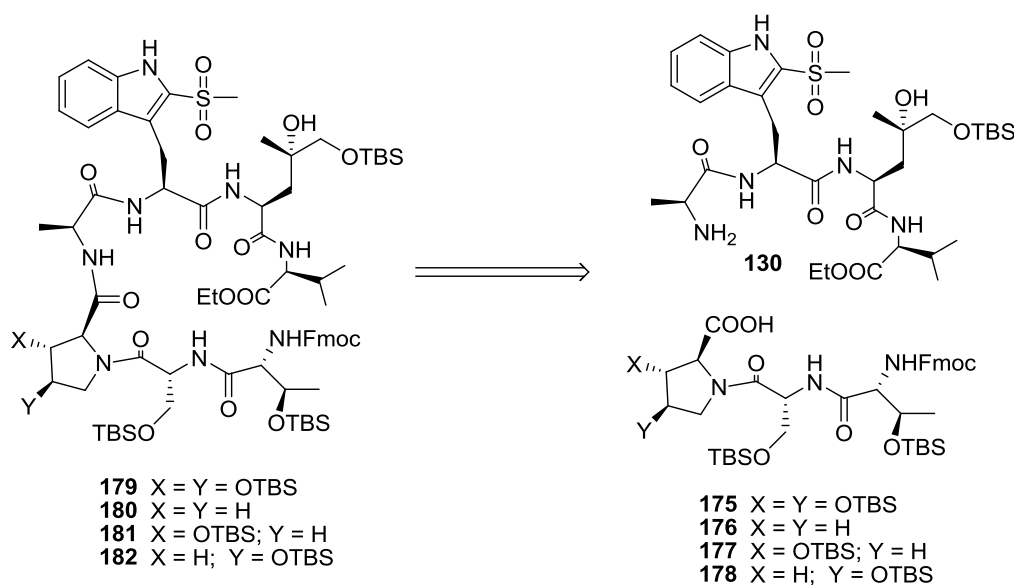
CHAPTER 4: FRAGMENT CONDENSATION AND CYCLIZATIONS

4.1 THE LINEAR HEPTAPEPTIDES

4.1.1 Overview

According to the retrosynthetic analysis presented in Chapter 2 (reiterated as Scheme 4.1), assembly of the linear heptapeptides involves [3 + 4] fragment condensations. In general, the synthesis of such oligopeptides could be achieved either through stepwise assembly or fragment condensation approaches. In a stepwise approach, the linear precursor is synthesized from one end to the other by adding one amino acid residue at a time to the growing sequence. Fragment condensation involves synthesizing the peptide fragments separately, followed by coupling them in a convergent fashion.

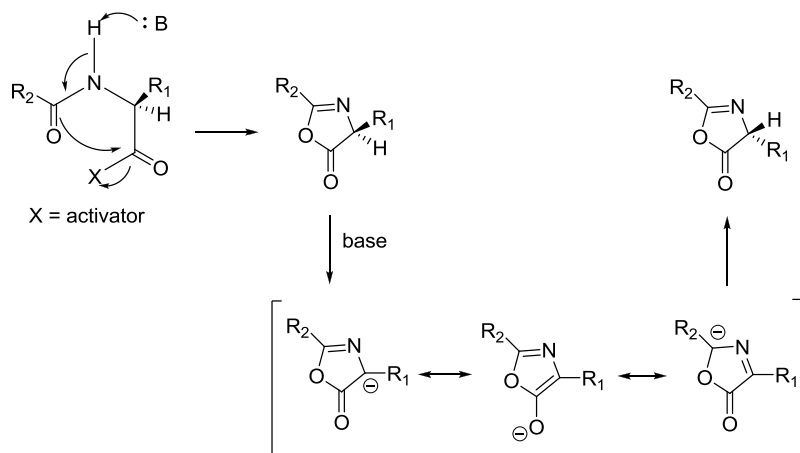
Scheme 4.1. Retrosynthetic analysis of allovroidin and analogs.



4.1.2 The Risk of Epimerization in Fragment Condensation

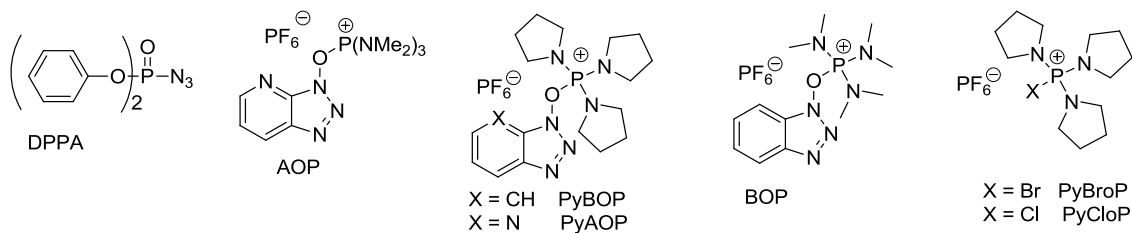
Having prepared our fragments, we were now ready to assemble the cyclization precursors through segment coupling. In general, segment couplings involving hindered peptides are prone to epimerization via oxazolone formation following acid activation (Scheme 4.2) *i.e.*, when R_2 = alkyl or peptidyl, base promoted enolization of the oxazolone intermediate occurs generating the undesired diastereomer. However, when R_2 = alkoxy (*viz-a-viz*, carbamate protected amino acid), then chances of oxazolone formation are low, and if generated, no epimerization occurs since the oxazolone intermediate is chirally stable and undergoes rapid aminolysis to give the desired product.

Scheme 4.2. Racemization through oxazolone.¹¹⁴

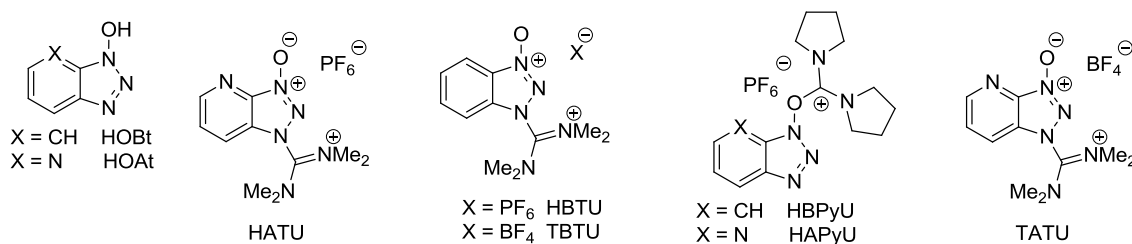


In addition to epimerization, the low coupling rates¹¹⁵ experienced in the coupling of hindered peptide fragments have often led to premature cleavage of base sensitive protecting groups such as Fmoc.¹¹⁶ However, our approach involves activation of non-epimerizable carboxyl components, bearing proline residues at their C-terminus. Furthermore, the emergence of new coupling reagents

(Figure 4.1), racemization suppressants and improved reaction conditions has had a great impact in the coupling of difficult segments.^{114, 117}



Examples of phosphorous based coupling reagents



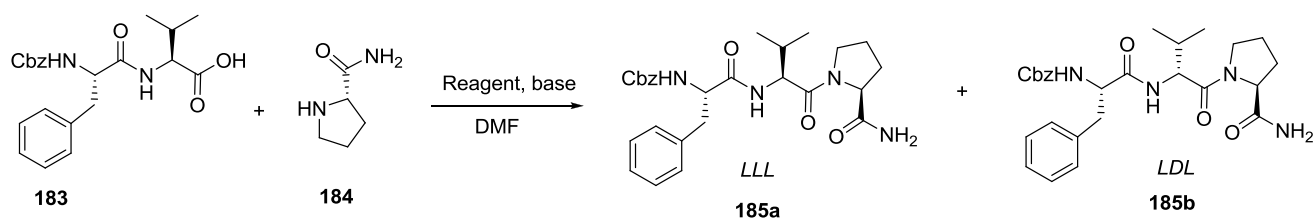
Examples of uranium/guanidinium-based coupling reagents

Figure 4.1. Selected phosphorous and uronium based coupling reagents

Studies by Carpino and co-workers have demonstrated the effect of various coupling reagents and base on the optical integrity of amino acid residues during peptide bond formation. The model peptide, Cbz-Phe-Val-Pro-NH₂, utilized by Carpino and co-workers involves coupling between sterically demanding residues thus rendering the Val residue susceptible to epimerization. According to Table 4.1, it can be seen that a combination of an appropriate coupling reagent, base and racemization

suppressant not only improves the yield but also minimizes the undesired racemization. In their investigation, a comparison between HOAt and HOBt as additives during carbodiimide-mediated couplings indicated that HOAt was better than HOBt at minimizing racemization when the reaction was conducted in DMF. For onium-based reagents, epimerization levels were noted to increase in the order of HAPyU < HATU < HBTU < BOP. The best result was obtained when collidine was used as a base.

Table 4.1. Effect of coupling reagent and base during peptide bond formation.¹¹⁸

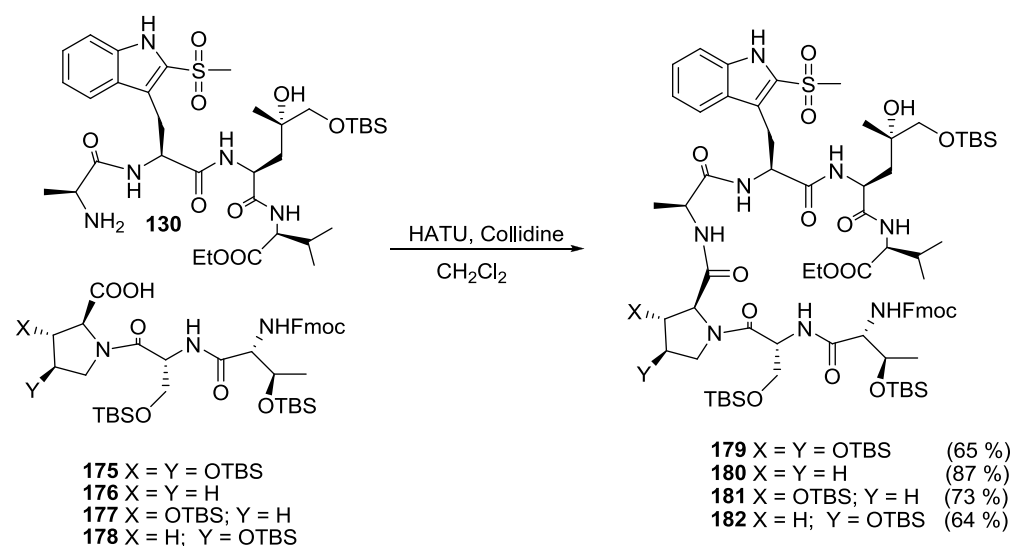


Coupling reagent	Base (equiv.)	Yield, %	LDL, %
EDC/HOAt	No base	85	4.7
EDC/HOBt	No base	87	18.9
HATU	DIEA (2)	86	13.9
HATU	Collidine (2)	83	5.3
HATU/HOAt	DIEA (2)	76	10.9
HATU/HOAt	Collidine (2)	72	2.4
HBTU	DIEA (2)	88	27.4
HBTU	Collidine (2)	81	14.2
BOP	DIEA (2)	84	30.4
BOP	Collidine (2)	81	13.9
HAPyU	DIEA (2)	89	10.8
HAPyU	Collidine (2)	87	3.5
HAPyU/HOAt	DIEA (2)	77	3.2
HAPyU/HOAt	Collidine (2)	76	1.6

4.1.3 Execution of the Condensations

We conducted the [3 + 4] fragment condensations between the tetrapeptide amine and the series of four tripeptide acids, using Carpino's HATU/collidine conditions, affording the corresponding linear heptapeptides in excellent yields (Scheme 4.3). Initial attempts at fragment condensation using PyBroP¹¹⁹ generated the linear heptapeptides in poor yields.

Scheme 4.3. The [3 + 4] fragment condensations.



It should be noted that the four linear heptapeptides were purified by flash column chromatography and analyzed by HPLC. The HPLC chromatograms indicated that the purity of each linear heptapeptides was greater than 90% (see experimental section for the HPLC traces). High resolution mass spectrometry confirmed the identity of each species. The ¹H NMR spectra of the linear heptapeptides were complicated by overlapping of signals, due to interconversion between the numerous conformations that are common to extended peptides in solution and therefore no individual assignments were made at this level.

4.2 THE CYCLIZATIONS

4.2.1 The Importance of Cyclic Peptides

Peptide cyclization is of great importance since it restricts the number of conformations in solution and thereby often enhances receptor binding affinities.¹²⁰⁻¹²² Also, the absence of ionizable C- and N-termini facilitates the crossing of lipid membranes resulting in better bioavailability necessary for therapeutic applications.^{123, 124} Furthermore, cyclic peptides have significant therapeutic potential due to their resistance to proteolytic degradation.¹²⁵

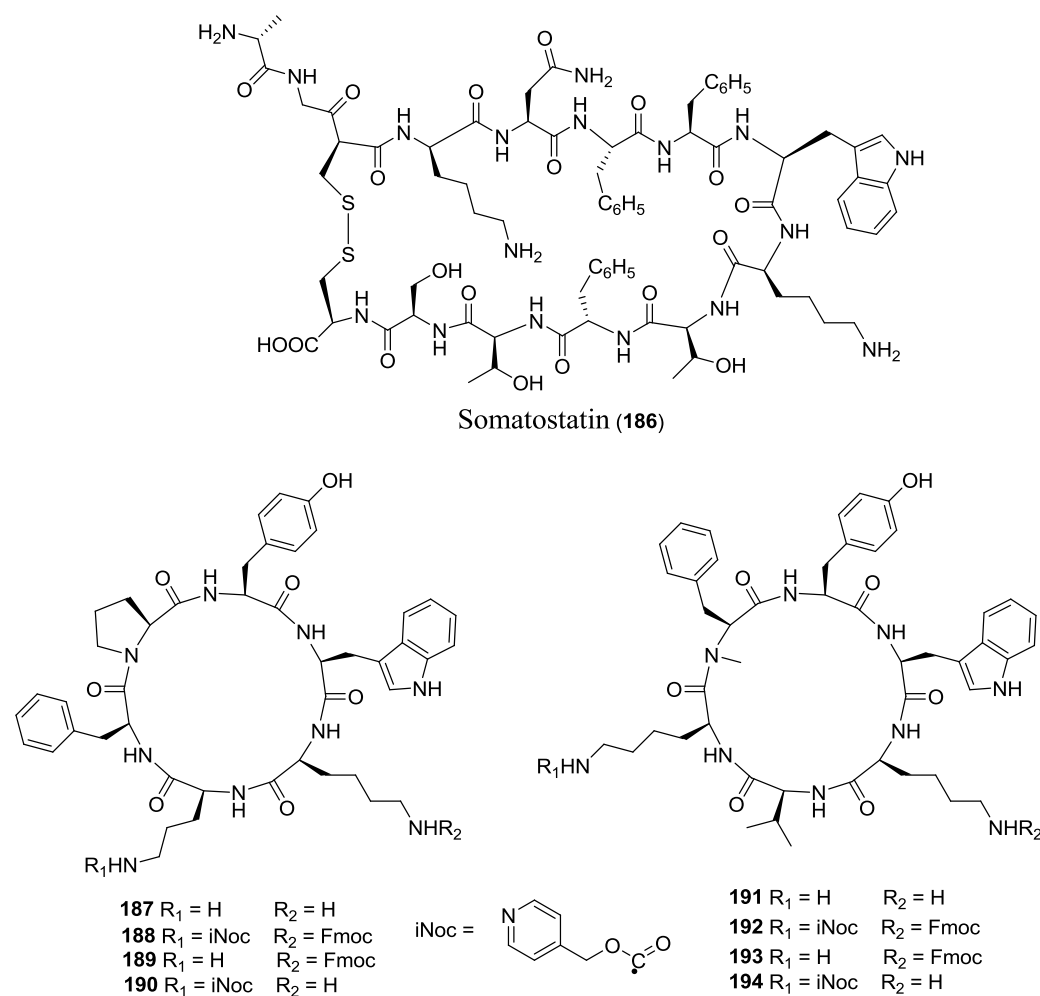


Figure 4.2. Examples of cyclic peptide drugs. Somatostatin¹²⁶ (**186**) along with hexapeptide analogs (**187-194**), synthesized by Hirschmann and co-workers.¹²⁴

4.2.2 Types of Peptide Cyclization

During the synthesis of cyclic peptides, the most challenging step is the cyclization reaction. Although numerous methods for peptide cyclizations have been developed,¹²⁷⁻¹³³ the intramolecular peptide bond formation remains a greater challenge than the preparation of the linear precursors. Among the various ways described for solution phase synthesis of cyclic peptides include the head to tail and side-chain to side-chain cyclizations (Fig. 4.3). The latter approach may involve formation of disulfide (Cys) or amide bonds (Lys in combination with Asp or Glu) between residue side-chains. The success of the two approaches is dependent on the availability of orthogonally protected linear precursors.¹²⁷ Other ways of peptide cyclization are head to side chain and side chain to tail. Some specific examples are given in Schemes 4.4-4.7 for illustration. In general, the choice of a cyclization approach is defined by the target molecule. For instance, during the synthesis of alloviroidin and analogs, we utilized a head to tail cyclization approach as directed by the structure of the cyclopeptides.

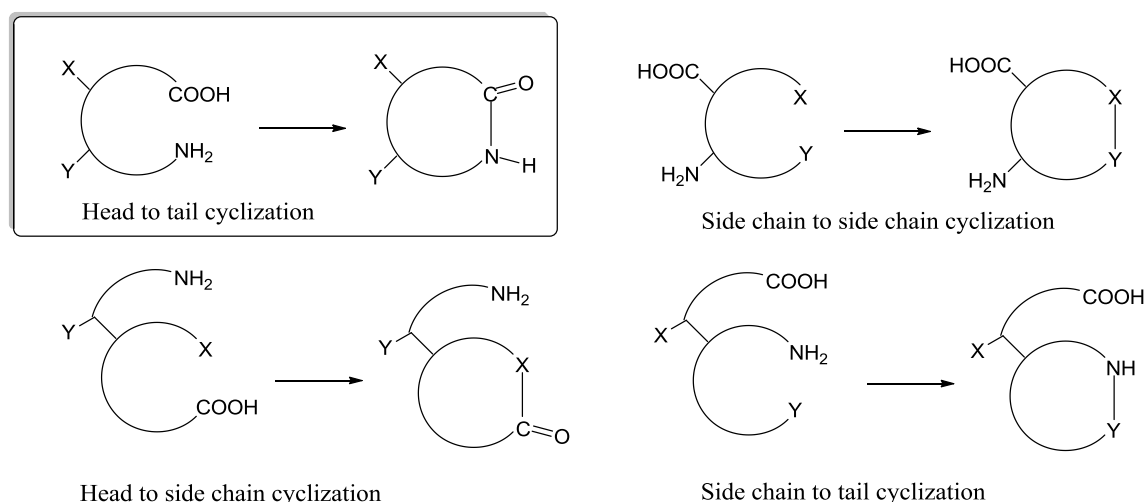
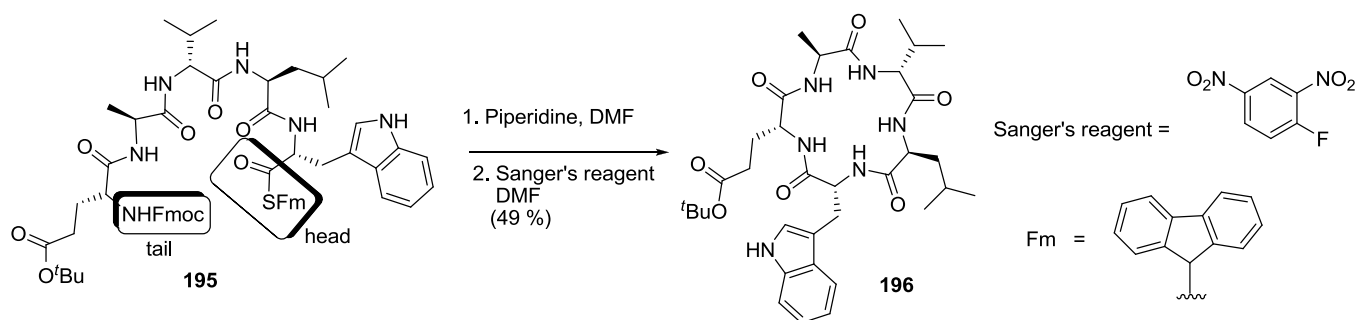
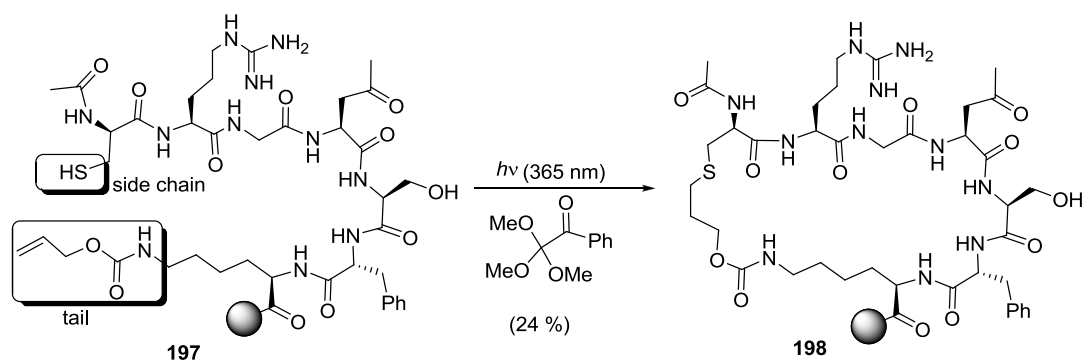


Figure 4.3. Examples of peptide cyclization approaches.

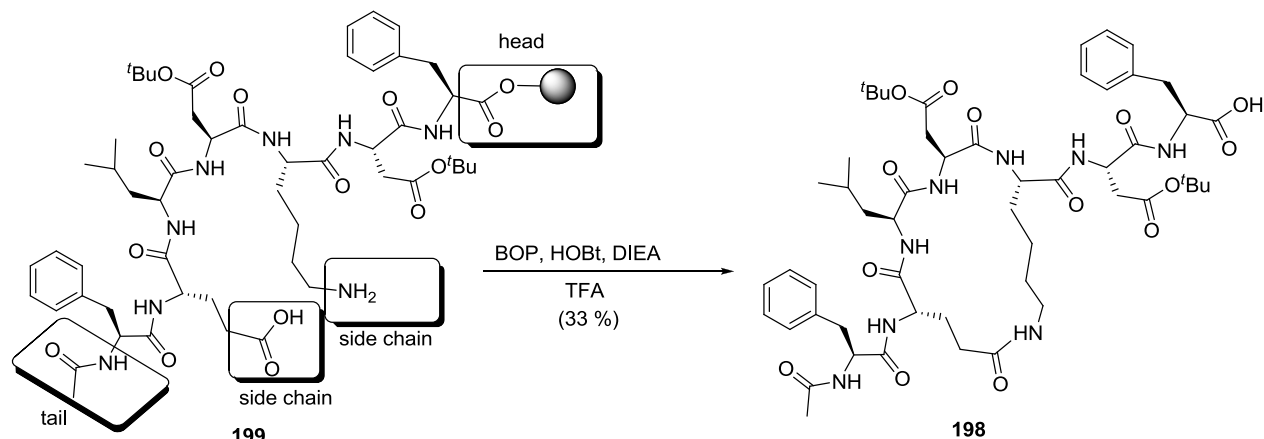
Scheme 4.4. Crich and Sasaki's head to tail cyclization of a pentapeptide.¹³⁴



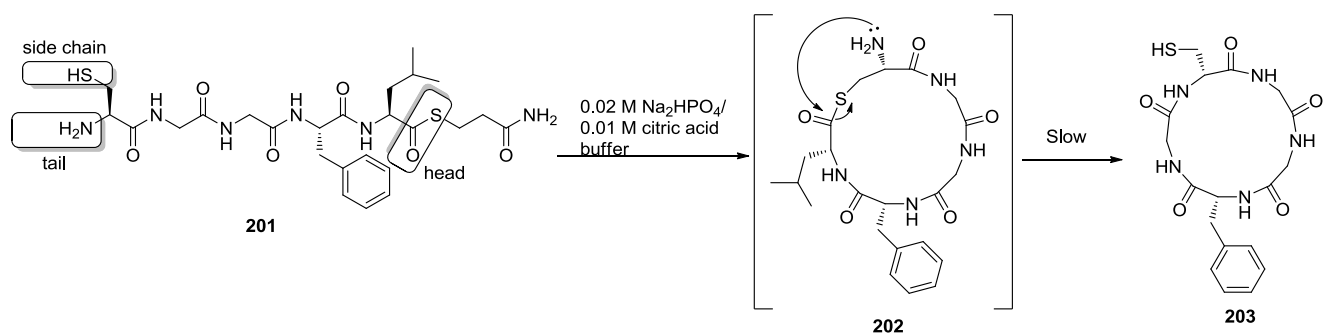
Scheme 4.5. Anseth and co-workers' side chain to tail cyclization on a solid phase.¹³⁵



Scheme 4.6. Smith and co-workers' side chain to side chain cyclization on a solid phase.¹³⁶



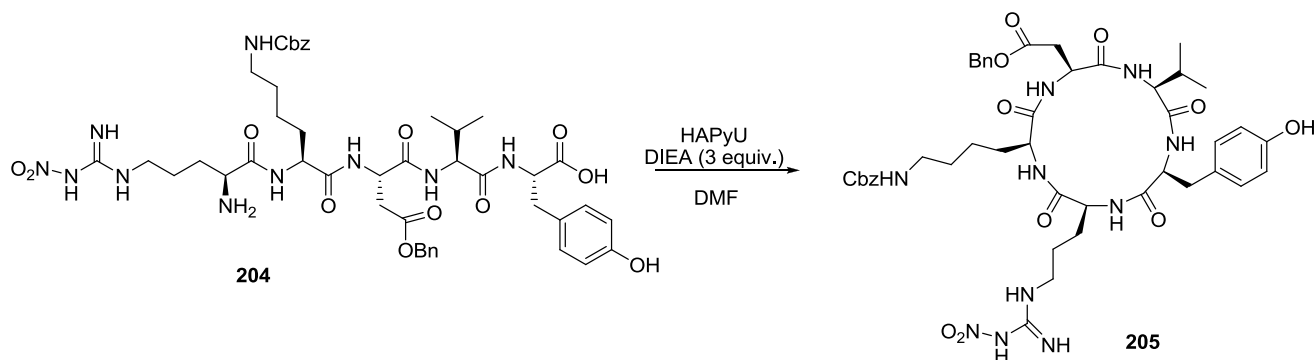
Scheme 4.7. Zhang and Tam's head to side chain cyclization.¹³⁷



4.2.3 Suppressing Epimerization of the C-Terminal Residue

Since peptide cyclizations are intramolecular reactions, a high dilution of 10^{-3} M or greater is required to suppress the formation of byproducts arising from dimerization and polymerization. Unfortunately, such dilute conditions also imply low concentration of reagents, resulting in sluggish reactions, with competitive peptide decomposition and epimerization compromising the yield and quality of the cyclomonomer.^{138, 139} During the cyclization of all *L*-penta- and hexapeptides using 1-hydroxy-7-azabenzotriazole-derived uronium and phosphonium reagents, Ehrlich and co-workers demonstrated that epimerization and cyclodimer formation could be minimized under highly dilute conditions. As demonstrated in Table 4.2, cyclodimer formation was reduced to 2 % when the concentration of **204** was 0.1 mM (Entry 3).¹³³

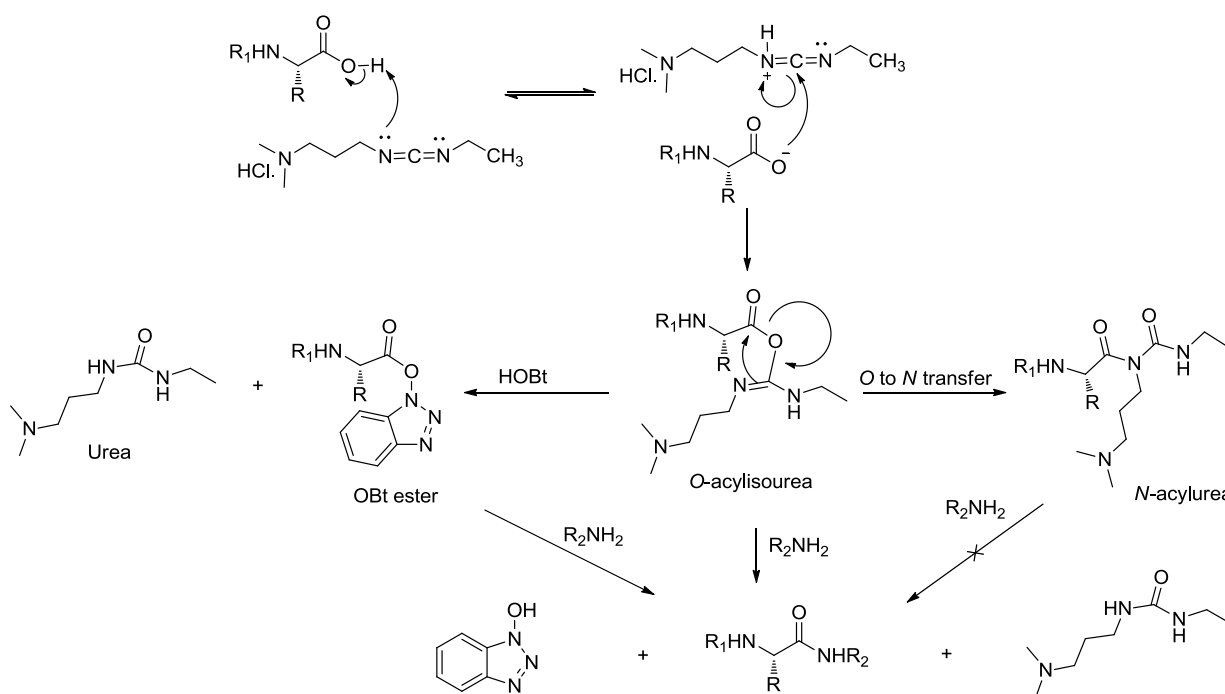
Table 4.2: Ehrlich and co-workers' cyclization of all *L*-pentapeptide.¹³³



Entry	Concentration of linear peptide (mM)	Cyclomonomer 205 (%)	D-Tyr-isomer (%)	Cyclodimer (%)
1	10	25	8.0	40
2	1	55	8.8	25
3	0.1	82	-	2

Traditionally, the extent of epimerization has been minimized by using azide or DPPA-mediated couplings;¹⁴⁰ however, these methods of activation are extremely slow.^{138, 141, 142} Carbodiimides used in combination with additives such as HOBt, HOAt, and *N*-hydroxysuccinimide (NHS) that form activated esters have also been utilized to effect peptide cyclizations. These reagents intercept and prevent the formation of an *N*-acylurea by reacting with the *O*-acylurea as shown in Scheme 4.8. Carbodiimides have the disadvantage of generating urea precipitates that often slow down peptide couplings.

Scheme 4.8. EDC activation.

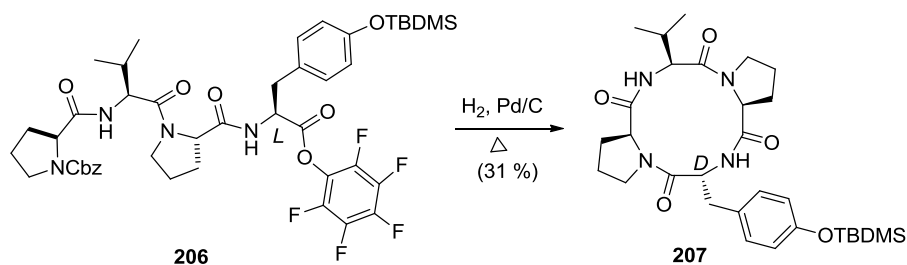


Several examples of peptide cyclizations have been reported using EDC/HOBt reagents, as compared to other carbodiimides.^{143, 144} The urea formed from an EDC mediated coupling is removed by aqueous extraction. In contrast, the dicyclohexylurea generated during *N,N'*-dicyclohexylcarbodiimide (DCC) mediated coupling reaction is difficult to remove using the standard aqueous work-up. Other reagents like TBTU¹⁴⁵ and BOP¹⁴⁶ are known to give improved yields for peptide cyclization,¹⁴⁷ but their use is limited due to unacceptable levels of epimerization.¹⁴⁸ The relatively new 1-hydroxy-7-azabenzotriazole HOAt-based reagents^{88, 149} have attracted considerable attention as serious alternatives to HOBt-based reagents and the traditional azide methods, which are too slow to be employed in conjunction with *N*-methyl peptides.¹³¹ The former improve cyclization rates relative to azide couplings in some cases but proceed with high levels of racemization.

4.2.4 Conformational Control to Facilitate Cyclization

Other key factors that dictate the success of a cyclization reaction are the linear precursor sequence and the choice of coupling reagent. This is illustrated by the attempts of Schmidt and Langner to synthesize the all *L*-isomer of tyrosinase inhibitor *cyclo*-[Pro-Val-Pro-Tyr].¹⁵⁰ According to Scheme 4.9, the carboxy terminus was activated as a pentafluorophenyl ester. Hydrogenolysis of the *N*-terminal Cbz group was expected to result in spontaneous cyclization. Unfortunately, epimerization of Tyr C α generated the *L, L, L, D* tetrapeptide that cyclized more readily than its all *L*-counterpart, resulting in the isolation of **207** in 31 % yield.

Scheme 4.9. Schmidt and Langner's *C*-terminal epimerization of all *L* residues.¹⁵⁰



Schmidt and Langner also demonstrated sequence dependence during cyclization after investigating ring closures at the various possible sites of the pentapeptide *cyclo*-[Pro-Ala-Ala-Phe-Leu]. According to Fig. 4.4, Schmidt and Langner were able to prepare the cyclopentapeptide in 21% yield after performing ring closure between alanine and phenylalanine residues. Cyclization at other possible sites gave rise to mixtures of monomers and dimers or no isolable product. It has also been shown that a linear sequence with *D* and *L* amino acids in alternate positions favors cyclization.^{133, 151-153}

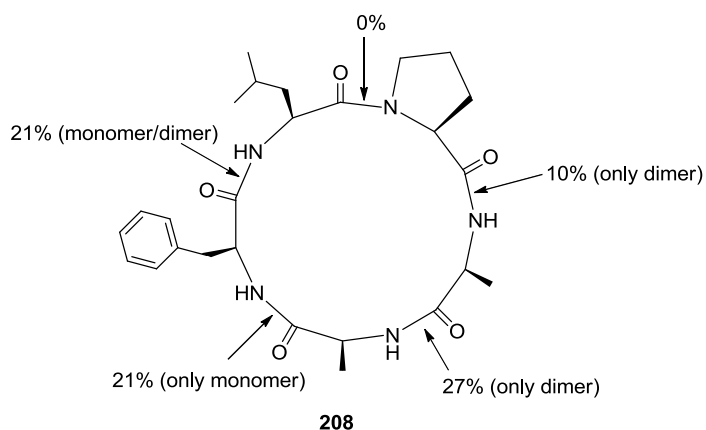
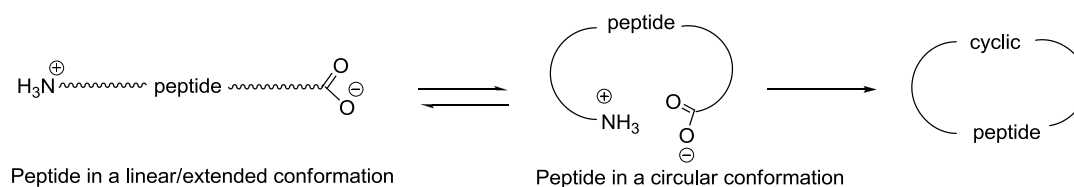


Figure 4.4. Schmidt and Langner sequence dependence cyclization.¹⁵⁰

The size of the ring to be closed also influences the ease with which an open chain precursor cyclizes. The cyclization of peptides with five residues is often difficult since dimerization occurs easily.^{154, 155} However, the cyclization of peptides containing seven to nine amino acids is considered much less residue-dependent and favored by the flexibility of the ring systems.¹²⁷ Small to medium-sized rings have difficulty accommodating the *Z* geometry necessary for cyclization.¹⁵⁶ Furthermore, the ease of cyclization is often enhanced by turn-inducing residues such as glycine, proline or *D*-amino acids.¹⁵⁷⁻¹⁵⁹ In order for a cyclization to occur, the activated linear peptide should adopt a circular conformation to bring the *N*- and *C*-termini in close proximity (**Scheme 4.10**).

Scheme 4.10. Extended and circular conformations of the peptide.



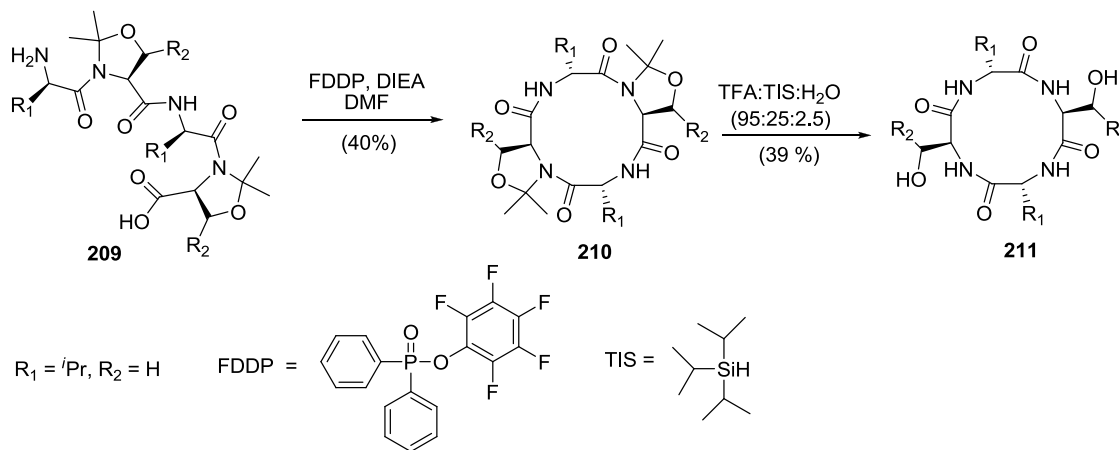
A planar transoid conformation of the peptide bond induces a rigid and extended conformation in the linear precursor making it difficult for cyclomonomer formation.¹³² Cyclizations involving all *D* or *L* peptides is challenging since these precursors prefer to adopt extended

conformations to minimize allylic strain.¹⁶⁰ Various strategies such as modification of the peptide bond or the use of external templates to influence conformational preorganization have been developed to overcome this problem.¹⁶¹ Ring closure kinetic studies by Daidone and Smith revealed that cyclization of longer peptides is enhanced by intramolecular hydrogen bonding and by the formation of β -sheet structures which bring the two termini close enough to cyclize.¹⁶² Rigid, extended conformations of shorter peptides were attributed to lack of intramolecular hydrogen bonds making cyclization of these peptides almost impossible.¹⁶²

Reverse turns in protein secondary structures have inspired chemists to develop ways of inducing turns in linear peptides to facilitate cyclic peptide synthesis.¹⁶³ This can be achieved by introduction of *cis* peptide bonds in the middle of the linear precursor to mimic β -turns.¹⁵⁶ The presence of *N*-methylated amino acids in peptides have the same turn inducing effect on the peptide backbone to that of proline.¹⁶⁴⁻¹⁶⁸

The use of pseudoprolines derived from serine and threonine as turn-inducers during synthesis of cyclic peptides has been documented by several groups.^{169, 170} When incorporated into peptides, pseudoprolines introduce cisoid conformations generating type-VI β -turn structures that favor cyclization.¹⁷⁰

Scheme 4.11. Jolliffe and co-workers' synthesis utilizing pseudoprolines as turn inducers.¹⁶⁹

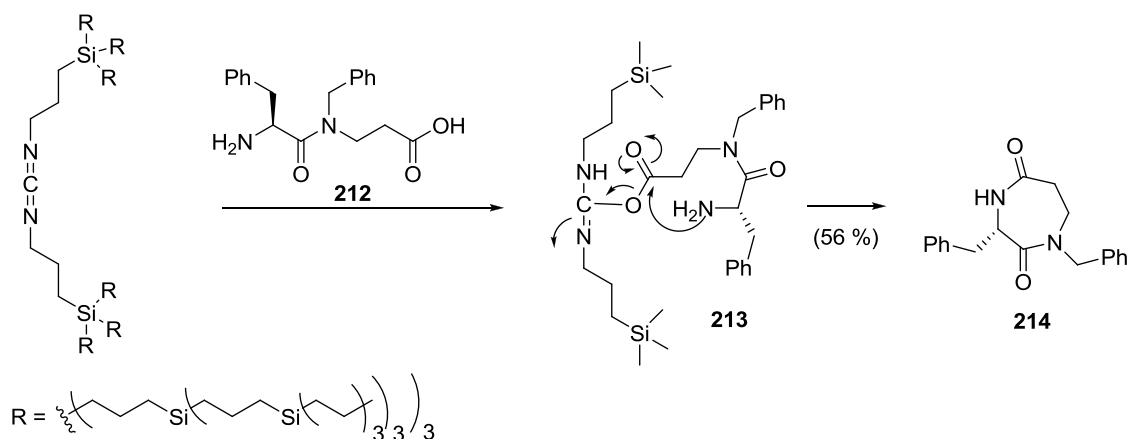


Studies have revealed that positioning the turn-inducing residue midway along the cyclization precursor could give better results than when it is at the terminal, although it is not possible to capitalize on this phenomenon for all peptide sequences.^{129, 132}

If possible, the cyclization site should not occur between sterically hindered amino acids such as *N*-methylated, α,α -disubstituted or β -branched residues. If the opportunity exists, cyclization should be engineered to occur between *D*- and *L*-residues since this facilitates the reaction.¹¹⁷ Brady and co-workers concluded in their study on the practical synthesis of cyclic peptides that the orientation of the *N*-terminal side chain along with the orientation of the amino group greatly influence the success of the cyclization.¹⁷¹

Another strategy for directing peptide cyclization involves the use of external templates as reaction cavities to accommodate and cyclize one linear peptide molecule at a time (Scheme 4.12).¹⁷² This isolates the peptide from the bulk solution, thereby minimizing chances of polymerization.

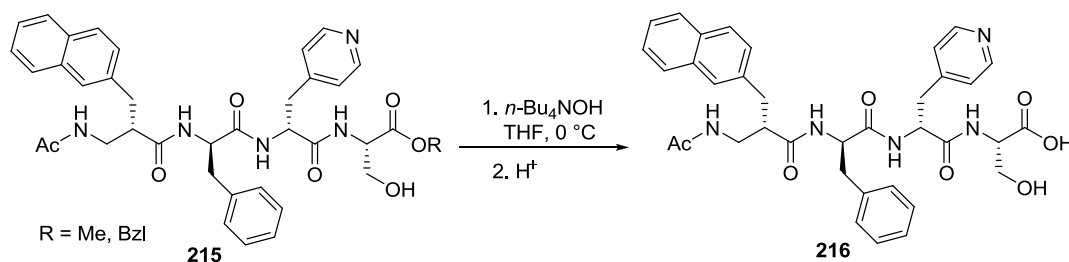
Scheme 4.12. van Maarseveen and co-workers' site isolation mechanism using carbosilane dendrimeric carbodiimide.¹⁷²



4.2.5 Cyclizations and Deprotections

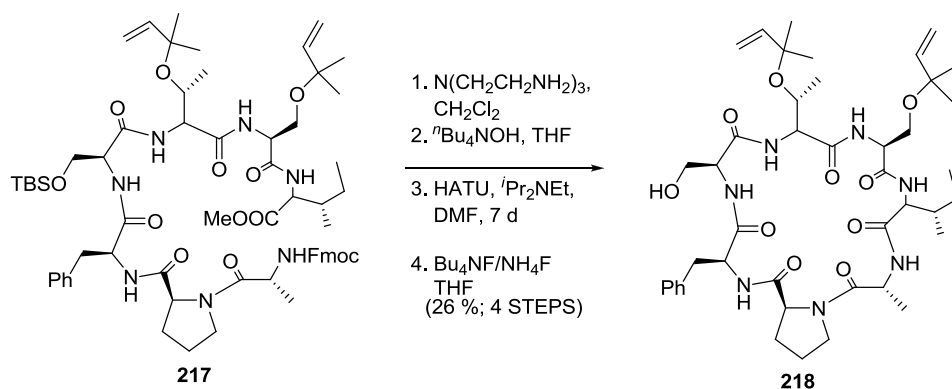
With the linear heptapeptide fragments in-hand, a prerequisite to the final cyclization is the liberation of the acid and amine functionality of the terminal residues. The Fmoc group in each linear precursor was cleaved by treatment with *tris*(2-aminoethyl)amine (TAEA) according to Scheme 4.15.⁹⁶ The presence of the side chain TBS ethers and the carboxyl ethyl ester enabled the purification of the heptapeptide amines by flash chromatography after a careful aqueous workup involving extraction from phosphate buffer (pH 5.5). We then hydrolyzed the ethyl ester with tetrabutylammonium hydroxide (TBAH) and subjected the deprotected heptapeptide amino acids to a phosphate buffer workup again before attempting cyclizations.¹⁷³ Our early attempts to hydrolyze the ethyl ester using potassium trimethylsilanolate¹⁷⁴ at low temperatures were plagued by silyl ether cleavage and incomplete ethyl ester removal. Extensive studies by Abdel-Magid and co-workers found the use of tetrabutylammonium hydroxide suitable for hydrolysis of polypeptide esters with minimum racemization risks as compared to alkali metal hydroxides (Scheme 4.13).¹⁷³

Scheme 4.13. Abdel-Magid and co-workers hydrolysis of polypeptide esters.



The progress of the hydrolysis reaction involving the proline analog was initially followed by HPLC analysis. Our choice of these conditions was guided by the final stages of Uto and Wipf's trunkamide A synthesis, in which a single TBS-protected serine residue was employed (Scheme 4.14).

Scheme 4.14. Wipf and Uto's synthesis of trunkamide A.¹⁷⁵



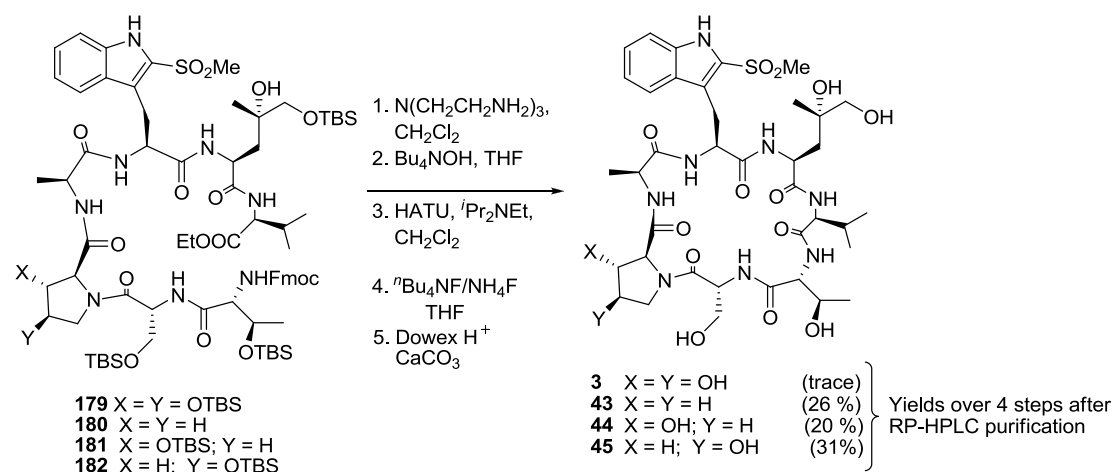
We then conducted our cyclizations under the HATU/DIEA-mediated coupling conditions. In each case, a solution of the linear precursor and the base were slowly added to a mixture of the coupling reagent and the base over a period of two hours via a syringe pump, to ensure high dilution. Indeed, slower addition afforded much cleaner reactions than when the addition was performed rapidly. We also compared DMF and dichloromethane as solvents for the cyclizations using a single syringe pump. Dichloromethane gave superior chemical yield, and also shortened the cyclization time from 48 h to 24 h. A similar solvent influence on cyclization was observed during the synthesis of aureobasidin A by Kurome and co-workers.¹⁷⁶ This phenomenon has been explained in terms of the solvation effect of the linear precursor whereby peptide interaction with the solvent through hydrogen bonding leads to either a circular or extended conformation.¹²⁸

It should be noted that cyclization of the 3-Hyp linear heptapeptide was more difficult compared to the other three and therefore the best yield was obtained upon conducting the reaction under high dilution using a dual syringe pump. With the dual syringe pump, the coupling reagent and the linear heptapeptide were independently added slowly to a solution of the base over a period of 2 h.¹⁷⁷

This parallel addition ensured that the concentration of the peptide remained constant and that the coupling reagent was active during peptide bond formation.

We concluded our syntheses by performing a global desilylation with tetrabutylammonium fluoride (TBAF), buffered with ammonium fluoride, affording the desired cycloheptapeptides with the recorded yields after reversed phase HPLC purification.

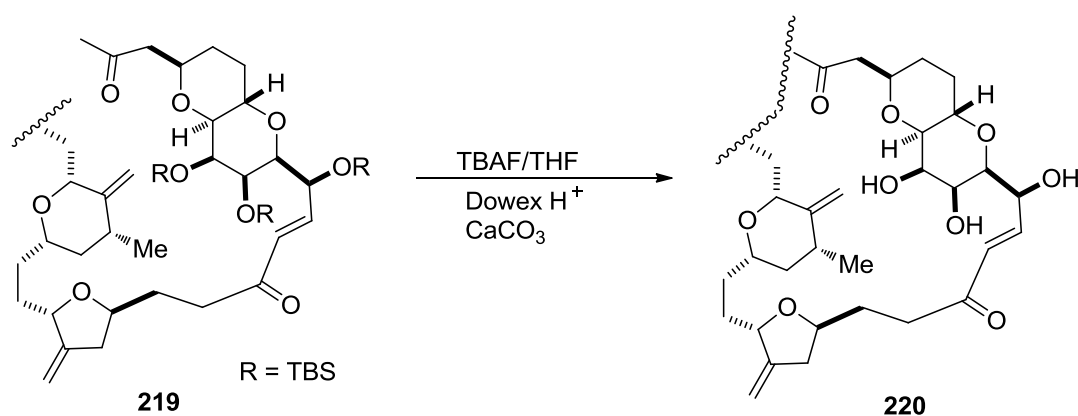
Scheme 4.15. Cyclizations and global desilylation.



The major problem encountered following the TBAF-mediated cleavage of the silyl ethers was the removal of the excess reagent and materials derived from TBAF that often require tedious aqueous workups to be eliminated. Neither an aqueous workup, nor reversed phase HPLC purification, were effective at removal of tetrabutylammonium ion salts from the silyl ether cleavage reaction and the “hangover” from ethyl ester hydrolysis with TBAH. The other challenge was posed by the polarity of our cyclic compounds since we would lose considerable amounts of the desired compounds during an aqueous workup, compromising our yields.

We were able to overcome this problem in the analogs by applying a workup procedure developed by Kishi and Kaburagi¹⁷⁸ who removed tetrabutylammonium salts at the conclusion of their synthesis of halichondrin. Their protocol involves the simultaneous addition of a commercially available sulfonic acid resin and calcium carbonate, followed by filtration (Fig. 4.5).¹⁷⁸ The resin/tetrabutylammonium salts, calcium fluoride and calcium carbonate are insoluble in THF and therefore can be removed by filtration, whereas water and TBSF are removed by evaporation leaving behind the desired alcohol (R-OH). However, the application of this protocol to the DHP containing cyclopeptide led to considerable loss of the product since we only recovered trace amounts of the natural product. We presume that the natural product could be either sticking to the resin or undergoing decomposition. Attempts to substitute CsF for tetrabutylammonium fluoride to deprotect the silyl ethers met with failure, *i.e.*, the reaction was sluggish and only generated decomposed products. Our hope was that this reagent would effect the deprotection without purification issues encountered with the ${}^n\text{Bu}_4\text{N}^+$ cation.

Scheme 4.16. Kaburagi and Kishi's synthesis of halichondrin.¹⁷⁸



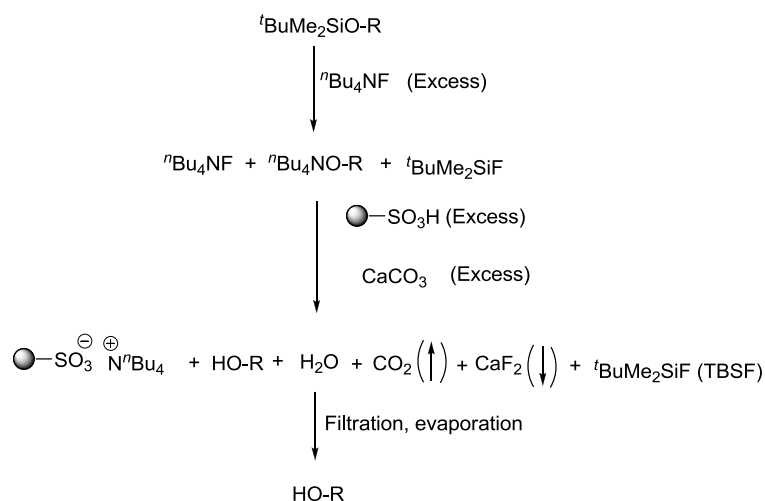


Figure 4.5. TBS deprotection and purification protocol.¹⁷⁸

A crude ^1H NMR analysis of our deprotected cycloheptapeptides, after applying Kishi's workup procedure, revealed less contamination by the TBAF derived materials, allowing for further purification by reversed phase HPLC.

From our results, we observed a significant variation in the cyclization yields for the four linear heptapeptides (Scheme 4.15). Cyclization involving the hyp-containing precursor gives the best yield. In contrast, the DHP heptapeptide provided the lowest yield. This trend suggests that the regio-, stereochemistry and degree of proline hydroxylation influence the backbone conformation which has a direct influence on cyclization. It appears that the *cis-trans* prolyl peptide bond isomerization favors *trans* for the DHP heptapeptide with hyp favoring the circular *cis* conformation required for cyclization. Also, the presence of hydroxyl groups on the pyrrolidine ring influence the structure of proline residues which is directly linked to the relative stability of the *cis-trans* ratios across the prolyl peptide bond.

4.2.6 Summary/Conclusions

In summary, the first total synthesis of alloviroidin (**3**) in trace amounts, along with that of three analogs with *L*-proline, *trans*-3-hydroxyproline or *cis*-4-hydroxyproline residue substituting for 2,3-*trans*-3,4-*trans*-dihydroxyproline in the natural product have been achieved via solution-phase head-to-tail cyclization. The linear heptapeptides were prepared via [3+4] fragment condensations between the series of four tripeptide acids **171-174** and the tetrapeptide amine **130**. Fragment condensations involving the tripeptide acids containing either *cis*-4-hydroxyproline or 2,3-*trans*-3,4-*trans*-dihydroxyproline residues were not as high yielding as for the proline or *trans*-3-hydroxyproline containing tripeptides due to the sterically hindered nature of the activated carboxyl termini residues.

We generated our target cyclopeptides by initiating the cyclizations using HATU. A dual syringe pump was used for slower addition of the linear precursors and the coupling reagent during the cyclization step. Cyclizations to produce the analogs containing *L*-proline or hyp residues proceeded in higher yields as compared to the 3-Hyp analog and the natural product. This trend is presumed to be influenced by the backbone conformation in the linear heptapeptide precursors with 3-Hyp analog having the least favorable conformation vis-à-vis.

Although the *tert*-butyldimethylsilyl group is one of the most utilized protecting group for alcohols, its application in peptide chemistry remains uncommon. In most cases, side chains of residues such as serine and threonine have been protected as *tert*-butyl ethers, especially in solid-phase peptide synthesis where the acid labile linker and side-chain protecting groups are cleaved in a single step. The successful utilization of TBS ethers in our synthesis demonstrates their application to peptide sequences with acid sensitive residues. The buffered conditions used for their global deprotection were compatible with the γ -hydroxylated dihydroxyleucine residue that would easily lactonize under standard acidic deprotection conditions.

4.3 EXPERIMENTAL SECTION

4.3.1 General Methods: As for Chapters 2 and 3 with the following additions and modifications:

NMR spectra were recorded on a Bruker AV-400-liquid or a Varian Inova-500 or a Varian system 700 spectrometer. Disodium 3-trimethylsilyl-1-propane-sulfonate (DSS) was used to reference ^1H NMR spectra run in 90% H_2O /10% D_2O .

Preparation of the phosphate buffer solution (pH 5.5, 50 mM): Monosodium phosphate (0.66 g) and disodium phosphate (0.06 g) were added to 100 mL of deionized water.

- **Pro heptapeptide 180.** Diisopropylethylamine (8 mg, 11 μL , 0.06 mmol, 1.2 equiv.) and HATU (21 mg, 0.05 mmol, 1.0 equiv.) were added to a solution of the tetrapeptide amine (40 mg, 0.05 mmol, 1.0 equiv.) and tripeptide acid (38 mg, 0.05 mmol, 1.0 equiv.) in CH_2Cl_2 (2 mL) at 0 $^\circ\text{C}$ under N_2 . The mixture was stirred and warmed to rt overnight, concentrated, and the product isolated by flash chromatography eluting with 4:1 EtOAc/Hex to give **180** (69 mg, 87 %). R_f 0.45 (4:1 EtOAc/Hex); $[\alpha]_{\text{D}}^{25}$ -33.7 $^\circ$ (c 1.0, CHCl_3). HRMS (+TOF) calcd for $\text{C}_{73}\text{H}_{115}\text{N}_8\text{O}_{16}\text{SSi}_3$ ($\text{M} + \text{H}$) $^+$: 1475.7454; obsd: 1475.7467. The purity of the heptapeptide was checked by HPLC on an Econosil silica column (10 mm diameter, 250 mm long) and a flow rate of 3 mL min^{-1} . The isocratic method used was 75% EtOAc in Hexanes. The heptapeptide was detected by UV absorption at 218 and 254 nm, R_T 21 min.

- **3-Hyp heptapeptide 181.** Diisopropylethylamine (13 mg, 17 μL , 0.10 mmol, 1.2 equiv.) and HATU (32 mg, 0.09 mmol, 1.0 equiv.) were added to a solution of the tetrapeptide amine (63 mg, 0.09 mmol, 1.0 equiv.) and tripeptide acid (75 mg, 0.09 mmol, 1.0 equiv.) in CH_2Cl_2 (3 mL) at 0 $^\circ\text{C}$ under N_2 . The mixture was stirred and warmed to rt overnight, concentrated, and the product isolated by flash chromatography eluting with 2:1 EtOAc/Hex to give **181** (99 mg, 73 %). R_f 0.40 (2:1 EtOAc/Hex);

$[\alpha]_{\text{D}}^{25}$ -13.7° (*c* 1.0, CHCl₃). HRMS (+TOF) calcd for C₇₉H₁₂₉N₈O₁₇SSi₄ (M + H)⁺: 1605.8268; obsd: 1605.8259.

• **4-hyp-heptapeptide 182.** Diisopropylethylamine (16 mg, 20 μL, 0.12 mmol, 1.2 equiv.) and HATU (46 mg, 0.12 mmol, 1.0 equiv.) were added to a solution of the tetrapeptide amine (90 mg, 0.12 mmol, 1.0 equiv.) and tripeptide acid (108 mg, 0.12 mmol, 1.0 equiv.) in CH₂Cl₂ (4 mL) at 0 °C under N₂. The mixture was stirred and warmed to rt overnight, concentrated, and the product isolated by flash chromatography eluting with 2:1 EtOAc/Hex to give **182** (125 mg, 64 %). *R_f* 0.40 (2:1 EtOAc/Hex); $[\alpha]_{\text{D}}^{25}$ -12.3° (*c* 1.0, CHCl₃). HRMS (+TOF) calcd for C₇₉H₁₂₉N₈O₁₇SSi₄ (M + H)⁺: 1605.8268; obsd: 1605.8259. The purity of the heptapeptide was checked by HPLC on an Econosil silica column (10 mm diameter, 250 mm long) and a flow rate of 3 mL min⁻¹. The isocratic method used was 66% EtOAc in Hexanes. The heptapeptide was detected by UV absorption at 218 and 254 nm, *R_T* 15 min.

• **DHP heptapeptide 179.** Diisopropylethylamine (8 mg, 10 μL, 0.06 mmol, 1.5 equiv.) and HATU (16 mg, 0.04 mmol, 1.0 equiv.) were added to a solution of the tetrapeptide amine (30 mg, 0.04 mmol, 1.0 equiv.) and tripeptide acid (42 mg, 0.04 mmol, 1.0 equiv.) in CH₂Cl₂ (2 mL) at 0 °C under N₂. The mixture was stirred and warmed to rt overnight, concentrated, and the product isolated by flash chromatography eluting with 1:1 EtOAc/Hex, then 2:1 EtOAc/Hex to give **179** (46 mg, 65 %). *R_f* 0.37 (1:1 EtOAc/Hex); $[\alpha]_{\text{D}}^{25}$ -18.5° (*c* 0.85, CHCl₃). HRMS (+TOF) calcd for C₇₃H₁₁₅N₈O₁₆SSi₃ (M + H)⁺: 1735.9042; obsd: 1735.9079. The purity of the heptapeptide was checked by HPLC on an Econosil silica column (10 mm diameter, 250 mm long) and a flow rate of 3 mL min⁻¹. The isocratic method used was 50% EtOAc in Hexanes. The heptapeptide was detected by UV absorption at 218 and 254 nm, *R_T* 14 min.

- **cyclo[-D-Thr-D-Ser-Pro-Ala-Trp(SO₂Me)-dihyLeu-Val] (43).** *Tris*-(2-aminoethyl)amine (48 mg, 49 µL, 0.329 mmol, 16.2 equiv.) was added to a solution of **180** (30 mg, 0.020 mmol, 1.0 equiv.) in CH₂Cl₂ (2 mL) at rt under N₂. The mixture was stirred for 30 min, diluted with EtOAc (15 mL) and washed with a phosphate buffer solution (pH 5.5, 10 mL). The aqueous layer was extracted further with EtOAc (4 × 15 mL). The organic extracts were combined, washed with brine (10 mL), filtered through MgSO₄ and concentrated. The residue was purified by flash chromatography eluting with 4:1 EtOAc/Hex, then 9:1 CH₂Cl₂/CH₃OH to give the amine (25 mg, 100 %) as a colorless foam.

This amine (25 mg, 0.020 mmol, 1.0 equiv.) was dissolved in a mixture of MeCN (1 mL) and H₂O (0.5 mL) and treated with tetrabutylammonium hydroxide (72 µL, 40 % wt in H₂O, 71 mg, 0.111 mmol, 5.5 equiv.) at 0 °C. The reaction mixture was stirred for 14 h, then diluted with CHCl₃ (40 mL) and washed with a phosphate buffer solution (pH 5.5, 15 mL). The aqueous layer was extracted further with EtOAc (4 × 15 mL). The organic extracts were combined, concentrated and used in the cyclization reaction without further purification (recovered 35 mg, theoretical yield 24 mg).

Diisopropylethylamine (5 µL, 3.8 mg, 0.029 mmol, 1.5 equiv.) was added to a solution of the crude linear amino acid heptapeptide (max., 0.020 mmol, 1.0 equiv.) in CH₂Cl₂ (8 mL). This solution was added over 2 h via a syringe pump to a stirring mixture of HATU (37 mg, 0.098 mmol, 5.0 equiv.) and DIEA (5 µL, 3.8 mg, 0.029 mmol, 1.5 equiv.) in CH₂Cl₂ (12 mL) at 0 °C under N₂. The mixture was stirred for 1 h at 0 °C, warmed to rt, and stirred for 2 d. This mixture was concentrated. The residue was diluted with EtOAc (30 mL), washed successively with 10 % citric acid, sat'd NaHCO₃ and brine (15 mL each). The aqueous layers were extracted further with EtOAc (3 × 15 mL). The organic extracts were combined, filtered through MgSO₄ and concentrated. The residue was purified by flash chromatography eluting with 15:1 CHCl₃/CH₃OH to give the cyclopeptide (15 mg, 65 %) as a colorless solid.

The TBS protected cyclopeptide (15 mg, 0.012 mmol, 1.0 equiv.) was dissolved in THF (1 mL) and cooled to 0 °C. This solution was treated with NH₄F (4.6 mg, 0.124 mmol, 10 equiv.) and TBAF (62 µL, 1M solution in THF, 0.062 mmol, 5.0 equiv.). The mixture was stirred at 0 °C for 16 h, diluted with MeOH (3 mL), followed by the addition of CaCO₃ (66 mg) and DOWEX 50WX8-400 H⁺ resin (200 mg). Stirring at this temperature was continued for 1 h and the mixture filtered through a pad of CeliteTM, rinsing thoroughly with methanol (30 mL). The filtrate was concentrated and the residue purified using RP-HPLC, eluting with MeCN and H₂O. The gradient method used was as follows (% acetonitrile in H₂O): 10-25% over 20 min; 25-35% over 10 min; 35% for 2 min; 35-10% over 3 min. The cyclopeptide was detected by UV absorption at 218 and 254 nm. The relevant fractions were combined and lyophilized to give **43** as a colorless solid (4 mg, 40 %). MALDI-TOF (+TOF) calcd for C₃₈H₅₆N₈O₁₃S(M + Na)⁺: 887.359; obsd: 887.397.

- **cyclo[-D-Thr-D-Ser-3-Hyp-Ala-Trp(SO₂Me)-dihyLeu-Val] (44).** *Tris*-(2-aminoethyl)amine (28 mg, 29 µL, 0.192 mmol, 16.2 equiv.) was added to a solution of **181** (19 mg, 0.012 mmol, 1.0 equiv.) in CH₂Cl₂ (2 mL) at rt under N₂. The mixture was stirred for 30 min, diluted with EtOAc (15 mL) and washed with a phosphate buffer solution (pH 5.5, 10 mL). The aqueous layer was extracted further with EtOAc (4 × 15 mL). The organic extracts were combined, washed with brine (10 mL), filtered through MgSO₄ and concentrated. The residue was purified by flash chromatography eluting with 4:1 EtOAc/Hex, then 9:1 CH₂Cl₂/CH₃OH to give the amine (15 mg, 94%) as a colorless foam.

The amine (14 mg, 0.010 mmol, 1.0 equiv.) was dissolved in a mixture of MeCN (1 mL) and H₂O (0.5 mL) and treated with tetrabutylammonium hydroxide (36 µL, 40 % wt in H₂O, 36 mg, 0.056 mmol, 5.5 equiv.) at 0 °C. The reaction mixture was stirred for 14 h, then diluted with CHCl₃ (30 mL) and washed with a phosphate buffer solution (pH 5.5, 10 mL). The aqueous layer was extracted further with EtOAc

(4 × 10 mL). The organic extracts were combined, concentrated and used in the cyclization reaction without further purification (recovered 22 mg, theoretical yield 13 mg).

A solution of the linear amino acid heptapeptide (13 mg, 0.010 mmol, 1.0 equiv.) in DMF (3 mL) and transferred into a syringe. A solution of HATU (14 mg, 0.038 mmol, 4.0 equiv.) in DMF (3 mL) was transferred into a second syringe. These two solutions were added over 2 h via a dual syringe pump to a stirring mixture of HATU (4 mg, 0.010 mmol, 1.0 equiv.) and DIEA (5 µL, 3.7 mg, 0.029 mmol, 3.0 equiv.) in DMF (3 mL) at 0 °C under N₂. The mixture was stirred for 1 h at 0 °C, warmed to rt, and stirred for 3 d. This mixture was diluted with EtOAc (25 mL), washed with 10 % citric acid (12 mL). The aqueous layer was extracted further with EtOAc (3 × 10 mL). The organic extracts were combined, washed with sat'd NaHCO₃ and brine (12 mL each), filtered through MgSO₄ and concentrated. The residue was semipurified by flash chromatography eluting with 2:1 EtOAc/Hex, then 9:1 CH₂Cl₂/CH₃OH to give the cycloheptapeptide (12 mg, contaminated with tetrabutylammonium salts) as a colorless solid.

The TBS protected cyclopeptide (12 mg, 0.009 mmol, 1.0 equiv.) was dissolved in THF (1 mL) and cooled to 0 °C. This solution was treated with NH₄F (4 mg, 0.125 mmol, 14 equiv.) and TBAF (63 µL, 1M solution in THF, 0.063 mmol, 7.0 equiv.). The mixture was stirred at 0 °C for 16 h, diluted with MeOH (3 mL), followed by the addition of CaCO₃ (66 mg) and DOWEX 50WX8-400 H⁺ resin (200 mg). Stirring at this temperature was continued for 1 h and the mixture filtered through a pad of CeliteTM, rinsing thoroughly with methanol (30 mL). The filtrate was concentrated and the residue purified using RP-HPLC, eluting with MeCN and H₂O. The gradient method used was as follows (% acetonitrile in H₂O): 10-25% over 20 min; 25-35% over 10 min; 35% for 2 min; 35-10% over 3 min. The cyclopeptide was detected by UV absorption at 218 and 254 nm. The relevant fractions were

combined and lyophilized to give **44** as a colorless solid (1.6 mg, 20 %). MALDI-TOF (+TOF) calcd for $C_{38}H_{56}N_8O_{14}S(M + Na)^+$: 903.353; obsd: 903.389.

- **cyclo[-D-Thr-D-Ser-4-hyp-Ala-Trp(SO₂Me)-dihyLeu-Val] (45).** *Tris*-(2-aminoethyl)amine (22 mg, 23 μ L, 0.151 mmol, 16.2 equiv.) was added to a solution of **182** (15 mg, 0.009 mmol, 1.0 equiv.) in CH_2Cl_2 (2 mL) at rt under N_2 . The mixture was stirred for 30 min, diluted with EtOAc (15 mL) and washed with a phosphate buffer solution (pH 5.5, 10 mL). The aqueous layer was extracted further with EtOAc (4 \times 10 mL). The organic extracts were combined, washed with brine (10 mL), filtered through $MgSO_4$ and concentrated. The residue was purified by flash chromatography eluting with 4:1 EtOAc/Hex, then 9:1 CH_2Cl_2/CH_3OH to give the amine (12 mg, 100 %) as a colorless foam.

The amine (12 mg, 0.009 mmol, 1.0 equiv.) was dissolved in a mixture of MeCN (1 mL) and H_2O (0.5 mL) and treated with tetrabutylammonium hydroxide (31 μ L, 40 % wt in H_2O , 31 mg, 0.048 mmol, 5.5 equiv.) at 0 °C. The reaction mixture was stirred for 14 h, then diluted with $CHCl_3$ (40 mL) and washed with a phosphate buffer solution (pH 5.5, 10 mL). The aqueous layer was extracted further with EtOAc (3 \times 10 mL). The organic extracts were combined, concentrated and used in the cyclization reaction without further purification (recovered 20 mg, theoretical yield 11 mg).

Diisopropylethylamine (2.2 μ L, 1.5 mg, 0.024 mmol, 1.5 equiv.) was added to a solution of the crude linear amino acid heptapeptide (11 mg, 0.008 mmol, 1.0 equiv.) in CH_2Cl_2 (4 mL). This solution was added over 2 h via a syringe pump to a stirring mixture of HATU (15 mg, 0.041 mmol, 5.0 equiv.) and DIEA (2.2 μ L, 1.5 mg, 0.024 mmol, 1.5 equiv.) in CH_2Cl_2 (4 mL) at 0 °C under N_2 . The mixture was stirred for 1 h at 0 °C, warmed to rt, and stirred for 2 d. This mixture was concentrated, diluted with EtOAc (20 mL) and washed with 10 % citric acid. The aqueous layer was extracted further with EtOAc (3 \times 10 mL). The organic extracts were combined, washed with sat'd $NaHCO_3$ and brine (10 mL each),

filtered through MgSO_4 and concentrated. The residue was purified by flash chromatography eluting with 15:1 $\text{CHCl}_3/\text{CH}_3\text{OH}$ to give the cyclopeptide (15 mg, the theoretical yield is 10 mg, contaminated with tetrabutylammonium salts) as a colorless solid.

The TBS protected cyclopeptide (10 mg, 0.007 mmol, 1.0 equiv.) was dissolved in THF (1 mL) and cooled to 0 °C. This solution was treated with NH_4F (3.9 mg, 0.105 mmol, 14 equiv.) and TBAF (52 μL , 1M solution in THF, 0.053 mmol, 7.0 equiv.). The mixture was stirred at 0 °C for 16 h, diluted with MeOH (3 mL), followed by the addition of CaCO_3 (66 mg) and DOWEX 50WX8-400 H^+ resin (200 mg). Stirring at this temperature was continued for 1 h and the mixture filtered through a pad of CeliteTM, rinsing thoroughly with methanol (30 mL). The filtrate was concentrated and the residue purified using RP-HPLC, eluting with MeCN and H_2O . The gradient method used was as follows (% acetonitrile in H_2O): 10-25% over 20 min; 25-35% over 10 min; 35% for 2 min; 35-10% over 3 min. The cyclopeptide was detected by UV absorption at 218 and 254 nm. The relevant fractions were combined and lyophilized to give **44** as a colorless solid (2.2 mg, 31%). MALDI-TOF (+TOF) calcd for $\text{C}_{38}\text{H}_{56}\text{N}_8\text{O}_{14}\text{S}(\text{M} + \text{Na})^+$: 903.353; obsd: 903.400.

- **cyclo[-D-Thr-D-Ser-DHP-Ala-Trp(SO₂Me)-dihyLeu-Val] (3).** *Tris*-(2-aminoethyl)amine (21 μL , 20 mg, 0.140 mmol, 16.2 equiv.) was added to a solution of **179** (15 mg, 0.009 mmol, 1.0 equiv.) in CH_2Cl_2 (2 mL) at rt under N_2 . The mixture was stirred for 30 min, diluted with EtOAc (15 mL) and washed with a phosphate buffer solution (pH 5.5, 10 mL). The aqueous layer was extracted further with EtOAc (4 \times 10 mL). The mixture was stirred for 30 min, diluted with EtOAc (15 mL), washed with brine and a phosphate buffer solution (pH 5.5) (10 mL each). The aqueous layers were extracted further with EtOAc (4 \times 10 mL). The organic extracts were combined, filtered through MgSO_4 and

concentrated. The residue was purified by flash chromatography eluting with 2:1 EtOAc/Hex, then 9:1 CH₂Cl₂/CH₃OH to give the amine (11 mg, 84 %) as a colorless foam.

The above amine (11 mg, 0.0073 mmol, 1.0 equiv.) was dissolved in a mixture of MeCN (1 mL) and H₂O (0.5 mL) and treated with tetrabutylammonium hydroxide (25 μ L, 0.040 mmol, 5.5 equiv. 40 % wt in H₂O) at 0 °C. The reaction mixture was stirred for 14 h, then diluted with CHCl₃ (25 mL) and washed with a phosphate buffer solution (pH 5.5, 10 mL). The aqueous layer was extracted further with EtOAc (4 \times 10 mL). The organic extracts were combined, concentrated and used in the cyclization reaction without further purification (theoretical yield is 10 mg, recovered 20 mg contaminated with tetrabutylammonium salts).

A solution of the linear amino acid heptapeptide (10 mg, 0.0067 mmol, 1.0 equiv.) in DMF (2.3 mL) and transferred into a syringe. A solution of HATU (10 mg, 0.0263 mmol, 3.9 equiv.) in DMF (2.3 mL) was transferred into a second syringe. These two solutions were added over 2 h via a dual syringe pump to a stirring mixture of HATU (3 mg, 0.0079 mmol, 1.1 equiv.) and DIEA (3.3 μ L, 2.6 mg, 0.0202 mmol, 3.0 equiv.) in DMF (2.3 mL) at 0 °C under N₂. The mixture was stirred and warmed to rt over 3 d and diluted with EtOAc (30 mL), washed successively with 10 % citric acid, satd NaHCO₃ and brine (15 mL each). The aqueous layers were extracted further with EtOAc (3 \times 15 mL). The organic extracts were combined, filtered through MgSO₄ and concentrated. The residue was semipurified by flash chromatography eluting with 2:1 EtOAc/Hex, then 9:1 CH₂Cl₂/CH₃OH to give the cycloheptapeptide (5 mg, 55 %, contaminated with tetrabutylammonium salts) as a colorless solid. *R_f* 0.33 (9:1 CH₂Cl₂/CH₃OH).

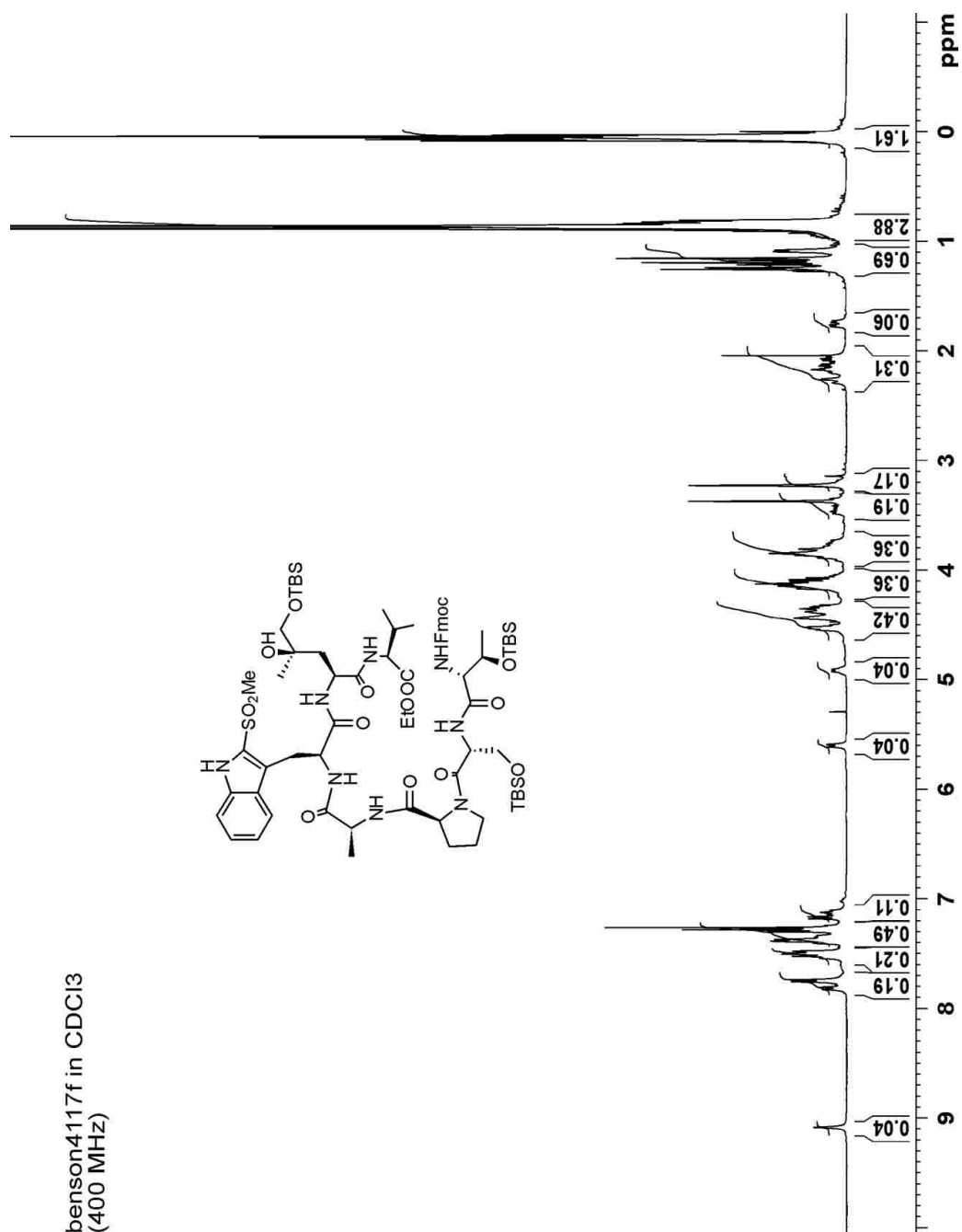
The TBS protected cyclopeptide (4 mg, 0.0027 mmol, 1.0 equiv.) was dissolved in THF (1 mL) and cooled to 0 °C. This solution was treated with NH₄F (3.4 mg, 0.1020 mmol, 38 equiv.) and TBAF (51 μ L, 0.051 mmol, 19 equiv. 1M solution in THF). The mixture was stirred at 0 °C for 16 h, diluted with

THF (3 mL), followed by the addition of CaCO₃ (138 mg) and H⁺ DOWEX 50WX8-400 (414 mg). Stirring at this temperature was continued for 1 h and the mixture filtered through a pad of CeliteTM, rinsing thoroughly with methanol (8 mL). The filtrate was concentrated and the residue purified using RP-HPLC, eluting with MeCN and H₂O. Purification of the final cyclopeptides utilized RP-HPLC on an Econosil C-18 column (10 mm diameter, 250 mm long) and a flow rate of 3 mL min⁻¹. The gradient method used was as follows (% acetonitrile in H₂O): 10-25% over 20 min; 25-35% over 10 min; 35% for 2 min; 35-10% over 3 min. The cyclopeptide was detected by UV absorption at 218 and 254 nm. The relevant fractions were combined and lyophilized to give trace amounts of **3** as a colorless solid. MALDI-TOF (+TOF) calcd for C₃₈H₅₆N₈O₁₅S(M + Na)⁺: 919.348; obsd: 919.399.

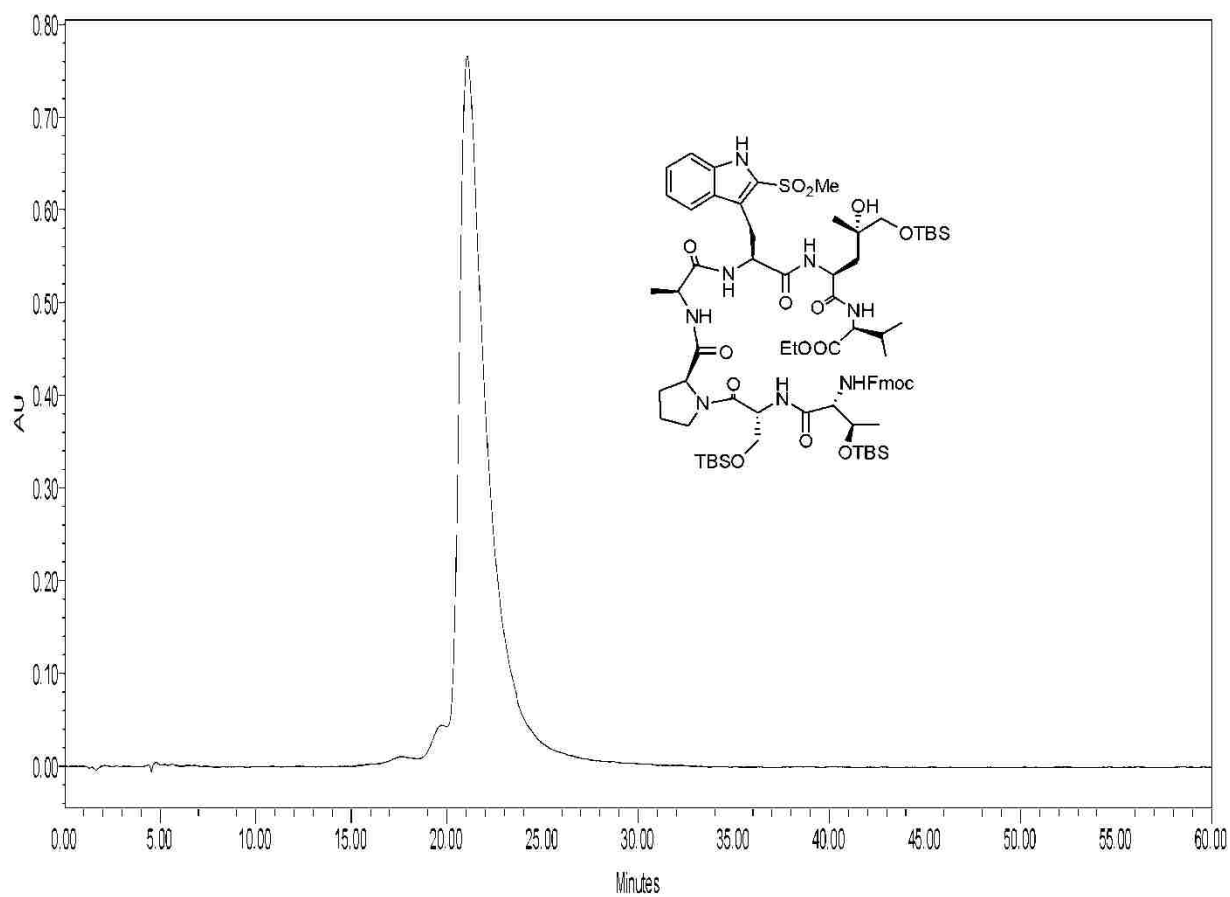
4.3.2 Spectra and HPLC Chromatograms

¹ H NMR spectrum of compound 180	203
HPLC chromatogram of compound 180	204
¹ H NMR spectrum of compound 181	205
HPLC chromatogram of compound 181	206
¹ H NMR spectrum of compound 182	207
HPLC chromatogram of compound 182	208
¹ H NMR spectrum of compound 179	209
HPLC chromatogram of compound 179	210
Monitoring the hydrolysis of ethyl ester using tetrabutylammonium hydroxide ...	211
¹ H NMR spectrum of compound 43	213
HPLC chromatogram of compound 43	214
¹ H NMR spectrum of compound 44	215
HPLC chromatogram of compound 44	216
¹ H NMR spectrum of compound 45	217
HPLC chromatogram of compound 45	218
HPLC chromatogram of compound 3	218

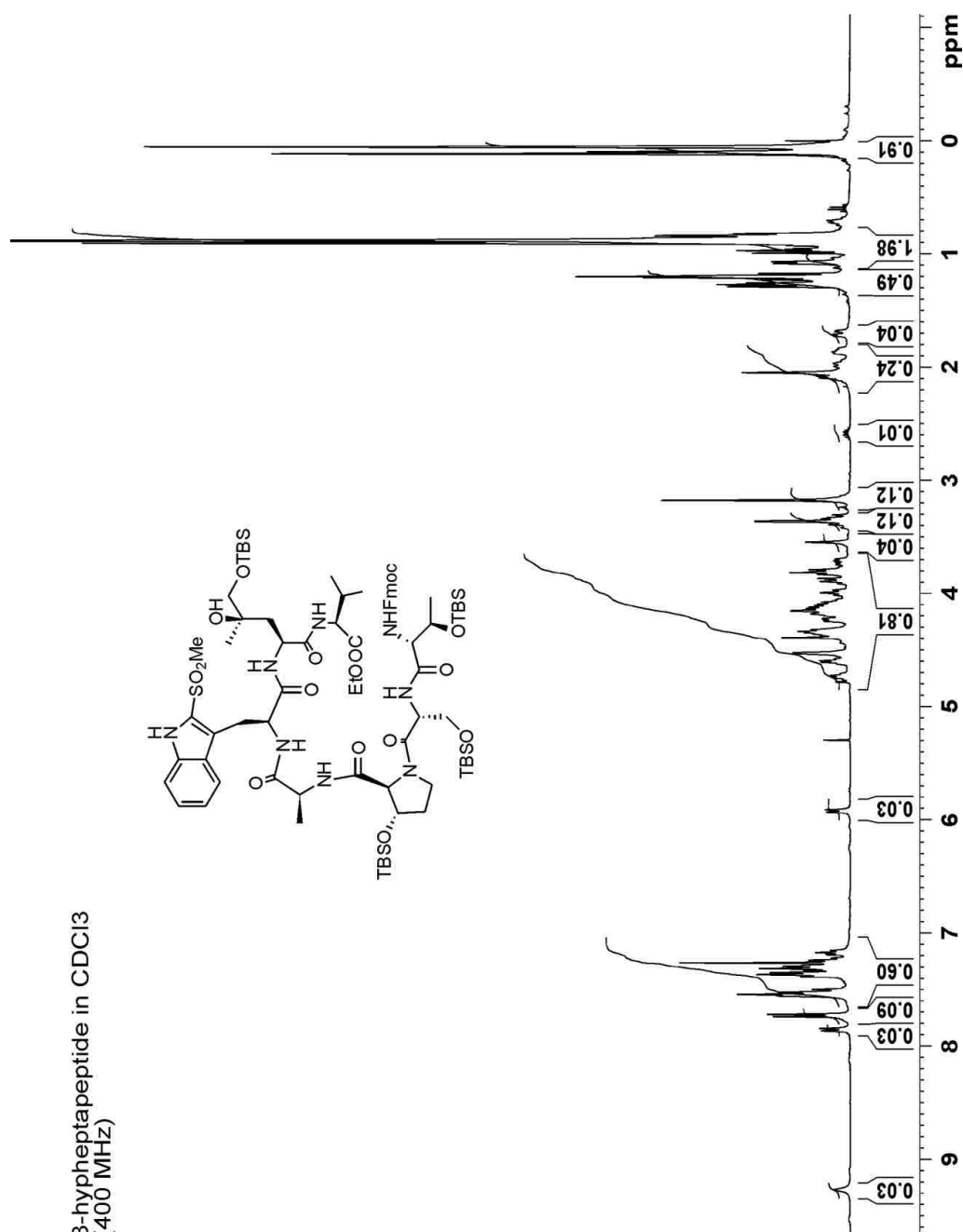
Pro heptapeptide (180)- ^1H NMR in CDCl_3 at 400 MHz



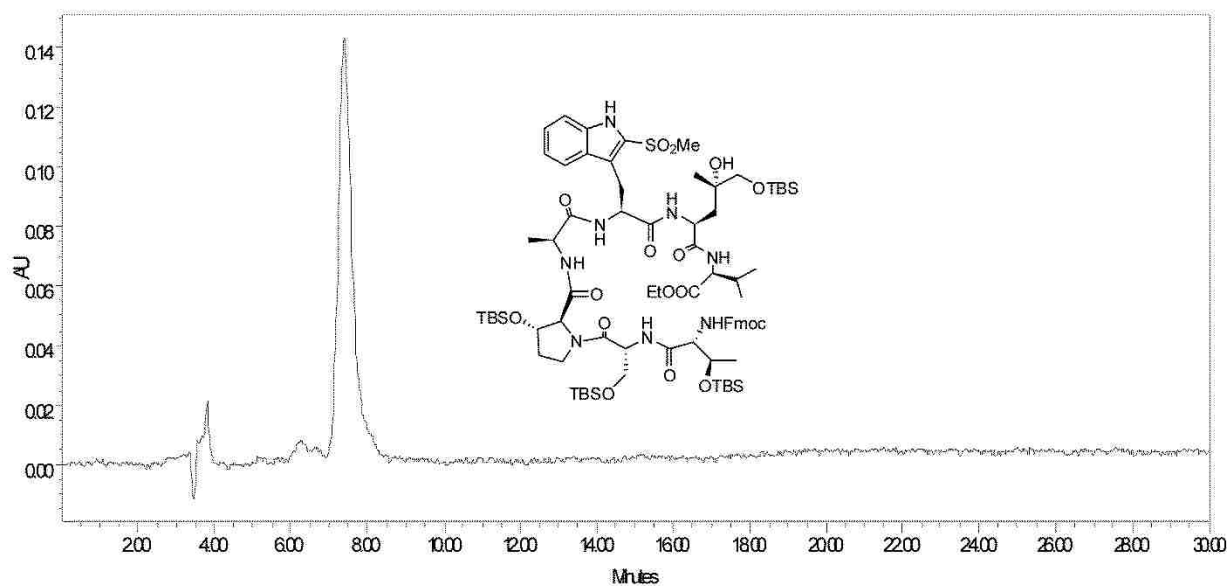
Proheptapeptide (180)- HPLC chromatogram at 254 nm, 75% EtOAc in Hexanes, 10 mm Econosil silica column, 3 mL min⁻¹ (99 % pure).



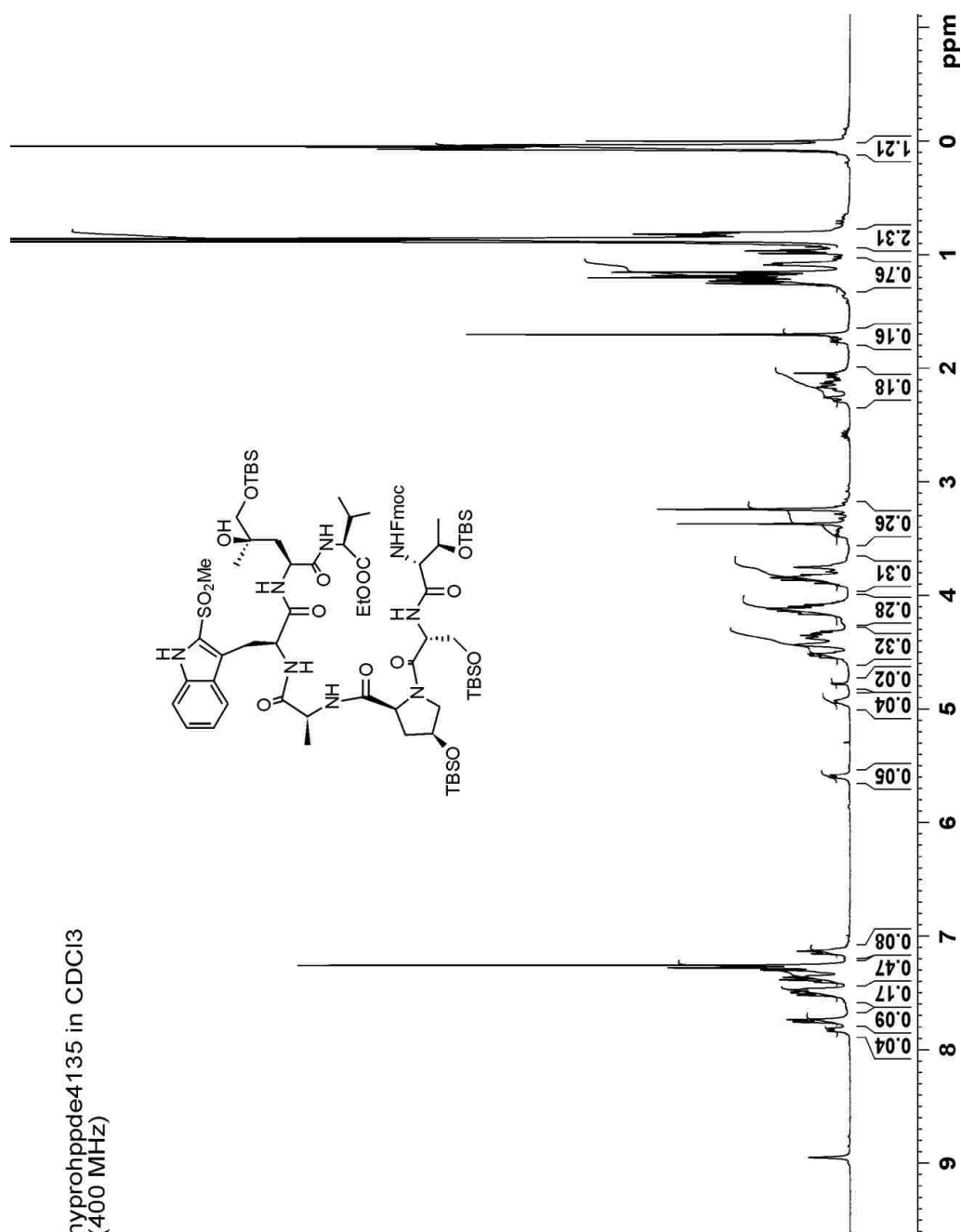
3-Hyp heptapeptide (181)- ^1H NMR in CDCl_3 at 400 MHz



3-Hyp heptapeptide (181)- HPLC chromatogram at 254 nm, 66% EtOAc in Hexanes, 10 mm Econosil silica column, 3 mL min⁻¹ (94 % pure).

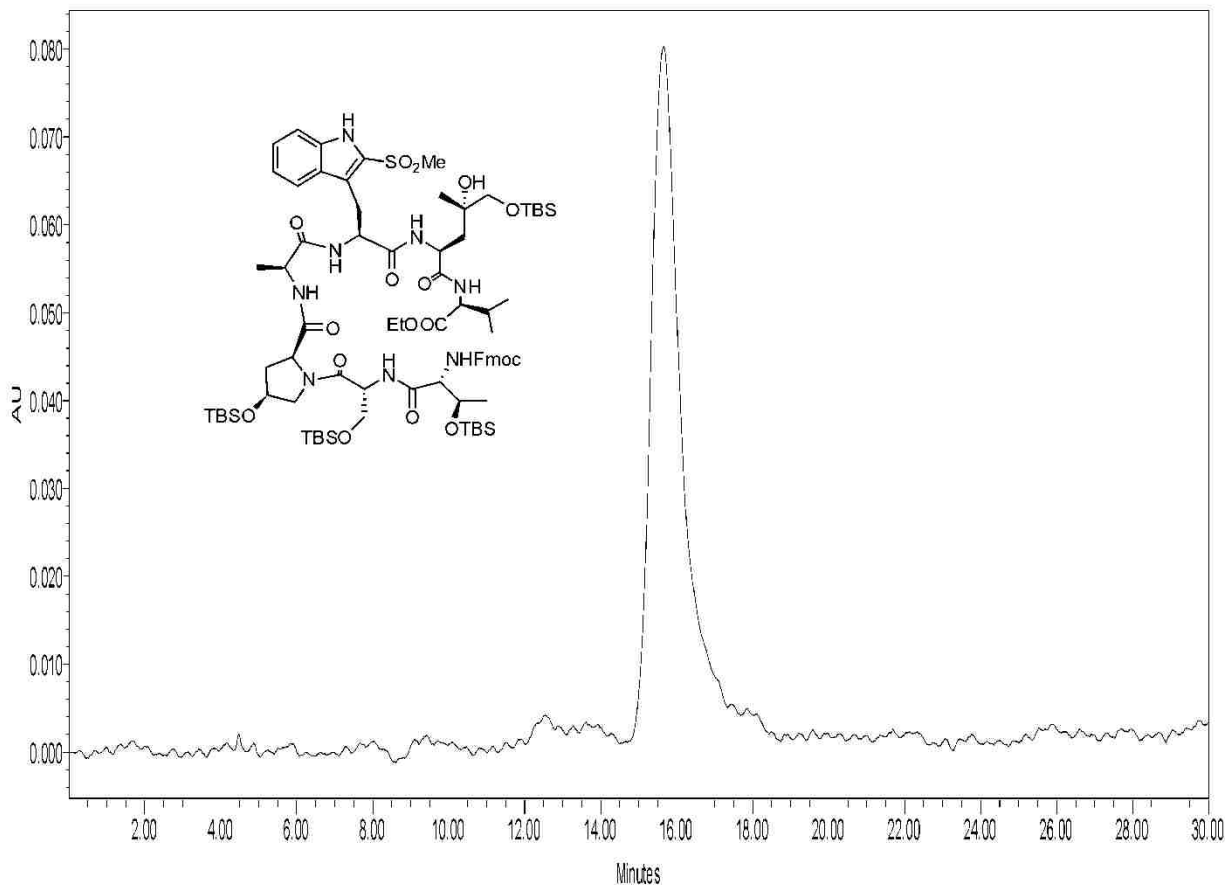


hyp-heptapeptide (182)- ^1H NMR in CDCl_3 at 400 MHz

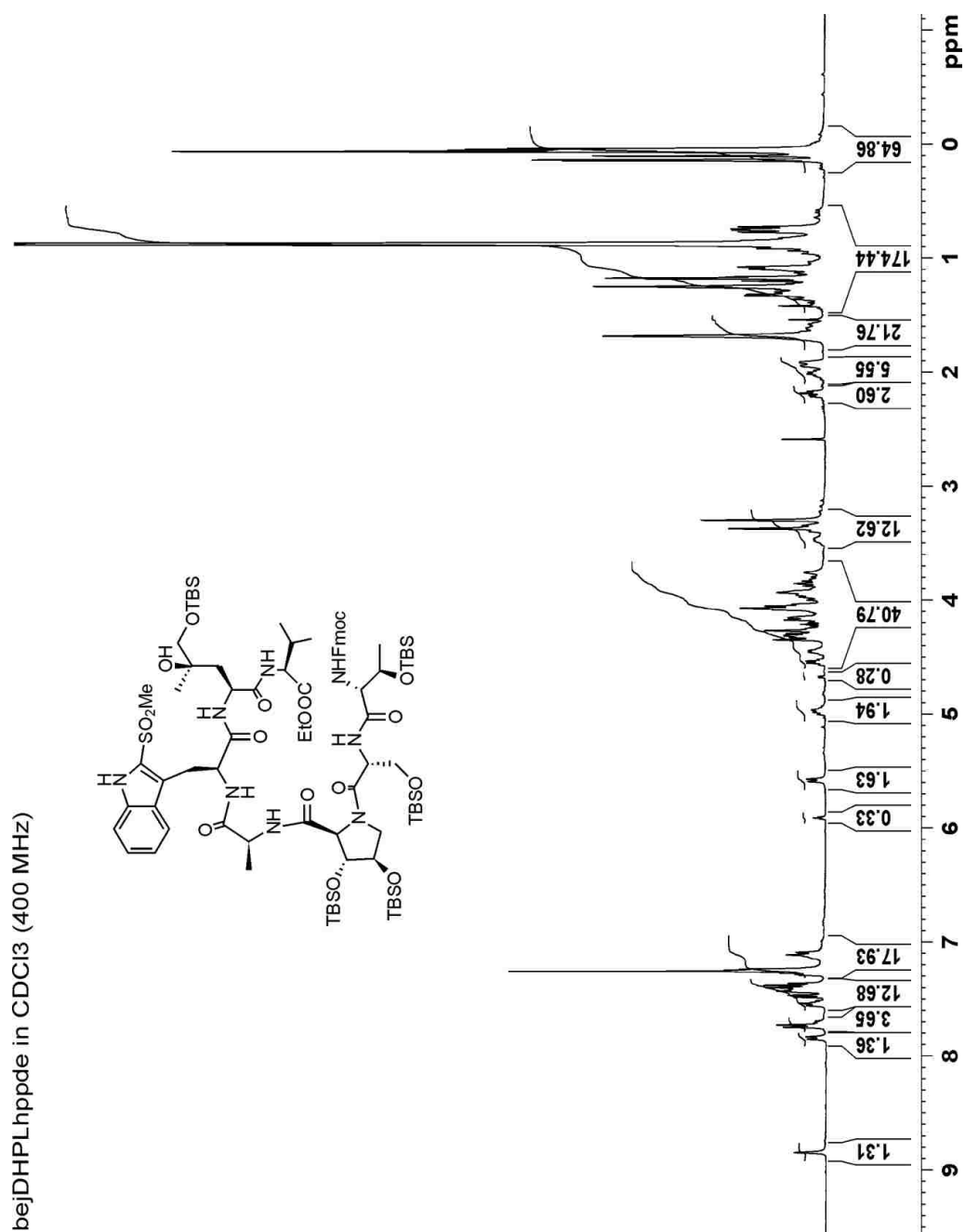


hypheptapeptide4135 in CDCl_3
(400 MHz)

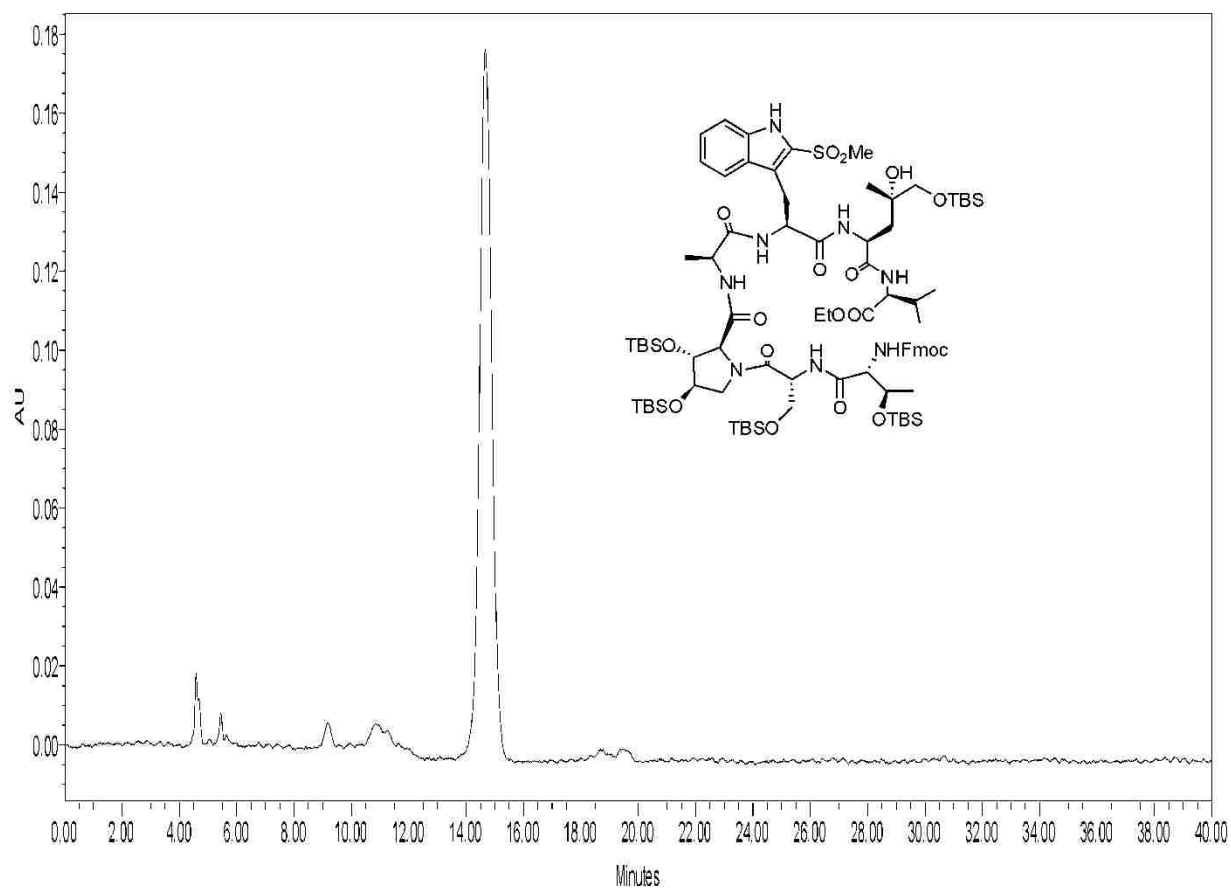
hyp heptapeptide (182)- HPLC chromatogram at 254 nm, 66% EtOAc in Hexanes, 10 mm Econosil silica column, 3 mL min⁻¹ (93 % pure).



DHP heptapeptide (179)- ^1H NMR in CDCl_3 at 400 MHz

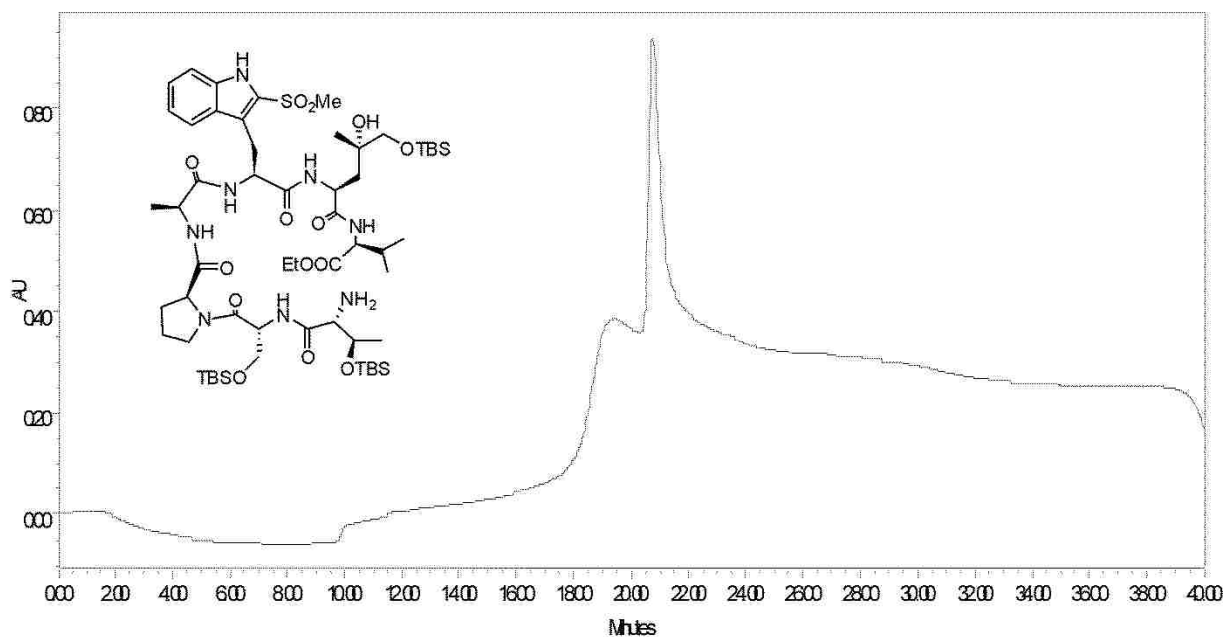


DHP heptapeptide (179)– HPLC chromatogram at 254 nm, 50 % EtOAc in Hexanes, 10 mm Econosil silica column, 3 mL min⁻¹ (90 % pure).

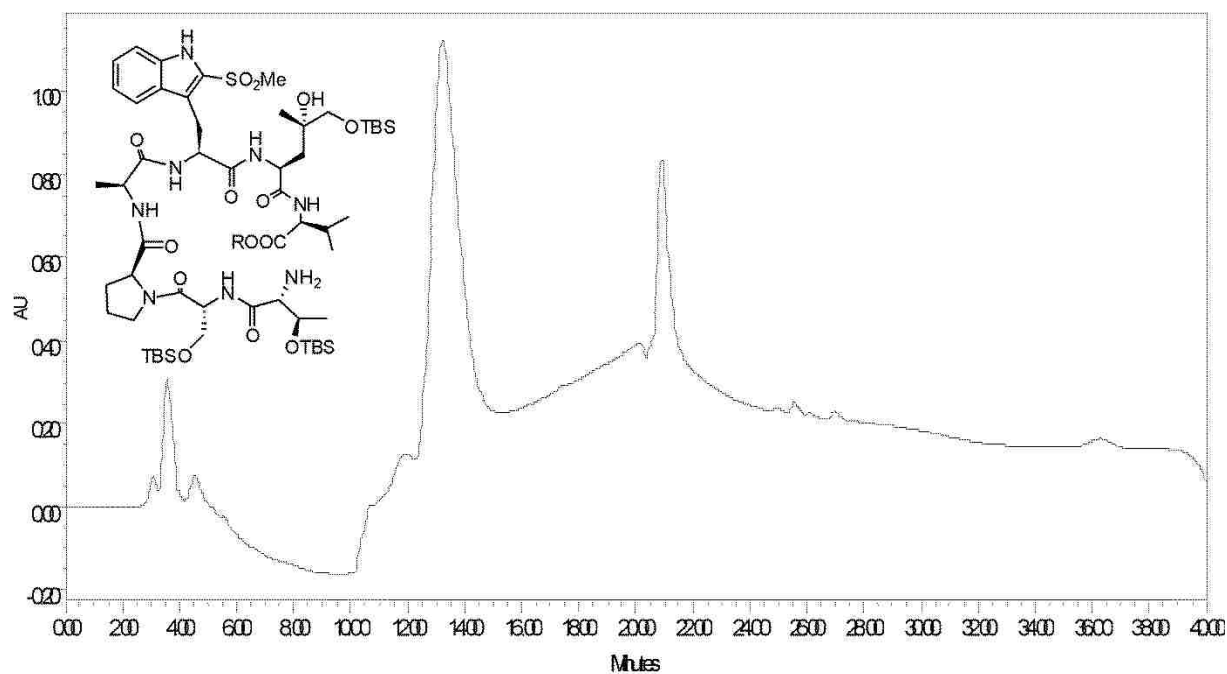


Monitoring the Hydrolysis of Ethyl Ester using Tetrabutylammonium hydroxide

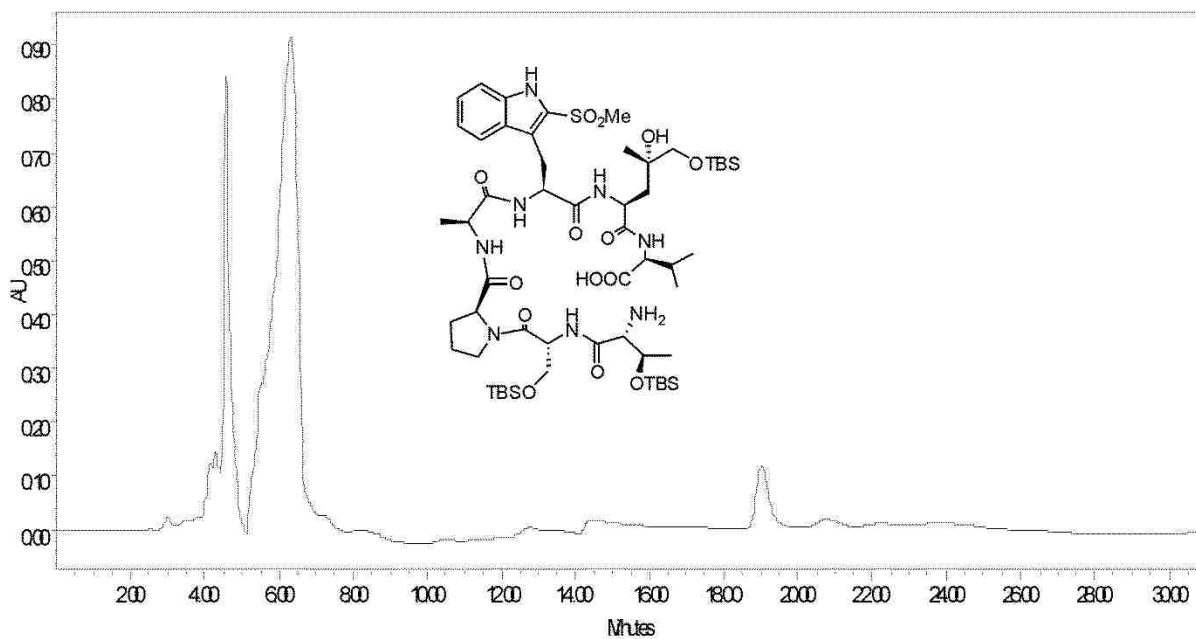
HPLC chromatogram of starting material at 218 nm, MeCN/H₂O, 4.6 mm Econosil C-18 column, 0.6 mL min⁻¹



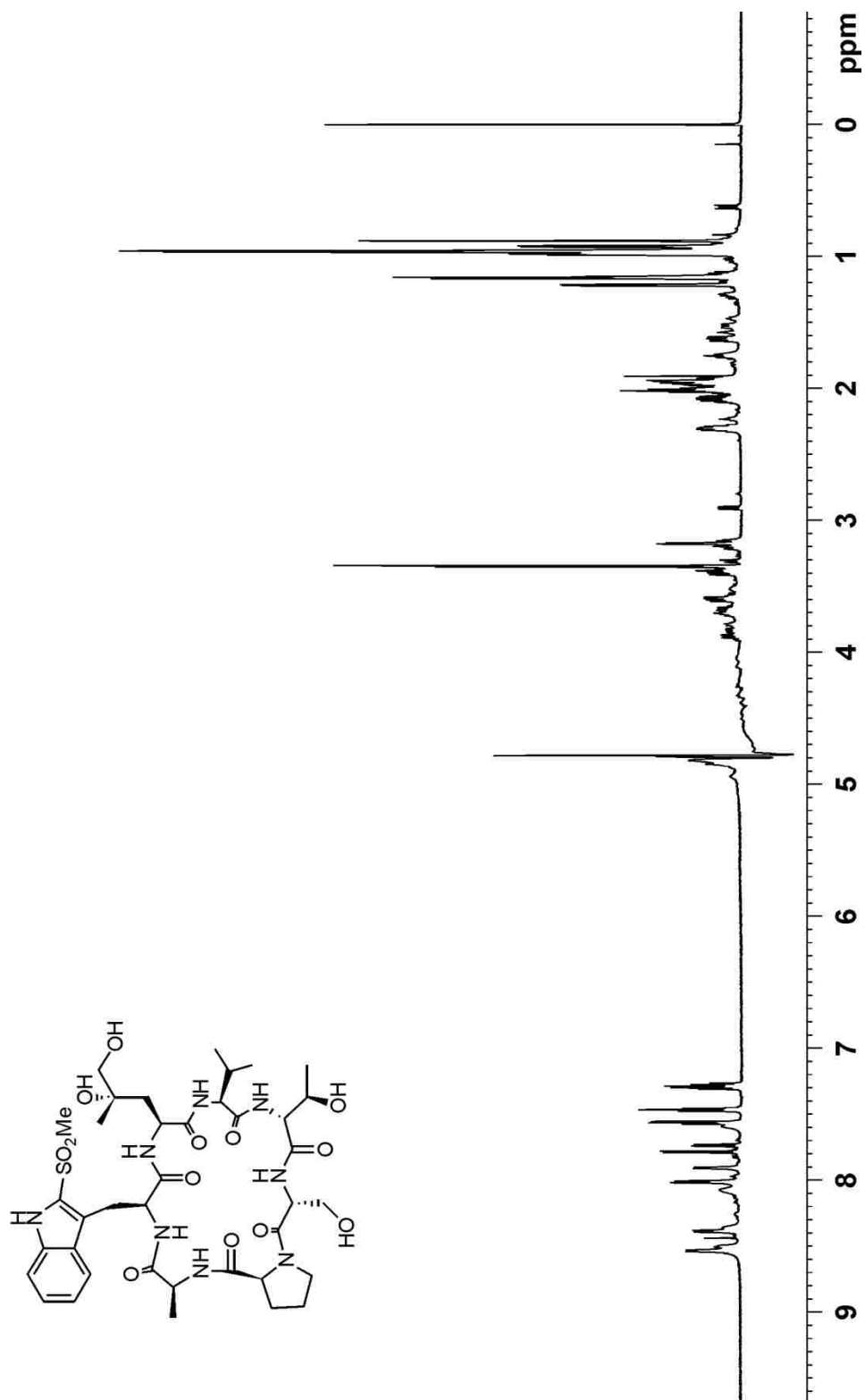
HPLC chromatogram of the reaction mixture after 6 h at 218 nm, MeCN/H₂O, 4.6 mm Econosil C-18 column, 0.6 mL min⁻¹



HPLC chromatogram of the reaction mixture after 9 h at 218 nm, MeCN/H₂O, 4.6 mm Econosil C-18 column, 0.6 mL min⁻¹

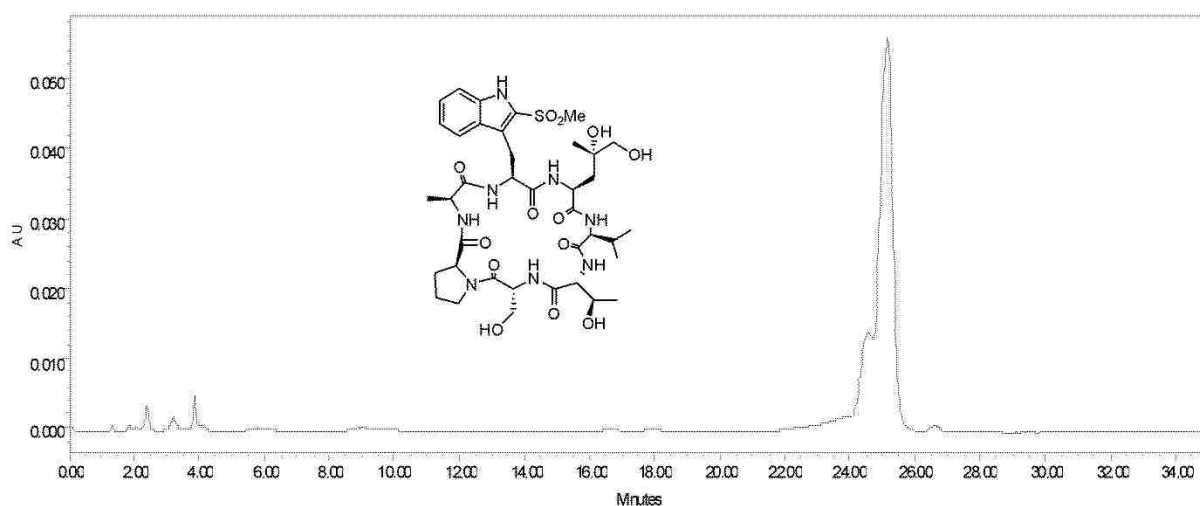


Proline analog (43) - ^1H NMR in 90% H_2O /10% D_2O at 700 MHz (pH 3.0)



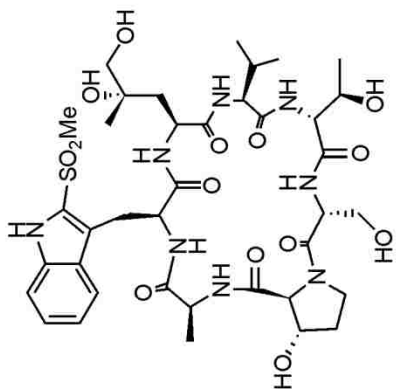
Proline Analog in 90% H_2O /10% D_2O (700 MHz, pH = 3.0, watergate suppression)

HPLC chromatogram of proline analog (**43**) at 254 nm, (% acetonitrile in H₂O): 10-25% over 20 min; 25-35% over 10 min; 35% for 2 min; 35-10% over 3 min, 4.6 mm Econosil C-18 column, 1 mL min⁻¹

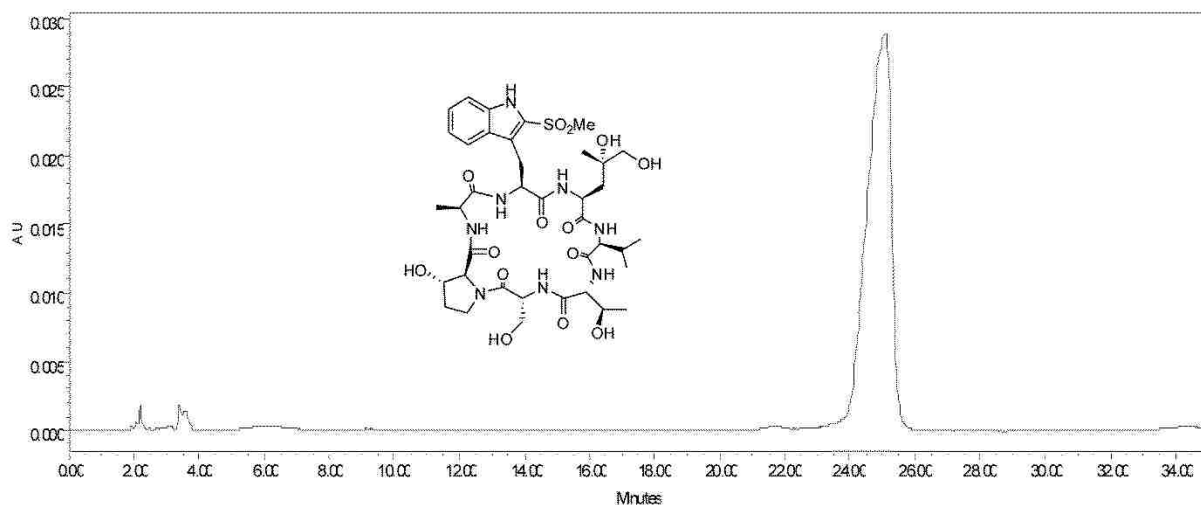


3Hyp Analog in 90% H₂O/10% D₂O
(700 MHz, pH 3.0)

Chemical structure of 3Hyp Analog is shown, featuring a complex molecule with multiple amide bonds, hydroxyl groups, and a sulfonamide group.

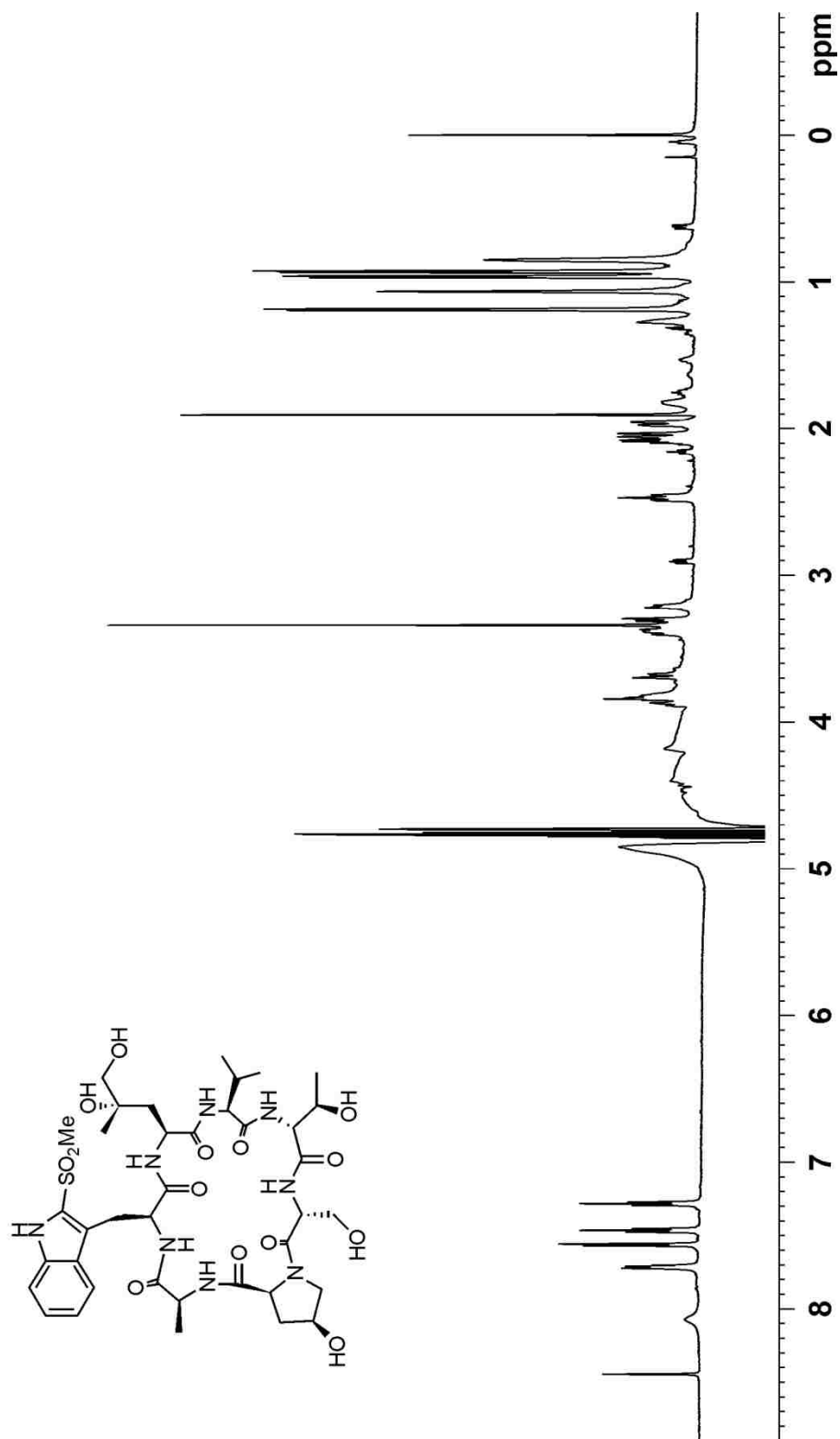


HPLC chromatogram of 3-Hyp analog (**44**) at 254 nm, (% acetonitrile in H₂O): 10-25% over 20 min; 25-35% over 10 min; 35% for 2 min; 35-10% over 3 min, 4.6 mm Econosil C-18 column, 1 mL min⁻¹

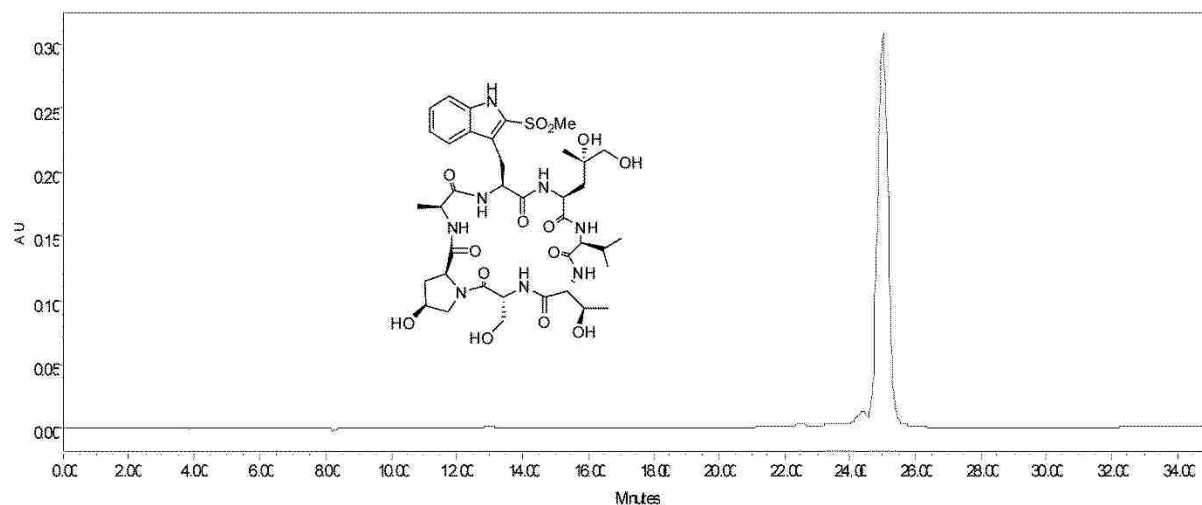


4-hyp analog (45) - ^1H NMR in 90% H_2O /10% D_2O at 700 MHz (pH 3.0)

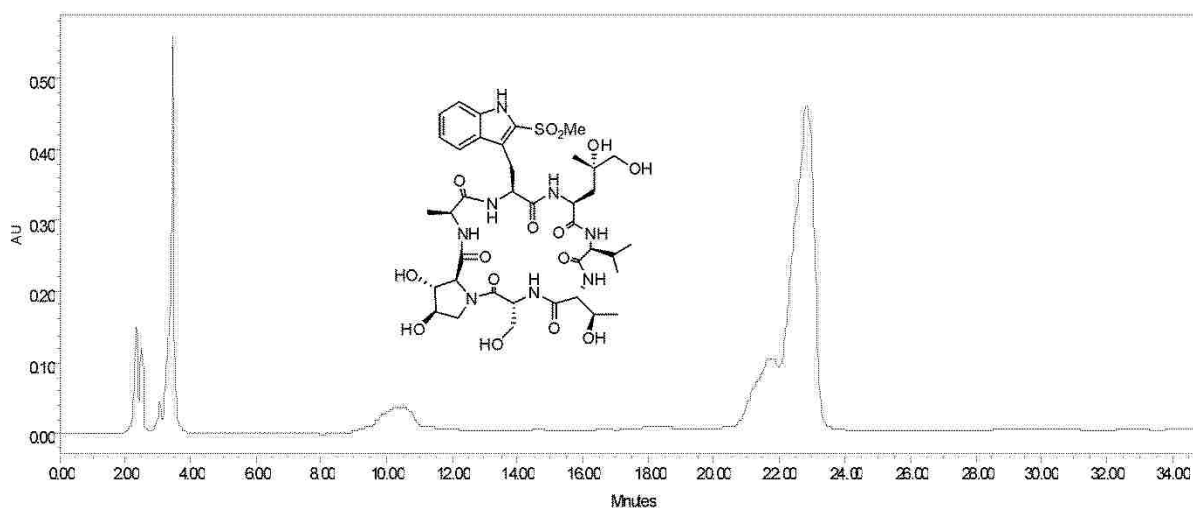
4-hyp Analog in 90% H_2O /10% D_2O water gate suppression
(700 MHz, pH 3.0)



HPLC chromatogram of 4-hyp analog (**45**) at 254 nm, (% acetonitrile in H₂O): 10-25% over 20 min; 25-35% over 10 min; 35% for 2 min; 35-10% over 3 min, 4.6 mm Econosil C-18 column, 1 mL min⁻¹



HPLC chromatogram of alloviroidin (**3**) at 254 nm, (% acetonitrile in H₂O): 10-25% over 20 min; 25-35% over 10 min; 35% for 2 min; 35-10% over 3 min, 4.6 mm Econosil C-18 column, 1 mL min⁻¹



CHAPTER 5: CONFORMATION

5.1 NMR, CD AND X-RAY STUDIES.

Circular dichroism¹ and NMR studies, as well as actin binding assays, have been used to study the conformation of phallotoxin and virotoxin analogs.^{179, 180} The Trp⁶ indole in phalloidin and virotoxins constitutes the chromophoric system responsible for the Cotton effects in the 250-320 nm range. Faulstich and coworkers¹ observed that the circular dichroism spectrum of phalloidin had two positive maxima at 217 and 235 nm. In contrast, the CD spectrum of viroisin has negative minima at 217 and 235 nm, an indication that the conformation of the indolyl thioether and sulfonyl angles is opposite (Fig. 5.1).

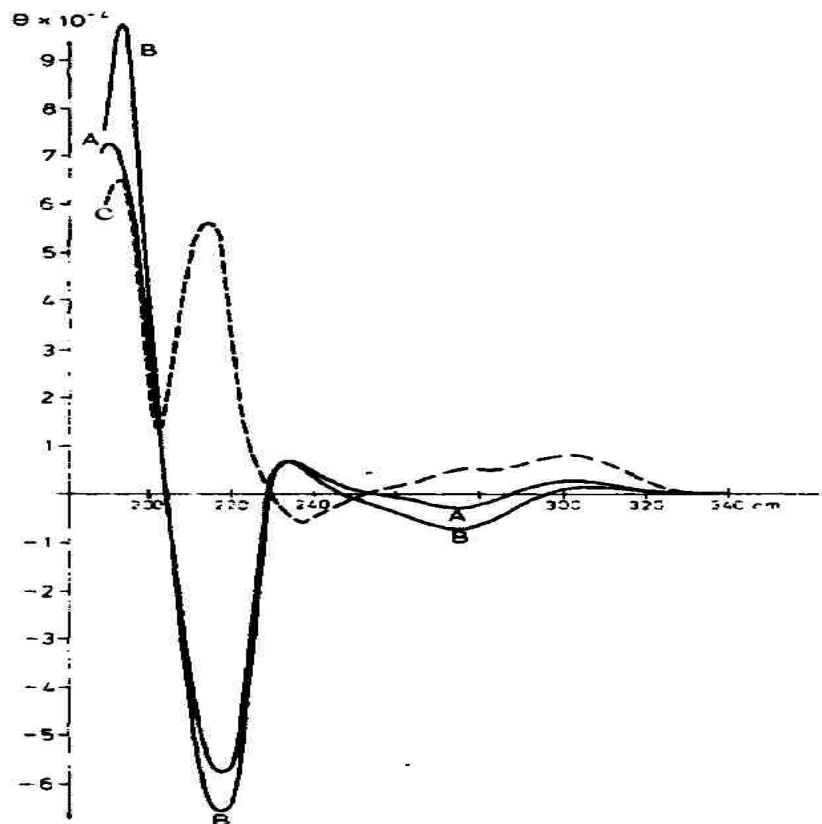


Figure 5.1. The CD spectra of viroidin (A), viroisin (B), and phalloidin.¹ Reprinted with permission from the American Chemical Society.

It has also been revealed that the conformation of monocyclic viroisin (Fig. 6) is similar to that of bicyclic phalloidin.^{30, 179} Through NMR studies, Kobayashi *et al.* demonstrated that both phallotoxins and virotoxins exist as a single conformer that is important for biological activity. Dethiophalloidin (Fig. 5.2) has several interconverting conformers, lacking almost all biological activity.¹⁷⁹

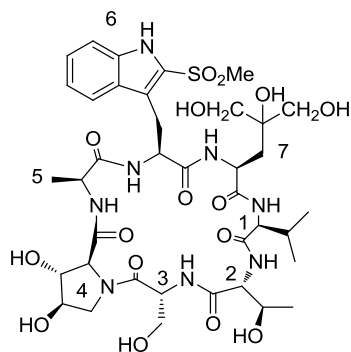
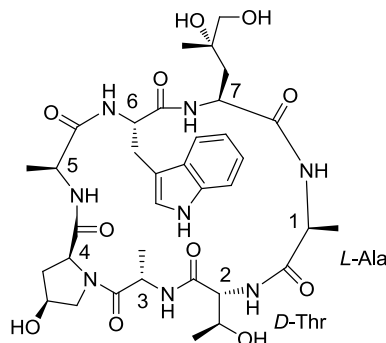


Figure 5.2. Viroisin (7)



Dethiophalloidin (221)

In general, geometric information can be derived from ¹H NMR spectra on the basis of the relationship between dihedral angles and vicinal coupling constants.¹⁸¹ Specifically, the coupling constant ³J_{NH α} between NH and H α is dependent on the torsion angle Φ and therefore gives information about the backbone conformation, while the H α and H β coupling constants describe the conformation of the side chain.¹⁸²⁻¹⁸⁶ Structures proposed for phalloidin and virotoxins were based on NMR data including ³J_{NH α} coupling constants, the temperature dependence of the NH proton signals, and rotating Overhauser effects (ROEs). Proton resonances were assigned on the basis of TOCSY and DQF-COSY spectra, and then HMQC and HMBC experiments were used to assign the aliphatic and aromatic carbon resonances. Interproton distances and the backbone dihedral angles were derived from the ROESY and coupling constant data respectively. Studies on the temperature dependence of amide proton chemical shifts provide information about hydrogen bonding. In general, temperature dependence of the NH resonance from a residue of a peptide is closely related to the rate of exchange (NH proton) with solvent

molecules. Specifically, a temperature gradient exceeding 4.0 ppb/K indicates an external NH orientation wherein the NH is exposed to solvent, and when the value is in the range of < 2 ppb/K, then either an intramolecular hydrogen bond is present or the NH may be buried within the peptide molecule (for peptides greater than 1 kDa).¹⁸⁷

5.1.2 Bhaskaran and Yu.¹⁸⁰

In 1994, Bhaskaran and Yu analyzed the conformation of viroisin (**7**) (Fig. 5.2) using two dimensional NMR and restrained molecular dynamics simulations. The values of the temperature gradients computed for the amide proton signals of viroisin were: 1.80 (Leu⁷), 2.21 (Val¹), 2.27 (Ala⁵), 4.14 (*D*-Ser³), 4.80 (*D*-Thr²), and 6.56 (Trp⁶) ppb/K. This indicated that the amide protons of Val¹, Ala⁵ and Leu⁷ residues participated in intramolecular hydrogen bonding. According to structures generated through computational studies, a hydrogen bond exists between either the Leu⁷ or Val¹ amide proton and the C=O group of Pro⁴. However, the dihedral angle values of the turn-forming residues did not match those observed for regular β turns, even though the hydrogen bond occurs between the C=O and NH of residues at *i*th and (*i*+3)th positions. These observations left no doubt that the closed loop of the structure obeys no typical structural pattern.

Probable conformations of viroisin in solution were derived from distance geometry and restrained molecular dynamics based on a set of distance constraints obtained from experimental data. The root-mean-square deviation values (0.065 nm for backbone atoms and 0.135 nm for all atoms) confirmed that viroisin has a highly ordered conformation in solution. Six structures generated from distance geometry and root mean square deviation methods revealed that the backbone of the molecule is folded into a dumbbell forming a convex surface at the central portion. This orients the Ala⁵ methyl group and the hydroxyl groups of the Pro⁴ residue to the convex side of the molecule, causing the Trp⁶

residue to protrude. The side chains of the Val¹ and Leu⁷ residues orient in the same direction, forming a hydrophobic domain for actin binding (Fig. 5.3). The hydroxyl group of Ser³ was oriented in a way that allowed a circular arrangement of other functional groups for binding to actin. These computational results are in agreement with the observed cross peaks between Ala⁵ methyl and Leu⁷ H_β protons in the NOESY spectrum.

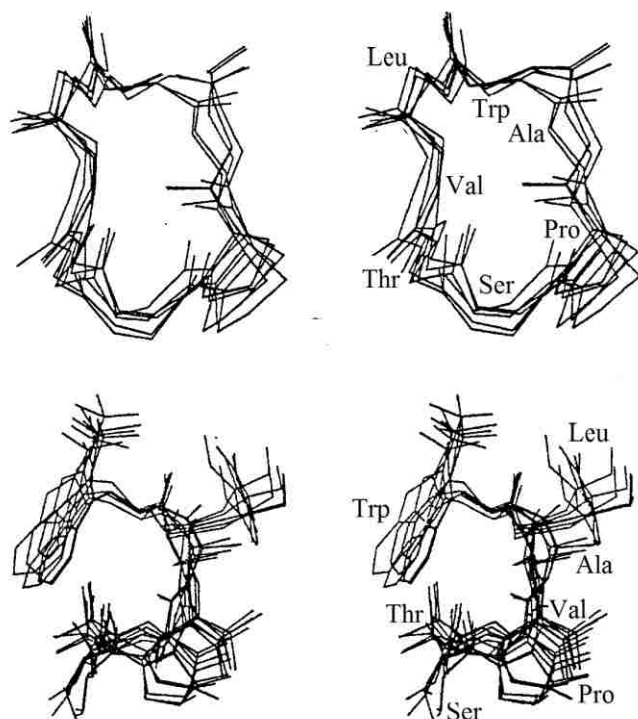


Figure 5.3. Stereo views of viroisin solution conformations showing side chain orientations.¹⁸⁰ Reprinted with permission from John Wiley and Sons.

5.1.3 Kobayashi and coworkers¹⁷⁹

In 1995, Kobayashi and coworkers studied the conformation of phalloidin and viroisin in solution using NMR and molecular modeling. The acyclic phalloidin derivatives, dethiophalloidin and secophalloidin (Fig. 5.4) were also studied, for comparison. In the ROESY spectra of both secophalloidin and dethiophalloidin, several sets of proton resonances exhibited positive cross peaks that were not due to scalar magnetization transfer, suggesting that major and minor conformers were

interconverting slowly on the NMR time scale. The spin systems of the minor conformers were assigned as 10 % for secophalloidin and 40 % for dethiophalloidin when these experiments were performed at 30 °C. In contrast, both phalloidin and viroisin existed as single conformers in solution.

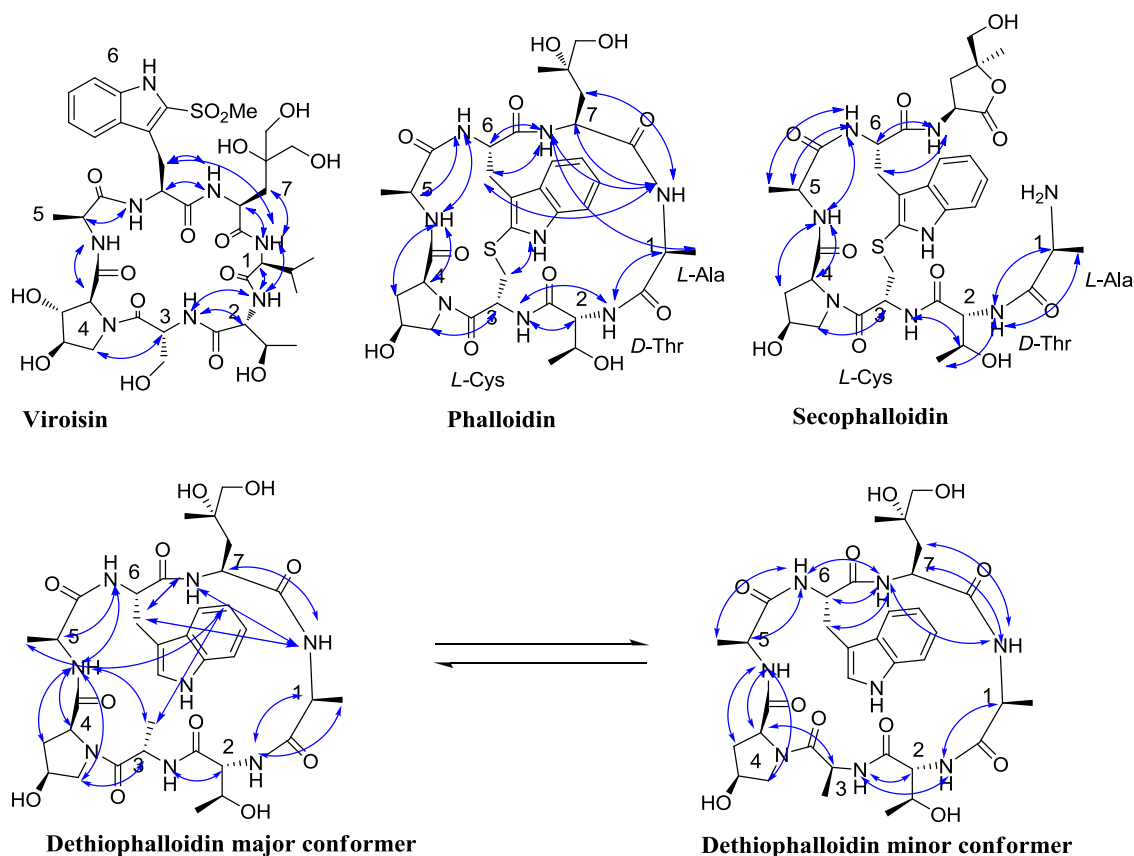


Figure 5.4. ROE correlations determined from 2D ROESY spectra.¹⁷⁹

The β -methyl resonances of Ala⁵/Ala¹ in phalloidin and Ala⁵/Val¹ in viroisin were temperature dependent, an observation not made for dethiophalloidin and secophalloidin. Kobayashi and co-workers attributed this temperature dependence of the toxic peptides' proton resonances of the methyl groups to the fluctuation of the Trp⁶ indole group at a rate faster than the NMR time scale, rather than by an overall change in their conformation.¹⁷⁹ Inter-proton distances confirmed that the motion of the Trp⁶ indole was rather negligible between 25 - 30 °C. It was therefore hypothesized that the shielding effect of the ring current would be sensitive to the distance between the Trp⁶ indole and Ala⁵ β -methyl

protons. The major difference between the proton resonances of the toxic and non toxic peptides was observed in the aliphatic region, *i.e.*, the Ala⁵ β -methyl proton resonances from phalloidin and viroisin exhibited a distinct up-field shift influenced by the ring current effect of the Trp-indole group. In contrast, the aliphatic proton resonances of secophalloidin and dethiophalloidin were relatively down-field. Secophalloidin displayed a 0.22 ppm up-field shift in the γ -methyl resonance of Thr², implying that the indole group has a different orientation to that of phalloidin.

The temperature-dependence of chemical shifts for the NH resonances of the Cys³ (-1.77 ppb/°C) and Trp⁶ (-0.37 ppb/°C) residues in phalloidin; Trp⁶ (-2.20 ppb/°C) in viroisin and Ala⁵ (-1.22 ppb/°C) in the major conformer of dethiophalloidin and Trp⁶ (-1.40 ppb/°C) in its minor conformer were not affected from 25 °C to 60 °C since they participate in intramolecular hydrogen bonding. The deuterium exchange rates of NH were also used to generate information related to hydrogen bonding. From the deuterium exchange kinetics experiment, the NH resonances of Cys³ and Trp⁶ in phalloidin were the only ones that were found to participate in hydrogen bonding. These findings indicated that phalloidin had the most rigid conformation, stabilized by a hydrogen bond involving Trp⁶ NH. Based on these results, viroisin's conformation was therefore believed to be slightly flexible, while the non-toxic peptides exhibited highly flexible conformations. Also, differences in chemical shifts of phalloidin and those of the major and minor conformers of dethiophalloidin were greater than 0.5 ppm for the α proton resonances of residues 3 and 6 and for the NH resonances of residues 2 and 6, implying that lack of the thioether bridge induces a large conformational change in the dethiophalloidin molecule. However, the difference in the chemical shifts of the major and minor conformers of dethiophalloidin was found to be small for the α proton resonances but relatively large for the NH resonances, supporting the argument that the two conformers were interconverting among different hydrogen bonding patterns. There was also a cross peak in the ROESY spectrum between Cys³/Ser³ H α and both Pro⁴ H δ , for both phalloidin

and viroisin, supporting the *trans* conformation of the peptide bonds between Cys³/Ser³ and Pro⁴ residues. The distinct cross peak between Ser³ H α and Pro⁴ H α in the ROESY spectrum of the minor conformer of dethiophalloidin confirmed that the Ser³/Pro⁴ peptide bond had a *cis* conformation.

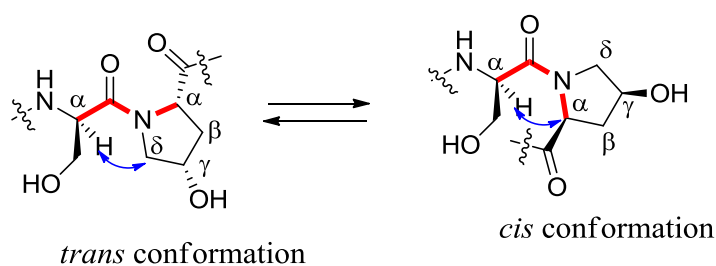


Figure 5.5. The *trans* and *cis* conformations of a *D*-serine-prolyl amide bond.

The dihedral angles of the lowest energy conformers for phalloidin and viroisin, as estimated using the protein health tool equipped in the QUANTA program were in agreement with the parameters determined by NMR. Phalloidin's final structure was found to possess a type-II- β -turn-like structure formed by the residues Cys³-Pro⁴-Ala⁵-Trp⁶, stabilized by a (*i*, *i*+3) hydrogen bond between the Cys³ C=O and Trp⁶ NH. This was further supported by a ROE cross peak between Pro⁴ C α H and Ala⁵ NH. Viroisin, on the other hand, adopts a conformation containing a distorted type-II- β -turn in the *D*-Ser³-Pro⁴-Ala⁵-Trp⁶ region, with a weak hydrogen bond between the *D*-Ser³ C=O and the Trp⁶ NH (Fig. 5.6). In general, β -turns,¹⁸⁸ also known as β -twist,¹⁸⁹ have a hydrogen bond between the main chain C=O of the first residue *i* and NH of the fourth amino acid (*i*+3). The difference between β -turns of type I and II is based on the backbone conformations of the residues at (*i*+1) and (*i*+2), represented by dihedral angles (Φ_{i+1} , Ψ_{i+1} and Φ_{i+2} , Ψ_{i+2}) respectively. The occurrence of *L*-proline at position *i*+2 leads to special β -turns due to higher preference of *cis* peptide bonds formed between proline and other residues.¹⁹⁰

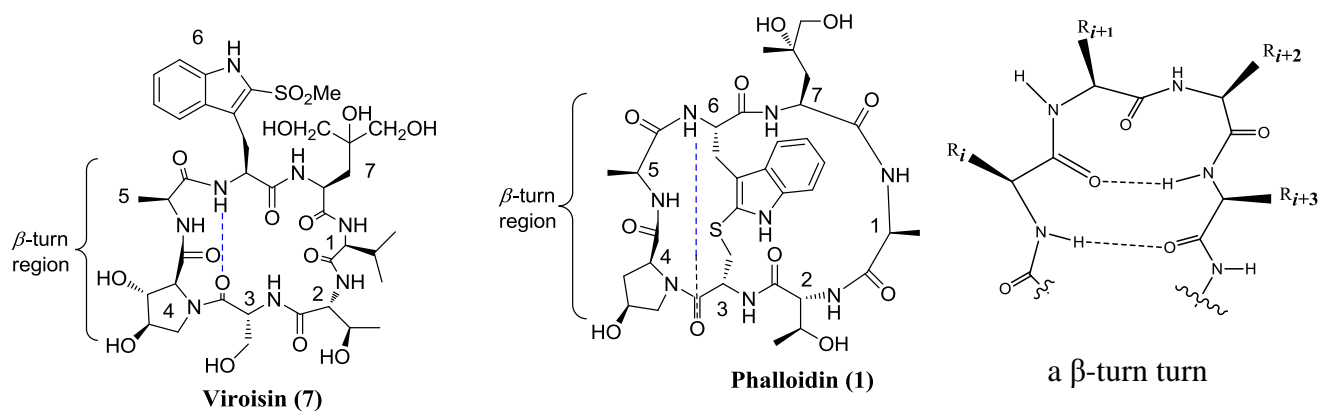
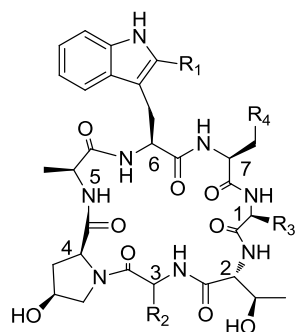


Figure 5.6. β -turn regions in viroisin and phalloidin.

Molecular modeling studies confirmed further that the Trp⁶ indole group in phalloidin's lowest-energy conformer is located above the β -methyl group of Ala⁵, being tightly fixed due to the rigidity of the bicyclic molecule. It was deduced that, since viroisin lacks a thioether bridge, the bulky methylsulfonyl group attached to the Trp⁶ indole residue is held into a hollow formed by the Val¹-D-Thr²-D-Ser³ segment, where the *D*-configuration of the Ser residue plays a major role in preventing interaction with its side chain.

5.1.4 Zanotti and coworkers³⁰

In 1999, Zanotti and coworkers demonstrated that the *D*-configuration of Ser played an important role in maintaining the phalloidin-like conformation of virotoxins. A viroidin analog with a *D*-serine in position 3, along with three other analogs, in which the *D*-serine residue was replaced by either a *D*-alanine, *L*-serine or *L*-alanine (Fig. 5.7), were synthesized and compared by NMR as well as in actin affinity assay. Other modifications to the natural product were the substitution of the dihydroxyproline and dihydroxyleucine residues with *cis*-4-hydroxy-*L*-proline (hyp⁴) and Leu⁷ respectively.



Analog	R ₁	R ₂	R ₃	R ₄
30	CH ₃ SO ₂	CH ₃ (<i>D</i> -)	CH ₃	CH(CH ₃) ₂
31	CH ₃ SO ₂	CH ₂ OH (<i>L</i> -)	CH ₃	CH(CH ₃) ₂
32	CH ₃ SO ₂	CH ₃ (<i>L</i> -)	CH ₃	CH(CH ₃) ₂

Figure 5.7. Viroisin analogs.³⁰

The NMR spectra of the analogs with *L*-configured amino acids at position-3 gave rise to 2-3 sets of signals, representing interconverting conformers. The analogs containing *L*-serine and *L*-alanine consisted of conformers in a ratio of 10:1 and 6:4:3, respectively. These conformers exhibited significant chemical shift differences of the backbone proton signals as compared to the *D*-serine containing analog. Those cyclic peptides containing *D*-configured amino acids at position-3 gave rise to a single set of signals.

Zanotti and coworkers demonstrated that changing the configuration of residue 3 from *D* to *L* caused a change in the backbone conformation of the molecule, resulting in low biological activity. It was speculated that the slow conformational transitions could be accounted for by the *cis/trans*-interconversions at the prolyl amide bond. This hypothesis was not proven since the ROE cross peaks in the region of CαH-CαH for the biologically inactive analogs could not be assigned due to overlapping and weak intensities of the signals.

The affinity for actin was based on the capacity of the analogs to displace demethylphalloidin from its binding site on filamentous actin. Omission of the dihydroxy-leucine residue and the extra hydroxyl group on the dihydroxyproline residue resulted in the loss of activity by a factor five.³⁰ A further reduction in the affinity for actin, by a factor of three, was observed for analogs lacking a β-

hydroxyl group in residue 3. Changing the configuration of *D*-serine to *L*-serine or substituting *L*-alanine for *D*-alanine sharply reduced the affinity for actin by a factor of 40 or >200 respectively.

5.1.5 Zanotti and coworkers³²

In 2001, Zanotti and coworkers investigated the solid state and solution conformation of a synthetic phallotoxin analog using X-ray diffraction, two-dimensional NMR and molecular dynamics calculations. The circular dichroism spectrum of the analog resembled that of phalloidin, with positive Cotton effects around 240 and 300 nm. The molecular model derived from the solid-state analysis indicated that all the peptide bonds were in the *trans*-conformation, with dihedral angles ranging from 168-180°. The macrocyclic heptapeptide was described as “bent” at the bridging points with the planes of the two rings forming dihedral angles of about 90.0(5)°. The indole ring was found to lie approximately in the plane of ring 1, containing the *cis*-4-hydroxyproline (hyp⁴)-Ala⁵ residues, resulting into an overall distorted “T” shape of the molecule.

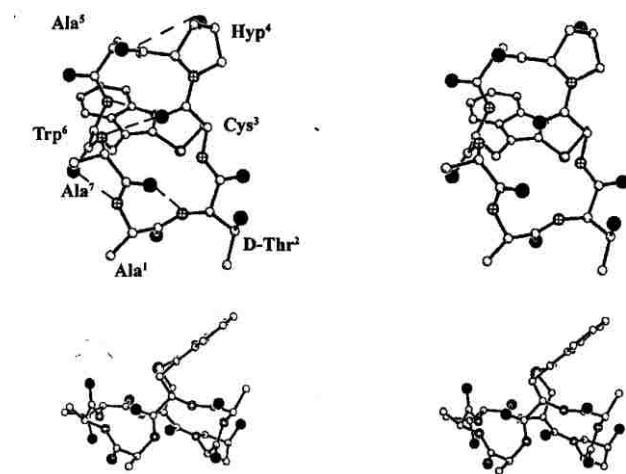


Figure 5.8. Stereodrawing of the molecular model of (Ala⁷)-phalloidin. Reprinted with permission from John Wiley and Sons.

The backbone conformation in the solid state was stabilized by a 4→1 hydrogen bond involving the Trp⁶ NH and the Cys³ CO, consistent with a type I β-turn, a 5→1 hydrogen bond between Ala⁷ NH and Cys³

CO, representing an α -turn of type Ia, a 3 \rightarrow 1 hydrogen bond between Ala¹ NH and Trp⁶ CO, consistent with an equatorial γ -turn, a 3 \rightarrow 1 hydrogen bond between D-Thr³ NH and Ala⁷ CO, described by an axial γ -turn, and an intramolecular hydrogen bond involving the Ala⁵ NH and hyp⁴-O ^{γ} residues (Figure 5.10). The α -turn and the two consecutive γ -turns observed in the solid-state were not present in solution due to high flexibility of ring 2. Relatively low temperature coefficient values for Cys³ NH and Trp⁶ NH residues further supported the involvement of these protons in hydrogen bonding. The $\chi^{1,1}$ and $\chi^{1,2}$ values (60° and -60°) of the D-Thr² side chain were in agreement with the g^- and g^+ conformations respectively. Torsion angles as obtained from X-ray analysis revealed that the hyp⁴ residue adopts an *endo*-type conformation, characterized by positive values for χ^1 and χ^3 and negative values for χ^2 and χ^4 .

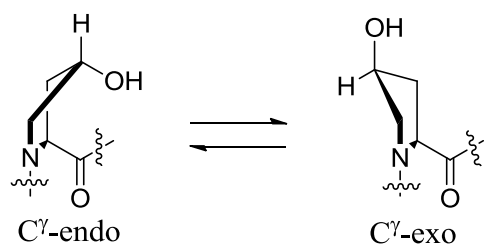


Figure 5.9. Conformations of hyp⁴ residue.

The observed χ^1 , $\chi^{2,1}$ and $\chi^{2,2}$ values of Trp⁶ indole were slightly different from those commonly found in proteins and small molecules, a deviation that was accounted for by the bridging effect, forcing the Cys³ side chain into uncommon conformational χ^1 angle of 28.6°.

The backbone dihedral angles from the molecular dynamics calculations were in agreement with the experimental Φ values of the Bystrovs' Karplus-type equation.¹⁹¹ Molecular dynamic studies *in vacuo* and water environments revealed a type I β -turn formed by Cys³-hyp⁴-Ala⁵-Trp⁶ and stabilized by a hydrogen bond between the Cys³ C=O and Trp⁶ NH residues. This region of the molecule was found to be very rigid during the molecular dynamics simulation. In contrast, the remaining part of the molecule (Ala⁷ to D-Thr²) was more flexible. The orientation of the Trp⁶ indole ring in the thioether

bridge was found to be pointing towards the hyp⁴-Ala⁵ segment, in both solid state and solution structures.

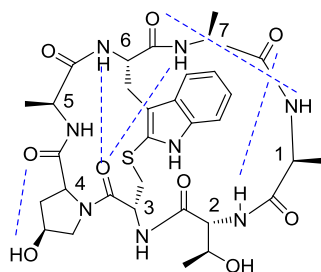
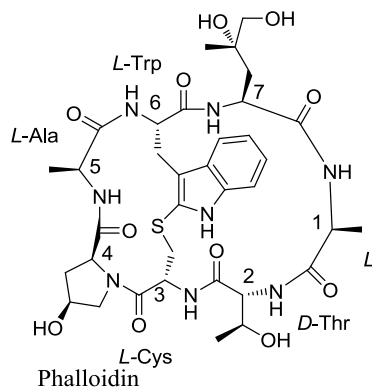


Figure 5.10. Intramolecular hydrogen bonds (dotted lines) observed by X-ray analysis.³²

5.1.6 Falcigno and Coworkers¹⁵

Falcigno and coworkers performed comparative conformational studies on synthetic derivatives of phalloidin, (Figure 5.11) in solution, using circular dichroism and restrained molecular dynamics based on NMR spectroscopy.



Analog	Residue 7	Residue 2	Residue 3
222	Ser (Bol)	<i>D</i> -Abu	<i>L</i> -Cys
223	Ala	<i>D</i> -Abu	<i>L</i> -Cys
224	Abu	<i>D</i> -Abu	<i>L</i> -Cys
225	Leu	<i>D</i> -Abu	<i>L</i> -Cys
33	Ala	<i>D</i> -Thr	<i>L</i> -Cys
226a	Ala	<i>L</i> -Thr	<i>L</i> -Cys
226b	Ala	<i>L</i> -Thr	<i>L</i> -Cys
227	Leu	<i>D</i> -Thr	<i>L</i> -Cys
228	Ala	<i>D</i> -Thr	<i>D</i> -Cys
229	Ser	<i>D</i> -Abu	<i>L</i> -Cys
230	Ser (caprylyl-ester)	<i>D</i> -Abu	<i>L</i> -Cys

226a and **226b** are atropisomers

Figure 5.11. Phalloidin analogs analyzed by Falcigno and co-workers.¹⁵

The synthetic analogs were designed to explore the importance of the chirality of *D*-Thr² and *L*-Cys³ residues, and the role of dihyLeu⁷ and Thr² side chains. Affinity for actin was measured on the basis of

the ability of the analog to displace [^3H]demethylphalloidin from its bound complex with F-actin. Analogs that had a significant difference in their affinities for actin with respect to phalloidin were selected for further conformational analysis in solution. From the circular dichroism spectra, a positive Cotton effect indicates that the value of the indolyl thioether angle is positive (*P* helical), while a negative Cotton effect describes *M* helical.

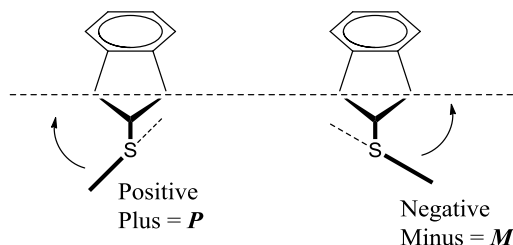


Figure 5.12. *P*- and *M*- helical configurations of a 2-indolylthioether⁶

Comparison of the circular dichroism spectra of the analogs revealed that both **228** and **226b** had positive Cotton effects, with **228** having two more maxima at around 292 and 300 nm. In contrast, analog **226a** was the mirror image of phalloidin with negative minima at around 250, 292 and 300 nm. Temperature dependence of the amide proton signals was obtained from one dimensional spectra recorded between 298 and 310 K. Small temperature coefficient values were recorded for Ala¹ NH and D-Thr² NH of analog **228**, Ala⁵ NH of analog **226a**, Trp⁶ NH, Ala¹ NH, and Ala⁵ NH of analog **226b**, indicating the participation of these amide protons in intramolecular hydrogen bonding.

Energy minimization and restrained molecular dynamics simulations were performed based on inter-proton distances computed from cross-relaxation rate values evaluated from the ROESY spectra. Data from restrained molecular dynamics simulation indicates that bicyclic analogs show atropisomerism according to whether the thioether bridge is up (U) or down (D) when the peptide chain is followed in a clockwise manner. The calculated conformational parameters of analogs **228** and **226b** were in good agreement with the NMR data, with both thioether bridges having a U-type structure. On the other hand, only a D-type model for analog **226a** matched the experimental data. The dihedral angles

of analog **228** were consistent with a backbone structure containing a type I β -turn formed by residues Trp⁶-Ala⁷-Ala¹-D-Thr² and stabilized by a hydrogen bond between Trp⁶ CO and D-Thr² NH. Also, this model had all the peptide bonds other than the Cys³-hyp⁴ bond in a *trans* conformation. The Ala⁵ methyl group of analog **228** was located in the anisotropy region of Trp⁶, an observation supported by the high field shift of the Ala⁵ methyl resonance.

The dihedral angles of analog **226a** were consistent with a type VIa β -turn in the Thr²-Cys³-hyp⁴-Ala⁵ region, stabilized by a hydrogen bond between Thr² CO and Ala⁵ NH residues. This model had all peptide bonds other than Cys³-hyp⁴ in a *trans* conformation. The Trp⁶ indole was oriented towards the hyp⁴ and Ala⁵ residues. Analog **226b**, on the other hand, had all peptide bonds in a *trans* conformation, with a type I β -turn formed by the residues Cys³-hyp⁴-Ala⁵-Trp⁶ and stabilized by a hydrogen bond between Cys³ CO and Trp⁶ NH. Again, the Trp⁶ indole ring was oriented towards hyp⁴-Ala⁵ residues.

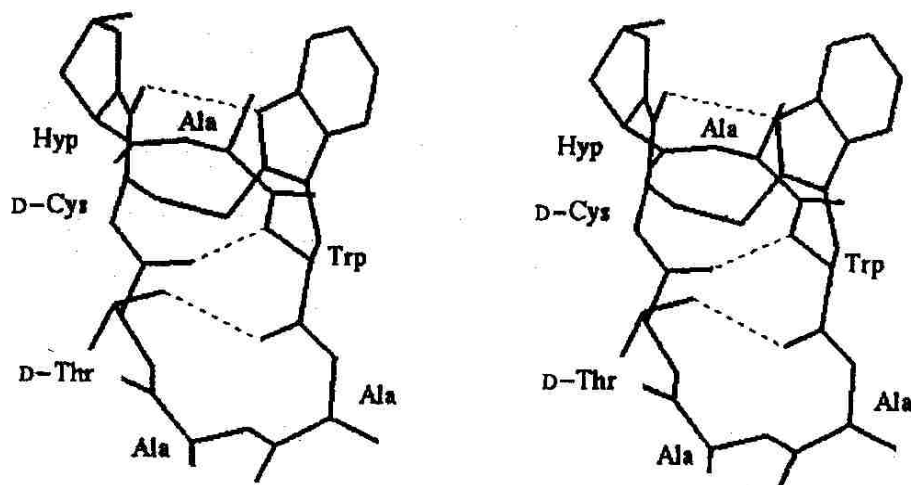


Figure 5.13. A stereodrawing of analog **226** illustrating a U-type structure. Intramolecular hydrogen bondings are shown by dotted lines.¹⁵ Reprinted with permission from John Wiley and Sons.

These studies demonstrated that neither the hydroxyl nor the carboxyl functional groups at the side chain of residue 2 had an impact on toxicity. The *D*-Thr² containing analogs were found to be more biologically active than their *D*-Abu² counterparts, supporting the requirement of a *D*-configured residue 2 with at least two carbon atoms for actin binding. Inversion of the configuration of residue 3 led to significant structural backbone changes characterized by the loss of activity.

5.2 CONFORMATION OF THE PROLINE CONTAINING TRIPEPTIDES

5.2.1 Overview

The conformation adopted by peptides depends on the sequence of amino acid residues along the chain. Prolyl residues, constrained by their pyrrolidine rings, have been known to influence the conformation of peptides and proteins.¹⁹² In general, most peptide bonds prefer to be in a *trans* orientation, however, the presence of either a proline or other secondary amino acid residue increases the population of the *cis* conformer (Fig. 5.14).

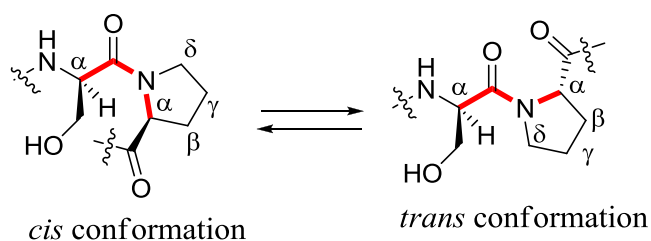


Figure 5.14. The *cis* and *trans* conformations of a *D*-serine-prolyl amide bond.

The *cis* to *trans* isomerization about the prolyl peptide bond plays an important role in protein folding and receptor binding. In solution, the pyrrolidine ring of the proline residue can either adopt the *C γ -endo* or *C γ -exo* or both interconverting ring pucker conformations (Figure 5.15). The ring pucker preference

influences the peptide main chain torsion angles and thereby the *cis-trans* isomerization of the amide bond.

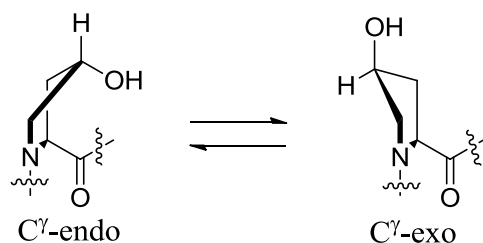
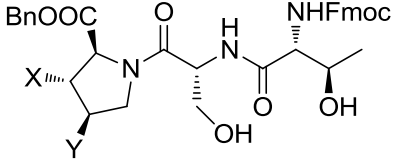


Figure 5.15. Conformations of hyp⁴ residue.

To investigate the conformational preference of the prolyl peptide bond in our linear peptides and how this influences the structure and ease of cyclization of the heptapeptides and the impact this would have on the conformation of the Ser³-Pro^{*}-Ala⁵-Trp⁶ (where Pro^{*} represents Pro, 3-Hyp, 4-hyp and DHP) peptide region, we determined the *trans-cis* ratios of the tripeptides with either unprotected side chains or with alcohols protected as TBS ethers. We reasoned that the TBS protected tripeptides (prepared in Chapter 3) would provide an insight into the conformation of the *D*-Ser³-Pro^{*} peptide bond in the cyclization precursors, while the fragments bearing free alcohols would help in the prediction of the conformation of the same region in alloviroidin and the analogs. We assigned the ¹H and ¹³C NMR resonances for the TBS protected compounds on the basis of COSY, HSQC, HMBC, and DEPT-135 experiments. The *trans* to *cis* ratios were determined by integration of well resolved signals in the ¹H NMR spectra of each isomer, followed by averaging of the integrals for each conformation (Tables **5.1** and **5.2**). The *cis* and *trans* conformations have been assigned before based on the chemical shifts of δ -carbons of the proline residues according to the findings of Lubell and co-workers who observed that the signal of the δ -carbon for the *cis* isomer is downfield of the *trans* isomer.¹⁹³ Our attempts to assign the two conformers using one dimensional GOESY¹⁹⁴ experiments at different temperatures were unsuccessful due to rapid interconversion between the conformers.

From Table 5.1, it can be seen that the *trans:cis* ratio for the prolyl peptide bonds vary with the degree, regio- and stereochemistry of proline hydroxylation.

Table 5.1. The *cis*-to-*trans* isomerization across the prolyl-serine peptide bond in CD₃OD (0.01M) at 25 °C and 400 MHz (m = multiplet).

 <p> 171 X = Y = OH 172 X = Y = H 173 X = OH; Y = H 174 X = H; Y = OH </p>	Compound	<i>trans:cis</i> ratio
	171	8.7:1
	172	4.4:1
	173	1.8:1
	174	2.1:1

We established the conformation of the prolyl ring puckers of the major isomers by comparing the observed $^3J_{\alpha\beta 1}$ and $^3J_{\alpha\beta 2}$ coupling constants with literature values.¹⁹⁵⁻²⁰¹ According to Cai and coworkers, both coupling constants for the C γ -exo conformer range between 7-11 Hz, giving rise to an apparent triplet, while in a derivative with a C γ -endo pyrrolidine, H α appears as a dd with coupling constants in the 6-10 Hz and 2-3 Hz ranges.²⁰² Tripeptide **171**, incorporating 2,3-*trans*-3,4-*trans*-3,4-dihydroxyproline has a stronger preference for the *trans* conformation and the pyrrolidine ring adopts the C γ -endo conformation on the basis of $^3J_{\alpha\beta}$ values of 7.8 and 4.4 Hz. The pyrrolidine ring in this conformation is stabilized by gauche interaction and hyperconjugation (Fig. 5.16). Raines and coworkers observed a similar *trans* conformation in *N*-acetyl-*trans*-4-hydroxyproline which has the C γ -*exo* pyrrolidine conformation.¹⁹⁵ Also, previous work in our group demonstrated that the *trans* conformation is favored in dipeptides containing 2,3-*trans*-3,4-*cis*-3,4-dihydroxyproline residue with the pyrrolidine ring preferring the C γ -*exo* conformation.³⁶

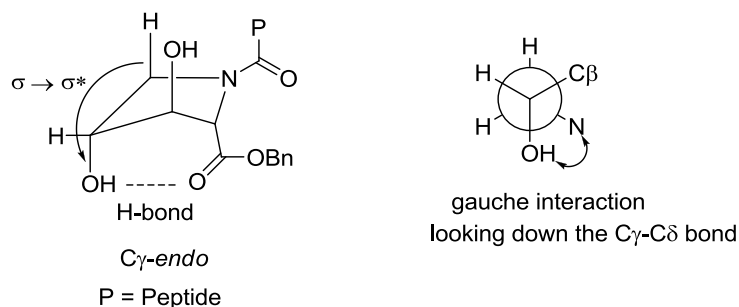


Figure 5.16. Pyrrolidine conformation in compound **171**.

In the case of tripeptide **172**, the equilibrium lies in favor of the *trans* isomer suggesting preference for the *exo* ring pucker conformation by the proline residue. However, this could not be established due to overlapping signals in the ^1H NMR spectrum.

The prolyl peptide bond in tripeptides **173** and **174** display increased *cis* character relative to compounds **171** and **172**. The pyrrolidine ring of compound **174** was assigned as *C γ -endo* pucker on the basis of $^3J_{\alpha\beta}$ values of 9.2 and 3.8 Hz. Inductive effects of the proline hydroxyl group in compounds **173** and **174** could be responsible for the increased *cis* ratio relative to that of **172**. The use of CD_3OD as a solvent interacts with the tripeptide's polar functional groups via intermolecular hydrogen bonding and thereby influencing the *cis*-to-*trans* isomerization across the prolyl-serine peptide bond.

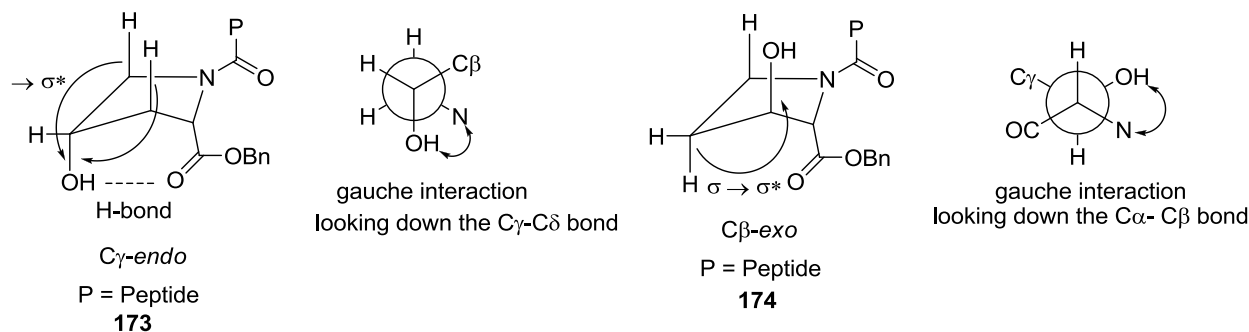


Figure 5.17. Pyrrolidine conformation in compounds **173** and **174**.

Interestingly, protecting the alcohols in the tripeptides as silyl ethers led to a drastic change in the *cis*-to-*trans* isomerization across the prolyl peptide bond for compounds **47-49**. According to Table 5.2, the observed increased levels of the *cis* isomer upon introduction of the bulky silyl groups can be explained

in terms of steric interactions. The pyrrolidine rings adopt conformations that minimize steric interactions between the bulky groups. The prolyl puckers of compounds **48** and **50** were assigned as *C γ -endo* pucker on the basis of $^3J_{\alpha\beta}$ values of 8.3, 3.6 Hz and 8.6, 5.0 Hz respectively.

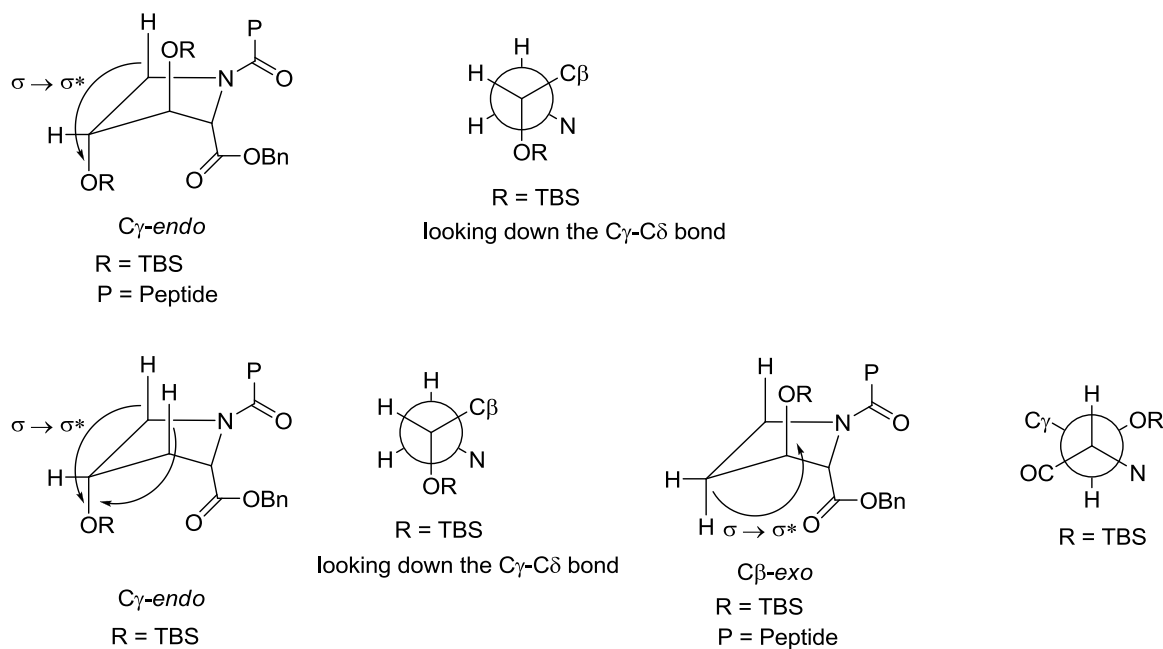
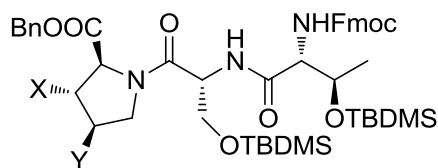


Figure 5.18. Pyrrolidine conformation in compounds **47**, **49** and **50**.

Increased levels of the *cis* isomer in the linear peptides facilitates cyclization and this explains the high chemical yield recorded during cyclization of the hyp containing heptapeptide.

Table 5.2. The *cis*-to-*trans* isomerization across the prolyl peptide bond (between *D*-Ser and Pro*) in CDCl₃ (0.01M) at 25 °C and 400 MHz. (ND = not determined, only a trace amount).



- 47** X = Y = OTBS
48 X = Y = H
49 X = OTBS; Y = H
50 X = H; Y = OTBS

Compound	<i>cis:trans</i> ratio	$^3J_{\alpha\beta}$ values (Hz)	Cyclization yield (% over four steps)
47	1:1.7	m	ND
48	1:5.5	8.3, 3.6	26
49	1:8.5	m	20
50	1:3	8.6, 5.0	31

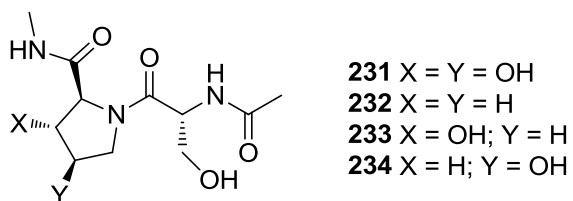
5.2.2 Computational Studies

In order to corroborate the *trans/cis* isomer ratios determined from NMR studies, we conducted computational studies of two conformations each of four acetylated dipeptides (Tables 5.3 and 5.4). Also, we hoped to find agreement on which of the two conformers is more stable and therefore the major conformer. We reasoned that these dipeptides would serve as a model for the Ser-Pro* (where Pro* is either DHP, Pro, 3-Hyp, or hyp) peptide bonds present in the tripeptides. We assumed that only the amide bond between the Ser and Pro* would exhibit conformational isomers. These dipeptides, by virtue of being smaller, possess less degree of freedom in comparison to the tripeptide fragments.

The *ab initio* and density functional calculations were performed using the Gaussian 09 package. Geometry optimizations for the *trans* and *cis* conformers of the dipeptides were carried out at the AM1, HF/3-21G and B3LYP/6-31g* levels. Frequency analyses were performed at the B3LYP/6-31g* level to verify the nature of the stationary points obtained and to calculate the zero point vibrational energies that were used to calculate Gibbs free energies in the gas phase at 298 K.

The energies of the two conformers per dipeptide are as shown in Table 5.3. According to Table 5.3, the predicted energies of the two conformers are in qualitative agreement with the experimental findings for the tripeptides (Table 5.1) with the exception of the DHP containing dipeptide, *i.e.*, the *trans* conformers are of lower energy and therefore favored over the *cis*. However, the calculated *trans/cis* ratios are poorly predicted by the B3LYP/6-31g* level. The discrepancy between experimental and calculated *trans/cis* ratios could be due to the difference in hydrogen bonding pattern involving either an amide or ester at the C-terminal of the Pro* residue in dipeptides and tripeptides respectively. This could also be due to the limitation of the method and basis set. The ratios could be improved by addition of diffuse and polarization functions to the basis set, *i.e.*, B3LYP/6-31+g*. The computed ratios should also be investigated in CH₃OH as this would incorporate the influence of hydrogen bonding.

Table 5.3. The energies and equilibrium constants ($K_{trans/cis}$) of the optimized dipeptide geometries.



Compound	<i>trans</i> (kcal/mol)	<i>cis</i> (kcal/mol)	(kcal/mol)	<i>K</i> (at 298K)
231	-656297.39	-656301.50	4.11	1.04×10^3
232	-561912.94	-561910.45	2.48	6.71×10
233	-609103.49	-609101.16	2.33	5.14×10
234	-609105.46	-609095.68	9.77	1.51×10^7

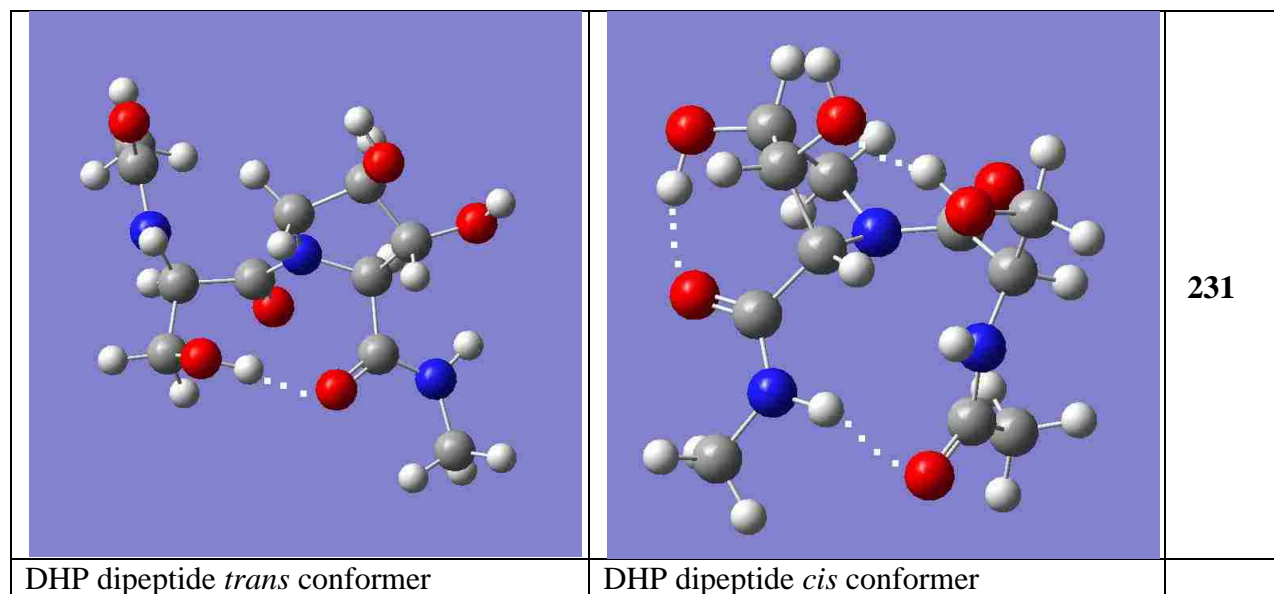


Figure 5.19 A. Optimized geometries of dipeptide **231**.

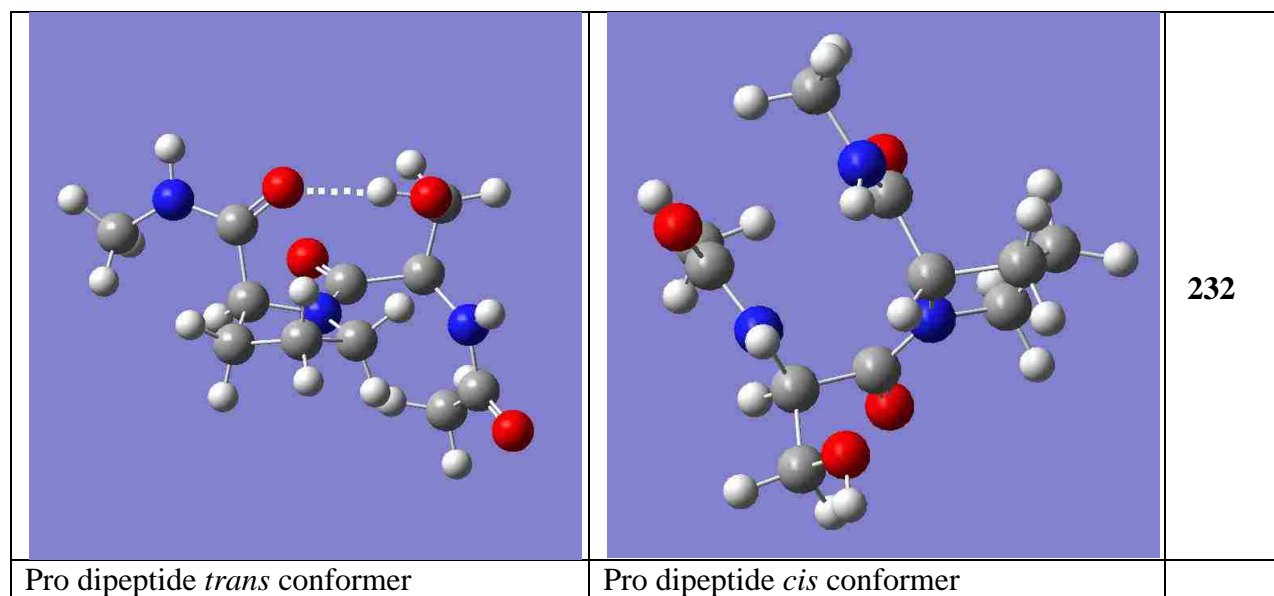


Figure 5.19 A continued. Optimized geometries of dipeptide **232**.

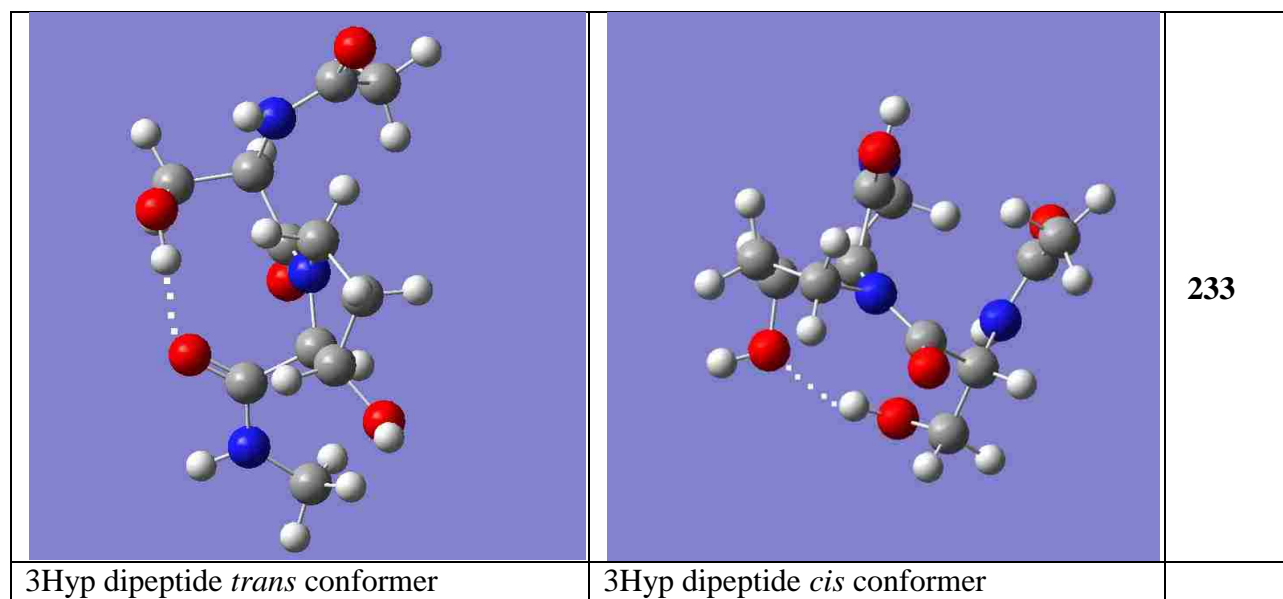


Figure 5.19 B. Optimized geometries of dipeptide **233**.

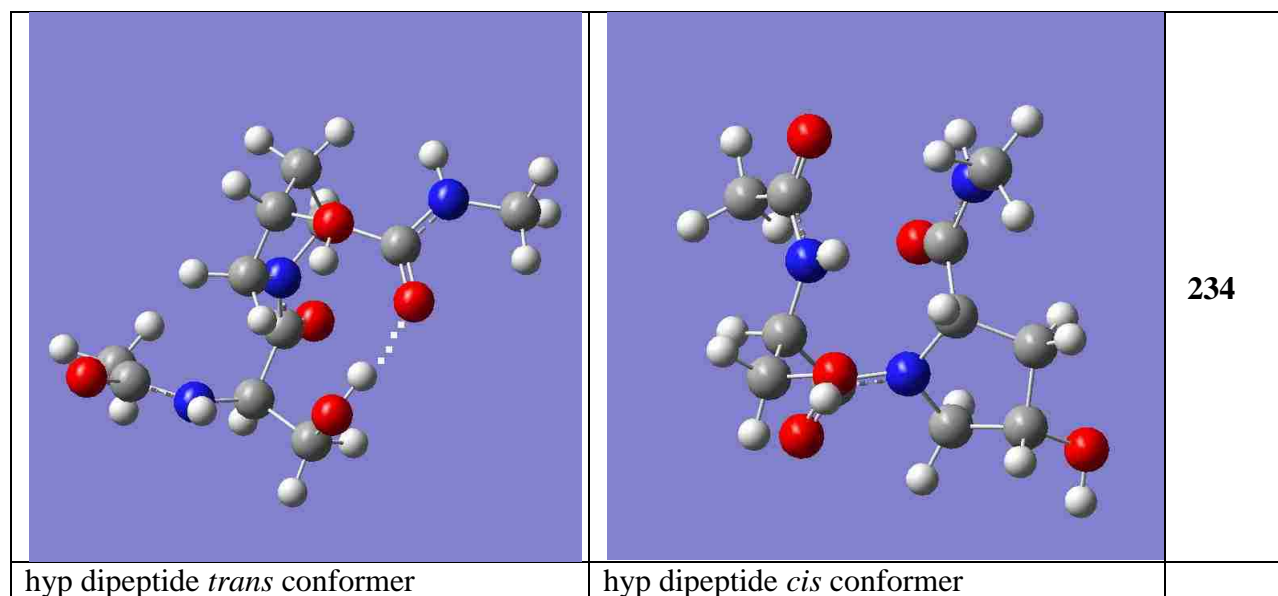


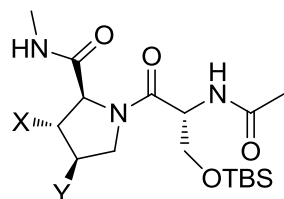
Figure 5.19 B continued. Optimized geometries of dipeptide **234**.

From Figure 5.19, the lowest energy conformations at B3LYP/6-31g* level are stabilized by varying degrees of hydrogen bonding. In the gas phase, the *cis* conformation in the DHP dipeptide is stabilized by three hydrogen bonds between DHP OH^β and Ser OH , DHP CO and DHP OH^γ , acetyl CO and acetyl amide NH . The *trans* conformer of the DHP dipeptide is stabilized by one hydrogen bond involving DHP CO and Ser OH . The *trans* conformer in the proline dipeptide is stabilized by a hydrogen bond between Pro CO and Ser OH . The 3-Hyp *trans* dipeptide conformer is stabilized by a hydrogen bond between 3-Hyp CO and Ser OH . However, a different hydrogen bonding pattern involving 3-Hyp OH and Ser OH is observed in the *cis* conformer. The *trans* conformer in the hyp dipeptide is stabilized by hydrogen bonding between hyp CO and Ser OH .

The calculated energies of the TBS protected dipeptides at the B3LYP/6-31g* level in the gas phase are as shown in Table 5.4. Even though the predicted energies of the two conformers are not in quantitative agreement with experimental findings, both theoretical and experimental results show

increased *cis* character but not in the same order. The increased *cis* character in both cases could be ascribed to the silyl ether protecting groups that break the hydrogen bonding pattern.

Table 5.4. The energies and equilibrium constants ($K_{trans/cis}$) of the optimized geometries.



235 X = Y = OTBS
236 X = Y = H
237 X = OTBS; Y = H
238 X = H; Y = OTBS

Compound	<i>trans</i> (kcal/mol)	<i>cis</i> (kcal/mol)	(kcal/mol)	<i>K</i> (at 298K)
235	-1647365.07	-1647345.88	19.19	1.22×10^{14}
236	-892270.86	-892267.42	3.43	3.34×10^2
237	-1269814.35	-1269811.64	2.70	9.65×10
238	-1269817.0	-1269813.98	3.01	1.65×10^2

The representative conformations of the TBS protected dipeptides optimized in the gas phase are presented in Figure 5.20.

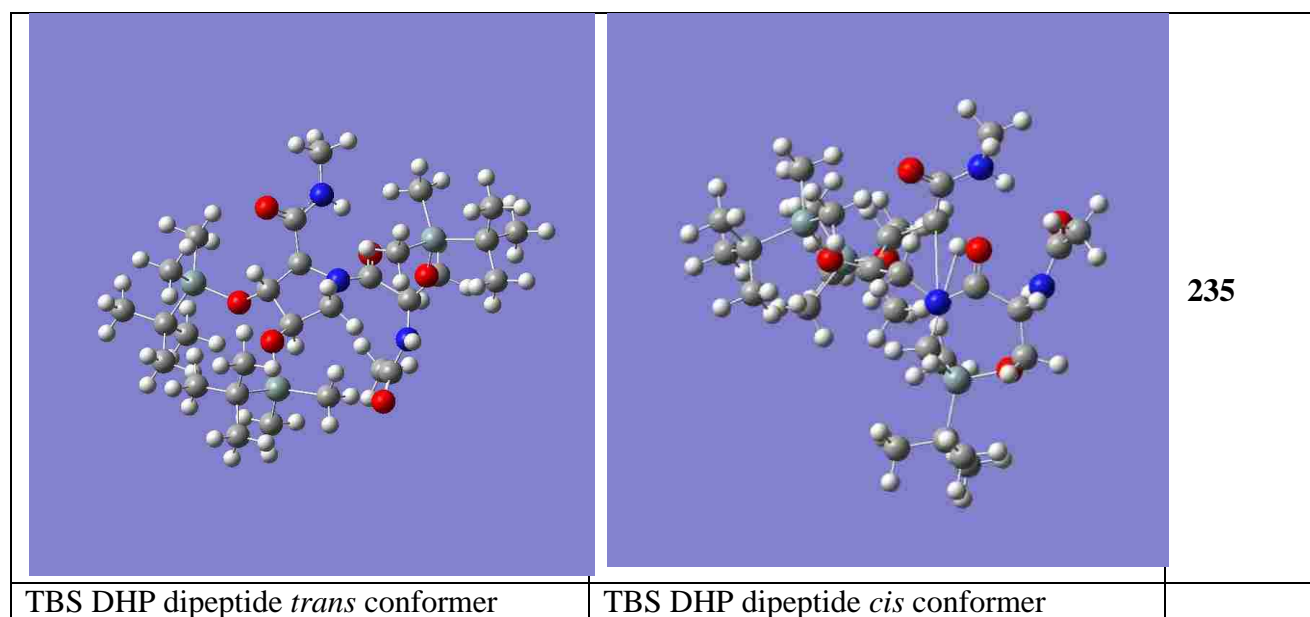


Figure 5.20 A. Optimized geometries of dipeptide **235**.

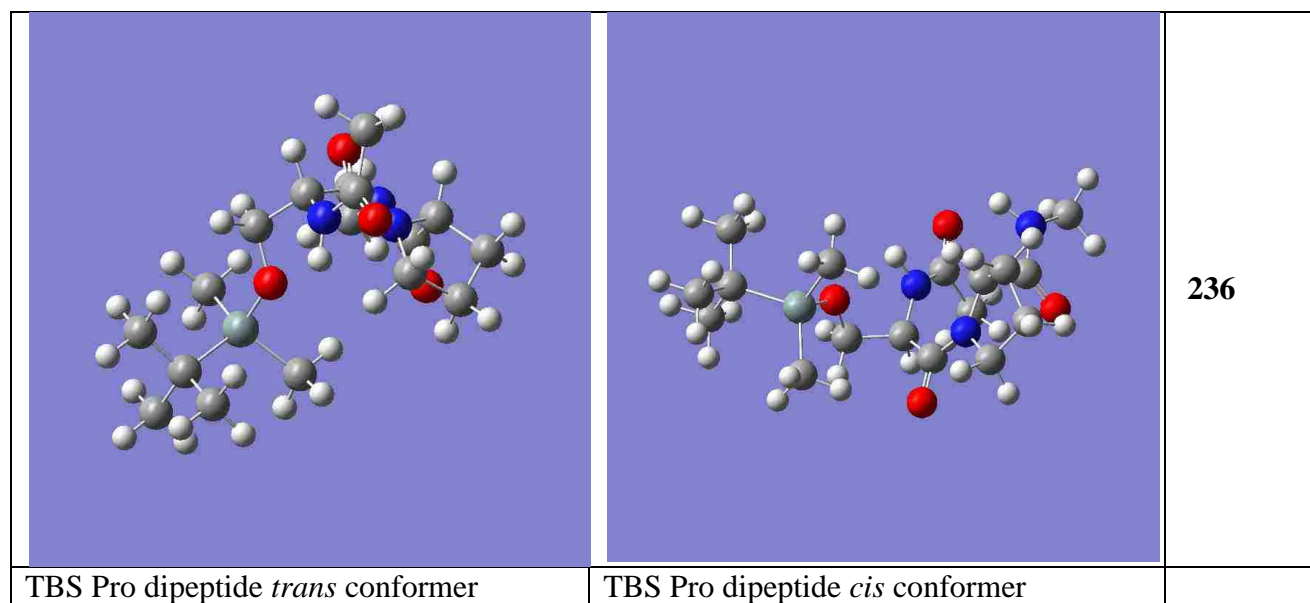


Figure 5.20 A continued. Optimized geometries of dipeptide **236**.

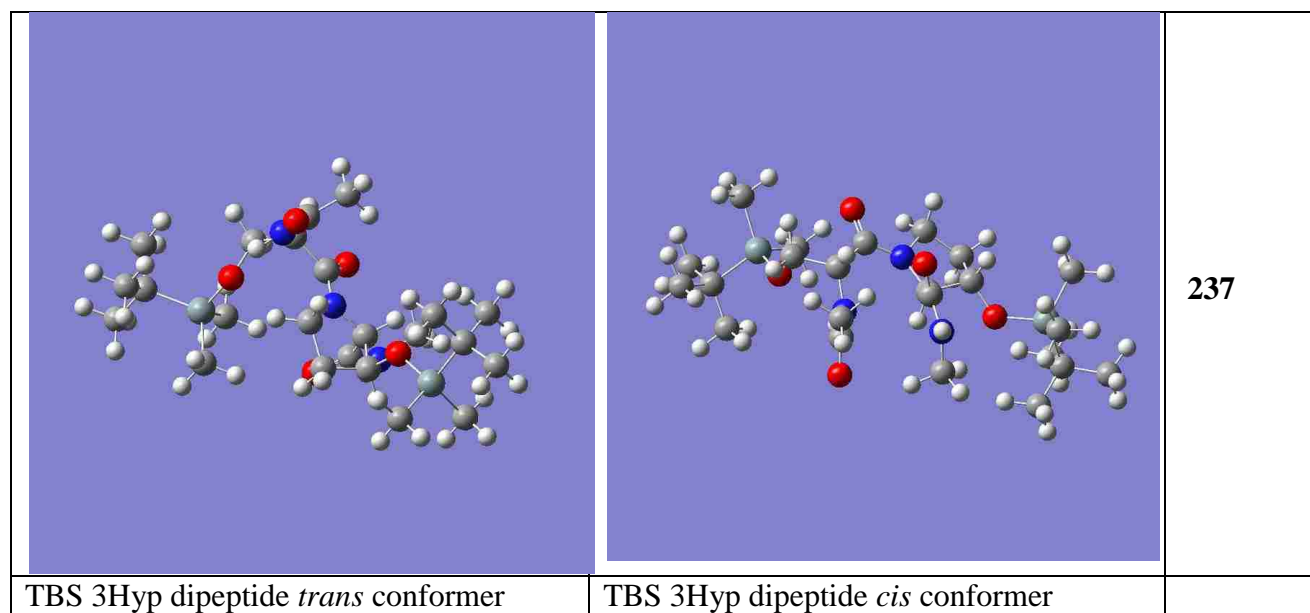


Figure 5.20 B. Optimized geometries of dipeptide **237**.

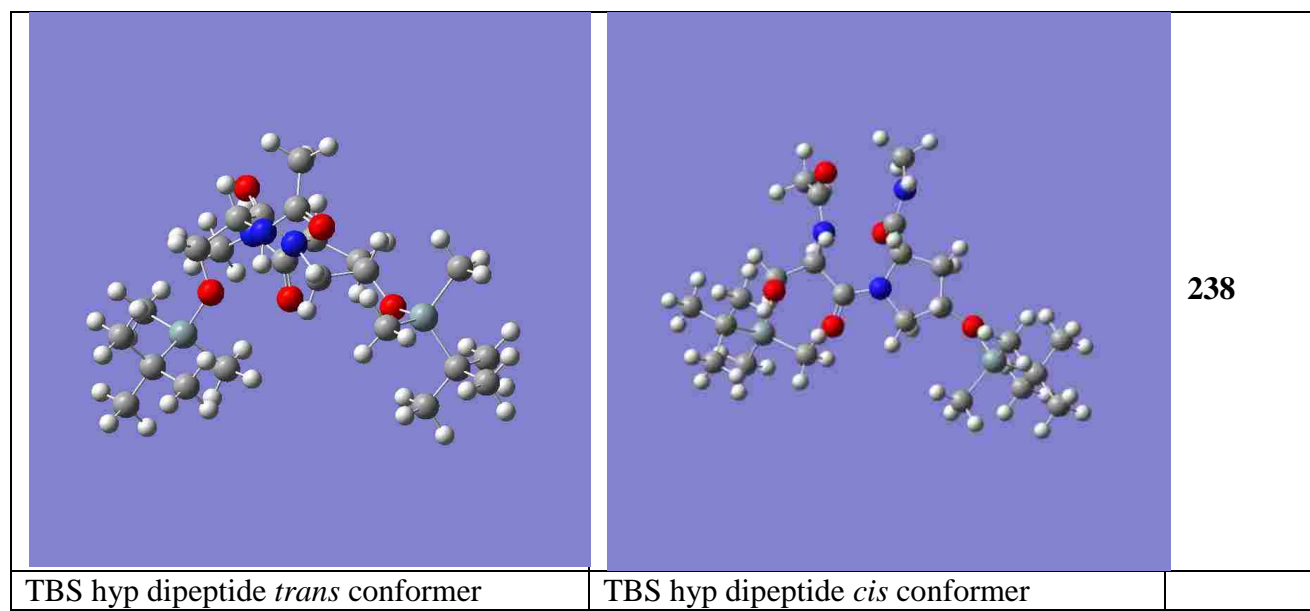


Figure 5.20 B continued. Optimized geometries of dipeptide **238**.

5.2.3 NMR Assignments and CD of Alloviroidin Analogs

To assign the spectra of the cycloheptapeptides, we conducted NMR studies in 90% $^1\text{H}_2\text{O}$ /10% $^2\text{H}_2\text{O}$, with $^2\text{H}_2\text{O}$ used for locking the sample. To further minimize the exchange of amide protons with the NMR solvent, we adjusted the pH of the medium to 3.0 according to Kobayashi and co-workers.¹⁷⁹ The proton resonances for compounds **43-45** presented in Table 5.5 were obtained from DQF-COSY and TOCSY spectra. The characteristically downfield chemical shift value of Ser³ H α facilitated the assignment of Ser³ H β . While the Ala⁵ H α was easily identified due to direct coupling to its methyl group. The Thr² methyl group was assigned based on coupling to its downfield H β . Similarly, the Val¹ and Trp⁶(SO₂Me) methyl groups were distinguished by the characteristic downfield chemical shift of Trp⁶(SO₂Me) methyl group that is not coupled to other protons.

Amide protons were assigned based on coupling to H α . The chemical shifts of the amide protons in the hyp analog and those of Trp⁶(SO₂Me) and HyLeu residues in the 3-Hyp analog were not observed in the spectra at 700 MHz spectrometer. We believe that this is due to the high rate of

deuterium exchange at high field. The proton signal of the Trp⁶ indole was observed further downfield in the ¹H NMR spectrum. The crosspeaks of the Trp⁶ ring were easily assigned in the TOCSY spectrum. The β methyl resonances of Ala⁵ in alloviroidin analogs exhibit a distinct downfield shift in comparison to those of toxic peptides reported in literature by Kobayashi and co-workers.¹⁷⁹ This implies that the Trp⁶ indole has a different orientation in the synthetic analogs and is not in close proximity with the Ala⁵ β methyl protons. Figures 5.21 and 5.22 represent the H α -NH cross peak regions in the TOCSY spectra of compounds **43** and **44** recorded at 25 °C.

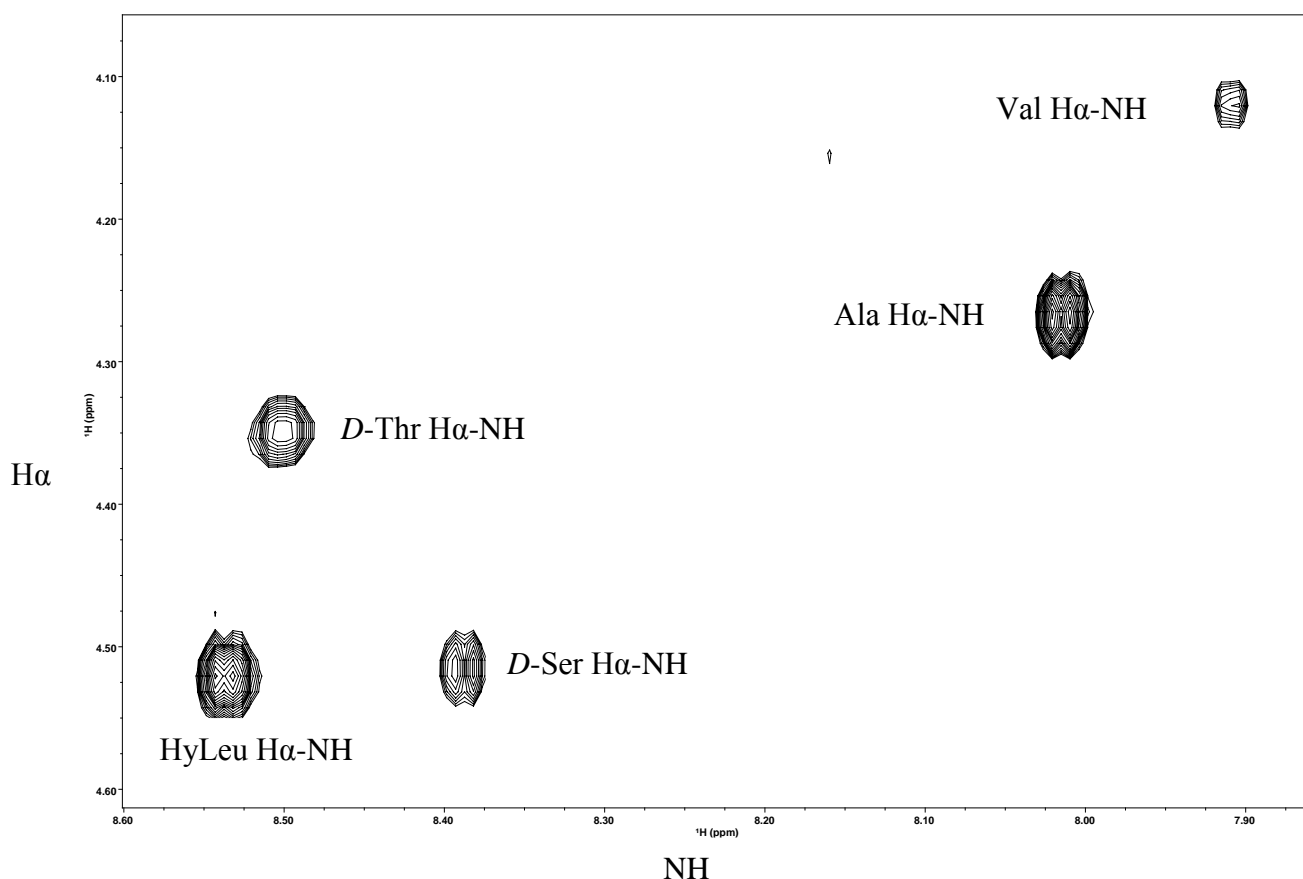


Figure 5.21. The H α -NH cross peaks in the TOCSY spectrum of compound **43** (proline-containing analog) in 90% H₂O/10% D₂O (pH 3.0) at 25 °C and 700 MHz.

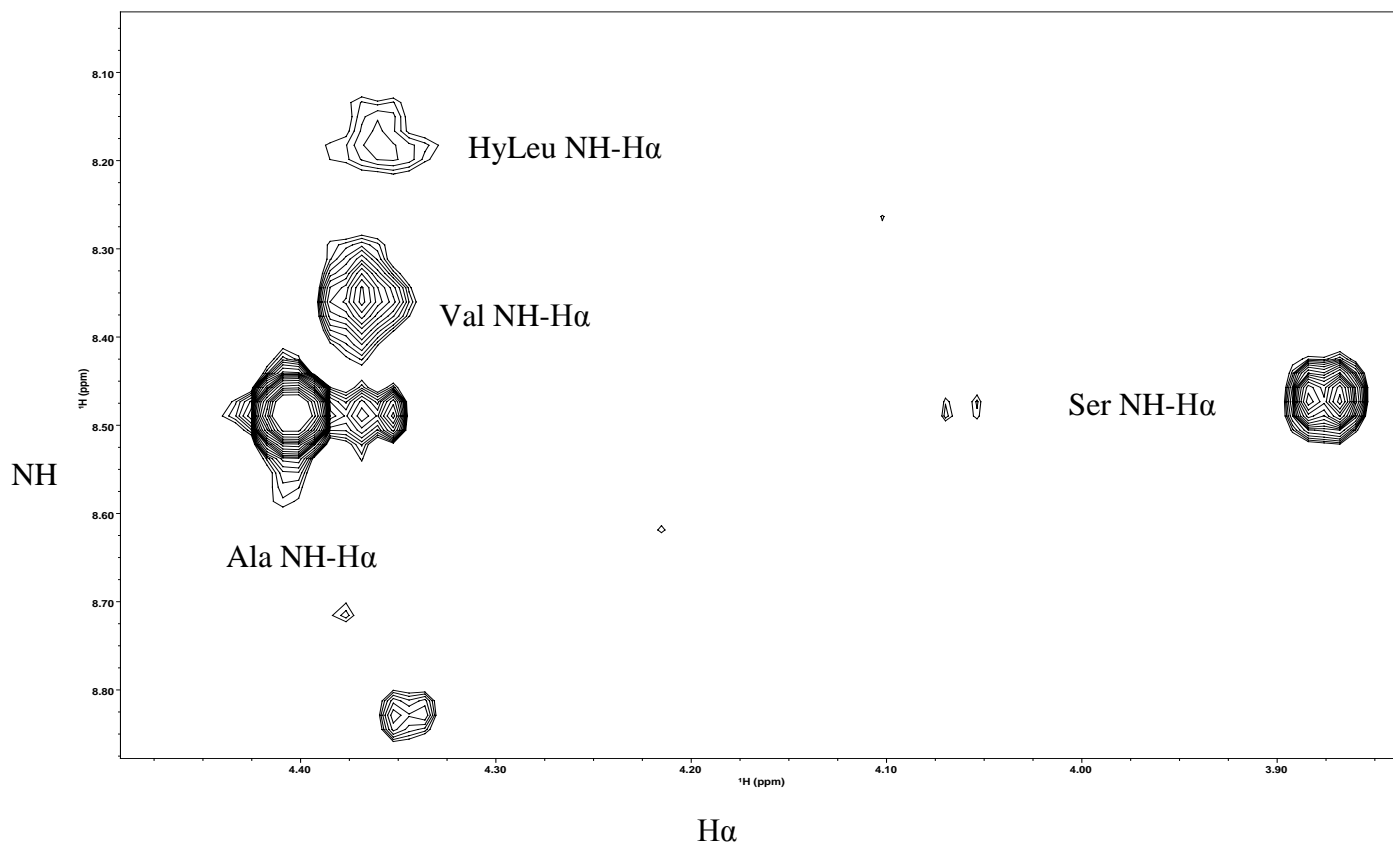


Figure 5.22. The NH-H α cross peaks in the TOCSY spectrum of compound **44** (3-Hyp-containing analog) in 90% H₂O/10% D₂O (pH 3.0) at 25 °C and 700 MHz (the unassigned cross peaks belong to the minor conformers).

Table 5.5. ¹H NMR chemical shifts of alloviroidin analogs (NH signals for compound **45** were not observed).

Cyclic Peptide	Residue	Chemical Shift (ppm) of:				
		NH	C α H	C β H	C γ H	Others
Proline Analog (43)	Val	7.91	4.11	2.15	0.98, 1.54	-
	<i>D</i> -Thr	8.50	4.78	4.34	1.22	-
	<i>D</i> -Ser	8.37	4.94	3.88, 3.85	-	-
	Pro	-	4.40	2.29, 2.31	1.99, 2.02	C δ H 3.81, 3.79
	Ala	8.01	4.26	2.07	-	-
	Trp (SO ₂ Me)	7.59	4.77	3.60, 3.40	-	SO ₂ Me 3.16
	HyLeu	8.53	4.52	1.62, 1.92	1.16	C δ H 3.83, 3.71

Table 5.5 continued. ^1H NMR chemical shifts of alloviroidin analogs (NH signals for compound **45** were not observed).

3Hyp Analog (44)	Val	8.36	4.37	2.06	0.99, 0.96	-
	<i>D</i> -Thr	8.53	4.79	4.36	1.24	-
	<i>D</i> -Ser	8.47	4.89	3.78, 3.87	-	-
	3Hyp	-	4.24	4.38	2.07, 2.13	C δ H 3.76, 3.86
	Ala	8.49	4.40	1.21	-	-
	Trp (SO ₂ Me)		4.76	3.86, 3.50	-	SO ₂ Me 3.18
	HyLeu	8.18	4.34	1.57, 1.93	1.29	C δ H 3.57, 3.70
hyp Analog (45)	Val		4.19	1.96	0.85, 1.83	-
	<i>D</i> -Thr		4.78	4.41	2.08	-
	<i>D</i> -Ser		5.00	3.86, 3.84	-	-
	hyp	-	4.60	2.46, 2.03	4.46	C δ H 3.81, 3.87
	Ala		4.42	1.19	-	-
	Trp (SO ₂ Me)		4.74	3.38, 3.68	-	SO ₂ Me
	HyLeu					C δ H

The upfield chemical shifts of Val¹ NH and Trp⁶(SO₂Me) NH at 7.91 and 7.59 ppm in the proline analog suggest their participation in intramolecular hydrogen bonding.

In the ROESY and NOESY spectra of the analogs, very weak resonances were observed making the assignment of the cross peaks unsuccessful. This could be due to rapidly inter-converting conformers on an NMR time scale. It is not clear why the flexibility of these cyclic peptides vary with the NMR field strength. We found out that the degree of conformation flexibility was greater on the high field 700 MHz spectrometer in comparison to the 250 MHz spectrometer.

To further examine the conformation of the cycloheptapeptides, circular dichroism of alloviroidin analogs **43** and **45** were measured in water. According to Figure 5.23 the hyp analog (**45**) exhibits a CD spectrum similar to that of other virotoxins,¹ specifically, two negative minima at 218 and 233 nm. In contrast, the proline analog (**43**) has negative minima at 196 and 214 nm. This observation indicates that virotoxins and the hyp analog (**45**) are likely to have similar conformations. It is important to note that the similarity in the CD spectra of virotoxins and the hyp analog (**45**) does not correspond to affinity for actin. The Cotton effect of the proline analog, however, exhibits marked backbone changes when compared to the natural virotoxins. These structural differences are presumed to be mainly due to isomerism about the Ser³-Pro⁴ peptide bond. These results suggest a relationship between CD and conformation interconversion, *i.e.*, there is the possibility that the Pro analog exists as a mixture of conformers.

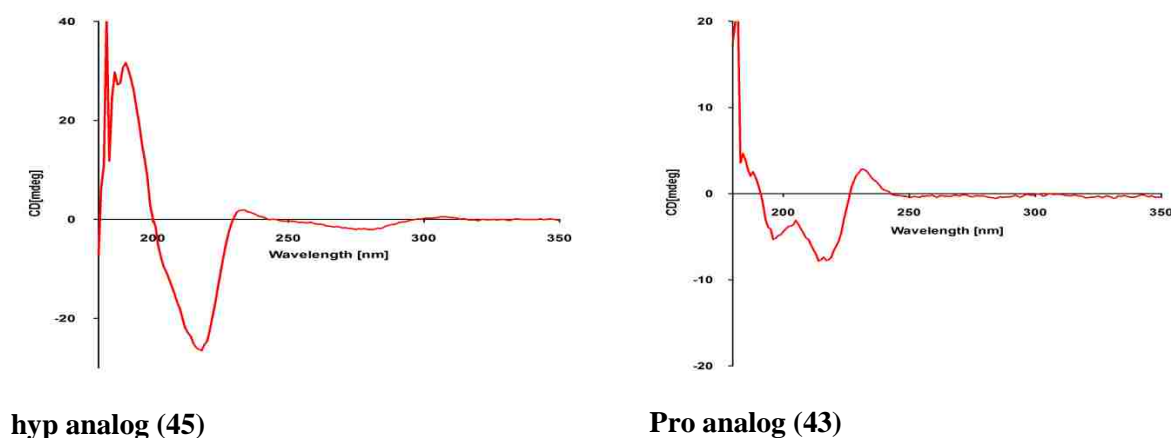


Figure 5.23. Circular dichroism spectra of hyp (**45**) and Pro (**43**) analogs in water (1.4×10^{-4} M).

5.2.4 Summary

In conclusion, we have examined the conformational preferences of the dipeptide fragments **231-238** using computational studies. These computational analyses indicate that the most stable

conformation of the dipeptides in the gas phase is *trans*. These findings on dipeptides are in qualitative agreement with our NMR findings on tripeptides **172-174** and **47-50**. However, the calculated *cis/trans* ratio values of the dipeptides are not in accord with the NMR results of the tripeptides. This could be explained in terms of the influence of the solvent on the *cis-trans* isomerization rotational barrier in solution through hydrogen bonding, the greater flexibility of longer tripeptide fragments and the two additional stereocenters introduced by the *D*-threonine residue.

These conformational studies on tripeptide fragments illustrate the influence of the degree and regiochemistry of proline hydroxylation on cyclization and the conformation of the cyclic heptapeptides. In particular, the TBS protected hyp residue was found to favor the *cis* conformation facilitating peptide cyclization. From these tripeptide conformational studies, there is a possibility that the conformational interconversions observed for the cyclic peptides could be explained in terms of the *cis/trans* isomerization across the prolyl peptide bond.

NMR experiments carried out on alloviroidin analogs have allowed proton assignment but have been unsuccessful at determining the solution structures. While ROESY and NOESY have been used by others for conformational analysis of similar analogs, only weak signals were observed in our spectra suggesting high conformational flexibility at high magnetic field. Further NMR studies at different field strengths and temperatures in combination with simulated calculations should be conducted to determine the conformation of the cyclic peptides.

Analysis of two cyclic peptides by CD spectroscopy in water revealed that the CD spectrum of the hyp analog is consistent with that of the natural virotoxins. This contrasts with the CD spectrum of the proline analog. The similarity in CD of the hyp analog with that of viroidin suggests that their conformation could be similar.

5.2.5 Future Work

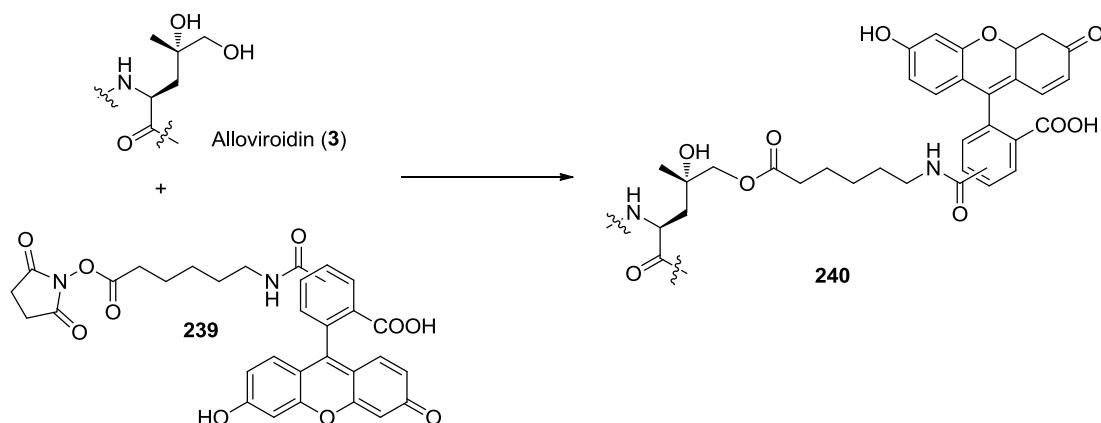
Given the weak signals in the NOESY and ROESY spectra of the cyclopeptides following NMR experiments at 700 MHz, we believe that performing these experiments at lower field strengths would slow down conformation interconversion and generate correlations that will be used to estimate interproton distances. Restrained energy minimizations should be performed to gain an insight into the structures of alloviroidin and analogs. Dihedral angles and distance restraints will be derived from DQF-COSY J values, ROESY and NOESY NMR data. Computational studies using SYBYL program will be used to generate structures that satisfy the NMR restraints. Energy minimization of each of the generated structures will allow them to relax to a local minimum energy. This will be achieved by heating the molecules followed by gradual cooling to enable the various conformations to relax to a minimum energy. Root mean square deviation will then be calculated for the superimposed structures.

Deuterium exchange NMR experiments will be conducted to ascertain which amide protons participate in hydrogen bonding. The cyclic peptides will be dissolved in D₂O and the rate of deuterium exchange will be measured by recording ¹H NMR and TOCSY experiments at different temperatures and time intervals. The amide protons of residues that are not involved in hydrogen bonding ought to be exchanged for ²H and this will be evident by the disappearance of H_N-H_α crosspeaks in the spectrum. The rate of exchange of the amide protons will be plotted against time to generate the rate constants that will be compared to values reported in literature.

The γ,δ-dihydroxyleucine residue, which has been shown not to be essential for actin binding, could serve as a handle for the attachment of a fluorophore to produce a new probe for visualizing actin dynamics. Derivatization of alloviroidin with a fluorophore (*e.g.*, **239**) will be achieved via ester bond formation with the primary alcohol of the dihydroxyleucine residue to deliver **240** (Scheme 5.1). The affinity of this conjugate for actin will be measured and compared to that of the commercially available

phalloidin fluorescein conjugate. In the event that this approach fails, the fluorescein could be incorporated into tetrapeptide **46** prior to fragment condensation and cyclization.

Scheme 5.1. Derivatization of alloviroidin with a fluorophore.



5.3 EXPERIMENTAL SECTION

5.3.1 General Methods: As for Chapter 4 with the following additions and modifications: For NMR studies, 2 mg of each cyclic peptide was dissolved in 200 μL of 90% H_2O /10% D_2O , pH 3.0 (the NMR solvent was prepared by mixing D_2O (10 mL) and HPLC grade H_2O (90 mL). The pH of the solvent mixture was adjusted to 3.0 using 0.1 M HCl and 1M NaOH solutions). Solvent suppression was done using WATERGATE sequence. The ROESY and NOESY experiments were performed at 150, 200, 300, 400, and 500 ms mixing times. Spectra assignment was achieved using Sparky and NMRViewJ software packages.

The *ab initio* and density functional calculation studies were performed using the Gaussian 09 package. Geometry optimizations for the *trans* and *cis* conformers of the dipeptides were carried out at the AM1, HF/3-21G and B3LYP/6-31g* methods and basis sets. Frequency analyses were performed at B3LYP/6-31g* level to verify the nature of the stationary points obtained and to calculate the zero point vibrational energies that were used to calculate Gibbs free energies in the gas phase at 298 K.

Circular Dichroism spectra (with sample concentrations of 1.4×10^{-4} M in water) were measured on a Jasco J-815 spectropolarimeter using a rectangular cell with a path length of 1 mm. Each measurement was the average result of three scans. Baseline spectrum of H₂O was subtracted.

REFERENCES

1. Faulstich, H.; Buku, A.; Bodenmüller, H.; Wieland, T., "Virotoxins: Actin-binding cyclic peptides of *Amanita virosa* mushrooms," *Biochemistry* **1980**, *19* (14), 3334-3343.
2. Little, M. C.; Preston, J. F. III., "The fluorimetric detection of amatoxins, phallotoxins, and other peptides in *Amanita suballiacea*," *Journal of Natural Products* **1984**, *47* (1), 93-99.
3. Bonnet, M. S.; Basson, P. W., "The toxicology of *Amanita virosa*: the destroying angel," *Homeopathy* **2004**, *93* (4), 216-220.
4. Bonnet, M. S.; Basson, P. W., "The toxicology of *Amanita phalloides*," *Homeopathy* **2002**, *91* (4), 249-254.
5. Nieminen, L.; Bjondahl, K.; Ojanen, H.; Mottonen, M.; Hirsimäki, P.; Hirsimäki, Y., "Sex differences in renal damage induced in the mouse by *Amanita virosa*," *Experimentelle Pathologie* **1977**, *14* (3-4), 136-140.
6. Wieland, T., "Peptides of poisonous *Amanita* mushrooms," *Springer-Verlag* **1986**, New York.
7. Gicquaud, C.; Turcotte, A.; Gruda, J.; Tuchweber, B., "In vivo and in vitro effects of peptide extracts from *Amanita virosa*," *Revue Canadienne de Biologie Experimentale* **1982**, *41* (1), 23-34.
8. Turcotte, A.; Gicquaud, C.; Gendreau, M.; St-Pierre, S., "Separation of the virotoxins of the mushroom *Amanita virosa* and comparative study of their interaction on actin in vitro," *Canadian Journal of Biochemistry and Cell Biology* **1984**, *62* (12), 1327-1334.
9. Wieland, O., "Changes in liver metabolism induced by the poisons of *Amanita phalloides*," *Clinical Chemistry* **1965**, *11* (2), 323-328.
10. Munekata, E.; Faulstich, H.; Wieland, T., "Peptide syntheses, LXI. Components of the green deathcap toadstool *Amanita phalloides*, LIII. Total synthesis of phalloin and [Leu⁷]-Phalloin," *Justus Liebigs Annalen der Chemie* **1977**, (10), 1758-1765.
11. Barak, L. S.; Yocum, R. R.; Nothnagel, E. A.; Webb, W. W., "Fluorescence staining of the actin cytoskeleton in living cells with 7-nitrobenz-2-oxa-1,3-diazole-phalloidin," *Proceedings of the National Academy of Sciences of the United States of America* **1980**, *77* (2), 980-984.
12. Wieland, T.; Miura, T.; Seeliger, A., "Analogues of phalloidin. D-Abu²-Lys⁷-phalloin, an F-actin binding analogue, its rhodamine conjugate (RLP) a novel fluorescent F-actin-probe, and D-Ala²-Leu⁷-phalloin, an inert peptide," *International Journal of Peptide and Protein Research* **1983**, *21* (1), 3-10.
13. Small, J. V.; Zobeley, S.; Rinnerthaler, G.; Faulstich, H., "Coumarin phalloidin: A new actin probe permitting triple immunofluorescence microscopy of the cytoskeleton," *Journal of Cell Science* **1988**, *89* (1), 21-24.

14. Faulstich, H.; Trischmann, H.; Mayer, D., "Preparation of tetramethylrhodaminy-phalloidin and uptake of the toxin into short-term cultured hepatocytes by endocytosis," *Experimental Cell Research* **1983**, *144* (1), 73-82.
15. Falcigno, L.; Costantini, S.; D'Auria, G.; Bruno, B. M.; Zobeley, S.; Zanotti, G.; Paolillo, L., "Phalloidin synthetic analogues: Structural requirements in the interaction with F-actin," *Chemistry A European Journal* **2001**, *7* (21), 4665-4673.
16. Wieland, T., "The toxic peptides from *Amanita* mushrooms," *International Journal of Peptide and Protein Research* **1983**, *22* (3), 257-276.
17. Wieland, T.; Deboben, A.; Faulstich, H., "Constituents of the green death cup. LVIII. Some dithiolanes derived from ketophalloidin usable in biochemical research," *Liebigs Annalen der Chemie* **1980**, (3), 416-424.
18. Wieland, T.; Hollosi, M.; Nassal, M., "Components of the green deathcap mushroom (*Amanita-phalloides*). LXI. δ -aminophalloin, a 7-analogue of phalloidin, and some biochemically useful derivatives, including fluorescent ones," *Liebigs Annalen der Chemie* **1983**, (9), 1533-1540.
19. Wulf, E.; Deboben, A.; Bautz, F. A.; Faulstich, H.; Wieland, T., "Fluorescent phallotoxin, a tool for the visualization of cellular actin," *Proceedings of the National Academy of Sciences of the United States of America* **1979**, *76* (9), 4498-4502.
20. Holmes, K. C.; Popp, D.; Gebhard, W.; Kabsch, W., "Atomic model of the actin filament," *Nature* **1990**, *347* (6288), 44-49.
21. Giganti, A.; Friederich, E., "The actin cytoskeleton as a therapeutic target: state of the art and future directions," *Prog Cell Cycle Res* **2003**, *5*, 511-525.
22. Fenteany, G.; Zhu, S., "Small-molecule inhibitors of actin dynamics and cell motility," *Current Topics in Medicinal Chemistry* **2003**, *3* (6), 593-616.
23. Hallen, H. E.; Luo, H.; Scott-Craig, J. S.; Walton, J. D., "Gene family encoding the major toxins of lethal *Amanita* mushrooms," *Proceedings of the National Academy of Sciences of the United States of America* **2007**, *104* (48), 19097-19101.
24. Luo, H.; Hallen-Adams, H. E.; Walton, J. D., "Processing of the phalloidin proprotein by prolyl oligopeptidase from the mushroom *Conocybe albipes*," *Journal of Biological Chemistry* **2009**, *284* (27), 18070-18077.
25. Munekata, E.; Faulstich, H.; Wieland, T., "Resynthesis of phalloidin and phallisin from the seco-compounds," *Angewandte Chemie-International Edition in English* **1977**, *16* (4), 267-268.
26. Boissonnas, R. A., "A new method of peptide synthesis," *Helvetica Chimica Acta* **1951**, *34* (3), 874-879.

27. Vaughan, J. R. Jr., "Acylalkylcarbonates as acylating agents for the synthesis of peptides," *Journal of the American Chemical Society* **1951**, 73 (7), 3547.
28. Wieland, T.; Bernhard, H., "Peptide synthesis. III. Use of anhydrides of N-acylated amino acids and derivatives of inorganic acids," *Annalen der Chemie-Justus Liebig* **1951**, 572 (1), 190-194.
29. Kahl, J. U.; Vlasov, G. P.; Seeliger, A.; Wieland, T., "Analogues of viroidin. Synthesis of four virotoxin-like F-actin binding heptapeptides with one less hydroxyl group in the dihydroxy-proline ring," *International Journal of Peptide and Protein Research* **1984**, 23 (5), 543-550.
30. Zanotti, G.; Kobayashi, N.; Munekata, E.; Zobeley, S.; Faulstich, H., "D-configuration of serine is crucial in maintaining the phalloidin-like conformation of viroisin," *Biochemistry* **1999**, 38 (33), 10723-10729.
31. Anderson, M. O.; Shelat, A. A.; Guy, R. K., "A solid-phase approach to the phallotoxins: Total synthesis of [Ala⁷]-phalloidin," *Journal of Organic Chemistry* **2005**, 70 (12), 4578-4584.
32. Zanotti, G.; Falcigno, L.; Saviano, M.; D'Auria, G.; Bruno, B. M.; Campanile, T.; Paolillo, L., "Solid state and solution conformation of [Ala⁷]-phalloidin: A synthetic phallotoxin analogue," *Chemistry A European Journal* **2001**, 7 (7), 1479-1485.
33. Schuresko, L. A.; Lokey, R. S., "A practical solid-phase synthesis of Glu⁷-phalloidin and entry into fluorescent F-actin-binding reagents," *Angewandte Chemie, International edition* **2007**, 46 (19), 3547-3549.
34. Taylor, C. M.; Jones, C. E.; Bopp, K., "The conversion of pentoses to 3,4-dihydroxyprolines," *Tetrahedron* **2005**, 61 (40), 9611-9617.
35. Edagwa, B. J.; Taylor, C. M., "Peptides containing γ , δ -dihydroxy-L-leucine," *Journal of Organic Chemistry* **2009**, 74 (11), 4132-4136.
36. Taylor, C. M.; Hardré, R.; Edwards, P. J. B., "The impact of pyrrolidine hydroxylation on the conformation of proline-containing peptides," *Journal of Organic Chemistry* **2005**, 70 (4), 1306-1315.
37. Mutter, M., "Macrocyclization equilibria of polypeptides," *Journal of the American Chemical Society* **1977**, 99 (25), 8307-8314.
38. Wieland, T.; Weiberg, O., "Amanita toxins. XIV. Synthesis of δ -hydroxyleucine hydrate," *Justus Liebigs Annalen der Chemie* **1957**, 607, 168-174.
39. Wieland, T.; Krantz, H., "The four isomeric γ -lactone of γ,δ -dihydroxyleucine," *Chemische Berichte* **1958**, 91, 2619-2626.
40. Sharpless, K. B.; Amberg, W.; Bennani, Y. L.; Crispino, G. A.; Hartung, J.; Jeong, K. S.; Kwong, H. L.; Morikawa, K.; Wang, Z. M.; Xu, D. Q.; Zhang, X. L., "The osmium-catalyzed asymmetric

dihydroxylation: A new ligand class and a process improvement," *Journal of Organic Chemistry* **1992**, 57 (10), 2768-2771.

41. Crispino, G. A.; Ho, P. T.; Sharpless, K. B., "Selective perhydroxylation of squalene: Taming the arithmetic demon," *Science* **1993**, 259 (5091), 64-66.

42. Turpin, J. A.; Weigel, L. O., "Enantioselective synthesis of the 6,8-dioxabicyclo [3.2.1] octane skeleton by asymmetric dihydroxylation," *Tetrahedron Letters* **1992**, 33 (44), 6563-6564.

43. Soderquist, J. A.; Rane, A. M., "(+)-Exo-brevicomine via an organometallic boulevard," *Tetrahedron Letters* **1993**, 34 (32), 5031-5034.

44. Tani, K.; Sato, Y.; Okamoto, S.; Sato, F., "Synthesis of optically active furfuryl alcohols and butenolides from *trans*-1-trimethylsilyl-3-alken-1-ynes via successive asymmetric dihydroxylation and hydromagnesiation reactions," *Tetrahedron Letters* **1993**, 34 (31), 4975-4978.

45. Jeong, K. S.; Sjo, P.; Sharpless, K. B., "Asymmetric dihydroxylation of enynes," *Tetrahedron Letters* **1992**, 33 (27), 3833-3836.

46. Crispino, G. A.; Jeong, K. S.; Kolb, H. C.; Wang, Z. M.; Xu, D. Q.; Sharpless, K. B., "Improved enantioselectivity in asymmetric dihydroxylations of terminal olefins using pyrimidine ligands" *Journal of Organic Chemistry* **1993**, 58 (15), 3785-3786.

47. Wang, Z. M.; Sharpless, K. B., "Asymmetric dihydroxylation of α -substituted styrene derivatives," *Synlett* **1993**, (8), 603-604.

48. Kolb, H. C.; Andersson, P. G.; Sharpless, K. B., "Toward an understanding of the high enantioselectivity in the osmium-catalyzed asymmetric dihydroxylation (AD). 1. Kinetics," *Journal of the American Chemical Society* **1994**, 116 (4), 1278-1291.

49. Kolb, H. C.; VanNieuwenhze, M. S.; Sharpless, K. B., "Catalytic asymmetric dihydroxylation," *Chemical Reviews* **1994**, 94 (8), 2483-2547.

50. Masamune, S.; Choy, W.; Petersen, J. S.; Sita, L. R., "Double asymmetric synthesis and new strategy for stereochemical control in organic synthesis," *Angewandte Chemie* **1985**, 24 (1), 1-30.

51. Cha, J. K.; Kim, N. S., "Acyclic stereocontrol induced by allylic alkoxy groups. Synthetic applications of stereoselective dihydroxylation in natural product synthesis," *Chemical Reviews* **1995**, 95 (6), 1761-1795.

52. Stork, G.; Kahn, M., "A highly stereoselective osmium tetroxide-catalyzed hydroxylation of γ -hydroxy α,β -unsaturated esters," *Tetrahedron Letters* **1983**, 24 (37), 3951-3954.

53. Reetz, M. T.; Strack, T. J.; Mutulis, F.; Goddard, R., "Asymmetric dihydroxylation of chiral γ -amino α,β -unsaturated esters: Turning the mismatched into the matched case via protective group tuning," *Tetrahedron Letters* **1996**, 37 (52), 9293-9296.

54. Hale, K. J.; Manaviazar, S.; Peak, S. A., "Anomalous enantioselectivity in the sharpless catalytic asymmetric dihydroxylation reaction of 1,1-disubstituted allyl alcohol derivatives," *Tetrahedron Letters* **1994**, 35 (3), 425-428.
55. Gardiner, J. M.; Bruce, S. E., "Unexpected diastereoselectivity in AD of an *L*-proline-derived 1,1-disubstituted alkene," *Tetrahedron Letters* **1998**, 39 (9), 1029-1032.
56. Wade, P. A.; Cole, D. T.; D'Ambrosio, S. G., "Diastereocontrol in the asymmetric dihydroxylation of chiral 3-alkenyl-4,5-dihydroisoxazoles," *Tetrahedron Letters* **1994**, 35 (1), 53-56.
57. Morikawa, K.; Sharpless, K. B., "Double diastereoselection in asymmetric dihydroxylation," *Tetrahedron Letters* **1993**, 34 (35), 5575-5578.
58. Albertson, N. F.; Archer, S., "The use of ethyl acetamidomalonate in the synthesis of amino acids. The preparation of *DL*-histidine, *DL*-phenylalanine and *DL*-leucine," *Journal of the American Chemical Society* **1945**, 67, 308-310.
59. Schmidt, U.; Schmidt, J., "The total synthesis of eponemycin," *Synthesis* **1994**, (3), 300-304.
60. Chenault, H. K.; Dahmer, J.; Whitesides, G. M., "Kinetic resolution of unnatural and rarely occurring amino acids: Enantioselective hydrolysis of *N*-acyl amino acids catalyzed by *acylase I*," *Journal of the American Chemical Society* **1989**, 111 (16), 6354-6364.
61. Dale, J. A.; Mosher, H. S., "Nuclear magnetic resonance nonequivalence of diastereomeric esters of α -substituted phenylacetic acids for determination of stereochemical purity," *Journal of the American Chemical Society* **1968**, 90 (14), 3732-3738.
62. Wang, Z. M.; Zhang, X. L.; Sharpless, K. B.; Sinha, S. C.; Sinhabagchi, A.; Keinan, E., "A general approach to γ lactones via osmium catalyzed asymmetric dihydroxylation. Synthesis of (-)- and (+)-muricatacin," *Tetrahedron Letters* **1992**, 33 (43), 6407-6410.
63. Braukmüller, S.; Brückner, R., "Enantioselective butenolide preparation for straightforward asymmetric syntheses of γ -lactones - Paraconic acids, avenaciolide, and hydroxylated eleutherol," *European Journal of Organic Chemistry* **2006**, (9), 2110-2118.
64. Wieland, T.; Georgi, V., "Components of immature *Amanita phalloides*. XXVIII. Synthesis of β -methyl- γ -hydroxyleucine and β -methyl- γ,δ -dihydroxyleucine two presumed amanitin precursors," *Justus Liebigs Annalen der Chemie* **1966**, 700, 133-148.
65. Goering, H. L.; Cristol, S. J.; Dittmer, K., "Unsaturated amino acids. II. Allylglycine, β -methallylglycine and crotylglycine," *Journal of the American Chemical Society* **1948**, 70 (10), 3310-3313.
66. Ersmark, K.; Feierberg, I.; Bjelic, S.; Hulten, J.; Samuelsson, B.; Aqvist, J.; Hallberg, A., "C-2-symmetric inhibitors of *Plasmodium falciparum* plasmepsin II: Synthesis and theoretical predictions," *Bioorganic & Medicinal Chemistry* **2003**, 11 (17), 3723-3733.

67. Sheradsky, T.; Knobler, Y.; Frankel, M., "Synthesis of peptides and of some polydipeptides of homoserine by an aminolactone method," *Journal of Organic Chemistry* **1961**, 26, 2710-2714.
68. Suzuki, M.; Owa, S.; Shirai, H.; Hanabusa, K., "Supramolecular hydrogel formed by glucoheptonamide of *L*-lysine: simple preparation and excellent hydrogelation ability," *Tetrahedron* **2007**, 63 (31), 7302-7308.
69. Bringmann, G.; Scharl, H.; Maksimenka, K.; Radacki, K.; Braunschweig, H.; Wich, P.; Schmuck, C., "Atropodistereoselective cleavage of configurationally unstable biaryl lactones with amino acid esters," *European Journal of Organic Chemistry* **2006**, (19), 4349-4361.
70. Hansen, K. K.; Grosch, B.; Greiveldinger-Poenaru, S.; Bartlett, P. A., "Synthesis and evaluation of macrocyclic transition state analogue inhibitors for α -chymotrypsin," *Journal of Organic Chemistry* **2003**, 68 (22), 8465-8470.
71. Kowalski, A.; Libiszowski, J.; Biela, T.; Cypryk, M.; Duda, A.; Penczek, S., "Kinetics and mechanism of cyclic esters polymerization initiated with tin(II)octoate. Polymerization of ϵ -caprolactone and *L,L*-lactide co-initiated with primary amines," *Macromolecules* **2005**, 38 (20), 8170-8176.
72. Pyring, D.; Lindberg, J.; Rosenquist, A.; Zuccarello, G.; Kvarnstrom, I.; Zhang, H.; Vrang, L.; Unge, T.; Classon, B.; Hallberg, A.; Samuelsson, B., "Design and synthesis of potent C2-symmetric diol-based HIV-1 protease inhibitors: Effects of fluoro substitution," *Journal of Medicinal Chemistry* **2001**, 44 (19), 3083-3091.
73. Rojo, I.; Martin, J. A.; Broughton, H.; Timm, D.; Erickson, J.; Yang, H. C.; McCarthy, J. R., "Macrocyclic peptidomimetic inhibitors of β -secretase (BACE): First X-ray structure of a macrocyclic peptidomimetic-BACE complex," *Bioorganic & Medicinal Chemistry Letters* **2006**, 16 (1), 191-195.
74. Ciapetti, P.; Taddei, M.; Ulivi, P., "CrCl₂ mediated allylation of N-protected α -amino aldehydes. A versatile synthesis of polypeptides containing an hydroxyethylene isostere," *Tetrahedron Letters* **1994**, 35 (19), 3183-3186.
75. Marshall, J. A.; Luke, G. P., "Stereoselective total synthesis of bengamide E from glyceraldehyde acetonide and a nonracemic γ -alkoxy allylic stannane," *Journal of Organic Chemistry* **1993**, 58 (23), 6229-6234.
76. Hutinec, A.; Ziogas, A.; El-Mobayed, M.; Rieker, A., "Spirolactones of tyrosine: synthesis and reaction with nucleophiles," *Journal of the Chemical Society, Perkin Transactions 1* **1998**, (14), 2201-2208.
77. Ben-Ishai, D.; Bernstein, Z., "Ureidoalkylations and oxyalkylation of aromatic compounds with glyoxylic acid derivatives," *Tetrahedron* **1977**, 33 (24), 3261-3264.
78. Faulstich, H.; Trischmann, H., "Peptide syntheses. XLVI. Synthesis of peptides of γ -hydroxyleucine," *Justus Liebigs Annalen der Chemie* **1970**, 741, 55-63.

79. Michl, K., "Facile racemization of N-acylated α -amino- γ -lactones," *Liebigs Annalen Der Chemie* **1981**, (1), 33-39.
80. Lipshutz, B. H.; Buzard, D. J.; Olsson, C.; Noson, K., "A modular route to nonracemic cyclo-NOBINs. Preparation of the parent ligand for homo- and heterogeneous catalysis," *Tetrahedron* **2004**, 60 (20), 4443-4449.
81. Benedetti, F.; Maman, P.; Norbedo, S., "New synthesis of 5-amino-4-hydroxy-2,6-dimethylheptanoic acid, a hydroxyethylene isostere of the Val-Ala dipeptide," *Tetrahedron Letters* **2000**, 41 (51), 10075-10078.
82. Corey, E. J.; Hopkins, P. B., "Diisopropylsilyl ditriflate and di-*tert*-butylsilyl ditriflate: New reagents for the protection of diols," *Tetrahedron Letters* **1982**, 23 (47), 4871-4874.
83. Schmidt, U.; Schmidt, J., "The synthesis of eponemycin," *Journal of the Chemical Society, Chemical Communications* **1992**, (7), 529-530.
84. Takase, S.; Itoh, Y.; Uchida, I.; Tanaka, H.; Aoki, H., "Total synthesis of amauromine," *Tetrahedron Letters* **1985**, 26 (7), 847-850.
85. Takase, S.; Itoh, Y.; Uchida, I.; Tanaka, H.; Aoki, H., "Total synthesis of amauromine," *Tetrahedron* **1986**, 42 (21), 5887-5894.
86. Dillard, R. D.; Bach, N. J.; Draheim, S. E.; Berry, D. R.; Carlson, D. G.; Chirgadze, N. Y.; Clawson, D. K.; Hartley, L. W.; Johnson, L. M.; Jones, N. D.; McKinney, E. R.; Mihelich, E. D.; Olkowski, J. L.; Schevitz, R. W.; Smith, A. C.; Snyder, D. W.; Sommers, C. D.; Wery, J. P., "Indole inhibitors of human nonpancreatic secretory phospholipase A₂. 1. Indole-3-acetamides," *Journal of Medicinal Chemistry* **1996**, 39 (26), 5119-5136.
87. Ponnusamy, E.; Fotadar, U.; Spisni, A.; Fiat, D., "A novel method for the rapid, nonaqueous *tert*-butoxycarbonylation of some ¹⁷O-labeled amino acids and ¹⁷O-NMR parameters of the products," *Synthesis* **1986**, (1), 48-49.
88. Carpino, L. A., "1-Hydroxy-7-azabenzotriazole. An efficient peptide coupling additive," *Journal of the American Chemical Society* **1993**, 115 (10), 4397-4398.
89. Carpino, L. A.; El-Faham, A., "Effect of tertiary bases on *O*-benzotriazolyluronium salt-induced peptide segment coupling," *Journal of Organic Chemistry* **1994**, 59 (4), 695-698.
90. Carpino, L. A.; Han, G. Y., "9-Fluorenylmethoxycarbonyl function, a new base-sensitive amino-protecting group," *Journal of the American Chemical Society* **1970**, 92 (19), 5748-5749.
91. Carpino, L. A.; Han, G. Y., "9-Fluorenylmethoxycarbonyl amino protecting group," *Journal of Organic Chemistry* **1972**, 37 (22), 3404-3409.

92. Carpino, L. A., "The 9-fluorenylmethoxycarbonyl family of base-sensitive amino-protecting groups," *Accounts of Chemical Research* **1987**, 20 (11), 401-407.
93. More, O'; Roy, A.; Sale, S., " β -Elimination of 9-fluorenylmethanol in aqueous solution: An E1cB mechanism," *Journal of the Chemical Society B: Physical Organic* **1970**, (2), 260-268.
94. More, O'; Roy, A., " β -Elimination of 9-fluorenylmethanol in solutions of methanol and tertiary-butyl alcohol," *Journal of the Chemical Society B: Physical Organic* **1970**, (2), 268-274.
95. More, O'; Roy, A., "Relationships between E2 and E1cB mechanism of β -elimination," *Journal of the Chemical Society B: Physical Organic* **1970**, (2), 274-277.
96. Carpino, L. A.; Sadat-Aalae, D.; Beyermann, M., "Tris(2-aminoethyl)amine as a substitute for 4-(aminomethyl)piperidine in the Fmoc/polyamine approach to rapid peptide synthesis," *Journal of Organic Chemistry* **1990**, 55 (5), 1673-1675.
97. Chakraborty, T. K.; Srinivasu, P.; Rao, R. V.; Kumar, S. K.; Kunwar, A. C., "Conformational studies of peptides containing *cis*-3-hydroxy-*D*-proline," *Journal of Organic Chemistry* **2004**, 69 (21), 7399-7402.
98. Gomez-Vidal, J. A.; Silverman, R. B., "Short, highly efficient syntheses of protected 3-azido- and 4-azidoproline and their precursors," *Organic Letters* **2001**, 3 (16), 2481-2484.
99. Martin, S. F.; Dodge, J. A., "Efficacious modification of the Mitsunobu reaction for inversions of sterically hindered secondary alcohols," *Tetrahedron Letters* **1991**, 32 (26), 3017-3020.
100. Dodge, J. A.; Trujillo, J. I.; Presnell, M., "Effect of the acidic component on the Mitsunobu inversion of a sterically hindered alcohol," *Journal of Organic Chemistry* **1994**, 59 (1), 234-236.
101. Gomez-Vidal, J. A.; Forrester, M. T.; Silverman, R. B., "Mild and selective sodium azide mediated cleavage of *p*-nitrobenzoic esters," *Organic Letters* **2001**, 3 (16), 2477-2479.
102. Garcia, A. L. L.; Correia, C. R. D., "Synthesis of dihydroxylated prolines and iminocyclitols from five-membered endocyclic enecarbamates. Total synthesis of the potent glycosidase inhibitor (2*R*, 3*R*, 4*R*, 5*R*)-2,5-dihydroxymethyl-3,4-dihydroxypyrrolidine (DMDP)," *Tetrahedron Letters* **2003**, 44 (8), 1553-1557.
103. Kim, J. H.; Long, M. J. C.; Kim, J. Y.; Park, K. H., "Stereodivergent and regioselective synthesis of 3,4-*cis*- and 3,4-*trans*-pyrrolidinediols from α -amino acids," *Organic Letters* **2004**, 6 (13), 2273-2276.
104. Angle, S. R.; Belanger, D. S., "Stereoselective synthesis of 3-hydroxyproline benzyl esters from *N*-protected β -aminoaldehydes and benzyl diazoacetate," *Journal of Organic Chemistry* **2004**, 69 (13), 4361-4368.

105. Kahl, J. U.; Wieland, T., "Synthesis of two naturally occurring diastereomeric dihydroxyprolines: 2,3-trans-3,4-trans-3,4-dihydroxy-l-proline and 2,3-cis-3,4-trans-3,4-dihydroxy-l-proline," *Liebigs Annalen der Chemie* **1981**, (8), 1445-1450.
106. Weir, C. A.; Taylor, C. M., "Synthesis of a protected 3,4-dihydroxyproline from a pentose sugar," *Organic Letters* **1999**, 1 (5), 787-789.
107. Taylor, C. M.; Barker, W. D.; Weir, C. A.; Park, J. H., "Toward a general strategy for the synthesis of 3,4-dihydroxyprolines from pentose sugars," *Journal of Organic Chemistry* **2002**, 67 (13), 4466-4474.
108. Corey, E. J.; Gras, J. L.; Ulrich, P., "New general method for protection of the hydroxyl function," *Tetrahedron Letters* **1976**, (11), 809-812.
109. Anderson, G. W.; Zimmerman, J. E.; Callahan, F. M., "The use of esters of *N*-hydroxysuccinimide in peptide synthesis," *Journal of the American Chemical Society* **1964**, 86 (9), 1839-1842.
110. Schlessinger, R. H.; Nugent, R. A., "Total synthesis of racemic verrucarol," *Journal of the American Chemical Society* **1982**, 104 (4), 1116-1118.
111. Martinez, J.; Tolle, J. C.; Bodanszky, M., "Side reactions in peptide-synthesis. 12. Hydrogenolysis of the 9-fluorenylmethyloxycarbonyl group," *Journal of Organic Chemistry* **1979**, 44 (20), 3596-3598.
112. Mandal, P. K.; McMurray, J. S., "Pd-C-induced catalytic transfer hydrogenation with triethylsilane," *Journal of Organic Chemistry* **2007**, 72 (17), 6599-6601.
113. Mirza-Aghayan, M.; Boukherroub, R.; Bolourtchian, M., "A mild and efficient palladium-triethylsilane system for reduction of olefins and carbon-carbon double bond isomerization," *Applied Organometallic Chemistry* **2006**, 20 (3), 214-219.
114. Han, S. Y.; Kim, Y. A., "Recent development of peptide coupling reagents in organic synthesis," *Tetrahedron* **2004**, 60 (11), 2447-2467.
115. Poulos, C.; Ashton, C. P.; Green, J.; Ogunjobi, O. M.; Ramage, R.; Tseggenidis, T., "Application of carboxylic-phospholanic mixed anhydrides to fragment coupling in peptide-synthesis," *International Journal of Peptide and Protein Research* **1992**, 40 (3-4), 315-321.
116. Wipf, P.; Heimgartner, H., "Synthesis of peptides containing α,α -disubstituted α -amino-acids by the azirine/oxazolone method: The (12-20)-nonapeptide of the ionophore alamethicin," *Helvetica Chimica Acta* **1990**, 73 (1), 13-24.
117. Humphrey, J. M.; Chamberlin, A. R., "Chemical synthesis of natural product peptides: Coupling methods for the incorporation of noncoded amino acids into peptides," *Chemical Reviews* **1997**, 97 (6), 2243-2266.

118. Carpino, L. A.; El-Faham, A.; Albericio, F., "Efficiency in peptide coupling: 1-Hydroxy-7-azabenzotriazole vs 3,4-dihydro-3-hydroxy-4-oxo-1,2,3-benzotriazine," *Journal of Organic Chemistry* **1995**, 60 (11), 3561-3564.
119. Frerot, E.; Coste, J.; Pantaloni, A.; Dufour, M. N.; Jouin, P., "PyBOP and PyBrOP: Two reagents for the difficult coupling of the α,α -dialkyl amino acid, Aib," *Tetrahedron* **1991**, 47 (2), 259-270.
120. Kessler, H.; Kutscher, B., "Synthesis and NMR investigation of cyclic pentapeptide analogs of thymopentin," *Tetrahedron Letters* **1985**, 26 (2), 177-180.
121. Chipens, G. I.; Mutulis, F. K.; Myshlyakova, N. V.; Misina, I. P.; Vitolina, R. O.; Klusha, V. J.; Katayev, B. S., "Cyclic analogues of bradykinin. IV. Structure-function relationships in the series of bradykinin cycloanalogues," *International Journal of Peptide and Protein Research* **1985**, 26 (5), 460-468.
122. Spear, K. L.; Brown, M. S.; Reinhard, E. J.; McMahon, E. G.; Olins, G. M.; Palomo, M. A.; Patton, D. R., "Conformational restriction of angiotensin II: Cyclic analogs having high potency," *Journal of Medicinal Chemistry* **1990**, 33 (7), 1935-1940.
123. Charpentier, B.; Dor, A.; Roy, P.; England, P.; Pham, H.; Durieux, C.; Roques, B. P., "Synthesis and binding affinities of cyclic and related linear analogs of CCK8 selective for central receptors," *Journal of Medicinal Chemistry* **1989**, 32 (6), 1184-1190.
124. Spanevello, R. A.; Hirschmann, R.; Raynor, K.; Reisine, T.; Nutt, R. F., "Synthesis of novel, highly potent cyclic hexapeptide analogs of somatostatin. Potential application of orthogonal protection for affinity chromatography," *Tetrahedron Letters* **1991**, 32 (36), 4675-4678.
125. Tyndall, J. D. A.; Nall, T.; Fairlie, D. P., "Proteases universally recognize beta strands in their active sites," *Chemical Reviews* **2005**, 105 (3), 973-999.
126. Vale, W.; Brazeau, P.; Grant, G.; Nussey, A.; Burgus, R.; Rivier, J.; Ling, N.; Guillemi, R., "Preliminary observations on the mechanism of action mode of somatostatin, a hypothalamic factor inhibiting the secretion of growth hormone," *Comptes Rendus Hebdomadaires Des Seances De L Academie Des Sciences Serie D* **1972**, 275 (25), 2913-2916.
127. Davies, J. S., "The cyclization of peptides and depsipeptides," *Journal of Peptide Science* **2003**, 9 (8), 471-501.
128. Li, P.; Roller, P. P.; Xu, J., "Current synthetic approaches to peptide and peptidomimetic cyclization," *Current Organic Chemistry* **2002**, 6 (5), 411-440.
129. Wipf, P., "Synthetic studies of biologically active marine cyclopeptides," *Chemical Reviews* **1995**, 95 (6), 2115-2134.

130. Anteunis, M. J. O.; Sharma, N. K., "BOP-Cl mediated cyclization of a linear precursor of virginiamycin S. Contra indication for using HOBt as racemization suppressor," *Bulletin Des Societes Chimiques Belges* **1988**, 97 (4), 281-292.
131. Wenger, R. M., "Synthesis of cyclosporine. Total syntheses of cyclosporin A and cyclosporin H, two fungal metabolites isolated from the species *Tolypocladium inflatum gams*," *Helvetica Chimica Acta* **1984**, 67 (2), 502-525.
132. Cavelier-Frontin, F.; Pepe, G.; Verducci, J.; Siri, D.; Jacquier, R., "Prediction of the best linear precursor in the synthesis of cyclotetrapeptides by molecular mechanic calculations," *Journal of the American Chemical Society* **1992**, 114 (23), 8885-8890.
133. Ehrlich, A.; Heyne, H. U.; Winter, R.; Beyermann, M.; Haber, H.; Carpino, L. A.; Bienert, M., "Cyclization of all-*L*-pentapeptides by means of 1-hydroxy-7-azabenzotriazole-derived uronium and phosphonium reagents," *Journal of Organic Chemistry* **1996**, 61 (25), 8831-8838.
134. Sasaki, K.; Crich, D., "Cyclic peptide synthesis with thioacids," *Organic Letters* **2010**, 12 (14), 3254-3257.
135. Aimetti, A. A.; Shoemaker, R. K.; Lin, C. C.; Anseth, K. S., "On-resin peptide macrocyclization using thiol-ene click chemistry," *Chemical Communications* **2010**, 46 (23), 4061-4063.
136. Liehr, S.; Barbosa, J.; Smith, A. B. III.; Cooperman, B. S., "Synthesis and biological activity of cyclic peptide inhibitors of ribonucleotide reductase," *Organic Letters* **1999**, 1 (8), 1201-1204.
137. Zhang, L.; Tam, J. P., "Synthesis and application of unprotected cyclic peptides as building blocks for peptide dendrimers," *Journal of the American Chemical Society* **1997**, 119 (10), 2363-2370.
138. Izumiya, N.; Kato, T.; Waki, M., "Synthesis of biologically active cyclic peptides," *Biopolymers* **1981**, 20 (9), 1785-1791.
139. Hale, K. J.; Cai, J.; Williams, G., "Total synthesis of 4-epi-A83586C. Epimerization in a macrolactamization mediated by BOP and DMAP," *Synlett* **1998**, (2), 149-152.
140. Shioiri, T.; Ninomiya, K.; Yamada, S., "Diphenylphosphoryl azide. A new convenient reagent for a modified Curtius reaction and for peptide synthesis," *Journal of the American Chemical Society* **1972**, 94 (17), 6203-6205.
141. Schmidt, R.; Neubert, K., "Cyclization studies with tetra- and pentapeptide sequences corresponding to β -casomorphins," *International Journal of Peptide and Protein Research* **1991**, 37 (6), 502-507.
142. Heavner, G. A.; Audhya, T.; Doyle, D.; Tjoeng, F. S.; Goldstein, G., "Biologically active conformations of thymopentin. Studies with conformationally restricted analogs," *International Journal of Peptide and Protein Research* **1991**, 37 (3), 198-209.

143. Boger, D. L.; Miyazaki, S.; Kim, S. H.; Wu, J. H.; Castle, S. L.; Loiseleur, O.; Jin, Q., "Total synthesis of the vancomycin aglycon," *Journal of the American Chemical Society* **1999**, *121* (43), 10004-10011.
144. Cao, B.; Park, H.; Joullie, M. M., "Total synthesis of ustiloxin D," *Journal of the American Chemical Society* **2002**, *124* (4), 520-521.
145. Knorr, R.; Trzeciak, A.; Bannwarth, W.; Gillesen, D., "New coupling reagents in peptide chemistry," *Tetrahedron Letters* **1989**, *30* (15), 1927-1930.
146. Castro, B.; Dormoy, J. R.; Evin, G.; Selve, C., "Peptide coupling reagents. IV. *N*-[oxytris(dimethylamino)phosphonium] benzotriazole hexafluorophosphate (BOP)," *Tetrahedron Letters* **1975**, (14), 1219-1222.
147. Felix, A. M.; Heimer, E. P.; Wang, C. T.; Lambros, T. J.; Fournier, A.; Mowles, T. F.; Maines, S.; Campbell, R. M.; Wegrzynski, B. B.; Toome, V.; Fry, D.; Madison, V. S., "Synthesis, biological activity and conformational analysis of cyclic GRF analogs," *International Journal of Peptide and Protein Research* **1988**, *32* (6), 441-454.
148. Benoiton, N. L.; Lee, Y. C.; Steinaur, R.; Chen, F. M. F., "Studies on sensitivity to racemization of activated residues in couplings of *N*-benzyloxycarbonyldipeptides," *International Journal of Peptide and Protein Research* **1992**, *40* (6), 559-566.
149. Carpino, L. A.; Elfaham, A.; Albericio, F., "Racemization studies during solid-phase peptide synthesis using azabenzotriazole-based coupling reagents," *Tetrahedron Letters* **1994**, *35* (15), 2279-2282.
150. Schmidt, U.; Langner, J., "Cyclotetrapeptides and cyclopentapeptides: Occurrence and synthesis," *Journal of Peptide Research* **1997**, *49* (1), 67-73.
151. Kessler, H.; Haase, B., "Cyclic hexapeptides derived from the human thymopoietin III," *International Journal of Peptide and Protein Research* **1992**, *39* (1), 36-40.
152. Tamaki, M.; Akabori, S.; Muramatsu, I., "Biomimetic synthesis of gramicidin S. Direct formation of the antibiotic from pentapeptide active esters having no protecting group on the side chain of the Orn residue," *Journal of the American Chemical Society* **1993**, *115* (23), 10492-10496.
153. Jacquier, R.; Lazaro, R.; Raniriseheno, H.; Viallefont, P., "Synthesis of HC toxin and related cyclopeptides containing the (*L*-Ala-*D*-Ala-*L*-Ada-*D*-Pro) sequence," *International Journal of Peptide and Protein Research* **1987**, *30* (1), 22-32.
154. Ehrlich, A.; Rothmund, S.; Brudel, M.; Beyermann, M.; Carpino, L. A.; Bienert, M., "Synthesis of cyclic peptides via efficient new coupling reagents," *Tetrahedron Letters* **1993**, *34* (30), 4781-4784.
155. Tang, Y. C.; Tian, G. L.; Ye, Y. H., "Progress in the study on synthetic method of cyclopeptide," *Chemical Journal of Chinese Universities-Chinese* **2000**, *21* (7), 1056-1063.

156. White, C. J.; Yudin, A. K., "Contemporary strategies for peptide macrocyclization," *Nature Chemistry* **2011**, 3 (7), 509-524.
157. Dale, J., "Conformational aspects of many-membered rings," *Angewandte Chemie-International Edition* **1966**, 5 (12), 1000-1021.
158. Kessler, H.; Kutscher, B., "Synthesis of cyclic pentapeptide analogs of thymopoietin. Cyclization with carbodiimide and 4-(dimethylamino)pyridine," *Liebigs Annalen der Chemie* **1986**, (5), 869-892.
159. Kessler, H.; Kutscher, B., "Peptide conformations. 40. Cyclic hexapeptide analogs of thymopoietin. Synthesis and conformational analysis," *Liebigs Annalen der Chemie* **1986**, (5), 914-931.
160. Hoffmann, R. W., "Flexible molecules with definite shape conformation design," *Angewandte Chemie International Ed.* **1992**, 104 (9), 1147-1157.
161. Blankenstein, J.; Zhu, J. P., "Conformation-directed macrocyclization reactions," *European Journal of Organic Chemistry* **2005**, (10), 1949-1964.
162. Daidone, I.; Neuweiler, H.; Doose, S.; Sauer, M.; Smith, J. C., "Hydrogen-bond driven loop-closure kinetics in unfolded polypeptide chains," *PLOS Computational Biology* **2010**, 6 (1).
163. Smith, J. A.; Pease, L. G., "Reverse turns in peptides and proteins," *Critical Reviews in Biochemistry* **1980**, 8 (4), 315-399.
164. Chatterjee, J.; Mierke, D.; Kessler, H., "N-methylated cyclic pentaalanine peptides as template structures," *Journal of the American Chemical Society* **2006**, 128 (47), 15164-15172.
165. Chatterjee, J.; Mierke, D. F.; Kessler, H., "Conformational preference and potential templates of N-methylated cyclic pentaalanine peptides," *Chemistry a European Journal* **2008**, 14 (5), 1508-1517.
166. Titlestad, K., "Cyclic tetra- and octapeptides of sarcosine in combination with alanine or glycine. Syntheses and conformation," *Acta Chemica Scandinavica Series B-Organic Chemistry and Biochemistry* **1977**, 31 (8), 641-661.
167. Dale, J.; Titlesta, K., "Cyclic oligopeptides of sarcosine (N-methylglycine)," *Journal of the Chemical Society D-Chemical Communications* **1969**, (12), 656-659.
168. Takeuchi, Y.; Marshall, G. R., "Conformational analysis of reverse-turn constraints by N-methylation and N-hydroxylation of amide bonds in peptides and non-peptide mimetics," *Journal of the American Chemical Society* **1998**, 120 (22), 5363-5372.
169. Fairweather, K. A.; Sayyadi, N.; Luck, I. J.; Clegg, J. K.; Jolliffe, K. A., "Synthesis of all-L cyclic tetrapeptides using pseudoprolines as removable turn inducers," *Organic Letters* **2010**, 12 (14), 3136-3139.

170. Dumy, P.; Keller, M.; Ryan, D. E.; Rohwedder, B.; Wohr, T.; Mutter, M., "Pseudo-prolines as a molecular hinge: Reversible induction of *cis* amide bonds into peptide backbones," *Journal of the American Chemical Society* **1997**, *119* (5), 918-925.
171. Brady, S. F.; Varga, S. L.; Freidinger, R. M.; Schwenk, D. A.; Mendlowski, M.; Holly, F. W.; Veber, D. F., "Practical synthesis of cyclic peptides, with an example of dependence of cyclization yield upon linear sequence," *Journal of Organic Chemistry* **1979**, *44* (18), 3101-3105.
172. Amore, A.; van Heerbeek, R.; Zeep, N.; van Esch, J.; Reek, J. N. H.; Hiemstra, H.; van Maarseveen, J. H., "Carbosilane dendrimeric carbodiimides: Site isolation as a lactamization tool," *Journal of Organic Chemistry* **2006**, *71* (5), 1851-1860.
173. Abdel-Magid, A. F.; Cohen, J. H.; Maryanoff, C. A.; Shah, R. D.; Villani, F. J.; Zhang, F., "Hydrolysis of polypeptide esters with tetrabutylammonium hydroxide," *Tetrahedron Letters* **1998**, *39* (21), 3391-3394.
174. Ohshita, J.; Taketsugu, R.; Nakahara, Y.; Kunai, A., "Convenient synthesis of alkoxyhalosilanes from hydrosilanes," *Journal of Organometallic Chemistry* **2004**, *689* (20), 3258-3264.
175. Wipf, P.; Uto, Y., "Total synthesis and revision of stereochemistry of the marine metabolite trunkamide A," *Journal of Organic Chemistry* **2000**, *65* (4), 1037-1049.
176. Inami, K.; Kurome, T.; Takesako, K.; Kato, I.; Shiba, T., "Site-specific ring opening of depsipeptide aureobasidin A in hydrogen fluoride," *Tetrahedron Letters* **1996**, *37* (12), 2043-2044.
177. Malesevic, M.; Strijowski, U.; Bachle, D.; Sewald, N., "An improved method for the solution cyclization of peptides under pseudo-high dilution conditions," *Journal of Biotechnology* **2004**, *112* (1-2), 73-77.
178. Kaburagi, Y.; Kishi, Y., "Operationally simple and efficient workup procedure for TBAF-mediated desilylation: Application to halichondrin synthesis," *Organic Letters* **2007**, *9* (4), 723-726.
179. Kobayashi, N.; Endo, S.; Kobayashi, H.; Faulstich, H.; Wieland, T.; Munekata, E., "Comparative study on the conformation of phalloidin, viroisin, and related derivatives in aqueous solution," *European Journal of Biochemistry* **1995**, *232* (3), 726-736.
180. Bhaskaran, R.; Yu, C., "NMR spectra and restrained molecular dynamics of the mushroom toxin viroisin," *International Journal of Peptide and Protein Research* **1994**, *43* (4), 393-401.
181. Karplus, M., "Contact electron-spin coupling of nuclear magnetic moments," *Journal of Chemical Physics* **1959**, *30* (1), 11-15.
182. Bystrov, V. F.; Ivanov, V. T.; Portnova, S. L.; Balashova, T. A.; Ovchinnikov, Y. A., "Refinement of the angular dependence of peptide vicinal NH-CαH coupling constant," *Tetrahedron* **1973**, *29* (6), 873-877.

183. Ramachandran, G. N.; Chandrasekaran, R., "Variation of NH-C α H coupling constant with dihedral angle in the NMR spectra of peptides," *Biopolymers* **1971**, 10 (11), 2113-2131.
184. Aubry, A.; Giessner-Prettre, C.; Cung, M. T.; Marraud, M.; Neel, J., "Geometric characteristics of H α -C α -NH sequence of 3-isoquinuclidone examined in different physical states. Effect on the vicinal coupling constant $J_{\text{H}\alpha\text{H}}$," *Biopolymers* **1974**, 13 (3), 523-536.
185. De Marco, A.; Llinas, M.; Wuethrich, K., "Analysis of the proton NMR spectra of ferrichrome peptides. I. The non-amide protons," *Biopolymers* **1978**, 17 (3), 617-636.
186. Barfield, M.; Gearhart, H. L., "Conformational dependence of vicinal hydrogen-nitrogen-carbon-hydrogen coupling constants in peptides," *Journal of the American Chemical Society* **1973**, 95 (2), 641-643.
187. Gierasch, L. M.; Rockwell, A. L.; Thompson, K. F.; Briggs, M. S., "Conformation- function relationships in hydrophobic peptides: Interior turns and signal sequences," *Biopolymers* **1985**, 24 (1), 117-135.
188. Ramachandran, G. N.; Venkatachalam, C. M., "Stereochemical criteria for polypeptides and proteins. IV. Standard dimensions for the *cis*-peptide unit and conformation of *cis*-polypeptides," *Biopolymers* **1968**, 6 (9), 1255-1262.
189. Benedetti, E.; Palumbo, M.; Bonora, G. M.; Toniolo, C., "On the oxy analogues to the 4 \rightarrow 1 intramolecularly hydrogen-bonded peptide conformations," *Macromolecules* **1976**, 9 (3), 417-420.
190. Richardson, J. S., "The anatomy and taxonomy of protein structure," *Advances in Protein Chem* **1981**, 34, 167-339.
191. Bystrov, V. F., "Spin-spin coupling and the conformational states of peptide systems," *Progress in Nuclear Magnetic Resonance Spectroscopy* **1976**, (10) Pt. 2, 41-82.
192. MacArthur, M. W.; Thornton, J. M., "Influence of proline residues on protein conformation," *Journal of Molecular Biology* **1991**, 218 (2), 397-412.
193. Beausoleil, E.; Sharma, R.; Michnick, S. W.; Lubell, W. D., "Alkyl 3-position substituents retard the isomerization of prolyl and hydroxyprolyl amides in water," *Journal of Organic Chemistry* **1998**, 63 (19), 6572-6578.
194. Stonehouse, J.; Adell, P.; Keeler, J.; Shaka, A. J., "Ultrahigh-quality NOE spectra," *Journal of the American Chemical Society* **1994**, 116 (13), 6037-6038.
195. Bretscher, L. E.; Jenkins, C. L.; Taylor, K. M.; DeRider, M. L.; Raines, R. T., "Conformational stability of collagen relies on a stereoelectronic effect," *Journal of the American Chemical Society* **2001**, 123 (4), 777-778.

196. Eberhardt, E. S.; Panisik, N.; Raines, R. T., "Inductive effects on the energetics of prolyl peptide bond isomerization: Implications for collagen folding and stability," *Journal of the American Chemical Society* **1996**, *118* (49), 12261-12266.
197. DeRider, M. L.; Wilkens, S. J.; Waddell, M. J.; Bretscher, L. E.; Weinhold, F.; Raines, R. T.; Markley, J. L., "Collagen stability: Insights from NMR spectroscopic and hybrid density functional computational investigations of the effect of electronegative substituents on prolyl ring conformations," *Journal of the American Chemical Society* **2002**, *124* (11), 2497-2505.
198. Renner, C.; Alefelder, S.; Bae, J. H.; Budisa, N.; Huber, R.; Moroder, L., "Fluoroproline as tools for protein design and engineering," *Angewandte Chemie International Edition* **2001**, *40* (5), 923-925.
199. Cadamuro, S. A.; Reichold, R.; Kusebauch, U.; Musiol, H. J.; Renner, C.; Tavan, P.; Moroder, L., "Conformational properties of 4-mercaptoproline and related derivatives," *Angewandte Chemie International Edition* **2008**, *47* (11), 2143-2146.
200. Sonntag, L. S.; Schweizer, S.; Ochsenfeld, C.; Wennemers, H., "The "azido gauche effect"-implications for the conformation of azidoproline," *Journal of the American Chemical Society* **2006**, *128* (45), 14697-14703.
201. Vitagliano, L.; Berisio, R.; Mastrangelo, A.; Mazzarella, L.; Zagari, A., "Preferred proline puckerings in *cis* and *trans* peptide groups: Implications for collagen stability," *Protein Science* **2001**, *10* (12), 2627-2632.
202. Cai, M. G.; Huang, Y.; Liu, J.; Krishnamoorthi, R., "Solution conformations of proline rings in proteins studied by NMR spectroscopy," *Journal of Biomolecular NMR* **1995**, *6* (2), 123-128.

APPENDIX: LETTERS OF PERMISSION



RightsLink®

Home

Account
Info

Help



ACS Publications

Title: Peptides Containing
γ,δ-Dihydroxy-L-leucine
Author: Benson J. Edagwa et al.
Publication: The Journal of Organic
Chemistry
Publisher: American Chemical Society
Date: Jun 1, 2009
Copyright © 2009, American Chemical Society

Logged in as:
Benson Edagwa
Account #:
3000400907

LOGOUT

PERMISSION/LICENSE IS GRANTED FOR YOUR ORDER AT NO CHARGE

This type of permission/license, instead of the standard Terms & Conditions, is sent to you because no fee is being charged for your order. Please note the following:

- Permission is granted for your request in both print and electronic formats.
- If figures and/or tables were requested, they may be adapted or used in part.
- Please print this page for your records and send a copy of it to your publisher/graduate school.
- Appropriate credit for the requested material should be given as follows: "Reprinted (adapted) with permission from (COMPLETE REFERENCE CITATION). Copyright (YEAR) American Chemical Society." Insert appropriate information in place of the capitalized words.
- One-time permission is granted only for the use specified in your request. No additional uses are granted (such as derivative works or other editions). For any other uses, please submit a new request.

BACK

CLOSE WINDOW

Copyright © 2012 Copyright Clearance Center, Inc. All Rights Reserved. [Privacy statement](#).
Comments? We would like to hear from you. E-mail us at customer@copyright.com



RightsLink

Home

Account
Info

Help



ACS Publications Title:

High quality High impact

Virotoxins: actin-binding cyclic
peptides of Amanita virosa
mushrooms

Logged in as:

Benson Edagwa

Account #:

3000400907

Author: Heinz Faulstich et al.

Publication: Biochemistry

Publisher: American Chemical Society

Date: Jul 1, 1980

Copyright © 1980, American Chemical Society

Logout

No charge permission and attribution

Permission for this particular request is granted for print and electronic formats at no charge. Figures and tables may be modified. Appropriate credit should be given. Please print this page for your records and provide a copy to your publisher. Requests for up to 4 figures require only this record. Five or more figures will generate a printout of additional terms and conditions. Appropriate credit should read: "Reprinted with permission from {COMPLETE REFERENCE CITATION}. Copyright {YEAR} American Chemical Society." Insert appropriate information in place of the capitalized words.

This permission does not apply to images that are credited to publications other than ACS journals. For images credited to non-ACS journal publications, you will need to obtain permission from the journal referenced in the Table/Figure/Micrograph legend or credit line before making any use of the image(s) or table(s).

BACK

CLOSE WINDOW

Copyright © 2011 Copyright Clearance Center, Inc. All Rights Reserved. [Privacy statement](#).
Comments? We would like to hear from you. E-mail us at customercare@copyright.com

**JOHN WILEY AND SONS LICENSE
TERMS AND CONDITIONS**

Aug 13, 2011

This is a License Agreement between Benson Edagwa ("You") and John Wiley and Sons ("John Wiley and Sons") provided by Copyright Clearance Center ("CCC"). The license consists of your order details, the terms and conditions provided by John Wiley and Sons, and the payment terms and conditions.

All payments must be made in full to CCC. For payment instructions, please see information listed at the bottom of this form.

License Number	2644470328175
License date	Apr 08, 2011
Licensed content publisher	John Wiley and Sons
Licensed content publication	Chemical Biology & Drug Design
Licensed content title	NMR spectra and restrained molecular dynamics of the mushroom toxin viroisin
Licensed content author	R. BHASKARAN, CHIN YU
Licensed content date	Apr 1, 1994
Start page	393
End page	401
Type of use	Dissertation/Thesis
Requestor type	University/Academic
Format	Print and electronic
Portion	Figure/table
Number of figures/tables	2
Number of extracts	
Original Wiley figure/table number(s)	figure2 and figure 5
Will you be translating?	No
Order reference number	
Total	0.00 USD

Terms and Conditions

TERMS AND CONDITIONS

This copyrighted material is owned by or exclusively licensed to John Wiley & Sons, Inc. or one of its group companies (each a "Wiley Company") or a society for whom a Wiley Company has exclusive publishing rights in relation to a particular journal (collectively "WILEY"). By clicking "accept" in connection with completing this licensing transaction, you agree that the following terms and conditions apply to this transaction (along with the billing and payment terms and conditions established by the Copyright Clearance Center Inc., ("CCC's Billing and Payment terms and conditions"), at the time that you opened your Rightslink account (these are available at any time at <http://myaccount.copyright.com>)

Terms and Conditions

1. The materials you have requested permission to reproduce (the "Materials") are protected by copyright.

**JOHN WILEY AND SONS LICENSE
TERMS AND CONDITIONS**

Aug 13, 2011

This is a License Agreement between Benson Edagwa ("You") and John Wiley and Sons ("John Wiley and Sons") provided by Copyright Clearance Center ("CCC"). The license consists of your order details, the terms and conditions provided by John Wiley and Sons, and the payment terms and conditions.

All payments must be made in full to CCC. For payment instructions, please see information listed at the bottom of this form.

License Number	2727311004838
License date	Aug 13, 2011
Licensed content publisher	John Wiley and Sons
Licensed content publication	Chemistry - A European Journal
Licensed content title	Solid State and Solution Conformation of [Ala7]-Phalloidin: A Synthetic Phallotoxin Analogue
Licensed content author	Giancarlo Zanotti, Lucia Falcigno, Michele Saviano, Gabriella D'Auria, Bianca Maria Bruno, Tiziano Campanile, Livio Paolillo
Licensed content date	Apr 1, 2001
Start page	1479
End page	1485
Type of use	Dissertation/Thesis
Requestor type	University/Academic
Format	Electronic
Portion	Figure/table
Number of figures/tables	1
Number of extracts	
Original Wiley figure/table number(s)	Figure 2
Will you be translating?	No
Order reference number	
Total	0.00 USD

Terms and Conditions

TERMS AND CONDITIONS

This copyrighted material is owned by or exclusively licensed to John Wiley & Sons, Inc. or one of its group companies (each a "Wiley Company") or a society for whom a Wiley Company has exclusive publishing rights in relation to a particular journal (collectively WILEY). By clicking "accept" in connection with completing this licensing transaction, you agree that the following terms and conditions apply to this transaction (along with the billing and payment terms and conditions established by the Copyright Clearance Center Inc., ("CCC's Billing and Payment terms and conditions"), at the time that you opened your Rightslink account (these are available at any time at <http://myaccount.copyright.com>)

Terms and Conditions

1. The materials you have requested permission to reproduce (the "Materials") are protected by

**JOHN WILEY AND SONS LICENSE
TERMS AND CONDITIONS**

Aug 13, 2011

This is a License Agreement between Benson Edagwa ("You") and John Wiley and Sons ("John Wiley and Sons") provided by Copyright Clearance Center ("CCC"). The license consists of your order details, the terms and conditions provided by John Wiley and Sons, and the payment terms and conditions.

All payments must be made in full to CCC. For payment instructions, please see information listed at the bottom of this form.

License Number	2727311406791
License date	Aug 13, 2011
Licensed content publisher	John Wiley and Sons
Licensed content publication	Chemistry - A European Journal
Licensed content title	Phalloidin Synthetic Analogues: Structural Requirements in the Interaction with F-Actin
Licensed content author	Lucia Falcigno,Susan Costantini,Gabriella Dapos;Auria,Bianca Maria Bruno,Suse Zobeley,Giancarlo Zanotti,Livio Paolillo
Licensed content date	Nov 5, 2001
Start page	4665
End page	4673
Type of use	Dissertation/Thesis
Requestor type	University/Academic
Format	Electronic
Portion	Figure/table
Number of figures/tables	1
Number of extracts	
Original Wiley figure/table number(s)	Figure 3
Will you be translating?	No
Order reference number	
Total	0.00 USD
Terms and Conditions	

TERMS AND CONDITIONS

This copyrighted material is owned by or exclusively licensed to John Wiley & Sons, Inc. or one of its group companies (each a "Wiley Company") or a society for whom a Wiley Company has exclusive publishing rights in relation to a particular journal (collectively WILEY). By clicking "accept" in connection with completing this licensing transaction, you agree that the following terms and conditions apply to this transaction (along with the billing and payment terms and conditions established by the Copyright Clearance Center Inc., ("CCC's Billing and Payment terms and conditions"), at the time that you opened your Rightslink account (these are available at any time at <http://myaccount.copyright.com>)

Terms and Conditions

1. The materials you have requested permission to reproduce (the "Materials") are protected by

VITA

Benson J. Edagwa received his Bachelor of Science degree in chemistry in 2005 from Moi University, Kenya. He was introduced to organic chemistry research in Prof. Paul Ndalut's laboratory, and his undergraduate thesis was on the anthelmintic value of pymac and diatomite. In the Fall of 2006, Benson was accepted into the doctoral program in the chemistry department at Louisiana State University, USA, where he is currently a doctoral candidate in organic chemistry working under the direction of Prof. Carol M. Taylor. His graduate dissertation work involves the first total synthesis of a virotoxin and three analogs to investigate the role of proline hydroxylation in the conformation and biological activity of these compounds. In the graduate school, Benson received the Charles Coates Travel Award and the Kiran Allam International Award for outstanding research and teaching in chemistry. He is a member of the American Chemical Society and the Kenyan Chemical Society.